CONTAINS PULLOUTS

Stratigraphy of the mid-Carboniferous boundary

Karen Braithwaite

Submitted in accordance with the requirements for the degree of Doctor of Philosophy

The University of Leeds
Department of Earth Sciences

October 1995

The candidate confirms that the work submitted is her own and that appropriate credit has been given where reference has been made to the work of others.

ABSTRACT

This study investigates the stratigraphy of the newly defined mid-Carboniferous boundary. The selection of the mid-Carboniferous stratotype section should reconcile problems between the different mid-Carboniferous biostratigraphies developed throughout the world and provide a standard against which other successions can be correlated.

The nature of the mid-Carboniferous boundary in the Clare Basin has been investigated. Various geochemical analyses have been conducted on a mid-Carboniferous section and it has been possible to construct a chart relating these various geochemical parameters to relative sea-level. It is shown that although deposition is complete through the interval, there is a geochemical expression of a lowstand during the lowest Chokierian. Additionally, doubt is cast on the presumption that all sediments deposited outside 'marine bands' are non marine. A model has been developed for mid-Carboniferous deposition in the Clare Basin. It is envisaged that the shelves of the Clare Basin were flooded during the early Namurian leading to an environment suitable for phosphate authigenesis. During a major regression in the Pendleian/lower Arnsbergian the phosphate was reworked into a lag. The lowstand of the basal Chokierian is marked by a thin lag on the shelves, whilst deposition was continuous in the basin centre. Later Chokierian times are marked by a widespread transgression.

The mid-Carboniferous stratotype has been chosen at Arrow Canyon, Nevada. Microfacies studies show that deposition was on a winnowed carbonate platform showing reworking of bioclasts. Faunal diversity and eveness studies have also been conducted on this section. No drop in diversity is seen at the mid-Carboniferous boundary, although a drop in eveness is seen, whether this relates to a specialised fauna or selective winnowing of bioclasts is unknown.

Correlations between America and western Europe show that conodonts are strongly facies controlled and it is unlikely that the appearance of *Declinognathodus noduliferus* is truly isochronous between sections, and thus is an unwise choice for defining the mid-Carboniferous boundary. Additionally it is suggested that Arrow Canyon was a poor choice for the stratotype section due to both the possibility of reworking, the presence of an unconformity in the section and possible doubts over the conodont record at this locale.

The *Rhachistognathus minutus* zone is recognized as a new conodont zone across the Arnsbergian/Chokierian boundary.

ACKNOWLEDGEMENTS

I would like to thank my supervisors Paul Wignall and John Varker for providing freely of their time, knowledge, and book collection throughout the course of my Ph.D., and also Rob Raiswell for assistance with all matters geochemical.

Additionally, many thanks go to Nick Riley at the B.G.S for identification of numerous poorly preserved specimens and general interest in the project, Alan Titus and family for introducing me to the mid-Carboniferous of southern Nevada, Ken Higgs for helping me to locate the Luggacurren section and John Pollard for trace fossil identification. Amoco, B.P. and Enron are thanked for funding the Nevadan field work.

All those who have bravely endured field work (and my driving), in particular Ham Smith, Greg Sambrook Smith, Paul Wignall, Chris Wibberley, Jo Wilkin, Tim Pointer, Ed Jones and Rob Nicolls are warmly thanked.

Numerous geochemists put up with my blundering around in the lab, particularly Dave ("where's that dirt come from?") Hatfield, Alan Gray, Simon Botrell, Rob Newton and Simon Dean.

The Sed lab inhabitants provided diversion (Julie Rodent, Mike Stewart and John Livesey) and dodgy jokes and general good humour (Neil Woodhouse). Miss Fitness 1995 (Jo Wilkin), Tim ("I can smell the rain") Pointer, Squadron Leader James Maunder, Jeff ("well I am a postdoc now...") Peakall and Chris Wibberley (probably the most expensive field assistant in the world) are especially thanked for their friendship and cynicism!

Other notable mentions include Jim ("I hate Inishcorker") Best, Nigel, Quentin, Ewan, Rob, Danni, Louise, Liddy, Julia, Golden Child and Andy who all either contributed or provided distraction.

This work could not have been completed without the encouragement and patience of Greg who provided a light at the end of a very dark tunnel!

But most of all, I would like to thank my parents who have always been willing to provide any necessary support in the furtherance of my education.

CONTENTS

LIST OF FIGURES

LIST OF TABLES

LIST OF PLATES

LIST OF ENCLOSURES

Chapter 1

INTRODUCTION

1.1 INTRODUCTION

Over the last two decades an intensive worldwide search for an uninterrupted section spanning the mid-Carboniferous boundary has taken place, with the ultimate goal to find a Global Boundary Stratotype Section and Point. Only at this stratotype is the 'golden spike' placed at a specific point in the section, representing a unique instant in time and a standard against which other sequences can be correlated (Bassett, 1990). This selection of the mid-Carboniferous boundary stratotype section should reconcile problems between the different mid-Carboniferous biostratigraphies developed throughout the world.

1.2 AIMS OF THE THESIS

This study aims to investigate the stratigraphy and changing palaeoenvironments across the mid-Carboniferous boundary, utilising a number of different approaches, from studies of the Clare Basin in western Ireland and at the mid-Carboniferous boundary stratotype at Arrow Canyon in Nevada, and at other sections within the Antler Basin.

There are four main objectives addressed in this study:-

- The Clare Basin is used as a case study to investigate depositional environments across the mid-Carboniferous boundary. Deposition was continuous across the mid-Carboniferous boundary in the basin centre, whilst on the basin shelves a phosphatized unconformity is present. Thus the basin was chosen with the objective to provide a model of mid-Carboniferous deposition utilising sedimentological, palaeontological and geochemical data.

- The mid-Carboniferous boundary stratotype at Arrow Canyon is examined to test the completeness of the section both at this locale and within a basinal context.

- With the decision on the choice of mid-Carboniferous boundary stratotype, ideally the problems of correlating the different biostratigraphic schemes that exist between America and western Europe should be solved. This assumption is examined and an attempt at biostratigraphic correlation is provided.

- The choice of both stratotype section and defining fauna are discussed and questioned in the light of developments over the last two decades since the inception of the search for a boundary stratotype.

1.3 APPROACHES USED IN THIS STUDY

A number of varied techniques were used in this study and are listed below.

- Detailed field logging of sections and utilisation of data collected from the literature has led to clarification of the depositional history of the Clare Basin, Ireland. Field logging of sections in the southern Antler Basin, Nevada facilitated correlation of the mid-Carboniferous throughout that basin, together with providing an insight into the completeness of the mid-Carboniferous boundary in this area.

- Intensive geochemical study has been employed to determine the palaeoenvironmental changes across the mid-Carboniferous boundary at a section in the Clare Basin. The geochemical methods used in this study were U/Th, C/S, degree of pyritization and reactive: total iron ratios. These methods allow the salinity, and degree of anoxia within this mid-Carboniferous basin to be investigated.

- Petrographic and S.E.M. study of thin and polished sections has been employed to elucidate the mode of formation of the phosphorite deposits of County Clare.

- Standard microfacies analysis was applied to petrographic samples taken from the mid-Carboniferous boundary stratotype at Arrow Canyon, Nevada, to elucidate the depositional palaeoenvironment. Statistical analysis (Shannon-Wiener Index) was applied to total counts of biodebris from the same samples to investigate faunal diversity changes around the mid-Carboniferous boundary.

- To facilitate comparison of the western European and American mid-Carboniferous biostratigraphies, range charts for selected conodont species have been produced for both regions. Integration of these charts with ammonoid occurrence data from both areas results in a cross-correlation of both the biostratigraphic schemes.

Many of these approaches have not been applied to the areas in question before. The integration of the detailed geochemical analysis has not previously been applied to ancient sediments, and is particularly applicable to the Irish section due to its good biostratigraphic control and thus known sea-level variations. A model for the mid-Carboniferous deposition in the Clare Basin is presented from the integration of a variety of data (e.g. sedimentological, palaeontological and geochemical).

The detailed study of the palaeoenvironment and faunal diversity changes across the mid-Carboniferous boundary at Arrow Canyon likewise has not been completed before.

1.4 BACKGROUND TO THE THESIS

1.4.1 Mid-Carboniferous stratigraphy

This work concentrates on the mid-Carboniferous stratigraphy of western Europe and America and thus the following description of the history of stratigraphic studies of the Carboniferous is primarily focused on these areas.

1.4.1.1. History of Carboniferous stratigraphic studies

Much interest has been focused on various aspects of Carboniferous geology and is largely due to the widespread economic coal deposits of the Westphalian. The first formal designation of the term Carboniferous was by

Conybeare and Phillips (1822) who also divided up the Carboniferous system into Carboniferous Limestone, Millstone Grit and Coal Measures. These divisions were initially adopted by workers in Europe, America and Russia, however numerous local stratigraphic terms were employed in Europe by the early twentieth century (Ramsbottom, 1991). A congress, with the stated objective to compare the stratigraphy of the Carboniferous in the different coal regions of Europe, was held at Heerlen in 1927. It was here that the notion of a single west European Carboniferous Classification was proposed. A further three congresses followed in 1935, 1951 and 1958. At the third congress in 1951 it was decided that the Carboniferous should remain as a system, although it would be divided into two subsystems, this was later rejected and the general opinion on the formation of a single worldwide classification was rather pessimistic! (Ramsbottom, 1991).

Separate to these meetings were the meetings of the International Geological Congress (I.G.S.). At the fourth meeting of the Heerlen Congress in 1958 the Heerlen temporary committee on Carboniferous Stratigraphy merged with the International Subcommission on Carboniferous Stratigraphy (S.C.C.S.) of the Commission on Stratigraphy of the I.G.S., resulting in a committee (S.C.C.S.) charged initially with the erection of a single classification for western Europe. When the International Union of Geological Sciences (I.U.G.S.) was founded in 1961 the Commission on Stratigraphy and the S.C.C.S. became part of the Union (Nudds and Palmer, 1990; Bouroz *et al.*, 1980).

Since the formation of the S.C.C.S. in 1961, the S.C.C.S. has become more formalised and bureaucratic with the formation of various committees and restrictions on voting rights. The S.C.C.S. has since its inception widened its field of research to investigate the Carboniferous both globally and in specific areas with the formation of Working Groups covering these specific topics. The ultimate aim of the S.C.C.S. is to select stratotypes representing specific chronostratigraphic horizons, that are applicable globally. Communication between members is biennially at Meetings of the S.C.C.S., held in conjunction with the International Carboniferous Congress (every four years) and at Field Meetings of the S.C.C.S. . The publication of the annual Newsletter on Carboniferous Stratigraphy also aids communication.

At present in western Europe the Carboniferous system is divided into five series which are then subdivided into stages based on their faunal content (Table 1.1).

Table 1.1 Chronostratigraphic classification for western Europe (from Wagner and Winkler Prins, 1991)

SYSTEM	SERIES	STAGES
C A R B O N I F E R O U S	Stephanian	C B Barruelian (A) Cantabrian
	Westphalian	D Bolsovian (C) Duckmantian (B) Langsettian (A)
	Namurian	Yeadonian Marsdenian Kinderscoutian Alportian Chokierian Arnsbergian Pendleian
	Viséan	Brigantian Asbian Holkerian Arundian Chadian
	Tournaisian	Ivorian Hastarian

The American Carboniferous, however is divided into two subsystems, the Mississippian and Pennsylvanian. These are further subdivided into series, these further subdivisions being based on both faunal and lithological characteristics (Wagner and Winkler Prins, 1991) (Table 1.2).

Table 1.2 Chronostratigraphic classification for North America (from Wagner and Winkler Prins, 1991)

SYSTEM	SUBSYSTEM	SERIES
CARBONIFEROUS	Pennsylvanian	Virgilian
		Missourian
		Desmoinesian
		Atokan
		Morrowan
	Mississippian	Chesterian
		Meramecian
		Osagean
		Kinderhookian

1.4.1.2 History of Carboniferous biostratigraphic studies

The mid-Carboniferous is typified in many regions of the world by siliclastic deposits, and thus biostratigraphic correlation between these deposits is principally limited to the three groups found in these facies: conodonts, goniatites and spores. Additionally brachiopod and foraminiferal schemes

have also been employed predominately in carbonate areas. In this study the ammonoid and conodont schemes are utilised and investigated.

Much of the early biostratigraphic work was principally based in England: Phillips (1832, 1836, 1841) and Brown (1841) being notable as the first workers to attempt a correlation in the Westphalian based on goniatites. Late nineteenth century work focused on the systematic description of faunas (e.g., Haug, 1898; Foord, 1903). These important works provided the basis for the milestone work of Bisat (1924) 'The Carboniferous Goniatites of the North of England and their Zones'. This presented a refined biostratigraphic zonation for the Viséan, Namurian and Westphalian, together with systematic descriptions of virtually all the Carboniferous ammonoids known at that time. Other works in the middle part of this century utilised this landmark work of Bisat and looked at areas of the zonation in more detail (e.g., Bisat, 1940; Bisat and Hudson, 1943; Hudson, 1945; Moore, 1945; Holdsworth, 1965) and also tried to correlate the scheme to regions both within and outside the British Isles (e.g., Bisat, 1928; Hodson, 1954a, 1957; Yates, 1962). The latter part of this century sees the work of ammonoid stratigraphy in Britain dominated by the work of Ramsbottom (e.g., 1962, 1969, 1977, 1978, 1979, 1980, 1981), with the development of schemes related to worldwide eustatic changes, and more recently by Riley (e.g. 1987, 1990, 1993, 1994) by the utilisation of a highly refined biostratigraphic zonation in sequence stratigraphical studies.

Although the ammonoids of predominantly the North American Midcontinent in the late nineteenth and early twentieth centuries were studied (e.g. Smith 1896, 1903; Girty, 1909, 1910), the works were predominantly of a descriptive nature. It was not until the work of Gordon (1964) that a zonation using these faunas was attempted. The various works of Gordon (e.g. 1968, 1969, 1970) and refinement of his biostratigraphic scheme dominated the American literature up until the 1970's. More recent works, principally by Saunders (e.g. 1973, 1975, 1977) have improved the biostratigraphic zonation, and attempted correlations with the western European stratigraphy. Present research is focusing on the newly discovered Chokierian age faunas from Nevada (Titus, 1992, 1993)

Early references to the occurrence of conodonts in mid-Carboniferous rocks in Britain were commonly incidental, and no attempt at zonation was made e.g., Moore (1863) Young (1880a, 1880b), Hinde (1900) and Smith (1900). It was not until the later part of this century that zonations were put forward for

Britain and Ireland, e.g., Rhodes *et al.*, (1969), Austin (1973) and Higgins (1975). Varker and Sevastopulo (1985) and Higgins (1985) have built on these earlier works and presented schemes applicable to the British succession. Comparisons with fauna both within and outside Europe have been made by numerous workers, however, correlation is hampered by facies control of the conodont faunas.

The presence of conodonts in strata in North America was not recognised until the 1920's (e.g. Bassler, 1925; Roundy, 1926). The following forty years saw the publication of predominately descriptive works primarily of samples collected from the mid-Continent. The first comprehensive zonation was proposed by Collinson *et al.*, (1962). An important work by Webster (1969) identified the existence of late Mississippian strata in Nevada and provided an extension of previous Mississippian zonations. Research from the seventies until the present day has been dominated by Lane (e.g. 1971, 1974, 1977, 1982, 1985), Rexroad (e.g. 1979, 1985) and Sandberg (e.g. 1979, 1980). Again, many of these workers have presented correlations with the western European zonation.

1.4.2 Geochronometry

There are predominantly three recent geochronometric schemes applied to the Carboniferous: Lippolt *et al.*, (1984) and Hess and Lippolt, (1986), Harland *et al.*, (1990) and the recent work of Claoué-Long *et al.*, (1993) and Riley *et al.*, (1994).

Figure 1.1 Recent geochronometric charts for the Carboniferous.

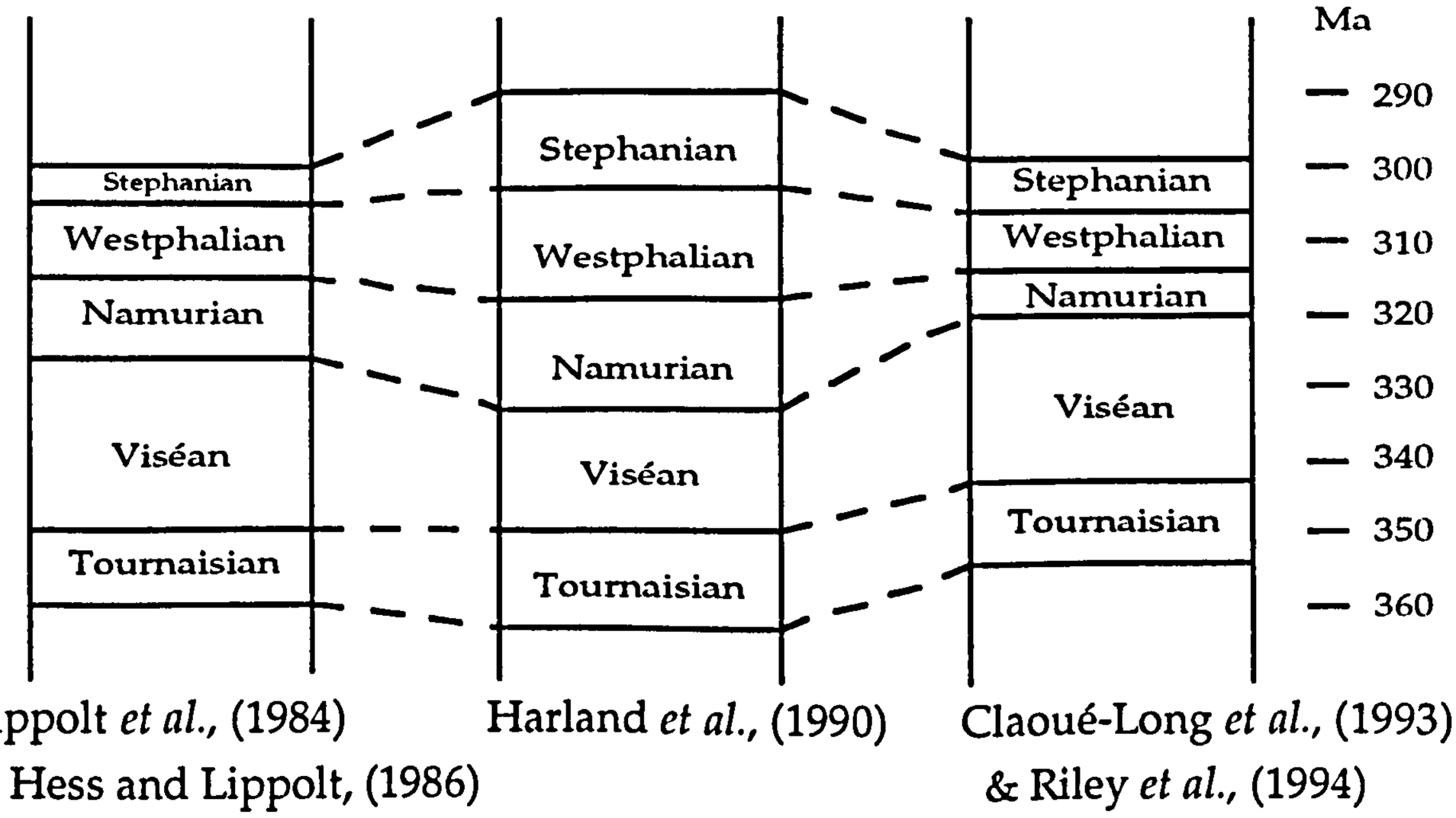

The most recent scheme (shown in Figure 1.1) shows a dramatic reduction in the age range of the Namurian and consequently will have implications for a wide range of applications to Carboniferous geology.

1.4.3 The mid-Carboniferous boundary

1.4.3.1. What is the mid-Carboniferous boundary?

The mid-Carboniferous boundary is a new boundary allowing worldwide correlation of the Carboniferous. Previously, the primary division of the Carboniferous was into five divisions in western Europe (Tournaisian, Viséan, Namurian, Westphalian and Stephanian). The mid-Carboniferous boundary now bisects the Carboniferous system into two subsystems, equivalent to the Mississippian and Pennsylvanian subsystems of the U.S.A.. However, the Mississippian-Pennsylvanian boundary as defined in North America does not have a formally accepted position (Wagner and Winkler Prins, 1991) and thus cannot be used as the stratotype.

1.4.3.2. When is the mid-Carboniferous boundary?

Through the work of the Subcommission on Carboniferous Stratigraphy it has been decided that the mid-Carboniferous boundary corresponds approximately to the time of change from *Eumorphoceras* to *Homoceras* goniatite faunas (Arnsbergian/Chokierian boundary in the Namurian of Great Britain). However, *Homoceras* was not considered a suitable taxon for worldwide recognition of the boundary as it was thought, until recently, to have been restricted to Europe, and thus not a suitable defining taxon worldwide (Saunders, 1984; Titus, 1992; Riley *et al.*, 1994).

Conodonts were one of the most widely distributed faunal groups during the Carboniferous and are therefore used to define the mid-Carboniferous boundary, with the first appearance of *Declinognathodus noduliferus* s.l. marking the level of the boundary (Saunders, 1984).

1.4.3.3 Why is the mid-Carboniferous boundary needed?

The mid-Carboniferous boundary is needed to allow worldwide correlation of the Carboniferous using a common classification scheme. Previously correlation was difficult, if not impossible, due to the development of regional classification schemes; correlation is supposedly now permitted by

using a widespread fauna as the defining biostratigraphic marker. The mid-Carboniferous marks a time of eustatic sea level low (Figure 1.2). Many areas show non-deposition and erosion lasting from late Arnsbergian to early Kinderscoutian times, for example a paleokarst showing relief of up to 100 m, extending over thousands of kilometres is developed on limestones of late Arnsbergian age in North Africa (Lemosquet *et al.*, 1983). As a consequence of this regressive period, significant changes in the fossil record are also seen at this level (Saunders and Ramsbottom, 1986) e.g., 82% of ammonoid genera became extinct between the end of the Arnsbergian and the end of the Alportian (Manger and Saunders 1982).

A stratotype defining the mid-Carboniferous boundary is therefore needed as a worldwide reference point. Work has progressed over the last ten years on the evaluation of potential stratotype sections by the mid-Carboniferous boundary Working Group of the Subcommission on Carboniferous Stratigraphy. A section at Arrow Canyon, Nevada was selected as the mid-Carboniferous boundary stratotype early this year (Lane, 1995).

1.4.4 General overview of the Carboniferous

1.4.4.1 Mid-Carboniferous Palaeogeography

During the Carboniferous, collision was occurring between Gondwanaland and Laurasia, (Leeder, 1988a; Besley 1988; Fraser and Gawthorpe 1990) and resulted in the formation of the Hercynian (Variscan) orogenic belt in western Europe and the Appalachian-Ouachita-Marathon orogenic belt in northern America. The assembly of the supercontinent Pangea resulted from the closure of the 'proto-Tethys' Ocean during the suturing of America and Eurasia (Laurasia) and Africa, South America, Antarctica and Australia (Gondwana) (Leeder, 1988a; Hatcher, 1988). Figure 1.3 shows the palaeogeography during mid-Carboniferous times. Laurasia was situated in a palaeoequatorial/low northern latitudes area, with Gondwana sited primarily in the lower parts of the southern hemisphere.

During the Viséan freely interconnected equatorial seas and extensive areas of shallow shelf seas were prevalent and led to the accumulation of large volumes of shallow-water carbonates at low-mid latitudes (Ross and Ross, 1985a). By the beginning of the Namurian the Hercynian-Appalachian orogeny had closed the equatorial seaway. Clastic debris began to be shed

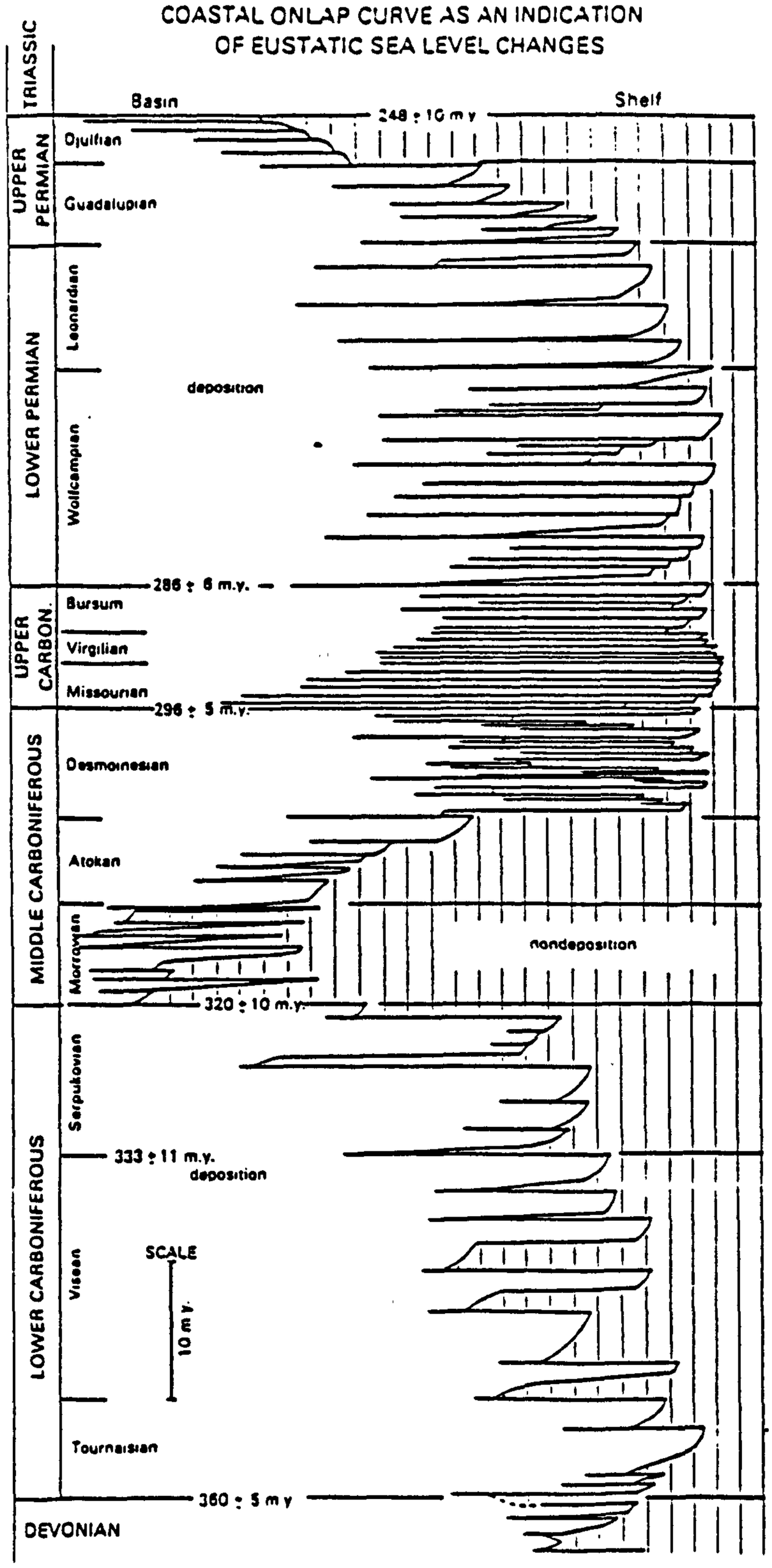

Figure 1.2. Coastal onlap curve for Carboniferous and Permian shelf sediments. The mid-Carboniferous boundary on this diagram occurs between the Serpukhovian and Morrowan stages). (From Ross and Ross, 1988).

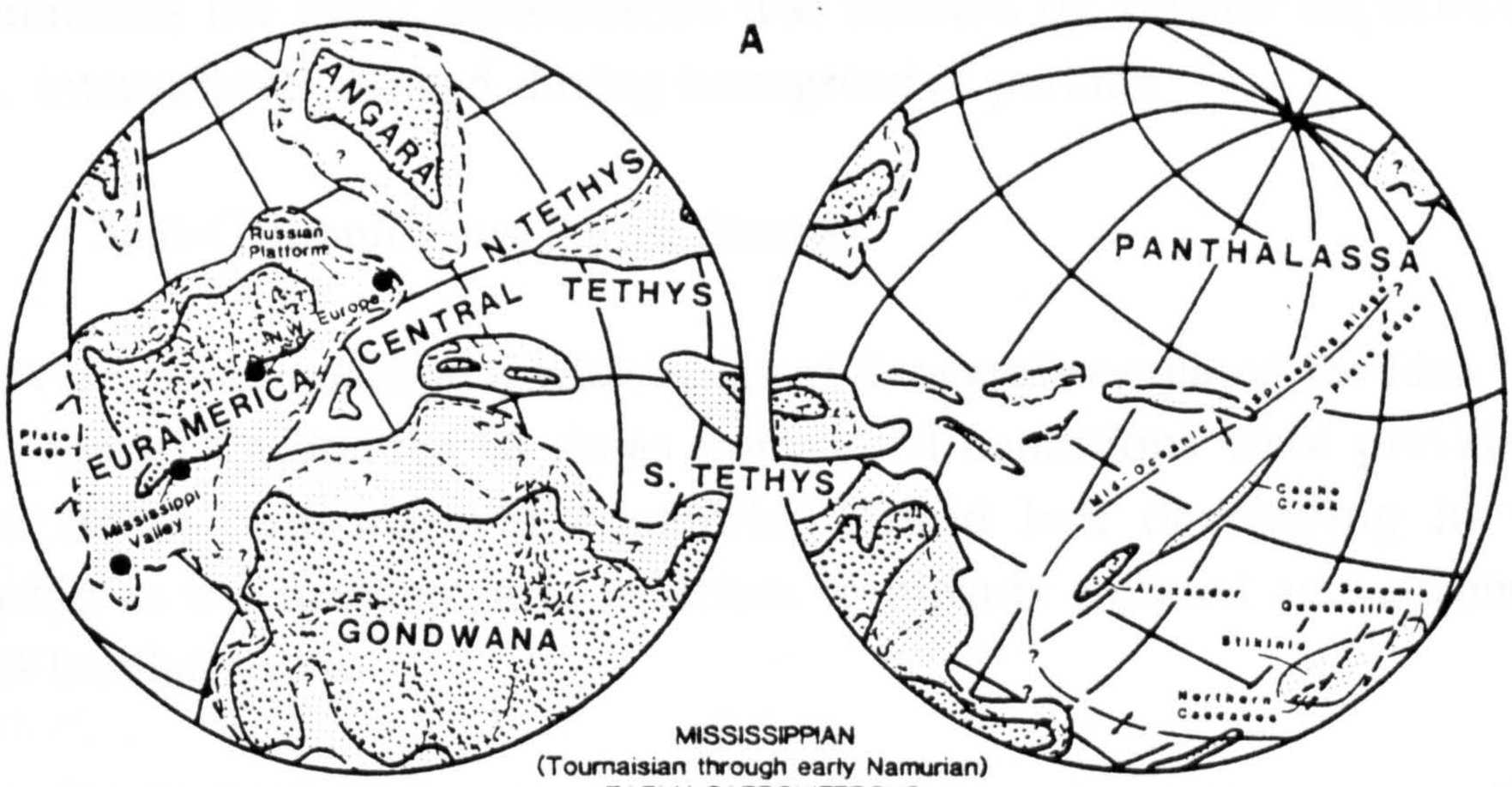

MISSISSIPPIAN
(Tournaisian through early Namurian)
EARLY CARBONIFEROUS

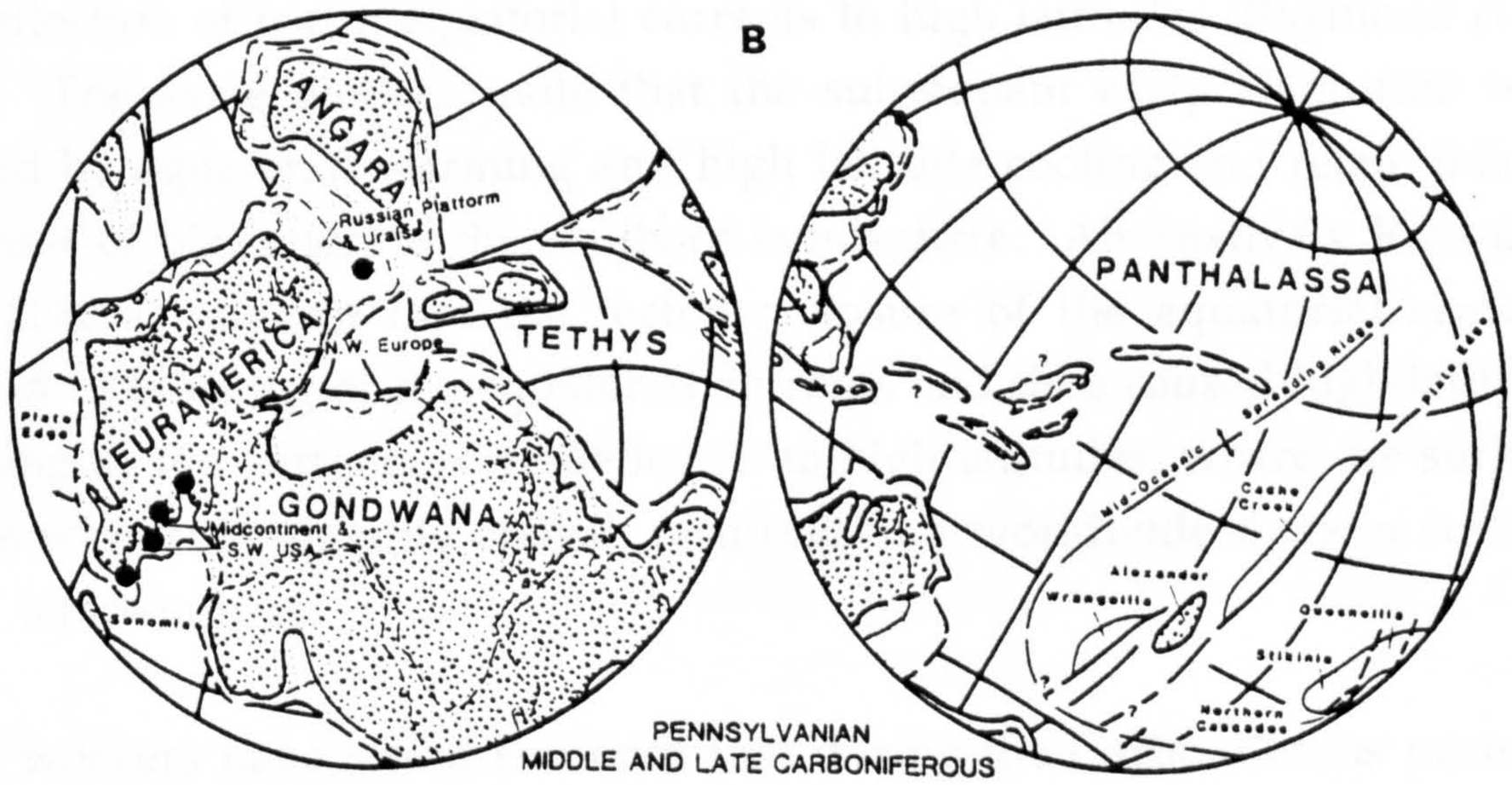

PENNSYLVANIAN
MIDDLE AND LATE CARBONIFEROUS

Figure 1.3. Mississippian and Pennsylvanian global palaeogeography. (From Ross and Ross, 1988).

from uplifted terranes (e.g., Fenno-Scandinavia, Appalachian-Ouachita Mountains) and led to the cessation of carbonate deposition in many areas. Ramsbottom (1980) has envisaged that the whole depositional area in the Carboniferous from the late Viséan was a vast, flat, low lying plain, virtually at sea-level and stretching from the USA, through Europe to the Urals. Thus, rather than the wide connected seas of the lower Carboniferous the mid-Carboniferous was marked by smaller depositional basins, intermittently linked during transgressive periods.

1.4.4.2 Mid-Carboniferous Palaeoclimate

Leeder (1988a) summarised a wide range of data and ventilated the idea that during Lower Carboniferous times monsoonal conditions were prevalent, with a broad, non-seasonal equatorial humid belt developing in the Namurian as the northern and southern continents collided and clustered around low latitudes.

High latitude warming occurred during the Viséan and the very earliest Namurian, and is attributed to the collision of Laurasia with Gondwana and the deflection of warm equatorial currents to high latitudes (Raymond *et al,* 1989). The same workers note that the subsequent early Namurian was marked by equatorial warming and high latitude cooling and relate this to the onset of glaciation in the southern hemisphere. Alternatively Ross and Ross (1985a) suggest that the tectonic closure of the equatorial seaway resulted in blocking of the equatorial currents and thus caused high-latitude warming as the currents were deflected to high latitudes, where the surface waters were subsequently cooled, resulting in a worldwide drop in surface water temperatures.

Many workers have found evidence that during the Carboniferous parts of Gondwana (and to a minor extent Laurasia) were glaciated (Crowell, 1982, Caputo and Crowell, 1985, Veevers and Powell, 1987; Frakes *et al.*, 1992)) with the glaciated areas laying predominantly within 45° of the Gondwanan palaeopole (what is now South Africa, South America and Antarctica). Glaciation was initiated in the late Devonian and three main events have been recognised by Veevers and Powell (1987): Fammenian, Viséan and Namurian.

1.4.4.3 Mid-Carboniferous Sedimentation and Cyclicity

Many workers have recognised cyclothemic deposition in the Carboniferous deposits of Europe, Urals, North Africa and North America (e.g. Saunders *et al.*, 1979.) These cycles are commonly asymmetric showing a rapid deepening followed by slow shallowing. The marine flooding event at the base of these transgressive-regressive cycles is often correlatable over vast distances (e.g. the *Homoceras beyrichianum* marine band has been recognised from the Urals, through Europe to western America).

Cyclical deposition in both the Dinantian and Silesian of western Europe has been documented by numerous workers, (notably Ramsbottom, 1969; 1973, 1977, 1979; Ramsbottom *et al.*, 1962; Calver, 1969; Holdsworth and Collinson, 1988 and Martinsen, 1990, 1993), with the cycles termed 'cyclothems', the smallest cycle seen within a mesothem (Ramsbottom, 1977) or 'minor lithological cycles' (Holdsworth and Collinson, 1988). Essentially each cyclothem consists of limestone/shale/coal or marine/non-marine shales with occasional sandstones, defined by a thin marine flooding surface at the base, termed a 'marine band'. Salinity is thought to be fully marine only at this horizon with a faunal cycle present in the marine band representing the change from non-marine strata to fully marine strata and back (Ramsbottom *et al.*, 1962). The marine portion of each of these cyclothems may only be a few cms thick and may represent only 5% of the total thickness of the cyclothem (Ramsbottom, 1969), however, from estimates of sedimentation rates and decompaction values Holdsworth (1966) argued that the time indicated by the deposition of the shaly deposits during marine bands may represent much of the time available for the formation of the entire cyclothem. Ramsbottom (1977, 1979) has also grouped these smaller scale cycles into larger mesothems, with an attempt to correlate these cycles worldwide made by Ross and Ross (1985b). However, the validity of these cycles is questioned by Leeder (1988a) and Holdsworth and Collinson (1988).

Similar cycles to those described from Europe have been documented from the Appalachians and Midcontinent U.S.A. (e.g., Wanless and Shepard (1936); Busch and Rollins (1984); Heckel (1977, 1986; Klein, 1990; Boardman and Heckel, 1989).

The controlling factor on this deposition has been linked to glacio-eustatic fluctuations during the Gondwanan glaciation by many workers (e.g.

Wanless and Shepard, 1936; Crowell, 1978; Veevers and Powell, 1987; Leeder 1988a), due to the asymmetric nature of the cycles, wide correlation, periodicity and apparent correlation with the initiation of ice-sheet growth in Gondwanaland. Other workers have also emphasised a tectonic influence for the origin of the cycles (e.g. Bott and Johnson, 1967; Klein and Willard, 1989). Ross and Ross (1985b) also mention that crustal processes such as changes in the volume of ocean basins by heating or cooling of the oceanic crust and increases or decreases in ocean trench activity or a combination of these and the above factors may be responsible for eustatic changes during the Carboniferous.

Previous estimates of the mean periodicity between marine bands (e.g., Leeder, 1988a) have used the Lippolt *et al.*, (1984) time scale in which the Namurian lasts 11 Ma and the stratigraphy of Ramsbottom (1969) of 64 marine bands in the Namurian, and resulted in a periodicity of 190 000 years. Heckel (1986) estimated the duration of Midcontinent major cyclothems as lying within the range 0.235 to 0.393 Ma, with the minor cyclothems recording a periodicity of 40 000 to 120 000 years. Similarly Veevers and Powell (1987) calculate a period of 250 000 to 375 000 of glacial boulder beds in western Australia, using the time scale of Harland *et al.*, (1982). This is further discussed in section 9.3.1.2.

It has been shown (Hays *et al.*, 1976; Imbrie *et al.*, 1984) that late Quaternary glacio-eustatic changes were related to the Milankovitch parameters of orbital cyclicity. The range of Carboniferous periodicity values has been attributed to a Milankovitch-type orbital eccentricity forced cyclicity with recurrence periods of 100 000 and 400 000 years by Busch and Rollins (1984), Collier *et al.*, (1990), Holdsworth and Collinson (1988) and Maynard, (1991), with the spread in values resulting from the sum of the combination of eccentricity, precession and obliquity cycles. (Additional distortion of the periodicity's calculated by different workers is likely to result from the use of different time scales). Further calculation yields an average sea-level rise of 45 m (range 37-105 m) from the 100 000 year periodicity, which is analogous to a 300-400 km transgressive landward shift in the position of the shoreline of the modern Mississippi delta (Collier *et al.*, 1990).

Thus, in summary the regions studied in this thesis were situated at low latitudes during the mid-Carboniferous. Palaeoequatorial deposits of the mid-Carboniferous are characterised by frequent (190 000 to 393 000 year) sea-level fluctuations. These periodic changes resulted in the formation of

cyclical deposits characterised by often deep water, marine transgressive deposits at the base followed by regressive shallower water or terrestrial/fluvial facies. Correlation between these cycles and between basins is facilitated by the presence of a distinctive marine biota at the base of the cycle, with commonly basins being linked infrequently and then, only during transgressive periods. A glacio-eustatic origin for these cyclothems due to Milankovitch-driven climatic fluctuations has been invoked by many workers.

1.5 OUTLINE OF THE THESIS

This introductory chapter examines the background and aims of the project.

Chapter 2 describes the western European and American biostratigraphic schemes used in this study. The history of the mid-Carboniferous boundary is discussed, together with the developments leading up to the final choice of stratotype.

Chapter 3 provides the geochemical methodology utilised in this study.

The geological background to the mid-Carboniferous of Ireland (predominantly the Clare Basin) is introduced in chapter 4. Studied mid-Carboniferous sections are described to provide an understanding of the basin history of the Clare Basin. Comparisons between the mid-Carboniferous biostratigraphy of western Ireland and northern Britain are made, together with inferences of sea-level changes.

Chapter 5 introduces current knowledge on the mode of formation and occurrences of phosphorite deposits. The nature of mid-Carboniferous phosphorite deposits of County Clare is described with a model provided for their formation.

Chapter 6 provides geochemical paleoenvironmental determination of the section spanning the mid-Carboniferous boundary at Inishcorker, County Clare, Ireland Various geochemical techniques are described and employed to determine geochemical facies through a period spanning the late Arnsbergian to early Alportian. The combination of a number of techniques elucidates the influence of sea-level changes on the Clare Basin during the mid-Carboniferous.

Using the work presented in chapters 4, 5 and 6 a model for the deposition of the mid-Carboniferous of the Clare Basin is presented in chapter 7.

Chapter 8 describes sections through the mid-Carboniferous of the southern Antler Basin. Using detailed microfacies analysis and statistical methods, the palaeoenvironment and faunal diversity across the mid-Carboniferous boundary stratotype section at Arrow Canyon is investigated. Cross correlation of the Arrow Canyon section with other sections in the Antler Basin is made.

Chapter 9 discusses the choice of both the mid-Carboniferous boundary stratotype and the defining faunal group. Previous cross correlation schemes between Europe and America are presented. An attempt at a cross-correlation between the two biostratigraphic schemes is made in the light of recent work.

Chapter 10 forms the conclusions to this thesis and reviews the findings of this work, together with some suggestions for future work.

Chapter 2

MID-CARBONIFEROUS BIOSTRATIGRAPHY AND THE MID-CARBONIFEROUS BOUNDARY

2.1 INTRODUCTION

This chapter explores the biostratigraphic background to the mid-Carboniferous boundary, both in Britain and North America. The history of the mid-Carboniferous boundary and the final choice of the mid-Carboniferous boundary stratotype are discussed.

2.2 MID-CARBONIFEROUS BIOSTRATIGRAPHY

2.2.1 British biostratigraphy

2.2.1.1 Ammonoid biostratigraphy

The ammonoid biostratigraphy of Great Britain has been extensively studied (e.g. Bisat, 1924, 1928; Moore, 1945; Ramsbottom *et al.*, 1962; Ramsbottom, 1977, 1979), and is the most complete ammonoid stratigraphy across the mid-Carboniferous in western Europe, if not the world. The most recent ammonoid biostratigraphy as defined by Riley (1993) and Riley *et al.*, (1994) (shown in Table 2.1) is used in this study. The ammonoids occur at discrete horizons ('marine bands') usually separated by barren strata from the succeeding marine band. The individual horizons are named after a distinctive ammonoid occurring at that horizon, although other ammonoids are commonly present.

2.2.1.2 Conodont biostratigraphy

The works of Rhodes *et al.*, (1969), Austin, (1973), Varker and Austin, (1974), George *et al.*, (1976), Johnston and Higgins, (1981), Metcalfe, (1981), Higgins and Varker, (1982), Varker and Sevastopulo (1985), and Riley (1990, 1993) have been used for determination of the Dinantian conodont zonation.

Stage	Index	Ammonoid horizon	Conodont Zone
YEADONIAN	G_1b^1	*Cancelloceras cumbriense*	*Idiognathoides sinuatus* - *Idiognathodus primulus (pt.)*
	G_1a^1	*Cancelloceras cancellatum*	
MARSDENIAN	R_2c^2	*Verneuilites sigma*	
	R_2c^1	*Bilinguites superbilinguis*	
	R_2b^5	*Bilinguites metabilinguis*	
	R_2b^4	*Bilinguites eometabilinguis*	
	R_2b^3	*Bilinguites bilinguis*	
	R_2b^2	*Bilinguites bilinguis*	
	R_2b^1	*Bilinguites bilinguis*	
	R_2a^1	*Bilinguites gracilis*	
KINDERSCOUTIAN	R_1c^4	*Reticuloceras coreticulatum*	*Idiognathoides corrugatus* - *Idiognathoides sulcatus*
	R_1c^3	*Reticuloceras reticulatum*	
	R_1c^2	*Reticuloceras reticulatum*	
	R_1c^1	*Reticuloceras reticulatum*	
	R_1b^3	*Reticuloceras stubblefieldi*	
	R_1b^2	*Reticuloceras nodosum*	
	R_1b^1	*Reticuloceras coreticulatum*	
	R_1a^5	*Reticuloceras dubium*	
	R_1a^4	*Reticuloceras todmordenense*	
	R_1a^3	*Reticuloceras subreticulatum*	
	R_1a^2	*Reticuloceras circumplicatile*	
	R_1a^1	*Hodsonites magistrorum*	
ALPORTIAN	H_2c^2	*Homoceratoides prereticulatus*	*Declinognathodus noduliferus*
	H_2c^1	*Vallites eostriolatus*	
	H_2b^1	*Homoceras undulatum*	
	H_2a^1	*Hudsonoceras proteum*	
CHOKIERIAN	H_1b^2	*Isohomoceras sp. nov.*	
	H_1b^1	*Homoceras beyrichianum*	
	H_1a^3	*Isohomoceras subglobosum*	
	H_1a^2	*Isohomoceras subglobosum*	
	H_1a^1	*Isohomoceras subglobosum*	*Rhachistognathus minutus*
ARNSBERGIAN	E_2c^4	*Nuculoceras nuculum*	*Gnathodus bilineatus bollandensis*
	E_2c^3	*Nuculoceras nuculum*	
	E_2c^2	*Nuculoceras nuculum*	
	E_2c^1	*Nuculoceras stellarum*	
	E_2b^3	*Cravenoceratoides nititoides*	
	E_2b^2	*Cravenoceratoides nitidus*	
	E_2b^1	*Cravenoceratoides edalensis*	
	E_2a^3	*Eumorphoceras yatesae*	
	E_2a^{2a}	*Cravenoceras gressinghamense*	
	E_2a^2	*Eumorphoceras ferrimontanum*	
	E_2a^1	*Cravenoceras cowlingense*	
PENDLEIAN	E_1c^1	*Cravenoceras malhamense*	*Kladognathus* - *Gnathodus girtyi simplex*
	E_1b^2	*Tumulites pseudobilinguis*	
	E_1b^1	*Cravenoceras brandoni*	
	E_1a^1	*Cravenoceras leion*	
BRIGANTIAN	P_2c	*Lyrogoniatites georgiensis*	*Gnathodus girtyi collinsoni*
	P_2b	*Neoglyphioceras subcirculare*	*Lochreia mononodosa*
	P_2a	*Lusitanoceras granosus*	*Gnathodus bilineatus*
	P_1d	*Paraglyphioceras koboldi*	
	P_1c	*Paraglyphioceras elegans*	
	P_1b	*Arnsbergites falcatus*	
	P_1a	*Goniatites crenistria*	
ASBIAN (pt.)	B_2b	*Goniatites globostriatus*	
	B_2a	*Goniatites hudsoni*	

Table 2.1 Late Brigantian and Namurian ammonoid stratigraphy and the cross correlation with ammonoid stratigraphy for western Europe.

The studies by Varker, (1964), Varker and Austin, (1974) and Higgins (1975, 1985) and Riley *et al.*, (1987) are used to define the Namurian and early Westphalian conodont biostratigraphy.

Although the current conodont zonation of the Brigantian and Namurian has primarily been developed from sections in England, it is commonly used as a standard western European biostratigraphy. In all cases both single and multielement species are referred to as cited in the relevant papers. The conodont zonation used in this study is shown in Table 2.1 and is discussed below.

***Gnathodus bilineatus* zone**

Recognised by the first appearance of *Gnathodus bilineatus* and *G. praebilineatus* together with the occurrence of *Synclydognathus cuspidatus, S. libratus, S. petilus, S. scalenus, Cavusgnathus cristatus, C. regularis, C. unicornis, Gnathodus girtyi girtyi, G. homopunctatus, Hindeodus? cf. cristulus, Lochriea commutata, Mestognathus beckmanni* and *Neoprioniodus singularis.*

The conodont assemblage zone ranges from the base of the *Goniatites hudsoni* (B_2a) to the early *Neoglyphioceras subcirculare* (P_2b) ammonoid zones (mid-Asbian to mid-Brigantian).

***Lochriea mononodosa* zone**

Recognised by the first appearance of *Lochriea mononodosa* and *Mestognathus bipluti* together with occurrences of *Synclydognathus cuspidatus, S. libratus, S. petilus, S. scalenus, Cavusgnathus cristatus, C. regularis, C. unicornis, Gnathodus bilineatus , G. girtyi girtyi, Hindeodus? cf. cristulus, Lochriea commutata* and *Neoprioniodus singularis.*

The first occurrence of *Polygnathus nodosus* occurs within this zone.

This conodont zone ranges from the early *Neoglyphioceras subcirculare* (P_2b) to the early *Lyrogoniatites georgiensis* (P_2c) ammonoid zones (mid- to late Brigantian).

***Gnathodus girtyi collinsoni* zone**

Recognised by the first occurrence of *Gnathodus girtyi collinsoni* together with the occurrences of *Synclydognathus cuspidatus, S. libratus, S. petilus, S. scalenus, Cavusgnathus cristatus, C. naviculus, C. regularis, C. unicornis, Gnathodus bilineatus , G. girtyi girtyi, G. girtyi rhodesi, Hindeodus? cf. cristulus, Kladognathus macrodentatus, Lochriea commutata, L. mononodosa, Mestognathus bipluti, Neoprioinodus parvus, N. singularis, Ozarkodina collinsoni* and *Polygnathus nodosus*

The *Gnathodus girtyi collinsoni* zone ranges from the early *Lyrogoniatites georgiensis* (P_2c) biohorizon to the base of the *Cravenoceras leion* (E_1a^1) marine band (late Brigantian to base Namurian).

***Kladognathus-Gnathodus girtyi simplex* zone**

Recognised by the first appearance of *Gnathodus girtyi simplex* and *G. girtyi soniae* together with occurrences of *Synclydognathus cuspidatus, S. petilus, S. scalenus, Cavusgnathus claviger, C. naviculus, Gnathodus bilineatus , G. girtyi girtyi, G. girtyi intermedius, G. homopunctatus, Kladognathus macrodentatus, Lochriea commutata, L. mononodosa, Mestognathus bipluti, Neoprioinodus spathatus* and *Polygnathus nodosus*

This conodont assemblage zone embraces the Pendleian Stage (E_1)

***Gnathodus bilineatus bollandensis* zone**

The lower limit of the zone is marked by the first appearance of *Gnathodus bilineatus bollandensis* together with occurrences of *Adetognathus unicornis, Cavusgnathus claviger, C. naviculus, Gnathodus bilineatus bilineatus, G. girtyi girtyi, G. girtyi intermediatus, G. girtyi soniae, Lochriea mononodosa* and *Polygnathus nodosus.*

The zone ranges from the base of the Arnsbergian (E_2) to the lower part of the *Nuculoceras nuculum* (E_2c^4) cyclothem.

***Rhachistognathus minutus* zone**

The base of the zone is delineated by the appearance of *Rhachistognathus minutus.* It appears as if this zone can be recognised by the

occurrence of *Rhachistognathus minutus* and *Adetognathus gigantus*. The zone ranges from within the lower part of the *Nuculoceras nuculum* (E_2c^4) cyclothem to the base of the *Isohomoceras subglobosum* (H_1a^2) marine band.

***Declinognathodus noduliferus* zone**

The base of the zone is marked by the appearance of *Declinognathodus inaequalis, D. lateralis, D. noduliferus* and *Neognathodus bassleri* together with *Adetognathus gigantus* and *Rhachistognathus minutus*. The first occurrence of *D. japonicus* occurs within this zone.

The *Declinognathodus noduliferus* zone ranges from the second *Isohomoceras subglobosum* marine band (H_1a^2) to top Alportian (H_2c^2).

***Idiognathoides corrugatus-Idiognathoides sulcatus* zone**

The base of the zone is marked by the entrance of *Idiognathoides corrugatus, I. macer, I. sinuatus* and *I. sulcatus* together with *Declinognathodus inaequalis, D. lateralis, D. noduliferus* and *Neognathodus bassleri*.

This conodont assemblage zone corresponds to the Kinderscoutian Stage (R_1 ammonoid zone).

***Idiognathoides sinuatus-Idiognathodus primulus* zone**

The base of the zone is marked by the entry of *Idiognathodus primulus*, together with the occurrence of *Declinognathodus lateralis, I. delicatus, Idiognathoides attenuatus, I. corrugatus, I. macer, I. sinuatus, I. sulcatus* and *Neognathodus bassleri*. The entry of *Streptognathodus nodosus* occurs within this zone.

This zone includes the Marsdenian (R_2), Yeadonian (G_1) and early Westphalian A Stages (*Gastrioceras subcrenatum*).

Except for the *Rhachistognathus minutus* zone, all other zones have been previously recognised in the works quoted above. This new zone is defined since it contains a distinct low diversity fauna. It is represented in the strata spanning the Arnsbergian-Chokierian boundary.

2.2.2 American biostratigraphy.

2.2.2.1 Ammonoid biostratigraphy

Unlike European Namurian ammonoid occurrences along particular horizons, the American ammonoids occur throughout the strata, thus the Chesterian and Morrowan ammonoid biostratigraphy is defined in terms of zones (cf. European Dinantian ammonoid zones) rather than marine bands.

The studies of Gordon, (1970), Saunders, (1973), Saunders *et al*,(1977), Manger and Saunders (1980), Webster *et al.*, (1984) and Titus (1992) have been used to determine the American ammonoid biostratigraphy. No early Pennsylvanian ammonoid zones are known from Nevada, and thus the Mississippian and very early Pennsylvanian zones are those of the Antler Basin (where a more complete record is available) and the younger Pennsylvanian zones are those of Midcontinent. A hiatus is present in the Midcontinent across the Mississippian-Pennsylvanian Boundary and thus any lower Pennsylvanian assemblages have been removed; likewise in Nevada an unconformity removed lower Pennsylvanian assemblages. Thus, the composite biostratigraphy presented in Table 2.2 provides the full known biostratigraphy across the boundary in America. (N.B. Cross correlations with the conodont biostratigraphy are poorly known in the late Chesterian).

2.2.2.2 Conodont biostratigraphy

The works of Collinson *et al.*, (1962), Lane (1967), Webster (1969), Dunn (1970), Collinson *et al.* (1971), Lane *et al.*, (1971), Lane and Straka (1974), Lane (1977), Sandberg *et al.* (1980), Lane and Baesemann (1982), Baesemann and Lane (1985), Lane, Baesemann, *et al.*, (1985), Weibel and Norby (1992) and Poole and Sandberg (1991) have been used to delineate the Chesterian and lower-middle Morrowan conodont stratigraphy of the U.S.A. Again, in all cases both single and multielement species are referred to as cited in the relevant papers. The conodont biostratigraphy is shown in Table 2.2.

***bilineatus* -Upper *Cavusgnathus* conodont zone**

The base is delineated by the first occurrence of *Gnathodus bilineatus*, other occurring conodonts include *Cavusgnathus regularis*, *Cavusgnathus unicornis*, *Cavusgnathus charactus*, and *Lochriea commutata*.

Sub-syst..	Series	Ammonoid Zone	Conodont Zone
PENNSYLVANIAN (pt.)	MORROWAN (pt.)	*Verneulites pygmaeus*	*symmetricus* (pt.)
		Arkanites relictus	
		Quinnites henbesti	*sinuatus* - *minutus*
		Retites semiretia	*noduliferus* - *primus*
		UNCONFORMITY	
		Homoceras beyrichianum - *Homoceras coronatum*	
		Isohomoceras suglobosum - *Isohomoceras diadema*	
MISSISSIPPIAN (pt.)	CHESTERIAN	*Delepinoceras thalassoide* - *Zephyroceras friscoense*	*muricatus*
		Stenoglaphyrites involutum	*unicornis*
		Eumorphoceras bisulcatum - *Cravenoceras richardsonianum*	*naviculus*
		Richardsonites merriami	
		Cravenoceras hesperium	
		Syngastrioceras barnettense	
		Lusitanoceras granosus	*bilineatus* - *Upper Cavusgnathus*
		Goniatites multiratus	

Table 2.2 Middle Carboniferous ammonoid stratigraphy and the cross correlation with conodont stratigraphy for the U.S.A.

***naviculus* zone**

The base of the zone is limited to the first occurrence of *Cavusgnathus naviculus* and the upper limit by the disappearance of *Cavusgnathus cristatus* and *Kladognathus primus.* Other occurring conodonts include *Cavusgnathus regularis, Cavusgnathus unicornis, Gnathodus bilineatus, Lochreia commutata* and *Gnathodus girtyi simplex.*

***unicornis* zone**

The top of the *Adetognathus unicornis* zone corresponds with the appearance of *R. muricatus* with the base defined by the appearance of the zonal name-bearer. Other conodonts noted as occurring within the *Adetognathus unicornis* zone include *Cavusgnathus altus, C regularis C. naviculus, C. unicornis, Gnathodus bilineatus, Lochriea commutata* and *G. girtyi simplex.*

***muricatus* zone**

Lower zone

The lower part of the zone is delineated by the occurrence of *R. muricatus* below *Adetognathus lautus.* Conodonts occurring within this zone are *Adetognathus unicornis, Cavusgnathus naviculus, C. unicornis, Gnathodus bilineatus, Lochriea commutatus,* and *G. girtyi simplex.*

Upper zone

The upper *muricatus* zone delineated by the appearance of *Ad. lautus. Gnathodus bilineatus, Gnathodus girtyi simplex* and *Adetognathus unicornis* are also present within the zone.

***noduliferus-primus* zone**

Lower zone

The base of the zone is marked by the first occurrence of *Rhachistognathus primus* or *Declinognathodus noduliferus.* The lower zone is divided into two parts, and is distinguished by the overlap in the upper ranges of *G. girtyi*

simplex and *G. bilineatus* cf. *bollandensis* and the lower ranges of *R. primus* and *D. noduliferus.*

Other conodonts occurring within the zone include *Adetognathus lautus, A. spathus, Lochrica commutata,* and *Rhachistognathus muricatus.*

Upper zone

The top of the zone is defined by the lowest occurrence of either *R. minutus* or *Id. sinuatus.*, and is defined as the range of *Declinognathodus noduliferus* and *Rhachistognathus* above *Gnathodus bilineatus* cf. *bollandensis* and *Gnathodus girtyi simplex. Adetognathus lautus,* and *Rhachistognathus muricatus* also occur.

***sinuatus-minutus* zone**

Lower zone

The base of the zone is defined with its lower limit coinciding with the first appearance of *Id. sinuatus* or *R. minutus,* the lower part of the zone is defined as the range of overlap of *R. primus* and *R. minutus.* Other conodonts include *Adetognathus lautus, Declinognathodus noduliferus and Rhachistognathus muricatus.*

Upper zone.

This zone is limited to the occurrence of *Id. sinuatus* or *R. minutus,* above the range of overlap of *R. primus* and *R. minutus,* prior to the first occurrence of *Neognathodus symmetricus.* It contains a similar fauna to the lower part of the zone.

***symmetricus* zone**

The *Neognathodus bassleri symmetricus* zone was defined as the range of the name-bearer below the first occurrence of *N. bassleri bassleri,* with other conodonts in the zone including *Adetognathus lautus, Declinognathodus noduliferus, Idiognathoides sinuatus, Rhachistognathus muricatus Rhachistognathus minutus*

***bassleri* zone**

The base is delineated by the first occurrence of *N. bassleri bassleri* and the top by the first appearance of *Idiognathodus sinuosus*. Other occurring conodonts include *Adetognathus lautus, Declinognathodus noduliferus, Idiognathoides sinuatus* and *Rhachistognathus minutus, Rhachistognathus muricatus.*

***sinuosus* Zone**

The zone is defined as the overlap in ranges of *Idiognathodus sinuosus* with *Neognathodus bassleri bassleri.* Other conodonts occurring within the zone include *Adetognathus lautus, Declinognathodus noduliferus, Idiognathoides sinuatus, Rhachistognathus minutus.*

Very recent work by Alan Titus (pers. comm. 1995) at the Nevada Test Site has led to the discovery of *Declinognathodus noduliferus* at a much lower position than it has previously been found (exact level not revealed). This new work and possible cross correlations between the British and American stratigraphies are presented and discussed in chapter 9.

2.3 THE MID-CARBONIFEROUS BOUNDARY

2.3.1 The need for a boundary.

To allow worldwide correlation for the Carboniferous System there needs to be a common classification. Previously, Carboniferous Stratigraphic schemes were developed on a regional basis, with three main schemes operating independently in western Europe, North America and the C.I.S. A proposal at the eighth International Carboniferous congress in Moscow (1975) for a unified international classification presented a scheme utilising established units from western Europe, the Soviet Union and North America (Bouroz *et al.*, 1977, 1978a, 1978b). By using previously defined units, it was felt that changes could be kept to a minimum. The original proposals for the subdivision of the Carboniferous utilised the Mississippian and Pennsylvanian subsystems with further subdivision into series and stages shown in Table 2.3 below.

Table 2.3. International Classification of the Carboniferous System proposed at the 8th International Carboniferous Congress in Moscow, 1975. (From Bouroz *et al*, 1977).

System	Subsystem	Series	Stage
Carboniferous	Pennsylvanian	Stephanian	Gzehlian Kasimovian
		Unnamed	Moscovian Bashkirian
	Mississippian	Mississippian	Serpukhovian Viséan Tournaisian

At the International Carboniferous Congress Meeting in Beijing, 1987 steps were taken to formally define the Carboniferous system. It was proposed that:

"The primary division of the Carboniferous shall be into two not three divisions, and that the boundary between the two divisions shall be taken at the level selected...as the mid-Carboniferous boundary and that each of the two divisions of the Carboniferous be recognised as a subsystem." (Engel, 1989).

A stratotype defining the mid-Carboniferous boundary is therefore needed as a worldwide reference point.

2.3.2 The level of the mid-Carboniferous Boundary

2.3.2.1 Preliminary ideas

The boundary between the Mississippian and Pennsylvanian has previously been investigated by a working group of the S.C.C.S. (initiated in 1971). It was found that the boundary between the two systems over much of the U.S.A. is marked by a regional unconformity and the group concluded that the Mississippian-Pennsylvanian boundary probably correlated with the base of the European *Reticuloceras* zone (Gordon and Mamet, 1978).

The 1975 proposal for the subdivision of the Carboniferous followed the ideas of the Mississippian-Pennsylvanian Working Group and defined the

mid-Carboniferous boundary as occurring at the base of the Kinderscoutian (R_1) in western Europe, with the appearance of *Reticuloceras*, although other possible levels such as at the base of the Chokierian (H_1) and Westphalian A (G_1) were also noted.

Brenckle *et al.*, (1977) proposed that the base of the H zone would be more uniformly recognised in both the ammonoid and conodont record.

Responding to a proposal of Bouroz *et al.*, (1977), a call was issued by the Subcommission on Carboniferous Stratigraphy to synthesise all available biostratigraphic data for all major mid-Carboniferous fossil groups to evaluate significant changes that might provide useful mid-Carboniferous boundary choices. A two-day symposium entitled 'The mid-Carboniferous boundary' was organised at the General Meeting of the Subcommission on Carboniferous Stratigraphy (S.C.C.S.) of the International Union of Geological Sciences in Leeds, September, 1981. Much of the biostratigraphic data evidence for the mid-Carboniferous boundary (Ramsbottom *et al.*, 1982) was presented and the results of the different fossil groups and preferred boundaries are shown in Table 2.4.

Table 2.4 Preferred boundaries for specific palaeontological groups from data presented at the mid-Carboniferous boundary meeting, Leeds, 1981 (Ramsbottom *et al*, 1982).

Fauna	Preferred boundary level
Ammonoids	basal Chokierian
Conodonts	basal Chokierian
Foraminifera	basal Chokierian and partly basal Kinderscoutian
Brachiopods	basal Kinderscoutian
Plant megafossils	within the upper Arnsbergian
Palynomorphs	within the upper Chokierian (Northern Europe) or basal Kinderscoutian (North America).
Corals	within the upper Alportian
Crinoids	between the basal Chokierian and basal Kinderscoutian

It thus appeared than the main candidates for the level of the mid-Carboniferous Boundary were at the base of the Chokierian (H_1) or at the base of the Kinderscoutian (R_1). As well as the biostratigraphic evidence it was noted that there was a lack of information of groups during the

Chokierian and Alportian, and also that these stages are commonly absent or show an impoverished fauna.

2.3.2.2 The mid-Carboniferous Working Group

At the Leeds Meeting it was decided to establish an ad-hoc working group of the S.C.C.S. under the chairmanship of Dr. Richard Lane to:-

"...investigate and evaluate the information available with regard to a possible 'lower/middle' Carboniferous boundary with emphasis on biostratigraphy from all parts of the world based on the information provided and views expressed at the 1981 symposium in Leeds." (Lane and Manger, 1985a; 1985b).

The procedure adopted by the ad-hoc committee in formalising the boundary was to first decide on the stratigraphic level and then subsequently examine potential stratotypes.

A comprehensive report by the ad-hoc committee was submitted at the next S.C.C.S. Meeting in Madrid 1983 where recommendations on the choice of biostratigraphic level were submitted (Lane, Bouckaert *et al.*, 1985) and later approved by the Titular Members of the S.C.C.S (Saunders, 1984):-

"1) The mid-Carboniferous boundary corresponds approximately to the time of change from *Eumorphoceras* to *Homoceras* faunas. However, the known distribution of *Homoceras* is not a suitable taxon for worldwide recognition of the boundary as it is restricted geographically to Europe and thus not a suitable defining taxon worldwide.
2) Conodonts were the most widely distributed faunal group during the Carboniferous and are therefore used to define the mid-Carboniferous boundary. The widespread conodont *Gnathodus girtyi simplex* gives rise to *Declinognathodus noduliferus* at approximately the same stratigraphic level. Thus, the first appearance of *Declinognathodus noduliferus* marks the mid-Carboniferous boundary. Where *Declinognathodus noduliferus* is absent (in the Gondwana realm) the top of the range of *Gnathodus girtyi simplex* approximates the same level.
3) Other species and separate fossil groups can also be utilised to recognise or approximate the mid-Carboniferous boundary. The foraminifers *Globivalvulina* sp. D, *Millerella pressa* and *Millerella marblensis* are important stratigraphic markers during the mid-Carboniferous.

Adetognathus lautus, Rhachistognathus primus and *Rhachistognathus minutus* were also noted as being useful marker conodonts."

Lane, Baesemann and Groves (1985) summarised the points against choosing the base of the Kinderscoutian as the mid-Carboniferous boundary. It was stated that the lower limit of the ammonoid *Reticuloceras* Zone is not consistent at three important type localities (type Kinderscoutian, type Morrowan and type Bashkirian). The base of the Kinderscoutian is defined by the appearance of *Reticuloceras circumplicatile* whilst the correlative base of the *Reticuloceras* Zone (*Retites semiretia*) in Arkansas contains *Reticuloceras tiro* and *R. wainwrighti* (and is dated as equivalent to the western European R_1b^2 ammonoid horizon, see section 9.2.1) The Bashkirian type section in C.I.S. does not even contain reticuloceratids.

Following the 1983 Madrid Meeting Richard Lane was charged with the formation and selection of an actual Working Group to begin deliberations for the selection of a stratotype. The working group consisted of 20 persons representing 12 countries. The biennial meetings of the S.C.C.S. since 1983 have provided much discussion on the merits of potential stratotypes together with more general discussion. Relevant field sites and potential stratotypes were visited in relation to these meetings at separate times by members of the working group.

2.3.3 Potential stratotype sections

Guidelines were issued to the Working Group for use in their evaluation of potential sections (Engel, 1990):-

1) The chosen potential locality should be fully accessible without logistical, political or other restrictions.
2) The section should be reasonably continuous (or composite) with good exposure, a lack of structural complexity, and a diverse and abundant fossil content.
3) Faunal studies of evolving lineage's should be completed or at least well-advanced; ideally they should include foraminifera, conodonts, ammonoids or spores where appropriate.
4) The chosen section(s) should have available fossil lists based on the first occurrence of relevant species on a sample-by-sample basis through the critical interval.

5) Each section will require information about its geological setting and the presence of any tectonic influences. The sedimentology needs to have been documented or at least be under active investigation.

In addition, as many fossil groups as possible should be present in the stratotype section to allow correlation with sections outside the subequatorial paleolatitudinal belt (where particular key fossil groups are not represented due to palaeoclimate or other differences). Companion studies also need to be undertaken in paralic or non-marine sections so that other fossil groups represented in these environments may be studied (Riley *et al.*, 1987).

A total of 11 sections have been proposed as potential stratotype sections since 1983 (Table 2.5).

For various reasons (e.g.. imprecise boundary location, political instability etc.) many of the sections were discounted leaving three main candidates:-

1) Stonehead Beck, Cowling, North Yorkshire, U.K.
2) Arrow Canyon, Nevada, U.S.A.
3) Aksu-1, Gissar Range, South Tien Shan, Uzbekistan.

2.3.3.1 Stonehead Beck, Cowling, West Yorkshire

The section at Stonehead Beck is situated 35km WNW of Leeds and occurs within a 40m thick section of the Sabden Shales. The exposed strata consist predominantly of shales with a thin sandstone at the base; occasional silty horizons also occur. Deposition was in a low energy basinal palaeoenvironment. The fauna is concentrated along discrete levels ('marine bands') often associated with calcareous nodules or beds, and consists of ammonoids, bivalves, gastropod spat, rare brachiopods and conodonts (not restricted to the so-called marine bands).

Ramsbottom *et al.*, (1983) first mentioned the section at Stonehead Beck as a possible reference section for the mid-Carboniferous boundary at the S.C.C.S. Meeting in Madrid 1983, and stated that the mid-Carboniferous boundary occurred at the base of the Chokierian. Riley *et al.*, (1987) formally proposed the section as a possible stratotype section and thoroughly studied the biostratigraphy (Figure 2.1). The conodont defined mid-Carboniferous boundary was re-evaluated as occurring 0.40 m below

Section	Reference	Facies	Fauna	Advantages	Disadvantages
Yushuliang, Eastern Gansu Province, China.	Skipp et al., 1989; Lane, 1988; Li *et al*,. 1987	Shallow marine and continental mixed carbonates and clastics.	Conodonts, ammonoids, megaflora.	Good access; good exposure.	Probable gap in the succession, structurally complicated.
Zhelvakovaya Valley, Donets Basin, Ukraine.	Skipp *et al.*, 1989.	Shallow marine and continental mixed carbonates and clastics.	Conodonts, ammonoids, foraminifera, spores.	Marine faunas and terrestrial spores.	Problematical access; poor exposure; imprecise boundary location.
Bechar Basin, Algeria.	Lemosquet *et al.*, 1983; Manger *et al.*, 1985.	Shallow marine mixed carbonate and clastics.	Conodonts, ammonoids, brachiopods, foraminifera	Highly fossiliferous	No correlation between faunal zones and various different groups; no sequence of ammonoids established.
Kal'muis, Donbass, Ukraine	Nemirovskaya *et al.*, 1990; Poletaev *et al.*, 1988.	Shallow marine and continental mixed carbonates and clastics.	Conodonts, ammonoids, foraminifera, brachiopods, corals, ostracods, bivalves, gastropods and algae	Wide range of fauna	Restricted conodont species; overlap of lower and upper Carboniferous conodonts; lack of ammonoids over boundary.
Col de Tantes, Haute Pyrénées, France.	Perret (1992)	Basinal carbonates.	Conodonts, crinoids, ostracods, goniatites, bivalves.	Good access (May-Nov!); good exposure	Highly metamorphosed; structurally complicated.
Granite Mountain, Nevada, U.S.A.	Gordon, 1983; Webster *et al.*, (1984);	Shallow marine carbonates.	Conodonts, foraminifera, bryozoa, brachiopods,	Good exposure, wide range of fauna.	Reworking of older conodonts at the mid Carboniferous boundary.
Baping, Guizhou Province, China	No details available.				
Guilin, Guangxi Province, China.	No details available.				
White Knob Mountains, Idaho, U.S.A.	Skipp *et al.*, 1983.	Shallow marine carbonates.	Conodonts, foraminifera, brachiopods, bivalves, corals, bryozoa.	Wide range of fauna.	Probable gap in the succession.
Stonehead Beck, North Yorkshire, England	See Text				
Arrow Canyon, Nevada, U.S.A.	See Text				
Aksu-1, Gissar Ridge, Uzbekistan.	See Text				

Table 2.5 Table showing potential candidate sections for the mid-Carboniferous boundary.

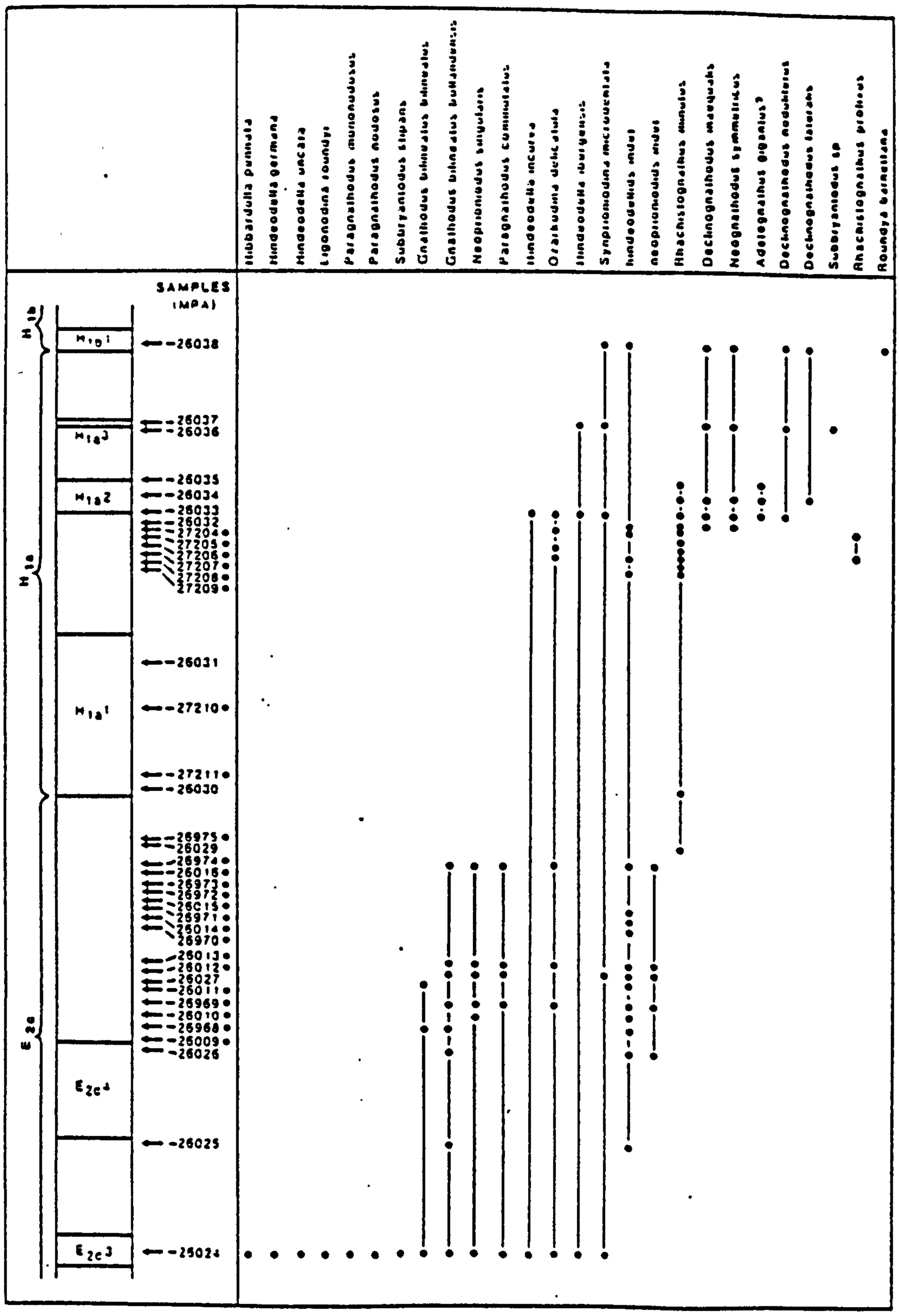

Figure 2.1 Conodont ranges across the mid-Carboniferous boundary at Stonehead Beck. Scale 1:240. (From Owens *et al.*, 1990). The mid-Carboniferous boundary is marked by the appearance of *Declinognathodus* s.l., which first appears in sample 26032.

the base of the H1a2 marine band (ie., 9.4 m above the Arnsbergian-Chokierian boundary), with the appearance of *Declinognathiodus inaequalis*.

The biostratigraphy for this section was refined by Varker *et al.*, (1990, 1994) and Owens *et al.*, (1990). It was found that the upper part of the *Gnathodus bilineatus bollandensis* zone was represented solely by *Rhachistognathus minutus*. The *Rhachistognathus* biofacies typically represents a shallow water fauna and additionally evidence for a shallower water environment at the close of the Arnsbergian is provided by the presence of the nearshore alga *Botryococcus* (Varker *et al.*, 1990, 1994; Owens *et al.* , 1990)

There is no change in the composition of miospore populations across the boundary at Stonehead Beck, with the boundary lying in the middle of the SO (*Lycospora subtriquetra-Kraeuselisporites ornatus*) zone. It has been noted (Owens, 1982) that two other miospore species may be important in delineating the boundary. *Schulzospora campyloptera* occurs up to 5 m below the Arnsbergian/Chokierian boundary and *Grandispora spinosa* has its youngest occurrence 16 m above the same boundary at Stonehead Beck.

There is good evidence that there is no break in deposition at the locality as, apart from there being no physical evidence of a break, there is a complete ammonoid and conodont zonal sequence. Geochemical work (Sr and clay mineral studies) by Riley *et al.*, (1994) also provided supporting evidence that there is continuous deposition through the mid-Carboniferous at this locality.

The section at Stonehead Beck is already the boundary stratotype for the Arnsbergian/Chokierian boundary (Ramsbottom *et al.*, 1981) and the type locality for *Isohomoceras subglobosum* (Bisat, 1924; Riley, 1987). The section has been bought by English Nature and designated a Site of Special Scientific Interest (S.S.S.I.) to guarantee its preservation (John Varker, *pers comm.*, 1995).

The section was visited by the working group in 1985 (Lane, 1988; Skipp *et al.*, 1989).

2.3.3.2 Arrow Canyon, Nevada.

The potential stratotype in Nevada is situated 80 km north-east of Las Vegas. Arrow Canyon exposes formations from late Devonian to Permian

in age with rocks of mid-Carboniferous age being represented by the Indian Springs and Bird Spring Formations. The Chesterian Indian Springs Formation (early Namurian) is 70 m thick and consists of interbedded limestones and shales in the lower part with bioclastic limestones in the upper. The Bird Spring Formation is 750 m thick and comprises sandy, cherty bioclastic limestones. The Bird Spring Formation ranges in age from Chesterian (late Mississippian) to Early Permian. Both formations are very fossiliferous with a shallow water fauna comprising conodonts, foraminifera, ostracods, bivalves, algae, brachiopods, bryozoa, corals and crinoids. The section at Arrow Canyon is further detailed in chapter 8.

Due to the virtually continuous exposure much work has been centred on the area. Langenheim and his students from the University of Illinois have published numerous reports on various aspects of the palaeontology and geology of the Arrow Canyon Section (e.g., Langenheim *et al.*, 1962; Langenheim and Langenheim, 1965). After being recognised from these early works as being one of the most depositionally complete exposures of Late Mississippian-Early Pennsylvanian strata in the USA, further biostratigraphic work (Webster and Lane, 1967; Webster, 1969) was conducted with the result that the section became the basis for conodont zonation in the USA (e.g., Lane and Baesemann, 1982).

Lane, Baesemann *et al.*, (1985) proposed Arrow Canyon as a potential stratotype due to its extensive exposure and completeness. The Mississippian-Pennsylvanian boundary occurs within the lower part of the Bird Spring Formation. The actual boundary shown by the presence of *Declinognathodus noduliferus* occurs " less than 1m below a conglomeratic horizon" (Lane, Baesemann *et al,*. 1985) in the lower part of the Bird Spring Formation within the top of a limestone bed, 85.4 m above the base of the Indian Springs (Webster *et al.*, 1985) (Figure 2.2). Prior to this work it was thought that the unconformity shown by the conglomerate marked the Mississippian/Pennsylvanian boundary.

There are multiple faunal events in the 9 m boundary interval which do not occur at the same stratigraphic levels. Foraminiferal and brachiopod zonation schemes have been erected for the Arrow Canyon section, however they do not coincide with each other nor with the conodont zonation.

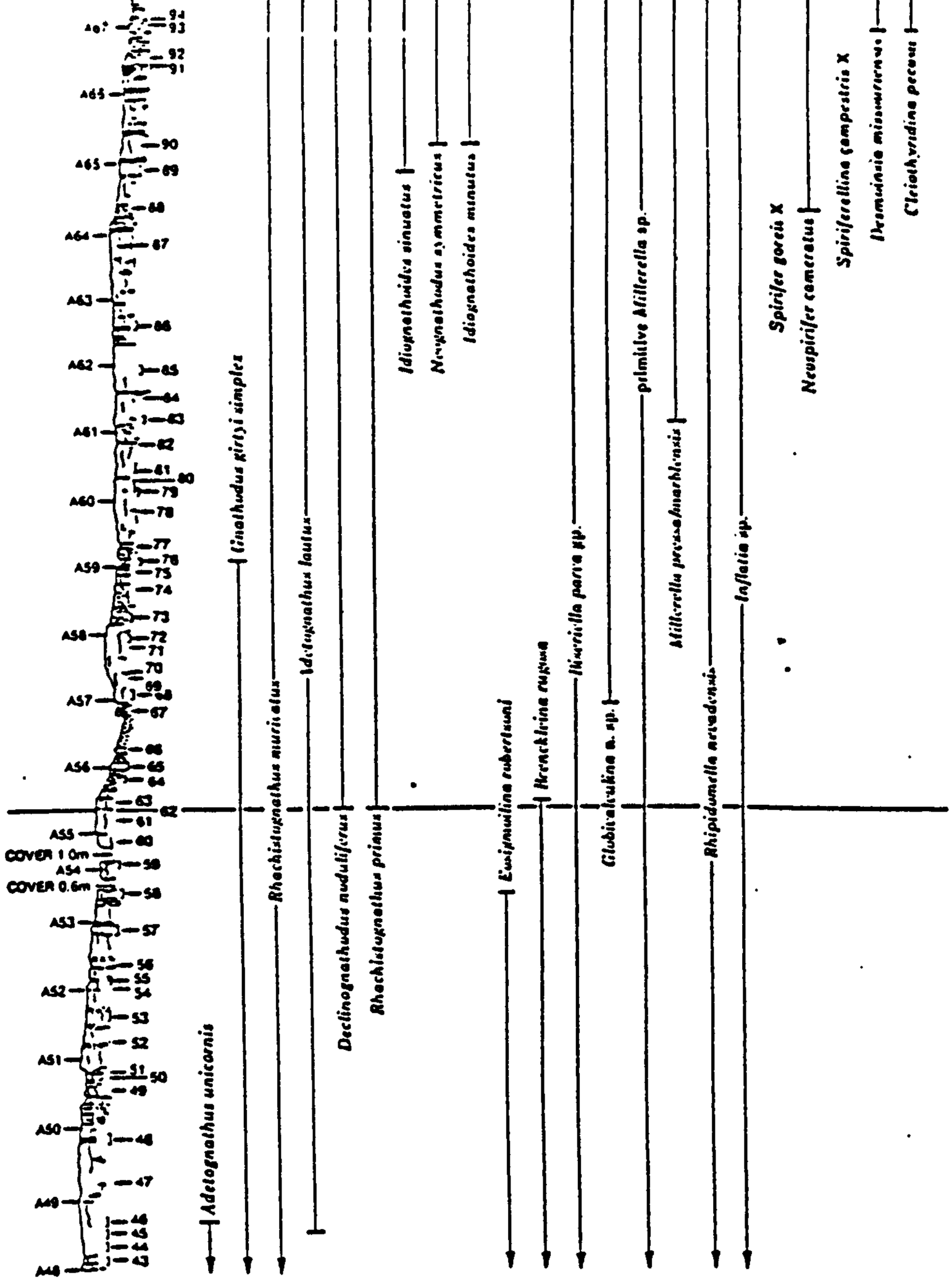

Figure 2.2 Ranges of important conodonts, foraminifera and brachiopods in a 30 m interval of the Bird Spring Formation across the mid-Carboniferous boundary at Arrow Canyon. 'A' numbers are spaced every 1.5 m. Numbers to the right of the stratigraphic column are sample positions. Taxa from *A. unicornis* to *Id. minutus* are conodonts, from *E. robertsoni* to *M. pressa* are calcareous foraminifera and the remainder are brachiopods. Sequence between A53 and A55 is not scale. (From Lane *et al.*, 1985).

The working group visited the section in 1989 and it was suggested that the section potentially was a good choice for the mid-Carboniferous boundary stratotype. However, it was noted that there were imperfections at the locality although these were stressed to be at the level of the conglomerate above the Mississippian-Pennsylvanian boundary (Engel, 1990).

2.3.3.3 Aksu-1 Section, Gissar Ridge, South Tien Shan, Uzbekistan.

The Aksu-1 section is situated in the Surchandarjinskaya district of Uzbekistan, on the south point of the Surkhantau Ridge (part of the Gissar Ridge), Tien Shan. Nemirovskaya and Nigmadganov (1992) proposed the 20 m thick section, which is exposed on the left bank of the Aksu River south of the village of Badava. The lower part of the section consists of micritic and interbedded cherts of the Badavinskaya Suite and contains *Eumorphoceras* ammonoids. The overlying Suffinskaya Suite is homoceratid-bearing and comprises interbedded shales, cherts and limestones (Figure 2.3).

A deep water fauna is present in the section at Aksu and includes conodonts, ammonoids, foraminifera, brachiopods and other groups. A co-occurrence on one bedding plane of the *Eumorphoceras* and *Isohomoceras* faunas is evident. The *Isohomoceras* faunas in this section also occur with *Idiognathoides* and *Neognathodus* conodont faunas and thus have a longer time range than the British sections.

It was suggested (Nemirovskaya and Nigmadganov, 1992) that the overlap in eumorphoceratid-homoceratid ammonoid ranges and the presence of intermediate conodont species (e.g., *Gnathodus postbilineatus*) suggest that the Aksu section is one of the most complete candidate sections,

Eva Paproth (Chairman S.C.C.S.) visited and reported to the Subcommission on the site in 1993

2.3.4 The decision

The procedure adopted by the I.U.G.S. Subcommission on Carboniferous Stratigraphy in the deciding a stratotype is detailed by Bouroz *et al.*, (1980). Basically the steps are as followed:-

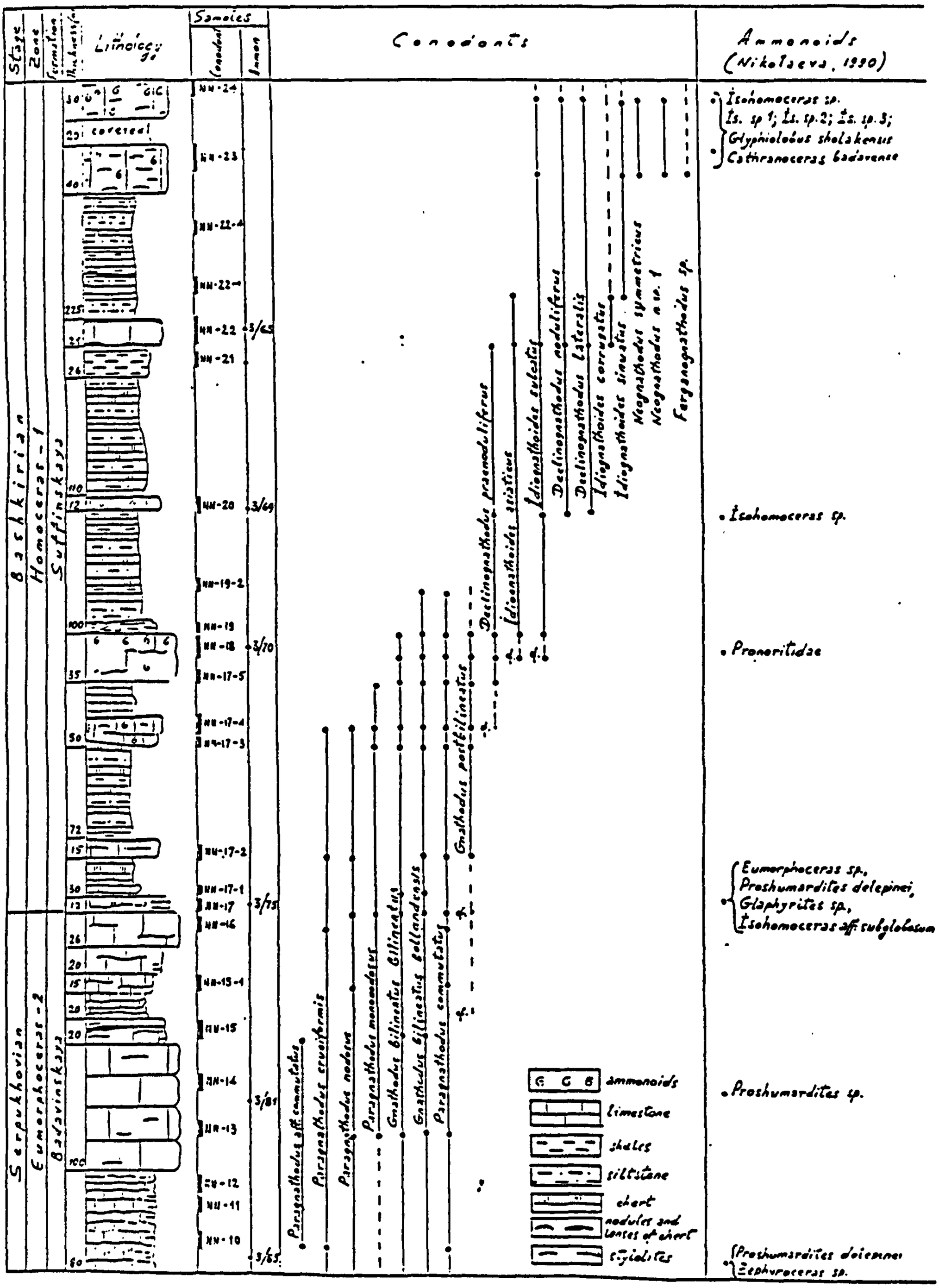

Figure 2.3 Conodont and ammonoid distribution across the mid-Carboniferous boundary of the Aksu-1 section, Gissar Ridge. Scale 1:50. From Nemirovskaya and Nigmadganov (1992).

1) After discussion at an S.C.C.S. meeting the merits of the various potential choices for stratotype sections, and the details for the stratotype candidates are published in the Newsletter on Carboniferous Stratigraphy.
2) A postal vote is then taken among the members of the working group. The Titular Members of the S.C.C.S. then have to approve/disapprove the selected candidate stratotype section
3) The result is then published and forwarded to the I.U.G.S. for ratification.

At the S.C.C.S. Meeting in Liège, Belgium in June 1993 much of the meeting dealt with mid-Carboniferous Boundary matters. A full review of the various proposed sections and their attributes was given by Richard Lane. It was decided to limit the decision on a stratotype to the three sections:- Stonehead Beck, U.K., Arrow Canyon, U.S.A. and Aksu-1, Uzbekistan with a postal vote to be concluded by 15th January 1994.

Extensive documents were circulated to all members of the working group. The sections were voted for in the order 1, 2 and 3 and the chosen candidate would be that with the lowest score of votes. However as shown in Table 2.6, both Arrow Canyon and Stonehead Beck had an equal number of first votes. It was then decided to conduct a second ballot with the choice narrowed to Arrow Canyon and Stonehead Beck. Arrow Canyon was chosen with 11 votes compared to Stonehead Beck's 8 votes.

As a consequence of the need to relocate the exact position of the boundary, a further vote was taken amongst the members of the working party, this was passed 13 to 5 (notably with Alan Higgins, Walt Manger, Bernard Owens, Eva Paproth and Bill Ramsbottom still disagreeing with the choice of stratotype.)

The proposition with supporting documentation was then passed to the Voting Membership of the Subcommission for ratification. The ballot closed on the 15th February 1995. The results are presented in Table 2.7.

Table 2.6. Results of the two postal ballots held by the mid-Carboniferous working group to decide the mid-Carboniferous boundary Stratotype. From Lane *et al.*, (1994). (A.C. = Arrow Canyon, S.B. = Stonehead Beck).

		1st Ballot			2nd Ballot	
Member	Country	A.C.	Aksu	S.B	A.C.	S.B.
Brenckle, P	U.S.A.	1	2	3	x	
Dvorak, J.	Czech.	2	3	1		x
Engel, B.	Aus.	2	3	1		x
Gastaldo, R.A.	U.S.A.	1	3	2	x	
Gibshman, N.	C.I.S.	1	3	2	x	
Higgins, A.C.	U.K.	3	2	1		x
Igo, H.	Japan	1	3	2	x	
Jing-zhi, Y.	China	2	1	3	x	
Lane, H.R.	U.S.A.	1	2	3	x	
Manger, W.	U.S.A.	2	3	1		x
Nemirovskaya, T.	C.I.S.	2	1	3	x	
Owens, B.	U.K.	2	3	1		x
Paproth, E.	G.R.	2	3	1		x
Perret, M.-F.	France	2	3	1		x
Ramsbottom, W.H.C.	U.K.	3	2	1		x
Rocha-Campos, A.	Brazil	1	3	2	x	
Skipp, B.	U.S.A.	1	2	3	x	
Yi-Ping, R.	China	2	1	3	x	
Zhi-hao, W.	China	1	2	3	x	
Total scores		32	45	37	11	8
No. of first votes		8	3	8		

Table 2.7. Subcommission vote on the mid-Carboniferous boundary (From Lane, 1995).

Member	Country	Yes	No
Brenckle, P	U.S.A.	x	
Chuvashov, B.	Russia	x	
Durante, M.	Russia	x	
Dutro, J.T., Jr.	U.S.A.	x	
Engel, B.	Aus.		x
Gonzalez, C.R.	Argentina	x	
Hongjun, G	China	x	
Igo, H.	Japan	x	
Kosanke, R.M.	U.S.A.	x	
Lane, H.R.	U.S.A.	x	
Laveine, J.P.	France	x	
Mamet, B.L.	Canada		x
Manger, W.	U.S.A.	x	
Paproth, E.	G.R.		x
Ramsbottom, W.H.C.	U.K.		x
Roberts, J.	Aus.	x	
Rocha-Campos, A.	Brazil	x	
Sevastopulo, G.D.	Ireland	x	
Shipu, Y.	China	x	
Wagner, R.H.	Spain	x	
Winkler Prins, C.F.	Holland	x	
Xingxue, L.	China	x	
Total scores		18	4

The decision of the Voting Members of the Subcommission confirmed the choice of Arrow Canyon as stratotype. The decision is now in the process of being formally recognised by the I.U.G.S.. (Engel, 1995).

The choice of both biostratigraphic marker and stratotype is further discussed in chapter 9.

2.4 SUMMARY

1. Conodont and ammonoid stratigraphies presented in this chapter form the basis for further discussions in the following chapters.

2. The mid-Carboniferous (or Mississippian/Pennsylvanian) boundary is marked by the first appearance of the conodont *Declinognathodus noduliferus* s.l.. The Mississippian/Pennsylvanian boundary approximates the Arnsbergian/Chokierian boundary, actually occurring slightly above it in the U.K., 40 cm below the H_1a^2 marine band.

3. The mid-Carboniferous boundary stratotype has been chosen within a shallow water carbonate sequence at Arrow Canyon, Nevada, U.S.A. The section is further detailed in chapter 8, and the wisdom of this choosing the section as stratotype is questioned in chapter 9.

Chapter 3

METHODOLOGY

3.1 INTRODUCTION

Palaeoenvironmental parameters such as oxygen levels and salinity were investigated using a series of lab. based (carbon analysis, sulphur analysis and iron analysis) and field based (gamma ray analysis) geochemical techniques. In addition, microfossils were extracted by acid digestion of rock samples.

Rock samples were mostly taken by a hand-held core-drill and where possible outer weathered rock was removed prior to coring to help prevent leached or oxidised samples being collected. To provide representative unbiased samples all rock samples were finely powdered using firstly a pestle and mortar followed by a mechanical ball mill. The samples were then stored in sealed bags. All machinery is thoroughly cleaned after each milling to prevent cross-contamination.

Carbon content (both total and inorganic) was determined by gas chromatography on a Carlo Erba Elemental Analyser model 1106, using the method of Krom and Berner (1983). Total sulphur was also determined by gas chromatography, with pyrite sulphur being determined using the method of Raiswell *et al.*, (1988), a modification of Canfield *et al.*, (1986). Reactive iron was determined by acid leaching (Berner, 1970) and measured by atomic absorption spectrophotometry. Total iron was determined by x-ray fluorescence spectrometery.

A portable gamma-ray spectrometer (Exploranium GR-256) was used in the field to measure amounts of Uranium, Thorium and Potassium applying the method of Myers and Wignall (1987).

A Camscan Series 4 scanning electron microscope (S.E.M.) was used to produce images of both specimens and polished sections, and also to

measure them quantitatively with an Link electron detection system (E.D.S.).

The methods of Varker (1987) and Collinson (1963) were used to digest rock samples for conodont analysis. The electromagnetic method of Varker (1987) was used to concentrate conodonts.

3.2 CARBON ANALYSIS

Both inorganic and total carbon contents for each sample were determined using gas chromatography on a Carlo Erba Elemental Analyser model 1106, applying the method of Krom and Berner (1983).

3.2.1 Principles of the Carlo Erba Elemental Analyser

The Carlo Erba Elemental Analyser is shown in diagram form in Figure 3.1. The machine contains two vertical quartz combustion/pyrolysis tubes, (used separately) surrounded by furnaces. The left tube is used for sulphur combustion and the right tube is used for carbon combustion (Figure 3.2). Samples (accurately weighed into small tin cups) are dropped at pre-set intervals (twelve minutes) into a the combustion tube, heated to 1030°C, through which a constant flow of helium is maintained. Flash combustion takes place as the helium stream is temporarily flushed with pure oxygen resulting in the oxidation of the tin cup. The resultant gases are quantified by being passed over chromium oxide (Cr_2O_3). The mixture of gases are transferred through a reduction reactor (filled with copper) at 650°C to eliminate excess oxygen, then it is introduced into the chromatographic column packed with Porapak QS and heated to 100°C. The individual components are then separated in the order N_2-CO_2-H_2O and are measured by a thermal conductivity detector with the response signal being interpreted by a computer to give a quantitative result. For further details on the operation and limits of the Carlo Erba Spectrometer see Al-Biatty (1990), Maynard (1991) and Dean (1994).

The elemental analyser is calibrated by standards (acetanilide (ACE) for carbon, %C=71.09, %H=10.36, %N=6.71), together with a international standard (PACS) and also blanks (empty cups). Standards should weigh between 0.7 - 1.5 mg, with rock samples between 1-3 mg. The standards and samples are accurately measured in small tin cups on a Sartorius Microbalance, before being sealed and placed in the sample carousel. All

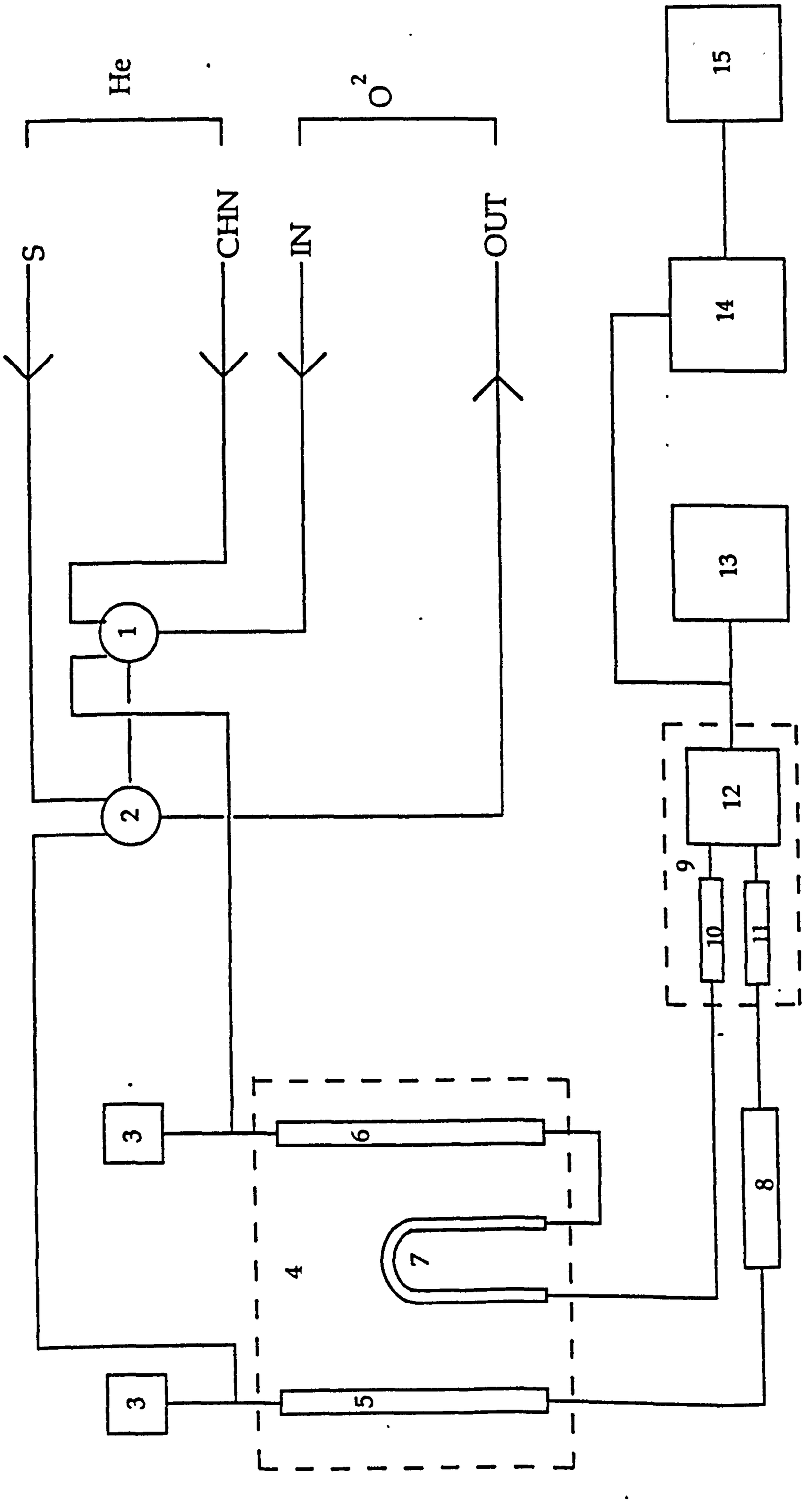

Figure 3.1. Schematic diagram of the Carlo Erba Elemental Analyser Model 1106, modified from Carlo Erba Strumentazione Short Notes.
1. Oxygen injection valve (S). 2. Oxygen injection valve (CHN). 3. Samplers. 4. Furnace. 5. Combustion reactor (S). 6. Combustion reactor (CHN). 7. Reduction reactor (S). 8. Water trap. 9. Thermostated oven. 10. Chromatographic column (CHN). 11. Chromatographic column (S). 12. Detector. 13. Recorder. 14. Integrator. 15. Computer.

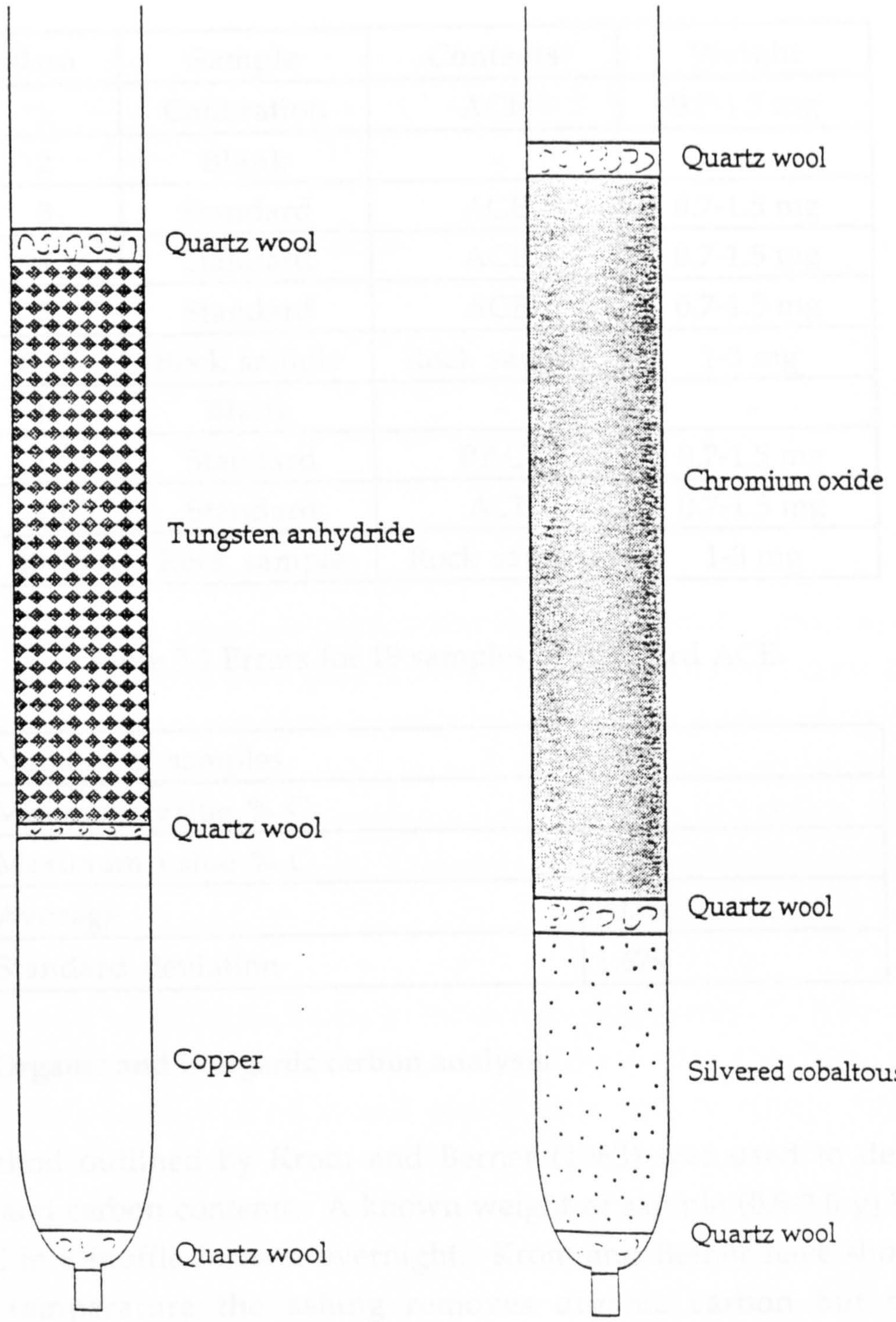

Figure 3.2. Combustion reactors for S and CHN, as used in the Carlo Erba Elemental Analyser, model 1106.

weights are entered into the computer for use in result calculation. When a batch of samples is processed a specific sequence of standards and blanks is followed as below:-

Table 3.1 Sequence of standards, blanks and samples used during each processing for carbon on the Carlo Erba Elemental Analyser, model 1106

Run	Sample	Contents	Weight
1	Calibration	ACE	0.7-1.5 mg
2	Blank	-	-
3	Standard	ACE	0.7-1.5 mg
4	Standard	ACE	0.7-1.5 mg
5	Standard	ACE	0.7-1.5 mg
6-15	Rock sample	Rock sample	1-3 mg
16	Blank	-	-
17	Standard	PACS	0.7-1.5 mg
18	Standard	ACE	0.7-1.5 mg
19-28	Rock sample	Rock sample	1-3 mg

Table 3.2 Errors for 19 samples of standard ACE.

Number of samples	19
Minimum value % C	67.86
Maximum value % C	74.45
Average	70.93
Standard deviation	1.679

3.2.2 Organic and inorganic carbon analysis

The method outlined by Krom and Berner (1983) was used to determine organic and carbon contents. A known weight of sample (0.5-2.0 g) is ashed at 450°C in a muffle furnace overnight. Krom and Berner have shown that at this temperature the ashing removes organic carbon but not any carbonate carbon present. Both inorganic carbon and total carbon contents for each sample were measured by gas chromatography on a Carlo Erba Elemental Analyser model 1106 (as described). After correction for weight loss during ashing, the difference in the two values is equivalent to the organic carbon content.

An alternative method to determine organic carbon is to remove carbonate by dissolution by reaction with 10% Hydrochloric acid. However, Dean (1994) found that this carbonate dissolution method is more prone to experimental error.

3.3 SULPHUR ANALYSIS

Total sulphur was determined using the Carlo Erba Elemental Analyser. Pyrite sulphur was determined using the method of Raiswell *et al.*, (1988), a modification of Canfield *et al.*, (1986).

3.3.1 Total sulphur determination

Total sulphur content is also measured with the Carlo Erba Elemental Analyser in a similar manner to carbon. Samples (accurately weighed into small tin cups) are dropped at pre-set intervals (12 minutes) into a vertical quartz tube, heated to 1020°C through which a constant flow of helium is maintained. Flash combustion takes place as the helium stream is temporarily flushed with pure oxygen resulting in the oxidation of the tin cups. The resultant gases are passed over tungsten trioxide (WO_3) achieving conversion to SO_2 and then passed over copper to remove excess oxygen. The mixture of gases are then introduced into a water trap of anhydrous magnesium perchlorate :$Mg(ClO_4)_2$, and then through a chromatographic column heated at 80°C, packed with Porapak QS where the SO_2 is separated from the other combustion gases. Measurement and calculation of results is as for the carbon method.

The elemental analyser is again calibrated by standards (Sulphanilamide (SAL) for sulphur, %C=41.84, %H=4.86, %S=18.62), together with an international standard (PACS) and also blanks (empty cups). Standards should weigh between 0.7 - 1.5 mg, with rock samples between 1-3 mg and are accurately measured in small tin cups on a Sartorius Microbalance, before being sealed and placed in order in the sample carousel. A small unweighed amount of vanadium pentoxide (V_2O_5) is added to the tin cup containing the rock sample to aid combustion. All weights are entered into the computer for use in result calculation. The same specific sequence of standards and blanks as for carbon determination is followed.

3.3.2 Pyrite sulphur determination

Pyrite sulphur was determined using the method of Raiswell *et al.*, (1988), a modification of the technique of Canfield *et al.*, (1986). Hydrogen sulphide produced from the reaction of chromous chloride with the sulphur in pyrite reacts with a known volume of copper sulphate solution producing copper sulphide and hydrogen sulphate (as shown by the equations below).

$$2CrCl_2 + FeS_2 + 4HCl \rightarrow 2CrCl_3 + 2H_2S + FeCl_2$$

$$H_2S + CuSO_4 \rightarrow CuS + H_2SO_4$$

By titration of ethylenediaminetetra-acetic acid disodium salt solution (EDTA) against the residual copper sulphate solution and against a standard known solution of known concentration, the amount of pyrite sulphur can be calculated.

1) Reagent and apparatus preparation

A Jones reductor is used to produce chromous chloride from chromic chloride. This reagent is then used to pyrite sulphur.

Jones reductor preparation

Eight grams of mercury (II) nitrate is weighed into a small beaker, 4-5 ml of concentrated nitric acid and 30-40 ml of distilled water are added and the mixture stirred until the mercuric acid is dissolved. The solution is diluted to 400 ml and poured into a larger beaker containing 400 g of granular zinc (30 mesh). The mixture is then stirred for approximately 10 minutes and is then decanted and washed three times with distilled water. The zinc amalgam is added to a Jones reducing column.

Chromous chloride preparation

200 ml of 10% Hydrochloric acid (HCl) is passed through the Jones reducing column (to activate the amalgam). This is followed by 200 ml of water.

A further 100 ml of HCl is passed through the column then 50 ml (i.e. a volume equal to half that of the storage bottle) of 2M chromic chloride (533 g chromium (III) chloride hexahydrate dissolved in 10% HCl and made up to one litre with 10% HCl), ensuring that the column is not exposed

between the additions. Under suction the solution is drawn through the column until the emerging liquid has changed from green to blue in colour, i.e., the solution has been reduced. The solution is then discarded and the collecting filter flask flushed with nitrogen. The suction is reactivated and the blue solution collected in the flask, with the top of the column being topped up with 10% HCl until the required volume is achieved.

A 100 ml storage bottle for the chromous chloride is flushed with nitrogen and the solution is quickly transferred to prevent oxidation.

2) Analysis of reduced inorganic sulphur by chromous chloride reduction

An accurately weighed powdered sample containing up to 50 mg of pyrite (usually between 0.3 and 2.0 g) is placed in a reaction vessel. 10 ml of absolute alcohol (ethanol) is added to the sample to prevent coagulation. The collecting head is connected and 25 ml of working copper solution (16.2 g copper {II} chloride /l) is accurately added by pipette.

The apparatus is transferred into a fume cupboard and onto a hotplate. A slow steady flow of nitrogen gas is passed into the apparatus via a nitrogen gas line. The apparatus is checked for leaks and when a flow rate of approximately 2 or 3 bubbles per second is achieved distilled water is added to the collecting head until only the top bulb is exposed (Figure 3.3). The system is left to flush to exclude oxygen for at least ten minutes.

Approximately 20 ml of concentrated hydrochloric acid and 40 ml of chromous chloride are added from a syringe through the addition tube. The solution is then simmered for at least 90 minutes.

After the apparatus has been allowed to cool, the solution and precipitate in the collection head are filtered through Whatman 12.5 cm no. 40 filter paper. Care is taken that all the residual copper sulphate solution is collected by washing the collecting head several times with hot water.

3) Determination of pyrite sulphur

A burette is washed with distilled water followed by 0.1M EDTA solution. To the copper sulphate solution sample approximately 70 ml of buffer solution (1M sodium acetate trihydrate adjusted to pH 5.5 with acetic acid) and a few drops of glycine cresol red indicator solution are added. This solution is

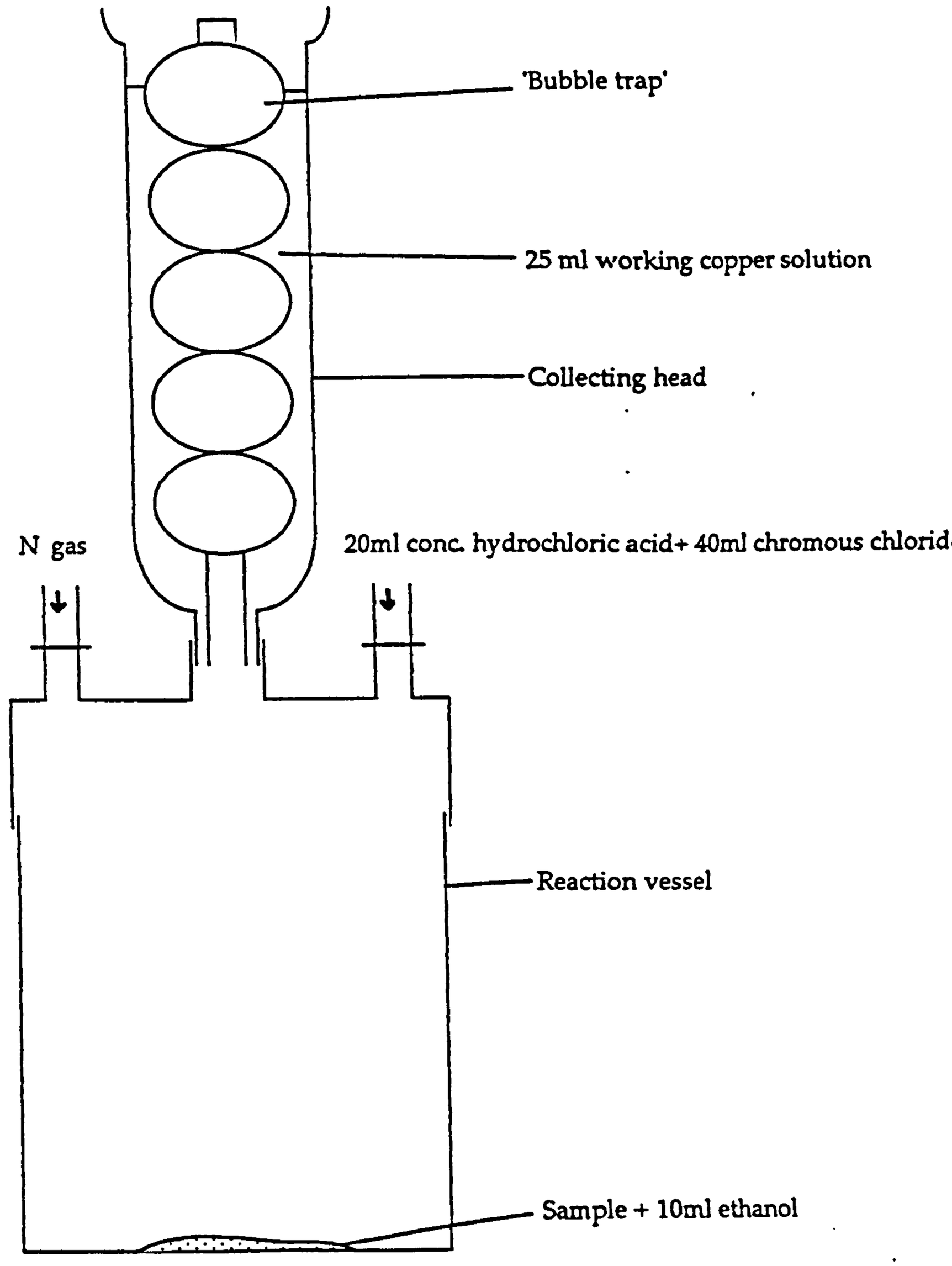

Figure 3.3. Apparatus used and reaction during the analysis of reduced inorganic sulphur by chromous chloride reduction.

then titrated against EDTA. The EDTA is also titrated against 25 ml blanks and against 25 ml of the standard copper solution (made to 6 g Cu/l with accurately measured copper (II) sulphate pentahydrate) for standardisation.

$$1\text{ml EDTA} = \frac{25}{\text{EDTA (standard)}} \times \frac{\text{g Cu}}{1000} \quad \text{g Cu}$$

but CuS =63.54 g Cu and 32.066 g S

$$\text{thus } 1\text{g Cu} = \frac{32.066}{63.54} = 0.50465848 \text{ g S}$$

$$\text{so 1ml EDTA} = \frac{25}{\text{EDTA (standard)}} \times \frac{\text{g Cu}}{1000} \times 0.50465848 \quad \text{g S}$$

$$\text{therefore \%S} = \frac{\text{EDTA (Blank-Sample) x g S/ml x 100\%}}{\text{wt of sample}}$$

and %S x 1.87087 =% FeS_2

3.4 IRON ANALYSIS

3.4.1 Pyrite iron

Pyrite iron contents were calculated from the amount of pyrite sulphur per sample (Pyrite iron % = 55.85/64.128 x S %).

3.4.2 Acid soluble iron

Acid soluble iron was calculated using the method of Raiswell *et al.*, (1988), a modification of Berner (1970), in which acid soluble iron (fine grained disseminated iron minerals such as limonite, ankerite, chlorite and haematite) is removed whilst the pyrite present in the sample is unaffected.

About 0.1 mg of sample is accurately weighed and placed in a test tube. 5 ml of concentrated (12M) HCl acid is added to the tube, which is then heated to boiling over a Bunsen burner for one minute. The solution is then simmered for one further minute, before the reaction is quenched by the addition of cold distilled water. The sample is then washed into a 250 ml volumetric flask and made up to volume with distilled water.

The samples are run on an atomic absorption spectrophotometer (AA), calibrated by standards. Briefly the AA works by flame combustion and is based upon the fact that elements (e.g., iron) absorb radiation strongly at discrete characteristic wavelengths, which coincide with the emission spectra lines for that particular element. The liquid sample is atomised in a flame photometer burner. A beam emitted from a cathode lamp traverses the flame and focuses on the entrance slit of a monochromator, which is set to read the intensity of the spectral line for iron. Light with this wavelength is absorbed by the iron atoms in the flame, and the degree of absorption is a function of the concentration of iron in the sample (Vogel, 1961). Six standards with concentrations of 0, 1, 2, 3, 4, 5 and 6 p.p.m. Fe are prepared with ferric nitrate solution. They are made to the same acidity as the samples. Further dilution of samples may be necessary if they are found to contain large amounts of iron.

Sample results from the A.A. are given in p.p.m. and are converted to Fe% by the following equation:-
Fe%= ppm x 10^{-6} x flask size (250 ml) x 100%/ weight of sample (g)

For dilutions, the flask size is doubled, or trebled etc. as appropriate.

3.4.3 Total iron

Total iron values were calculated using X-ray fluorescence spectrometry. Briefly, this method involves the heating of 0.4 g of sample (previously ashed at 1000°C) with 4 g of flux 110 (in a platinum and gold alloy crucible) to 1000 °C in a muffle furnace. The crucible contents are made up to 4.4 g with additional flux. The crucible and its contents are then heated over flame to remelt the sample. When fully molten the glass is poured into a pre-prepared 40 mm diameter copper ring and left to cool.

The glass ring is analysed in the spectrometer. A beam of x-rays irradiates a glass and the beam is absorbed by the elements composing the sample. Each major element will absorb a different particular wavelength. The spectrometer calculates total weight percentages from the amount of absorption of the particular wavelengths.

Results are expressed as oxides of the particular elemnts, and thus recorrection for weight loss and to provide a value for solely the major element have to be made.

3.5 GAMMA-RAY SPECTROMETRY

Concentrations of uranium, thorium and potassium were measured with a portable gamma-ray spectrometer (the Exploranium GR-256). The method as described in Myers and Wignall (1987) was used.

The three radioactive elements U, Th and K (and some of their associated daughter products) all emit gamma radiation whose energy is characteristic of the emitting isotope. The abundance of the three elements can be determined by measuring the intensity and energy of the gamma radiation. Authigenic uranium can be calculated by a simple equation.

3.5.1 Theory

During radioactive decay three types of common decay products are produced, alpha particles, beta rays and gamma radiation. Gamma radiation is a high energy form of electromagnetic radiation. Because gamma rays have no electrical charge and no mass they are capable of penetrating more than 30 cm of 'earth type' materials (Hansen, 1975). Gamma rays travel at the speed of light and have a frequency directly proportional to the energy of the radiation. They interact with matter in three principal modes - compton scattering, photoelectric absorption and pair production.

As a radioactive isotope decays along a decay series, it passes through various intermediate isotopes ultimately to a stable end product. The isotopes each emit gamma ray energy. Thus in both the gamma ray and the thorium decay sequence there are a large number of energy peaks or gamma ray lines. To be of use in gamma ray spectrometry a line for an isotope of each decay series (for U, Th and K) is measured. The line must be isolated from adjacent lines and have a high yield (a high number of photons emitted for each 100 disintegrations per isotope). The most useful line for the uranium series is that of bismuth-214 (with an energy of 1.76 MeV and a yield of 19%). Thalium-208 (with a yield of 100% and energy of 2.62 MeV) is the useful thorium sequence line. Potassium-40 has a single line at 1.46MeV (Figure 3.4).

3.5.2 Radiation detection by the Exploranium GR-256 spectrometer

The Exploranium GR-256 (with GPS-21 detector) is a microprocessor based

Isotope	Symbol	Atomic number	Energy in Mev, (% yield)
Uranium-238	U	92	
Thorium-234	Th	90	0.09 (15), 0.06 (7), 0.03 (7)
Protactinium-234	Pa	91	1.01 (2), 0.77 (1), 0.04 (3)
Uranium-234	U	92	0.05 (28)
Thorium-230	Th	90	
Radium-226	Ra	88	0.19 (4)
Radon-222	Rn	86	
Polonium-218	Po	84	
Lead-214	Pb	82	0.35 (44), 0.24 (11), 0.29 (24), 0.05 (2)
Bismuth-214	Bi	83	**Most useful energy at 1.76 (19), amongst many peaks.**
Polonium-214	Po	84	
Lead-210	Pb	82	
Bismuth-210	Bi	83	0.05 (4)
Polonium-210	Po	84	
Lead-206	Pb	82	

Isotope	Symbol	Atomic number	Energy in MeV, yield (%)
Thorium-232	Th	90	0.06(24)
Radium-228	Ra	88	
Actinium-228	Ac	89	Many peaks, none important
Thorium-228	Th	90	
Radium-224	Ra	88	
Radon-220	Rn	86	
Polonium-216	Po	84	
Lead-212	Pb	82	0.30 (5), 0.24 (82), 0.18 (1),).12 (2)
Bismuth-212	Bi	83	Many peaks, none important
Polonium-212	Po	84	
Thallium-208	Tl	81	**Most useful energy at 2.62 (100), amongst many peaks**
Lead-208	Pb	82	

Isotope	Symbol	Atomic number	Energy in MeV, (% yield)
Potassium-40	K	19	1.46 (11)

Figure 3.4. Radioactive decay series of U-238, Th-232 and K-40, together with gamma radiation with energy in MeV and percentage yield.

instrument with 256 channels spread equally over the entire gamma-ray spectrum.

The detector absorbs the gamma radiation and converts it to a light flash or a scintillation. This light flash is received by a photomultiplier tube that converts the light flash into a voltage proportional to the intensity of the flash. The console separates the voltage into a number of classes dependant upon magnitude, therefore providing an energy spectrum of the incident gamma rays.

A sodium iodide crystal is used as the detector in the GPS-21 detector, as it has high density and good transparency resulting in high absorption of gamma rays and effective transmission of energy to the photomultiplier tubes. Gamma ray energy is transferred to an electron in the crystal as kinetic energy. The electron ionizes a short path length in the crystal (with a resultant scintillation or flash of light) as it slows down. The intensity of the scintillation is proportional to the energy of the incident gamma ray.

Temperature variations cause changes in the power supply voltage and in the amplification characteristics of the photomultiplier tubes and varies the energy stability of the spectrometer channels or windows. To increase the stability of the spectrometer steps such as thermal insulation of components and cooling of power supplies together with high quality electronics are implemented. A reference source (cesium-137) is used to maintain automatic gain control. This source has a known energy and a electronic circuit correlates spectrometer output with the known source energy.

A correction is also made to the measured counts for the time taken to register a photoelectric interaction and the pulse to proceed to the photomultiplier tube. This time is called 'dead time' as the system cannot measure simultaneous interactions so corrections must be made, especially at high count rates.

3.5.3 Concentration determination and data correction

The Exploranium GR-256 calculates the concentration of the elements Th, U and K by applying corrections and sensitivity constants to the measured values. The relationships are defined by the following equations:-

$$Th\ (ppm) = C_{Th}\ (N_{Th} - S_1N_U - S_2N_{Cos} - b_{Th})$$

$U\ (ppm) = C_U\ (N_U - S_3N_{Th} - S_4N_{Cos} - b_U)$
$K\ (\%) = C_K\ (N_K - S_5N_{Th} - S_6N_U - S_7N_{Cos} - b_K)$

where C_{TH}, C_U and C_K are sensitivity constants relating the response to the abundance of the decaying isotope,
N_{TH}, N_U, N_K and N_{cos} are observed counts per unit time in the Tl^{208}, Bi^{214}, K^{40} and cosmic ray channels,
S_n coefficients are the compton stripping ratios,
bTH, bU and bK are the background counts in the various channels.

Both the sensitivity constants and the stripping values must be determined experimentally with the crystal and for each different geometrical relationship between the crystal and radiation source.

The background effects of atmospheric and cosmic sources can be ignored during hand held portable surveys as the signal derived from recording so close to the source is so strong. Therefore the equations above can be rewritten:-

$Th\ (ppm) = C_{Th}\ (N_{Th} - b_{Th})$
$U\ (ppm) = C_U\ (N_U - S_3N_{Th} - b_U)$
$K\ (\%) = C_K\ (N_K - S_5N_{Th} - S_6N_U - b_K)$

3.5.4 Field procedure

Before initial use (and at yearly intervals) the gamma ray spectrometer is calibrated with pads containing known concentrations of K, U and Th. Outcrops were chosen to study using the guide-lines mentioned by Myers and Wignall (1987):-

1) Unweathered sections to minimise the effect of leaching of K and U .
2) Sections of constant moisture as variable moisture content can alter the emanating power of the rock.
3) The geometry of the section studied should be a flat area of at least 3 m diameter (i.e., approximates the geometry of the calibration pads).
4) The rock should be in a state of radioactive equilibrium (otherwise the gamma rays emitted by 214Bi and 208Tl cannot be used to measure the concentration of the U and Th parents). Equilibrium can be assumed for the U series if the rocks are more than one million old and can always be assumed for the Th series.

Ideally the first of these criteria is rarely met, but loose material and scree was cleared away from sections prior to gamma ray analysis.

When the detector is placed in contact with the rock, it measures a bowl shaped area 10 cm deep, with a radius of 50 cm (Maynard, 1991) (Figure 3.5). Therefore, the greatest resolution is achieved by placing the detector on top of a bedding plane. In the field, however, it was generally found that it was easier to measure at right angles to bedding. Measurements were taken at least every metre through the thickness of the strata. The detector was left to accumulate counts for 120 seconds. Maynard (1991) found that with a count of two minutes a precision of better than 2% could be obtained for shale and mudstone lithologies.

3.5.5 Calculation of results

Values for total counts, uranium (ppm), thorium (ppm) and potassium (%) can be read directly from the display monitor. Authigenic uranium can be calculated as described in Myers and Wignall (1987) and Wignall and Myers (1988).

All thorium in the rock is present in the detrital clay fraction, unlike uranium which may be detrital, or authigenic. The crustal average Th/U ratio is 3.5 (Adams and Weaver 1958). Myers and Wignall (1987) calculated an average Th/U of 3.9±0.7 from 154 low organic carbon marine and deltaic mudstone. They subsequently calculated the detrital uranium for each reading by dividing the thorium value by three. A Th/U ratio of three was assumed so that significant values of authigenic U were measured.

Thus, $U_{authigenic} = U_{actual} - U_{detrital}$

where $U_{detrital} = Th/3$

3.6 SCANNING ELECTRON MICROSCOPY

A Camscan Series 4 Scanning Electron Microscopy (S.E.M.) was used to produce images based on specimen topography. The fossil specimens are first coated with a thin film of gold to improve conductivity whilst polished sections were coated with carbon. Briefly, the electron-optical lens system of the S.E.M. focuses a beam of electrons emitted from an electron gun into a fine probe which impinges on the surface of the specimen, where the electron-specimen interactions result in a number of emission signals from which images can be derived (Lloyd, 1987). An E.D.S. X-ray detection system

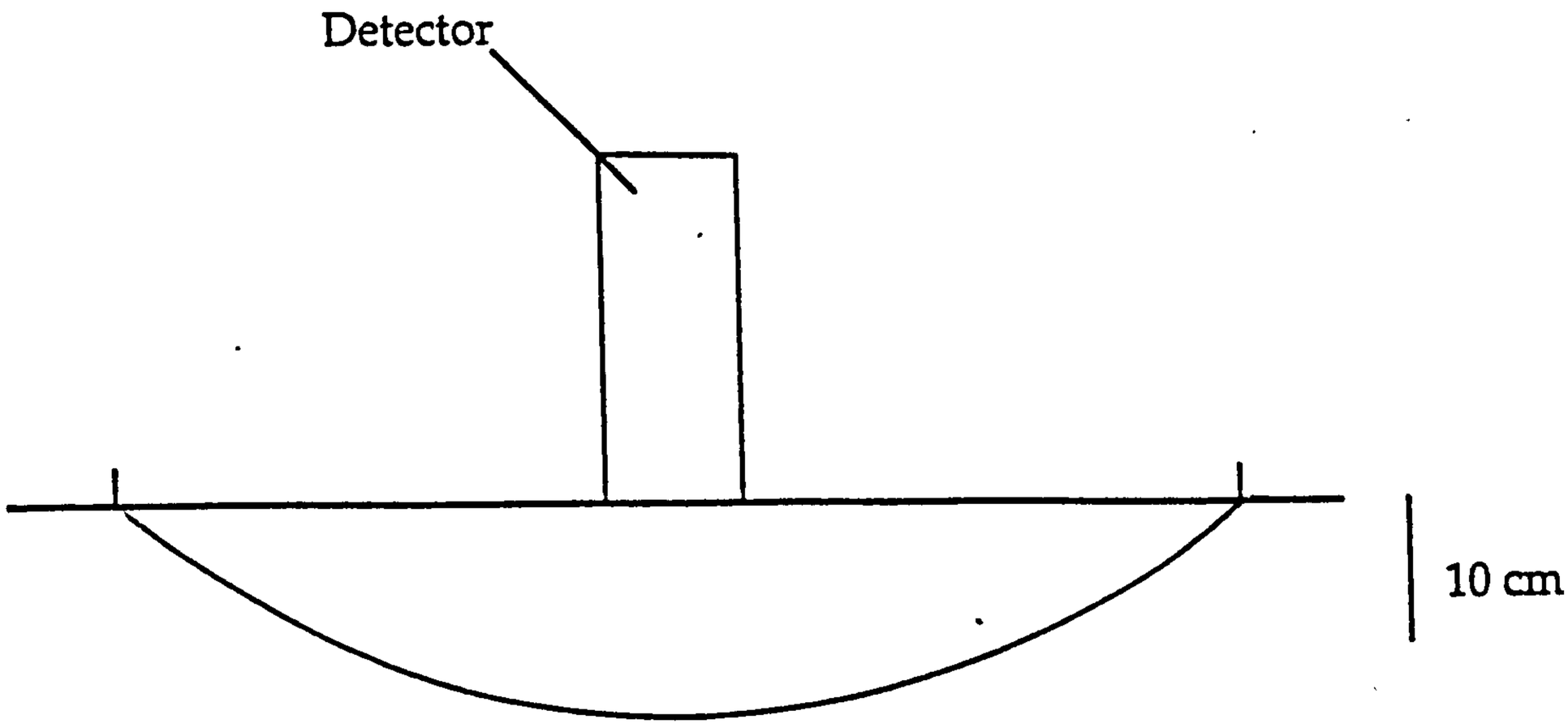

Figure 3.5. Area of effective sample measured by the Gamma-ray spectrometer.

was used to quantitatively measure composition (an electron beam emitted form a gun interacts with atoms in the sample displaying electrons from with the atoms of the sample. This displacement produces x-rays with wavelengths characteristic of the sample atom.

3.7 CONODONT EXTRACTION AND CONCENTRATION

The methods of Varker (1987) and Collinson (1963), (described in Austin (1987)) were used to extract conodonts, together with the magnetic concentration method of Varker (1987).

Samples of approximately 1.5 kg in size were collected and manually broken into smaller fragments (approximately 3-5 cm). The sample is then thoroughly dried for 24 hours in an oven at between 75-100°C. The samples were then placed in a plastic bucket and immersed in paraffin for at least two days, (Varker, 1987). The paraffin is then decanted (and is cleaned and reused) and the bucket filled with warm water. It also appeared that disintegration of the rock was increased slightly with the addition of a detergent such as 'Fairy'. The paraffin method works by physical disaggregation of the shales by the water replacing paraffin in the pores. The residues are then sieved using mesh sizes of 150 μm and 850 μm. It is important that any disaggregated residue is washed carefully through sieves as the paraffin may contain conodonts.

The remaining residue is then treated with acetic acid diluted to 10-15% in warm water (Collinson, 1963) to remove any carbonate. Again any residues are sieved with 150 μm and 850 μm size mesh.

The residues were hand picked for conodonts, although if a large amount of residue was recovered then the electromagnetic separation method of Varker (1987), a modification of Dow (1960) was used. The electromagnetic method relies upon the fact that apatite has a low susceptibility to magnetism (Figure 3.6).

Firstly pyrite and limonite are removed from the residue by passing a magnet (wrapped in tissue) over the surface. The residue is then passed through a Frantz isodynamic magnetic separator. The side slope and forward slope are set at 10°. The residue is then fed into the hopper and the magnetic field increased until 30-50% of the residue passes down the divider and is removed as the magnetic fraction. This 'magnetic' fraction is stored

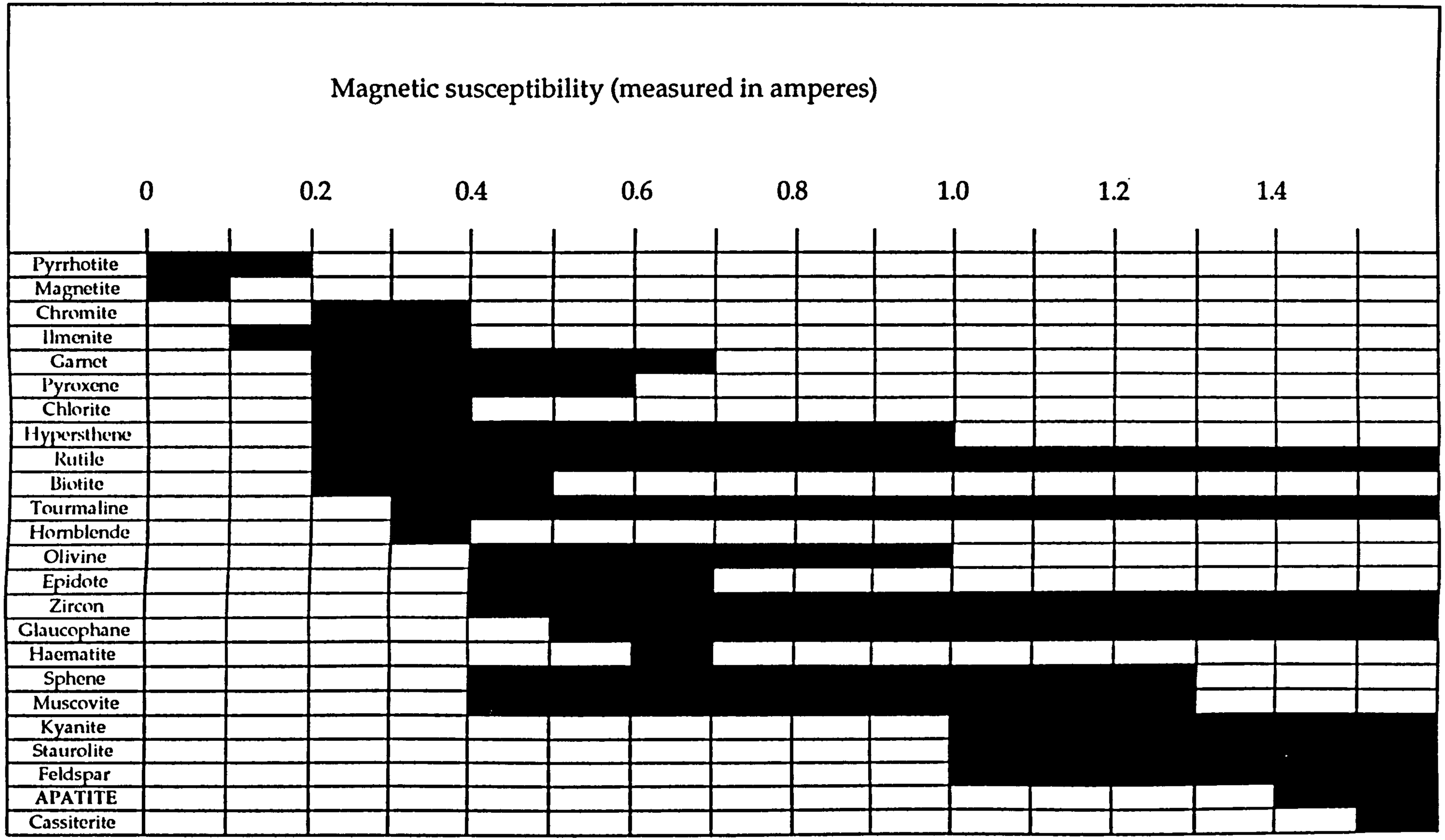

Figure 3.6. Extraction ranges of various minerals at different ampages for a side slope of 15° on the Frantz isodynamic magnetic separator.

and the process repeated with the remaining residue until a final 'non magnetic' fraction reaches a size that is manageable enough to be hand-picked. The final 'non magnetic fraction' is hand picked and if this contains conodonts, then the 'magnetic' residues must be inspected (in reverse order) until they contain no conodont specimens.

3.8 CURATION

All figured and referenced macrofossil, microfossil and trace fossil specimens are stored with the Department of Earth Sciences at the University of Leeds. Likewise all figured and referenced rock specimens, petrographic thin sections and geochemical samples and powders are also stored at this location.

Chapter 4

IRISH CARBONIFEROUS STRATIGRAPHY

4.1 HISTORY OF IRISH CARBONIFEROUS RESEARCH

4.1.1 County Clare/Northern Kerry

Griffith (1838) and Weaver (1840) were amongst the first individuals to investigate the geology of the County Clare/Northern Kerry region (Figure 4.1) in the mid nineteenth century and classified the strata as Coal Measures. The first detailed mapping of the area (at a scale of one inch to one mile) was undertaken in the middle of the nineteenth century by the British Geological Survey. Between 1859 and 1862 several 1 inch maps and memoirs covering the geology of the region were published:-

Map 114. Ballyvaughan. 1862. (Revised 1868, 1882).
Map 122. Hag's Head. 1862. (Revised 1882).
Map 123. Ennistimon. 1862. (Revised 1882).
Sheet Memoir 114, 122, 123. F.J. Foot, 1863.
Map 131. Mullagh. 1860. (Revised 1882).
Map 132. Ennis. 1860. (Revised 1882).
Sheet Memoir 131, 132. F.J. Foot, 1860.
Map 140. Loop Head. 1859. (Revised 1882).
Map 141. Kilrush. 1859. (Revised 1881).
Sheet Memoir 140,141. F.J. Foot, 1860.
Map 142. Foynes. 1859. (Revised 1882).
Sheet Memoir 142. G.H. Kinahan and F.J. Foot, 1860.
Map 150. Kerry Head. 1859.
Map 151. Listowel. 1859. (Revised 1881).
Sheet Memoir 150, 151. F.J. Foot, 1859.

In the earliest editions of the maps the units described were named the Carboniferous Limestone followed by the Coal Measures, which contained a

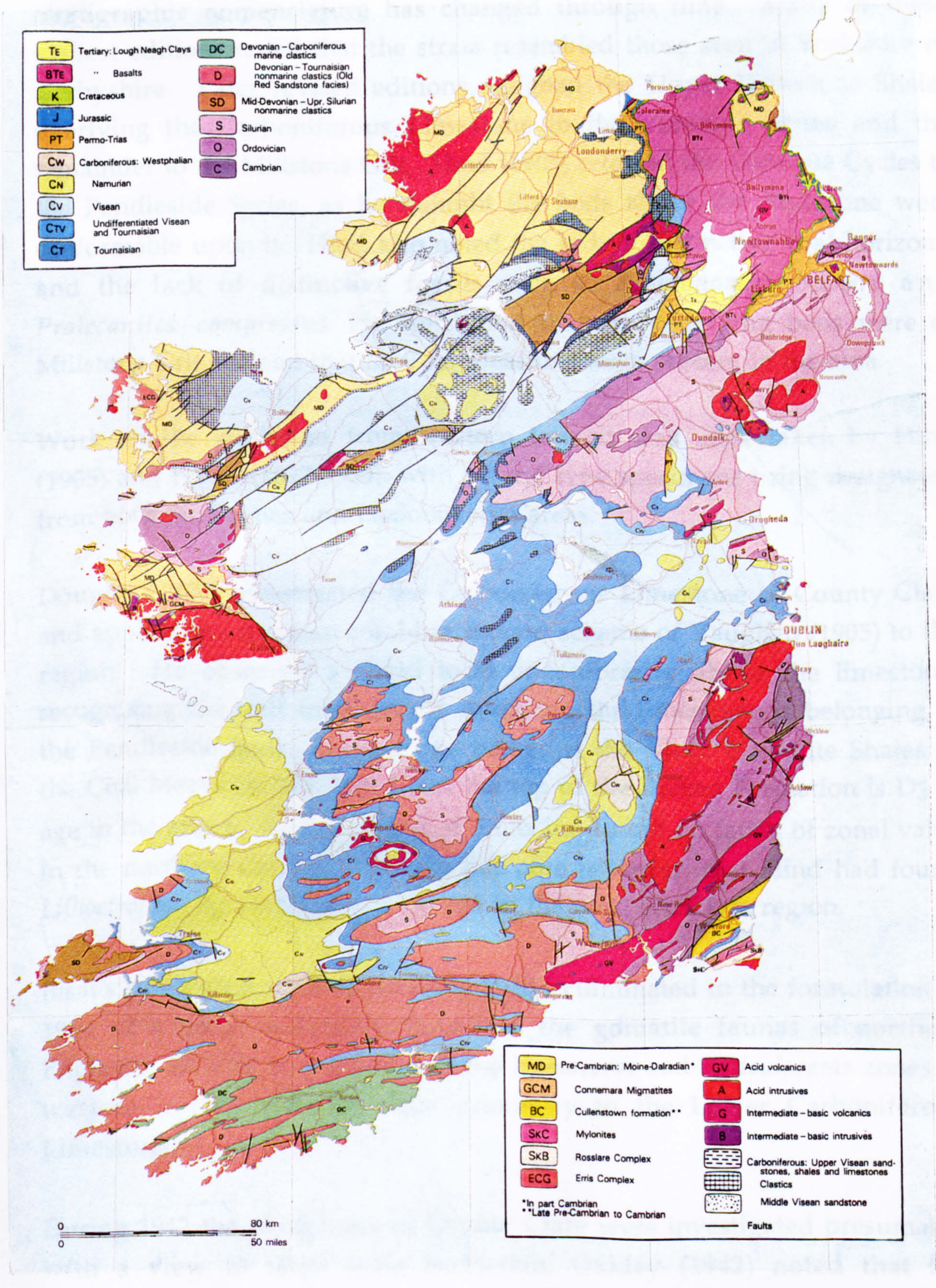

Figure 4.1 Simplified geological map of Ireland. The Namurian strata of County Clare are shown to the middle left of the map, and the Leinster coalfield occurs between Kilkenny and Carlow in the bottom right of the map. From the Geological Survey of Ireland (1979).

basal unit named the Upper Limestone Shales. Tables 4.1 and 4.2 show how stratigraphic nomenclature has changed through time. Many of these earliest editions noted that the strata resembled those seen in Yorkshire or Derbyshire. Later revised editions assigned the Upper Limestone Shales overlying the Carboniferous Limestone to the Yoredale Series and the remainder to the Millstone Grit. Hind (1905) referred the Yoredale Cycles to the Pendleside Series, as he thought the beds above the limestone were conformable upon it. Hind also noted the lack of distinctive coal horizons, and the lack of distinctive fossils such as *Posidonomya becheri* and *Prolecanites compressus*. He concluded that the overlying beds were of Millstone Grit age and that no Coal Measures were present in the area.

Work on the goniatites from western Ireland was undertaken by Hind (1905) and Foord (1897-1903), with several type specimens being designated from both the Foynes and Lisdoonvarna areas.

Douglas (1909) investigated the Carboniferous Limestone of County Clare and applied the Avonian coral-brachiopod scheme of Vaughan (1905) to the region. He observed a slight local unconformity above the limestone, recognising the unit immediately overlying the limestone as belonging to the Pendleside Series although he named it the Black Goniatite Shales of the Coal Measures. He noted that the top of the Burren Formation is D_3 in age in the area to the north-west of Ennis but found no fauna of zonal value in the northern Clare region. He did note however, that Hind had found *Lithostrotion* sp., indicating a D_2 age in the northern Clare region.

Bisat's pioneering work in the early 1920's culminated in the formulation in 1924 of a zonal succession based on the goniatite faunas of northern England. He also recognised that the *Homoceras* and *Reticuloceras* zones of western Ireland were in close proximity to the Lower Carboniferous Limestone.

During 1942 the phosphates of County Clare were investigated presumably with a view to large scale extraction, Oakley (1942) noted that the phosphorite appeared to belong to the E zone after finding a goniatite of *Homoceras* age immediately above the phosphate.

The first publication of Hodson's extensive work on the County Clare area (1954a) concerned the post-Carboniferous limestone beds in northern Clare. Hodson

Geological Survey 1860	Geological Survey 1882	Hind 1905	Hodson 1954b	Lewarne 1959	Rider 1974	Martinsen 1989	This work	
Grits and Shales (Coal Measures) Lower Flagstone Series (Coal Measures)	Lower Coal Measures (Gannister Beds) Flagstone Series (Millstone Grit)	Flagstone Series (Millstone Grit)	Upper Sandy Shale and Sandstones Sandstone Lower Sandy Shales and Sandstone	Inishcorker Sandstone Series	Central Clare Group:- Cyclothems	Central Clare Group:- Cycle V Cycle IV Doonlicky Cycle Kilkee cycle Tullig cycle	Cycle V Cycle IV Doonlicky Cycle Kilkee cycle Tullig cycle	Central Clare Group
Shale Series (Coal Measures)	Shale Series (Yoredale Beds)	Shale Series with goniatites (Pendleside Series)	Foynes Shales (Millstone Grit)	Clare Shales	Shannon Group:- Gull Island Formation Ross (Sandstone) Formation Clare Shale Member	Shannon Group:- Gull Island Formation Ross (Sandstone) Formation Clare Shale Member	Gull Island Formation Ross (Sandstone) Formation Clare Shale Member	Shannon Group
Upper Limestone	Upper Limestone	Carboniferous Limestone	Upper Limestone	Carboniferous Limestone	Carboniferous Limestone	Carboniferous Limestone	Inishtubrid Beds	Carboniferous Limestone

Table 4.1 Table showing changes in Formation names through time for rock units outcropping around the Shannon estuary area.

Geological Survey 1863	Geological Survey 1883	Hind 1905	Douglas 1909	Hodson 1954a	Lewarne 1959	Hodson and Lewarne 1961	O'Connor and Pyne 1986	This Work	
Black Shales (Coal Measures) Grits and Flags (Coal Measures)	Lower Coal Measures (Gannister Beds) Flagstone Series (Millstone Grit)	Flagstone Series (Millstone Grit)		Hag's Head Flagstone Group Hag's Head Shale Group Moher Shales Doonagore Flagstone Group Doonagore Shale Group Cronagort Sandstone	Doonagore Shale Series Cronagort Sandstone Series Fisherstreet Slumped Series	Cronagort Sandstone Group Fisherstreet Slumped Beds		Moher Shale Member	Kilkee Cyclothem
								Doonagore Flagstone Member Doonagore Shale Member	Tullig Cyclothem
								Cronagort Sandstone Member Fisherstreet Slumped Member	Gull Island Formation
Upper Limestone (Coal Measures)	Shale Series (Yoredale Beds)	Shale Series with Goniatites (Pendleside Series)	Black Goniatite Shales of the Coal Measures (Pendleside Series)	Clare Shales:- Upper or Sandy Shale Group Middle or Goniatite Shale Group Lower or Phosphate Group (Millstone Grit)	Clare Shales:- Shales with hard ribs Goniatite Shales Phosphate	Clare Shales:- Ribbed Beds Goniatite Shales Phosphorite Shales	Clare Shale Formation:- Ribbed Shale Member Goniatite Shale Member Phosphorite Shale Member Cahermacon Shale Member	Ribbed Shale Member Goniatite Shale Member Phosphorite Shale Member Cahermacon Shale Member	Clare Shale Formation
							Magowna Limestone Formation		Magowna Limestone Formation
Carboniferous Limestone	Upper Limestone	Carboniferous Limestone	Upper Limestone	Carboniferous Limestone	Carboniferous Limestone	Carboniferous Limestone	Burren Formation		Burren Formation

Table 4.2 Table showing changes in Formation names through time for rock units outcropping around the northern Clare area.

primarily dealt with the Clare Shales but also defined the overlying sandstone and siltstone beds. He recognised that part of the Lower Carboniferous Limestone (D3 of Douglas, 1909) was missing in the area (finding *Lithostrotion* coral indicating D2 age near to the top of the limestone) and that a phosphatic horizon was often welded to the top of the Limestone. He named the condensed shales succeeding the D2 limestone as the Clare Shales; these were then subdivided into the Lower or Phosphate Group, the Middle or Goniatite Shale Group and the Upper or Sandy Shale Group. Northerly overstep was noticed in these shales. The succeeding sand- and siltstones were also named: the Cronagort Sandstone, Doonagore Shale Group, Doonagore Flagstone Group, Moher Shales, Hag's Head Shale Group, and Hag's Head Flagstone Group.

Hodson (1954b) recognised that all the strata lying above the Limestone belonged to the Millstone Grit Series, as the Pendleside Series is Viséan and lower Namurian in age, naming the shales exposed near the centre of the basin at Foynes the Foynes Shales. He also recognised that there was an unconformity at the base of the Namurian that varied temporally throughout the basin. A later paper by Hodson (1957) delimited the lateral extent of the marine bands by comparison of faunas and successions found in County Clare with those of Britain, Belgium and Germany.

Gill Lewarne (1959) a student of Hodson's, set about trying to correlate the junction of the Lower and Upper Carboniferous in Clare and Limerick. By detailed logging of numerous sections she was able to prove both the temporal and spatial extent of the unconformity at the base of the Clare Shales. Interbedded shales and limestones found on an island in the centre of the Carboniferous basin were named the Inishtubrid beds and are of uncertain age (probably B2 or P1); these were preceded by her 'Striped Limestones'. She re-evaluated the classification of Hodson (1954a) of the sandstones above the Clare Shales. The Sandy Shale Group of Hodson was removed and replaced with the term 'Shales with hard ribs and nodules', which constituted the highest unit in the Clare shales. These were followed by the Fisherstreet Slumped Sandstone series and then the Cronagort Sandstone and succeeding beds of Hodson. Lewarne also investigated the presence of 'spongolites' in the E2 of Limerick and Clare and the presence of starfish traces (*Asteriacites* sp.) in the Ross Formation.

Further papers with Hodson (Hodson and Lewarne, 1961) expanded upon the biostratigraphical framework presented by Hodson previously with slight refinement of the names of certain members of the succession.

O'Brien (1953) investigated the phosphorite bands mainly around the Doolin-Noughavel area and recognised a succession of beds.

The top Carboniferous Limestone Beds were assigned a P_2 age by Clarke (1966) on the basis of its coral content.

Rider (1974) investigated primarily the strata overlying the Clare Shales and established a lithostratigraphy that could be used basin wide. He also compared the area with the modern Mississippi delta. The lowest Namurian Group, the Shannon Group, was subdivided firstly into the Clare Shale Member and their overlying and also lateral equivalent strata-the Ross Sandstone Formation, followed by the Gull Island Formation. The overlying strata were assigned to the Central Clare Group and were described as cyclothemic in nature.

O'Connor and Pyne (1986) assessed the quality and volume of the phosphorite deposits in northern Clare, introducing two new Member names, the Magowna Limestone Formation (lying unconformably upon the Burren Formation) which is unconformably overlain by the Cahermacon Shale Member, part of the Clare Formation occurring directly beneath the Phosphate Shale Member. No type sections nor ages were assigned to these two members.

More recent research in the late eighties has centred upon the evolution of the basin fill with particular focus upon the depositional and soft sediment deformational processes (Collinson *et al.*, 1991; Martinsen, 1989; Martinsen and Bakken, 1990; Pulham, 1989). The names of the cyclothemic deposits of the Central Clare Group (Tullig, Kilkee, Doonlicky, Cycle IV and Cycle V) appear to have entered the literature with the work of Martinsen (1989) and Pulham (1989). The current research (Elliot and Pulham, 1990; Davies and Elliot, 1994a and 1994b; Strogen, 1994) involves the application of sequence stratigraphical concepts and the use of a portable gamma-ray spectrometer to the upper parts of the Shannon Group (Ross Sandstone and Gull Island Formation) and the lower part of the Central Clare Group (Tullig cyclothem) with a view to assessing reservoir quality.

4.1.2 Leinster Coalfield

The first accounts of the Leinster Coalfield area (Figure 4.1) were by Griffith (1814) who produced a map and report on the mining potential of the Coalfield. During the mid-late nineteenth century a map and memoir concerning the area were published:-

Map 128. Athy. Part of Queen's County and the County of Kildare. 1858 (Revised 1878, 1901)
Sheet Memoir 128. J. Beete Jukes, G.H. Kinahan and J. O'Kelly, 1859.

The first map and memoir referred to the strata as Upper Limestone overlain by Coal Measures with a Lower Shales Series. The maps were revised and a memoir of the geology of the Leinster Coalfield was written by Hardman in 1881. The rocks of the area were divided on a similar basis to those of County Clare with the Upper Limestone being followed by a Shale Series (Yoredale Beds) and then a Flagstone Series (Millstone Grit); these were succeeded by the Lower and Middle Coal Measures. Cherty beds lying conformably beneath the Yoredale Series were assigned to the Upper Limestone.

The bivalve faunas of the Coalfield were extensively studied and compared with those retrieved from similar aged sites in Britain by Eager (e.g. 1956). Nevill (1956) evaluated the stratigraphy of the Leinster Coalfield and recognised that the oldest Namurian deposits were shales.

The most recent work conducted in the area is that of Higgs (1986) who subdivided and described the Namurian succession and correlated the area with other sections in Ireland. Higgs recognised that the chert member previously assigned to the Upper Limestone was in fact Arnsbergian in age. He also established type sections for the new Formations he defined. The Luggacurren Shale Formation succeeds the Carboniferous Limestone and comprises of four Members;- the Coonbeg Chert Member, Glen View Shale Member, Black Trench Limestone Member and Knockahonagh Member.

4.2 BASIN DEVELOPMENT AND TECTONICS

The Clare Basin - alternatively called the Shannon Trough (Sevastopulo, 1981; Strogen, 1988), Foynes Basin (Haszeldine, 1988) and the Western Irish Namurian Basin (Martinsen, 1989; Collinson *et al.*, 1991) - was an asymmetrical basin with its axis running ENE-WSW roughly along the present-day River Shannon (Figure 4.2). It had a deep central trough 10-20 km wide, with gently shelving slopes to the north and south (Martinsen, 1989). It has been suggested that the Clare Basin was a half-graben at depth (Strogen, 1988) with the Pre-Cambrian basement of Galway extending southwards to provide a stable platform on which the shelf areas were developed, at least in County Clare (Hodson, 1954a).

Subsidence of the Clare Basin was initiated during the late Courceyan and became more rapid towards the end of the Dinantian, with the extrusion of locally abundant alkaline basalt lavas and volcaniclastics in the Limerick area (Shelford, 1967; Deeny, 1982; Strogen, 1988). By the Arundian the area had evolved into a carbonate ramp system and was dominated until Asbian times by shallow water sediments. Towards the end of the Asbian the deposition of 'striped limestones' (interpreted as having formed by calcite replacement of evaporites (Sevastopulo, 1981) or algal mats (Thorn, 1958)) was followed by Brigantian basinal shales and calciturbidites (Inishtubrid Beds) deposited in northern Kerry (Strogen, 1994). Shelf limestones developed to the north and south. During the lowest parts of the Namurian black shale deposition occurred in the basin centre, whilst a hiatus and accumulation of phosphate occurred on the basin shelves. Turbiditic sandstones were followed by the final basin-fill of prodelta and delta top sandstones in the upper Namurian.

During the Carboniferous continental collision was occurring between Gondwana and Laurasia (Leeder, 1988a; Leeder and McMahon, 1988). Back-arc extension of the lithosphere resulted in N-S extension and E-W trending faults with reactivation of older inherited Caledonian structures (Soper *et al.*, 1987, Gawthorpe *et al.*, 1989). Suggestions that the subsidence in the Clare Basin was centred on reactivation of the Silvermines-Navan lineament that lay above the Iapetus suture zone (or a zone of fractures) have been proposed by numerous workers (Deeny, 1982; Leeder, 1982; Coller, 1984; Sanderson, 1984; Haszeldine, 1988; Strogen, 1988; Martinsen, 1989; Collinson *et al.*, 1991); (Figure 4.3). Haszeldine (1984) alternatively

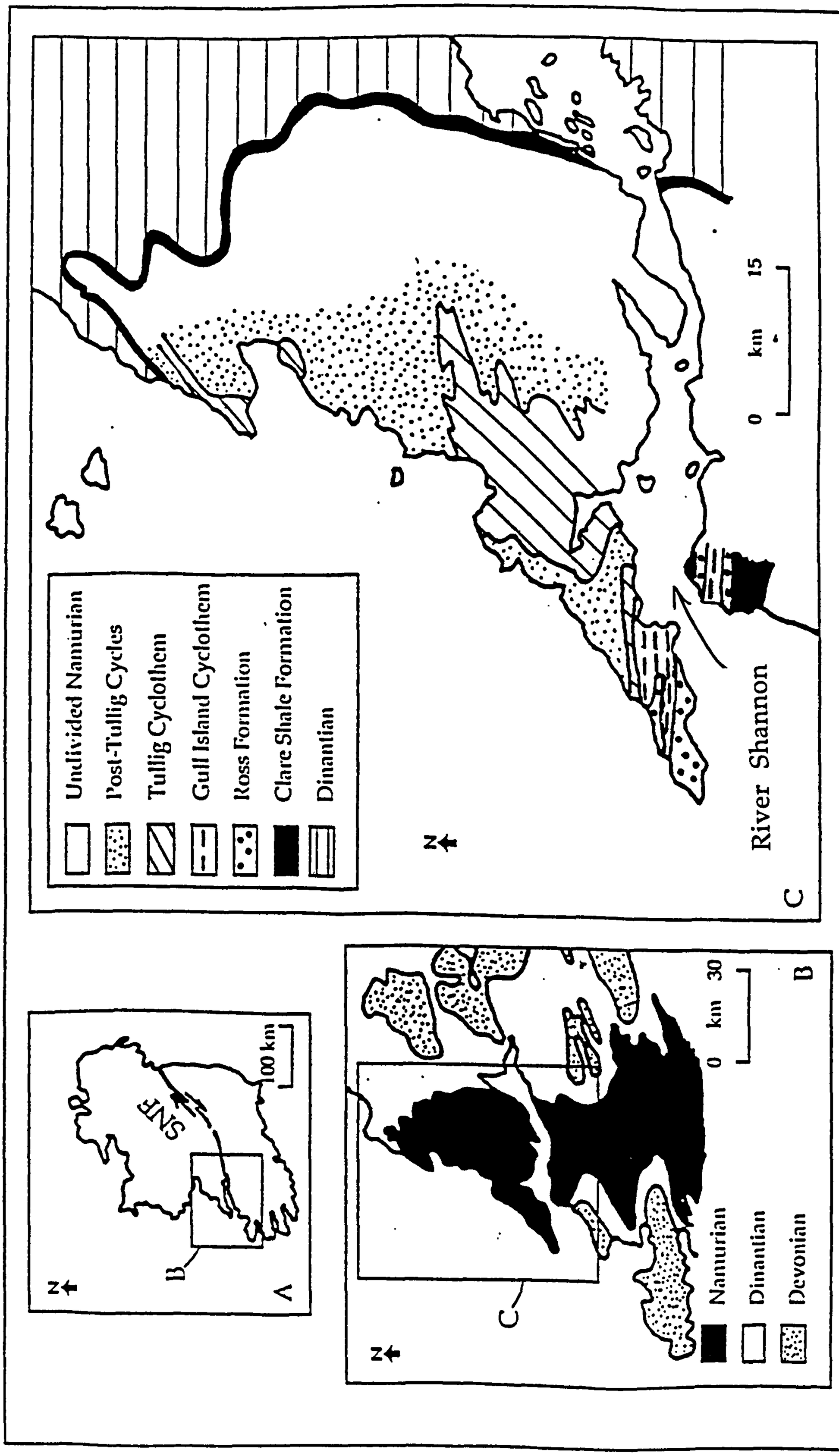

Figure 4.2 Location of the Clare Basin and sketch geological map. After Collinson *et al.*, 1991.

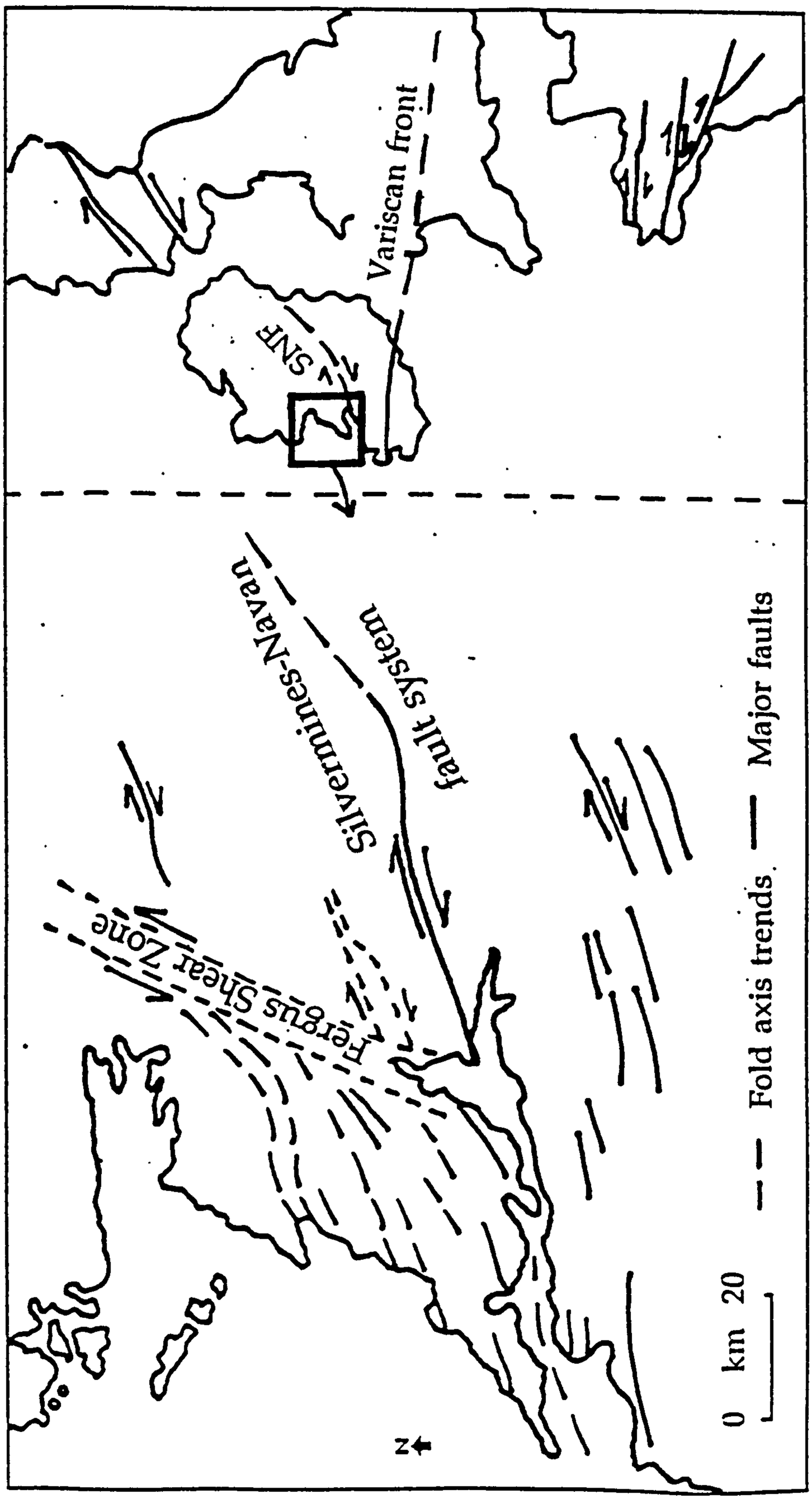

Fold axis trends — Major faults

Figure 4.3 Regional structure map. After Coller (1984) and Sanderson (1984).

suggested that the most dominant extensional stress-field during the Carboniferous was aligned perpendicularly to that proposed by the advocates of the back-arc extension model, i.e. E-W to NW-SE and that this is related to the opening of the proto-Atlantic during the late Carboniferous (although this rifting may have been initiated during the late Silurian according to Haszeldine, 1988). Whether the dominant structural control is one of purely Carboniferous extension or transtension is a matter for debate.

Leeder (1982) suggested that the trend and structure of the Clare Basin was controlled by the inheritance of the trace of the Caledonian Iapetus closure line, with subsidence controlled by Hercynian processes (Figure 4.4). Thus the alkaline-basalt volcanics are probably related to mantle partial melting during active extension in the Viséan (Leeder and McMahon, 1988), followed by basin sag during the Namurian. Marginal uplift would provide the westerly source of sediment (Leeder, 1988a). Deeny (1982) argued similarly, that the alkaline-basalt volcanics were related to an attempted Devono-Carboniferous separation of two crustal plates along the Iapetus suture line with the Shannon area gravity anomaly of >20 mgals possibly representing evidence for a 'frozen ocean spreading centre embryo' (*sic*) which terminated activity for some unknown reason (Figure 4.5)

Haszeldine (1984) dismissed the Leeder/Deeny models as not being able to account for the new N-S (i.e. non-inherited) orientations of the Carboniferous nor the faster subsidence rates in the Namurian than the Dinantian. Strogen (1988) rejected the extensional model by suggesting that the stretching (beta) values calculated for the Limerick area would not be enough for the threshold value for the outbreak of volcanics solely by extension alone. He implied that the behaviour of the Clare Basin is much more suggestive of a strike-slip controlled basin. The evidence for this being that the basin is strongly asymmetric (with control by not the Iapetus suture itself, but a broad fracture zone), and the sporadic nature of the volcanics.

Haszeldine (1984, 1988) suggested that the stresses imposed by the opening of the proto-Atlantic were prevalent, initially beginning in the late Silurian. Alkaline volcanics in the Clare Basin would be related to areas of tension and thinned crust, with the westerly sourcing of sediment seen in the late Namurian of the Clare Basin related to uplift caused by crustal fracturing. Recent work by Tate (1993) on the offshore Porcupine Seabight Basin proves north-south extensional structures that therefore would appear to validate

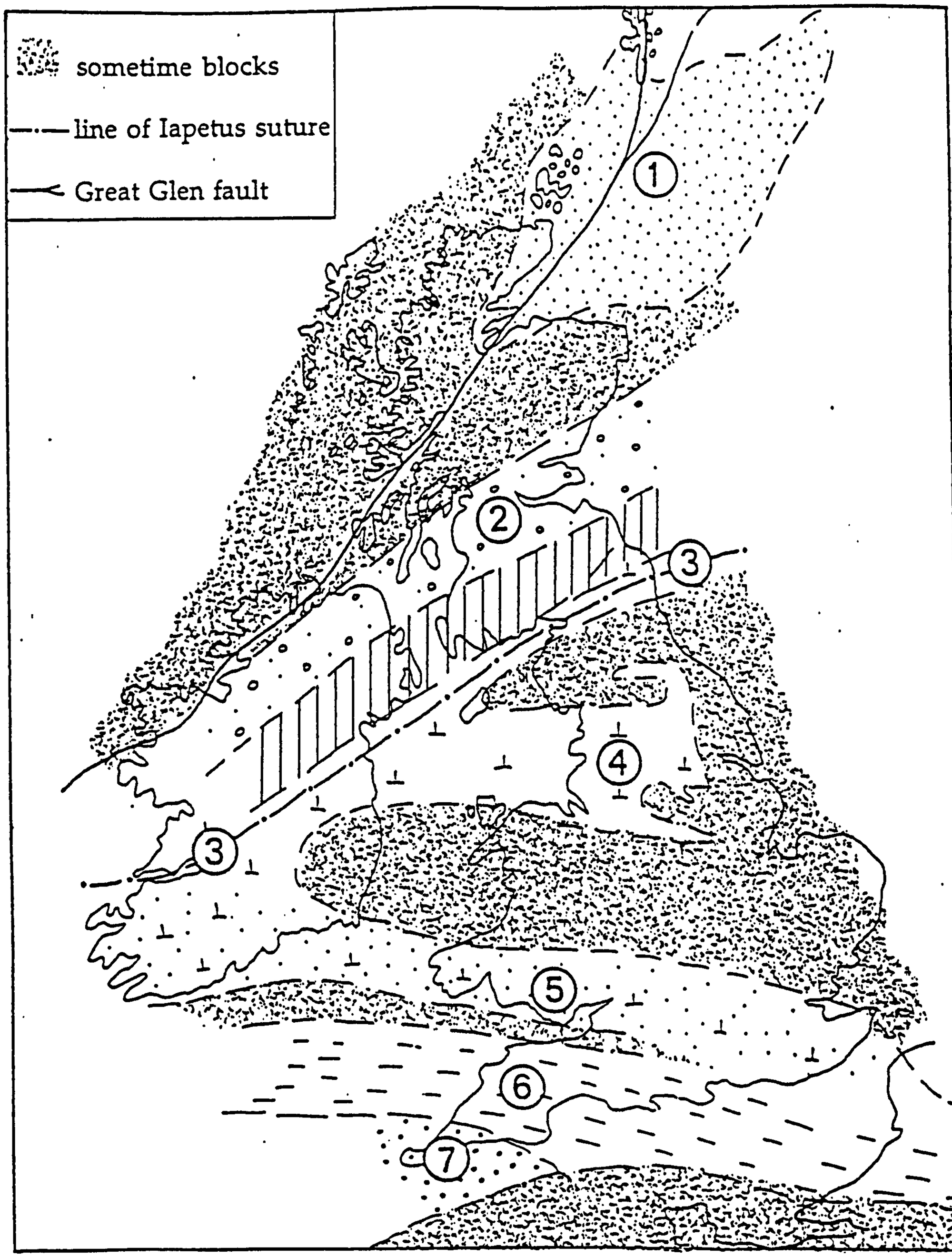

Figure 4.4 The major Upper Palaeozoic basinal areas of the British Isles, together with the location of (sometime) blocks, the Iapetus suture and Great Glen fault system. 1 = Orcadian (M-U O.R.S.); 2 = Midland Valley Basin (M Sil.-U Carb.); 3 = Northumberland-Solway-Dublin-Clare basins along the line of the Iapetus suture; 4 = S. Pennine and smaller basin; 5 = S. Wales-S. Ireland basin; 6 = Rheno-Hercynian zone of S.W. England-Belgium-Germany; 7 = S. Cornish flysch trough. From Leeder (1982).

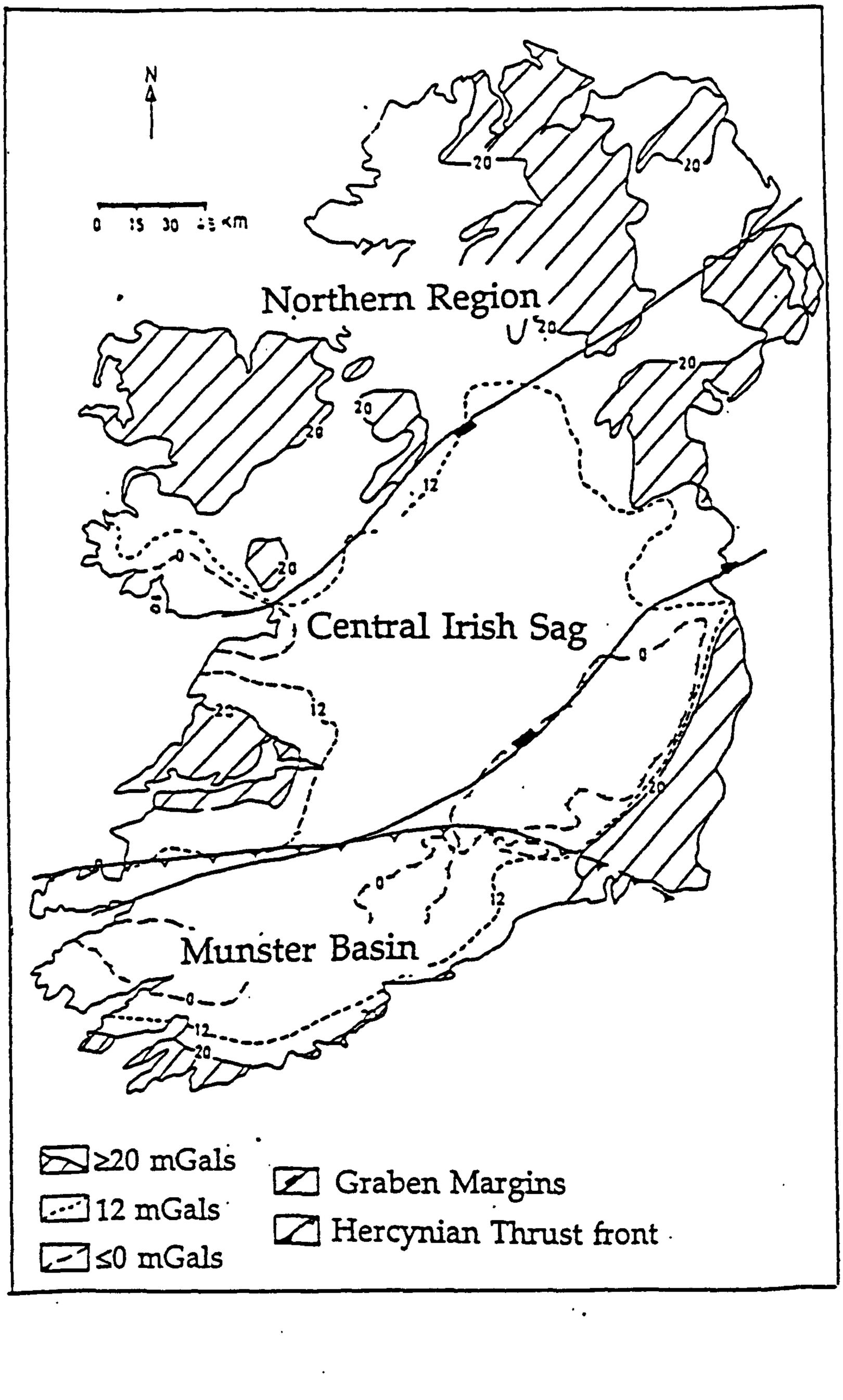

Figure 4.5 Irish regional gravity, the postulated rift margins and suggested Hercynian thrust front. From Deeny (1982).

Haszeldines proto-Atlantic opening. It is interesting to note that Tate also recognised a mid-Namurian unconformity and he suggested that this could represent erosion and non-deposition during east-west to north-south basin realignment. Leeder (1988a) refuted the transtension model as he stated that no proto-Atlantic rifting started until the lower Permian, and that the transcurrent structural lineation may be related to transtension/transcurrent tectonic episodes along the NE continuation of the Maritime Canadian Crustal Shear zone.

Coller (1984) suggested that movement on ENE-WSW trending Silvermines-Navan faults was due to a large normal (extensional) as well as dextral horizontal (transcurrent) movement component, considered to be a result of transcurrent shearing in an overall extensional regime. This model appears to best clarify the features observed in the Clare Basin being able to explain the 'embryonic' rifting of the Clare Basin with development of volcanics but with also strike-slip movement on faults, ultimately to produce a transtensional basin. The two stress-fields affecting the area (Boyce *et al.*, 1983; Martinsen, 1989) being those due to the proto-Atlantic rifting of Haszeldine (1984, 1988) and the stress caused by the subduction of Gondwana beneath Laurasia (Leeder, 1982, 1988a).

4.3 GENERAL STRATIGRAPHY OF THE CLARE BASIN

The total thickness of Namurian sediment in the Clare Basin is 1600 m (Pulham, 1989). Incipient metamorphism of the sediments has been noted by Brindley and Gill (1958) by the conversion of thin coal seams to anthracite and the secondary silicification of sandstones and siltstones. The Namurian sequence has been subjected to strong thermal effects (Croker, 1994), with conodonts retrieved from the Lisdoonvarna area showing Conodont Alteration Index Values of 5.0.

The earliest Namurian deposits in the Clare Basin are those of the marine-band bearing Clare Shale Formation, extensively studied by Hodson (1954a, 1954b) and Hodson and Lewarne (1961). The Clare Shales are dark-grey to black, often with calcareous nodules and beds and also septarian nodules. Marine bands are commonly associated with the nodular horizons, from which some well-preserved goniatites can be retrieved.

Differential subsidence resulted in the deep central trough accumulating at least 215 m of the Clare Shale Formation (Hodson and Lewarne, 1961) with

probable continual deposition from Dinantian times, whilst the gently dipping shelves to the north and south show much more condensed and incomplete sections resting unconformably on the limestone below. The succession north of the River Shannon in County Clare shows northerly onlap of shales, such that at the northern margin only 12 m of the Clare Shales is present (Figure 4.6).

The differential subsidence of the basin also resulted in the 'funnelling' of the turbiditic Ross Formation down the centre of the Clare Basin, and the deposition of 380 m (Collinson *et al.*, 1991) of silts and fine grained sands above the Clare Shales in the centre of the basin. These 380 m of axial sediments are equivalent to the top parts of the thin (12 m) Clare shale succession on the flanks of the basin. The Ross Formation lies between the *Homoceras undulatum* (H_2b^1) and *'Hudsonoceras' ornatum* or *Reticuloceras dubium* (R_1a^5) marine bands (Collinson *et al.*, 1991; Sevastopulo, 1981), with the formation occurring earlier in the west of the basin axis than in the east (Sevastopulo, 1981).

The Ross Formation displays many sedimentary structures typical of turbidity flows such as flute and sole marks and rippled tops to sandstone beds. It also shows soft sediment deformation in the form of slides and slumps and spectacular water-escape structures (Gill and Keunen, 1958). The palaeocurrents in the Ross Sandstones appears to have been dominantly from the south-west (i.e., parallel to the basin axis), although other directions are seen at the base (from the south-east) and in the upper parts (from the north-west) (Collinson *et al.*, 1991).

The Gull Island Formation overlies the Clare Shale Formation in the north and the Ross Formation in the axial regions, and lies between the *Reticuloceras dubium* and *Reticuloceras stubblefieldi* marine bands (Rider, 1974). It thins from 550 m near the basin centre to probably 130 m in the north (Collinson *et al.*, 1991), where it is known as the 'Ribbed Beds' (deformed by the Fisherstreet Slide) and Cronagort Sandstone (Hodson and Lewarne, 1961). The Gull Island Formation consists of turbiditic sandstones mainly at the base, overlain by siltstones and fine-grained sandstones. The intense soft-sediment deformation in this formation (slumps, slides and water escape structures) has been detailed by Gill and Keunen (1958), Gill

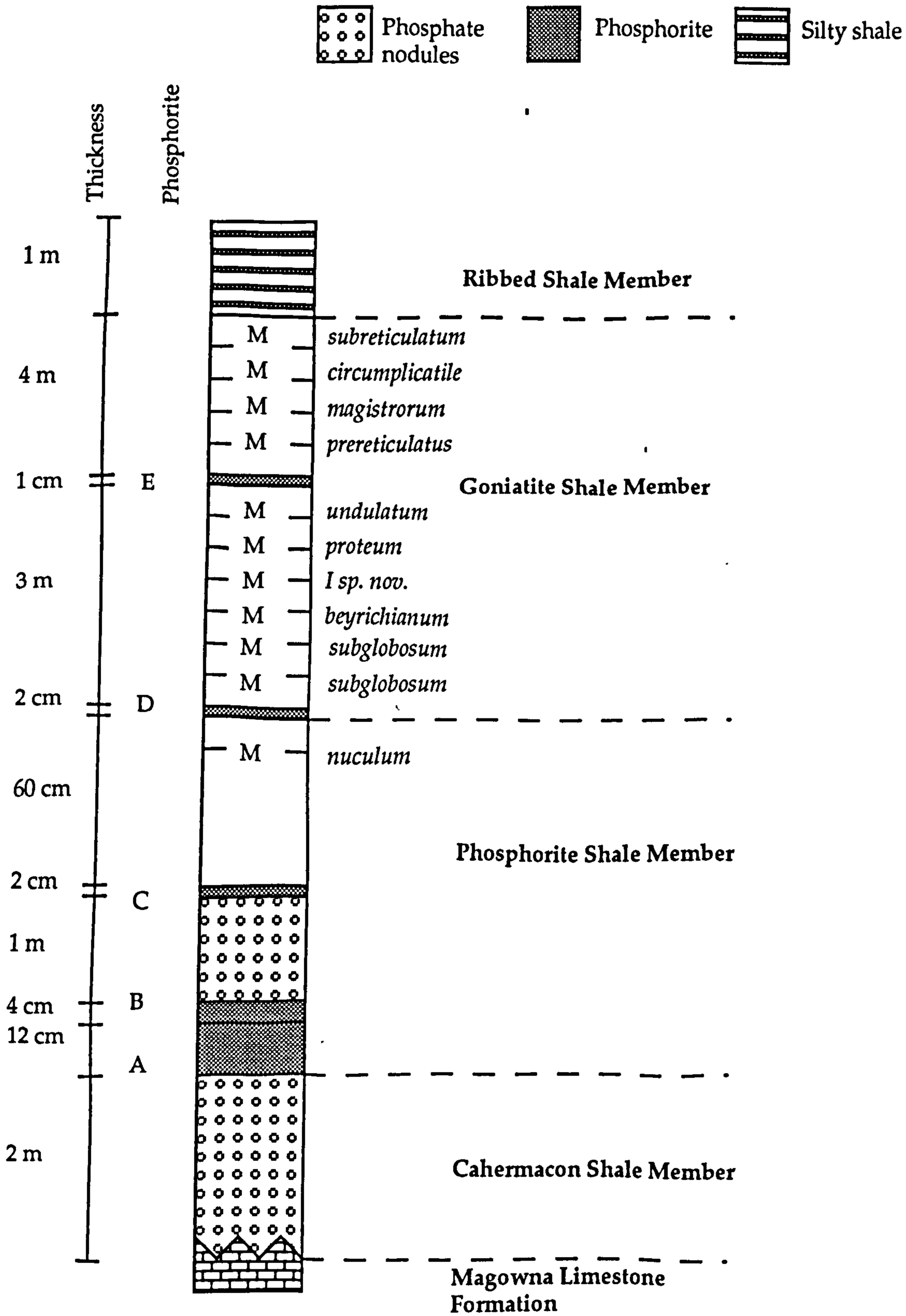

Simplified stratigraphic log through the Clare Shales in northern County Clare, (not to scale).

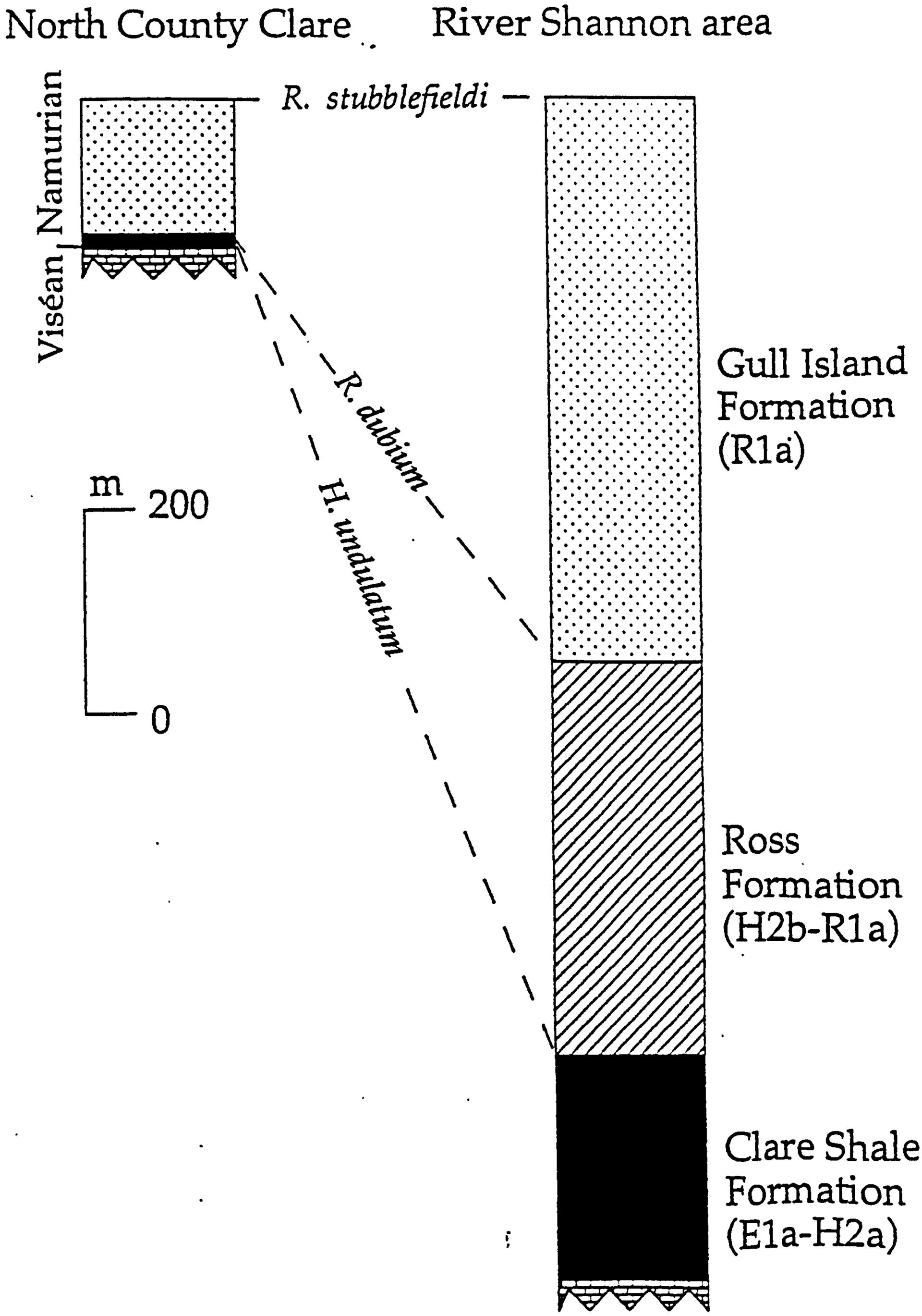

Figure 4.6 Early Namurian stratigraphy of the Clare Basin.

(1979), and Martinsen, (1989). The palaeocurrents within the Gull Island Formation also appear to have been dominantly from the south-west and again evolving to be from the north-west in the upper parts of the formation (Collinson *et al.*, 1991). The soft sediment deformation in the Ross Formation and Gull Island Formations indicate a palaeoslope dipping to the ESE-SE in County Clare (Collinson *et al.*, 1991).

Both the Ross Formation and Gull Island Formation sandstones are sourced from the west, possibly from a region of uplift related to proto-Atlantic rifting (Haszeldine, 1984, 1988) or marginal uplift (Leeder, 1988a). Leeder (1988b) also suggested that the major clastic influx at this time, (which is also seen in the northern England basins) may have been caused by climatic change from arid to humid conditions resulting in drainage system growth. Above the Gull Island Formation there is a transition into the deltaic cyclothems of the Central Clare Group. These cyclothems range from 100-200 m thick and are described by Pulham (1989) and Rider (1974) and were probably deposited in a more uniformly subsiding basin (Collinson *et al.*, 1991).

4.4 BIOSTRATIGRAPHIC DETAILS OF SECTIONS.

The Clare Basin is used as a case study to investigate deposition across the mid-Carboniferous. Whilst it is known that deposition in the basin centre was continuous over the mid-Carboniferous boundary, the timing and nature of the hiatus on the basin margin is especially poorly understood. Thus the basin was chosen with the objective to provide a model of mid-Carboniferous deposition.

The sections detailed from County Clare are described from north to south geographically (Figure 4.7). Sample numbers are noted in brackets.

The ammonoid and conodont biostratigraphies as presented in sections 2.2.1.1 and 2.2.1.2. are used in determining the biostratigraphy of the studied sections. Only fossiliferous beds are mentioned in the following text.

4.4.1 Ballydonohoe Bridge

The section near Ballydonohoe Bridge is exposed in small cliffs in the meanders of the stream approximately 600 m upstream from the bridge.

Location	Grid Ref
County Clare	
Ballydonohoe Bridge	R135992
St Brendans Well	R147985
St Catherines Caves	R093977
Roadford	R083972
Ballyshanny House	R187954
Lough Raha	R251870
Magowna Castle	R293820
Shallee	R281688
Paradise House	R284624
Inishcorker	R268581
County Limerick	
Foynes	R262499
County Kerry	
Ballybunion	Q858410
County Laois	
Luggacurren	S586882

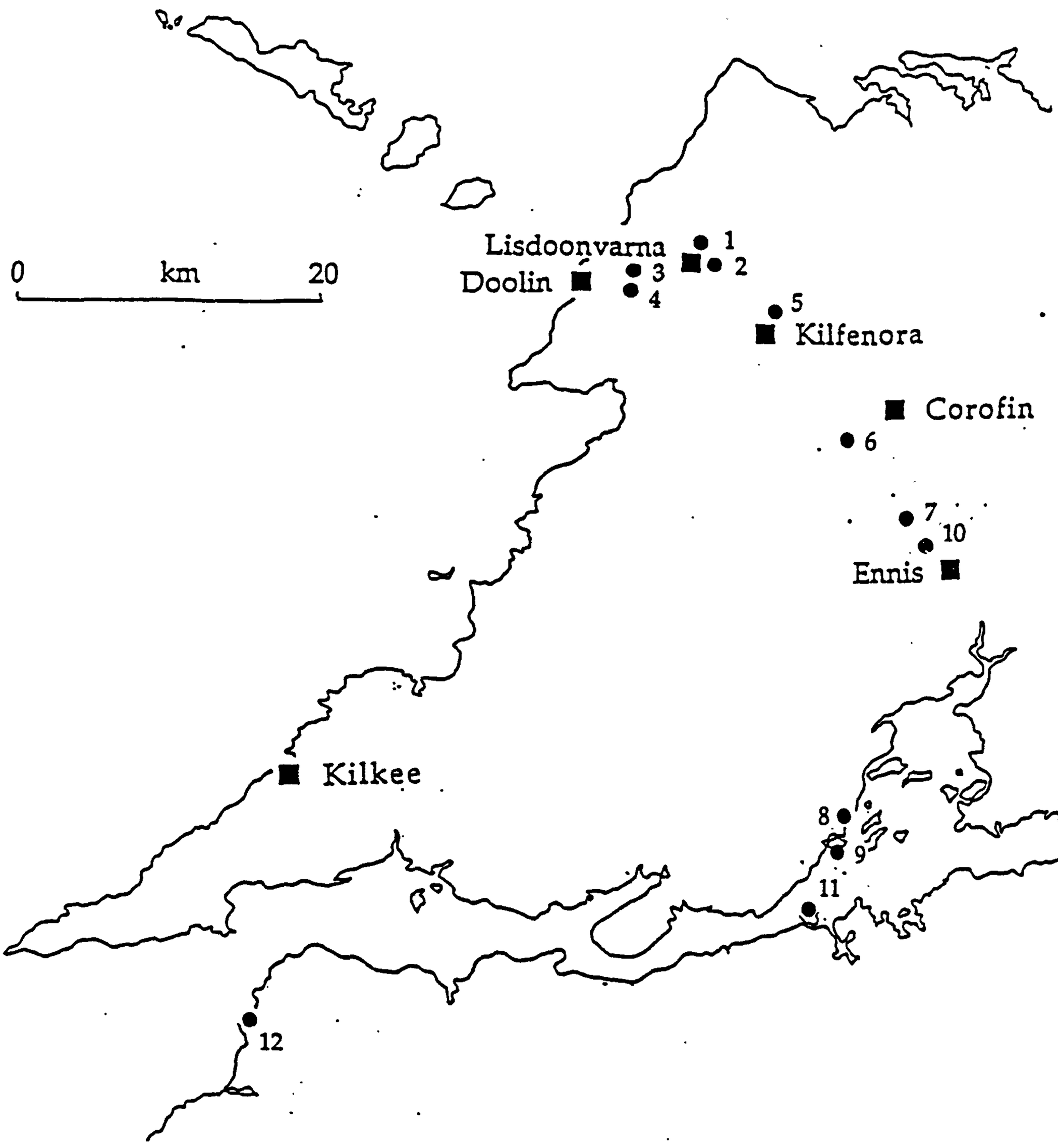

Figure 4.7 Location map for localities described or shown on the chronostratigraphic diagram. 1 = Ballydonohoe Bridge; 2 = St. Brendans Well; 3 = St. Catherines Caves; 4 = Roadford; 5 = Ballyshanny House; 6 = Lough Raha; 7 = Magowna Castle; 8 = Paradise House; 9 = Inishcorker; 10 = Shallee; 11 = Foynes; 12 = Ballybunnion

Two sections were measured and a composite section constructed. (Figures 4.8 and 4.9).

The top of the limestone can be seen forming the streambed. Developed on top of the basal limestone is a coarsening-up pyritic crinoidal packestone (BDB3, BDBC1). This displays an undulose top surface and varies in thickness from 3-7 cm. A 3-5 cm pyritic phosphate then caps the limestone (BDB4).

The top 6 cm of a 33cm thick bed of pyritic platy-papery medium grey shale 37 cm above the basal limestone horizon, displays horizons of profuse variably articulated *Posidonia corrugata* and *Selenimyalina variabilis* (BDB1, BDB6) .

Very rare poorly preserved unidentifiable bivalves occur in a 35 cm thick bed of medium grey flaky-platy shale 1.11 m above the top of the limestone .

A very weathered, thin shelled goniatite band (40 cm thick) occurs 1.85 m above the limestone surface associated with a platy-papery dark grey shale.

Although no thick-shelled goniatites were found in this examination, Lewarne (1959) found *Homoceras beyrichianum* in close association with *H.* aff. *subglobosum* from outcrops in the same stream presumably only a short stratigraphic distance above the measured outcrops. Hodson (1954a) notes that the *H.* aff. *subglobosum* found in the *Homoceras beyrichianum* band was probably a variation of Haug's (1898) *beyrichianum* (var. *tenuistriata*), thus it is difficult to decide whether Lewarne found the H_1b^1 or H_1b^2 horizon. At Roadford and at Inishcorker the *Homoceras beyrichianum* (H_1b^1) horizon is preceded by a thin-shelled goniatite horizon; the thin-shelled goniatite band found in this survey may equate with that horizon. Thus, although the *Posidonia corrugata* indicates an age older than the Chokierian, the presence of these goniatites of latest Chokierian show that a non sequence of at least H1a is present in the area. The occurrence of the pre-Chokierian bivalves above the phosphate horizons also proves that phosphate development must be of Arnsbergian or older age at this location.

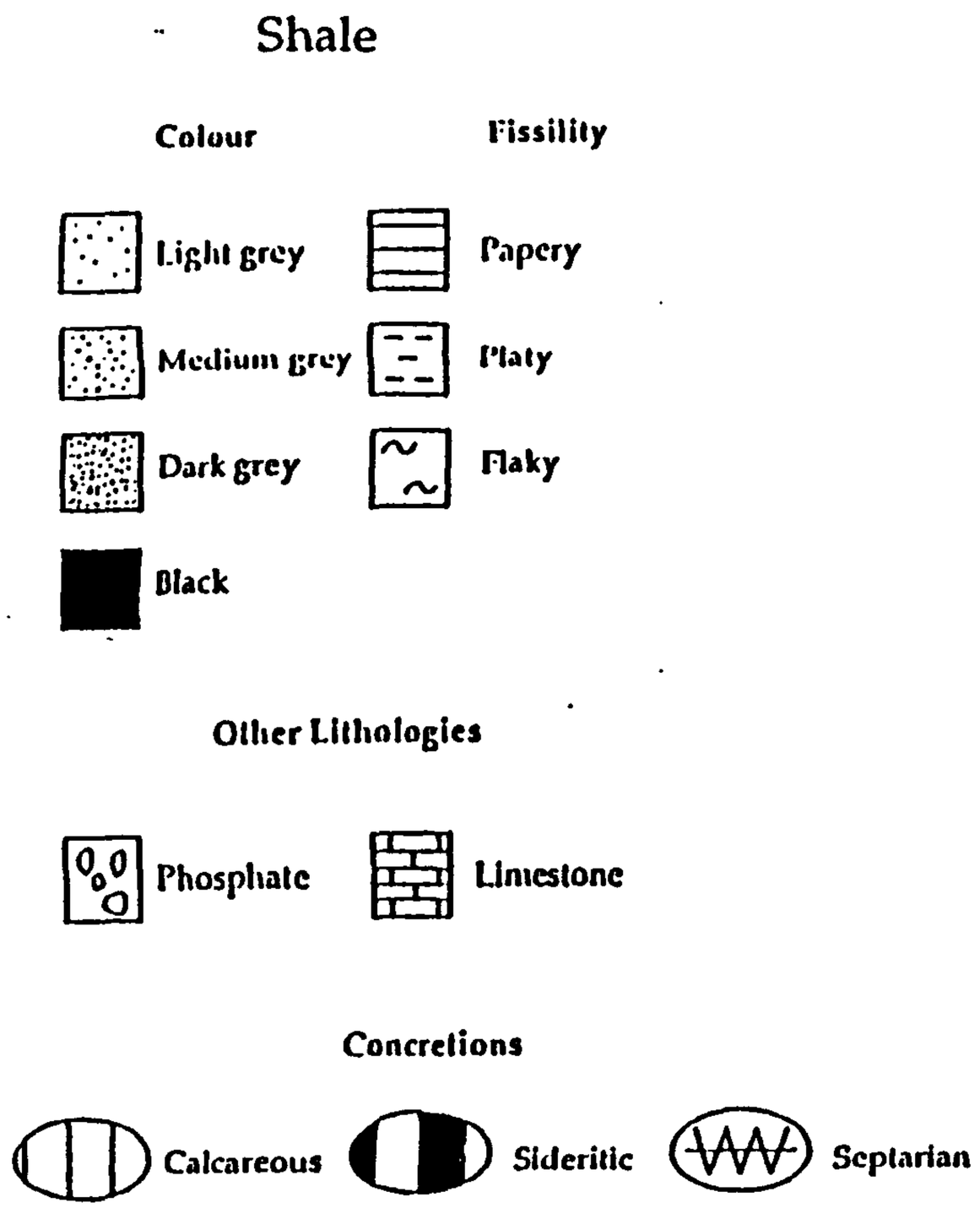

Figure 4.8 Key to sedimentary logs.

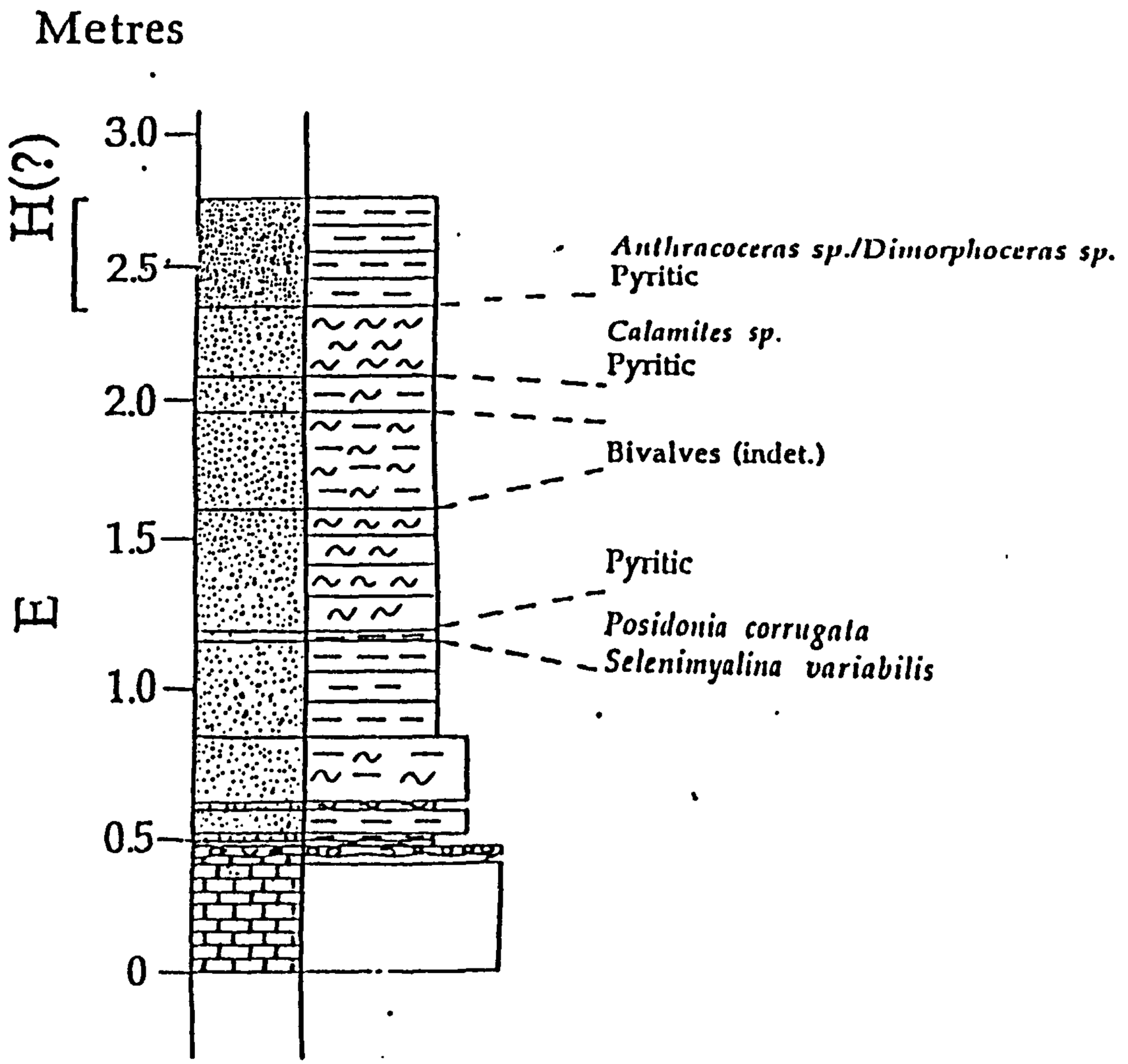

Figure 4.9 Sedimentary log of the outcrop at Ballydonohoe Bridge.

4.4.2 St Brendan's Well

This section is well exposed in cliffs in the Gowlaun stream just below a farm, approximately 100 m upstream from the road bridge. The river passes over the top surface of Dinantian limestones during heavy rains but often disappears completely during drier weather (Plate 4.1). Figure 4.10 shows the sedimentary log constructed from this outcrop.

A 5-12 cm phosphatic lag (SBWP) is developed on top of the undulose surface of the limestone (SBWL), this is followed by a more friable phosphate (SBWtopP) 3 cm thick.

Rare scattered poorly preserved indeterminable bivalves are found 1.39 m above the limestone in a 10 cm thick dark grey pyritic paper shale (SBW7). At 1.49 m above the limestone a 24 cm thick well cemented dark grey-black paper shale contains scattered *Caneyella semisulcata* (SBW9). This bivalve is also present in a 30 cm thick dark grey flaky shale (SBW11) 44 cm further up the succession and in a 9 cm thick medium grey flaky shale 2.47 m above the limestone (SBW13). The 5cm thick rusty black paper shale following this horizon also contains the same bivalves (SBW14).

The H_1b^1 goniatite band containing *Homoceras beyrichianum* occurs 2.90 m above the limestone and is preserved within calcareous bullions 15 cm thick. (SBWB). The 39 cm thick rusty dark grey flaky shale following this cemented horizon contains scattered *Caneyella sp.* bivalves and indeterminate goniatites (SBW19).

Further barren nodules and shales follow up into the cliff as far as is accessible. Hodson (1954a) also noted *proteum, undulatum* and *prereticulatus* levels from this locality.

A sample taken from the top of the Dinantian limestone yielded the conodonts:- *Gnathodus bilineatus bilineatus, Synclydognathus cuspidatus, Lochreia nodosa., Hindeodella* sp., *Neoprioniodus cuspida, Cavusgnathus* sp., and *Ozarkodinia delicatus.* There are no conodonts diagnostic of a single conodont zone, but the age provided by conodonts must range from the *Gnathodus bilineatus* zone (B_2a-mid Asbian) to the lower part of the *Gnathodus bilineatus bollandensis* zone (top E_2c^3- upper Arnsbergian) (see chapter 2 for discussion on conodont zones).

Plate 4.1 View north-west of the outcrop at St. Brendans Well.

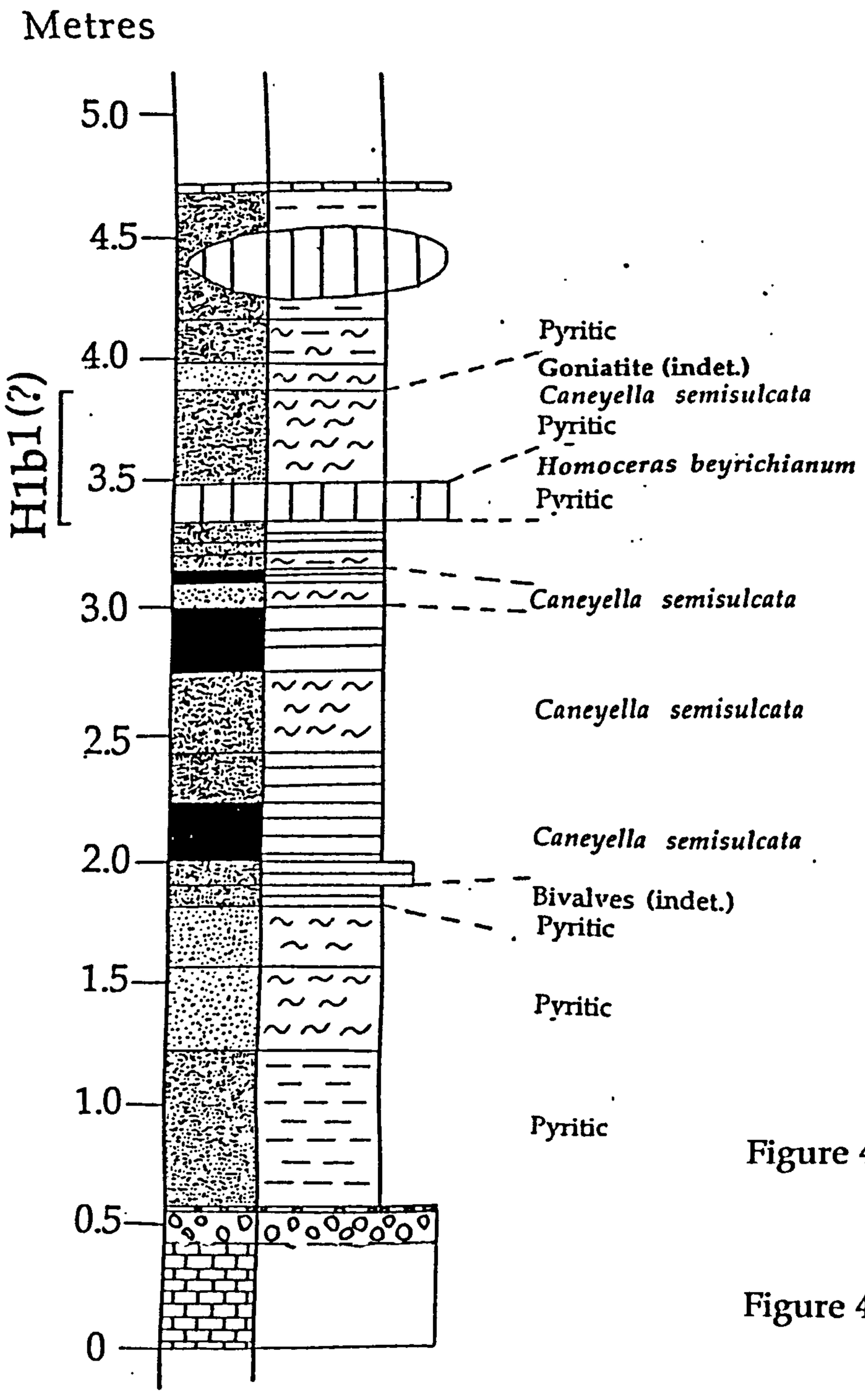

Figure 4.10 (Left). Sedimentary log of part of the outcrop at St. Brendans Well.

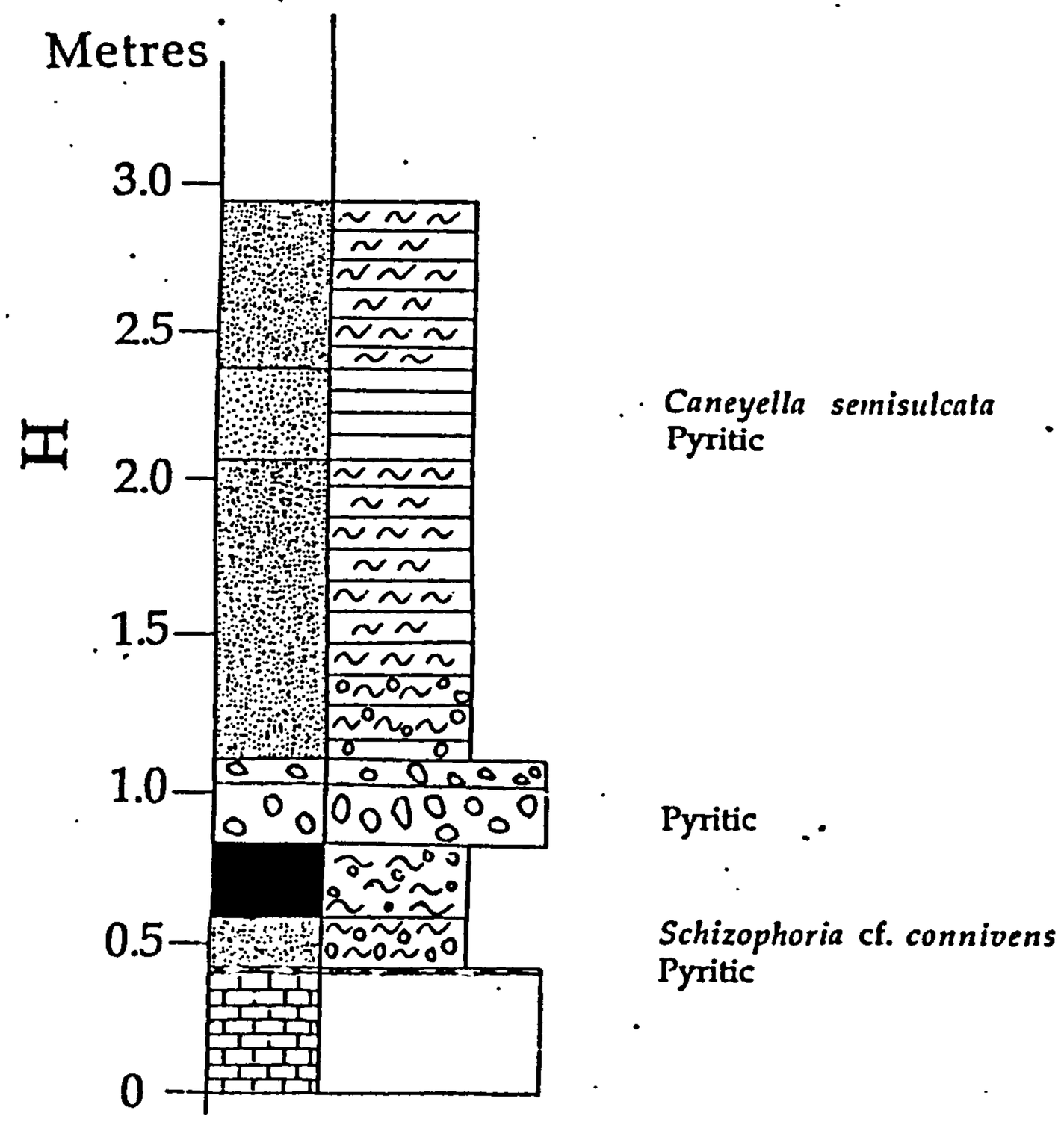

Figure 4.11 (Above). Sedimentary log of part of the outcrop at St. Catherines Cave.

Thin section studies of the upper phosphate horizon at this locality also showed the presence of a spumelline radiolaria cf. *Entactinosphaera* sp.

The phosphate development and non sequence at St Brendan's Well are pre- upper Chokierian in age.

4.4.3 St Catherine's Caves

This small section is exposed in the small stream leading from St Catherine's caves, on the northern side of the road leading to Lisdoonvarna from Knockfin Crossroads. The exposure is very close to the road. The strata are horizontally bedded. The sedimentary log is shown in Figure 4.11.

The top of the Dinantian limestone forms a step in the stream. The undulose top of the limestone is pyritic (ISC1). The 21-27 cm thick dark grey flaky shale overlying the limestone contains *Schizophoria* cf. *connivens*. brachiopods (ISC2, ISCC1). Large ovoid phosphate nodules occur especially near the base of the shale unit up to 1.5 cm in size. The overlying 25 cm pyritic black flaky shale also shows similar nodules (ISCC2). This unit is overlain by a 17-25 cm thick hard band of phosphate (ISC3) with a 6 cm thick horizon of 'knobbly' phosphate (ISC4) developed directly above it.

1.67 m above the limestone surface a 30 cm thick medium grey paper shale contains rare scattered *Caneyella semisulcata* bivalves (ISC5).

Schizophoria connivens has been documented as occurring in E1 strata from northern England by Pocock (1968). Thus, a Pendleian age is given to the strata below the phosphate with the presence of *Caneyella semisulcata* at the top of the section showing that the shales above the phosphate are of post-Arnsbergian age.

4.4.4 Roadford

The section occurs in small cliffs south of the Aille River approximately 350 m west of Roadford (Figure 4.12). The horizontally bedded section was measured next to scree from the old phosphate mines. At the time of visiting the water level was fairly high in the river so accessibility for the lowest horizons was poor.

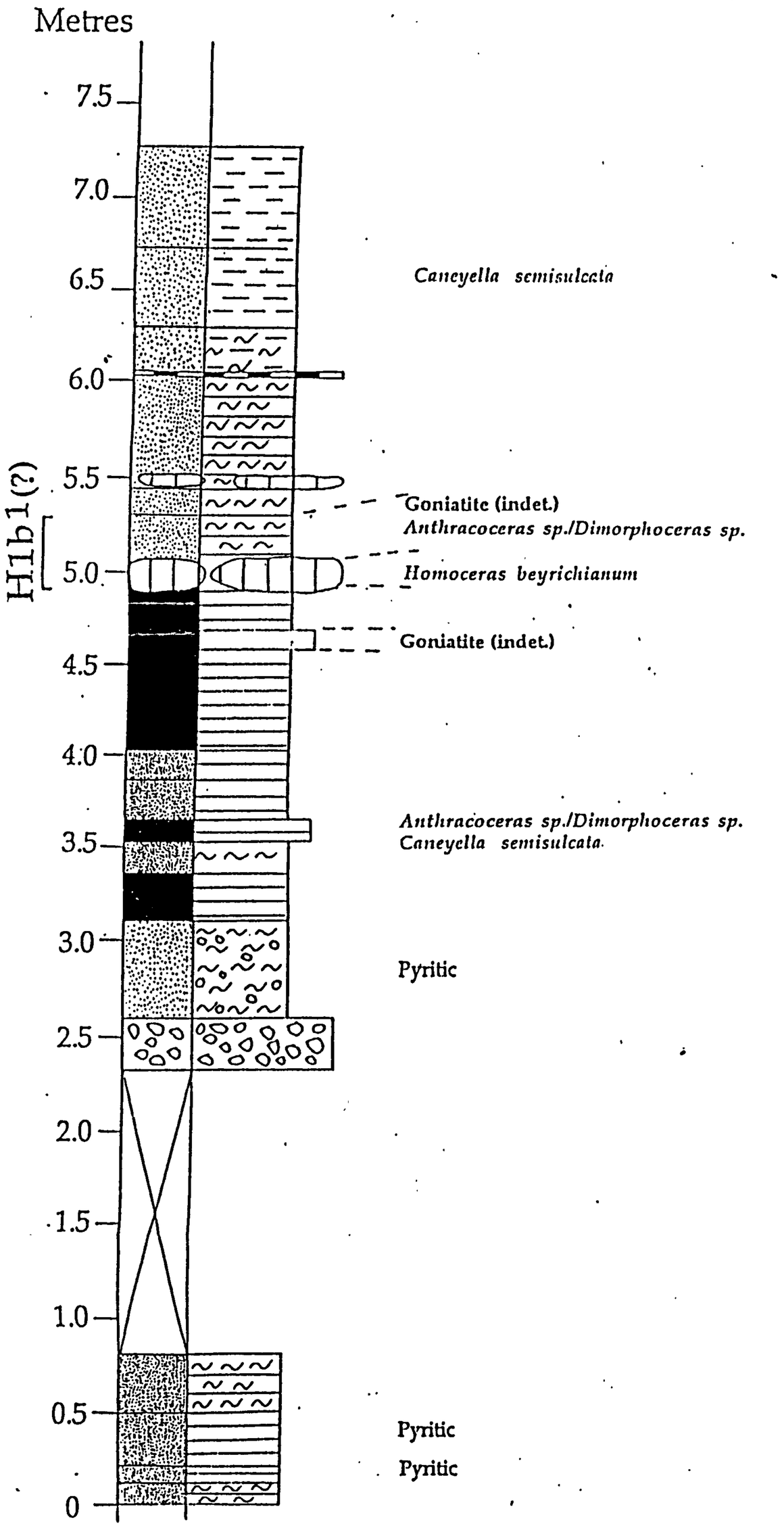

Figure 4.12 Sedimentary log of part of the outcrop at Roadford.

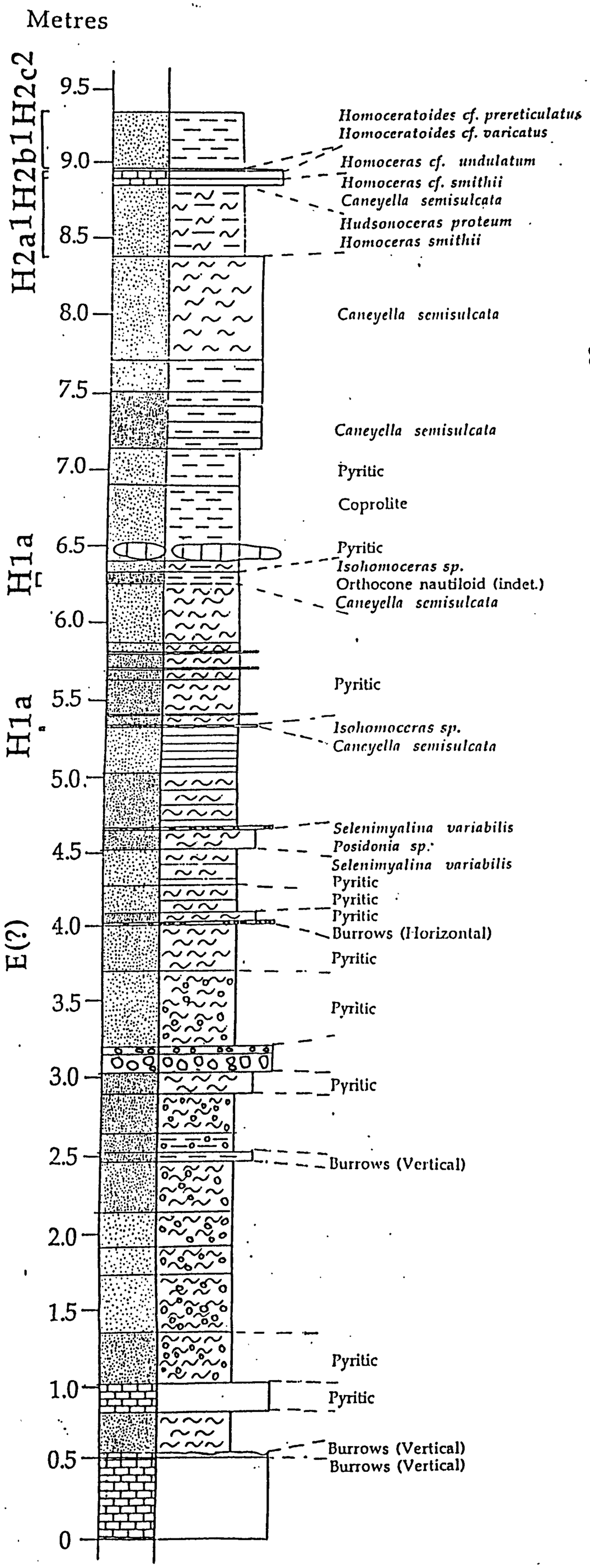

Figure 4.13 Sedimentary log of part of the outcrop at Ballyshanny House.

The lowest 82 cm of the outcrop is composed of barren nodular shales (R1),. 1.5m of outcrop is then obscured by scree. Approximately 2.22m above the base of the outcrop the very top parts of a >28 cm thick pyritic phosphate horizon is exposed (R2).

3.54 m above the base of the logged section very rare thin shelled-goniatites (R4) are present along with rare *Caneyella semisulcata* bivalves in a well cemented black paper shale.

Traces of goniatites (R5) occur within a well cemented black paper shale at 4.59 m above the base of the logged section.

The H_1b^1 (*Homoceras beyrichianum*) marine band is preserved within a calcareous pyritic nodule 17 cm thick set in black paper shale at 4.91 m above base (R6) The following 24 cm of flaky-papery medium grey shale shows very rare poorly preserved goniatites (R7).

A lone indeterminate pectinid bivalve was found preserved in 42 cm of medium grey platy shale 6.24 m above the base.

Hodson (1954a) noted many different variations of *H. beyrichianum* found from this locality including one (his *H.* aff. *subglobosum*) which he later referred to as *Homoceras beyrichianum* var. *tenuistriatum*. However, the samples collected in this study show little variation.

4.4.5 Ballyshanny House

The sections at Ballyshanny House occur roughly 400 m north of the House at a place where a stream runs into Poulnagolum pothole (Plate 4.2). Sections occur for over 200 m upstream. The log is constructed from a composite section and is shown graphically in Figure 4.13.

The top surface of the limestone is exposed near a small waterfall forming the rim to the pothole. The limestone shows quite a diverse fauna comprising small coral heads, crinoids, trilobites (indet. pygidium) and shelly debris (BWH1). The top surface of the limestone is bioturbated and hummocky, the burrows appear to be generally associated with the hummocks and penetrate down from the bed above. John Pollard (pers. comm., 1995) has suggested that they may be *Chromatichnus wegberensis*

Plate 4.2 View of the lower part of the stream section at Ballyshanny House. The top of the limestone surface provides the bed to the stream (in the lower part), this is seen outcropping to the bottom left of the Plate. Outcrops of the Clare Shale Formation occur on the banks upstream of this point.

Plate 4.3 Top surface of the limestone at Ballyshanny House showing large orthocone nautiloids and preferential preservation of cemented burrows.

(described from the Carboniferous by Donaldson and Simpson, (1962)). These traces are thought to be allied to *Zoophycos* sp., a deep water trace. The top surface of the limestone also shows current aligned giant *Orthoceras* sp. specimens up to 30 cm long (Plate 4.3). From four readings the average palaeocurrent direction is to 212°.

A 0.5-3 cm thick slightly bioclastic limestone (BWH2; BWHC1) also shows sections through *Chromatichnus* burrows that show a pyritic and dolomitic halo around the burrow (Plate 4.4). These tubes reach down at least 4 cm into the limestone and average 4 per 100 cm^2. A 19 cm thick pyritic phosphatic limestone (BWH3) is separated from the basal massive limestone surface by 27 cm of shale (BWHC2).

Further small amounts of bioturbation (pyrite lined and very similar to that seen in the top of the limestone) is present in an 8 cm thick medium-dark grey platy shale 1.90 cm above the limestone surface (BWH5).

Shales between the bioturbated shale and the overlying phosphate band contain pyrite and phosphate nodules (BWH6, BWHC6).

At 2.49 m above the basal limestone a 11 cm thick pyritic phosphatic conglomerate is evident (BWH7), this is overlain by a 4 cm thick more friable phosphate horizon (BWH8) (Plate 4.5).

A 6 cm bed of medium grey flaky shale, which contains a thin (1cm) phosphatic and pyritic lag at the base, occurs at 3.48 m above the limestone. There also appears to be some horizontal burrowing within the shale (BWH9).

Rare *Selenimyalina variabilis* bivalves are found in a 25 cm thick medium grey flaky-papery shale 3.74 m above the limestone (BWH10). This is followed by a well cemented flaky shale 12 cm thick with *Posidonia corrugata* and *Selenimyalina variabilis* bivalves (BWH11). A thin (3 cm) phosphate lag (BWH12) follows the bivalve-containing shale.

At 4.78 m above the limestone a 1 cm thick, cemented medium-grey shale horizon yields *Isohomoceras* sp. goniatites and *Caneyella semisulcata* bivalves (BWH13). A similar fauna (BWH15) is seen in a 7 cm thick dark

Plate 4.4 View of a section through a sample of limestone (taken from the uppermost Dinantian limestone horizon at Ballyshanny House). Note pyrite lining and paler coloured dolomitic halo to the burrow.

Plate 4.5 View of an outcrop at Ballyshanny House showing two prominent horizons in the waterfall, the lower is that of the well cemented bioturbated shale and the upper prominent horizon is the lowest phosphorite (A). (Gamma-ray detector for scale is 30 cm long).

grey platy shale at 5.71 m above the massive limestone. The two marine bands are therefore assigned to the H1a chronozone.

Specimen BWH16 from a 32 cm thick, well-cemented, dark grey platy paper shale, at 6.66 m above the limestone contains *Caneyella semisulcata* bivalves, 20 cm above this horizon, a 62 cm thick well cemented pyritic medium grey flaky shale contains the same species of bivalve.

The marine band H_2a^1 containing *Hudsonoceras proteum* and *Homoceras smithii* (BWH17) is associated with a 43 cm thick, flaky-platy, medium grey shale at 7.80 m above the limestone. Specimen BWH18 taken from immediately above this horizon shows a thin (8cm thick) micritic limestone horizon with *Caneyella semisulcata* and *Homoceras* cf. *smithii*. The overlying 5 cm thick horizon is a shale with a thin phosphatic top (BWH19); the shale is packed with specimens of *Homoceras* cf. *undulatum* diagnostic of the H_2b^1 marine band.

The H_2c^2 marine band containing *Homoceratoides* cf. *prereticulatus* and *Homoceratoides* cf. *varicatus* occurs at the top of the measured section in a 37 cm thick medium grey platy shale (BWH20).

Disintegration of a sample of shale taken from directly above the limestone (BWH6) provided a single, rather poor specimen of the conodont *Gnathodus bilineatus*. A pyritic nodule horizon (BWHC20) at 5.87 m above the basal limestone provided the following conodonts on disintegration:- *Hindeodella ibergensis, Hindeodella incurva,* and *Synprioniodina microdentata,* and also numerous sponge megasclere spicules. This conodont fauna is similar to that described from the Alportian of County Clare by Austin (1972). Thin section work on specimen BWH4 (taken from 1.35m above the basal limestone) provided a spumelline radiolarian cf. *Entactinosphaera* sp very similar to those described from Derbyshire by Holdsworth (1966a, 1966b).

No goniatites of H1b age were recognised during this study. However, Graham *et al.*, (1986) recognize one *Homoceras beyrichianum* horizon, but neither of the *Isohomoceras* levels.

The succession at this locality is, in the lower parts, of pre-Chokierian age (shown by the presence of the bivalve *Posidonia corrugata*). Above this there are at least two datable disconformities in the section:-

1) There are two horizons containing *Isohomoceras* sp. goniatites. It appears that the *I*. sp. nov. (H_1b^2) marine band is commonly associated with *Homoceras beyrichianum*. This goniatite is not present, and the fact that there are two horizons of *I*. sp. assigns these bands to the H_1a. There are only two rather than three *Isohomoceras* levels present; thus a non depositional event must have taken place at some point during H_1a.
2) The *Vallites eostriolatus* (H_2c^1) marine band is also absent.

4.4.6 Lough Raha

The section near Lough Raha, approximately 800 m WNW of the Lough occurs in a stream section running down the north side of a field approximately 40 m to the south-west of a fork in the road (Plate 4.6). The dip of bedding is 8° to the south-west. The sedimentary log is shown in Figure 4.14.

The lowest parts of the succession comprise flaky barren shales. At 3.17 m above the base of the logged section thin-shelled goniatites together with *Posidonia* sp. bivalves are present in a 22 cm thick dark grey paper shale (DC3).

The H_2a^1 marine band occurs at 3.57 m above the base and is associated with a rusty weathering, 34 cm thick, papery-flaky shale (DC4), and contains *Hudsonoceras proteum, Homoceras smithii* and a goniatite similar to *Ramasites* sp. The 36 cm thick dark grey flaky shale following this marine band contains rare scattered *Caneyella semisulcata* (DC5). The overlying *Homoceras undulatum* marine band (H_2b^1) is 61 cm thick and present in a dark grey flaky-papery shale (DC6). *Caneyella semisulcata* bivalves are present in abundance in the lower part of this marine band.

The H_2c^1 (*Vallites eostriolatus*) marine band occurs with *Caneyella semisulcata* (some associated with wood fragments) immediately overlying the H_2b1 band and is preserved in a 29 cm thick dark grey flaky-papery shale (DC6a). The overlying 62 cm of dark grey paper shale contains the H_2c^2 (*Homoceratoides prereticulatus*) marine band together with very rare *Dunbarella* sp. bivalves (DC7).

Plate 4.6 View to the north of the outcrop at Lough Raha. The *Hudsonoceras proteum/Homoceras smithii* marine band occurs in the rusty weathering shale to the middle-right of the Plate.

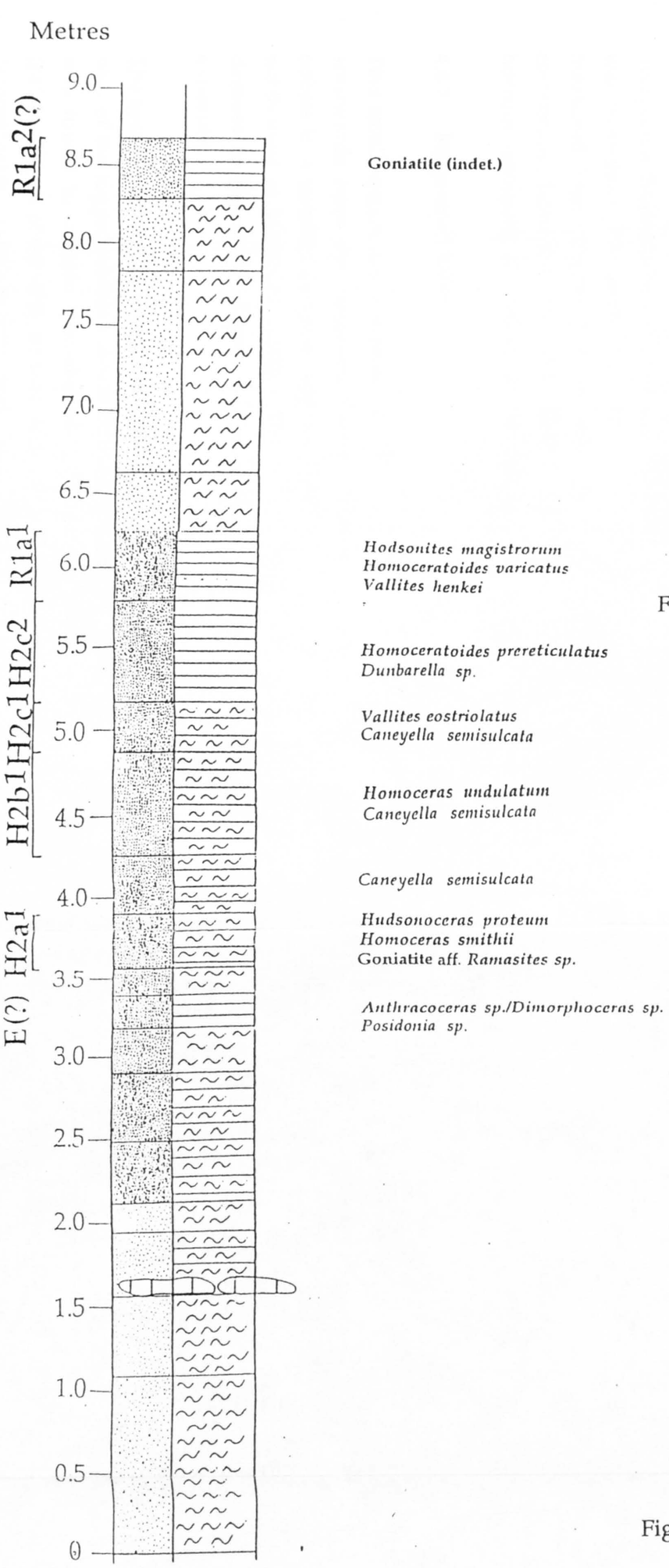

Figure 4.14 Sedimentary log of the outcrop at Lough Raha.

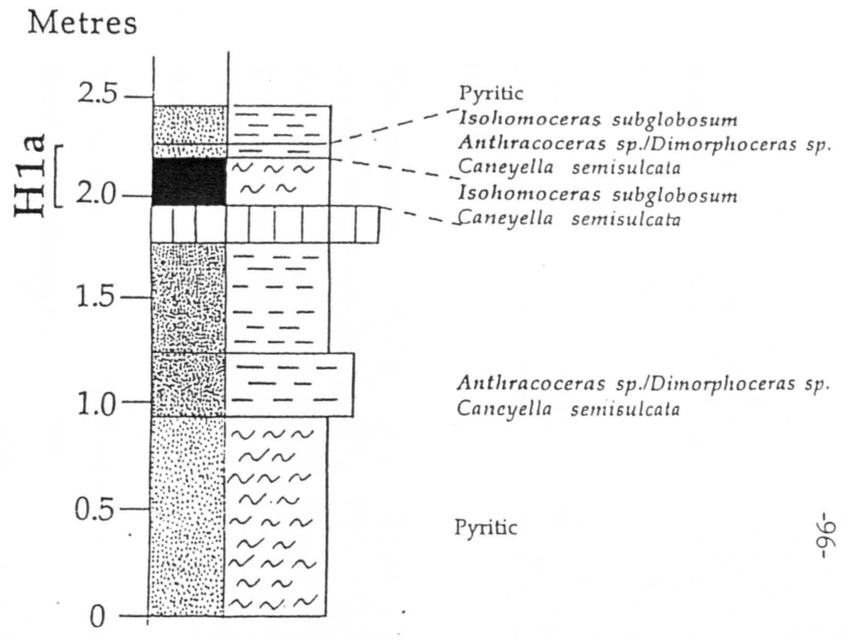

Figure 4.15 Sedimentary log of part of the outcrop at Magowna Castl

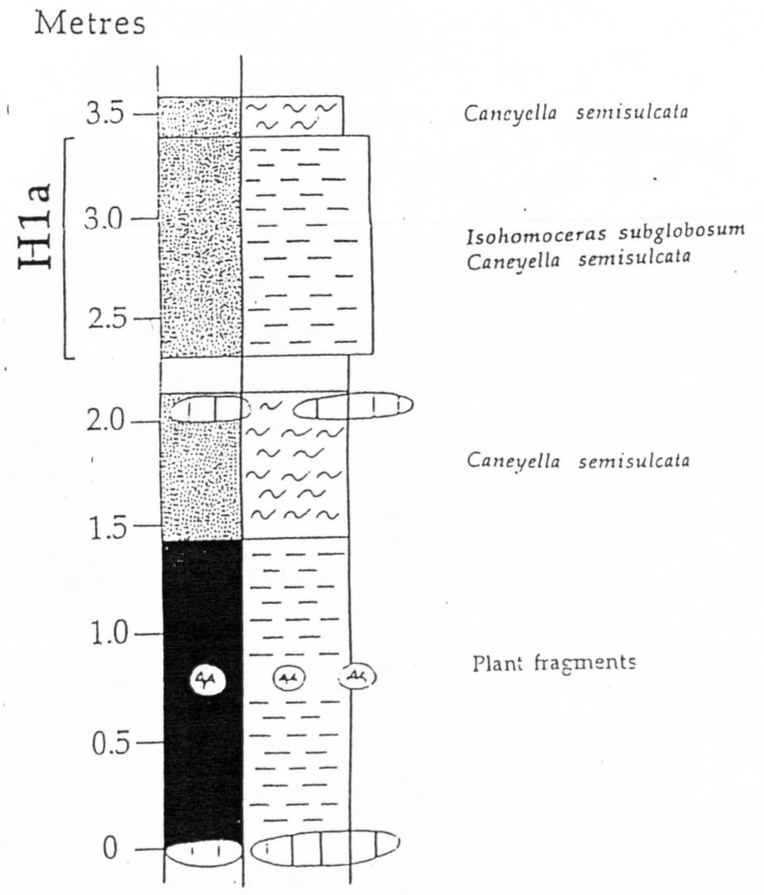

Figure 4.16 Sedimentary log of part of the outcrop at Paradise House.

The dark grey paper shale overlying the *prereticulatus* marine band is 46 cm thick and contains goniatites diagnostic of the *Hodsonites magistrorum* marine band (R_1a^1):-*Hodsonites magistrorum, Homoceratoides varicatus* and *Vallites henkei.*

The 37 cm thick, very weathered, dark grey paper shale at the top of the section contains goniatites but these were too badly preserved to be identified.

The presence of *Posidonia* sp. bivalves in the lower part of the section appears to indicate an age older than the Chokierian assuming that they are *Posidonia corrugata* as no other species of this genus occurs in the British Isles until mid-R_1 time. The goniatite horizon occurring above this level is the H_2a^1 marine band, thus a non sequence may be present at this locality cutting out at the whole of the Chokierian.

The section at Lough Raha displays the H_2c^1 (*Vallites eostriolatus*) marine band, this has not been recorded in County Clare before.

Lewarne (1959) also measured a section very close to this locality (at the overgrown Poulnagolloor pothole adjacent to the field in which the section was measured). Her section appears much more condensed than the section measured here and she did not recognise the *proteum, undulatum* nor *eostriolatus* horizons. She did however find a *Homoceras beyrichianum* horizon, unusually not associated with calcareous nodules.

4.4.7. Magowna Castle.

This small section lies in a small stream to the south side of a road leading westwards from the Magowna Castle-Ahaun Bridge Road. The section occurs in a treacherous gorge approximately 50m from the roadside, 500m north-west of Magowna Castle. The dip of bedding at this outcrop is 4 degrees to the west. Figure 4.15 shows the sedimentary log from this exposure.

The lowest parts of the measured section are pyritic shales. 93 cm above the base of the logged section a 30 cm thick dark grey platy well-cemented shale was found to contain thin-shelled goniatites and *Caneyella semisulcata* (MC1). 73 cm above this horizon a 22 cm thick, black flaky shale contains *Isohomoceras subglobosum* and *Caneyella semisulcata* (MC2). The

overlying 7 cm thick dark grey platy shale contains *Isohomoceras subglobosum*, thin-shelled goniatites and *Caneyella semisulcata* (MC3). This marine band is thus assigned to one of the three H_1a horizons. The strata to the top of the exposure are barren.

Approximately 30 m upstream a muddy limestone horizon 28 cm thick was found to contain well-preserved *Homoceras beyrichianum* of the H_1b^1 marine band.

Lewarne (1959) recorded interbedded shales and limestones overlying the Carboniferous Limestone downstream of this exposure and assigned them to the E_1, although she did not recover any goniatites at this locality However, during this study unusual 40 cm long vertical burrows (branching at base cf. *Thallasinoides* sp.) where recognised in the top 1m of Carboniferous Limestone. A specimen of the ammonoid *Lyrogoniatites georgiensis*, indicative of terminal Brigantian times (P_2c) was collected from the limestone directly above the bioturbated limestone at Magowna during this study. It is unknown whether this unusual bioturbated horizon correlates with that at Ballyshanny House. These interbedded shales and limestones (above the Carboniferous Limestone) are very probably the Magowna Formation of O'Connor and Pyne (1986).

4.4.8. Paradise House

The section studied at Paradise House is exposed on the shore in the southern reaches of the River Fergus. The short section was measured approximately 100 m to the north-west of the path leading down from Paradise House. Undoubtedly there is much more section semi-exposed (beneath seaweed) at this locality but time and cover permitted only a small section to be logged (Figure 4.16). The dip of bedding at this locality is 35 degrees to the north-west.

A flaky, dark grey, pyritic shale with small calcareous nodules near the top was found to contain *Caneyella semisulcata* bivalves. A well-cemented, platy, dark grey shale 17 cm higher contained *Isohomoceras subglobosum* and *Caneyella semisulcata* bivalves (PH1). The overlying dark grey flaky shale (19 cm thick) also contained the same bivalves. This marine band is H_1a in age and may correspond to the H_1a^2 marine band found at Inishcorker (the H_1a^1 and H_1a^3 bands are found associated with calcareous nodules).

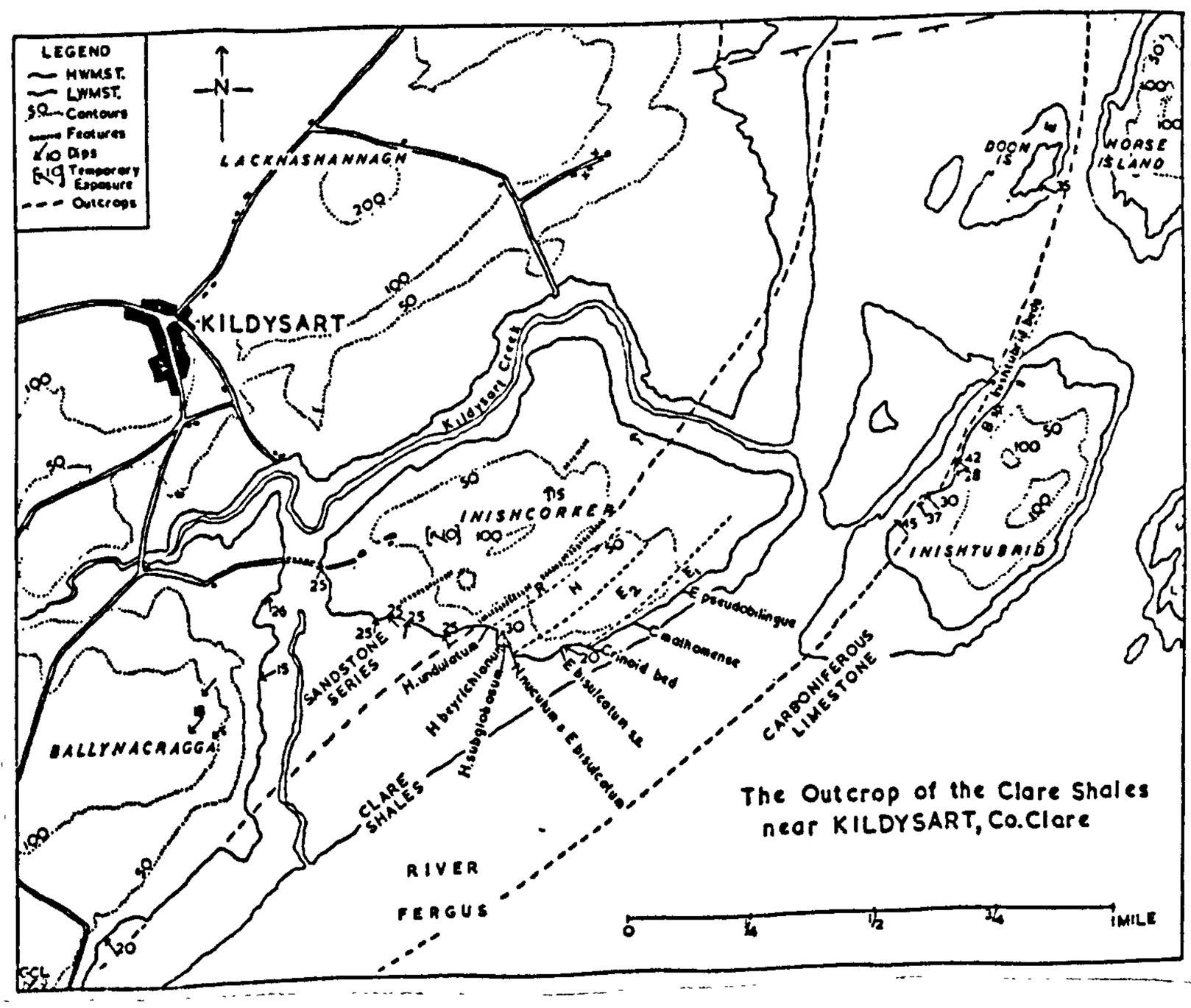

The Outcrop of the Clare Shales near KILDYSART, Co. Clare

Location map for the section logged at Inishcorker. (From Hodson and Lewarne, 1961).

Lewarne (1959) logged this section and found marine bands ranging from *Isohomoceras subglobosum* to *Reticuloceras circumplicatile* in age in the Clare Shales, although she did not recognise all the faunal bands present in this interval (this is likely to be a function of collection difficulty at this locality).

4.4.9 Inishcorker

The small island of Inishcorker lies near to the mainland village of Kildysart on the north side of the Shannon. It lies in the southern reaches of the River Fergus, close to the confluence with the River Shannon, and is accessible by a small causeway at low tide. A section in the Clare Shales spanning the mid-Carboniferous is superbly exposed in the low coastal cliffs on the south of the island (Plate 4.7). The dip of the bedding is approximately twenty degrees to the north-west. Figure 4.17 shows the sedimentary log of the succession.

The lowest parts of the succession at Inishcorker are barren and pyritic. Curious paired vertical pyrite tubes (cf. *Arenicolites* sp.) on average 30 cm long (up to 60cm maximum) and between 2 to 5 cm apart appear at certain levels in the lowest part of the succession (Plate 4.8). Their origin is enigmatic and may be diagenetic (as no other evidence for benthos is seen at this horizon) or possibly biogenic (although the organism involved would have to tolerate extremely low O_2 levels).

The lowest bivalve horizon occurs 17.00 m above the base of the logged succession in a 6 cm cemented horizon and consists of rare *Actinopteria regularis* bivalves (IN3). The lowest Namurian goniatite band exposed at Inishcorker is an *Anthracoceras* sp./*Dimorphoceras* sp. horizon, which is considered to be equivalent to the lowermost *Nuculoceras nuculum* (E_2c^2) marine band of northern England. This occurs 22.65 m above the base of the logged succession and is preserved in a 8 cm thick pyritic, carbonate cemented horizon. This marine band contains, in addition to the goniatites, *Posidoniella vetusta* bivalves and cypridinid ostracods (IN4).

The E_2c^3 (*Nuculoceras nuculum*) marine band occurs between 29.25 and 30.65 m. The basal 37 cm is a hard, dark grey, platy shale containing

Plate 4.7 View of much of the outcrop on the southern side of Inishcorker. The E_2c^3 marine band occurs in strata dipping to the left on the right-hand side of the Plate. The sandstones of the Ross Formation can be seen on the far left of the Plate.

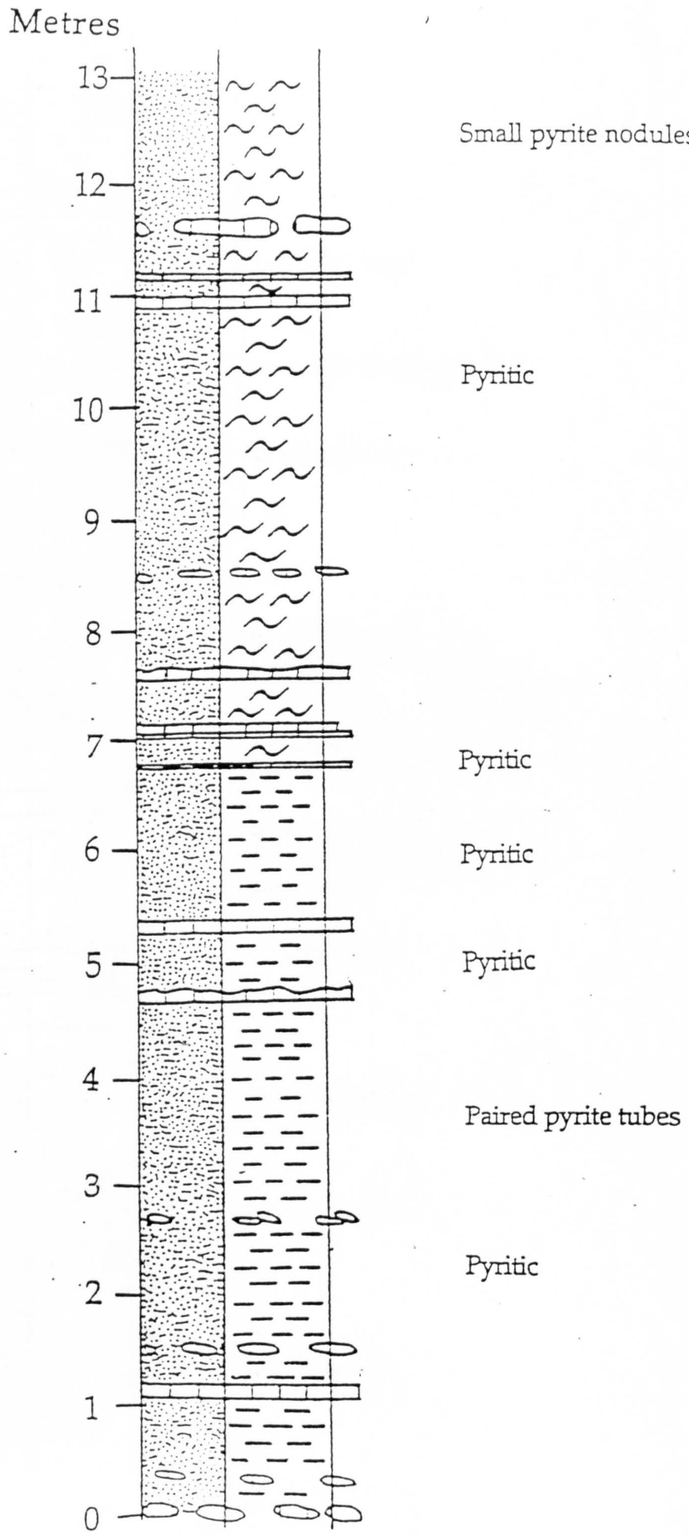

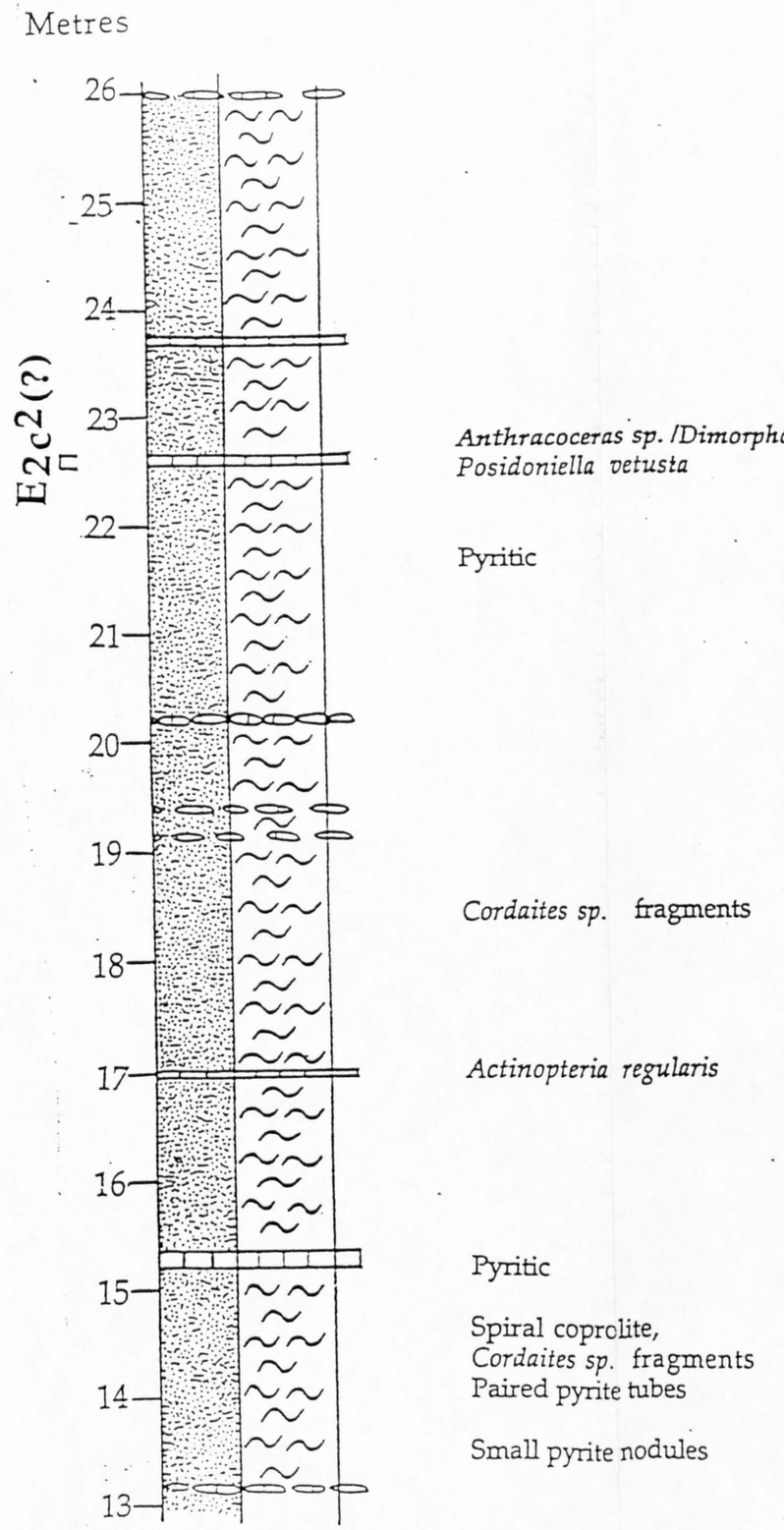

Figure 4.17 Sedimentary log of part of the outcrop at Inishcorker.

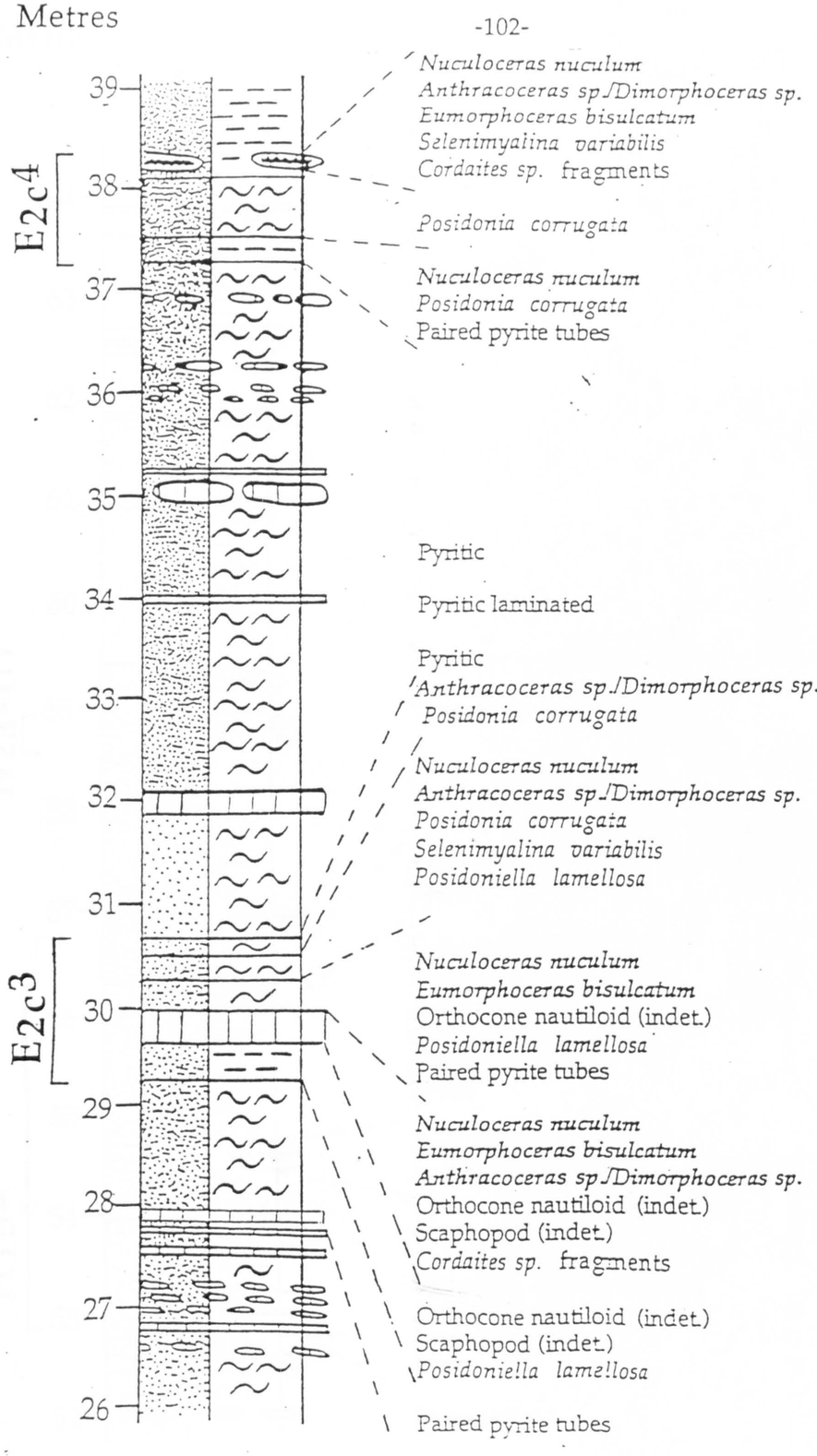

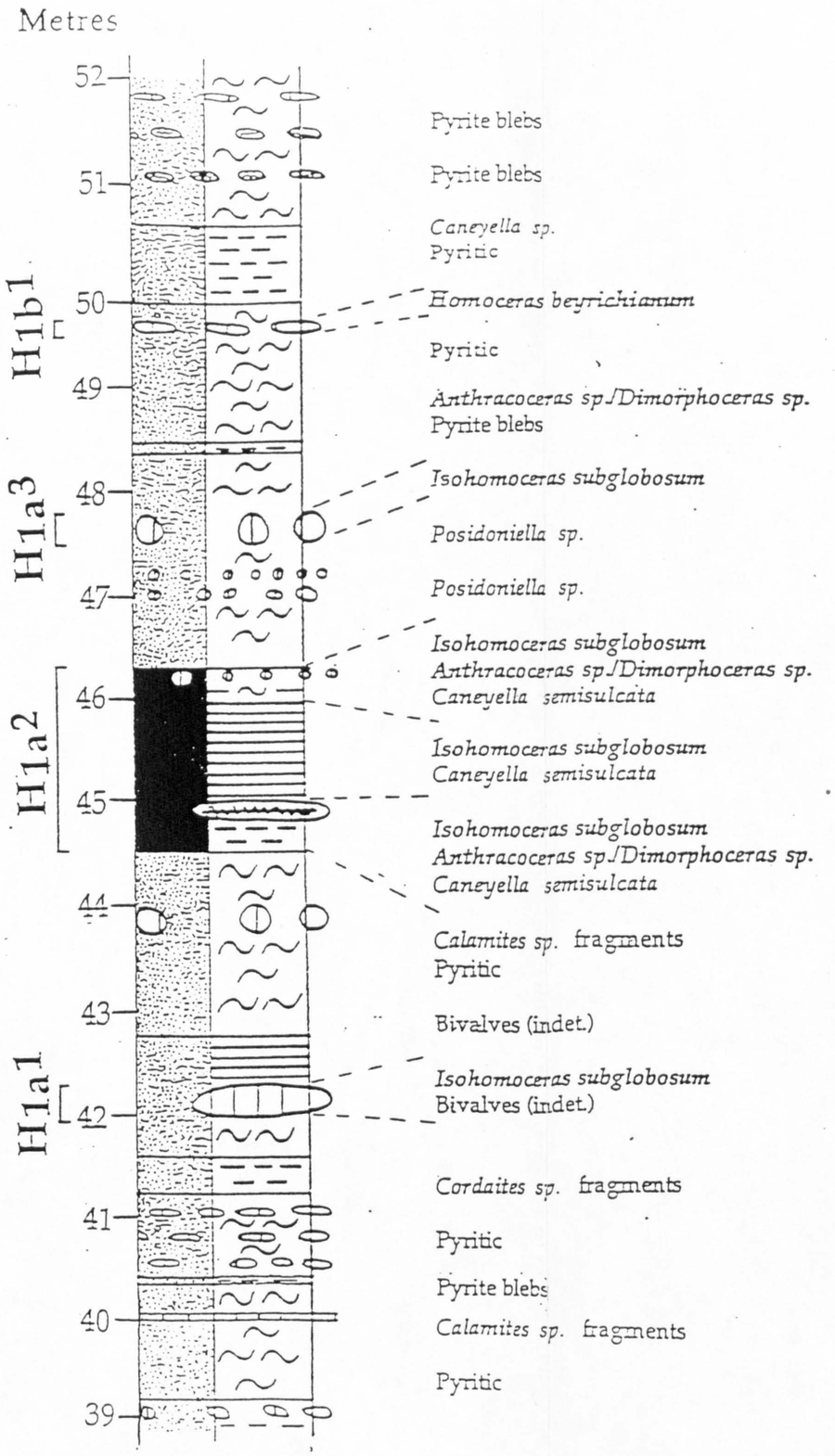

Figure 4.17 Continued.

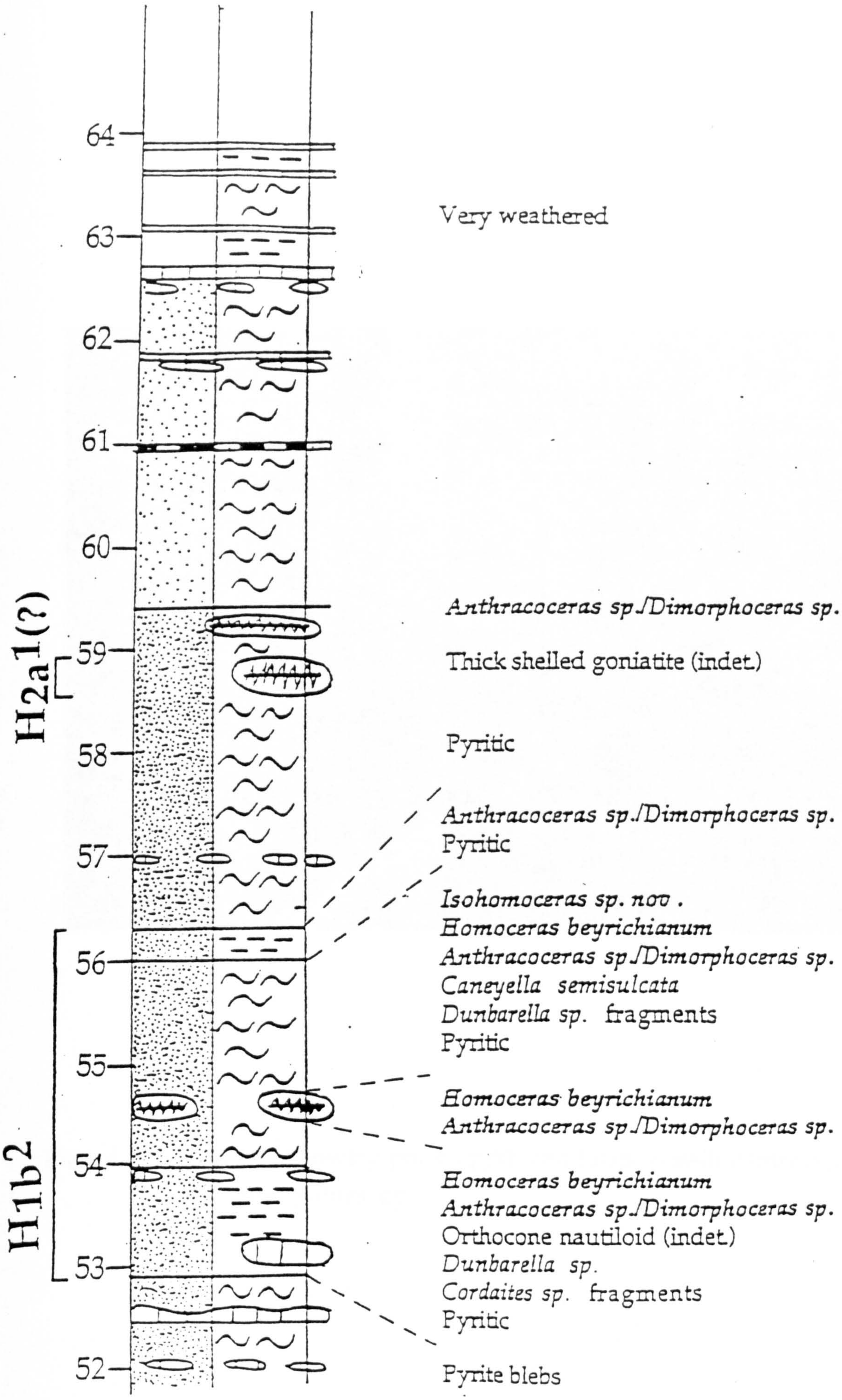

Figure 4.17 Continued.

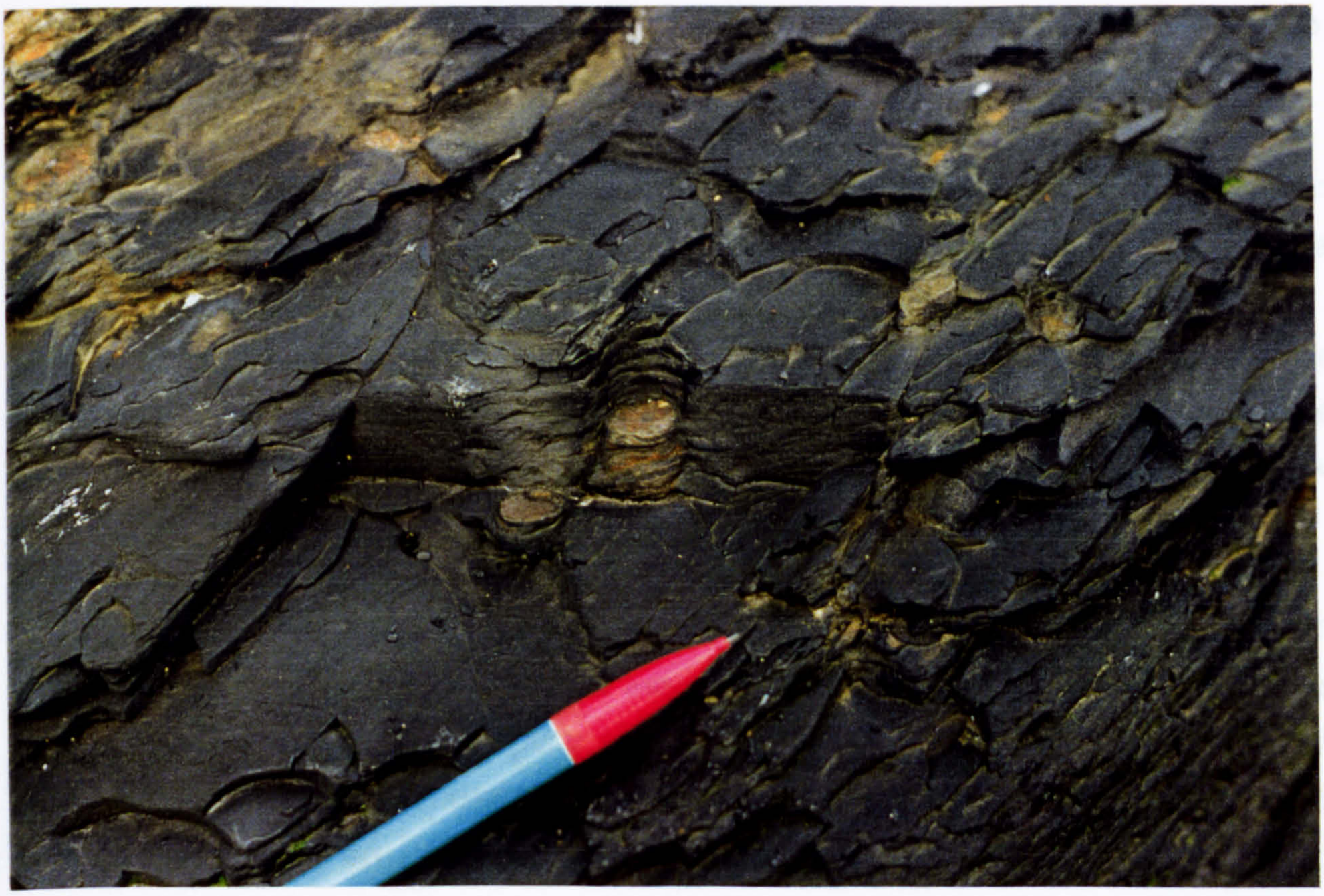

Plate 4.8 Plate showing paired pyritized tubes, possibly burrows cf. *?Arenicolites* sp.

orthocone nautiloids (indet.), scaphopods (indet.) and *Posidoniella lamellosa* bivalves (IN6). This is followed by 33 cm of limestone with the diagnostic goniatite *N. nuculum,* together with *Eumorphoceras bisulcatum, Anthracoceras* sp./*Dimorphoceras* sp. ammonoids and further orthocone nautiloids and scaphopods (IN7). The succeeding 70 cm of dark grey flaky shales show a diverse fauna of *N. nuculum, E. bisulcatum, Anthracoceras* sp./*Dimorphoceras* sp. ammonoids, orthocone nautiloids (indet.), *Posidonia corrugata, Selenimyalina variabilis* and *Posidoniella lamellosa* (IN8, RIN20, RIN21, RIN22). The very upper part of the marine band is 15 cm thick and contains*Anthracoceras* sp./*Dimorphoceras* sp. ammonoids and *Posidonia corrugata* (IN9).

The uppermost *Nuculoceras nuculum* marine band (E_2c^4) occurs between 37.25 m and 38.35 m in dark grey flaky and platy shales together with a septarian nodule horizon. The fauna consists of *N. nuculum, E. bisulcatum, Anthracoceras* sp./*Dimorphoceras* sp. ammonoids, *Posidonia corrugata* and *Selenimyalina variabilis* (IN10, IN11). The centre of the marine band is devoid of ammonoids, *Posidonia corrugata* constituting the only fauna.

The oldest Chokierian ammonoids of the H_1a^1 marine band occur 42.00 m above base in a 30 cm thick band associated with large calcareous bullions and dark grey flaky and papery shales (Plate 4.9) (IN12, RIN1, RIN2). This band shows an impoverished fauna consisting of *Isohomoceras subglobosum* and an indeterminate bivalve.

The succeeding H_1a^2 marine band, ranging from 44.50 to 46.30 m above base, contains *Isohomoceras subglobosum, Anthracoceras* sp./*Dimorphoceras* sp. ammonoids and *Caneyella semisulcata* bivalves preserved as compressions in a black paper shale with septarian and calcareous nodules (IN13, IN14, IN15, RIN3, RIN4, RIN5).

Two small calcareous nodule horizons at around 47.00m contain a bivalve fauna of *Posidoniella* sp.

The topmost *Isohomoceras subglobosum* (H_1a^3) band occurs in a horizon of small calcareous nodules at 47.65 m with the fauna being restricted to the diagnostic ammonoid (RIN6, RIN7).

Level of the mid-Carboniferous boundary ($H1a^2$)

Plate 4.9 View north-east of the upper Arnsbergian and lower Chokierian strata at Inishcorker. The $H1a^1$ marine band occurs at the horizon of the weathered-out bullion to the middle-left of the Plate. The mid-Carboniferous boundary (at $H1a^2$) is present in the small cliff to the left of the Plate.

Between the H_1a^3 and the H_1b^1 marine bands there is a 12 cm dark grey platy shale horizon at 48.45 m bearing thin-shelled ammonoids (*Anthracoceras* sp./*Dimorphoceras* sp.) (IN17).

The 27 cm thick H_1b^1 *Homoceras beyrichianum* marine band, containing only the definitive goniatite is found from the top of the calcareous bullions at 49.55 m. The overlying shale contains *Caneyella* sp. bivalves at its base (IN18, RIN8, RIN9).

The H_1b^2 marine band is the thickest band exposed at Inishcorker being 3.45 m thick and is developed from 52.95 m above the base. Although this band corresponds with the *Isohomoceras* sp. nov. band of Riley *et al.* (1987), the lower half of the marine band contains a fauna of *Homoceras beyrichianum, Anthracoceras* sp./*Dimorphoceras* sp., orthocone nautiloids (indet.) and *Dunbarella* sp. (IN 19, RIN10, RIN11, YARI3, YARI4), whilst the top 1.60 m of the band shows an *Isohomoceras* sp. nov. dominated assemblage but also with *H. beyrichianum, Anthracoceras* sp./*Dimorphoceras* sp., *Caneyella semisulcata* and *Dunbarella* sp (RIN12, YARI1, YARI2). The upper 26 cm of the marine band contains only *Anthracoceras* sp./*Dimorphoceras* sp (RIN13). The marine band fauna is associated with dark grey flaky and platy shales with calcareous and septarian nodules.

Towards the top of the logged sequence the shales become very weathered with large septarian nodules at 58.55 m containing indeterminable goniatites, possibly corresponding to the H_2a^1 (*Hudsonoceras proteum*) marine band (RIN14).

The section at Inishcorker displays three *Isohomoceras subglobosum* marine bands, this has not been recorded previously in Ireland. There also appear to be two marine bands containing *Homoceras beyrichianum*- at Inishcorker, with the upper horizon also containing *Isohomoceras* sp. nov. Thus, unlike the northern England biostratigraphy, the Irish ammonoid biostratigraphy shows the development of two *Homoceras beyrichianum* bands, the upper of which is probably equivalent (as shown at Inishcorker) to the *I.* sp nov. (H_1b^2) marine band (Braithwaite, 1994).

4.4.10 Luggacurren.

The section at Luggacurren is exposed in a stream approximately 1 km south of Luggacurren village, County Laois upstream of a confluence with a tributary. The sedimentary log is shown in Figure 4.18.

At the base of the measured section the lowest 92 cm of medium-dark grey flaky-papery shale shows small horizontal pyritized burrows (cf. *Planolites* sp.) (LUG1). This is followed by a very well cemented 12 cm thick pyritic dark grey mudstone containing *Posidonia corrugata* bivalves (LUG2, RLUG5). 2 cm of medium grey limestone with *Posidonia corrugata* bivalves and small plant fragments (LUG3, RLUG3) and pyritized burrows as below separates this horizon from the overlying 8 cm of shale (Plate 4.10). This shale is pyritic and slightly calcareous containing *Nuculoceras nuculum, Selenimyalina variabilis* and *Posidonia corrugata* (LUG4).

A 10 cm thick, dark grey, well cemented, calcareous horizon (LUG5, RLUG6) shows *Nuculoceras nuculum,* and orthocone nautiloids and is assigned to the E_2c^4 horizon. The following 16 cm of medium-dark grey well cemented shale shows *Caneyella semisulcata* bivalves.

1.92 m above base a 10 cm thick paper shale shows rare scattered *Caneyella semisulcata,* together with an indeterminate goniatite (LUG7) *Caneyella semisulcata* bivalves are also present in the more cemented 10 cm of shale directly above this horizon. The H_1a^2 marine band occurs above the shale in a dark grey pyritic limestone 15 cm thick showing *Isohomoceras sp.* goniatites. The following 17 cm of black, flaky-papery shale also shows *Isohomoceras sp.* goniatites (LUG8) and shows increasing cementation upwards.

The H_1a^3 marine band is present 3.50 m above the base of the measured section and is associated with a well-cemented, medium grey, platy shale and contains *Isohomoceras* sp., orthocone nautiloid (indet) and *Caneyella semisulcata* bivalves. (LUG10). The succeeding 19 cm (of a similar facies) contains the same fauna together with *Posidoniella* sp. bivalves, *Cordaites* sp. plant fragments and the partial remains of an indeterminate actinopterygian fish (LUG11, LUG12).

Plate 4.10 General view upstream of the outcrop at Luggacurren. The E_2c^4 limestones form prominent steps in the stream-bed.

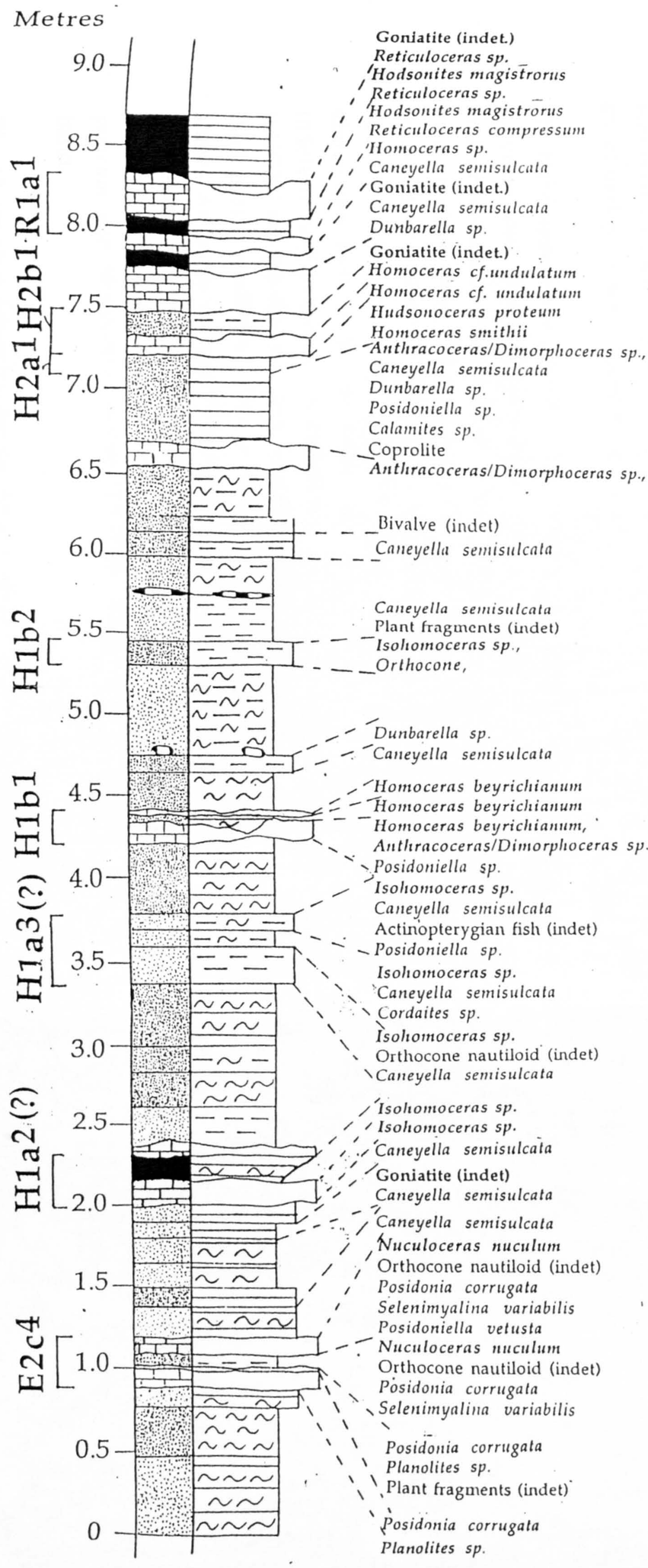

Figure 4.18 Sedimentary log of part of the outcrop at Luggacurren.

At 4.33 m above the base of the section, the *Homoceras beyrichianum* marine band occurs in a 13 cm thick limestone and contains the definitive goniatite together with *Anthracoceras sp/Dimorphoceras* sp. and *Posidoniella* sp. bivalves (LUG13). The following 3 cm of dark grey flaky shales also contains *Homoceras beyrichianum* goniatites (LUG14). The 3 cm thick cementstone overlying this also contains *Homoceras beyrichianum* goniatites (LUG15). The succeeding 25 cm thick dark grey flaky shale shows scattered *Caneyella semisulcata* bivalves at the top. This is followed by 11 cm of dark grey platy cemented shale with *Dunbarella sp.* bivalves (LUG16).

The H_1b^2 marine band occurs at 5.42 m above the base and is associated with a pyritic, well-cemented platy shale. The fauna comprises *Isohomoceras sp.* and orthocone nautiloids (indet.) (LUG17). The following 33 cm thick medium-dark grey platy shale contains plant fragments and *Caneyella semisulcata* bivalves (LUG18). Similar bivalves are seen scattered at 5.93 m above the base in a 22 cm light-medium grey platy-flaky shale. At 6.26 m above the base a 12 cm thick dark grey platy shale shows small indeterminate bivalves. *Anthracoceras* sp. */Dimorphoceras* sp. goniatites (LUG20) are present at 6.68 m above the base in a semi-continuous 13 cm thick pyritic mudstone. The overlying 53 cm thick dark grey paper shale shows *Anthracoceras* sp./*Dimorphoceras* sp. goniatites and *Dunbarella* sp. *Posidoniella* sp. bivalves, fragments of *Calamites* sp, and a coprolite at the base (LUG21), whilst the very top parts of the shale contain *Hudsonoceras proteum* and *Homoceras smithii* (LUG22a) indicating the H_2a^1 marine band.

The 13 cm thick irregular, pyritic, limestone horizon succeeding the shales contains *Homoceras cf. undulatum* marine band (LUG22b). Sample LUG23 taken from the overlying 14 cm thick dark grey papery-platy shale also contains *Homoceras cf. undulatum* goniatites.

The following 27 cm semi-continuous pyritic limestone contains indeterminate goniatites (LUG24). This limestone horizon is superseded by 9cm of black paper shale containing an indeterminate goniatite and *Caneyella semisulcata* and *Dunbarella* sp. bivalves (LUG25).

The 11 cm thick irregular limestone (LUG26) contains *Homoceras* sp. and *Caneyella semisulcata* and is separated from an overlying limestone horizon by a 10 cm thick well cemented paper shale containing *Hodsonites magistrorum, Reticuloceras compressum* goniatites of the R_1a^1 marine

band. The following limestone is irregular and 10-29 cm thick and contains *Hodsonites magistrorum* and *Reticuloceras* sp. goniatites (LUG28). The 35 cm thick dark grey-black paper shales overlying the limestone contains *Reticuloceras* sp. and an indeterminate goniatite (LUG29).

The logged section is very similar to that shown by Higgs (1986), although it is evident from this study that there are two *Isohomoceras sp.* horizons which are presumed to be the higher two. Also *Homoceras beyrichianum* was not found to be present in the H_1b^2 marine band, and so in this respect the fauna is the same as the marine band in Britain, ie., there is no *Homoceras beyrichianum* as seen in the H_1b^2 band in County Clare. The other differences are that the *proteum-smithii* horizon was proved at this locality as was the *magistrorum* horizon. There is no evidence of either the *eostriolatum* or *prereticulatus* horizons, although admittedly these horizons could be represented by the indeterminate goniatite horizons.

The evidence from this locality therefore appears to affirm the stratigraphy as seen in the Clare Basin, with evidence of a non-sequence during the early Chokierian resulting in the absence of the lowest H_1a marine band.

4.5 DISCUSSION

4.5.1 Biostratigraphy in County Clare

The section at Inishcorker exhibits the, as yet, most biostratigraphically complete mid-Carboniferous section in Ireland. Thus it is taken that this section displays the full biostratigraphy through the mid-Carboniferous in Ireland.

The revised ammonoid biostratigraphy through the mid-Carboniferous in Ireland, although very similar to that of northern England, shows some differences. Table 4.3 shows the revised ammonoid stratigraphy through the mid-Carboniferous in Ireland as ascertained during this study.

The lowest goniatite band exposed at Inishcorker is an *Anthracoceras* sp./*Dimorphoceras* sp. horizon, which is considered to be equivalent to the lowermost *Nuculoceras nuculum* (E_2c^2) marine band of northern England.

Amm. Hor. Index	Ammonoids
R1a1	Hodsonites magistrorum, Homoceratoides varicatus, Reticuloceras compressum
H2c2	Homoceratoides prereticulatus, Homoceratoides varicatus
H2c1	Vallites eostriolatus
H2b1	Homoceras undulatum
H2a1	Hudsonoceras proteum, Homoceras smithii
	Anthracoceras sp/Dimorphoceras sp.
H1b2	Isohomoceras sp. nov., Homoceras beyrichianum
H1b1	Homoceras beyrichianum
	Anthracoceras sp/Dimorphoceras sp.
H1a3	Isohomoceras subglobosum
H1a2	Isohomoceras subglobosum
H1a1	Isohomoceras subglobosum
E2c4	Nuculoceras nuculum, Eumorphoceras bisulcatum
E2c3	Nuculoceras nuculum, Eumorphoceras bisulcatum
	Anthracoceras sp./Dimorphoceras sp.

Table 4.3 Table showing ammonoid stratigraphy for the mid-Carboniferous of County Clare determined in this study.

Faunal Band	Ammonoids
I	R. subreticulatum
H	R. circumplicatile
G	R. circumplicatile, Ht. varicatus
F	R. aff compressum
E	Ht. aff. prereticulatus
D	H. undulatum
C	Hu. proteum, H. smithii
B	H. beyrichianum
A	H. beyrichianum, H. aff. subglobosum

Table 4.4 Table showing ammonoid stratigraphy of Hodson (1954a).

Ammonoids
Hd ornatum
R. paucicrenulatum
R. subreticulatum, Ht. divaricatus
R. circumplicatile
R. circumplicatile, Ht. varicatus
H. magistrorum
Ht. prereticulatus
H. eostriolatum
H. undulatum
Hu. proteum, H. smithii
Dimorphoceras
H. beyrichianum
H. beyrichianum
Dimorphoceras sp.
H. subglobosum
H. subglobosum
N.nuculum
N. nuculum, E. bisulcatum
Ct. sp
Ct. nitidus
E. bisulcatum
C. malhamense
E. pseudobilingue
C. leion

Table 4.5 Table showing ammonoid stratigraphy of Lewarne (1959).

This lowest *Nuculoceras nuculum* horizon has not been found in Ireland, and thus appears to be represented by the thin-shelled goniatite horizon.

Unlike occurrences in northern England, *Homoceras beyrichianum* occurs at two levels in County Clare, the upper of which also contains *Isohomoceras* sp. nov.; this may correlate to the *I.* sp. nov. band of Riley *et al.*, 1987. The original stratigraphy for County Clare as defined by Hodson (1954a) is shown in Table 4.4. Lewarne (1959) extended the stratigraphy and recognised further marine bands in the Clare Shales, in counties Clare, Kerry and Cork. Her zonation is shown in Table 4.5.

Hodson (1954a) stated that it was possible that more than two faunal bands containing *H. beyrichianum* existed in the lower parts of the Clare Shales with a complex of marine bands containing an evolving fauna. He suggested that faunal band A may be an intermediate band between the H_1a (*I. subglobosum*) and H_1b (*H. beyrichianum*) zones. Hodson (1954a) noted many different variations of *H. beyrichianum* including one (his *H.* aff. *subglobosum*) which he later referred to as *Homoceras beyrichianum* var. *tenuistriatum*. Therefore, when referring to Hodson's work it is quite difficult to distinguish the H_1b^1 and H_1b^2 marine bands. I have decided in this work to identify the H_1b^2 marine band only by the additional presence of *Isohomoceras subglobosum*.

This work has confirmed the existence of the *eostriolatum* band in County Clare (at Lough Raha); it has been recognised from the Clare Shales in Limerick by Lewarne (1959). Hodson did not recognise the H_2c^1 marine band (*V. eostriolatum*) but did find a homoceratid in his faunal band E, which he noted as a form with characters intermediate between *H. eostriolatum* and *H. henkei*.

4.5.2 Spatial extent of the marine bands in County Clare

Hodson and Lewarne (1961) described the fill of the Clare Basin as showing increasing northerly onlap onto the shelves with time; this still holds true. However, from correlation with the aid of the marine bands, it is evident that at least three unconformities have occurred on the margins of the Clare Basin, one directly above the Dinantian limestone, one during the Pendleian/mid-late Arnsbergian and one spanning the mid-Carboniferous boundary. A fourth possible unconformity occurred during *eostriolatum* times, although the evidence for this from outcrops is scanty.

Deposition was probably continuous in the centre of the Clare Basin, although it should be noted that not all the British ammonoid horizons are present. Hodson (1954b) however, suggested from thickness relationships in the vicinity of Foynes Island, that there was probably an unconformity somewhere between the late Dinantian and upper Arnsbergian. Lewarne (1959) noted the occurrence of the lowest Namurian ammonoid band (*C. leion*) directly above the limestone in the Magowna area, (and the same marine band has been recognised at Kilnamona in this study, (less than 2 km SE of Magowna)), although Lewarne also speculated that there was probably an unconformity in the Arnsbergian in this area.

Conodonts taken from the top limestone at St Brendan's Well unfortunately did not yield any particularly diagnostic conodonts (those that were retrieved were indicative only of a range between the *Gnathodus bilineatus* zone (B_2a-mid Asbian) to the lower part of the *Gnathodus bilineatus bollandensis* zone (top E_2c^3 - upper Arnsbergian)). However Clarke (1966) recognised corals of a P_2 age in the area. The *Cravenoceras leion* horizon found in the distal shelf area at Kilnamona, has not been noted during this work from study of outcrops in a more proximal shelf region, therefore it is presumed that the non depositional hiatus/ erosion occurring on the proximal shelf area has obliterated any evidence of the Pendleian, with the lowest marine band present pertaining to the *Isohomoceras* chronozone. At the St. Catherine's Cave locale the shale immediately above the limestone has been assigned to the Pendleian (E1) by the presence of *Schizophoria* cf. *connivens* brachiopods which have been noted from the E_1 and R_1 of Britain by Pocock (1968).

Thus it appears that the eroded shelf margin area very probably correlates with a lowstand of sea level, when deposition was confined to the basin centre, probably during the late Brigantian-early Pendleian, prior to the major regression that formed the main phosphorite bed on the shelves. Graham *et al.*, (1986) recognised a single *Nuculoceras nuculum* horizon lying above the phosphorite horizon in the Cahermacon area so it is likely that this constrains the major phosphorite bed (second unconformity) to between the earliest Pendleian and mid-late Arnsbergian (this is also proved

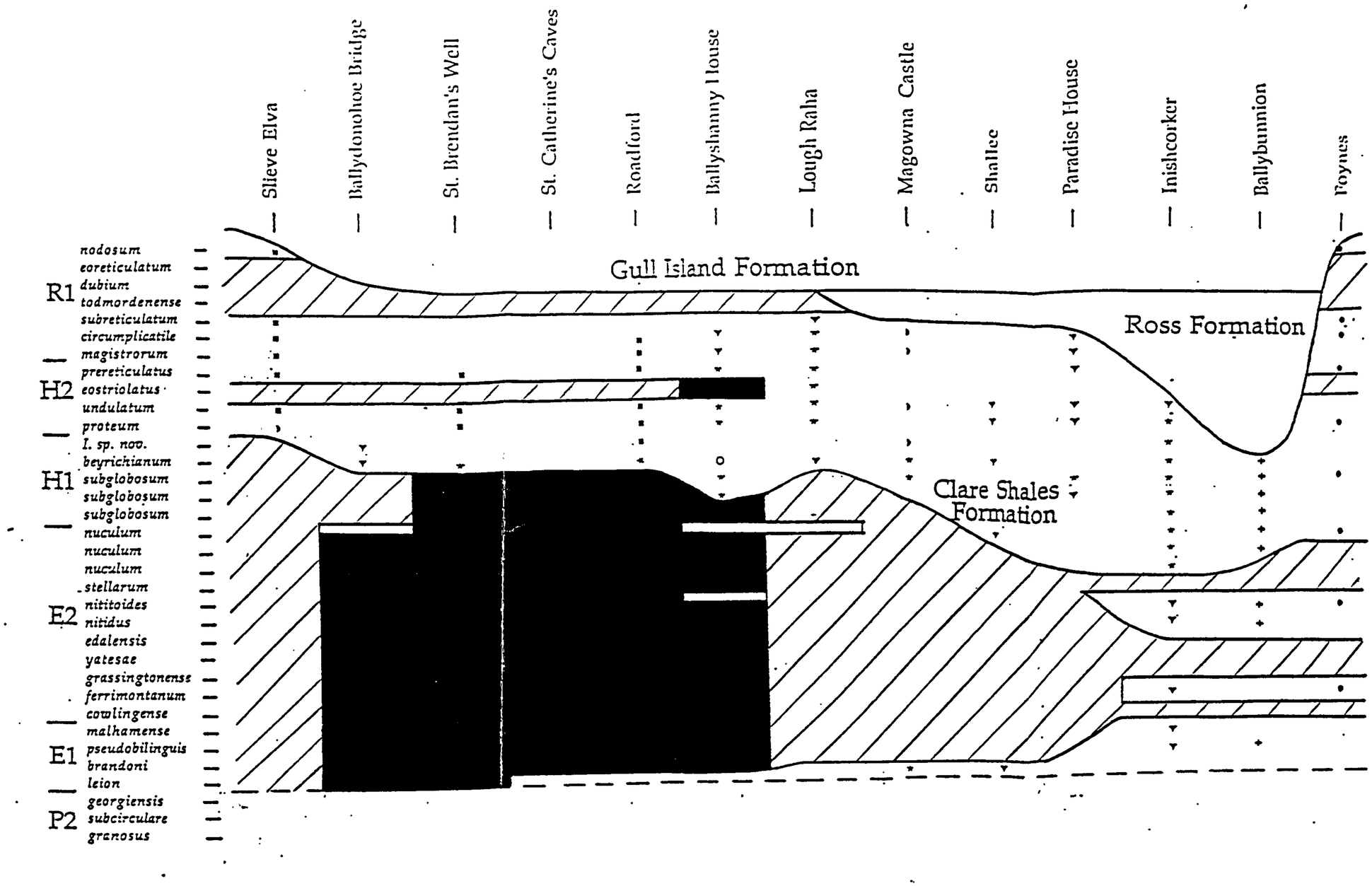

Figure 4.19 Chronostratigraphic diagram of the Clare Basin. Dashed line indicates uncertain age of the top of the Dinantian, (although it is probable that deposition is continuous through the Dinantian/Namurian boundary in the Shannon Estuary area). The age of the major phosphatization and/or erosion event(s) (shown in black) can only be constrained to pre-Chokierian in age and thus the diagram shows the range of time over which this event could have occurred. Periods of the poorly dated Pendleian/Arnsbergian shale deposition in northern Clare are shown, although again deposition could have occurred at any point (as there is no proven ammonoid horizons) so the ages given in the diagram are purely arbitrary. Diagonally shaded areas represent periods of non deposition and/or erosion.

It should be noted that much of the data is poor; this is due to a combination of poor exposure and also the fact that the biostratigraphy used is that of Riley *et al.*, (1994) and thus some absences of marine bands represent horizons unknown to the various authors at the time of writing. Thus, it may be possible that in fact lower Chokierian aged strata are present at Lough Raha and Magowna Castle.

by the presence of the pre-Chokierian *Posidonia corrugata* above the phosphorite).

The third unconformity is not marked by a phosphate lag (except possibly at Ballyshanny House) and spans at least the lower Chokierian (*Isohomoceras* chronozone) in proximal areas. Thus, the mid-Carboniferous Boundary, as shown by goniatites, is restricted to the centre of the Clare Basin.

The phosphatic lag horizon at Ballyshanny House between the *undulatum* and *prereticulatus* marine bands represents the shelf expression of a regression during *eostriolatum* times when the marine band is confined solely to the distal shelf area (Lough Raha) and probably the central basinal area.

The chronostratigraphic diagram (Figure 4.19) shows how the geographical limits of marine bands vary with time (see chapter 7 for a fuller discussion). The positions of the small amounts of *Posidonia corrugata* bearing shales are arbitrary and in fact could have occurred at any time during the Pendleian and Arnsbergian. Similarly the time-range over which the phosphatization/erosion occurred is shown is poorly dated. Many hiatuses are shown on the chronostratigraphic diagram, and some, particularly around the Foynes area are probably due to poor data. Also it should be noted that the time axis has used the standard British stratigraphy of Riley *et al.*, (1994) (see Table 2.1), so some of the marine bands will have been unknown to the various authors. It appears that the general stratigraphy throughout the Namurian of Ireland shows essentially the same succession of marine bands as Britain. Yates (1962) proved the existence of a complete succession spanning *Cravenoceras leion* to *Cravenoceratoides nititoides* marine bands on Slieve Anierin, County Leitrim. The *stellarum* horizon has been proven in the Summerhill Basin (Nevill, 1957), with the mid-Carboniferous succession being shown in this work.

The lower *beyrichianum* horizon is commonly the oldest marine band above the limestone/phosphorite at many of the localities on the shelf area. Therefore, it is not until latest Chokierian times that sea-level had recovered from lowstand of the Pendleian and Arnsbergian to allow marine band deposition on the shelf. The chronostratigraphic diagram also shows clearly how the Ross Formation is funnelled down the central axis of the basin, with gradual onlap up the sides of trough.

4.5.3 Comparisons to other Irish sections

Both Sevastopulo (1981) and Higgs (1986) have provided comprehensive comparisons of Namurian stratigraphy throughout Ireland and the reader is referred to these works for thorough accounts.

A non-sequence spanning the early Namurian is seen in many regions of Ireland. Shelford (1963) recognises a non-sequence ranging from D_2 to R_1 times (although this is rather poorly dated) with mudstones overlying a pitted Dinantian limestone surface in County Tipperary. Nevill (1956) and Higgs (1986) both recognised a mid-Namurian unconformity in the Leinster Coalfield with spongolitic cherts and shales of the Coonbeg Member (probably E_2b age) resting on the Dinantian limestone.

However, continual deposition through the Dinantian into the Pendleian is evident at a few exposures. Yates (1962) described a virtually continuous section from Slieve Anierin in County Leitrim, the faunas are very rich and comprise all of the lower Namurian horizons of Riley *et al.*, (1994). Jackson (1965) described the Kingscourt inlier, County Cavan and again at this locality there is no break between the Dinantian and the Namurian in the south of the area, although in the north of the area a break occurs such that late Arnsbergian strata rest on D_1 limestones. The Chokierian, Alportian and lower Kinderscoutian in the Kingscourt area are represented by sandstones. Nevill (1957) noted that the Summerhill Basin also showed continuous deposition from the Dinantian, with Arnsbergian beds showing a thick chert development and the Chokierian strata being represented by black shales. Unfortunately the beds spanning the mid-Carboniferous boundary are poorly exposed and unfossiliferous.

Work from scattered exposures in northern County Cork by Morton (1965) showed a similar succession to that seen in shelf areas of County Clare, with the absence of the *eostriolatum* marine band. Reconnaissance work during this study proved the area to be extremely poorly exposed.

The mid-Carboniferous boundary therefore appears to be only continuous in the centre of the Clare Basin, with many regions showing either non-sequences with younger strata resting on the Dinantian or with sand development during the Chokierian and Alportian.

4.5.4 Comparisons with the British biostratigraphy

Ramsbottom (1977) defined eleven mesothems, each eustatically driven and bounded by unconformities on cratonic (i.e. shelf) areas (Figure 4.20). Each mesothem consisted of several smaller cycles or cyclothems, each containing a single marine band, with the highest cyclothem in any mesothem having the greatest geographical extent Thus Ramsbottom proved that certain mesothems were restricted in their extent, in particular the N3 and N5 mesothems and the lowest part of N6.

The N3 cyclothem consists of the E_2c zone (*Nuculoceras nuculum*), restricted in northern England to the basin centre, with the close of the cycle seeing the demise of many of the common lower Namurian fauna (e.g., *Eumorphoceras* sp., *Nuculoceras* sp., *Cravenoceratoides* sp, *Glaphyrites* sp., *Kazarkhoceras* sp. and *Posidonia corrugata*.)

The N4 cycle comprises the Chokierian stage (H_1) and begins with a transgression of *Isohomoceras subglobosum*-bearing beds. The upper parts of the mesothem (*Homoceras beyrichianum*) is very widespread. A major regression occurs at the top of the cycle.

The N5 cycle comprising the lower and middle parts of the Alportian (*Hudsonoceras proteum* (H_2a) and *Homoceras undulatum* (H_2b)) also has limited distribution. The lowest faunal band of N6 (*Vallites eostriolatum*) has extremely limited distribution. The base of this cycle sees significant new entries among ammonoids (*Vallites* sp., *Homoceratoides, Reticuloceras* sp and *Hodsonites* sp.), bivalves (*Dunbarella rhythmica* and *Posidonia obliquata*) and conodonts.

When comparing the Irish data to those of Ramsbottom there are very clear similarities. The widespread transgression at the base of the Namurian is shown in the Clare Basin by the presence of *Cravenoceras leion* at Kilnamona. The N3 to N5 mesothems are very similar to those documented from the British succession with the N3 cycle restricted to the basin, the N4 cycle showing widespread transgression of the *beyrichianum*-containing beds, and the N6 cycle showing extremely limited distribution of the *Vallites eostriolatum* marine band, being represented, at least on the distal shelf area by a thin phosphatic lag.

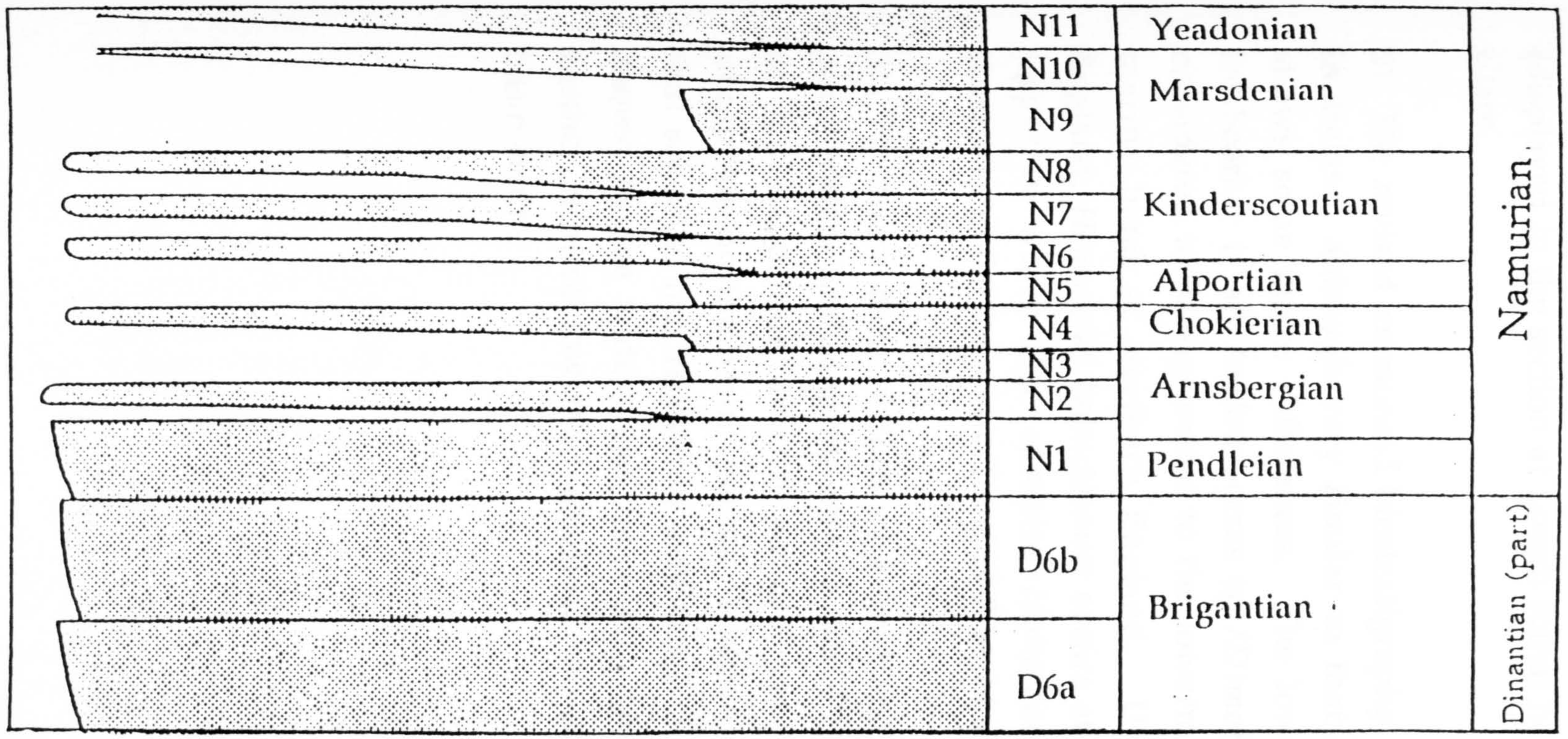

Figure 4.20 The eleven mesothems and their extent in northern Britain. From Ramsbottom (1977).

4.6 CONCLUSIONS

1) The section at Inishcorker exhibits the, as yet, most biostratigraphically complete mid-Carboniferous section in Ireland. Thus it is taken that this section displays the full biostratigraphy through the mid-Carboniferous in Ireland. The range of the H_2c^1 (*Vallites eostriolatus*) marine band (displayed in the section at Lough Raha) has also been extended to County Clare.

2) The revised ammonoid biostratigraphy through the mid-Carboniferous in Ireland, although very similar to that of northern England, however shows some minor differences. The lowest goniatite band exposed at Inishcorker is an *Anthracoceras* sp./*Dimorphoceras* sp. horizon, which is considered to be equivalent to the lowermost *Nuculoceras nuculum* (E_2c^2) marine band of northern England. Unlike occurrences in northern England, *Homoceras beyrichianum* occurs at two levels in County Clare, the upper of which also contains *Isohomoceras* sp. nov.; very probably correlates to the *I.* sp. nov. band of Riley *et al.*, 1987.

3) The Clare Basin witnessed a lowstand during the late Pendleian and Arnsbergian, confining the marine bands to the basin centre with a period of non-deposition and/or erosion resulting in the accumulation of phosphate on the basin shelves. It was not until latest Chokierian times that sea-level had recovered sufficiently to allow deposition on the shelf shown by the widespread *Homoceras beyrichianum*-bearing horizon. A further relative lowstand confined the *eostriolatum* marine band to the basin centre.

Chapter 5

THE PHOSPHORITES OF THE CLARE SHALE FORMATION

5.1 INTRODUCTION

The phosphorite present in County Clare occurs in three forms - as epigenetic replacement, pristine phosphate and reworked phosphate grains. There are two main occurrences of the phosphorite, in the Cahermacon Shale and in the Phosphorite Shale Members, with a thin lag also developed in the Goniatite Shale Member of the Clare Shale Formation. Towards the north of the area the phosphorite rests directly upon the undulose top of the Magowna Formation, but towards the basin a 3.5 m thick shale unit is developed (the Cahermacon Shale Member) between the limestone and the phosphorite (Graham *et al.*, 1986). A further thin phosphorite deposit lies directly on this basal phosphate. The two upper phosphorite horizons (exposed at Ballyshanny House) are much thinner than the basal horizon and are lenticular in shape and more impersistant. The topmost phosphorite horizon lies within the Goniatite Shale Member of the Clare Shale Formation, above the first occurrence of goniatites in the section.

The exact composition of the phosphate mineral has not been determined. E.D.S. proved that the phosphate present is in the form of calcium phosphate and thus rather than refer to any particular "species" of the phosphatic minerals the general term phosphate, apatite or calcium phosphate is used.

(N.B. For ease of use, all plates are contained within a pocket at the back of this thesis).

5.2 MAGOWNA FORMATION

The topmost horizon of the Magowna Formation appears at all outcrops to be undulose, and this eroded surface was almost certainly developed prior to phosphorite deposition. The bioturbated surface at Ballyshanny (Plate 5.1) is poorly dated with no indicative conodonts present, nor any ammonoids. However, a specimen of the ammonoid *Lyrogoniatites georgiensis*, indicative of terminal Brigantian times (P2c) was collected from the limestone directly above the bioturbated limestone at Magowna. It is not known whether this unusual horizon correlates with that at Ballyshanny House.

Petrographic investigation of samples from the top surface of the limestone show evidence of replacement by phosphate. Generally the patches of limestone replaced by phosphate are small and rounded-subrounded (0.2 mm), although some larger irregular patches up to 1.25 mm in size are present in samples from the St Catherine's Cave locality (Plates 5.2 and 5.3). The patches show brown phosphate primarily replacing the matrix of the rock with remnants of bioclasts (in particular bivalve and ostracod fragments) clearly visible. Many samples of the limestone show slight neomorphism of the micrite adjacent to the phosphatized areas.

5.3 CLARE SHALE FORMATION

5.3.1 Forms of phosphate

5.3.1.1 Cahermacon Shale Member

Phosphate occurs in the Cahermacon Shale in three forms (microbially mediated phosphatization, pellets and epigenetic replacement).

a) Microbial mediated phosphatization.

i) Associated with nodules

The nodules seen in sample ISCC1 (Plate 5.4) and also in the field at St. Catherine's Cave and Ballyshanny House measure 0.8-2 cm in size. They are rounded to ovoid in shape and occur scattered throughout the shale, which is smooth and appears somewhat contorted around the nodules. These nodules resemble large pyrite framboids but petrography shows that they are microbially-mediated phosphate grains. Microbial coatings on grains, (e.g. radiolarian tests) have been phosphatized. Similar grains have been attributed to being microbially influenced phosphatic structures by

many workers (e.g. Soudry and Lewy, 1988, 1990; Jarvis, 1992). The margins of the nodule are diffuse rather than sharp in thin section. Interstitial matrix consists of fine grained phosphate, organic matter and calcite. Pyrite is present as a coat on the phosphatized grains or as a fill in the interstitial pores.

ii) Un-associated with nodules

Much of the mass of sample BWH4b (Plates 5.5, 5.6 and 5.7) was found to contain a botryoidal/collomorphic growth form to the phosphate virtually identical to that seen in ISCC1 (see above). One area of the sample clearly shows a botryoidal microbial growth which has been phosphatized.

b) Pellets

Phosphate is also present in the shale in the form of rounded to elongate pellets (0.2-0.7 mm in size) of calcium phosphate (Plate 5.8). These are commonly associated with microbial growth (as stringers, BWH5) or nodules (ISCC1). These may be completely replaced areas of sediment or perhaps phosphatized faecal pellets.

c) Epigenetic replacement?

Samples BWH6 and BWHC6 both show curious aggregate grains comprising lath-shaped crystals up to 1 mm in size . The crystals show high relief, tabular, colourless calcium phosphate with inclusions of organic matter; rather high amounts of quartz are also present. The individual phosphate laths show replacement by a brown form of calcium phosphate, generally of the crystals closest to the margins of the aggregate grains; this appears to have taken place dendritically (Plates 5.9-12). The laths show a thin prismatic wall structure when seen under back scattered S.E.M. (Plate 5.13). The grains are set in a matrix of cubic pyrite and are rounded which may show that some reworking has occurred, although, from observations of the contact between the pyrite and the grains, it may well be possible that dissolution of the grain margins has taken place concurrent with pyrite growth, and thus the rounding of the grains is entirely a secondary feature related to diagenesis. In fact is it possible to recognise laths that are crosscut by the pyrite, and thus the rounding is entirely a result of pyrite invasion.

No similar phosphatic structures have been seen in the literature and neither Joe MacQuaker nor Ian Jarvis (pers. comm., 1994) have recognised anything similar during their studies of phosphates. The origin for these

grains is therefore enigmatic. However, megasclere sponge spicules were obtained from a nodule higher in the succession during breakdown for conodont extraction (Plate 5.14). The lower Namurian shows the development of a widely developed siliceous mudrock (comprising numerous sponge spicules) throughout Ireland (Lewarne, 1959; Sevastopulo, 1981; Graham *et al.*, 1986; Higgs, 1986). The spicules recovered from the nodule show very similar sizes to the phosphate grains, and therefore possibly may have been replaced by phosphate. Pyrite emplacement would have taken place within the voids between grains, and is possibly synchronous with silica dissolution and phosphate precipitation. The geochemical changes in the environment for these processes to occur is likely to be highly complex involving fluctuations in the oxygen levels and pH of the microenvironment.

5.3.1.2 Phosphorite Shale Member

There has been some previous investigation into the phosphorites of County Clare. Oakley (1942) noted occurrences at Roadford (Toomullin), Noughavel and Kilfenora and described the occurrence of the phosphorite as lenticular. He recognised that the phosphorites had a complex genetic history, being repeatedly reworked with two or three distinguishable generations of apatite and collophane. O'Brien (1953) found five phosphate horizons, each of which lay further south than its predecessor. This was related to a southwards migrating shoreline. O'Brien postulated a diagenetic origin for much of the phosphatic material.

Hodson (1954a) noted the variable thickness and lithology of the phosphorites over northern Clare and assigned them to the Phosphate Group, later the Phosphorite Shale of the Clare Shale Formation (Hodson and Lewarne, 1961). He stipulated that there were two types of phosphate deposits forming in two different anoxic environments. The 'pebbly' phosphates were envisaged to form on a submerged ridge whilst the more 'uniform' beds were postulated to form in an 'offshore lagoon'. Thus he described the mid-Carboniferous in Clare as being an environment of quiet lagoons separated by submerged ridges which cut off any oxygenating waters possibly rising upslope from the basin centre.

O'Connor and Pyne (1986) analysed samples and found the R.E.E. and U content (~150 p.p.m.) to be similar to those of phosphorite occurrences elsewhere.

The four phosphorite beds (A to D) assigned to the Phosphorite Shale Member show a range of component grains and complex internal stratigraphies. They range in grain size from arenites to granular gravels, with textures ranging from wackestones to grainstones. All are dominated by a high pellet and bioclast content. The beds range in thickness from 1 cm to 12 cm.

a) Grains

i) Pellets

The pellets range in size from 0.05-3.0 mm and vary from rounded to subangular (Plate 5.15). They consist of brown cryptocrystalline calcium phosphate and may contain inclusions (endogangue) comprising pyrite or calcitic debris. The pyrite is usually in the form of very fine grained disseminated pyrite and/or as thin coating around the grains. The pellets containing calcite laths are generally more irregular in shape. Some of the pellets, especially those associated with pyrite may show a faint internal structure reminiscent of that seen in the microbially influenced phosphate (Plate 5.16 and 5.17).

Thus, it is supposed that there may be two different origins for these grains, phosphatized faecal pellets (with or without calcite laths) and pellets formed by a reworking of a precursor phosphate, including those formed by phosphatization of bacterial elements and from epigenetically replaced limestone.

ii) Bioclasts

Many of the samples contain conodonts; these show selective winnowing, and consist predominantly of robust platform elements (Plates 5.18, 5.19 and 5.20). Bone debris is present in varying amounts, often replaced in part by pyrite (Plates 5.19, 5.20 and 5.21). Phosphatized radiolarian tests (Plate 5.22) also occur as do phosphatized or chertified spines, possibly sponge spicules. Generally the bioclasts show low-moderate amounts of abrasion.

iii) Lithoclasts

There are two main phosphatic lithoclasts occurring within the phosphorite, composite grains and grains showing a botryoidal/collomorphic growth form.

Composite grains are present in a few samples; they show reworking from a previous phosphorite. Often, (Plates 5.23 and 5.24) they show subrounded -angular clasts of phosphorite set in matrix. The grains are commonly rimmed by pyrite. Clasts seen in BWH8 show a precursor phosphorite containing many grains of pyrite. Samples SBWP and BDB4 show a composite grain, 3 mm in size, containing 0.5 mm rounded, calcite-lath containing pellets of a slightly darker calcium phosphate set in a lighter brown matrix also containing laths (Plates 5.25 and 5.26). The origin is assumed to be epigenetic replacement of a pelleted limestone (c.f. ISCC1)

Grains exhibiting a botryoidal growth form are subrounded-subangular and vary in size from 1 - 7 mm (Plates 5.27 and 5.28). They are light brown in colour in plane polarised light showing clear bioclasts (phosphatized radiolaria and conodonts). Pyrite cubes may be present . Under crossed nicols a coarse microcrystalline calcium phosphate is seen growing collomorphically around the clast. The phosphate growth appears to be highly influenced by the bioclasts and from comparison with the phosphates formed in the shale is probably also influenced by microbial coatings on grains. Similar phosphate grains have been attributed to replacement of microbial structures (e.g. Soudry and Lewy, 1988, 1990; Jarvis, 1992).

iv) Other lithoclasts

Pyrite is present as detrital grains and is usually rounded-subrounded. Size varies from 0.25-0.75 mm. Quartz is also present in most samples and occurs as grains up to 0.75 mm in size. Single crystal and composite grains occur. A mixed source (igneous, recrystallized, stretched and schistose metamorphic) is evidenced by both straight and varying degrees of undulose extinction.

b) Matrix (exogangue)

The exogangue comprises cryptocrystalline phosphate, fine grained quartz and pyrite. Growth of the cubes of pyrite have taken place prior to the matrix emplacement. Samples taken from St. Brendan's Well show a coarse equant calcite cement.

c) Authigenic growth

Sample BWH7 shows actual phosphate growth within the lag (Plates 5.29 and 5.30). Bacterial growth attached to pyrite grains was then phosphatized prior to matrix emplacement. The matrix of this sample also contains

phosphatized radiolarian test and again the collomorphic growth of phosphate associated with the radiolaria is similar to the bacterial influenced growth seen in previous grains.

Sample SB2 taken from 1m above the phosphate at St Brendan's Well shows an ovoid nodule 1.5cm in size. The centre of this nodule also shows cubic pyrite used as a substrate for a bacterial colony.

5.3.1.3 Goniatite Shale Member

A thin lag (horizon E) occurs in the this Member between the *undulatum* and *prereticulatus* marine bands. The component grains are very similar to those seen in the underlying phosphorites.

5.3.2 Spatial variations of the phosphorites.

As previously mentioned there are five phosphorite horizons lying above the Magowna Limestone Formation; these can be correlated by their component grains and thicknesses.

Phosphorite horizon A

This is the lowest unit present in the area. This is shown by samples BDB4, ISC3, SBWP and BWH7 and measures 6, 6, 5-12 and 11 cm in thickness at the respective localities and shows consistent fining up (Plate 5.31). The base of the lag is bulbous or erosive in nature. The top of the lag shows some vertical burrowing. Grains characteristic of this horizon are 'botryoidal' grains, composite grains and pellets containing calcite debris. Rounding in the grains appears to increase northwards. The diagenetic history is varied between outcrops. Isopachous calcium phosphate is seen in samples towards the north of the Clare Basin. Pyrite rims are present around some grains. Cubic pyrite is ubiquitous in the matrix. A dissolution event is fairly common in the phosphorite prior to a later pyrite, phosphate or quartz fill. Calcite cement is present in samples taken from St. Brendan's Well. Authigenic growth of phosphate associated with a bacterial mat is evident in a sample from St. Catherine's Well. (ISC3).

Phosphorite Horizon B

This unit lies directly on top of horizon A, but is not developed at the Ballydonohoe bridge locality. Thickness is fairly constant at 3 or 4 cm. The base of the unit is planar or erosive in a proximal area, and the top again is relatively planar. Grains present on the top surface of the phosphate show that polishing and truncation occurred after phosphorite deposition. Common grains in the deposit comprise 'botryoidal' grains and pellets containing calcite debris. Again diagenetic history is varied although commonly pyrite rims to grains are present prior to a cubic pyrite growth. Some dissolution of bioclasts or grains has taken place prior to a later pore fill of pyrite, phosphate or quartz. There is some calcite cement present in horizon B at St. Brendan's Well.

Phosphorite Horizon C

This horizon is developed at Ballyshanny House (BWH9) where it occurs as a 2 cm lag. Rounded clasts of a 'botryoidal' origin are evident as are copious conodonts. The shale overlying the phosphate shows horizontal burrowing.

Phosphorite Horizon D

A 2 cm phosphate lag occurs only at Ballyshanny house (BWH12). Clasts include pellets, 'botryoidal' clasts and bioclasts. Conodonts are present showing isopachous phosphate cement (Plate 5.32). Cubic pyrite growth predated matrix emplacement. Some dissolution of presumably calcitic debris took place prior to a late stage microcrystalline cement. Large amounts of pyrite are present at this horizon and in reflected light is seen to replace phosphatic debris such as conodonts (possibly, these are dissolution and void fill events by pyrite). Burrowing is evident in the phosphate horizon and is filled with an acicular pyrite.

Phosphorite Horizon E

The uppermost phosphatic lag occurs only at Ballyshanny House and is 1 cm thick. It consists of subangular pellets. Bioclasts are very common and comprise copious amounts of conodonts showing isopachous phosphate cement (Plate 5.33). Pyrite rimmed grains and cubic pyrite grains are present. Some small amounts of microcrystalline phosphate growth has taken place in the voids.

5.4 DISCUSSION ON GENERAL PHOSPHATE FORMATION

5.4.1 Concentration of phosphorus, calcium, fluorine and carbonate ions

For phosphate (in the form of carbonate fluorapatite) to form, there needs to be a source of the component ions in the environment. The marine environment is supplied with phosphate from weathering products carried in solution by rivers. There is also an oceanic supply with phosphate ions carried in solution or suspension. Localised increases in the concentration of phosphorus in the sediment are provided by the biomass of marine organisms such as algae, phytoplankton or fish debris or from the presence of phosphate-bearing particulate iron (or manganese) (Föllmi, 1990). Accumulation of organic matter will occur in an anoxic environment where the phosphates present in the biomass will not be liberated by oxidation. Released phosphate from the oxic decomposition of organic matter absorbs on iron oxyhydroxides, carbonates and clay minerals, (Krom and Berner, 1980, 1981; Jarvis, 1992). Phosphorus is released from the reduction of this particulate iron (Fe oxyhydroxides converting to FeS and FeS_2) in the anoxic environment. Glenn and Arthur (1990) and Föllmi, (1990) also suggested a mechanism involving this PO_4^{3-} 'pump and shuttle' (Schaffer, 1986). In their model particulate iron and manganese oxyhydroxides settle through the water column and scavenge PO_4^{3-}. Beneath the redox boundary the hydroxides are dissolved and release their PO_4^{3-}, the reduced metal cations then diffuse back into the bottom waters and become re-oxidised (and thus prone to absorbing more phosphate). Repetitive cycling may result. Föllmi (1990) mentioned that bioturbation is necessary to irrigate the sediment. He emphasised that the release of PO_4^{3-} from decaying organic matter is possibly a minor influence on phosphogenesis since phosphogenesis occurs prior to putrefaction of microbial colonies and other organisms.

It has also been suggested that alkaline volcanism may provide phosphorus fluorides to the environment (e.g., Baturin, 1988).

It has been shown by numerous workers (e.g., Nathan, 1990), that organic matter trapped in phosphate grains is primarily humic acids. Humic acids form early in diagenesis (after the formation of fulvic acids) near the sediment water interface by condensation of monomers produced by enzymic degradation of organic matter. Phosphorus itself is liberated from organic matter during the transition from fulvic acids to humic acids

(Nissenbaum, 1979). The humic acids are unstable and readily evolve by polymerisation into kerogen. In a highly reducing environment the humic acid stage may be absent, but if the environment is too oxidising the organic matter will be lost (Slansky, 1986). Thus it can be assumed that the phosphate particles form in regions where the humic acids are most plentiful and stable - the slightly reducing to moderately oxidising environment associated with the oxygen minimum layer (pycnocline). In this environment drastic changes in the solubility of phosphate will occur and there will be a supply of phosphate from both upward diffusing porewater and from within the water column (Arthur and Jenkyns, 1981). Many workers (e.g. Arthur and Jenkyns, 1981; Loughman; 1984, Föllmi, 1990) have recognised, from facies relationships in the geological record, that the site of phosphate authigenesis is often associated with deposition in low or fluctuating oxygen conditions in the top few cms of the sediment, adjacent to the paleopycnocline. Loughman (1984) also noted an absence of pyrite and light $\partial^{13}C$ values (which he attributed to the incorporation of CO_2 produced by bacterial oxidation) which may also testify to a moderately oxidising environment. But although a source for phosphate may be available there are certain other environmental parameters that need to be satisfied before apatite precipitation takes place.

Martens and Harris (1970) showed that Mg^{2+} ions inhibit apatite precipitation by the blocking of Ca^{2+} sites in the crystal lattice. With a pH of 7.5-8 apatite precipitation could only take place with a Ca/Mg ratio ≥5.2, (below this an amorphous magnesian phosphate is formed); seawater has a ratio of 0.2. The Ca/Mg ratio may be elevated to allow phosphate formation by the high organic content of the mud (e.g. chlorophyta have a ratio >5.2), the formation of Mg-rich minerals (such as montmorillonite or dolomite) or the liberation of NH_3 during bacterial oxidation of organic matter (Curtis, 1980; Misi and Kyle, 1994). Gulbrandsen *et al.*, (1984) later showed that crystallisation of carbonate-fluorapatites is time dependant, and that the effects of Mg inhibition are overcome, with the amorphous phosphate recrystallising to crystalline magnesian phosphate and then carbonate-fluorapatite over 10-100 years. Thus Mg ion inhibition may not be as important (especially when applied to the geological record) as initially thought.

5.4.2 Formation of sedimentary apatites

1) Biogenesis

Calcium phosphate is concentrated in the skeletons of fish and other vertebrates, conodonts and shells of some inarticulate brachiopods.

2) Direct precipitation

It was once thought (Kazakov, 1939) that direct chemical precipitation took place when cold supersaturated waters rose from depth and met warmer waters with a higher pH value and lower CO_2 partial pressure. Workers such as Gulbrandsen (1969) and Martens and Harris (1970) have now discredited this idea with the findings that the pH in these warmer waters would stimulate $CaCO_3$ precipitation and that Mg ions inhibit apatite precipitation below a certain Ca/Mg ratio.

There appear to be two methods of phosphatization, either by the means of an intermediate stage involving gels or by the direct growth of apatite. Baturin (1974) recognised various stages of growth in nodules from the southern African margin and postulated the growth of gels of calcium phosphate from saturated interstitial solution, which then harden and dehydrate. Burnett (1977) noticed direct precipitation of small rosettes of apatite crystals in Recent deposits off the Peruvian and Chile coast. Martens and Harris (1970) showed that the gel forms at lower Ca/Mg ratios than direct apatite precipitation. The process of direct precipitation probably starts when a suitable nucleation site (calcitic debris, radiolaria, bone debris, quartz, feldspar or dolomite crystals) acts as a catalyst to apatite precipitation. This diversity of 'seed' surfaces may be explained by the coating of the surface by humic acids (Slansky, 1986). Lateral flow of ions will continue apatite growth.

3) Epigenesis.

Ames (1959) showed that a very low concentration of phosphate may be enough to trigger replacement of carbonate. The need for a high Ca/Mg ratio may be obverted if the interstitial pore waters is different from those of the marine environment; also calcite passes into solution prior to crystallisation of apatite. Jarvis (1992) suggested that a low pH is necessary for carbonate dissolution and noted that a lowering of pH could be caused by hydrogen ion production caused by oxic decomposition of organic matter, oxidation of H_2S by sulphide-oxidising bacteria or ion production associated with simultaneous iron and sulphate reduction during pyrite formation.

4) Microbial mediation.

Bacteria are very commonly associated with recent phosphate deposits and have been noted from many ancient phosphate deposits (e.g. Riggs, 1979; Soudry and Champetier 1983; Southgate, 1986; Abed and Al-Agha, 1989; Lewy, 1990; Jarvis, 1992). Lamboy (1990), also concluding that a major role is played by bacteria in the formation of phosphatic deposits, noted two types of phosphatized microbial remains - lamellar crusts and dispersed ovoid bacteria and botryoidal communities - from the Cretaceous chalks of France. Williams and Reimers (1983) suggested that the sulphur-oxidising bacteria (*Beggiatoa* and *Thioploca*) control the growth of phosphatic laminae and nodules in the Miocene Monterey Formation

5.4.3 Formation of a phosphorite deposit

1) Reworking.

Reworking is mainly mechanical by the transport of a pre-existing deposit with the winnowing of clays and other fine particles (e.g. Jarvis,1980; Baird, Brett and Kirchgasser, 1988; Baird and Brett 1986, 1991; Föllmi, 1990.) Repeated episodes of reworking, burial, phosphogenesis and re-exposure have been termed Baturin Cycles by Mullins and Rasch (1985). Biological reworking may also take place by phospho-micritization by Schizomycophyta or by boring of grains (Jarvis, 1980; Soudry, 1979 in Slansky (1986).

Baird and Brett (1986), Slansky (1986), Baird, Brett and Kirchgasser, (1988) and Glenn and Arthur (1990) noted that during transgression, internal waves may concentrate phosphatic deposits (Figure 5.1). This has led to the development of the Baird and Brett model internal wave erosion model. In this scenario, a concentration of pyrite and phosphate lag occurs due to erosion associated with internal waves along the pycnocline. As the waves propagate upslope and break, the energy is dissipated and thus erosion is concentrated on the outer slope (Taylor, 1993). Erosion would have taken place due to abrasion and carbonate dissolution (under conditions of carbonate undersaturation and/or low pH). Seafloor erosion would therefore be associated with the onset of anaerobic conditions and this would be reflected in the rock record with the phosphatic deposit overlying shallow water deposits with black shales developed above it.

Baturin (1971), and many other workers, (e.g. Jarvis, 1980; Loughman, 1984; Glenn and Arthur, 1990), attributed the growth of phosphate nodules to periods of transgressions with the concentration of the nodules during

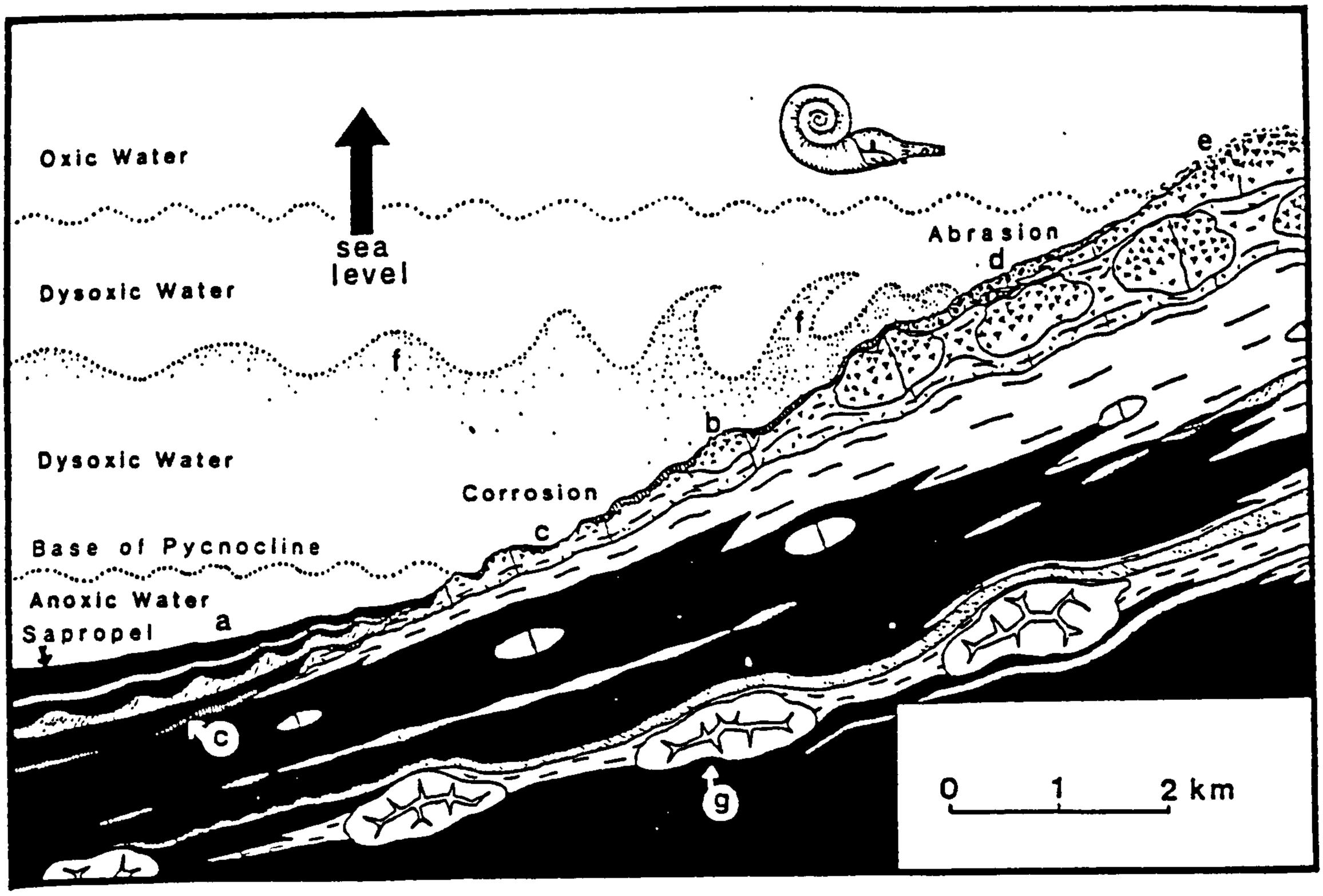

Figure 5.1 The Baird and Brett erosion model. The diagram shows the process of mechanical erosion and corrosion of concretionary carbonate deposits during a transgression event. Internal wave-impingement on the palaeoslope is believed to have been a significant factor in the submarine erosion process. These waves generate turbulence on the slope, removing fines, and exposing carbonate material for corrosional attack in dysoxic water. Residual early diagenetic pyrite and phosphatic debris is concentrated as a tractional placer in lenses. Upslope migration of the pycnocline produces a widespread, gently-inclined unconformity which is progressively buried by overlapping black muds and silts as water deepens. Key: (a) black muds; (b) concretionary wackestone truncated by corrosion; (c) reworked detrital pyrite (corrosion residue); (d) packstone veneer of mixed pyrite-calcareous debris; (e) living auloporid thicket; (f) internal wave-train impinging palaeoslope; (g) septarian concretions marking stratigraphic position of similar cycle developed further upslope. From Baird and Brett (1991).

regression when they were affected by wave action (either storm waves or internal waves as the pycnocline retreats downslope). Miller *et al.*, (1988) and Miller (1991) have recognised scour features in mudrocks from episodic basinward currents related to eustatic fall in the Devonian of New York State. Again, he attributed these erosive currents as storm driven in origin.

Table 5.1. Differences between the transgressive and regressive models in a basinal setting

	Transgressive	Regressive
Strata beneath phosphorite	Grey/bioturbated shales	Black shales
Strata overlying phosphorite	Black shales	Grey/bioturbated shales
Truncation of underlying units	Increases downslope	Increases upslope

2) Epigenesis of pre-existing non phosphatic particles
Substitution by calcium phosphate is commonly associated with calcareous debris.

3) Cavity fill
The micro-environments provided by cavities may provide a local chemistry to facilitate phosphate formation by epigenesis or direct precipitation.

4) Phosphatization of faecal pellets.

5) Direct precipitation
This will occur when a suitable surface acts as a catalyst to apatite precipitation.

5.4.4 Paleoenvironment and rates of phosphate sedimentation .

Estimates for the rate of phosphate sedimentation range from 100 000 to 50 million years per metre of phosphorite. Baturin (1970), from estimates of phytoplankton productivity calculated a maximum rate of accumulation of 100 000 to 150 000 years per metre of deposit. Föllmi (1990) recognised accumulation rates of 5-50 million years per metre of deposit from the Helvetic mid-Cretaceous phosphorite deposits. Slansky (1986) suggested that the slow rates of phosphorite accumulation would require condensed sedimentation and a high degree of stability in the palaeogeography of the

basin and its supply of organic matter (allowing slow burial of the organic matter). He also noted that the lack of supply of terrigenous matter could result from a dry climate, flat land or sediment bypass.

Many workers (e.g. Jarvis, 1980; Vail, 1987; Föllmi, 1990) noted that phosphogenesis correlates with maximum flooding surfaces and condensation. Riggs *et al.*, (1985) demonstrated, from Miocene deposits on the Atlantic Coast of the U.S.A., that phosphogenesis reached a maximum on the maximum portion of the rising sea-level. They also noted that the duration of the highstand is an important factor in the controlling the amount of phosphate concentrated in the environment. Transgressive periods may be favourable to phosphorite formation in a number of ways, as well as limiting sediment supply by the reduction in relief and increasing the area of the highly fertile continental shelf available for the formation of phosphorite deposits, there will be an increase in the thickness of the oxygen minimum layer. Thus, there will be deposition and preservation of phosphate-containing organic rich black shales. As the phosphate deposits form near the pycnocline they will be associated with black shales forming beneath the pycnocline, and more oxygenated and possibly bioturbated deposits forming above it.

Arthur and Jenkyns (1981) also correlated phosphorite accumulation with warm climates which would result in increased weathering (and therefore release of phosphorus), and also the development of widespread oxygen-depleted waters (due to decreased rates of ocean circulation and low levels of oxygen solubility). Misi and Kyle (1994), following the phosphatization model of Cook and Shergold (1986), suggested that phosphatization events could follow a major period of glaciation: a major expansion of organic productivity would result from the large volume of nutrient rich waters following the glacial period.

5.5 MODEL FOR THE FORMATION OF THE PHOSPHORITE DEPOSITS OF COUNTY CLARE

5.5.1 Types of phosphate sediment

a) Samples from the top surface of the limestone show evidence of epigenetic replacement by phosphate.

b) Pristine phosphates are present in the form of nodules, ?epigenetically replaced sponge spicules, or mats. These are particularly prevalent in the Cahermacon Shale Member and above phosphorite horizons A and B.

c) Reworked phosphates show a wide variety of phosphatic clasts with different generations of phosphatic cement. This suggests repetitive cycles of burial, phosphogenesis, erosion and reworking.

5.5.2 Spatial and temporal trends associated with the phosphorite deposits.

Three different sedimentary regimes associated with the phosphorite deposits can be recognised in the Clare Basin.

a) Fine grained , dark, laminated shales. These shales together with small calcareous nodules are present across the entire outcrop of the Clare Shale Formation and they are the only facies present in the centre of the basin. They are predominantly unfossiliferous but are punctuated by thin fossiliferous horizons (marine bands) dominated by nektonic fauna (ammonoids and orthocone nautiloids). Both in the marine bands and also at other discrete levels benthic bivalves are present. These horizons probably represent short lived colonization events by an opportunistic species in an otherwise anoxic bottom environment. This facies appears to be the normal or background sedimentation between phosphatic events. It is envisaged to form predominantly beneath an anoxic lower water column.

b) Fine grained, dark grey, often convoluted shales with nodules, mats and grains of phosphate. As previously explained authigenic phosphate formation occurs in fluctuating oxygen conditions associated with the pycnocline with precipitation of the phosphate occurring within the top few cms of the sediment. This facies occurs on the distal shelf, and not in the basin centre itself. It only occurs in the lower part of the Clare Shale Formation.

c) The third sedimentary regime comprises reworked phosphates. The lowest and thickest horizon (A) shows bioturbation in which burrows are predominantly vertical. This shows that the oxygen conditions were highly fluctuating and, at least at one point, the oxic/anoxic interface retreated into the sediment.

5.5.3 Model for the genesis of the phosphorite deposits of the Clare Shale Formation

The marine bands present in the Clare Shale Formation represent chronostratigraphic horizons providing correlation throughout the basin, although unfortunately, no marine bands are present within the Cahermacon Shale or Phosphorite Members. However, on a large scale northwards onlap of the Dinantian Limestone by the Clare Shale Formation is evident. The Clare Basin appears to have had only limited connections to the open sea (Ziegler, 1982) and appears to have been a stagnant backwater of the main northern European Basins. The lack of visible bioturbation (outside phosphorite horizons) and epibenthos indicates anaerobic or at the best quasi-anaerobic conditions in the sediment (see section 7.3.1). Sedimentation rate throughout the basin is low. Deposition in the basin centre was continuous from the Dinantian, whilst in the north of the basin a hiatus developed either through subaerial exposure or by submarine erosion and sediment bypass. No evidence of vadose or phreatic cements is present in the topmost limestone (although this level may have conceivably been eroded).

The top of the Dinantian limestone is poorly dated and it is unknown whether the development of the undulose topography (developed prior to Clare Shale deposition in the distal shelf - at Ballyshanny House) took place during the lower Namurian or late Brigantian.

Epigenetic replacement of the limestone surface took place during contact with transgressive phosphate-rich waters during the Pendleian or Arnsbergian. Local micro-environments in the lithified limestone were susceptible to phosphatization by local enrichments in Ca rather than Mg ions. Carbonate dissolution prior to apatite precipitation may have been aided by a lowering of pH caused by hydrogen ion production related to oxic decomposition of organic matter, oxidation of H_2S by sulphide-oxidising bacteria or ion production associated with simultaneous iron and sulphate reduction during pyrite formation.

There were probably four sources for the phosphate in the environment.

a) Oxic decay of organic matter.
b) Phosphorous released from P-bearing particulate iron compounds (ferric oxyhydroxides) during reduction.

c) Fluvial input from weathered hinterlands.
d) Volcanism occurring at the south-eastern limits of the basin (Strogen, 1988) may provide further phosphorous to the environment.

Flooding of the shelf led to a shallow hemipelagic environment with low sedimentation rates. The low sediment influx is probably a function of proximal trapping of the sediment, sediment bypass down the deep axis of the Clare Basin and low sediment input from the possible limestone bedrock to the north. Expansion of the oxygen minimum zone up onto the shelf led to fluctuating oxygen levels in the sediment, favourable to phosphate authigenesis in the organic-rich Cahermacon Shale Member

Phosphate growth in the Cahermacon Shale appears to have been bacterially influenced both within the nodules and as separate regions in the sediment. Bacteria have been recognised in modern environments (e.g. Rossenberg and Diaz, 1993; Larkin, *et al.*, 1994; Fossing *et al.*, 1995) and are associated with low oxygen environments. It is possible that sulphur-reducing bacterial mats (*Beggiatoa* and *Thioploca*), present at the sediment water interface in the stagnant conditions of the Clare Basin exert a major influence on phosphate authigenesis. Larkin *et al.*, (1994) has shown that the diameter of the bacterial filaments is up to 500µm; this compares well with the size of filaments seen in thin section. Pyrite formation in the sediment would occur post-phosphate growth in more anoxic conditions. Further repeated transgressive rises led to establishment of zones of phosphate authigenesis further away from the basin centre. Regressive periods would lead to the migration of the O_2 minimum layer resulting in the lowering of the oxic/anoxic boundary to the sediment surface or just below it. Burrowing such as seen at Ballyshanny House (BWH5) resulted, however, no colonisation of an exaerobic bivalve facies is evident, possibly due to removal during erosional emplacement of the overlying phosphate pelleted shale.

There is no sedimentary record preserved below phosphorite horizon A to the north of the area, but it seems probable that one of two different scenarios could have operated in the region. Firstly erosion by storm or internal waves associated with the pycnocline was taking place during decreased rate of sedimentation, alternatively authigenic phosphate growth took place in shale that was later removed during erosion associated with the deposition of phosphorite A.

The major phosphorite of phosphorite horizon A is associated with an erosional base and grading up of clasts. Clasts show a slight increase in rounding proximally pointing to more prolonged winnowing. Undoubtedly the accumulation of this deposit took place over a great period of time and reworked many older, lithified deposits together with pyrite clasts exhumed from the underlying shales. However, two different mechanisms could be invoked for the formation of the phosphorite deposit with the concentration of resistant phosphate and the winnowing of fines by both storm waves and the impingement of the pycnocline (and internal waves) associated with a drop in sea level, or alternatively by shelf erosion during transgression as the pycnocline moved upslope.

Various lines of evidence suggest that the deposit was formed during a relative fall in sea level with the smearing out of a previously formed deposit:-

a) Increase in the phosphorite matrix occurs distally. This probably represents offshore winnowing of fines further out into the basin.

b) Botryoidal type pellets are quite rare distally and so it is assumed that erosion was not quite as strong in this area to exhume the precursor nodules from the underlying shale. These grains are possibly therefore only eroded out of the more proximal deposits and not reworked far out into the basin.

c) Rare burrowing in the top of the phosphorite shows oxic or dysoxic conditions were present in the top of the sediment (Plate 5.34). Polished blocks of phosphorite A commonly show the preservation of a 'pyrite front', which appears to bioturbated in the top 4 cm of the rock. Biorturbation could pre- or post-date pyritization.

d) Clasts showing calcite laths are very similar to patches of epigenetic phosphatization seen forming in the limestone. The clasts occur in phosphorite deposits all over the shelf suggesting that they must be originally derived from a landward source. There would not be a source for them if they were derived from accumulation and reworking by transgressive internal waves (as the limestone is overlain by shale in the distal area). Similarly there is no source for composite grains.

e) Fluctuating oxygen levels in the sediment are shown by the growth of pyrite in the matrix and also by the authigenic microbially influenced growth of phosphate.

f) Proximal deposits show a enrichment in Th containing heavy minerals (47.3 ppm.) compared to 11.2 ppm in distal environments. Additionally authigenic U values are higher in the more distal environment reflecting lower oxygen conditions and a greater environmental stability. This is an indication of prolonged winnowing of fines and concentration of heavy minerals in the more proximal shelf area.

Thus it is envisaged that the phosphorite A horizon formed during a prolonged regressive interlude with offshore transportation of a pre-existing proximally deposited phosphorite. Oxygen levels fluctuated but were generally low (shown by pyrite formation within the sediment and microbially influenced phosphate authigenesis), with bioturbation indicating the establishment of dysoxia in the sediment at times. Some slight increase in grain size at the top of the deposit may indicate amalgamation of reworking events or reactivation of the reworking mechanism. Conodont and bone debris present is not highly abraded and is interpreted as stratigraphic rather than sedimentary accumulation of these bioclasts, i.e., they are not reworked from deposits (except when included in composite grains). Winnowing of the more fragile conodont elements has taken place. This could indicate that the rather rounded phosphate grains have gained their shape in a more high energy (proximal) environment before being transported out onto the more distal shelves of the basin. The more angular grains seen distally have been moved out of the zone of abrasion. It is thus suggested that the regressive retreat of the pycnocline and associated internal waves impinging on the shelf and also storm waves led to the reworking and accumulation of phosphorite A. The shallowly dipping shelves of the lower Namurian could have been easily eroded by this mechanism and chemical dissolution in the poorly oxic waters would also explain the absence of a limestone lag. Prolonged erosion seen in the north of the area would have occurred if the pycnocline was static at this level for a period of time in the absence of sediment supply. Relatively deep water conditions were still present over the shelf, particularly in the more distal regions, where only infrequent periods of agitation of the phosphate clasts induced stagnant conditions within the sediment. Background 'dropout' of the bioclasts in the low energy conditions explains the observed low abrasion seen in the condensed deposits. Sedimentation rate was

effectively zero for a long period of time during the accumulation of this deposit. It could be expected that increased sedimentation rates would result during a regression, but it is likely that sediment bypass was a major factor at this time. Little sediment was derived from the north where presumably limestone dominated landscapes were in evidence, the siliclastics derived from the hinterlands to the west were confined to the basin centre.

Phosphorite horizon B contains much less matrix and the grains are relatively well rounded over the entire shelf area, although this horizon is absent to the north of the area. The clasts present in his horizon are similar to horizon A and indicate reworking from a precursor phosphorite deposit, although again conodont debris shows low abrasion and probably represent prolonged periods of stratigraphic bioclast accumulation with sporadic intervals of higher energy reworking. No bioturbation is evident in the horizon, and the horizon is commonly overlain by phosphatic shale. The low amounts of matrix in this horizon could result from increased environmental energy or reworking of a mature phosphorite. The presence of relatively lowly abraded bioclast suggest that a low energy environmental regime was dominant, and thus it seems likely that horizon B formed by reworking of a mature phosphorite with further concentration of phosphate grains and winnowing of fines. A distal source for the phosphorite is unlikely due to the nature of the grains, and also Horizon A does not show an erosive top. It is conceivable however that the horizon A in a more proximal position could be reworked, the decreased thickness of the A horizon to the very north of the area may testify to this model. Thus horizon B is likely to have formed during regression with prolonged reworking in a proximal area and deposition with minor amounts of erosion removing any transgressive shales in the more distal area of the shelf.

Following the regression that formed horizon B the oxygen minimum zone migrated upslope and phosphate authigenesis occurred over the shelf.

The third phosphorite horizon (horizon C) was only evident at the Ballyshanny House locale during this study. Clasts comprise reworked pellets and conodonts. This lag is interpreted as forming due to regressive reworking in a similar way to that envisaged for the formation of lag A, as the shale lying directly over the phosphatic lag is bioturbated, showing an increase in the oxygen level in the sediment, presumably brought about as the oxic/anoxic boundary migrated downslope.

Phosphorite horizon D occurs between the last Arnsbergian and the first Chokierian faunas at Ballyshanny House. It is very similar in nature to horizon C. Horizon D also shows bioturbation. It could be speculated that this lag was formed due to regressive reworking associated with a fall in sea-level at the base of the Chokierian, together with stratigraphic accumulation related to reduced sedimentation rates during this time (see chapter 6) as the phosphorite comprises a condensed assemblage of conodonts and pellets presumably concentrated due to low sedimentation rates. During this study phosphorite D was only recognised at Ballyshanny House although Graham *et al*,(1986) recognised this and horizon C at St. Brendan's Well, thus showing these phosphate accumulation events are a shelf wide phenomena.

Phosphorite horizon E is probably the shelf expression of the lowstand associated with the *eostriolatum* marine band, which is confined to the basin centre. Very low sedimentation rates occurred during *eostriolatum* times. Again, the mechanism for the accumulation is equivocal. It is likely that the extremely depressed sedimentation rate is a major factor in the accumulation of phosphorite at this horizon. Four marine bands occur in the space of 1 m and therefore testifies to the low sedimentation rate at this interval.

5.6 CONCLUSIONS

1) Authigenic phosphate is present in four forms in the topmost Magowna Formation and Clare Shale Formation.

a) Epigenetic replacement of the limestone.

b) Microbial mediated phosphate nodules and random areas of sediment.

c) Pellets.

d) Possible epigenetic replacement of sponge spicules (?).

2) Flooding of the shelf led to a shallow hemipelagic environment with low sedimentation rates. The low sediment influx is probably a function of proximal trapping of the sediment, sediment bypass down the deep axis of the Clare Basin and low sediment input from the limestone highlands to the north. Expansion of the oxygen minimum zone up onto the shelf led to fluctuating oxygen levels in the sediment, favourable to phosphate authigenesis in the organic-rich Cahermacon Shale Member

3) Up to five phosphatic lag horizons are evident on the northern shelf of the Clare Basin. The lowermost two horizons show clasts pertaining to a precursor phosphorite horizon and are interpreted as smearing out of a previous lag onto the shelf area. The mechanism for their formation is interpreted as reworking by internal waves associated with the impingement of the pycnocline on the shelf as it moves downslope during regression. Additionally reworking may have been facilitated by bringing the sediment surface to within storm wave base. Evidence for regressive rather than transgressive accumulation is shown by the presence of clasts derived from the underlying limestone (which cannot be derived from the basin centre) and also bioturbation above the phosphorite (indicating an increase in oxygen levels).

The two thin lags (C and D) do not show reworking of a prior phosphorite horizon and solely accumulation and reworking of shale derived phosphatic material such as bioclast and nodules, it is likely therefore that erosion and time available for accumulation at this point was not as prolonged as for horizon A. Low sedimentation rates may be a major factor in the accumulation of these two thin horizons. Both lags are interpreted to have formed during regression. Horizon D separates Arnsbergian and Chokierian faunas and may represent the shelf expression of the mid-Carboniferous lowstand.

A thin lag between the *undulatum* and *prereticulatus* marine bands represent the shelf expression of the restricted *eostriolatum* marine band.

4) The overall model for the Clare Basin phosphorite deposition envisages a major transgression during the early Namurian resulting in the rise of the oxygen minimum zone upslope. This leads to phosphate formation across the shelf. The top of the Magowna Formation is bathed in phosphate rich waters and local replacement occurs. A major regression at some time during the Pendleian or Arnsbergian led to the development of a phosphatic lag that shows prolonged reworking and smearing out a lithified phosphorite (presumably deposited in a more proximal environment) out across the shelf. Reworking is probably by deep storm waves together with internal waves associated with the drop of the pycnocline downslope. In the proximal areas erosion was strong and the lag rests directly on the limestone, having removed any shale deposited in the north, in the more distal area the lag rests upon the phosphatic shale. A subsequent later

regression removed any transgressive shales and deposited a thin further lag.

Following a transgression the oxygen minimum zone was again perched high up on the shelves of the Clare Basin and led to phosphate growth in a more proximal area. Two further lag accumulations were formed (the upper of which separates Arnsbergian from Chokierian faunas), these were possibly associated with regressions, although it is likely that extremely low sedimentation rates were a factor in their accumulation. Authigenic phosphate growth was terminated during Chokierian times.

A further thin lag during *eostriolatum* times represents the regression associated with this interval.

Chapter 6

GEOCHEMICAL PALAEOENVIRONMENTAL ANALYSIS

6.1 INTRODUCTION

Various geochemical techniques have been applied to samples from the section at Inishcorker to determine palaeoenvironmental changes across the mid-Carboniferous boundary. The section displays black and dark grey shales with distinct marine horizons. Additionally the use of a portable gamma-ray spectrometer has been applied to selected sections (of those described in chapter 4).

Many of the geochemical methods for determining palaeoenvironment result from the analyses and correlations of organic carbon with pyrite and its component ions. To understand the interrelationships in the C-S-Fe system, the formation, diagenesis and inorganic geochemistry of black shales are briefly discussed, together with a background to the use of U, Th and K radioisotopes in palaeoenvironmental analysis.

6.2 BLACK SHALE FORMATION

For a thorough review of black shale sedimentology and geochemistry the reader is referred to Wignall (1994) and Arthur and Sagemann (1994).

Tyson (1987) defined black shales as 'dark coloured, fine grained mudrocks having the sedimentological, palaeoecological and geochemical characteristics associated with deposition where oxygen-deficient or oxygen-free bottom conditions prevailed at the sediment-water interface'.

Some of the most important controls on black shale formation are the degree of bottom water oxygenation and the primary production and rate of supply of organic matter (O.M.) to the sediment and its preservation.

The terminology for low oxygen regimes is shown in Table 6.1.

Table 6.1. Terminology for low oxygen regimes and the resulting biofacies in marine environments. After Tyson and Pearson, (1987).

Oxygen level ml/l	Oxygenation regime	
	Facies	Biofacies
8.0-2.0	Oxic	Aerobic
2.0-0.2	Dysoxic	
2.0-1.0	moderate	Dysaerobic
1.0-0.5	severe	
0.5-0.2	extreme	
0.2-0.0	Suboxic	Quasi-anaerobic (probably corresponds to exaerobic)
0.0 (free H_2S)	Anoxic (= euxinic)	Anaerobic

Prolonged contact with oxygen results in oxidation of the organic matter (O.M.). Oxygen depletion occurs when oxygen demand created by the decay of metabolizable O.M. exceeds the rate of oxygen supply (Tyson and Pearson, 1991).

Downward mixing of oxygenated surface waters is restricted by stratification of the water column due to density interfaces (pycnoclines) produced by temperature (thermocline), salinity (halocline) or chemical (chemocline) gradients. Development of the water column stratification is at a maximum when the thermocline and/or halocline is most developed. In mid-latitudes this development is seasonal, being dependant on the duration and intensity of insolation during the spring and summer, the background winter water temperature and the frequency, duration and magnitude of mixing. (Tyson and Pearson, 1991). Additionally, topographic controls are important in producing prolonged periods of anoxia, e.g. in silled or enclosed basins where overturn of the stratified water column is low or impossible and where a strong pycnocline will be evident.

Organic flux is an important control on the formation of black shales, there are two differing models on the origin and accumulation of high amounts

of organic matter: the so-called preservation versus production debate (Table 6.2).

Proponents of the preservation theory suggest that organic matter accumulates and is preserved in anoxic environments (e.g. Tyson, 1987; Canfield, 1989; Wignall, 1991). Alternatively the productivity model predicts a high rate of organic matter flux (caused by increased productivity) to the seafloor with the rate of burial exceeding rate of oxidation (Calvert, 1987; Pederson and Calvert, 1990).

Table 6.2. Depositional conditions in the preservation and productivity models for organic matter accumulation. From Wignall (1994).

	Preservation	Productivity
Water column	**Stratified, slow overturn of water column**	**Well mixed**
Primary productivity	**Low-moderate (1-100 g/cm²/yr)**	**High (200-600 g/cm²/yr)**
Sedimentation rate	**Low (10-100 cm²/1000 yr)**	**Usually high (1-10m²/1000 yr**

6.3 DIAGENESIS IN FINE GRAINED SEDIMENTS

During burial diagenesis both physical and chemical changes take place. At deposition the initial assemblage of sedimentary particles will be a mix of components with different chemical stabilities. The least stable components are first to react, followed in sequence by those with lower reactivities. In an organic-rich mudrock, the zones reflect the sequential use of oxidants during bacterial breakdown of organic matter. There are primarily four zones of diagenesis present in sediments deposited in oxidised bottom waters, with the oxic zone being absent in sediments deposited in anoxic bottom waters (Wignall, 1994). Table 6.3 shows the reactions occurring in each of the diagenetic zones, with successive oxidants being utilised as supply of the oxidants is cut off with depth.

Zone	Depth	Schematic equation	Selected mineralogical changes
Oxic	mm-cm	$CH_2O + O_2 \rightarrow$ $CO_2 + H_2O$ (Bacterial aerobic respiration)	Clay exchange reactions. Phosphate fixation by ferric hydroxides.
Denitrification	mm-cm	$5CH_2O + 4NO_3^- \rightarrow$ $4HCO_3^- + 3H_2O + 2N_2 + CO_2$ (Nitrate used as an oxidant)	
Sulphate reduction	1-10 cm	$2CH_2O + SO_4^{2-} \rightarrow$ $2HCO_3^- + H_2S$ (sulphate used as an oxidant)	Hydrated iron oxides reduced. Iron monosulphides precipitated. Pyrite formation. Local concretion formation.
Methanogenic	?	$2CH_2O \rightarrow CH_4 + CO_2$	

Table 6.3. Diagenetic zones. After Curtis (1980) and Wignall (1994)

6.4. INORGANIC GEOCHEMISTRY

6.4.1 Pyrite Formation and C-S-Fe relationships

Pyrite precipitation occurs from the reaction of dissolved Fe^{2+} or detrital iron complexes with dissolved sulphide, as shown by the equation below, (e.g., Berner, 1970, 1982, 1984; Goldhaber and Kaplan, 1974; Berner and Raiswell, 1983; Raiswell and Berner, 1985; Canfield, 1989; Canfield *et al.*, 1994).

$$Fe^{2+} + H_2S \rightarrow FeS + 2H^+$$
$$FeS + S_0 \rightarrow FeS_2$$

H_2S is produced by the reduction of sulphate by bacteria using O.M. as a reducing agent and energy source (Berner, 1984).

Pyrite is not commonly formed directly, rather metastable iron sulphide minerals (mackinawite ($FeS_{0.9}$ to $FeS_{0.95}$) and greigite (Fe_3S_4)) form intermediate stages (Canfield and Raiswell, 1991).

There are four main limiting factors in pyrite formation :-

1) Deposition and preservation of bacterially decomposable organic matter .
2) Sulphate concentration in the water column
3) Sulphide availability in the sediment.
4) Availability of iron minerals that are reactable with H_2S.

1) Organic matter

Both the amount and type of organic matter delivered to the site of deposition influences the amount of pyrite formation (Middleburg, 1991). The organic supply limits the rate and amount of bacterial sulphate reduction (Westrich, 1983).

Organic matter comprises a variety of compounds, each with differing reactivities to sulphate. In rapidly depositing sediments, i.e., those underlying areas of high productivity or in euxinic environments, the more reactive organic compounds are buried into the subsurface zone of sulphate reduction, before they can be destroyed by aerobic processes. Consequently there is abundant H_2S to react with iron minerals. In sediments that are

slowly deposited or occur in low productivity environments, much organic matter is destroyed aerobically and as a result the small amount of organic matter preserved contains poorly reactable compounds. In these circumstances there is little H_2S production and little reaction with iron minerals (Berner and Raiswell, 1983).

Organic carbon and iron contents often correlate positively due to the association of colloidal organic matter and colloidal iron-oxides with clay grains. Deposition of more clay entails the deposition of more organic matter and more iron (Raiswell and Berner, 1985).

2) Sulphate concentration

Pyrite formation is limited in freshwater environments as sulphate concentrations are less than 1% of that found in oceans (average 28 mmol/l SO_4^{2-}) (Berner and Raiswell, 1984). Sulphate in the marine environment is not thought to be a limiting factor on pyrite formation (Berner, 1978, 1984).

3) Sulphide availability

Pyrite formation may be initially limited in marine or euxinic sediments when all available sulphide has reacted with the readily reactive iron oxides and iron oxyhydroxides. Then, as the more stable iron minerals slowly react, hydrogen sulphide can no longer be removed from the sediment (by fixation as pyrite) at the same rate as sulphate reduction. Hydrogen sulphide can then be lost from the sediment before reaction with the poorly reactive iron minerals; thus pyrite formation may also partly depend on the relative rates of sulphate reduction compared to rates of sulphide reaction (Canfield *et al.*, 1992). However, sulphide availability will only be a limiting factor when there is a mechanism to facilitate loss of H_2S from the system. Berner and Westrich (1985) note that loss of H_2S from the sediment may occur due to the oxidation of reduced sulphur compounds by oxygen introduced into the sediment by bioturbation. Bioturbation may also introduce physical pathways into the sediment to facilitate further H_2S loss; upward movement of methane bubbles may also strip H_2S from the system.

3) Iron mineralogy

The concentration of solid-phase iron and its reactivity toward sulphide are among the most important factors limiting pyrite formation (Canfield *et al.*,

1992). In silicate-poor environments such as carbonates, iron has a limiting effect on pyrite formation due to the low concentration of iron minerals. An iron mineral assemblage can also be defined as reactive or poorly reactive. Reactive iron is the fraction which readily reacts with sulphide, (Berner, 1970; Berner 1984; Raiswell and Berner 1985; Canfield 1989). The highly reactive oxide minerals are the most important Fe phases in early diagenetic pyrite formation, and when reactive iron is abundant, pore water sulphide may be exhausted by rapid reaction with the oxides.

Consequently, studies of modern sediment show that time is also a crucial factor in iron mineral reaction, with the poorly reactive iron sheet silicates reacting much more slowly than iron oxyhydroxides (Canfield *et al.*, 1992) (Table 6.4). Hydrogen sulphide can be lost from the sediment without reaction with the poorly reactive iron minerals; thus pyrite formation depends on the relative rates of sulphate reduction compared to rates of reaction of sulphide with iron minerals (Canfield *et al.*, 1992).

Table 6.4 Reactivity of iron minerals towards hydrogen sulphide. From Canfield, *et al.*, (1992)

Iron mineral	Reactivity k ($yr.^{-1}$)	Half life $t_{1/2}$
Ferrihydrite	2200	2.76 hr.
Lepidocrocite	>85	<2.94 days
Goethite	22	11.5 days
Hematite	12	21 days
Magnetite	6.6×10^{-3}	105 yr.
'Reactive' silicates	3×10^{-3}	231 yr.
Sheet silicates	8.2×10^{-6}	84530 yr.
Ilmenite, Garnet, Augite, Amphibole	«8.2×10^{-6}	»84530 yr.

6.4.2 Radiogenic isotopes

It was first noticed by Adams and Weaver (1958) that marine shales are more radioactive than non-marine deposits, with a correlation seen between the U/Th ratios and the bottom water anoxia of shales. This relationship is due to the variation in concentration of three isotopes (K, Th and U).

Potassium is largely contained in the detrital feldspar, mica grains and soil clays (such as illite) produced from the weathering of a granitoid source rock. Some K also goes into solution and clays continue to absorb K during transport and upon deposition. (Heier and Billings, (1972) in Myers and Wignall (1987)).

Uranium and thorium are mostly contained in accessory minerals and as surface coatings on minerals. Both may be leached during transport and weathering, and absorbed by clays (Tieh *et al.*, 1980). Therefore both Th and U are present in accessory minerals and clay grade material. However, U can also be removed from solution and formed authigenically. Uranium, unlike Th, is soluble. In oxidising environments it is found in the U^{6+} oxidation state as the highly soluble UO_2^{2+} uranyl ion (Cochran *et al.*, 1986). Under anoxic conditions the U^{4+} ion is stable. Shaw *et al.*, (1994) recognise two mechanisms for the concentration of U in sediments, from recent studies on the Chesapeake Bay sediments. Firstly there is aerobic uptake of U by bio-matter in the surface water, which is then preserved under anoxic conditions associated with a rise in productivity. Secondly, there is uptake of reduced U^{4+} from the water column by suspended particles in anoxic water. Alternatively, Borovec *et al.*, (1979) suggested that uranium can be fixed by oxidation-reduction reactions following humic acid absorption of the uranyl ions. Anderson *et al.*, (1989a, 1989b) also suggested direct precipitation of U within the sediments as a possible mechanism for authigenic uranium concentration.

6.5 GEOCHEMICAL INDICATORS OF PALAEOENVIRONMENT

6.5.1 Carbon, Sulphur and Iron relationships.

6.5.1.1 C/S ratios as palaeosalinity indicators

Berner and Raiswell (1984) used the relationship between total organic carbon and pyrite sulphur to distinguish ancient marine from freshwater sedimentary rock (Figures 6.1 and 6.2). This relationship derives from the fact that much less diagenetic pyrite is formed in organic-rich sediment deposited in freshwater than marine sedimentary regimes. Pyrite formation is limited in freshwater environments as sulphate concentrations are less than 1% of that found in oceans (average 28 mmol/l SO_4^{2-}). Pyrite sulphur content in freshwater rocks is low and relatively independent of organic carbon content. In contrast marine sediments show a good correlation

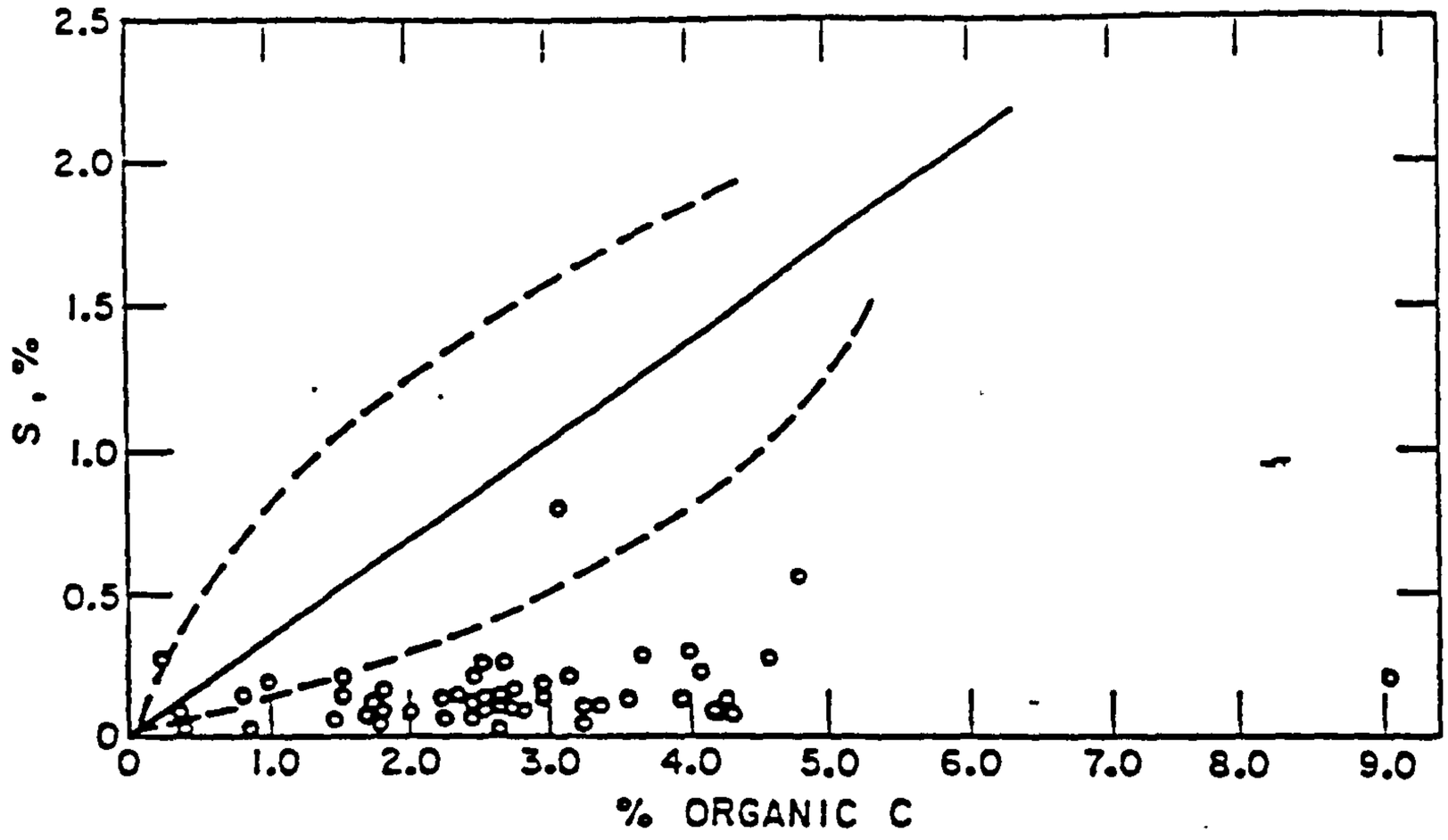

Figure 6.1 Plot of %C v. %S for Carboniferous non-marine sediments. region enclosed by dashed line represents present day normal marine sediments. (From Berner and Raiswell, 1984).

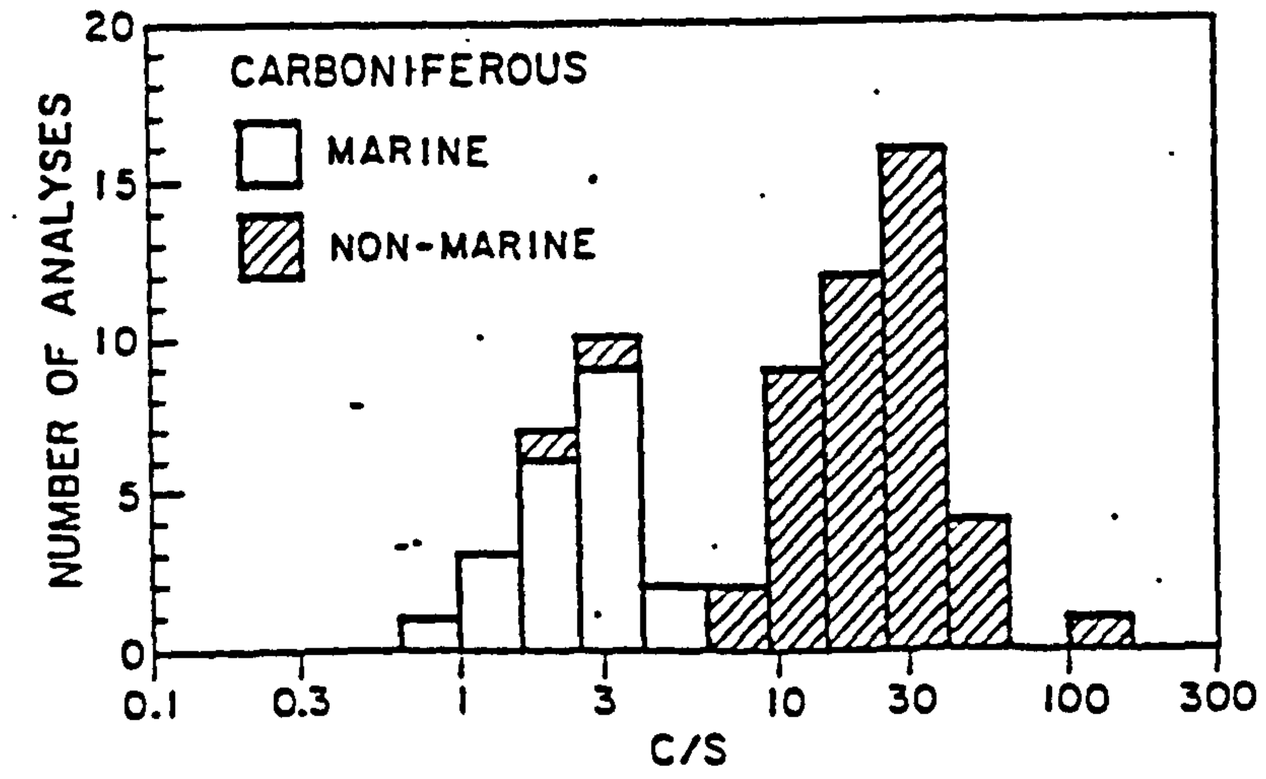

Figure 6.2 Frequency distribution of C/S ratio for marine and non-marine Carboniferous strata. (From Berner and Raiswell, 1984).

between carbon and pyrite sulphur, with the average C/S ratio of modern marine sediments at 2.8±1.5. It is probable that the C/S ratio is constant as a constant fraction of the available organic matter in the sediment is metabolizable to H_2S (Berner and Raiswell, 1983). Berner and Raiswell (1984) showed that marine rocks (>18‰ salinity) are characterised by low C/S ratios (0.5-5.0) and freshwater by high C/S values (>10).

However, the C/S method is restricted in its use since:-

1) The C/S method cannot be applied to rocks low in T.O.C. (<1%).

2) Pure limestones are low in iron minerals and so pyrite formation is limited by iron availability and thus the C/S method is not applicable.

The C/S method was initially thought not to be applicable to sediments deposited in euxinic environments, i.e., where there is H_2S in the water column. Under these conditions pyrite can form in the water column, independently of the organic carbon content of the sediment. The C/S plot will thus have a positive intercept on the sulphur axis, indicating the presence of syngenetic pyrite (Raiswell and Berner, 1985; Dean, 1994). However, it is now thought (Rob Raiswell, pers. comm., 1995) that the C/S value in an euxinic sediment will be the maximum possible, since the pyrite sulphur value will reflect the limitation of pyrite formation by organic carbon or iron.

Further work by Raiswell and Berner, (1987) established the relationship between the C/S ratio and the amount of organic carbon loss during burial (Figure 6.3). Progressive carbon loss during burial occurs by microbial methanogenesis, thermal maturation, and low grade metamorphism, whilst pyrite sulphur values remain constant. By comparison with thermal maturity indicators (e.g., vitrinite reflectance, conodont colour index) Raiswell and Berner showed that there was a clear relationship between the loss of carbon during burial and reduction in the C/S value. It was demonstrated that by normalising the organic carbon content to pyrite sulphur (so that C/S = 2.8) carbon loss during burial could be calculated. The C/S method for calculation of depositional organic carbon contents can only be applied to sedimentary rocks showing evidence of deposition under normal marine conditions.

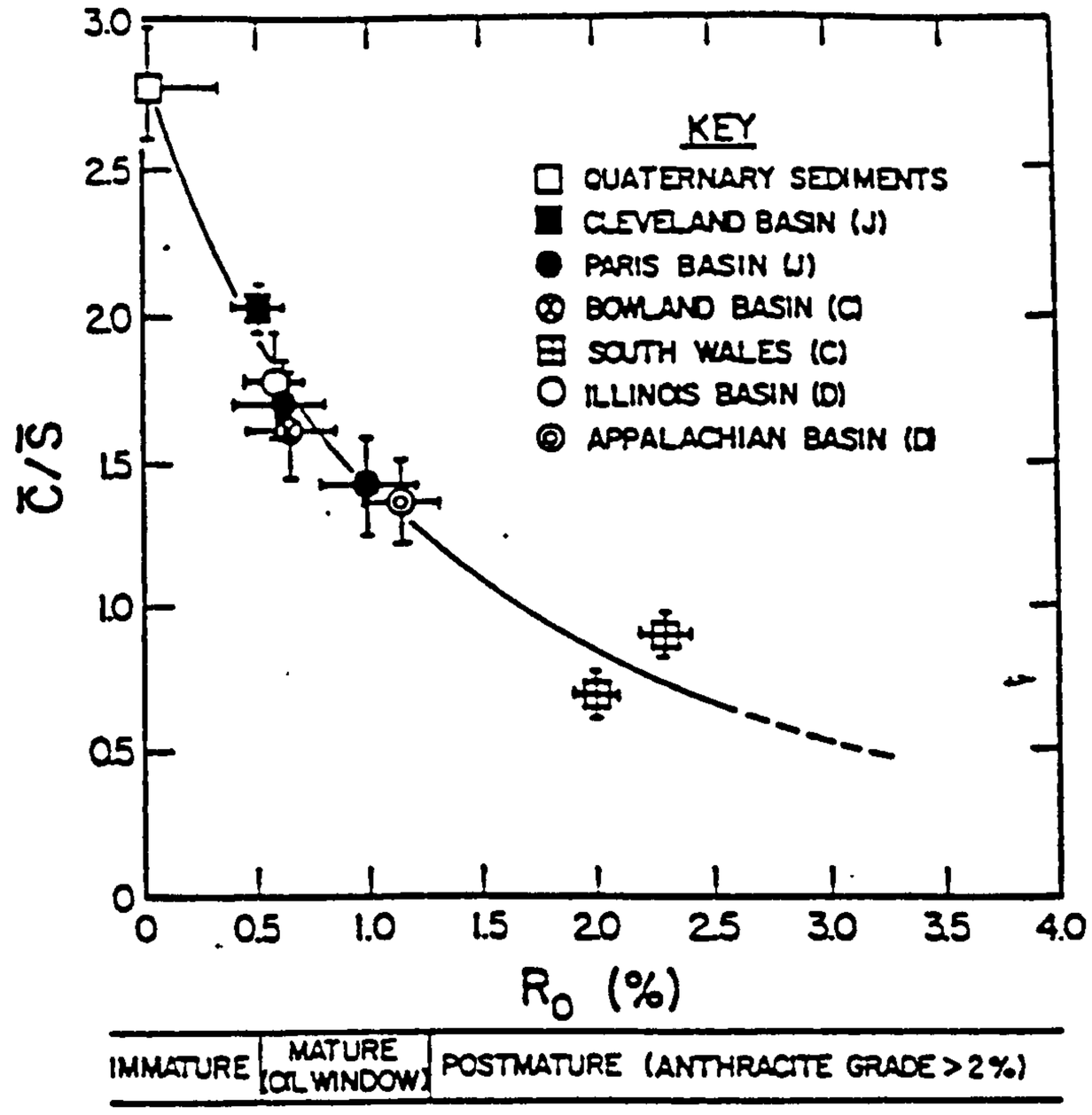

Figure 6.3 Plot of mean C/S for normal marine sediments v. vitrinite reflectance (R_o). Error bars represent standard deviation. (From Berner and Raiswell, 1987).

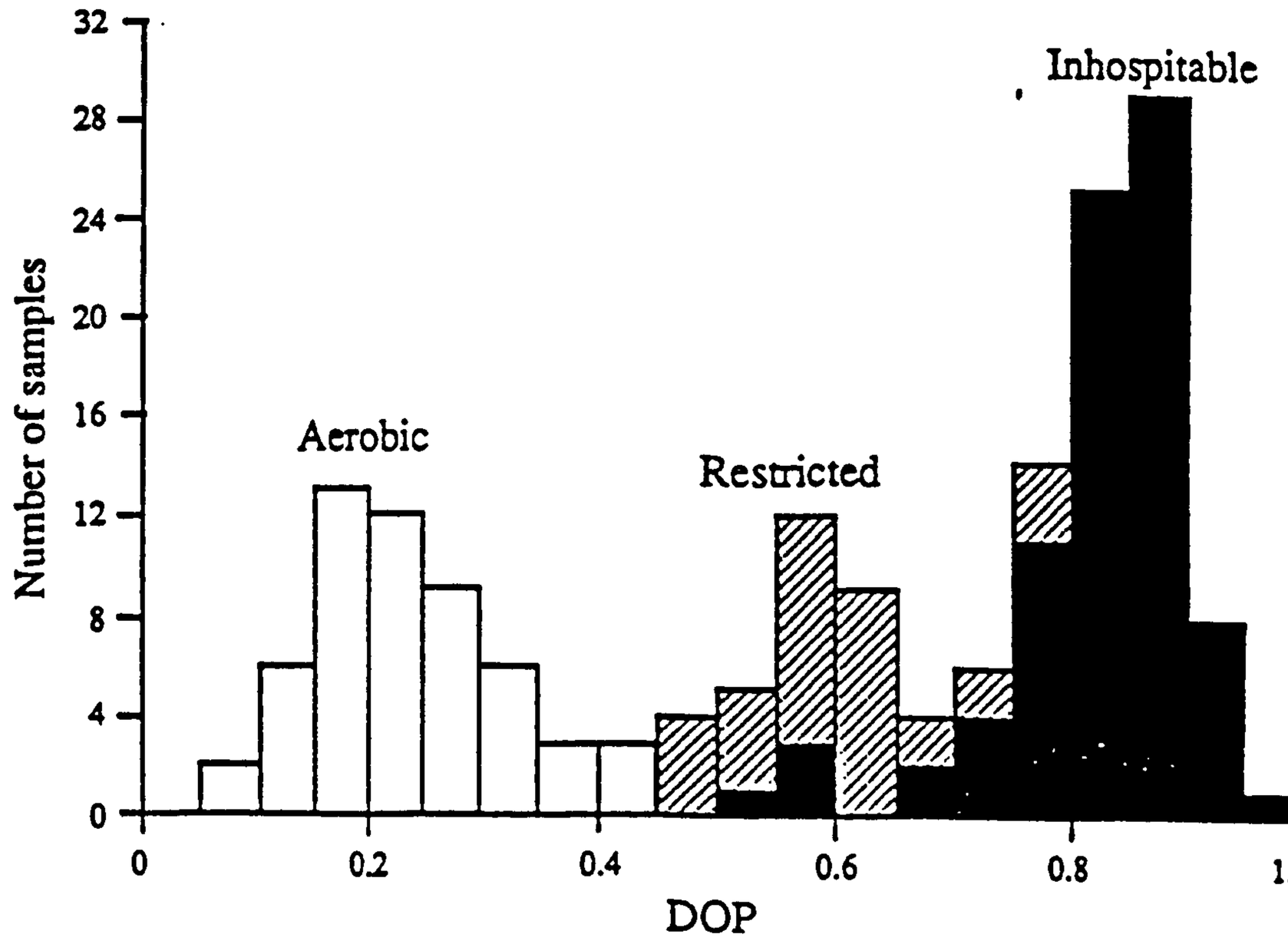

Figure 6.4 Histogram showing variation in DOP with the degree of oxygenation of the bottom water. (From Raiswell *et al.*, 1988).

6.5.1.2 Degree of Pyritization as an indicator of palaeo-oxygenation.

Raiswell *et al.*, (1988) used degree of pyritization (D.O.P.) (Berner, 1970) for recognising the degree of bottom water oxygenation in an organic-rich sediment (Figure 6.4). D.O.P. is the ratio of pyritic Fe to reactive Fe (pyritic Fe + acid-soluble Fe). D.O.P. is thus a measure of the amount of iron that has reacted compared the total available for reaction and is related to the amount of H_2S and reactive minerals in the sediment.

Raiswell *et al.*, (1988) were able to distinguish three palaeo-oxygenation categories: aerobic (showing D.O.P. <0.45), restricted (0.45≤ D.O.P. <0.75) and inhospitable bottom (D.O.P. ≥0.75).

Raiswell *et al.*,(1988) stipulated some provisos in applying the D.O.P. method:-

1) Organic carbon content should not obviously be a limiting factor in pyrite formation, i.e., samples with appreciable organic matter should be used (>0.15%).
2) Fresh samples should be used to minimise the loss of pyrite sulphur due to pyrite oxidation.
3) Sediments should contain less than 65% biogenic skeletal debris ($CaCO_3$ or silica) (Raiswell and Berner, 1986) so that they contain sufficient iron content.
4) No additions or losses of sulphide sulphur should have occurred as a result of maturation or metamorphism. Evaporites or rocks containing high sulphate contents are susceptible to H_2S formation during high-temperature sulphate reduction and should be avoided.
5) Iron carbonate concretions should be avoided as iron migration may result in large amounts of acid extractable iron being added to the sediment.
6) The method can only be applied to sediments younger than the Devonian due to the presence of a highly reactive organic carbon phase in Devonian and older rocks.

Under anoxic conditions seawater sulphate is reduced to H_2S, which reacts with detrital iron minerals and eventually forms pyrite (Berner, 1984). In normal marine sediments (those deposited beneath an oxygenated water column) pyrite formation occurs in the anoxic environment beneath the sediment-water interface. In a normal marine environment an increase in organic carbon appears to be matched by an increase in detrital iron oxides

(present in siliclastic debris), and therefore an increase in H_2S production is equalled by higher reactive detrital iron content. However, pyrite formation in a normal marine environment is limited by the amount of organic matter which can be utilised by sulphate-reducing bacteria, and also the risk of oxidation (e.g. by bioturbation), of the pyrite and organic matter.

Euxinic sediments are deposited beneath an H_2S bearing water column, thus iron minerals can also react with the H_2S in the water column prior to deposition. These sediments show no limitation of pyritization by reoxidation, however there can be limitation by the amount of reactive iron or organic carbon content. The resulting C-S and D.O.P. plots are shown in Figure 6.5.

Raiswell and Berner (1985) showed how D.O.P. clarifies the C/S plot:-
1) An intercept on the S axis and correlation between C and S (C-S plots) and positive correlation between D.O.P. and total organic carbon (T.O.C.) reflects carbon-limitation during diagenetic pyrite formation (Figure 6.5A and 6.5C).
2) An intercept on the S axis and constant value of D.O.P. reflects iron-limited pyrite formation with all pyrite possibly being syngenetic (Figure 6.5B and 6.5D).
3) An intercept on the S axis with constant S level (independent of T.O.C). D.O.P is independent of carbon content and reflects iron-limited pyrite formation, possibly indicating syngenetic pyrite formation.

Raiswell *et al.*, (1994) have also noted that there is also a correlation between D.O.P. values and the reactivity and length of exposure time of the iron minerals to sulphide. Thus a low value for D.O.P. may indicate either sulphide or iron limitation (due to consumption of all reactive iron minerals). Iron limitation will occur once the reactive iron minerals (iron oxides (except magnetite) and iron oxyhydroxides) have been used, because the remaining iron minerals are slow to react (Canfield *et al.*, 1992; Canfield *et al.*, (in prep.)) . Hydrogen sulphide will be lost from the sediment without reaction with the poorly reactive iron minerals; thus pyrite formation depends on the relative rates of sulphate reduction compared to rates of sulphide reaction (Canfield *et al.*, 1992).

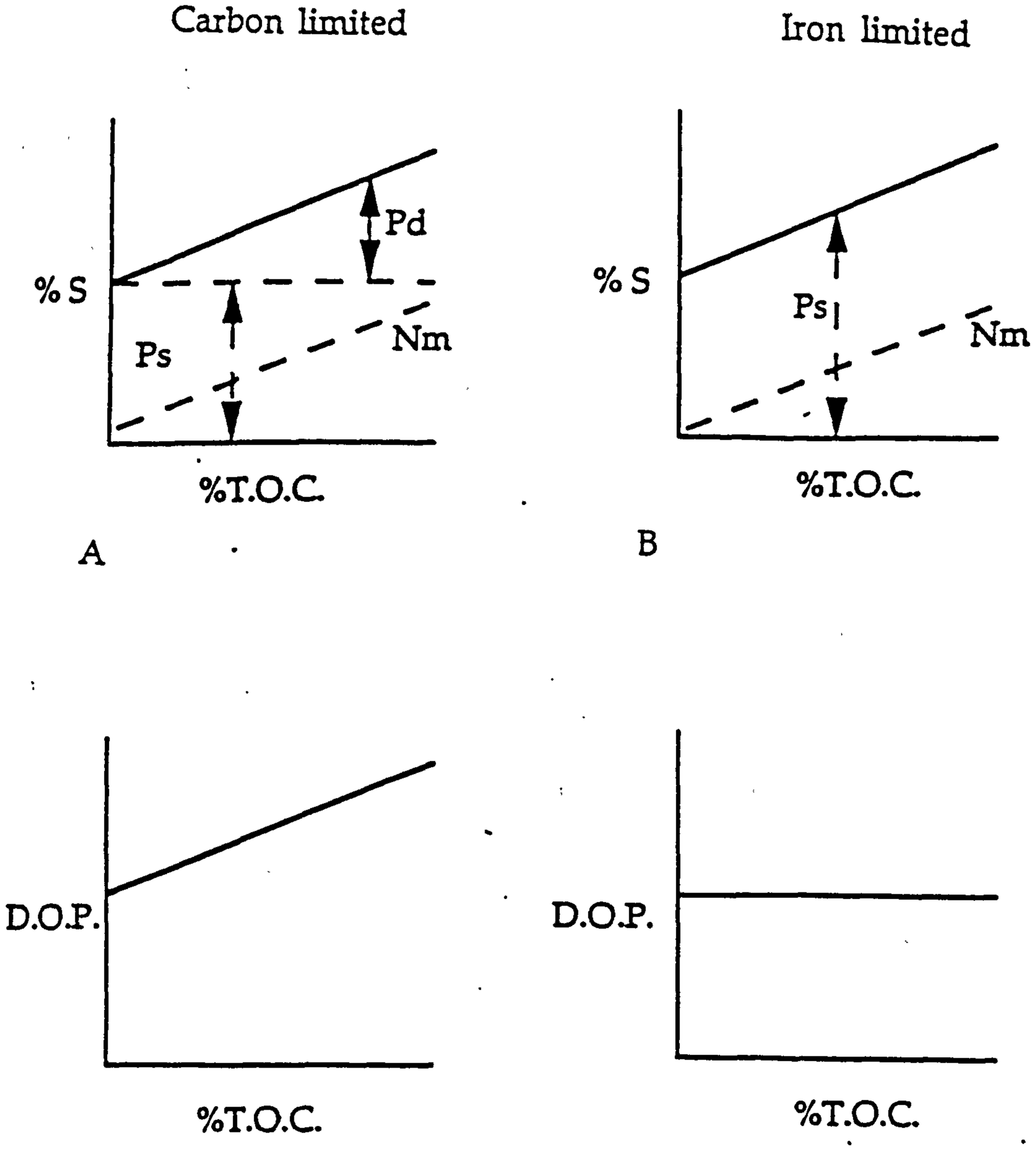

Figure 6.5 A, C. Idealised plot of %T.O.C. v. %pyrite sulphur (A), and %T.O.C. v. DOP (C) for carbon limited sediments. (Ps = syngenetic pyrite, Pd = detrital pyrite, Nm = normal marine line).
B, D. Idealised plot of %T.O.C. v. %pyrite sulphur (B), and %T.O.C. v. DOP (D) for iron limited sediments.
(From Raiswell and Berner, 1985).

6.5.1.3 Reactive iron

Canfield *et al.*, (in prep) and Raiswell (in prep) have investigated the relationship between the D.O.P. and the type of iron minerals present in specific environments. By utilising data from modern environments (e.g., F.O.A.M. site, Gulf of Mexico, Santa Barbara Basin and the Black Sea) it was found that there is a distinct correlation between the amount of reactive iron and total iron; this is related to bottom-water oxygenation and environment (Figure 6.6). Anoxic or sulphidic environments show a relatively higher reactive iron content compared to dysaerobic environments for the same amount of total iron. In the euxinic environment iron will be present as detrital and dissolved iron species (within the water column) (Figure 6.7). The iron-oxide coat surrounding detrital grains is dissolved at the chemocline (Rob Raiswell, pers comm., 1995). The chemocline will be preferentially and most intensely developed in the basin centre (due to lower amounts of mixing of the stratified water column), at the boundary between H_2S bearing waters and poorly oxygenated waters. Although there will be horizontal transport of the reduced iron along the chemocline, there will an overall net diffusion of the iron in solution (Fe^{2+}) downwards to the sediment. There is therefore an increased reactive iron (in the form of Fe^{2+}) input to the sea-floor beneath development of a strong chemocline in euxinic basins. In comparison, reducing conditions will be only poorly developed in dysaerobic conditions. Consequently, very little iron will be taken into solution and thus relatively less reactive iron will be provided to the seafloor. The detrital iron (comprising poorly reactive species such as sheet silicates) will provide a much larger proportion of the iron present.

6.5.2. Radiogenic isotopes as palaeo-oxygenation indicators.

Myers and Wignall (1987) investigated the relationship between palaeoecology and gamma-ray spectrometry to evaluate palaeo-oxygen levels. Gamma-ray spectrometry measures the abundance of K, Th and U in a rock.

Potassium and thorium are present in the detrital clay fraction of a mudrock (with other K and Th carriers such as heavy minerals or feldspar being mostly deposited en route to the site of clay deposition). Uranium is also present in this detrital fraction, although it may also be present in the form

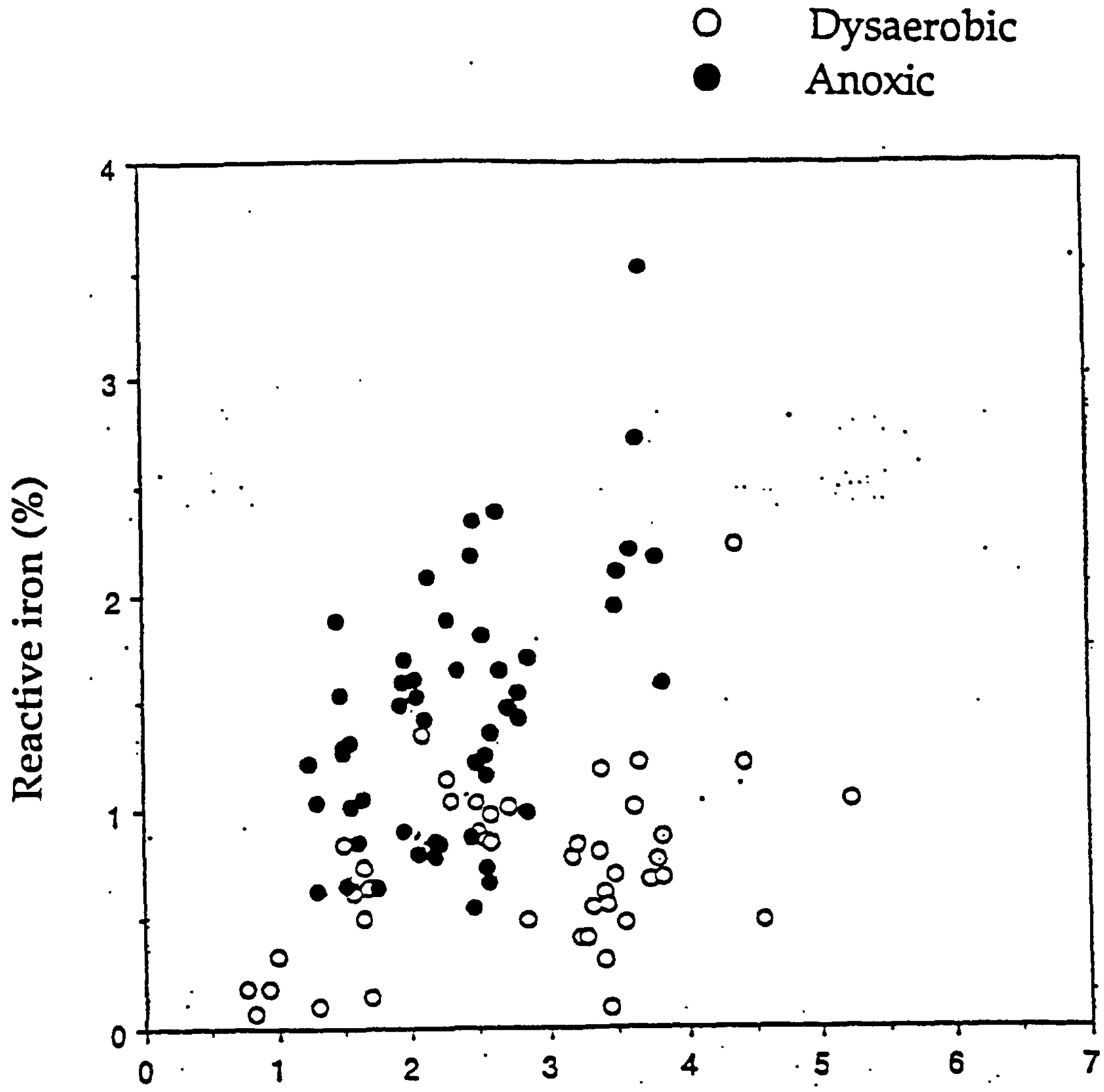

Figure 6.6 Reactive v. total iron plot for dysaerobic sediments and anoxic sediments. (From Raiswell, in prep.).

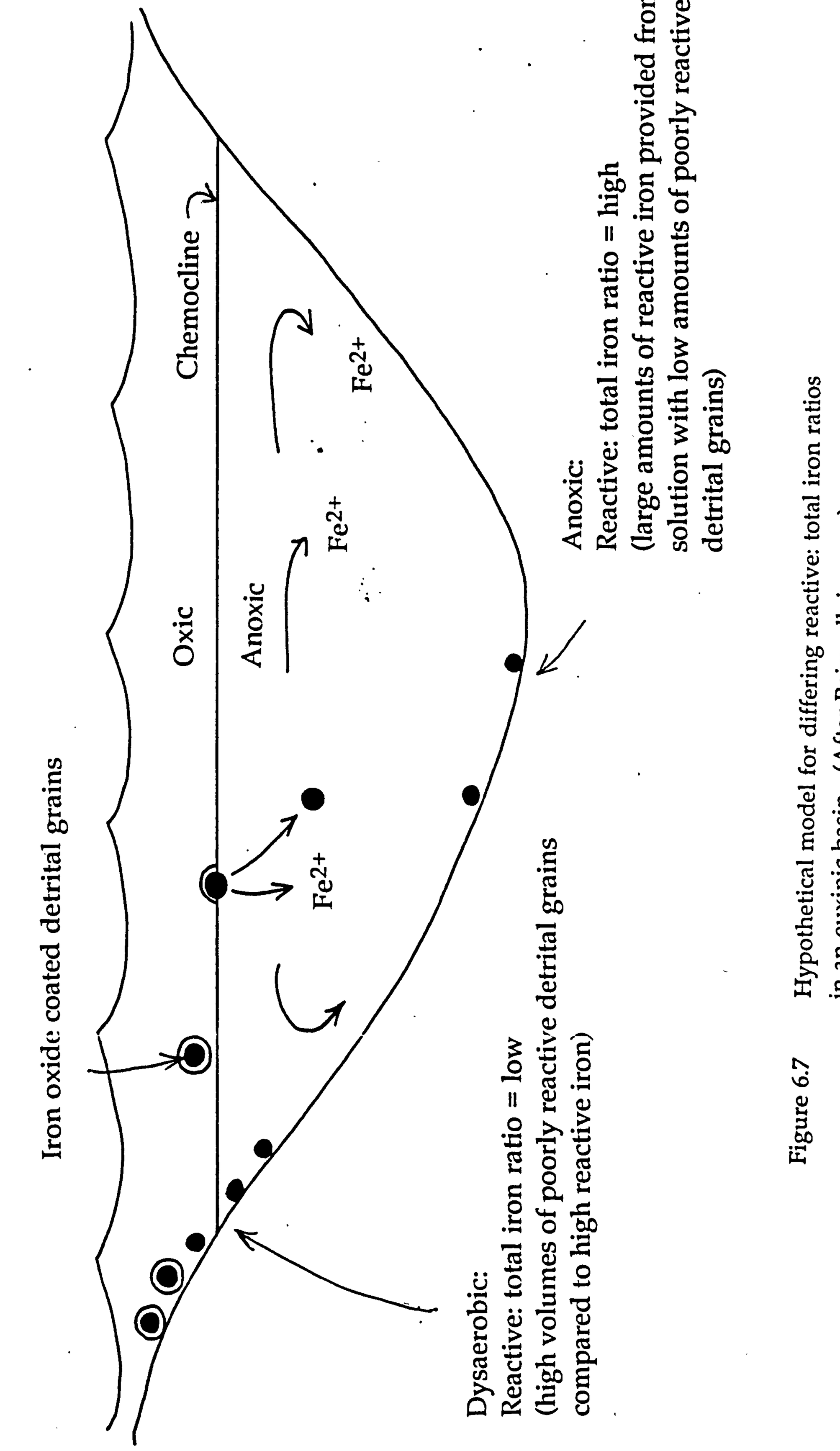

Figure 6.7 Hypothetical model for differing reactive: total iron ratios in an euxinic basin. (After Raiswell, in prep.).

of authigenic uranium which is precipitated from solution under anoxic conditions.

As Th is therefore relatively immobile compared to U, there must be a relationship between the detrital Th, detrital U and authigenic U (assuming all Th is present as a detrital fraction).

The average crustal Th/U ratio is 3.5 (Adams *et al.*, 1959). Myers and Wignall (1987) calculated an average Th/U of 3.9±0.7 from 154 low organic carbon marine and deltaic mudstone. They subsequently calculated the detrital uranium for each reading by dividing the thorium value by three. A Th/U ratio of three was assumed so that significant values of authigenic U were measured.

Thus, $U_{authigenic} = U_{actual} - U_{detrital}$
where $U_{detrital} = Th/3$

Authigenic U contents can be used to qualitatively compare the degree of anoxia of sections.

6.6. GEOCHEMICAL PALAEOENVIRONMENTAL ANALYSIS ACROSS THE MID-CARBONIFEROUS BOUNDARY AT INISHCORKER.

6.6.1 INTRODUCTION

Various geochemical techniques have been applied to samples at 1 m intervals over a 36 m section at Inishcorker. This spans the mid-Carboniferous Boundary and ranges from E_2c^2 to H_2a^1 in age.

The section at Inishcorker was chosen for intensive geochemical study as it is the most complete of all the studied sections through the mid-Carboniferous. The locality also shows high erosion rates which reduces the time available for weathering of any susceptible mineral complexes (e.g., pyrite) in collected samples. To further reduce the influence of weathering, fresh samples were obtained with a portable handheld corer.

Clear alternations between 'marine band' and 'non-marine' strata are evident. As previously discussed (section 1.4.4.3) many workers have held the opinion that strata outside marine bands are deposited in non-marine

conditions. In this study, as in many previous studies, the palaeontologically barren strata in between the marine bands are termed 'non-marine'. However, geochemical investigation of the section at Inishcorker tests this assumption.

6.6.2 Results and interpretation

6.6.2.1 C-S-Fe relationships

Values of carbon/sulphur ratios were calculated using re-corrected values of T.O.C. A vitrinite reflectance of 4.7% (46 analyses of sample INGC1) has been determined (James Maynard, pers comm. 1993) and would correspond to a C/S ratio of <0.5 for normal marine sediment (after Raiswell and Berner) (Figure 6.3). Rather than assume that the marine bands were deposited in 'normal marine' conditions (cf. Raiswell and Berner), and hence have a C/S ratio of 0.5, it is assumed that there has been a 70% loss of organic carbon through maturation (Berner and Raiswell, 1984) for all samples, rather than by re-correction using a decreased C/S ratio. It should also be noted that pyrite sulphur values are consistently less than total sulphur values; this discrepancy can be accounted for by the presence of organic S, elemental sulphur and the weathering effect of pyrite by oxidation (Canfield *et al.*, 1986).

The corrected C/S values obtained from the Inishcorker samples range from 1.37 to 97.78 (Table 6.5). Using a value of below 5.0 to indicate marine deposition, 43.75% of values calculated from both 'marine band' and non-'marine bands' appear to predict deposition under normal salinities (i.e. C/S <5). A further 43.75% show values falling in the range 5.0-10.0, no conclusions can be drawn as to the palaeosalinity of these samples, as a clear division of marine from freshwater environments can only be drawn at a value of 10 (Berner and Raiswell (1984), although it is possible that they may indicate brackish waters, (however, re-interpretation of these results is necessary when deposition was in euxinic conditions (see below)). Berner and Raiswell (1984) formulated their model from data collected from predominantly unweathered borehole samples. Thus, if it can be assumed that pyrite sulphur recovery is incomplete (due to the reasons detailed above) then it is possible that true C/S ratios will show a slight decrease form the calculated values.

Ammonoid zone	Sample	Total C (%)	Inorg C (%)	TOC (%)	Original TOC (%)	Total S (%)	Pyrite S (%)	FeS2 (%)	Acid Fe (%)	Pyrite Fe (%)	Reactive Fe (%)	D.O.P.	C/S	Original C/S	Ua (ppm)	Total iron (%)	Reactive/Total iron
H2a1m	16	0.6900	0.0000	0.6900	2.9667	2.4200	2.1579	4.0372	0.1903	1.8793	2.0696	0.9080	0.4124	1.3748	4.4700	4.6300	0.4471
H1b2	15	2.5100	0.0000	2.5100	8.3667	3.8300	1.5784	2.9530	0.8711	1.3746	2.2457	0.6121	1.5902	5.3007	5.6000	n/a	n/a
H1b2m	14	2.6000	0.4441	2.1600	7.2000	5.0800	2.5730	4.8137	0.1793	2.2407	2.4200	0.9259	0.8395	2.7983	6.5000	5.9100	0.4095
H1b2m	13	2.8800	0.0105	2.8700	9.5667	3.0700	2.2337	4.1685	0.0587	1.9366	1.9953	0.9705	1.2906	4.3021	6.7000	n/a	n/a
H1b2m	12	6.7400	1.5900	5.1500	17.1667	2.4600	1.8780	3.5135	2.7378	1.6358	4.3733	0.3740	2.7423	9.1409	8.8300	7.1400	0.6125
H1b1	11	1.3200	0.0937	1.2300	4.1000	3.5200	2.7954	5.2298	0.2408	2.4344	2.6752	0.9100	0.4400	1.4667	9.9700	n/a	n/a
H1b1	10	1.1100	0.0000	1.1100	3.7000	1.3800	0.9750	1.8241	0.1284	0.8491	0.9775	0.8686	1.1385	3.7949	4.4000	3.6600	0.2671
H1b1m	9	1.6700	0.0212	1.6500	5.5000	1.8300	1.2059	2.2580	0.8496	1.0511	1.9007	0.5630	1.3671	4.5571	4.7200	4.4100	0.4310
H1a3	8	1.8300	0.0527	1.7800	5.9333	1.9400	1.5974	2.9885	0.3071	1.3911	1.6982	0.8192	1.1143	3.7144	6.1700	3.5600	0.4770
H1a3m	7	5.0000	0.0224	4.9800	16.6000	3.0400	2.2808	4.2671	1.3396	1.9883	3.3259	0.5972	2.1834	7.2781	7.4100	n/a	n/a
H1a2	6	4.4500	0.7362	3.7100	12.3667	2.4600	1.9628	3.7096	0.5946	1.7268	2.3214	0.7439	1.8711	6.2370	6.9200	n/a	n/a
H1a2m	5	6.1800	0.0323	6.1500	20.5000	1.4200	0.2389	0.4470	0.5874	0.2081	0.7908	0.2632	25.7430	85.8100	6.8700	2.7100	0.2917
H1a2m	4	5.8300	0.0333	5.8000	19.3333	2.7000	1.4046	2.6278	1.4845	1.2232	2.7077	0.4518	4.1299	13.7643	8.4000	3.4400	0.7871
H1a1	3	1.7900	0.5779	1.2100	4.0333	2.7200	1.8446	3.4510	0.2376	1.6064	1.8440	0.8712	0.6560	2.1866	9.5000	4.6200	0.3991
H1a1	2	2.1200	0.0628	2.0600	6.8667	2.8300	2.0580	3.8503	0.3929	1.7923	2.1852	0.8202	1.0010	3.3366	7.8000	4.8700	0.4487
H1a1m	1	6.2000	2.5482	3.6500	12.1667	3.0400	2.0687	3.8703	0.0979	1.8016	1.8995	0.9485	1.7644	5.8813	6.0300	5.3700	0.3537
E2c4	20	2.2300	0.0632	2.1700	7.2333	1.9900	0.8228	1.5394	0.1791	0.7166	0.8957	0.8000	2.6373	8.7911	4.0300	4.0100	0.2234
E2c4	21	1.9600	0.0635	1.9000	6.3333	2.6200	1.4625	2.7361	0.1255	1.2736	1.3991	0.9103	1.2991	4.3305	4.7300	4.6100	0.3035
E2c4	22	3.2200	0.9308	2.2900	7.6333	2.0800	1.7210	3.2198	0.3487	1.4988	1.8475	0.8113	1.3306	4.4354	7.3700	4.4000	0.4199
E2c4m	23	9.0900	0.0461	9.0400	30.1333	3.7500	2.5583	4.7842	1.4859	2.2279	3.7138	0.5999	2.5335	11.7787	11.5700	4.7800	0.7770
E2c3	24	1.8900	0.0114	1.8800	6.2667	1.6100	1.1546	2.1601	0.1938	1.0055	1.1993	0.8384	1.6283	5.4276	3.0000	n/a	n/a
E2c3	25	2.6900	0.0210	2.6700	8.9000	1.3300	1.1400	2.1328	1.1330	0.9928	2.1258	0.4670	2.3421	7.8070	4.7000	n/a	n/a
E2c3	26	1.8600	0.0000	1.8600	6.2000	1.3300	1.0224	1.9128	0.1221	0.8904	1.0125	0.8794	1.8192	6.0642	2.9300	4.0500	0.2500
E2c3	27	1.3900	0.0000	1.3900	4.6333	0.9000	0.4331	0.8103	0.4052	0.3772	0.7824	0.4821	3.2094	10.6981	3.3300	3.5900	0.2179
E2c3	28	1.2100	0.0000	1.2100	4.0333	1.4000	0.5965	1.1160	0.2522	0.5195	0.7717	0.6732	2.0285	6.7617	5.2300	3.9700	0.1944
E2c3	29	1.4000	0.0105	1.3900	4.6333	1.6700	0.7709	1.4423	0.3140	0.6714	0.9854	0.6813	1.8031	6.0103	3.2700	n/a	n/a
E2c3m	30	6.0700	0.0215	6.0500	20.1667	2.6500	2.0611	3.8561	0.1796	1.7950	1.9746	0.9090	2.9353	9.7844	20.8000	3.8500	0.5129
E2c2	31	0.7700	0.0000	0.7700	2.5667	2.0500	0.2290	0.4284	0.0967	0.1994	0.2961	0.6735	3.3624	11.2082	5.9600	n/a	n/a
E2c2	32	1.1100	0.0104	1.1000	3.6667	0.1400	0.0375	0.0702	0.1011	0.0327	0.1338	0.2442	29.3333	97.7778	2.3700	4.7500	0.0282
E2c2	33	1.6200	0.0731	1.5500	5.1667	0.8000	0.6667	1.2473	0.4896	0.5806	1.0702	0.5425	2.3249	7.7496	2.3000	n/a	n/a
E2c2	34	1.2200	0.0000	1.2200	4.0667	1.0900	0.7181	1.3435	0.1448	0.6254	0.7702	0.8120	1.6989	5.6631	0.6000	3.8500	0.2000
E2c2	35	4.8600	0.0000	4.8600	16.2000	3.7500	2.8627	5.3557	0.3503	2.4930	2.8433	0.8768	1.6977	5.6590	5.4300	n/a	n/a
E2c2	36	1.9700	0.0000	1.9700	6.5667	2.1600	1.6005	2.9943	0.1175	1.3938	1.5113	0.9223	1.2309	4.1029	n/a	4.1700	0.3624
E2c2	37	1.0100	0.0000	1.0100	3.3667	3.1500	2.4034	4.4964	0.2359	2.0930	2.3289	0.8987	0.4202	1.4008	n/a	n/a	n/a

Table 6.5 Table showing geochemical results for each sample. Marine band samples (defined by faunal content) are shown shaded.

The C-S graphs show positive intercepts on the pyrite sulphur axis of the graph (Figure 6.8), indicating that there has been some syngenetic pyrite formation. C/S values can however be used in this scenario. In an euxinic environment it is highly likely that pyrite formation will be limited due to iron or carbon contents. Therefore, it is probable that the value calculated as the C/S ratio for a sample in an euxinic environment is the maximum value attainable due to inflation of the C/S value since pyrite sulphur is limited. Thus values falling in the range 5-10 may in fact represent limited pyrite formation in a marine environment (in which case 78% of the section is then re-interpreted as marine).

It could be argued that there may be some diagenetic alteration of the 'non marine' sediments to produce the high pyrite sulphur values. This diagenetic alteration may be by mobilization of organic sulphur during early burial or by additions due to hydrothermal or other external processes (Rob Raiswell, pers. comm., 1995). However, it would then be expected that the pyrite sulphur values would be more uniform throughout the sampled section. Thus, this study assumes that all the pyrite is formed during early diagenesis.

The D.O.P. varies from values of 0.24 to 0.97 through the section. 9% of samples show values indicating deposition in aerobic conditions (D.O.P$\leq$0.45), whilst 56% of the samples show a D.O.P. value of $\geq$0.75.

Thus it appears that there are two separate mechanisms for pyrite formation.

In the 'non marine' environments it appears that deposition occurred within a euxinic basin at most times. A positive intercept on the sulphur axis shows that there was commonly both syngenetic and diagenetic pyrite formation, ie. there is free H_2S in the water column allowing reaction with detrital iron minerals before burial. Diagenetic pyrite formation appears to have been carbon-limited, shown by the correlation of both pyrite S and D.O.P with T.O.C (statistical confidence levels of 98.6% and 67% respectively) (Figures 6.8 and 6.9). However, although these sediments have been interpreted as 'non marine' by palaeontological methods (cf. Ramsbottom *et al.*, 1962) in fact geochemical analysis indicates that at least 60% of the samples show deposition in marine waters, with the majority of the rest of the samples showing values falling in the ambiguous 5-10 range. It may be that as the basin is intensely stratified at most times, the less dense

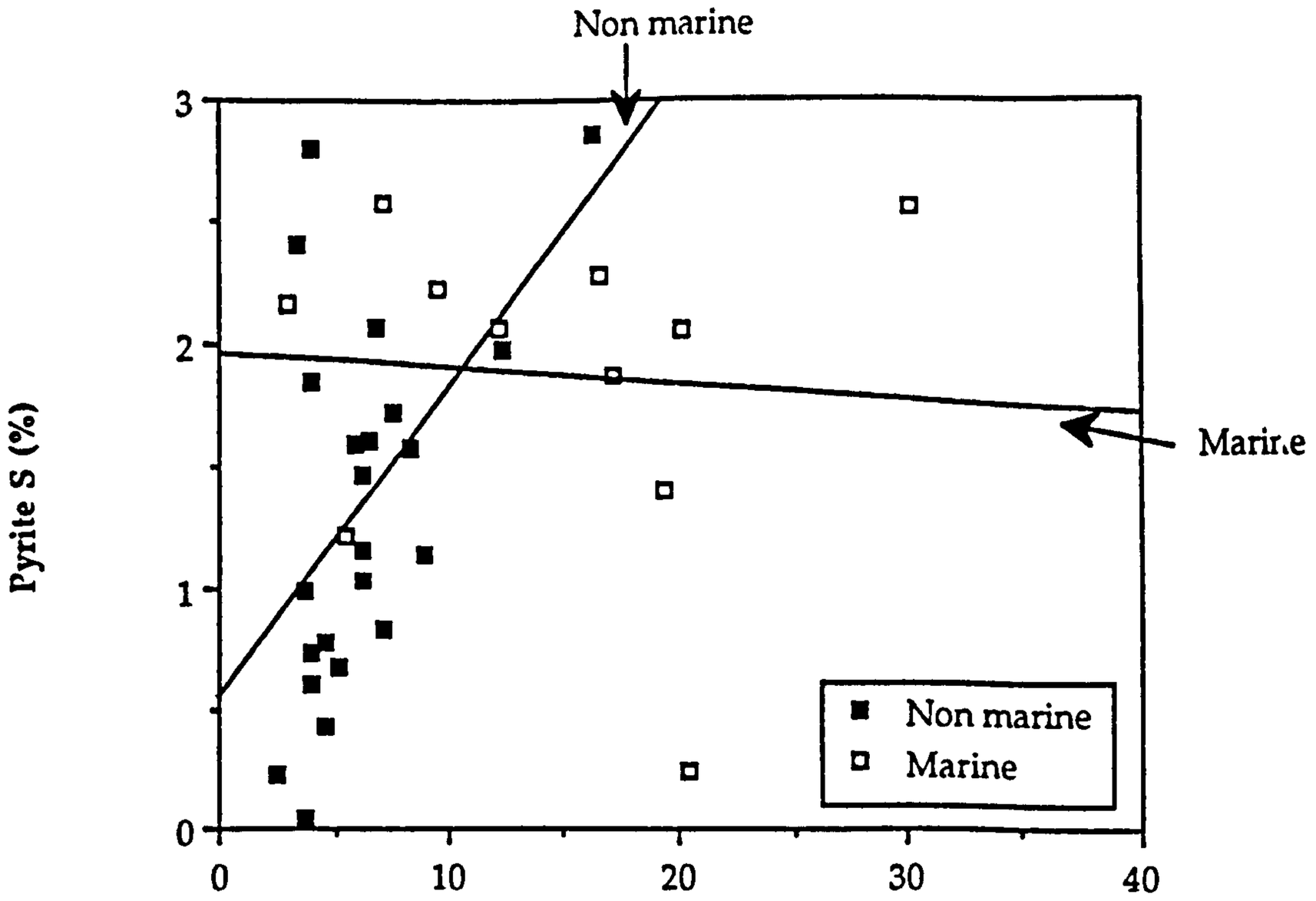

Figure 6.8 Graph showing %T.O.C v. %pyrite sulphur for marine and 'non-marine' samples from Inishcorker.

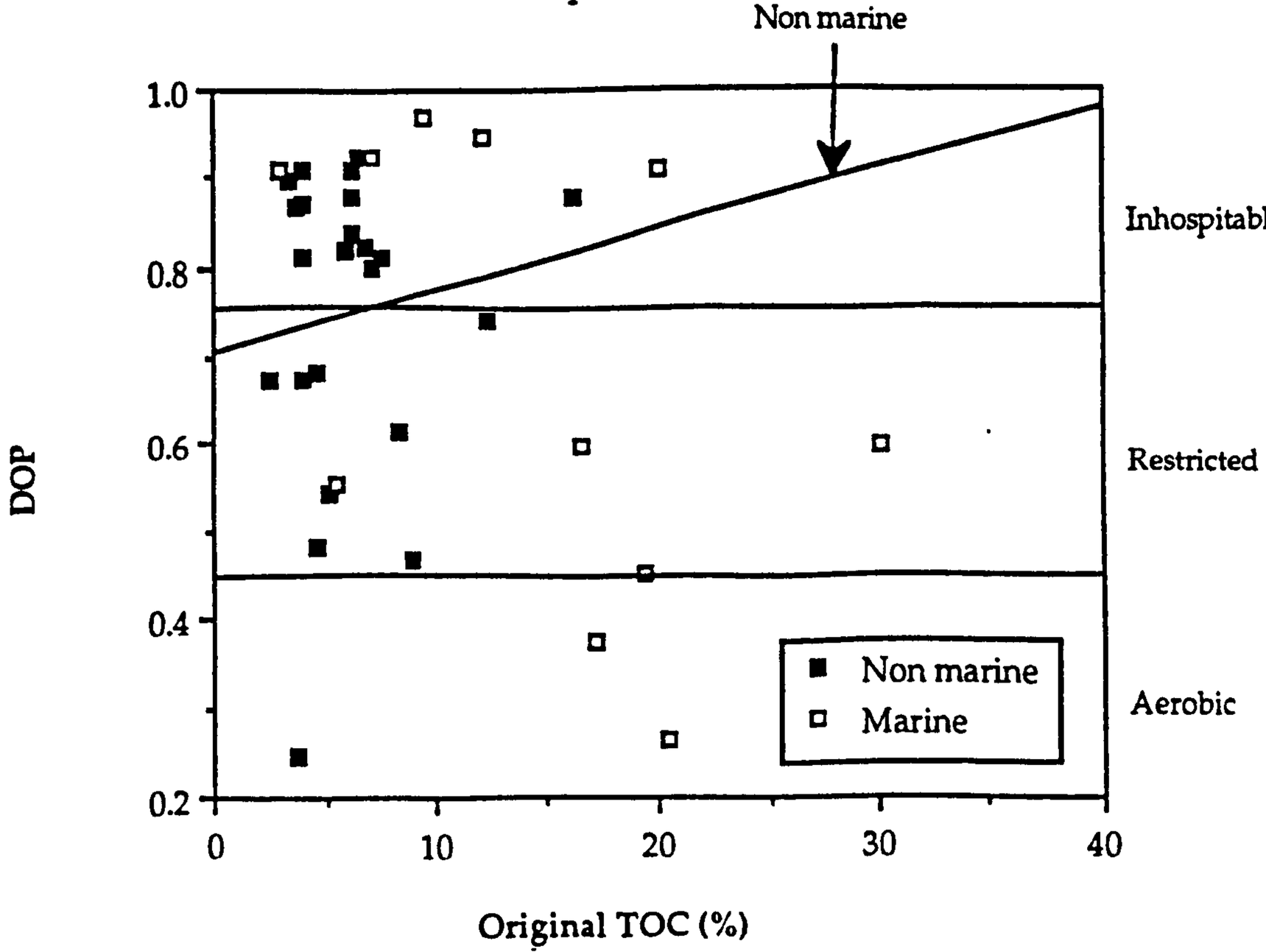

Figure 6.9 Graph showing %T.O.C. v. DOP for marine and 'non-marine' samples from Inishcorker.

freshwater entering the basin is in fact 'floating' on top of euxinic marine waters and only at times of mixing is freshwater sulphate concentrations an important control on pyrite formation. This is further discussed in chapter 7.

'Marine band' deposition shows a slight negative correlation between T.O.C. and pyrite sulphur. Once again a positive intercept is seen indicating syngenetic pyrite formation in a H_2S bearing water column (however, there is statistically only 62% confidence in this correlation). The negative correlation may indicate iron limited pyrite formation. With increased T.O.C. there is decreased pyrite formation, possibly this may have resulted from increased hydrogen sulphide loss from the sediment. In this case it is possible that all pyrite formed is produced syngenetically. The D.O.P. results show wide spread on the graph and no conclusions can be drawn.

Total organic carbon varies from 0.77 to 9.05 % through the section (which corrects to a range of pre-maturation values of 2.57% to 30.13%) the greatest organic carbon content is coincident with the E_2c^4 marine band. Total organic carbon peaks coincide with marine band development and are likely to be due to one or a combination of the following factors:-

1) Higher productivity
2) Higher preservation
3) Less dilution by sediment input.

High D.O.P. values tend to suggest that preservation in anoxic bottom waters was the most important factor in organic matter content for many of the marine bands. However, many of the Chokierian marine band samples show surprisingly low D.O.P. values and may suggest high productivity with more oxic, nutrient rich waters being present in the water column. However enigmatically no corresponding increase in benthic fauna (as might be expected) is seen with the decrease in D.O.P. values. Obviously as marine bands are equated with maximum flooding surfaces and therefore with sea-level highs it is expected that there is less dilution of the organic carbon by sediment, as sediment input to the basin will be trapped in a proximal position.

The graph of reactive versus total iron (Figure 6.10) shows separation of the two fields of 'non-marine' and marine strata (statistically significant at >99%). Marine band samples generally show higher reactive/total iron values than

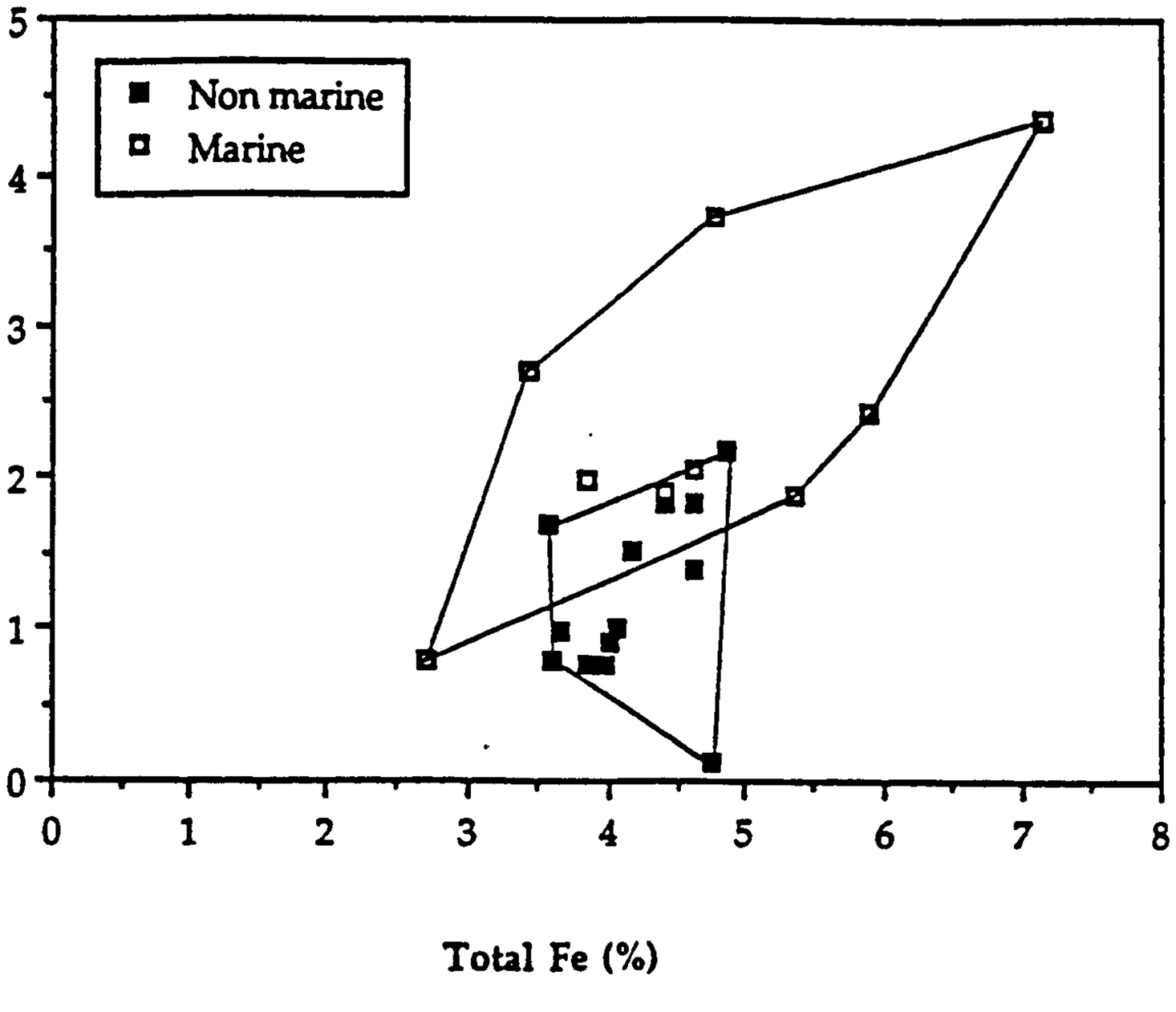

Figure 6.10 Graph showing %total Fe v. %reactive Fe for marine and 'non-marine' samples from Inishcorker.

'non-marine' samples. The average 'non marine' Fe: Fe ratio is 0.2917 and the average value for the marine sample is 0.5136.

Comparison with Raiswell (in prep) shows that reactive/total iron values from the 'non-marine' samples from Inishcorker plot in his dysaerobic field (Figure 6.6). But, D.O.P. values for these Inishcorker samples show that in the majority of cases deposition is in the 'inhospitable bottom' category. Thus, although the Raiswell model shows separation of fields for sediments with differing oxygen levels, a similar relationship also results from the nature of the iron complexes available. This can be related to the proximity of the sediment source and the spatial extent of the chemocline. If, as in the Clare Basin, there is a well developed chemocline at the top of the oxygen minimum layer separating H_2S-bearing from poorly oxic waters at most times, then the reactive/total iron value is influenced by detrital sediment input. Although the section at Inishcorker was deposited in the basin centre, fluctuations in the relative sea-level would have led to deposits indicative of both proximal and distal environments due to increased sediment input, and the differing extent of the chemocline, both of which are ultimately a function of sea-level.

An area more proximal to the sediment source is likely to receive more detrital iron although possibly still receiving the dissolved Fe^{2+} from the water column. Additionally however, it is possible that distal environments may show depressed ratios if there is a mechanism which allows deposition of large volumes of detrital iron in the basin centre, e.g. turbidites.

Reactive iron content depends on the stability and extent of the chemocline. The reduced spatial area of the chemocline at low sea-level and its lower position in the water column, will decrease the amount of dissolved Fe^{2+} added to the water column.

Relative sea level will effectively be the ultimate control on reactive: total iron ratios.

At low sea-level, it is envisaged that greater volumes of detrital deposits will reach the basin as a larger area is being eroded to fill a smaller basin. There is also the likelihood that increased freshwater run-off will ultimately increase mixing in the water column and therefore decrease chemocline stability (reducing amounts of Fe in solution).

At high sea-level, it is likely that the water column will be stratified leading to a stable chemocline and large amounts of reactive iron in solution. Sediment is likely to be trapped in proximal areas, allowing low amounts of detrital iron into the basin. The relatively high values of total iron for the marine bands is probably a function of the low sedimentation rate, i.e. the time available for detrital accumulation. However, it is possible that at extreme highstand that mixing of the water column occurs due to large scale oceanographic processes being set up because of the greater areal extent of the basin. Barriers between basins will be submerged and it is possible that the basin will receive both sediment and basinal waters from neighbouring regions.

6.6.2.2 Radioisotopes

Marine sediments show relative higher concentrations than non-marine sediments, with a peak of 20.8 ppm. Uranium peaks at marine bands reflect decreases in sedimentation rates therefore increasing the time available for U fixation (due to low dilution by sediment), increased chemocline stability (therefore increasing dissolved U in water column) and also increased organic contents. Marine sediments at Inishcorker show positive correlation between authigenic uranium and T.O.C., reflecting the role of organic matter in authigenic uranium precipitation (significance >95%) (Figure 6.11). 'Non marine sediments' do not show significant statistical correlation between T.O.C. and U, reflecting the fact that U contents are independent of T.O.C., thus, such factors such as sediment dilution may be important.

Th values can be of use in determining detrital input . As Th is present in the detrital fraction, changes in the amount of Th can be used as a crude qualitative measure of detrital input to the basin. Thus increases in Th may indicate increased detrital input i.e., there is less dilution of detrital heavy minerals by clays, (due to proximity to the sediment source, or due to selective sorting).

Values measured from marine horizons plot towards the U corner of the K-Th-U ternary diagram (Figure 6.12) and this trend is due to the combination of decreased detrital input together with increased uranium content (higher authigenic values).

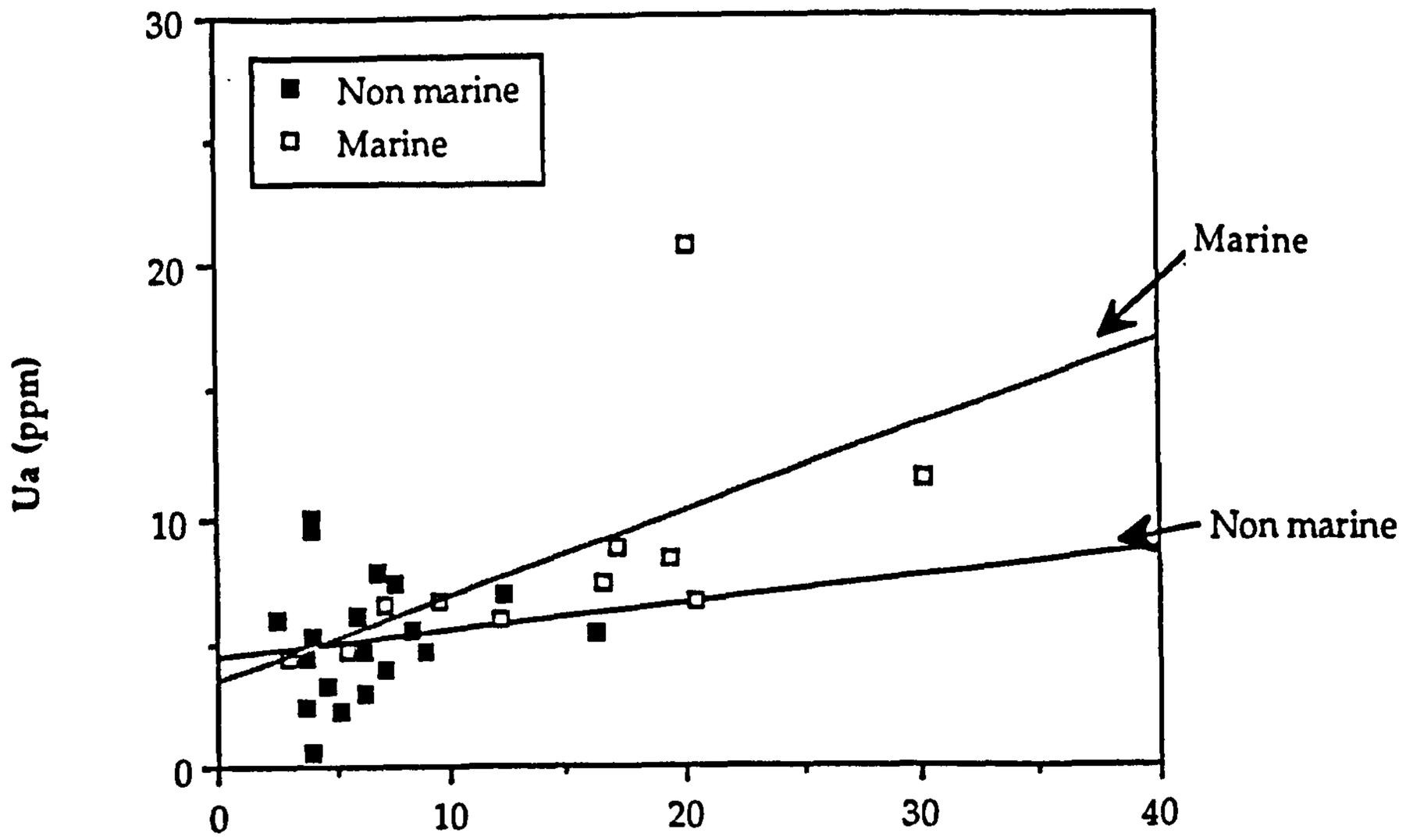

Figure 6.11 Graph showing %T.O.C. v. Ua (ppm) for marine and 'non-marine' samples from Inishcorker.

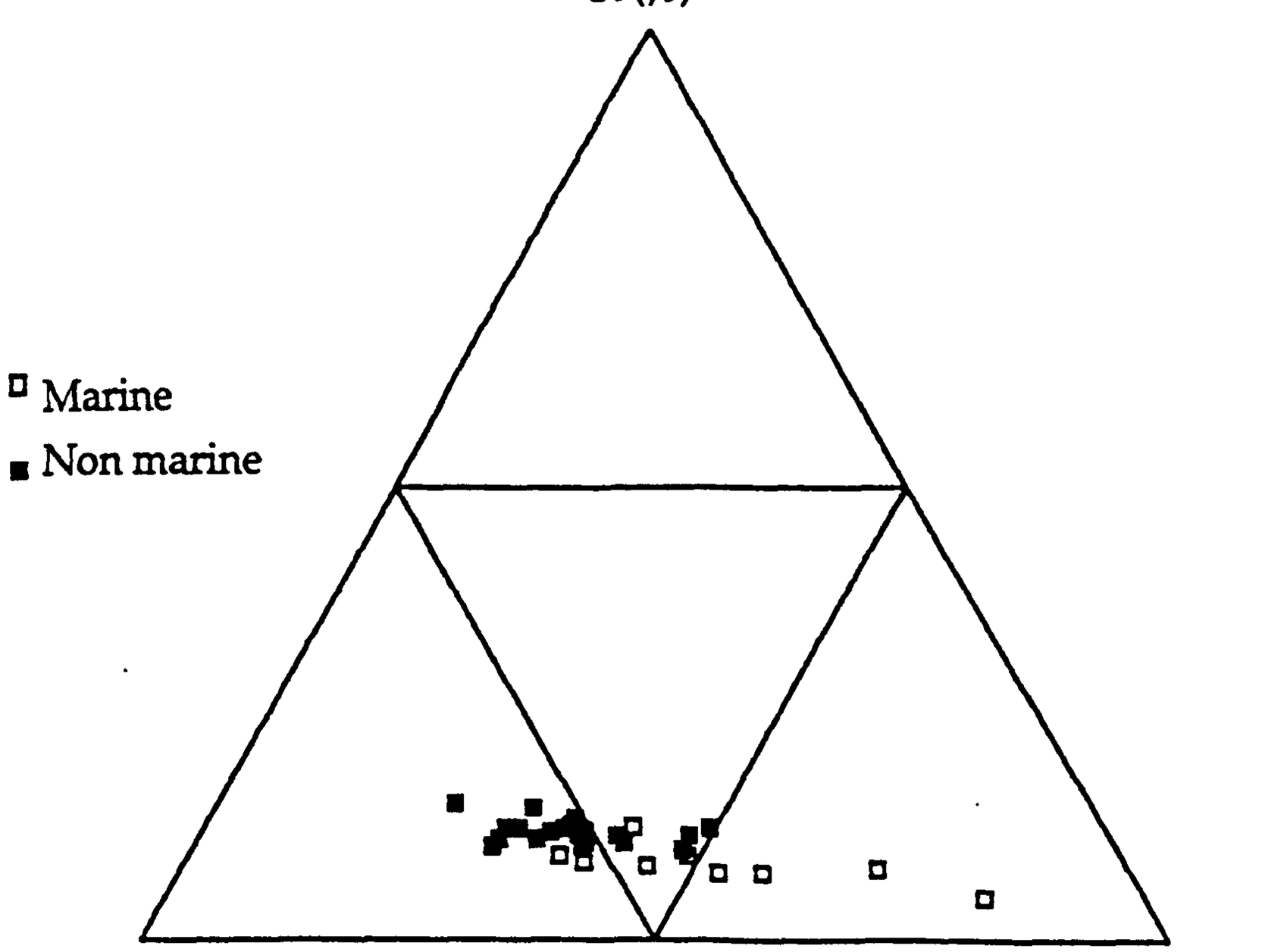

Figure 6.12 Ternary diagram showing U, Th (ppm) and %K for marine and 'non-marine' samples from Inishcorker.

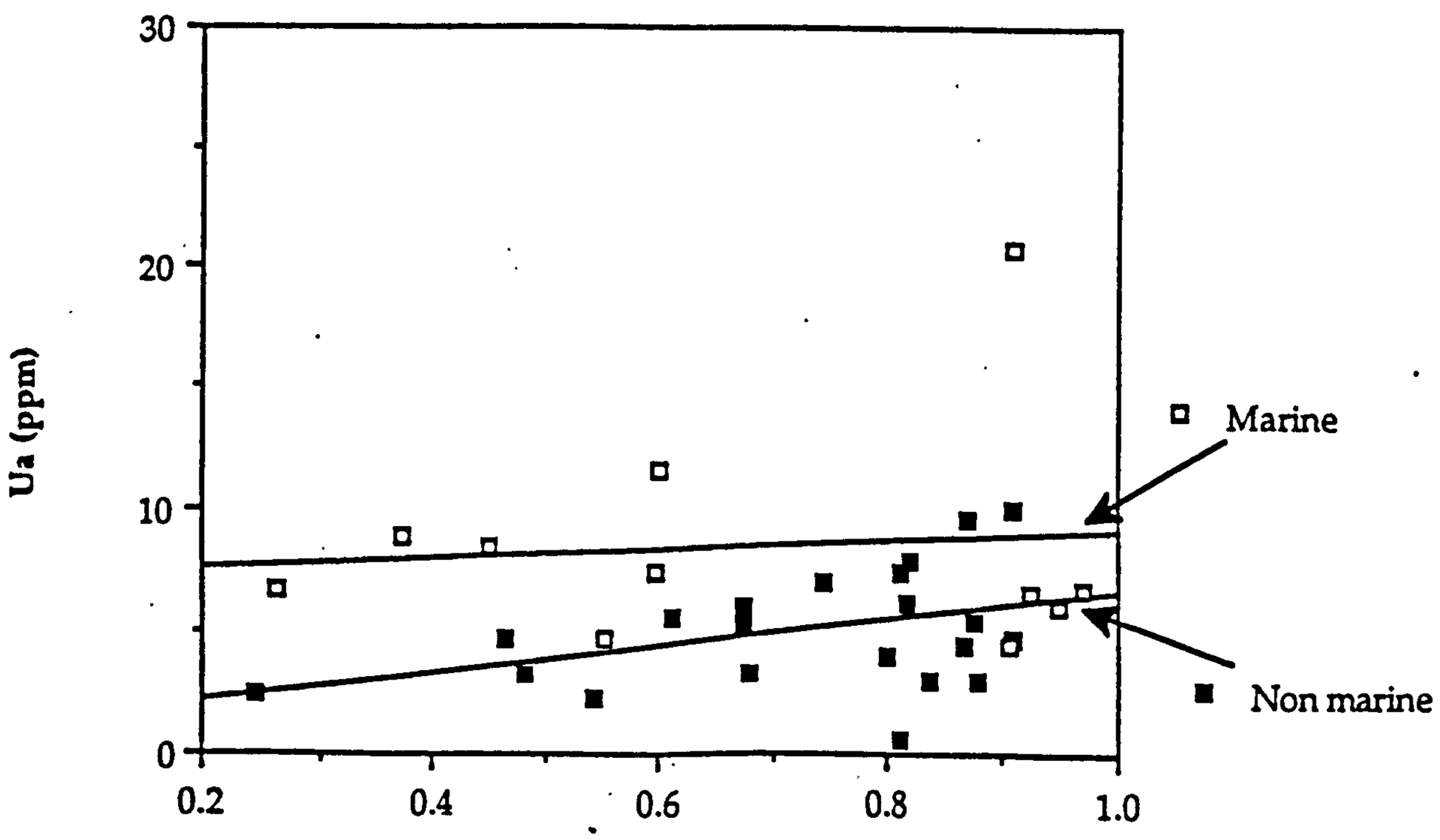

Figure 6.13 Graph showing D.O.P. v. Ua (ppm) for marine and 'non-marine' sediments from Inishcorker.

Marine sediments show higher average values of Ua for the same D.O.P. when compared to non marine sediments (Figure 6.13). Although D.O.P. values indicate anoxia in the environment, at any particular high D.O.P. value marine sediments show higher Ua values (than for non-marine strata), probably due to increased thickness of the oxygen minimum layer and therefore increased Ua in solution.

6.6.2.3 Relationship of the C-Fe-S and radioisotope geochemical techniques to sea-level.

By comparing D.O.P., reactive Fe/total Fe values, and detrital input it is possible to select a finite set of variations and relate these to sea-level. These are described in the Table 6.6. It is assumed that during low sea-level that the spatial extent of the chemocline (and thus the amount of Fe in solution) is a main controlling factor on reactive iron.

Table 6.6. Relationship between sea-level, D.O.P., reactive iron/total iron value and detrital input.

Sea-level	D.O.P.	Reactive/total Fe value	Detrital input	Scenario
High	High	High	Low	A Stratified basin
	High	Low	High	B Stratified basin
	Low	Low	Low	C Mixed basin
	Low	Low	High	D Mixed basin
	Low*	High	Low	E Mixed basin
	Moderate	Low	High	F Semi-mixed basin
	Moderate	High	Low	G Semi-mixed basin
Low	High	Low	High	H Stratified basin
	High	Low	Low	I Stratified basin
	Low	Low	High	J Mixed basin
	Low	Low	Low	K Mixed basin

* only feasible at extremely high sea-level, when sedimentation rates are minimal.

6.7. TEMPORAL TRENDS IN GEOCHEMICAL PARAMETERS THROUGH THE MID-CARBONIFEROUS AT INISHCORKER

6.7.1 Introduction

Reactive iron: total iron ratios are determined as high or low by using the average of the two average values for both marine and non-marine sediments (0.4026). It is assumed that organic carbon type does not vary through the section. When reviewing the following discussion the reader is referred to Tables 6.5, 6.6, 6.7 and 6.8 and Figure 6.14.

6.7.2 E_2c^2 cyclothem

Deposition in the lower part of the cyclothem was in a stratified euxinic basin (shown by high D.O.P. and enrichment in Ua). Maximum salinity values suggest a marine influence on deposition.

The upper part of the cyclothem shows deposition in restricted and aerobic environments probably in a variably mixed basin. This could relate to a period of instability and full mixing of the water column at a time of relative sea level low during the last stages of the cyclothem, when the ever-decreasing thickness of the water column could become increasingly deeply mixed. C/S ratios also indicate that freshwater was present at these times in the water column.

Detrital input was fairly high and increased towards the top of the cyclothem (shown by Th). Ua shows a slight drop towards the top of the cyclothem, probably also a response to decreased T.O.C. and decreased anoxia in the basin. Reactive/total iron values are low throughout the cyclothem and this is likely to be a function of detrital input and restricted chemocline extent.

It appears that the results may indicate either a relative sea-level high or relative low (B or H) at the base of the cycle (Table 6.6). However, as previously discussed increased detrital input is assumed to enter the basinal setting either during lowstand or by turbidite processes (which may occur at relative low or high stands). There is no evidence of turbidite processes occurring this early in the Clare Basin and thus it is assumed that detrital input is high due to increases related to lowstand. Towards the top of the cyclothem it appears that freshwater (possibly previously existing as a less

Method	Use	Criteria
D.O.P.	Palaeo-oxygenation.	Aerobic (D.O.P. <0.45), restricted (0.45≤D.O.P. <0.75) and inhospitable bottom (D.O.P. ≥0.75).
C/S	Palaeosalinity.	Marine (C/S 0.5-5.0) and freshwater (C/S values >10).
Ua	Palaeo-oxygenation.	Qualitative comparison between readings (increased Ua results from increased or prolonged anoxia).
Th	Detrital input	Qualitative comparison between readings (increased Th results from increased detrital input).
Reactive/ non reactive iron	Palaeo-oxygenation and detrital input.	Qualitative comparison between values (high values results from decreased detrital input and/or increased chemocline stability).
T.O.C.	Palaeo-oxygenation	Qualitative comparison between values (increased T.O.C. results from increased productivity or preservation).

Table 6.7 Summary of use and interpretation of geochemical methods.

Cyclothem	D.O.P.	T.O.C.	Reactive/ total Fe	Ua	C/S	Detrital input	Productivity v. preservation?	Sea-level.
H_1b^2	Low (aerobic) at base, increases towards top of marine band, then decreases to top of cyclothem.	Peak at marine band.	High at marine band.	Minor peak at marine band.	Marine and ?brackish.	Low at base, increased detrital input to top of cyclothem.	Productivity.	High. Oxic waters due to mixing (due to water influx/oceanographic processes) at base of marine band, followed by stagnancy as sea-level falls. Breakdown of chemocline at the end of the cycle.
H_1b^1	Moderate (restricted) during marine band, increases towards top of cyclothem.	No distinct changes.	High at marine band.	No distinct changes.	Marine.	Low, increases towards top of cyclothem.	Preservation.	High. Mixing at base due to water influx/oceanographic processes, then prolonged anoxia.
H_1a^3	Moderate (restricted) during marine band, increases towards top of cyclothem.	Peak at marine band.	n/a	No distinct changes.	Marine.	Low, increases towards top of cyclothem.	Productivity.	Rising. Mixing at base due to water influx/oceanographic processes. Increased detrital input as sediment routes are re-established.
H_1a^2	Moderate (restricted) during marine band, increases towards top of cyclothem.	Peak at marine band.	Generally high.	No distinct changes.	Marine and ?brackish.	Low.	Productivity.	Moderate-rising. Mixing at base due to water influx/oceanographic processes followed by sediment starvation in a well-stratified basin.
H_1a^1	High (euxinic).	Slight rise at marine band.	Low	No distinct changes.	Marine.	Low.	Preservation.	Low. Condensed deposits related to sediment starvation in a well-stratified basin.
E_2c^4	Moderate (restricted) during marine band, increases towards top of cyclothem.	Peak at marine band.	High at marine band.	Peak at marine band, decreases towards top of cyclothem.	Marine.	Low, increases towards top of cyclothem.	Productivity.	High. Mixing at base due to water influx/oceanographic processes, then prolonged anoxia.
E_2c^3	High (euxinic) at base, fluctuates to top of cyclothem.	Peak at marine band.	High at marine band.	Peak at marine band, decreases towards top of cyclothem.	Marine and ?brackish.	Increased input towards centre of cyclothem.	Preservation.	Moderate-rising. More prolonged anoxia.
E_2c^2	High (euxinic) at base, decreases to restricted and aerobic at top.	Peak at centre of cyclothem.	Constant low.	Peak at base, decreases towards top of cyclothem.	Marine at base, freshwater towards top of cyclothem.	Increased detrital input to top of cyclothem.	Preservation.	Low. High detrital input, and breakdown of chemocline and freshwater input at the end of the cyclothem.

Table 6.8. Table showing a summary of geochemical characteristics and interpreted sea-level changes for each cyclothem.

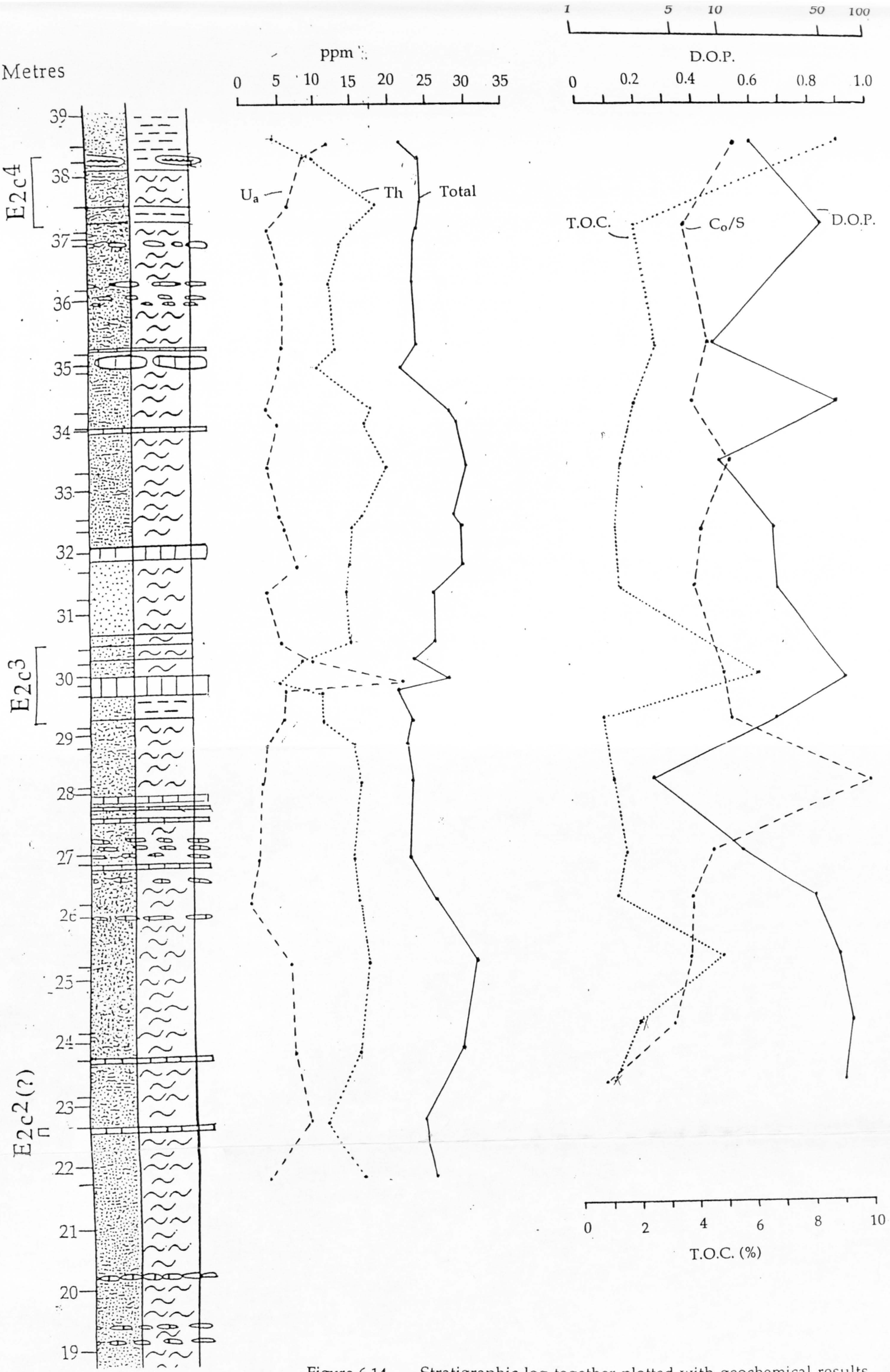

Figure 6.14 Stratigraphic log together plotted with geochemical results. Lower part of the section at Inishcorker.

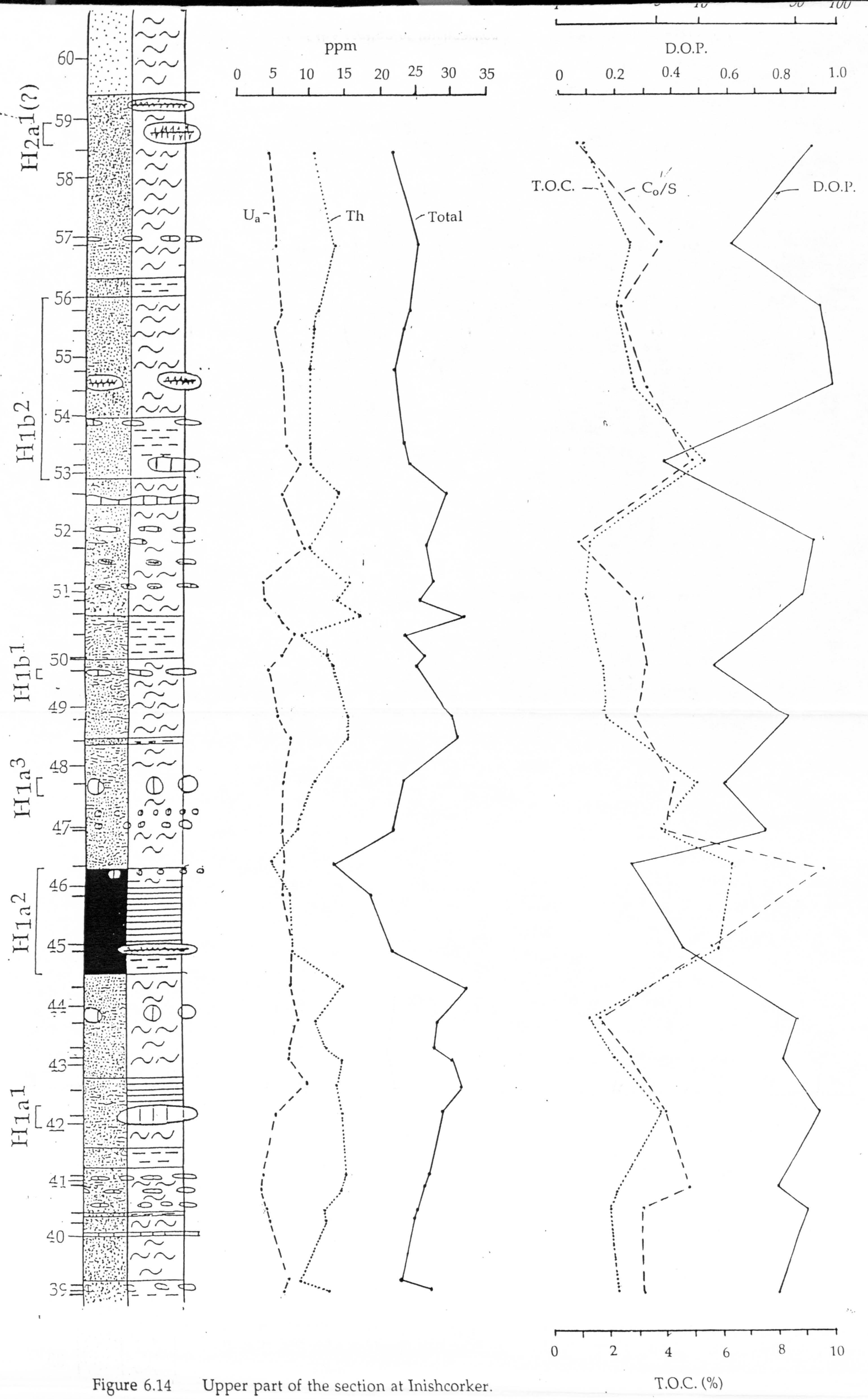

Figure 6.14 Upper part of the section at Inishcorker.

dense layer on top of the euxinic marine waters) is mixed to the base of the water column and influences pyrite diagenesis

6.7.3 E_2c^3 cyclothem

Deposition during the lower part of the cyclothem (at the marine band) was in a euxinic stratified basin (high D.O.P. high Ua) which consequently led to preservation of high amounts of organic matter. It is likely that the eustatic sea-level maximum during marine band development (and therefore increased chemocline stability and extent) and the corresponding depressed sedimentation rate conspire to allow more reactive Fe and Ua in solution and longer periods for U fixation.

The 'non marine' part of the cyclothem shows fluctuations in D.O.P. which indicate deposition in restricted and inhospitable bottom conditions with a short-lived anoxic event developed in the centre of the cyclothem, although it is not matched by either increases in Ua or T.O.C. Intermediate C/S ratios (5-10) are ambiguous and may reflect brackish water development, although some of the maximum C/S ratios associated with the euxinic 'non marine' sediments suggest marine conditions were prevalent.

Sediment input was fairly high in the lower part of the 'non marine' portion of the cyclothem, although it reduced towards the top. Reactive/total iron values are low throughout the 'non-marine' part of the cyclothem and this again is likely to be a function of detrital input and restricted chemocline extent.

Relative sea-level appears to have been higher than in the previous cyclothem. More prolonged anoxia occurs throughout the cyclothem and may indicate the presence of a thick water column resistant to surficial mixing processes. It is likely that scenario A applies (Table 6.6).

6.7.4 E_2c^4 cyclothem

Marine band deposition was in a restricted environment (moderate D.O.P. moderate Ua). However, extremely high amounts of T.O.C. (corrected values of 30%) are preserved, perhaps due to high productivity in a partially overturned nutrient-rich water column. Reduced detrital input in the lower part of the cyclothem results in a high reactive/total iron value.

Mixing may have been induced at high sea-level, when the basin had its greatest areal extent, by the establishment of large scale oceanic processes (e.g. gyres) within the basin, or due to the influence of an enormous volume of presumably colder, denser waters entering the basin as land connections were submerged during maximum transgression.

Towards the upper part of the cyclothem, as sea-level became lower, increased detrital input (and reduced chemocline extent) resulted in a decrease in reactive/total values and probable dilution of organic matter. Deposition in the upper part of the cyclothem was within an euxinic environment as sea-level fell and the large scale processes waned. A marine influence however is seen in these barren sediments; this may be related to the establishment of a well-stratified basin, with dense anoxic marine waters occupying a position at the base of the water column.

Sea-level was at a maximum during this cyclothem shown by low detrital input and long-lasting anoxia (scenario G).

6.7.5 H_1a^1 cyclothem

Deposition in the H_1a^1 cyclothem was in an euxinic stratified basin as indicated by high D.O.P. values. Detrital input fluctuated but was very low. Reactive/total detrital iron ratios are also generally low. Thus, as little sediment was reaching the depositional site, it is probable that the restricted spatial extent of the chemocline was a dominant factor on the low reactive /total iron values (and additionally Ua values). T.O.C. values are low and may reflect low nutrient availability in the stagnant waters. C/S values reflect marine deposition and thus the establishment of a well stratified water column.

Therefore comparison with Table 6.6 indicates a relative sea-level low (scenario I). It is probable that the chemocline was confined to the very basin centre. The low detrital input would result from sediment diversion away from the Clare Basin at extreme eustatic minima; the Clare Basin during the early Chokierian is thus effectively a stagnant lake.

6.7.6 H_1a^2 cyclothem

The H_1a^2 marine band shows deposition in a restricted environment. Both decreased sediment input and increased chemocline extent conspired to

increase the reactive/total iron ratios. It may be that the moderate D.O.P values may be induced by mixing during a high sea-level stand by the establishment of large scale oceanic processes or a large influx of cold dense waters within the basin in a similar way to that seen in the E_2c^4 marine band.

The marine band is unusually thick and may represent the re-establishment of sediment routes into the basin at high-stand or a prolonged period of marine deposition. The upper part of the marine band provides evidence of deposition in an aerobic environment together with high amounts of T.O.C. It therefore appears that marine band deposition culminated with the water column mixing.

However, the later part of the cyclothem sees a return to stagnancy, and possibly the establishment of brackish bottom waters. Increases in reactive iron are also seen probably reflecting greater chemocline stability, possibly reflecting restriction of the basin once again as sea-level fell during the upper part of the cyclothem. Consequently preservation potential of organic carbon is high.

The upper part of the marine band culminated in a breakdown in the chemocline stability and resultant complete overturn of the water column. It may be that links with adjacent basins were made and a great influx of water entered the basin. It may have alternatively been due to oceanographic processes. Sea-level fell higher in the cyclothem and detrital input increased as mixing decreased as the basin lost its interbasinal connections and the large scale processes waned, and once again the basin became stratified.

Scenario G appears to be applicable to the H_1a^2 marine band, i.e. sea level is rising from the major lowstand of H_1a^1.

6.7.7 H_1a^3 cyclothem

The base of the H_1a^3 cyclothem shows increased T.O.C. with deposition in restricted bottom waters (shown by Ua and D.O.P). Reactive iron content is high and is likely to be related to decreased sediment input during marine band formation. Again partial overturn may be related to large scale oceanographic processes being set up during maximum transgression or the influx of cold marine waters.

The upper 'non marine' part of the cyclothem shows deposition in inhospitable environment (high D.O.P.) with a corresponding increase in gamma-ray Th reflecting increased sedimentation rates in a more stagnant environment. Again C/S reflects a marine influence on diagenesis.

Further rise in sea-level is indicated at the base of the H_1a^3 cyclothem with a return to a mixed water column (due to greater oceanographic processes and possibly fresh, cold, seawater input). Scenario G appears to be relate to this cyclothem. Sea-level was rising during late *Isohomoceras* times with increased detrital input as sediment routes were re-established into the basin during later parts of the cyclothem (and the turbidite fronted Ross delta progrades).

6.7.8 H_1b^1 cyclothem

Similar to previous cyclothems the base of the marine band shows a decrease in D.O.P. to a restricted environment and thus partial overturn of the water column. No peak is seen in Ua. A relatively high reactive/total iron value is seen indicating depressed detrital input.

The upper part of the cyclothem shows fluctuations in the gamma-ray Th signature and thus detrital input. D.O.P. however is high and reflects the return of stagnant conditions as sea-level dropped and mixing processes and marine connections were lost. Marine conditions are dominant throughout the cyclothem and may reflect the great volume of marine waters assumed to enter the basin at this time, or again stratification of the water column.

Further rise is seen in the H_1b^1 cyclothem with mixing of the water column and decreased detrital input due to similar processes as for H_1a^3 (scenario G). Falling sea-level at the close of the cyclothem resulted in further stagnancy and increased detrital input.

6.7.9 H_1b^2 cyclothem

The base of the marine band shows a low Ua and low D.O.P. (aerobic). Reactive/total Fe is high (relating to decreased detrital input at the very base of the marine band). Productivity is probably the dominant control on T.O.C. contents, presumably due to the formation of a nutrient-rich water column as the stratification was overturned (due to processes as mentioned in previous sections). The upper parts of the marine band indicate anoxic

deposition although no peak is seen in T.O.C. nor Ua perhaps reflecting deposition in distal stagnant nutrient poor environment with dilution by sediment (as the H_1b^2 cyclothem is very thick indicating high sedimentation rates during its deposition).

Non-marine strata show decreases in D.O.P. which are related to increased water column mixing, and consequently a increase in C/S is seen possibly relating to the influence of brackish waters on pyrite formation.

Sea-level highstand occurred in the marine band base with cold, oxic waters added to the basin. Full mixing of the water column occurred. Detrital input was low but increased as sea-level drops (and the turbidite-fronted Ross delta progrades). Stagnancy occurred as sea level dropped and mixing processes waned, although it was re-established towards the top of the cyclothem as the chemocline broke down. Scenario E is likely to be applicable.

The relationships between sea-level, marine band and the mid-Carboniferous boundary will be further addressed in chapter 7. Interbasinal connections and the overall basin history of the Clare Basin are also discussed.

6.8. SPATIAL TRENDS IN AUTHIGENIC URANIUM CONTENT THROUGHOUT THE CLARE BASIN.

On the shelf area the gamma-ray signatures from strata occurring below the phosphorite have been measured at Ballyshanny (Figure 6.15). Detrital input was steady. Ua contents increase up towards the phosphorite with the sediment directly below the phosphorite showing values of 68 ppm. It appears that the basin is stagnant in the shelf area throughout deposition of the phosphorite shales. Ua values are probably related to high anoxia and incorporation of U in the phosphorite nodules. As no definite age can be assigned to the phosphorite horizon it is unknown whether this period correlates to any of the sections at Inishcorker, although it is unlikely. The phosphorite horizon shows a peak of 85.5 ppm. at Ballyshanny House. Th content is very high in the proximal shelf region at St. Brendan's Well (44 ppm) and consequently U is lower (63.6 ppm) (Figure 6.16). This high amount of detrital Th is very probably related to hydraulic sorting of the heavy minerals in a more proximal area (see section 5.5.3). A slow drop-off in the gamma-ray signatures after the phosphorite occurs.

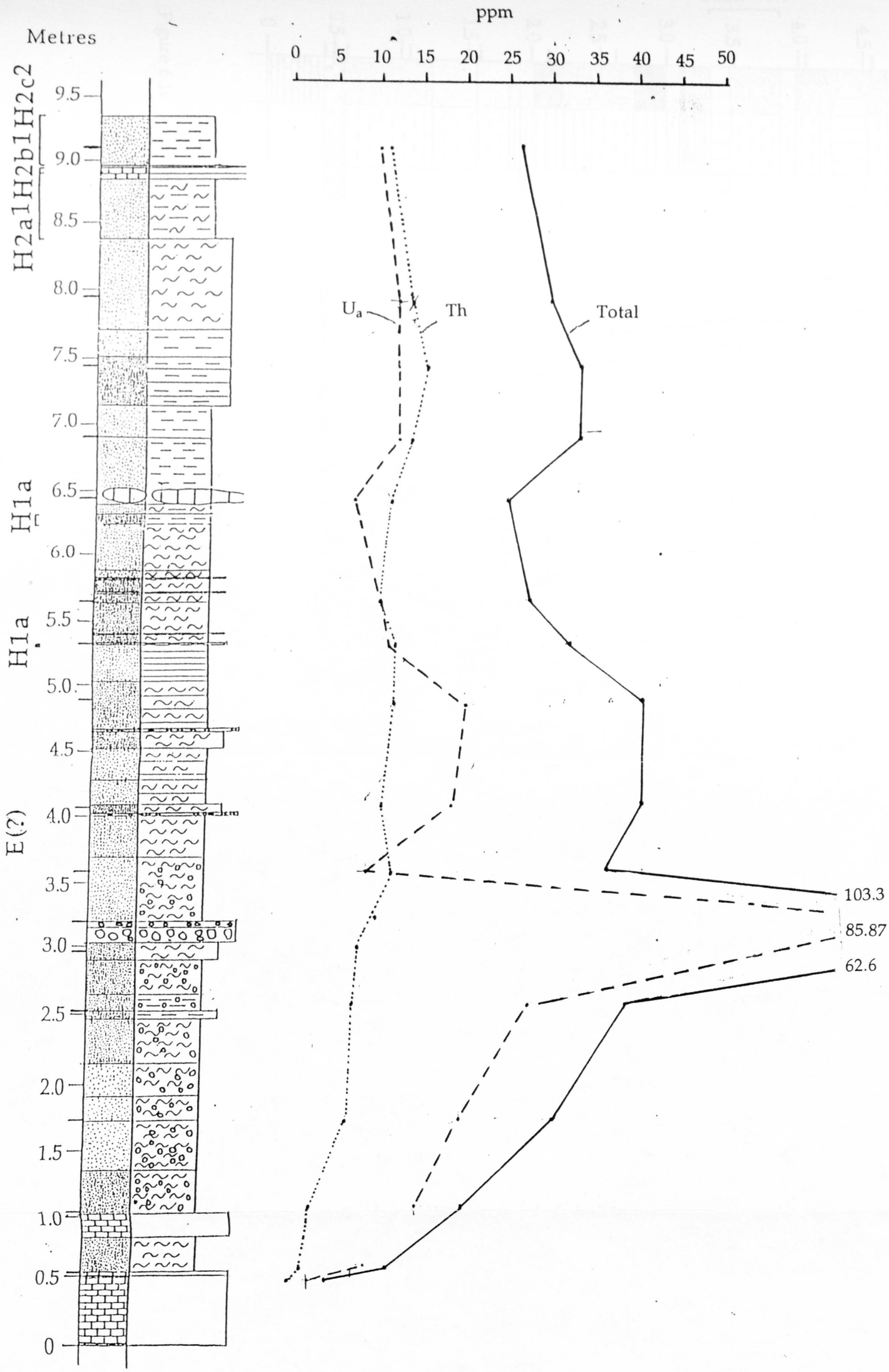

Figure 6.15 Stratigraphic log and gamma-ray spectrometry data measured at Ballyshanny House.

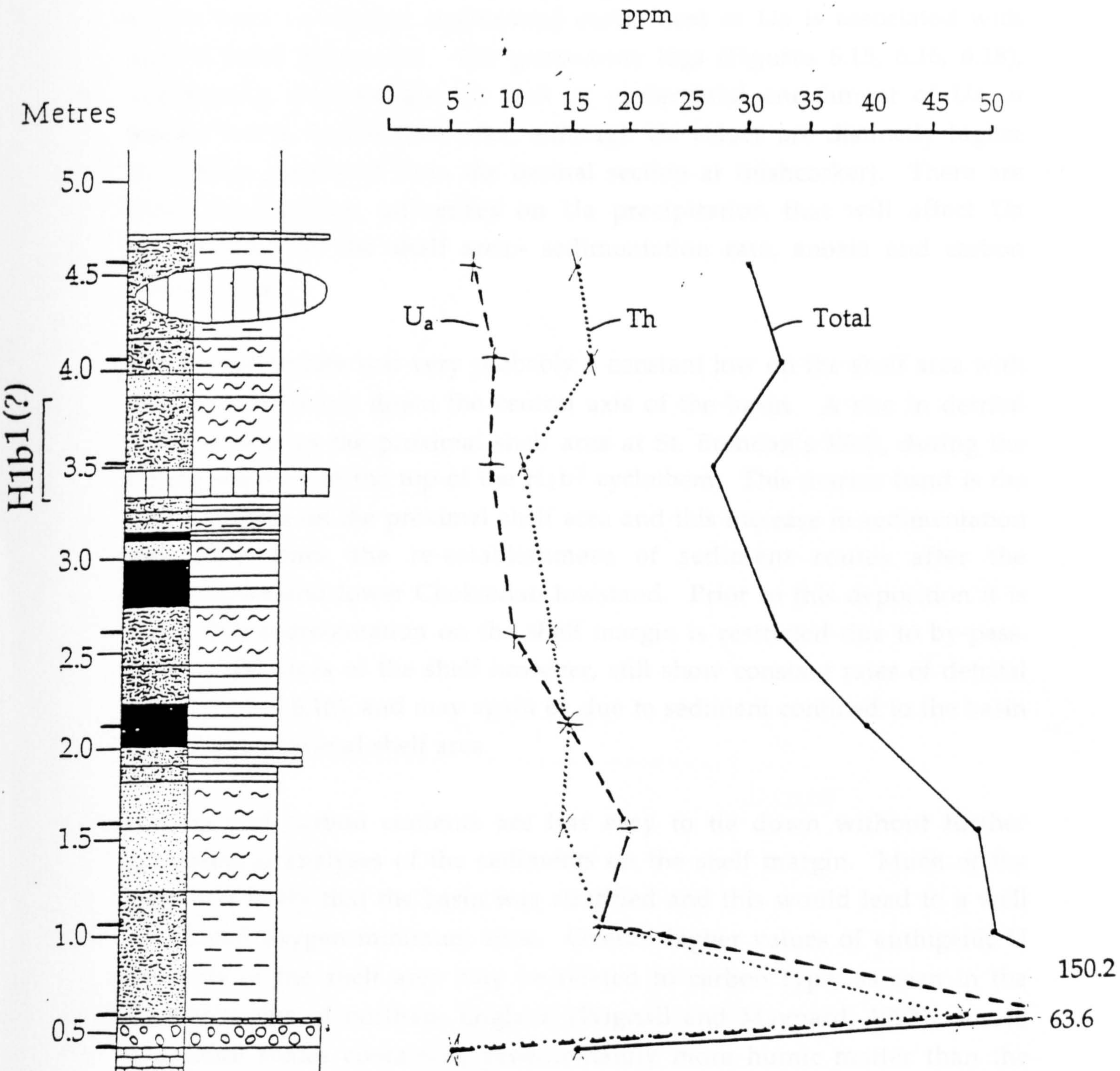

Figure 6.16 Stratigraphic log and gamma-ray spectrometry data measured at St Brendans Well

The ternary diagram for all post-phosphorite gamma-ray values (Figure 6.17) shows no distinct preferential enrichment in Ua is associated with marine band deposition. The gamma-ray logs (Figures 6.15, 6.16, 6.18), additionally demonstrate the lack of preferential enrichment of Ua in marine bands on the shelf area, although Ua values are distinctly higher than those measured from the basinal section at Inishcorker). There are three predominant influences on Ua precipitation that will affect Ua precipitation on the shelf area:- sedimentation rate, anoxia and carbon content/type.

Sedimentation rate was very probably a constant low on the shelf area with sediment diversion down the central axis of the basin. A rise in detrital input is seen in the proximal shelf area at St. Brendan's Well, during the falling sea-level at the top of the H_1b^1 cyclothem. This marine band is the oldest present on the proximal shelf area and this increase in sedimentation rate may mark the re-establishment of sediment routes after the Arnsbergian and lower Chokierian lowstand. Prior to this deposition it is likely that sedimentation on the shelf margin is restricted due to by-pass. More distal areas of the shelf however, still show constant rates of detrital input (Figure 6.18), and may again be due to sediment confined to the basin centre and proximal shelf area.

Anoxia and carbon contents are less easy to tie down without further geochemical analyses of the sediments on the shelf margin. Much of the time it is likely that the basin was stratified and this would lead to a well developed oxygen minimum zone. Overall higher values of authigenic U contents in the shelf area may be related to carbon type, as seen in the Carboniferous of northern England (Wignall and Maynard, 1993), due to nearshore shales containing predominantly more humic matter than the distal shales. Thus, a combination of both constant low oxygen levels and carbon type may lead to generally high values of authigenic uranium precipitation. The lack of preferential enrichment of Ua in the later Chokierian and early Alportian marine bands (also seen interestingly in the basinal deposits) is enigmatic, although it may be a function of sedimentation rate and prolonged anoxia.

The Luggacurren section shows a section similar to that in the Clare Basin (Figures 6.19 and 6.20). Unlike the sections present on the shelves of the Clare Basin the Luggacurren section shows a gamma-ray signature similar to that observed at Inishcorker. Definite Ua peaks correlate to marine band

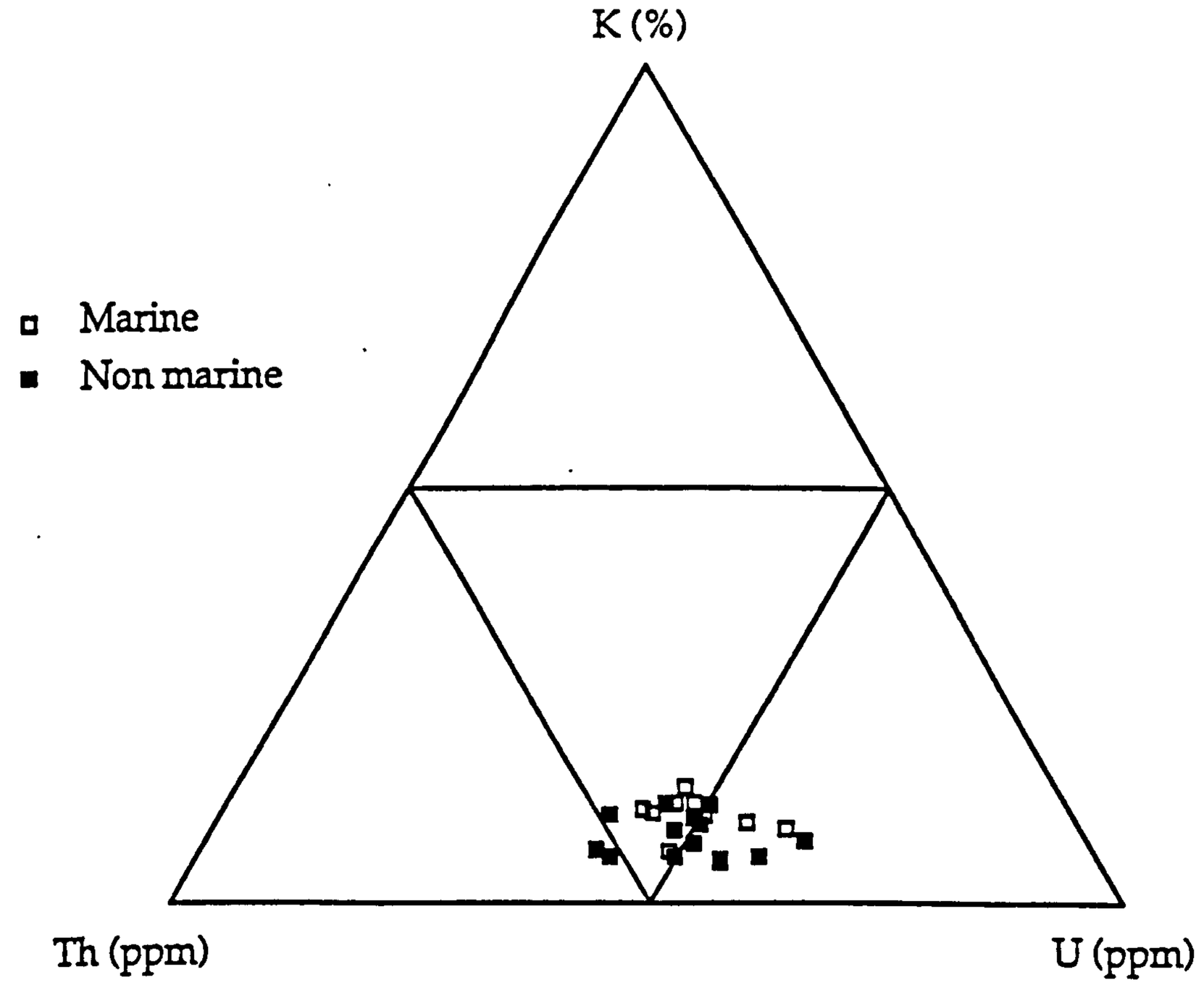

Figure 6.17 Ternary diagram showing U, Th (ppm) and %K for all post-phosphorite marine and non-marine readings at sampled localities in County Clare.

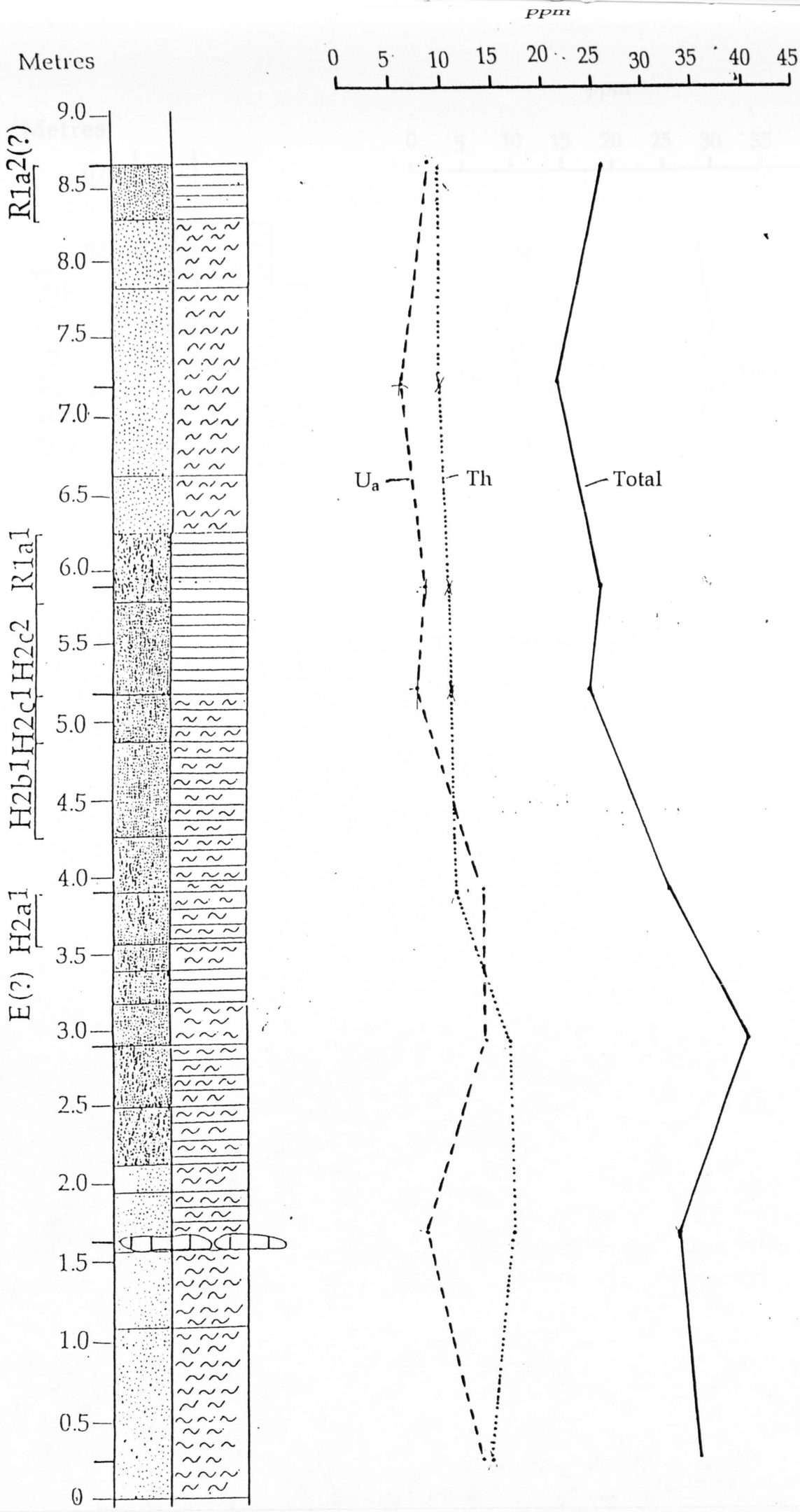

Figure 6.18 Stratigraphic log and gamma-ray spectrometry data measured at Lough Raha.

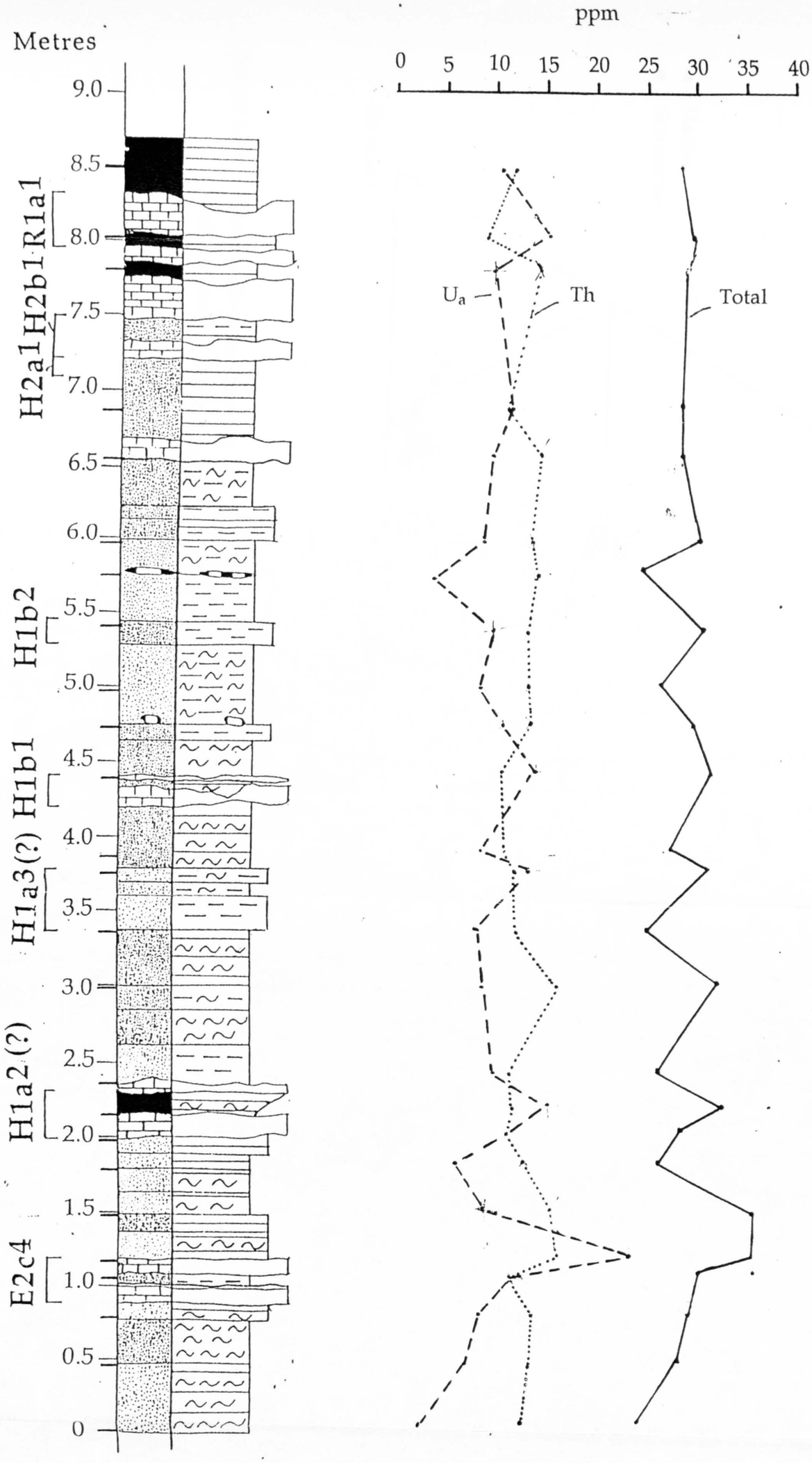

Figure 6.19 Stratigraphic log and gamma-ray spectrometry data measured at Luggacurren.

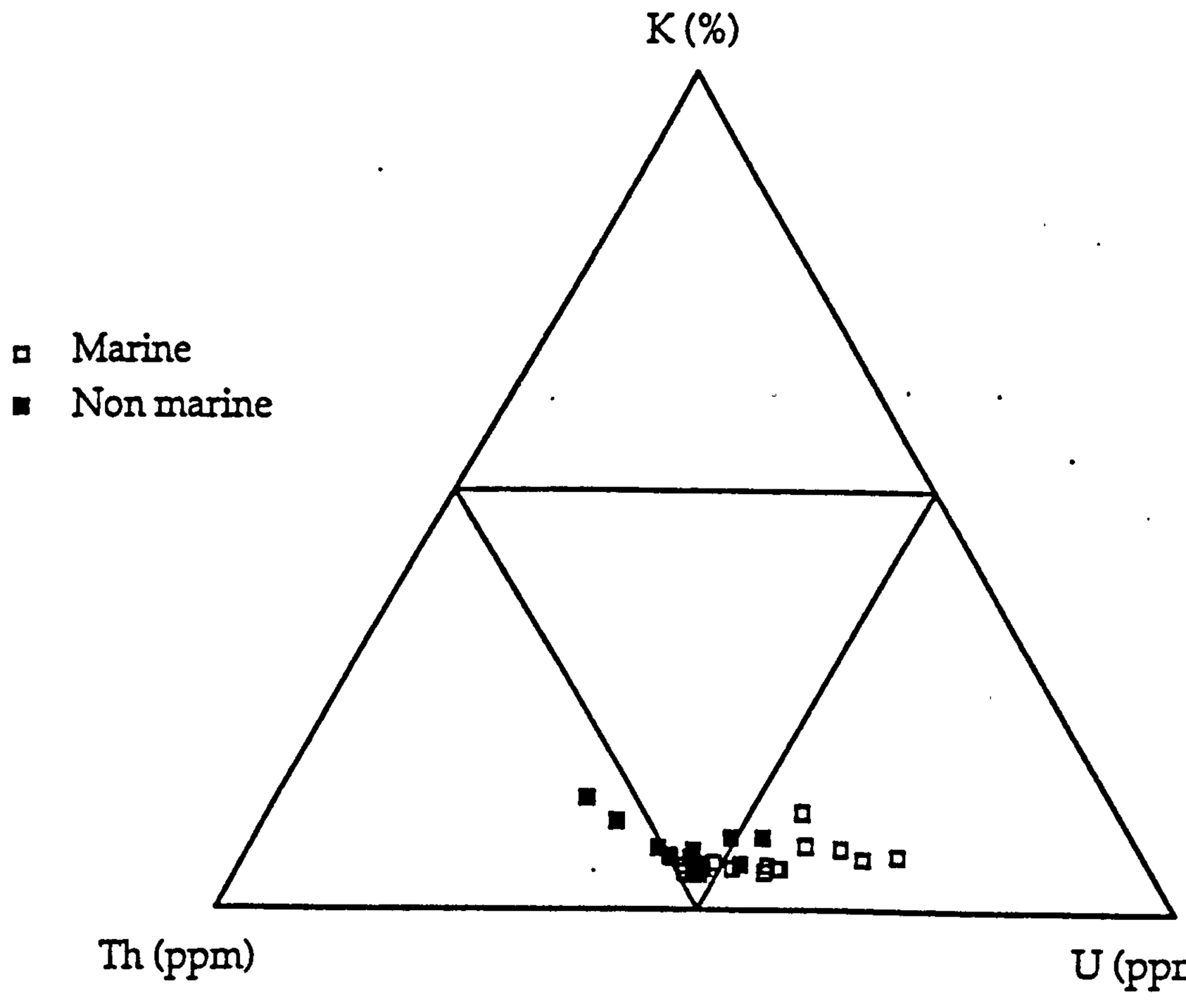

Figure 6.20 Ternary diagram showing U, Th (ppm) and %K for marine and 'non-marine' strata at Luggacurren.

development. Th values fluctuate and can also be related to increased detrital input in the upper parts of the cyclothems.

6.9 CONCLUSIONS

1) Distinct geochemical differences are seen between 'non-marine sediments' and 'marine bands' in the centre of the Clare Basin

'Non marine' sediments show pyrite formation comprising both syngenetic and diagenetic components with diagenetic pyrite being carbon-limited. Much of the iron available for pyrite formation is contained in the detrital fraction. The assumption that sediments deposited outside marine bands are non marine appears to be incorrect for sediments deposited in the Clare Basin. For much of the mid-Carboniferous the Clare Basin appears to have been euxinic, thus the stratification of the water column exerts a major control on pyrite formation, with little influence of freshwater sulphate values. It is envisaged that the freshwater entering the basin exists as a 'pool' floating on the surface of denser marine waters. Only at times of mixing (commonly towards the end of cyclothems when a decreasing thickness of water column can be easily mixed) do sediments show a brackish or freshwater influence on pyrite formation.

Marine sediments also show syngenetic pyrite formation, which is limited by iron availability. It is possible that no diagenetic pyrite formation occurs. Iron available for pyrite formation is mostly provided from reactive iron in solution.

2) Overall, shelf sediments show a distinct enrichment in authigenic uranium compared with the more basinal deposits; this is probably related to the incorporation in phosphorite complexes in the pre-Chokierian aged strata. Chokierian and later strata probably owe their enrichment to the type of organic carbon present. No preferential enrichment is seen between marine and non marine sediments in later Chokierian strata this is enigmatic, but may be a function of sedimentation rate and prolonged anoxia.

3) By comparing values of D.O.P, reactive iron: total iron ratios and sedimentation rates a correlation chart between sea level and these geochemical parameters has been produced. When applied to the values

obtained from the Inishcorker section, relative sea-level changes can be deduced.

Th upper Arnsbergian shows a rise in sea-level with a maximum reached in the E_2c^4 cyclothem. The base of the Chokierian however, is marked by a dramatic fall in sea-level, probably with sediment routes completely diverted away from the Clare Basin. The mid-Carboniferous sees the Clare basin as effectively a stagnant lake. A rise in sea-level is then seen through the Chokierian, with the H_1b^1 and H_1b^2 (*Homoceras beyrichianum* and *Isohomoceras sp. nov.* marine bands) showing extremely high sea-level stand.

It thus appears that the global lowstand that in many places marks the mid-Carboniferous boundary (defined as the change from *Eumorphoceras* to *Homoceras* sp. ammonoids) can be distinguished geochemically in a basinal setting even if deposition is continuous through the boundary.

Chapter 7

MODEL FOR THE DEPOSITION OF THE MID-CARBONIFEROUS CLARE SHALE FORMATION IN COUNTY CLARE.

7.1 INTRODUCTION

This chapter acts to assemble and summarise the data presented in the previous three chapters, and determine the major controls on sedimentation during mid-Carboniferous times in the Clare Basin, and also provide a model for deposition during the early and middle parts of the Namurian for the Clare Basin.

7.2 CONTROLS ON DEPOSITION OF THE CLARE SHALE FORMATION

There are three main controls on the deposition of the Clare Shale Formation: basin configuration, extent of sea-level changes and sediment supply.

7.2.1 Basin configuration

The bathymetric framework, interbasinal connections and basinal energy are inherently controlled by the basinal morphology.

7.2.1.1 Bathymetric framework

Rapid subsidence occurred in the centre of the Clare Basin during Viséan and early Namurian times, whilst the stable shelves to the north in County Clare subsided more slowly (Strogen, 1988). This led to the starvation of the northern shelves as clastic deposits were preferentially funnelled down the axis of the Clare basin during the early Namurian, so that dramatic variations are seen in the thickness of the Clare Shale Formation, with 12 m

of shale in the northern part of the County in comparison to 215 m of strata in the Shannon area.

Deposition during the middle and upper Namurian (from the Ross Formation onwards) is thought to have been in a more uniformly subsiding basin (Collinson *et al.*, 1991). Basin-fill only reached base-level during deposition of the Tullig cyclothem in the Marsdenian. Variations in thickness of deposits between northern and southern County Clare are seen throughout the Namurian e.g. the Gull Island Formation is 550 m in the basin centre whilst only 130 m is developed to the north) (Collinson *et al.*, 1991) however later cyclothemic deposits show less contrast in thickness. It may be that some differential subsidence was still occurring during the later parts of the Namurian or that the effects of inherited topography are still seen during the upper Namurian.

7.2.1.2 Interbasinal connections

The Clare Basin seems to have had no direct open sea connections during mid-Carboniferous times (Ziegler, 1982). The basin appears to have been bounded to the south by the Leinster High and the Galway High to the north (Hodson, 1957; Sevastopulo, 1981). To the east of the basin it is probable that a palaeo-topographic high was in evidence (and thus the Clare Basin is effectively silled), although this hypothesis is based on the very few exposures of Namurian rocks between the Clare Basin and the Leinster Basin, (e.g., Shelford (1963) recognised an unconformity spanning late Dinantian to Marsdenian times in the Limerick Basin). Thus, it appears that the depositional basins during the mid-Carboniferous in Ireland were small and separated from each other by shallow and emergent areas of low relief, as envisaged for the basins of northern England (Holdsworth and Collinson, 1988).

Holdsworth and Collinson (1988) also suggested that marine incursions may have involved marine connections being developed via Poland and Russia, a distance of over 2000 km.

Therefore, except at times during marine band formation, it is highly likely that the Clare Basin had no interbasinal connections and appears to have been a stagnant backwater of the main northern European Basins.

7.2.1.3. Basinal energy.

Basinal energy in the Clare Basin was likely to be influenced by:-

a) Wave processes (Pulham, 1989).

b) Highstand establishment of oceanic processes such as mesoscale eddies (Brown *et al.*, 1993).

c) Breaking of internal waves.

d) Sinking plumes of dense water (Gade and Edwards, 1980).

e) Boundary mixing between different water masses.

f) Thermohaline currents driven from oceanic connection and aided by freshwater plumes or surface evaporation (Collinson, 1988).

There is no evidence of tidal processes in the Clare Basin. It is likely that the long distance, shallow water connections between the Clare Basin and any open ocean would severely damp tidal flow (Collinson, 1988).

From computer modelling of the Cretaceous Interior Seaway of North America Jewell (1993) was able to model the effect of storms on a stratified water column. If it is assumed that during a relative sea-level high the Carboniferous basins of western Europe were linked into a seaway of comparable size to that of the Cretaceous of North America, then it can be shown that winter storms can mix up to 200 m down into the stratified water column. This may provide an estimate of the minimum depth of water attained during the marine band deposition in the mid-Carboniferous of the Clare Basin (Heckel (1991) estimates a minimum depth of 100-200 m for the deep water deposition of Pennsylvanian cyclothems in the U.S.A.)

7.2.2 Sea-level changes and salinity

Changes in sea-level during the Namurian are commonly thought to have been glacially driven (see section 1.4.3.3). Individual cyclothems show fluctuations in sea-level with the development of a marine band at the base representing deposition within fully saline conditions developed at maximum water depth within that cycle. It is also noted that sea-level changes may be of varying amplitude between cyclothems (Ramsbottom, 1969). Heckel (1991) noted that fluctuations in the Gondwanan ice-sheet would easily have been capable of producing sea-level rises in the order of 200-250 m.

During high sea-level the low-relief barriers between basins would be submerged and it is possible that the basin would receive both sediment (in suspension) and basinal waters from neighbouring regions. Additionally these connections between basins allowed the free migration of fauna. During the sea-level highstand associated with marine band deposition (e.g. *Homoceras beyrichianum* marine band) free connections between basins ranging from the Urals to western America were forged. It is likely that the water column would have been virtually permanently stratified, due to both salinity and temperature gradients, as in equatorial regions today. The greater depth of water may also have resulted in a stratification of the water column due to the increased thickness of the water column that would have been unmixed by predominantly surficial wind-driven mixing processes. However, at extreme highstand, mixing of the water column may have occurred due to large scale oceanographic processes being set up due to the greater areal extent of the basin and/or large volumes of colder, denser, oxygenated waters enter the basin. Sedimentation rates would be low as the sediment becomes trapped in proximal areas. Both these mechanisms conspire to provide high values of organic carbon within the sediment, as high productivity may result from partial overturn of the water column or from the influx of fresh waters into the basin; low sedimentation rates allow low dilution of the organic carbon added to the sediment.

During lowstand it is likely that greater volumes of detrital deposits would reach the basin. Increased freshwater run-off would also enter the basin. This, the reduction in any large scale oceanographic processes, and the reduced oceanic exchange developed at high sea-level, may however, result in thermohaline stratification of the water column (Heckel, 1991). During later parts of the cyclothem, complete breakdown of the stratification may occur as the basin becomes fully freshwater and turbulent wind-driven processes mix an ever decreasing thickness of water column. At extreme lowstand very low sedimentation rates may result if sediment diversion due to channel avulsion away from the basin takes place.

Salinity variations are a function of both the extent of the sea-level change (and thus the amount of saline water brought into the basin during maximum flooding), the amount freshwater discharge into the basin and the intensity of the stratification of the water column. During maximum flooding the effect of dilution by the freshwater was masked by the high volumes of fully saline basinal waters developed as oceanic connections were forged when the low-relief topographic highs were submerged.

Additionally the lower density freshwater may have been able to float on the denser saline waters (Holdsworth and Collinson, 1988). During lower base-levels the oceanic connections were lost and the basin would have become desalinated as freshwater entered a restricted basin. Holdsworth and Collinson (1988) have calculated that an 'average' British Carboniferous basin could become desalinated in as little as 32 years. Salinity variations are further discussed in sections 7.3.1 and 7.3.2.1.

7.2.3 Sediment supply

Sediment supply during deposition of the Clare Shale Formation shows a constant source (shown by Figure 6.12). The shales represent fall-out from suspension under quiet conditions. Increased sedimentation rates in the centre of the basin occurred towards late Chokierian times, prior to the arrival of the turbidites of the Ross Formation. Palaeocurrent measurements in both the Ross Formation and Gull Island Formation indicate sourcing from the west (Collinson *et al.*, 1991), possibly from a region of uplift related to proto-Atlantic rifting (Haszeldine, 1984, 1988) or marginal uplift (Leeder, 1988a). As the Clare Shale Formation represents deposition of pro-delta sediments of the Ross/Tullig Delta, it is envisaged that they share the same source.

However, all three factors are intimately linked and conspire to heavily influence the style of mid-Carboniferous sedimentation in the Clare Basin. Thus, ultimately these three influences will control:-

1) Water column stratification and thus oxygen availability.
2) Relative sea-level changes and salinity levels.
3) Sediment supply routes to the basin.

7.3 ENVIRONMENT OF DEPOSITION

The use of two different geological disciplines provide clues to the depositional environment of the Clare Shale Formation.

7.3.1 Palaeoecology

The dominant controls on fauna within the Clare Basin are the salinity and oxygen content of the basinal waters. The lack of fauna outside marine bands is likely not to be a taphonomic phenomenon but related to these palaeoenvironmental parameters.

A salinity control on Carboniferous fauna has been documented by numerous workers (e.g. Ramsbottom *et al.*, 1962, Holdsworth, 1966a). Indeed, fauna in the middle Carboniferous cyclothems is concentrated in the 'marine band' at the base of the cyclothem in the Clare Basin (except for bedding-plane accumulations of bivalves (discussed below)). Marine bands formed at maximum transgression, when land connections to the northern England Basins were submerged and nektonic/nektobenthic ammonoid fauna migrated into the basin (Tanabe *et al.*, 1995). Sediment input to the basin at these times was very depressed and the marine band accumulated over a long period of time, represented now by a thin interval of rock. It is envisaged that only during 'marine band' deposition were basinal waters fully marine and allowed a commonly diverse nektonic/nektobenthic community to flourish. Ramsbottom *et al.*, (1962) from detailed investigation of core have recognised faunal cycles, which they related to salinity. These are shown in Figure 7.1. Maximum salinity is represented by a thick-shelled goniatite phase, with barren strata thought to represent deposition in fresh or very slightly brackish water. These cycles cannot be recognised in the Clare Basin, however, with instead rather rapid changes from 'marine'- to 'non marine' strata being evident. It appears from palaeontological evidence therefore, that the barren strata between 'marine' bands are non marine, however, geochemical evidence suggests this was not the case. In mid-Carboniferous strata in Britain, Riley *et al.*, (1987) and Varker (1994) have documented occurrences of conodonts (which are assumed to be marine organisms) outside of goniatite-containing strata, thus also suggesting that these barren strata are marine. It appears likely that the control on marine band formation is much more complex than simple salinity changes. It is probable that benthic oxygen levels were also an important factor in marine band formation; possibly the development of the 'thick-shelled' goniatite phase is related to the establishment of oxic marine waters as colder, denser, oxygenated marine waters entered the basin at maximum transgression. The conodont fauna may have lived at a higher position in the water column where oxic conditions persisted for a longer time.

'Occluded cycles' (those showing missing fauna (i.e. missing marine bands), but with no physical evidence of erosion) may represent the persistence of low salinity or a sedimentary regime unfavourable to goniatite preservation, (Holdsworth and Collinson, 1988). However, very low oxygen levels may also be a factor (discussed in section 7.3.2.3).

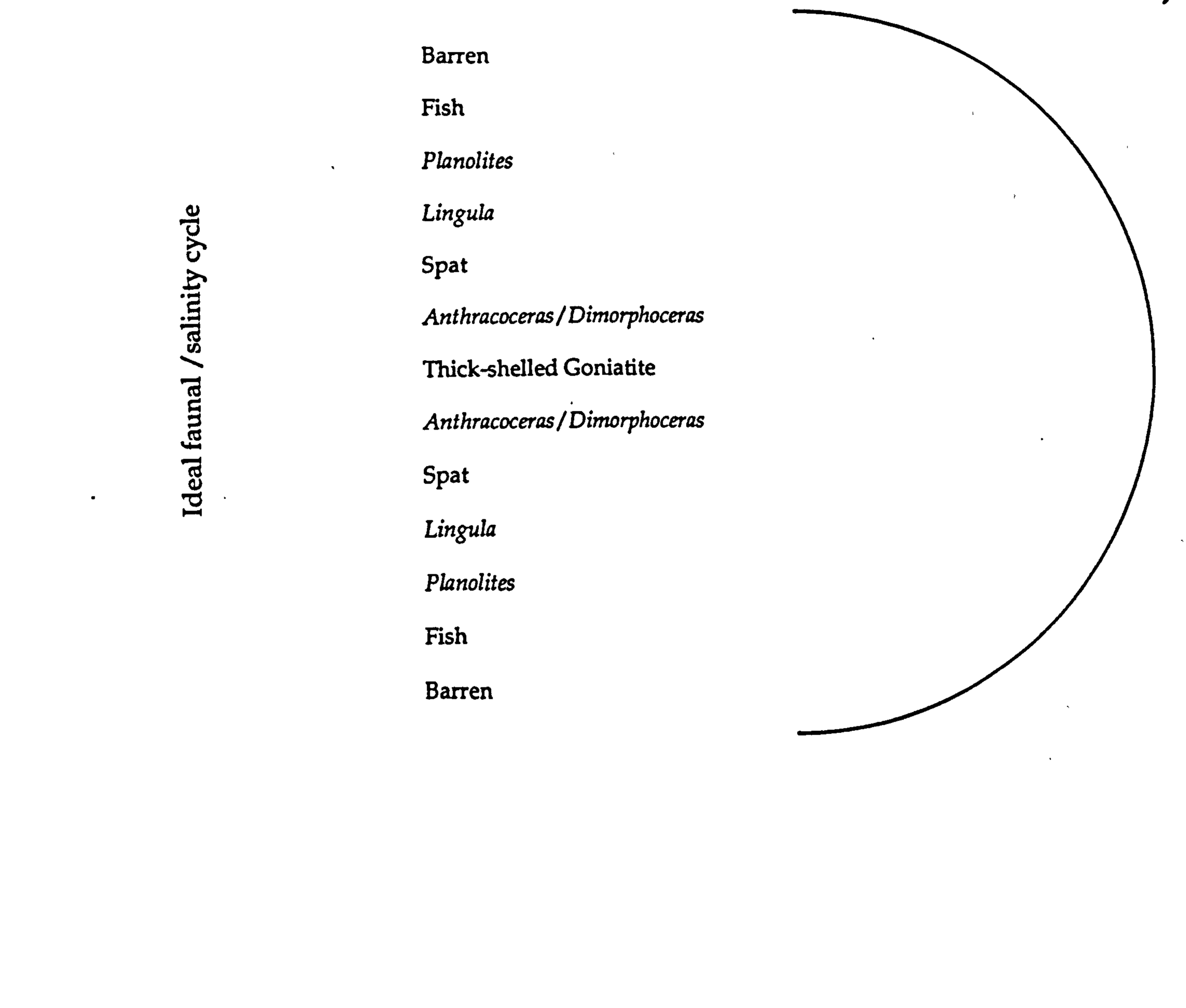

Figure 7.1 Ideal faunal salinity cycle. (From Ramsbottom *et al.*, 1962).

The lack of visible bioturbation (outside phosphorite horizons) indicates anaerobic or at the best quasi-anaerobic conditions in the sediment, i.e. the oxic/anoxic boundary is perched at the sediment water interface or in the water column. Bedding plane accumulations of benthic marine bivalves, (seen unassociated with marine bands in the north of the area), are often dominated by one species, e.g. *Posidonia corrugata*. These faunal concentrations probably represent an exaerobic biofacies of opportunistic epibenthos, developed during periodic oxygenation events (Antia and Wood, 1977). It appears that the basin is commonly stratified and euxinic. However, a poorly or non-stratified water column has been shown to have been present at times of maximum transgression (during marine band development), possibly due to oceanographic processes or from overturn of the water column by dense cold marine waters entering the basin. These events could have been brought about by the breakdown of the stratified water column leading to short-lived oxygenation episodes at the seafloor. Additionally the water column overlying the northern shelf areas may have been of sufficient thickness to allow mixing by storms. The lack of goniatites associated with these bivalve assemblages may be due to shallow water depths, or the geologically instantaneous period of oxygenation.

Late Arnsbergian marine bands are quite diverse, comprising up to four benthic species, and pertain to oxygen-related biofacies (O.R.B.) 4 (poikilotopic biofacies) representing periodic oxia (Wignall, 1994). Commonly marine bands through the Chokierian display faunas comprising only ammonoids and thus represent anaerobic biofacies or O.R.B. 2 of Wignall and Hallam (1991), interpreted as indicating anaerobic conditions at the sea-floor.

7.3.2 Geochemistry

Geochemical techniques have allowed the qualitative determination of salinity, detrital input and oxygen levels and quantitative determination of organic carbon values across the mid-Carboniferous boundary in the centre of the Clare Basin.

7.3.2.1 Salinity

The assumption that sediments deposited outside 'marine bands' in County Clare are non marine appears to be incorrect. It appears probable that the development of a well-stratified water column led to denser marine waters

occupying a level at the base of the water column, with any freshwater entering the basin efetively 'floating' as a less dense layer on top of the euxinic marine waters. Only at times of complete overturn of the water column (which commonly occurred towards the end of cyclothems) did freshwater reach the bottom levels of the water column and manifest a non-marine diagenetic signature.

7.3.2.2 Detrital input

The shale deposition associated with the mid-Carboniferous deposits of County Clare is considered to represent fall-out from suspension under quiet conditions, however, a crude estimation of variations in detrital input can be made.

Sedimentation rates were at a minimum during the lowest Chokierian in the basin centre and detrital input was low. Geochemical analysis suggests that sediment starvation at this time was due to sediment diversion during a sea-level low, rather than condensation associated with high sea-level.

Sedimentation rate was very probably a constant low on the shelf area with sediment diversion down the central axis of the basin. A rise in detrital input was seen in the proximal shelf area at St. Brendan's Well, during the falling sea-level at the top of the *Homoceras beyrichianum* cyclothem. This marine band is the oldest present on the proximal shelf area and this increase in sedimentation rate may mark the re-establishment of sediment routes after the Arnsbergian and lower Chokierian lowstand, prior to this deposition it is likely that sedimentation on the shelf margin is restricted due to by-passing.

7.3.2.3 Oxygen levels

Stratification of the water column due to salinity, density or temperature contrasts resulted in the Clare Basin being euxinic, both during marine band deposition and at times outside marine band deposition. During marine band deposition it is likely that thermohaline stratification of a thick water column resulted. Overturn of this stratification in the basin centre may have occurred, initially due to the influx of cold dense waters as land connections were broken and oceanic connections were forged during maximum transgression. It is also possible that large scale current processes were set up during the basin greatest areal extent.

Stratification was also evident during 'non-marine' deposition and may have resulted from the less dense freshwater entering the basin and 'floating' on top of denser marine euxinic waters. Total breakdown of this thermohaline stratification may have occurred when the basin was fully flushed of its marine waters. Additionally, as sea-level shallowed towards the top of cyclothems, wind-driven or storm mixing would reach deeper as the thickness of the water column diminished. However, at least during the H_1a^1 cyclothem, it is probable that channel avulsion led to low amounts of freshwater entering the Clare Basin and prolonged thermocline stratification resulted in what was effectively a vast stagnant lake.

Only gamma-ray spectrometry was conducted on the sections deposited on the northern shelves of the basin and this proves prolonged periods of anoxia.

7.3.2.4 Organic carbon

Peaks in total organic carbon values coincide with marine bands. These peaks may be due to increased preservation or productivity during periods associated with marine band deposition.

High D.O.P. values tend to suggest that preservation in anoxic bottom waters is the most important factor in organic matter content for many of the marine bands. However, many of the Chokierian marine band samples show surprisingly low D.O.P. values which may suggest high productivity with more nutrient rich waters being present in the water column (possibly related to overturn of the stratification at high sea-level stand).

By combining these various geochemical parameters, an estimation of sea-level changes can be ascertained. These have been described in section 6.7, and are also further discussed below.

7.4 MODEL FOR DEPOSITION IN THE CLARE BASIN DURING THE MID-CARBONIFEROUS

The model is presented in picture form in Figure 7.2

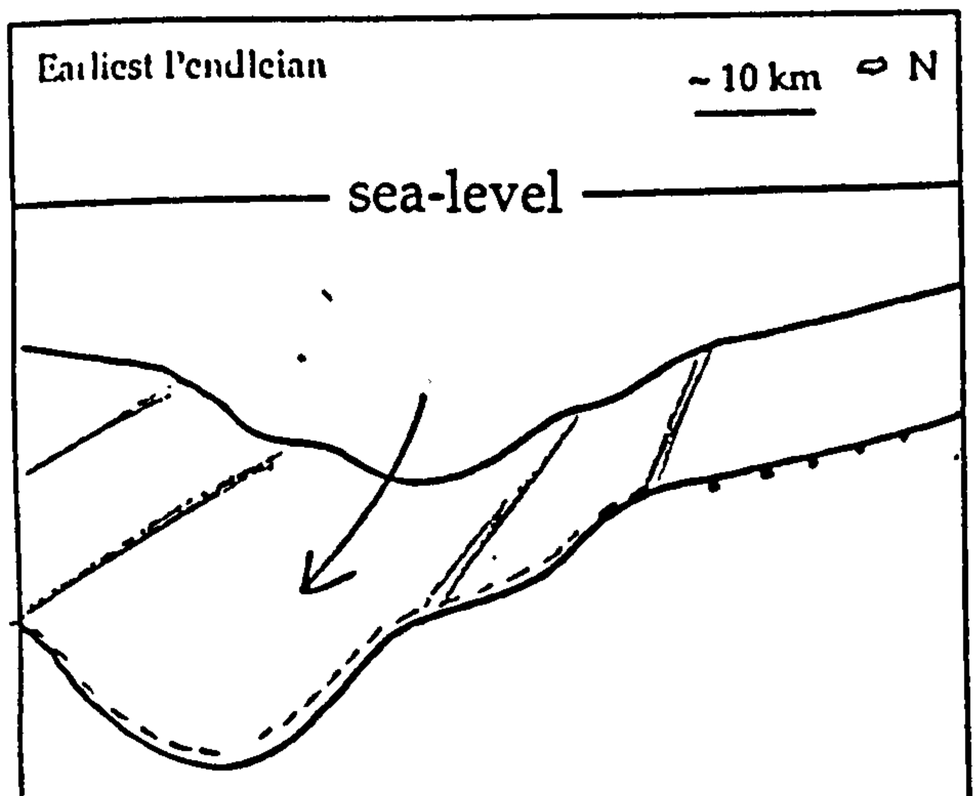

- Transgression perches oxygen minimum zone upslope.
- Epigenetic replacement of top surface of Dinantian limestone.
- Low sedimentation rates on the northern shelves.
- Continuous deposition across Dinantian/Namurian boundary in basin centre. Possible erosion/non deposition in proximal areas.

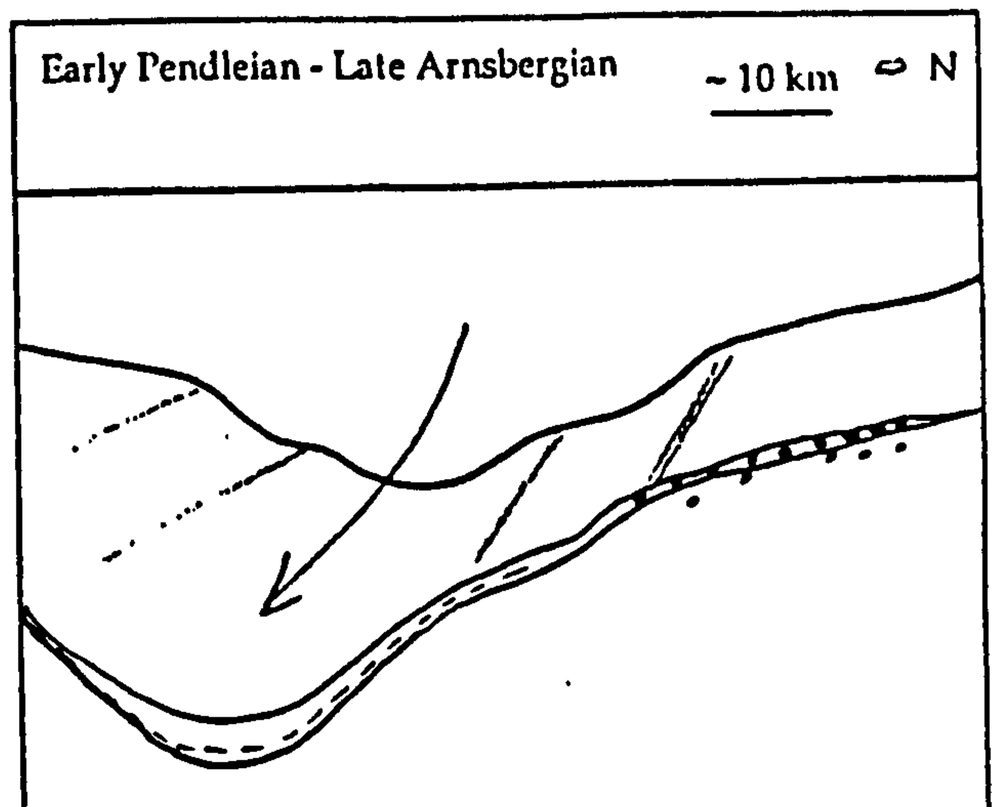

- Phosphate authigenesis in the fluctuating oxygen conditions developed in the shallow hemipelagic environment on the northern shelves.
- Depressed sedimentation rates on the northern shelves
- Possible erosion/non deposition in proximal areas.
- Probable continuous deposition in the basin centre.

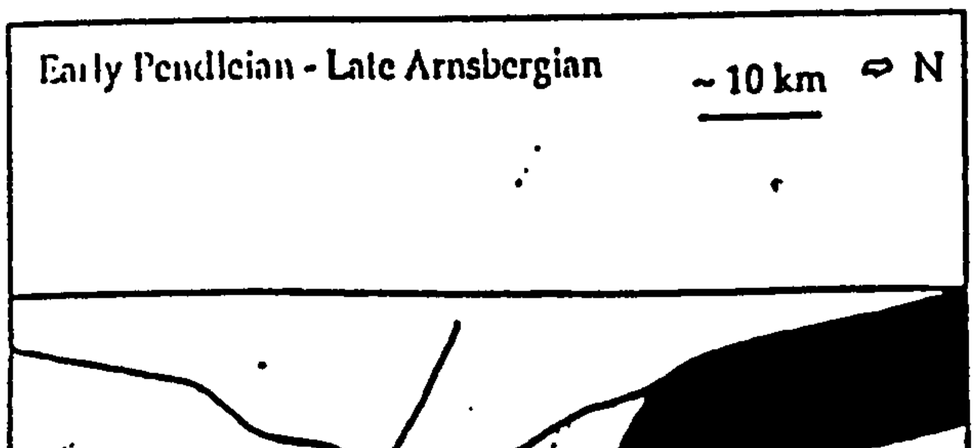

- Regression leads to erosion and reworking of precursor phosphorite out towards the basin centre due to deep storm waves or regressive retreat of the pycnocline.
- Prolonged winnowing of fines in proximal areas.
- Low sedimentation rates and low oxygen levels on the northern shelves.
- Probable non deposition on distal shelf areas, with probable continuous deposition in the basin centre.

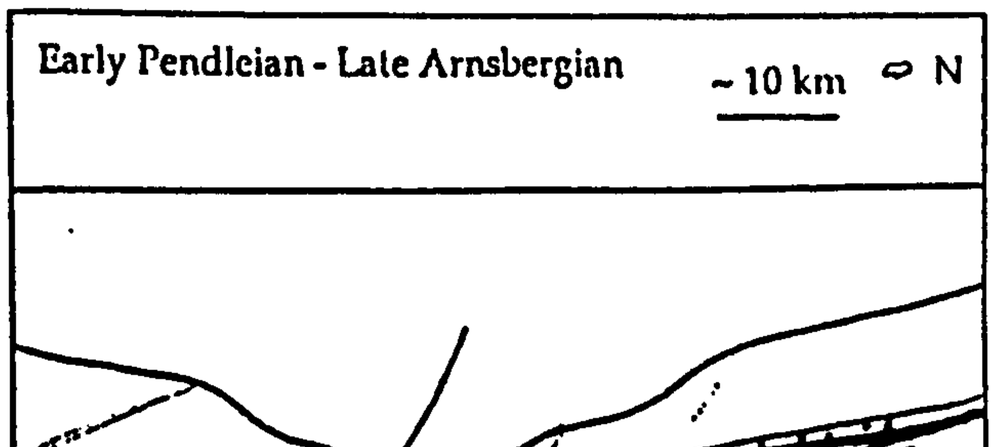

- Transgression perches oxygen minimum zone upslope
- Low sedimentation rates and low oxygen levels on the northern shelves.
- Probable continuous deposition in the basin centre.

Figure 7.2 Cartoons depicting deposition through the mid-Carboniferous in the Clare Basin. Dashed lines represent marine bands (although not all marine bands are shown). Black areas represent phosphatic lag development. Black dots represent phosphate authigenesis or epigenesis. Solid horizontal line represents sea-level.
Thickness not to scale on northern shelves.

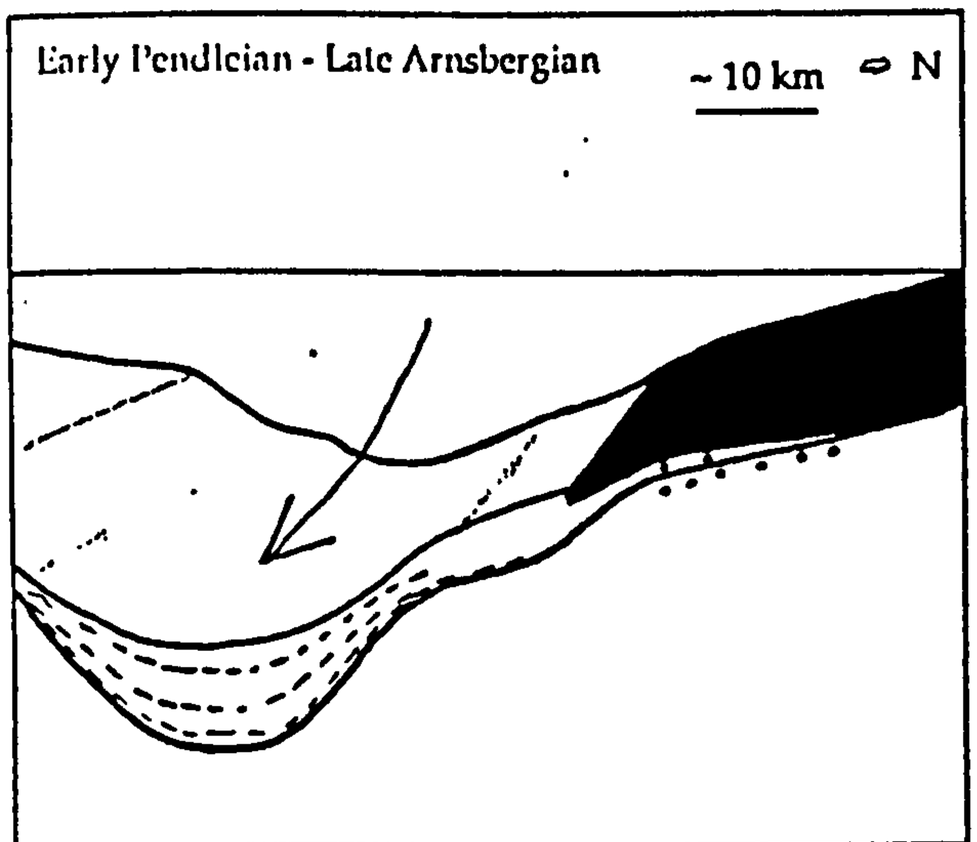

- Regression leads to erosion and reworking of precursor phosphorite out towards the basin centre due to deep storm waves or regressive retreat of the pycnocline and removes any previously deposited transgressive shales.
- Low sedimentation rates and low oxygen levels on the northern shelves.
- Probable continuous deposition in the basin centre.

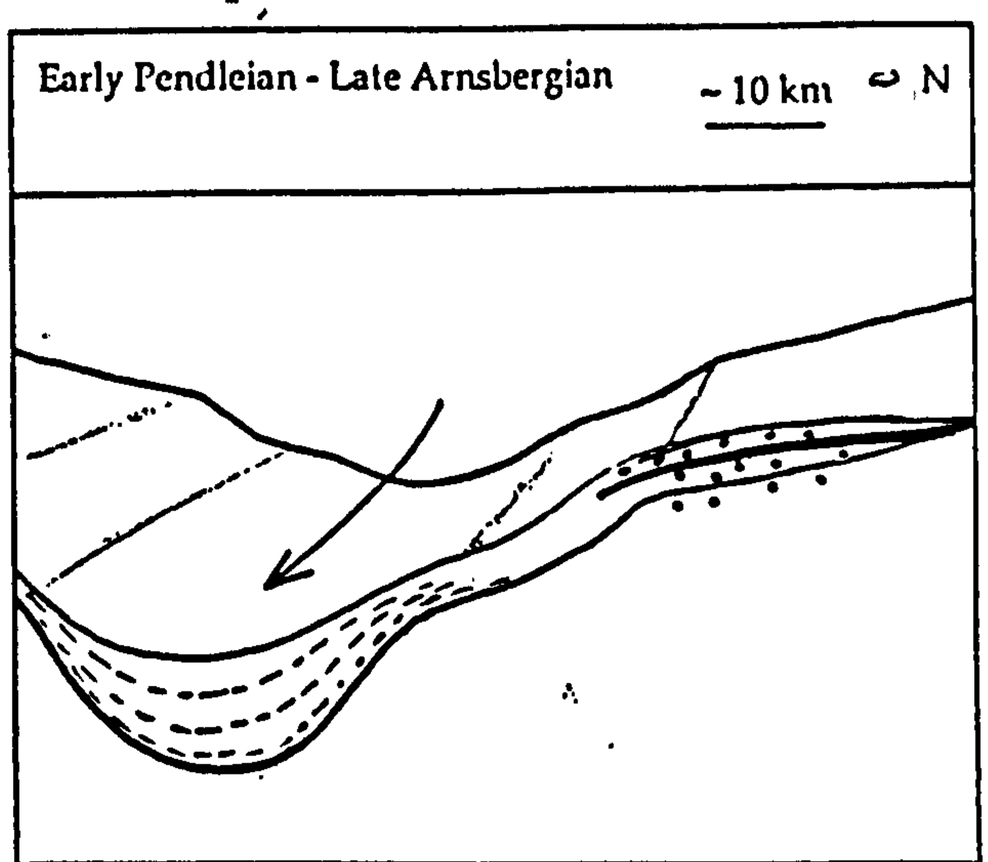

- Transgression perches oxygen minimum zone upslope and results in further phosphate authigenesis.
- Possible erosion/non deposition in proximal areas.
- Low sedimentation rates and low oxygen levels on the northern shelves.
- A short-lived regressive event leads to a thin biorturbated phosphatic lag.
- Probable continuous deposition in the basin centre.

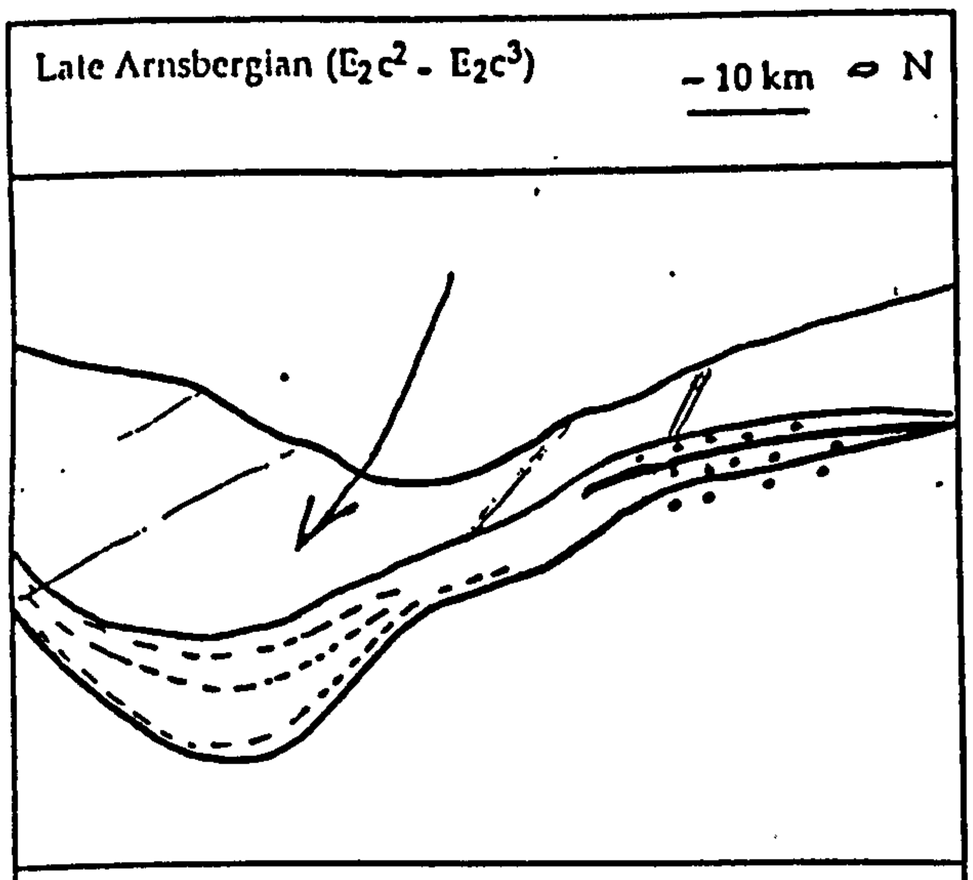

- Sea-level is rising towards the end of the Arnsbergian, however, no marine bands reach up onto the shelf.
- Stable stratified water columns persist.

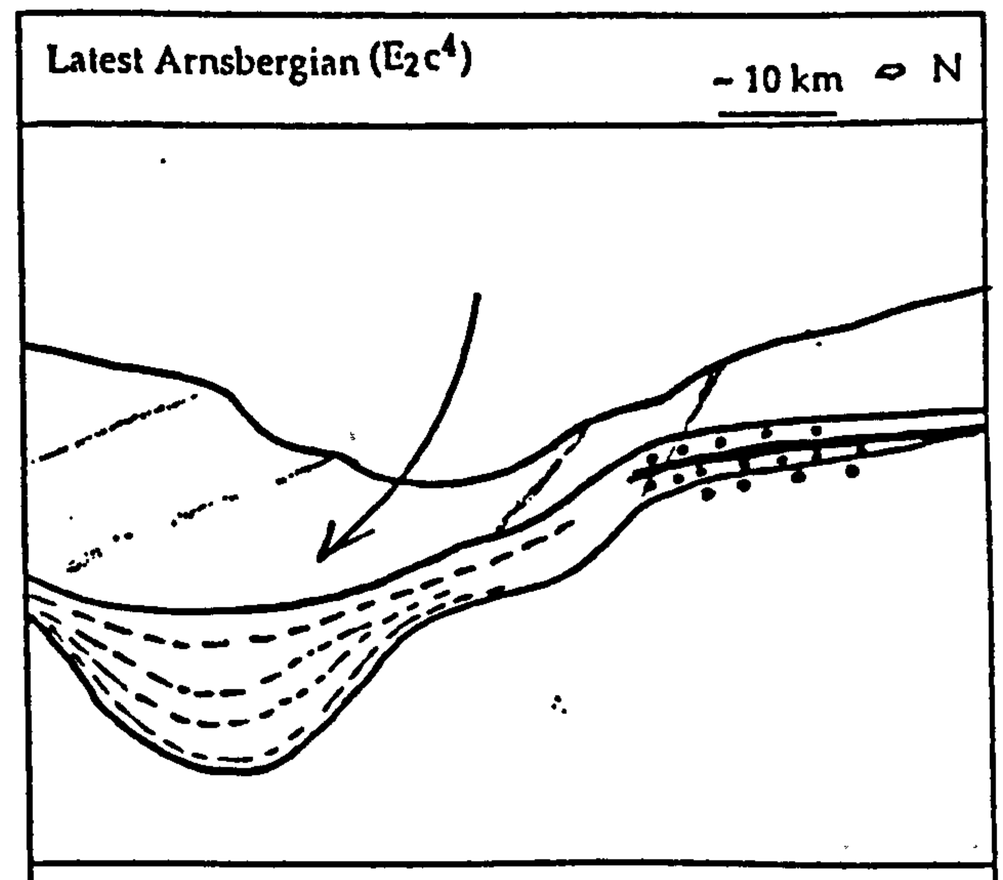

- Relative sea-level high
- Poorly mixed basin during marine band formation results from large scale oceanic processes, or influx of vast volume of cold, oxygenated waters entering the basin and results in high productivity.
- Low sedimentation rates and low oxygen levels on the northern shelves.
- Marine band reaches up onto the distal shelf areas.

Figure 7.2 Continued.

Earliest Chokierian (H_1a^1)

~ 10 km ⇦ N

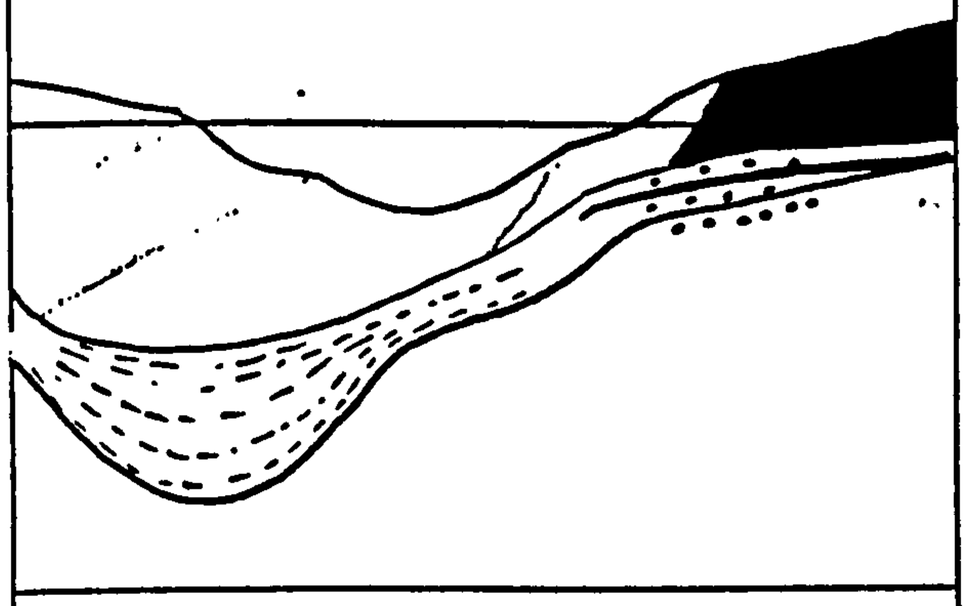

- Extreme sea-level low.
- Very depressed sedimentation rate probably due to sediment diversion away from the basin.
- Well stratified water column.
- Thin phosphatic lag forms on the northern shelf.

Early Chokierian (H_1a^2 - H_1a^3)

~ 10 km ⇦ N

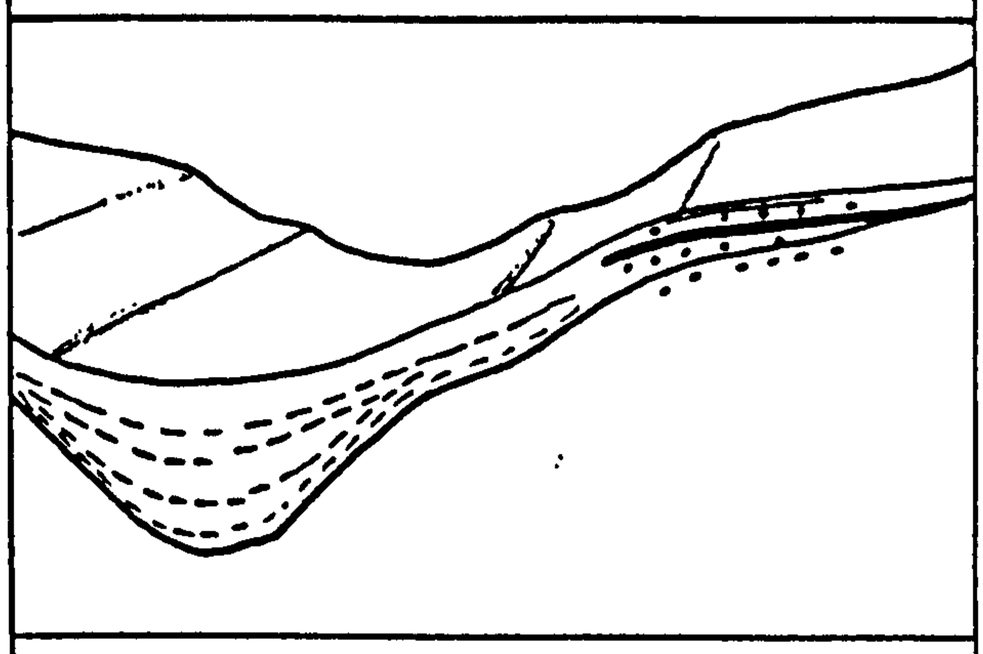

- Sea-level rises from the low of the early Chokierian.
- Poorly mixed basin during marine band formation results from large scale oceanic processes, or influx of vast volume of cold, oxygenated waters entering the basin.
- Increased sedimentation rate as sediment routes into the basin are re-established during marine band formation.
- Low sedimentation rates and low oxygen levels on the northern shelves.
- Marine bands reach up onto the distal shelf areas.

Late Chokierian (H_1b^1 - H_1b^2)

~ 10 km ⇦ N

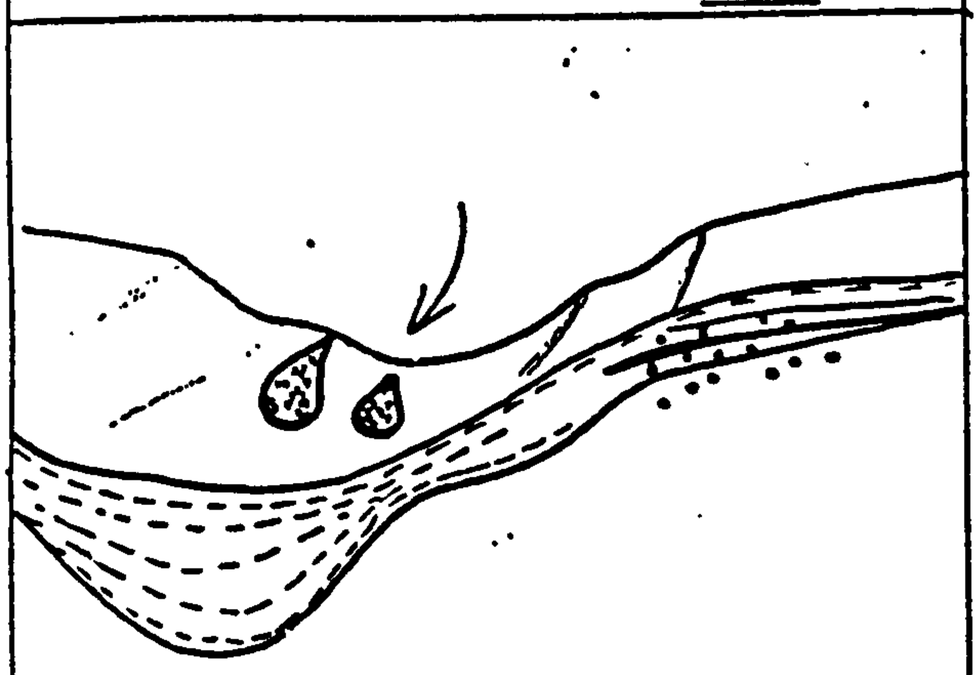

- Relative sea-level high.
- Increased sedimentation rate in basin centre as Ross delta progrades. Low sedimentation rate on the northern shelf.
- Marine bands reach up to proximal shelf areas.
- Predominantly well stratified water column due to great thickness of water column.

Alportian and later

~ 10 km ⇦ N

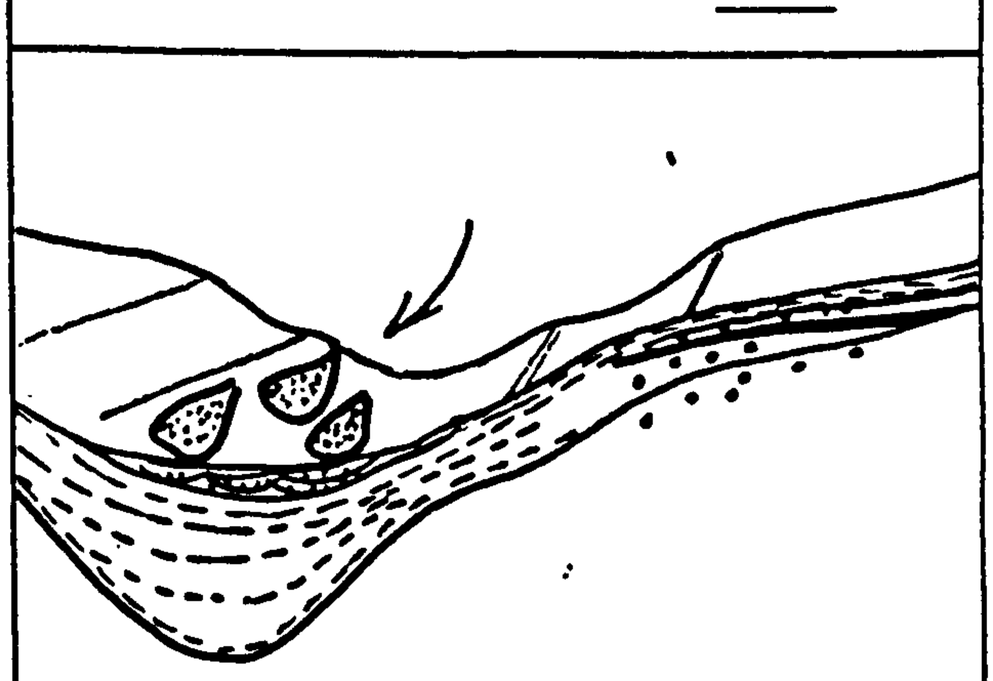

- Increased sedimentation rate in the basin centre as Ross delta progrades. Low sedimentation rate on the northern shelf.
- Relative sea-level high results in deposition of marine bands on the northern shelf.
- Regression associated with the eostriolatum marine band is shown as a phosphatic lag on proximal shelf areas.

Figure 7.2 Continued.

7.4.1 Earliest Pendleian (*C. leion*)

The presence of the oldest Namurian ammonoid horizon (*C. leion*) has been noted above the limestone at Magowna and Kilnamona (very distal shelf margin) directly above the Dinantian limestone. It is also probable that deposition across the Dinantian-Namurian boundary was continuous in the basin centre (Figure 7.2). There is no evidence of any lower Namurian strata in proximal shelf areas, and the Cahermacon shale in the more distal areas is undated. The top of the Dinantian limestone is also poorly dated and it is not known whether the development of the undulose topography (developed prior to Clare Shale deposition in the distal shelf area at Ballyshanny House) took place during the lower Namurian or late Brigantian. The hiatus observed in the north of the area may have formed either through subaerial exposure (although no evidence of vadose or phreatic cements is present in the topmost limestone), or by submarine erosion and sediment bypass, at any time up to the deposition of the lowermost phosphorite horizon.

The initial rise of the pycnocline upslope must have occurred early in the Pendleian. The intensely bioturbated limestone at Ballyshanny House displaying *Chromatichnus wegberensis* may represent the transgressive reworking of the limestone (this species is thought to be allied to *Zoophycos* sp., a deep water trace (Donaldson and Simpson, 1962)).

A model is envisaged for the Clare Basin in that a major transgression at the base of the Pendleian resulted in the rise of the oxygen minimum zone upslope. The top of the Magowna Limestone Formation would have been bathed in phosphate-rich waters and epigenetic replacement of the limestone surface took place in the absence of sediment supply, during contact with transgressive phosphate-rich waters during the Pendleian (or possibly Arnsbergian in more proximal areas).

7.4.2. Early Pendleian (*E. brandoni*) to late Arnsbergian (*N. stellarum*)

As stated above the Cahermacon Shale and Phosphate Members of the Clare Shale Formation are extremely poorly dated. Both Lewarne (1959) and Graham *et al.*, (1986) mention finds of a single *Nuculoceras nuculum* horizon above the phosphate on the northern shelves. This study assigns deposition of the three lowest phosphorite horizons to sometime within the Pendleian or lower Arnsbergian. No comparative sections are known

in the basin centre, although it is likely that shale deposition persisted throughout the interval (Lewarne, 1959; Hodson and Lewarne, 1961). Sedimentation rates were extremely depressed on the shelves of the Clare Basin as sediment was preferentially funnelled down the deep axis of the Clare Basin.

It is envisaged that the flooding of the shelf during the lower Pendleian (as detailed in section 7.4.1) led to a shallow hemipelagic environment with low sedimentation rates. Expansion of the oxygen minimum zone up onto the shelf led to fluctuating oxygen levels in the sediment, favourable to bacterially-influenced phosphate authigenesis in the Cahermacon Shale Member (now only preserved in the distal shelf area and also at the St. Catherine's Cave locale). It is unknown what depositional processes were taking place in a more proximal position on the shelves. However it is probable that either erosion by storm or internal waves associated with the pycnocline was taking place during decreased rate of sedimentation, or, alternatively authigenic phosphate growth took place in shale that was later removed during erosion.

The shelves of the Clare Basin during the lower Namurian would have been suitable for phosphate deposition in a number of ways (compare with section 5.4):-

1) Terrigenous input was reduced due to sediment bypass down the axis of the Clare Basin.
2) Widespread transgression additionally limited sediment input and increased the area of the continental shelf available for the phosphorite formation. A corresponding increase in the thickness of the oxygen minimum layer would have increased preservation potential of phosphorus-rich organic matter.
3) Warm mid-Carboniferous climates resulted in increased weathering (and therefore release of phosphorus), and also the development of widespread oxygen-depleted waters (due to decreased rates of ocean circulation and low levels of oxygen solubility).
4) A major expansion of organic productivity would result from the large volume of nutrient rich waters following the early Namurian glacial period (see section 1.4.4.2).

Deposition of the lowermost phosphorite horizon (A) is speculated to have taken place during a prolonged regressive interlude with offshore

transportation of a pre-existing proximally deposited phosphorite out into the basin. Erosion and reworking of the precursor phosphorite may have been facilitated by the regressive retreat of the pycnocline and associated internal waves impinging on the shelf and also the increased influence of storm waves as sea-level lowered. Prolonged winnowing of fines and concentration of heavy minerals occurred in the more proximal shelf area and may have been due to the pycnocline being static at this level for a long period of time in the absence of sediment supply. Additionally, erosion in the north of the area probably removed any previously deposited shale and here the lag rests directly upon limestone. Oxygen levels fluctuated but were generally low with the establishment of dysoxia in the sediment at times. Relatively deep water conditions were still present over the shelf, particularly in the more distal regions, where stagnant conditions persisted and only infrequent periods of agitation disturbed the phosphate clasts. Sedimentation rate was effectively zero for a long period of time during the accumulation of this deposit. It could be expected that increased sedimentation rates would result during a regression, but it is likely that sediment bypass was a major factor at this time. In the proximal areas erosion was strong and in the more distal area the lag rests upon the phosphatic shale

It is likely that deposition of an interval of transgressive shales followed deposition of this lower phosphorite. A thin second phosphorite horizon (B) similarly formed during a subsequent regression removing any transgressive shales.

Following the regression that formed horizon B, the oxygen minimum zone migrated upslope and phosphate authigenesis occurred over the shelf. Formation of a very thin, bioturbated phosphatic lag (C) was probably due to a short lived regressive event.

The very distal parts of the shelf area show no phosphate development, however, a non-sequence is present throughout the interval (Figure 4.19). This may represent the distal loss of erosive energy during the regressive events associated with phosphorite deposition.

7.4.3 Late Arnsbergian (E_2c^2-E_2c^4 cyclothems)

The E_2c^2 cyclothem saw deposition in the basin centre initially in a stratified euxinic basin during marine band development, with deposition towards

the top of the cyclothem in a variably mixed basin. Sea-level was relatively low in the E_2c^2 cyclothem.

The E_2c^3 cyclothem shows deposition in a euxinic basin during marine band formation. Relative sea-level appears to have been higher than the previous cyclothem. More prolonged anoxia occurred throughout the cyclothem and may indicate the presence of a thick water column resistant to mixing processes. Salinity throughout the cyclothem was fully marine or brackish.

The E_2c^4 cyclothem shows a relative sea-level high developed throughout the cyclothem. However, marine band deposition was in a poorly mixed basin. Mixing may have been induced at high sea-level, when the basin had its greatest areal extent, by the establishment of large scale oceanic processes within the basin or due to the influence of an enormous volume of presumably colder, denser waters entering the basin as land connections were submerged during maximum transgression. As mixing processes waned, deposition was within an euxinic basin. A fully marine signature is seen throughout the cyclothem and reflects the well-stratified nature of the water column. It is speculated that the *Nuculoceras nuculum* marine band observed on the basin shelves to the north belongs to this later cyclothem, and thus only during the latest Arnsbergian had the sea-level recovered from the regressive interlude of the lower Namurian to allow marine band deposition on the shelves. At other times it is likely that deposition on the shelves was dominated by low salinity, poorly oxic/anoxic conditions.

7.4.4 Early Chokierian (H_1a^1-H_1a^3 cyclothems)

The lower Chokierian (H_1a^1) shows extremely restricted deposition after the sea-level high of the late Arnsbergian. Deposition throughout the lowermost Chokierian was in a euxinic basin. Sediment input was extremely depressed and may have resulted from sediment diversion away from the Clare Basin at extreme eustatic minima; the Clare Basin during the early Chokierian is thus effectively a stagnant lake. The fourth phosphorite horizon (D) occurs between the last Arnsbergian and the first Chokierian faunas at Ballyshanny House. It could be speculated that this lag was formed due to regressive reworking associated with a fall in sea-level at the base of the Chokierian.

The later H_1a marine bands show deposition in poorly mixed waters and thus the sea-level is envisaged to have risen quite dramatically from the lowstand of the basal Chokierian, with the establishment of large scale oceanic processes or a large influx of cold dense waters within the basin in a similar way to that seen in the E_2c^4 marine band. The H_1a^2 marine band is unusually thick in the basin centre and may represent the re-establishment of sediment routes into the basin at high-stand. However, the later parts of the H_1a^2 and H_1a^3 cyclothem saw a return to stagnancy, possibly reflecting restriction of the basin once again as the basin lost its interbasinal connections and the large scale processes waned, and once again the basin became stratified as sea-level fell during the upper part of the cyclothem.

The two *Isohomoceras subglobosum* marine bands seen on the distal shelf area at Ballyshanny House are assigned to the later H_1a cyclothems, and thus it is shown that there was a quite rapid recovery from the mid-Carboniferous lowstand to allow deposition on the shelves. Shelf deposition during this time appears to have been condensed and the marine bands are very thin and contain an extremely sparse fauna. It is probable that the marine event on the shelves was very short-lived with a quick return to conditions unfavourable for goniatites (e.g. drop in salinity, water depth or oxygen levels)

7.4.5 Late Chokierian (H_1b^1 and H_1b^2)

Both the *Homoceras beyrichianum* and *Isohomoceras sp. nov* cyclothems are widespread and thus a relative sea-level high is postulated to have occurred during deposition of these cyclothems. Fully marine waters were developed at the base of the water column throughout this interval and testify to the establishment of a well-stratified water-column.

The H_1b^1 cyclothem probably shows the greatest relative sea-level high with prolonged anoxia following marine band deposition in a partially overturned water column. The *Homoceras beyrichianum* horizon is commonly the oldest marine band above the phosphorite at many of the localities on the shelf area. Therefore, it was not until latest Chokierian times that marine band deposition occurred on the proximal shelf area.

The succeeding H_1b^2 cyclothem shows anoxic conditions developed towards the end of marine band deposition, with mixing of the water column as sea-level fell towards the end of the cyclothem. The H_1b^2 cyclothem is very

thick indicating high sedimentation rates during its deposition, possibly related to progradation of the turbidite-fronted Ross delta.

Although these cyclothems exist on the shelf area, it is evident that low sedimentation rates still persisted, presumably with sediment bypass down the basin axis. Conditions on the shelf area were established which allowed goniatites to flourish, no benthic fauna is seen during these marine bands and may relate to very poorly oxic/anoxic conditions being prevalent at the sediment-water interface.

7.4.6 Early Alportian (H_2a^1 and H_2b^1 cyclothems)

The lower Alportian cyclothems show widespread distribution and thus sea-level is interpreted to have been relatively high. Marked differences in sediment supply are shown throughout this interval between the shelf and basin axis areas. For example the *undulatum* and *proteum* marine bands are separated by 15.36 m of silty shales in the basin area (Hodson and Lewarne, 1961) compared to a 0.36 m thickness of shale on the shelf area (at Lough Raha). These differences can be assigned to the imminent advance of the Ross turbidites.

7.4.7 Mid-Alportian (H_2c^1 cyclothem)

The mid-Alportian shows a lowstand of sea-level, probably with the *eostriolatum* marine band confined to the basin centre. Very low sedimentation rates occurred during *eostriolatum* times and throughout the later Alportian and are possibly related to sediment bypass.

7.4.8 Alportian and later

The later Alportian shows further transgression, with the entire sequence of known Namurian marine bands being present until the R_1a^3 (*Reticuloceras subreticulatum*). A conspicuous gap between the R_1a^3 and R_1b^1 strata (*Reticuloceras eoreticulatum*) may represent high sediment influx associated with the deposition of the Ross and Gull Island Formations or a prolonged period of desalination.

7.5 DISCUSSION

7.5.1 Possible modern analogues for the Clare Basin

It appears that the Clare Basin was predominantly anoxic, although fluctuations in oxygen content are seen. It is likely that marine connections were lost at times outside maximum transgression, and freshwater input to the basin occurred during non-marine periods, although this freshwater probably floated as a less dense horizon on top of the anoxic marine bottom waters.

There is no modern analogue that shows repetitive marine input on the scale seen in the Clare Basin. Howevér the Black Sea may be used as an analogue for euxinic deposition. The Black Sea is a deep, enclosed basin and displays long term anoxia, with the dissolved H_2S being present below 150 m in the water column (Arthur and Sagemann, 1994). A pycnocline/chemocline/halocline is present at 250 m depth (Canfield *et al.*, in prep.). The basin is almost landlocked and is connected to the Mediterranean by a link which may be less than 30 m deep. The basin also receives huge amounts of freshwater from northern rivers. Circulation is poor due to the highly stratified nature of the water column and sedimentation rates are also low. The Black Sea in comparison to the Clare Basin therefore shows deposition in a brackish stratified basin, with low detrital input and high preservation of organic matter. Wignall (1994) describes the applicability of this basin as an analogue to ancient black shales and notes that a drawback to the Black Sea is its great depth. He suggests that ancient black shales were likely to have accumulated in shallower basins (such as the Clare Basin) and thus would be more susceptible to eustatic/climatic and storm effects.

Additionally an analogue such as fjord (a shallow stratified, silled basin which is subject to storm mixing with the redox boundary fluctuating above and below the sediment water interface) may be applicable to deposition on the northern shelves of the Clare Basin, and at times of mixing during marine band deposition.

Gade and Edwards (1980), from studies of deep water renewal in fjords, note two particular features that may be applicable to the Clare Basin, with its deep axis and presumably shallow water connection to the northern England Basins and ultimately the ocean. Firstly these workers note that

the sudden influx of cold, dense oxygen rich waters may result in uplift of the bottom waters of the basin. These are likely to be nutrient-rich and therefore phytoplankton blooms may occur, further reducing the oxygen levels in the basin. However, in some cases uplift of the deep oxygen-depleted water may bring H_2S up to the water surface resulting in fish-kills (Ozretich, 1975). Secondly, these authors note (from observation of multiple-linked fjords) that if renewal is density linked then intrusion to multiple basins may lead only to partial renewal, particularly if the renewing water derives from a neighbouring stagnant basin (and thus contains little O_2).

Is there an analogue here for the very poorly developed stunted juvenile ammonoids seen in the British and Irish Basins, particularly across the mid-Carboniferous boundary? If at maximum transgression during the sea-level low of early Chokierian times, a stagnant water column was overturned, then this may explain both the lack or reduction in diversity of benthic fauna during marine band development and the restricted size of the ammonoids. Additionally as the Clare Basin was effectively the last in a chain of basins linking to the ocean (which possibly lay in the southern C.I.S. area, Holdsworth and Collinson, 1988), then its water supply was likely to differ considerably from normal marine waters as it would assume the signature of pervious basinal waters. Only during highstand of sea-level (e.g. late Arnsbergian or late Chokierian would the basinal waters approach a chemistry and oxygen level similar to that of the open ocean.

Recent experimental flume modelling of depositional systems (Wood *et al.*, 1993; Koss *et al.*,1994) has clarified the effects of a major sea-level fall (to below the shelf-slope break) on detrital input to a depositional system. These workers have found that following a rapid substantial fall, coarse sediment is effectively ponded on the old shelf area. The only detrital input to the basin will be from reworking of the previous fine grained slope deposits as the edge of the shelf is incised. Eventually however, headward erosion of the incised valleys will reach the stranded coarse deposits and the coarse sediment will enter the basin. The important point in their work is that there is a distinct time-lag between the lowstand and the transport of coarser-grained debris into the basin. This could explain the lag of detrital input into the basin associated with the mid-Carboniferous lowstand during the $H1a^1$ cyclothem. It can also be speculated that the vast volumes of coarser detritus entering the system with the deposition of the Ross turbidite-fronted delta during early Alportian times in the Clare Basin may

represent both the timelag between the major fall in sea-level and the entrance of coarse deposits into the basin.

7.5.2 The mid-Carboniferous boundary in the Clare Basin.

As previously mentioned (section 2.2.1.2) the mid-Carboniferous boundary as defined by conodonts occurs in the British Stonehead Beck section (the only section with refined conodont and goniatite control) at the base of the H_1a^2 marine band. The very lowest Chokierian (H_1a^1) at this basinal section displays a poor, impoverished, shallow-water conodont fauna (Varker *et al.*, 1990, 1994; Owens *et al.*, 1990). Other sections throughout both Ireland and Europe commonly show the absence of at least one of the early Chokierian marine bands, or representation of the Chokierian by a sand unit or unconformity, e.g., Owens *et al.*,(1990) from studies of a section 20 km from the proposed stratotype at Stonehead Beck, have found E_2c^4 and early H_1 strata to be represented by a 2-5 cm thick sandstone horizon. Saunders and Ramsbottom (1986) have documented the 'mid-Carboniferous eustatic event' throughout the world and have found a hiatus to range from E_2b to at least H_1b in sections fromNorth Africa, Poland and China to U.S.A.

It appears that the Inishcorker section shows geochemically the expression of the lowstand immediately prior to the mid-Carboniferous boundary (as defined by ammonoids). Major extinctions are seen at the end of the Arnsbergian (Saunders and Ramsbottom, 1986; Ramsbottom, 1980) with a dramatic change to homoceratid-dominated ammonoid faunas, with a slight time lag (of one marine band) seen in the change from gnathodid to declinognathodid conodont faunas. Ramsbottom (1980) suggested that during periods of intense ecological restriction and increased environmental stress (i.e. major eustatic lowstand) saltations in ammonoid evolution occurred. Holdsworth and Collinson (1988) have related this to 'overheating' of restricted provinces, and suggested that only in certain basins were the ammonoids immured from temperature changes. Thus, major entrances of fauna seen in the rock record reflect extra-province, cool water adaptation. Additionally these authors note that regression-induced separation of population centres during eustatic low may be a catalyst for evolutionary change.

Whatever the evolutionary catalyst was, it was likely to affect other faunas, including conodonts. If the faunal turnover was related to the major sea

level fall and speciation was synchronous, it may be that the ammonoid and conodont record is out of phase due to facies control of the conodonts within and between the western European basins or related to different migration rates of the two faunas from the basin in which these animals survived the mid-Carboniferous extinction.

7.6. SUMMARY

1) Major controls on mid-Carboniferous deposition in the Clare Basin were basin configuration, sediment supply and the extent of sea-level changes. These combined to influence water column stratification, oxygen availability and sediment routes to the basin.

2) A model combining various lines of evidence (predominantly including palaeontological and geochemical), has been developed for mid-Carboniferous deposition in the Clare Basin.

The earliest Namurian shows a major transgression over the shelf area, resulting in a poorly oxygenated shallow sea, with conditions favourable to phosphogenesis. This was followed by a period in which deposition appears to have been predominantly confined to the basin centre with prolonged erosion resulting in the deposition of a phosphate lag. Fluctuations in sea-level led to the reactivation of the erosive mechanism during relative lowstand, interspersed with low energy shale deposition during succeeding sea-level highs.

The late Arnsbergian saw a relative increase in sea-level until a high at the end of the stage. This was followed by a dramatic fall at the beginning of the Chokierian. Repeated rises in sea-level occurred until the late Chokierian, when eventually the entire shelf area was transgressed.

3) The mid-Carboniferous boundary is only preserved in the centre of the Clare Basin; this is likely to have been due to the immediately preceding lowstand of the H_1a1.

Chapter 8

MID-CARBONIFEROUS STRATIGRAPHY OF SOUTHERN NEVADA

8.1 INTRODUCTION

The mid-Carboniferous boundary stratotype section has been chosen at Arrow Canyon, Nevada (Lane, 1995), within the Carboniferous Antler Basin. In this chapter detailed microfacies analysis is described from the section spanning the mid-Carboniferous interval at Arrow Canyon resulting in palaeoenvironment determination. Diversity changes across the boundary are investigated by using diversity and eveness analysis (Shannon-Wiener function). The Arrow Canyon section and the mid-Carboniferous stratigraphy are re-evaluated in the light of very recent Carboniferous biostratigraphic developments.

A further three sections are described from the southern part of the Antler Basin for comparison with the mid-Carboniferous Boundary section at Arrow Canyon (Figure 8.1).

8.2 BASIN DEVELOPMENT AND TECTONICS

The Antler orogen was initiated during the late Devonian (Frasnian), by the collision of an accretionary arc system with the passive margin of North America (Moores, 1970; Speed and Sleep, 1982; Burchfield and Royden, 1991; Goebel, 1991; Smith *et al.*, 1993), the accretionary prism of the arc system being underthrust by the continental slope and outer shelf of the passive margin. Vertical loading and downflexing of the continental shelf by the emplacement of the allochthon created the Antler foreland basin with sediment being derived from these highlands (Speed and Sleep, 1982).

The convergence of the accretionary prism provided a Mississippian Mountain belt with a parallel, north-east-south-west aligned, asymmetrical structural trough up to 400 km wide. A maximum thickness of sediments

Location	Grid Ref
Clark County	
Arrow Canyon	114°46′40″, 36°44′12″
Indian Springs	115°41′40″, 36°31′20″
Frenchman Mountain	114°59′40″, 36°11′40″
Nye County	
Syncline Ridge	116°10′00″, 37°2′30″
Lincoln County	
Kane Springs Wash	114°38′05″, 37°9′10″

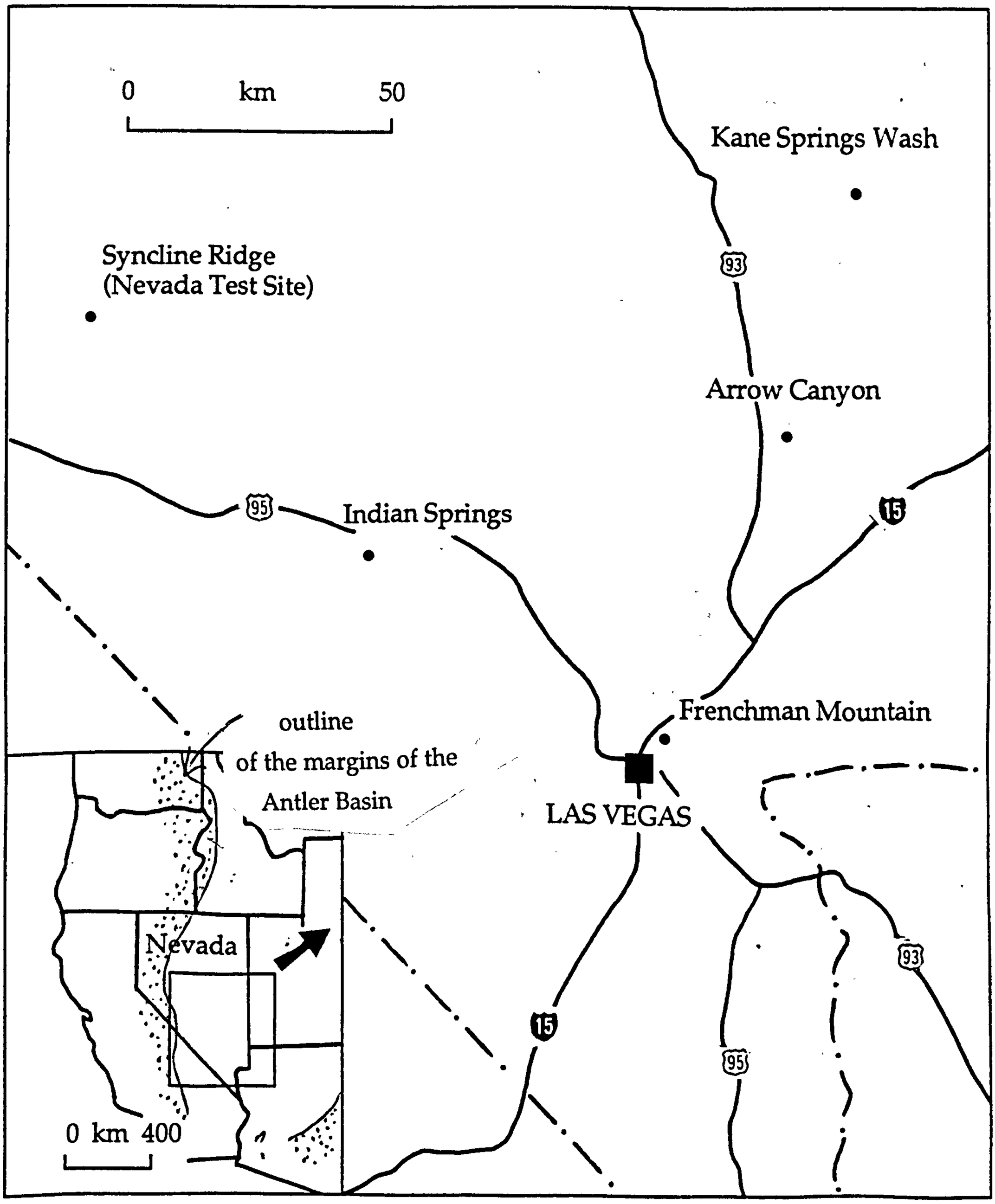

Figure 8.1 Location map of sections visited and/or mentioned in the text.

of 3.5 km in the west of the trough, thinning to <1 km to the east. The foreland basin developed on a continental shelf which had earlier accumulated shoal water carbonates and siliclastic sediments ranging from Cambrian to Late Devonian in age. Early in the Mississippian, sediment from the Antler Highlands was transported west to a postulated trough, a relict forearc basin that lay between the highlands and magmatic arc, and east to the foreland basin. During the lower Mississippian deep marine deposits accumulated in a starved basin (Poole, 1974). Later in Mississippian time, the foreland basin became filled with the eastward prograding molasse system. The molasse facies change across the region from alluvial and deltaic deposits in the area of the western trough to prodelta shallow marine siliclastic deposits in the former starved basin and on the carbonate shelf. Sediment derived from the west was transported through deltaic distributary channels, with sediment derived from the east being transported through bypass channels cut into the carbonate platform (Poole and Sandberg, 1977; Sandberg and Gutschick, 1980; Harbaugh and Dickinson, 1981; Stevens *et al.*, 1991) (Figure 8.2).

During the mid-Mississippian the highlands were further uplifted and the foreland basin widened. As the highlands continued to rise early foreland basin deposits lapping onto the lower prism slope were uplifted and resedimented (Speed and Sleep, 1982).

By the end of the Mississippian the highlands were much reduced and sedimentation was increased to the west. Load reduction resulted in regional uplift of both the highland and foreland basin and caused the foreland basin to become shallow or subaerial. Peritidal carbonates and evaporite carbonate deposits formed at the margins of the cratonic platform. During the latest Mississippian a few embayments encroached on the platform from marginal seas. However, the sediment source to the west existed until mid-Pennsylvanian times. Siliclastic sedimentation waned in the late Mississippian and early Pennsylvanian, and gradually gave way to carbonate sedimentation (Trexler and Nitchman, 1990).

The original distribution of Carboniferous rocks has been modified by major west-to-east thrusting during the Lower Triassic (Golconda Thrust) and the middle Cretaceous to lower Tertiary Sevier and Laramide orogonies. Middle Tertiary through Holocene block faulting (Basin and Range Province) has segmented all older structures (Larson and Langenheim, 1979).

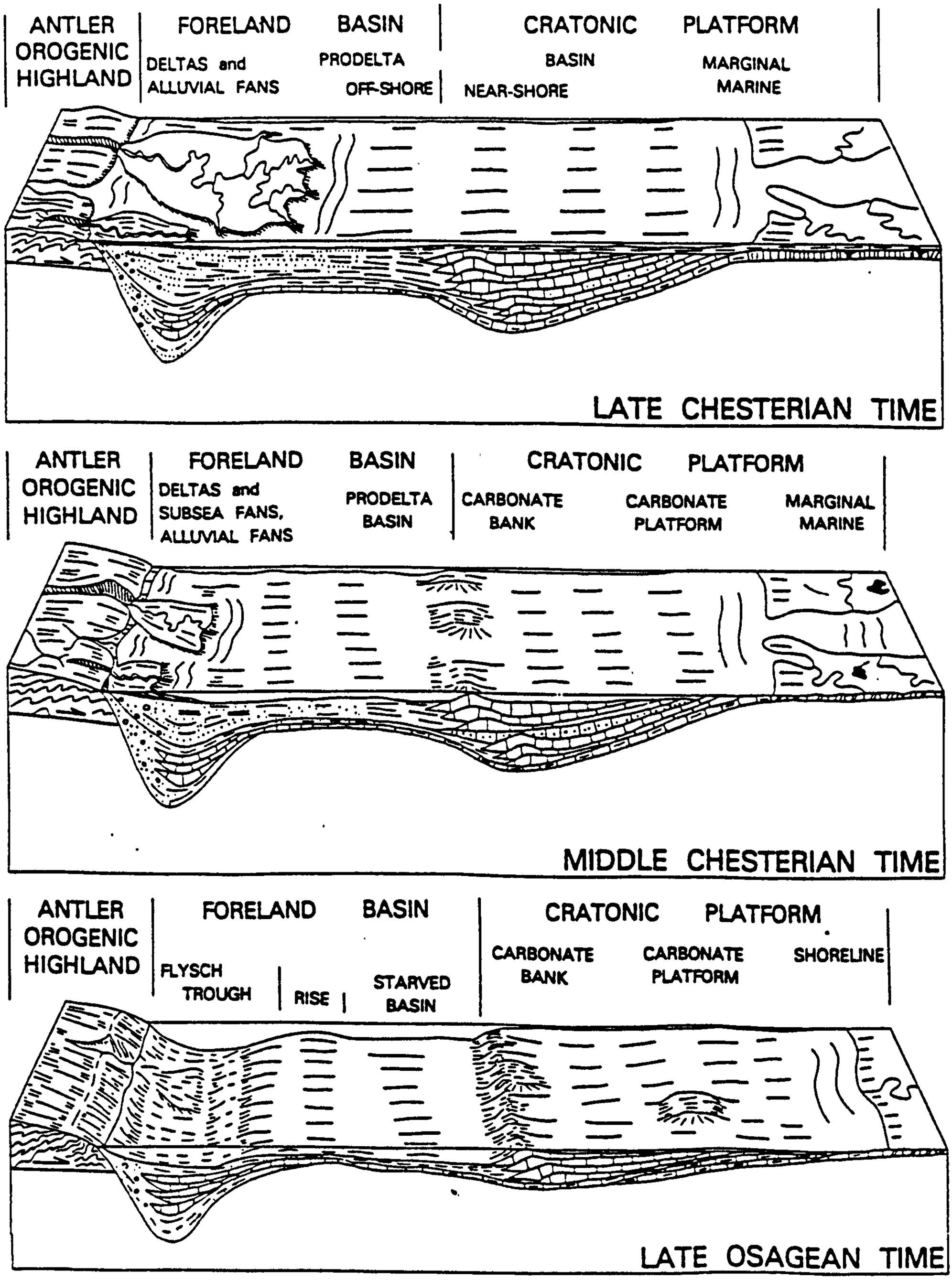

Figure 8.2 Evolution and palaeogeography of the Antler basin during the Upper Mississippian (From Stevens *et al.*, 1991).

8.3 STRATIGRAPHY OF THE ANTLER BASIN

The stratigraphy of the southern Antler Basin is shown in Figure 8.3, with the location of the studied sections in Figure 8.1. Mississippian Formations in southern Nevada comprise the shelf carbonates of the Yellowpine Limestone Formation unconformably overlain by the Battleship Wash Formation. The mixed clastic and carbonate basin margin deposits of the Indian Springs Formation unconformably overly the Battleship Wash Formation or lie directly on the Yellowpine Limestone where the Battleship Wash Formation has been removed by erosion (Langenheim *et al.*, 1962; Langenheim and Langenheim, 1965; Webster, 1969; Poole and Sandberg, 1991).

The Indian Springs passes up conformably into shelf limestones of the Bird Spring Formation (or its lateral equivalent the Callville Limestone Formation). In west of the study area the Bird Spring Formation equivalent, the Tippipah Limestone Formation, unconformably overlies the Indian Springs Formation, (Gordon and Poole, 1968; Webster *et al*, 1984).

Towards the north of the study area at Kane Springs the flysch deposits of the Chainman Shale Formation are conformably overlain by the Indian Springs Formation, which pass up conformably into the Bird Spring Formation (Webster, 1969). The Test Site section shows the lateral basinal equivalents of the upper Mississippian Formations and lower Pennsylvanian portion of the Bird Spring Formation; the Eleana Formation. This unit is unconformably overlain by the Tippipah Limestone.

8.4 ARROW CANYON

The mid-Carboniferous boundary stratotype section at Arrow Canyon crops out within a canyon on the northern end of the Arrow Canyon Range, Clark County, Nevada. It is reached by a jeep track (following the wash) leading off a paved road from State Highway 168 (see Webster *et al.*, 1985) for a full description of the directions to the locality.

Due to the extreme aridity and rugged topography, the rocks are essentially completely exposed (Plate 8.1). The section was logged in this study from the top surface of the Battleship Wash Formation, for a total height of 121.15

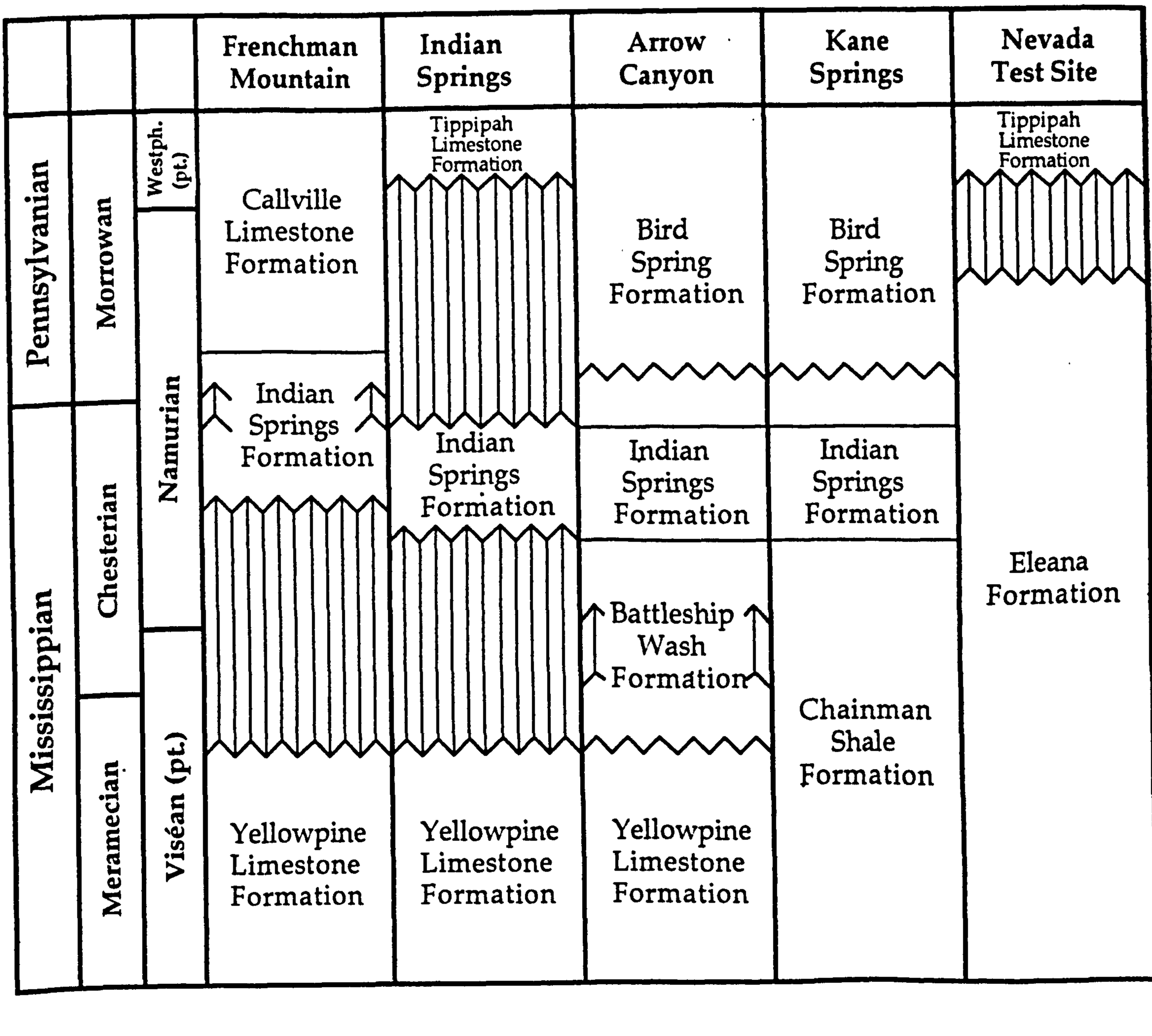

Figure 8.3 Stratigraphy of the southern Antler Basin (After Webster *et al.*, 1984).

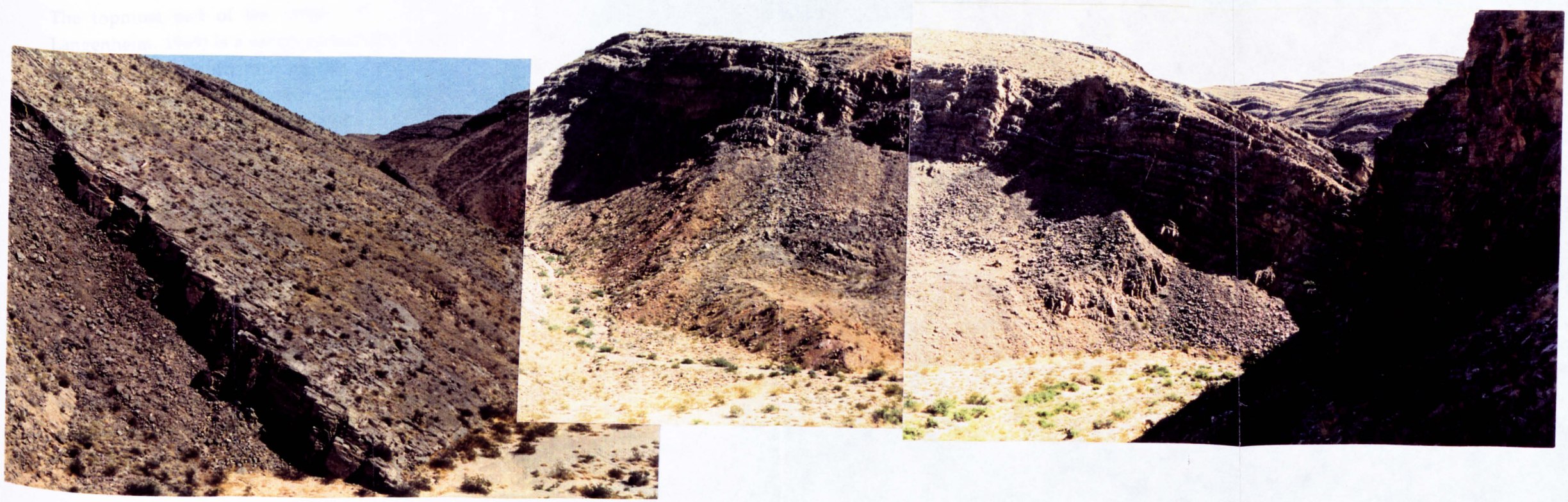

Plate 8.1 View north-east of the mid-Carboniferous strata at Arrow Canyon. The bedding plane to the left of the Plate is the top of the Battleship Wash Formation. The Indian Springs Formation weathers rusty yellow in the centre of the Plate. The mid-Carboniferous boundary lies within the Bird Spring Formation which forms the cliffs to the right of the Plate. Height of cliffs apprximately 200 m.

m, passing the mid-Carboniferous boundary at 85.6 m (Enclosure 1). The rocks investigated comprise the Indian Springs and Bird Spring Formations, dipping approximately 20-40° to the ESE, and crop out approximately 75 m from the narrow mouth of the gorge. Outcrops were measured on both sides of the canyon and a composite section has been constructed through the Indian Springs Formation and lower part of the Bird Springs Formation (Enclosure 1).

8.4.1 Description of the section at Arrow Canyon

The topmost bed of the Battleship Wash Formation (Langenheim and Langenheim, 1965) is a sandy grainstone, containing crinoid and brachiopod debris together with rare corals. The undulose top surface displays abundant casts of *Stigmaria* sp. (identified as *Stigmaria ficoides* and *Stigmaria wedingtonensis* by Pfefferkorn, (1972)). These casts are up to 2 m long and are filled with sand from the bed above.

The overlying Indian Springs Formation (Webster and Lane, 1967) is 69.85 m thick with a 25 cm thick greeny yellow weathering fine grained sandstone at the base of the formation. This horizon contains much carbonaceous debris, although no *Stigmaria* were present.

From this horizon until approximately 43 m above the base, the Indian Springs shows cyclic repetitions of varicoloured (red, grey and purple) 9-12 m thick weathering shales capped by 1-2 m thick orange-weathering biopackstones to biograinstones, the top surfaces often showing phosphatic clasts and abundant brachiopod debris.

The 52 cm thick marker conglomerate of Webster (1969) occurs at 31.33 m above the base of the Indian Springs and comprises subangular limestone chert and phosphatic clasts up to 7 cm in size. Reworked Devonian goniatites are present in the limestone (Alan Titus, pers comm., 1992).

The upper part of the Indian Springs is less well exposed and consists of yellow and orange weathering tabular cross-bedded and symmetrically rippled fine-medium grained sandstones overlain by interbedded marls and bioclastic sandy limestones.

The base of the Bird Spring Formation (Langenheim *et al.*, 1962; Webster, 1969) is drawn at 69.85 m above the base of the Indian Springs Formation at

the first occurrence of 'clean' cherty limestones. The basal 13.91 m of the formation shows predominantly cherty biograinstones, containing a fauna dominated by crinoid ossicles and brachiopod fragments. At 83.76 m above the base of the Indian Springs Formation a 41 cm thick interval displays friable yellow marl and limestone containing well preserved bryozoa together with articulated brachiopods and crinoid debris. This unit is overlain disconformably by a 2.28 m thick grainstone sequence which in turn is terminated by a 34 cm thick conglomerate interval at 86.04 m above the base of the Indian Springs Formation (Plates 8.2 and 8.3). The conglomerate interval contains three individual fining up beds, the top of which are sandy and display symmetrical ripples. Clasts comprise angular-subrounded chert and limestone fragments up to 5 cm in size. This is overlain by a 51 cm thick interval of calcareous siltstones. A further 2.10 m thick clastic horizon lies erosively upon this siltstone. At the base this consists of a cross-bedded carbonate-cemented sandstone and passes up into a cross-bedded sandy grainstone.

The following 32.16 m of Bird Spring Formation to the top of the measured section comprises cherty bioclastic limestones. The basal part of the Bird Spring above the conglomerate consists of biograinstones. The interval between 92.6 to 108.8 m above the base of the Indian Springs Formation shows a sequence of mudstones and wackestones with rare packstones and grainstones.

The upper part of the logged sequence shows a return to biograinstone facies. A cross-bedded unit overlain by a thin limestone conglomerate horizon occurs at 111.86 m above the base of the Indian Springs Formation.

8.4.2 Biostratigraphy of the Arrow Canyon section

The biostratigraphy has been quite extensively studied on the section particularly by Langenheim and his numerous masters and doctoral students at the University of Illinois at Urbana-Champaign (e.g., Brill, 1963; Coogan, 1964; Langenheim and Langenheim, 1965; Cassity and Langenheim, 1966;). This has led to the development of several conflicting numerical bed identification schemes (e.g., Amoco brass-tagged beds, Webster and others painted schemes). Unfortunately, however, no real synthesis of the biostratigraphic data has been forthcoming, except for over a very short interval spanning the boundary.

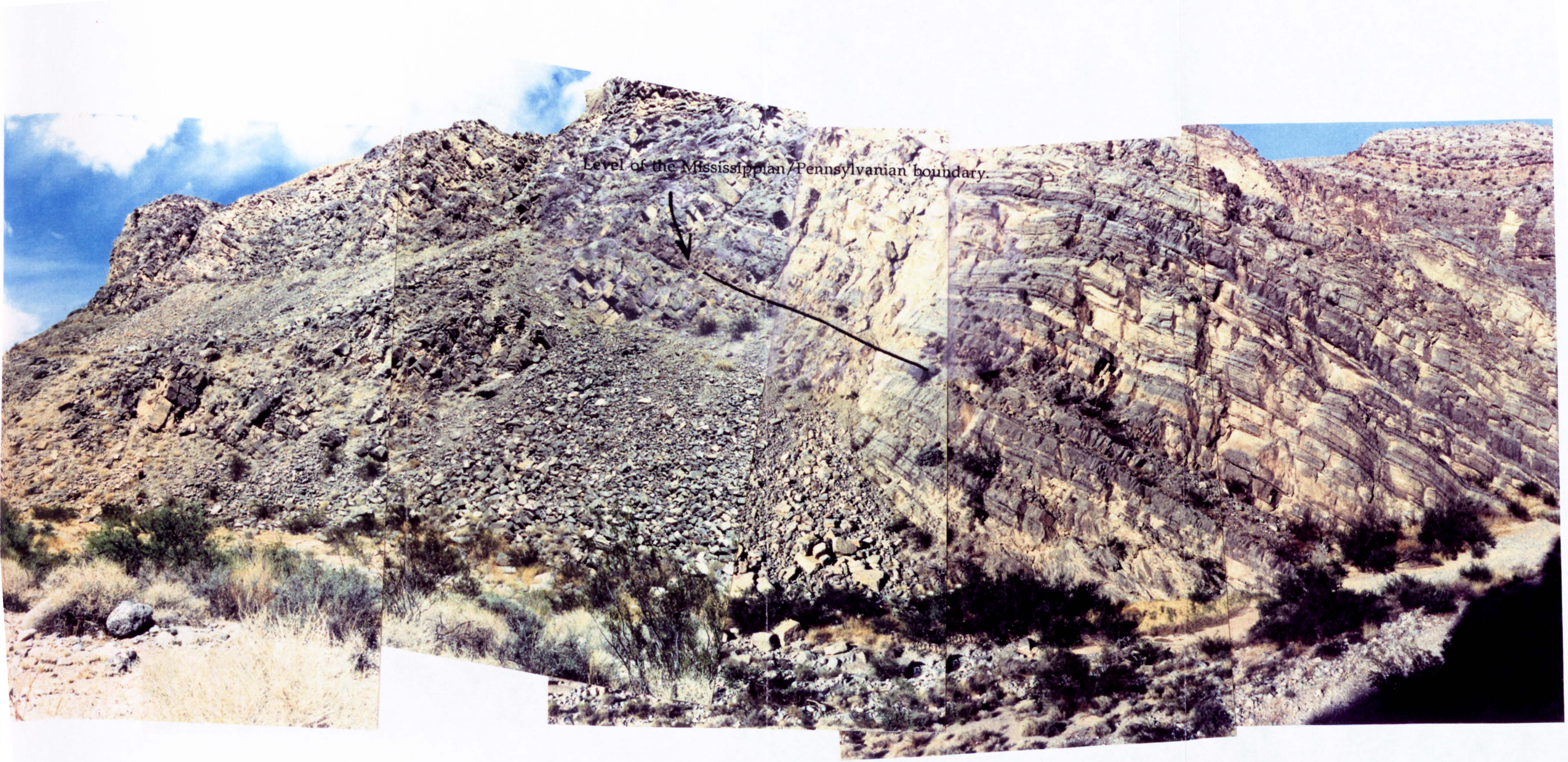

Plate 8.2 View north-east of the mid-Carboniferous strata at Arrow Canyon. Section measured in this study up through the Bird Spring Formation on the middle left of the diagram up to the mid-Carboniferous boundary at the top of the scree slope in the centre of the Plate. Post boundary strata measured along canyon floor.

Plate 8.3 View north of the boundary strata at Arrow Canyon.

Work on the conodonts of the succession (Webster, 1969) initially led to the belief that the Mississippian-Pennsylvanian boundary equated to the conglomerate horizon developed within the lower part of the Bird Spring Formation. Further work by Lane, Baesemann, *et al.*, (1985) led to the position of the boundary being displaced to "less than one metre below the conglomerate", within the top of the limestone bed 85.4 m above their logged base of the Indian Springs Formation (Lane, Baesemann, *et al.*, 1985, p 434), (this equates to the bed I have measured at 85.6m.) However, recent work by Uwe Brand (Nick Riley, pers comm., 1995) has recognised the appearance of the boundary defining conodont beneath its previous documented occurrence at the base of the bed (the exact height has not been disclosed).

The foraminiferal biostratigraphy of the Arrow Canyon section has been documented by Brenckle (1973) and Brenckle *et al.*, (1982) They noted that changes in the foraminiferal assemblages did not coincide directly with the conodont-defined boundary. Lane, Baesemann, *et al.*, (1985) also briefly discussed the brachiopod fauna and did not recognise any distinct changes over the boundary interval.

8.4.3 Facies Interpretation of the mid-Carboniferous at Arrow Canyon

8.4.3.1 Battleship Wash and lower and middle Indian Springs Formations

Deposition of the Battleship Wash Formation is envisaged as being within a nearshore, peritidal environment (Poole and Sandberg, 1991). The uppermost horizon of the Battleship Wash Formation representing a forested beach or carbonate mudflat deposit, possibly overlain by a palaeosol at the base of the transgressive Indian Springs Formation.

Several 9-12 m thick cycles are evident in the Indian Springs Formation, and comprise a thin layer of phosphate pebbles, followed shales occaisionally grading up into silt, capped, in the lower part of the section, by limestone (or once a conglomerate). Towards the top of the Indian Springs the cycles become capped by cross-bedded sandy units.

The cycles probably represent small scale transgressive-regressive cycles, with a transgressive phosphatic lag developed during the sea-level high at the base of the cycle. The sandy units at the top of the Indian Springs may

represent mouth bar deposits, developed at the top of the regressive cycle as the area becomes more proximal to the prograding delta.

These cycles appear to be similar to the 'minor lithological cycles' or 'cyclothems' documented from Britain (e.g., Ramsbottom, 1977, 1979; Holdsworth and Collinson, 1981; Read, 1991; Maynard and Leeder, 1992), however, the lack of faunal data makes the analysis of salinity fluctuations uncertain.

8.4.3.2 Upper Indian Springs and lower Bird Springs Formations

Microfacies analysis

Microfacies analysis has been conducted in this study on thin sections and acetate peels on samples taken from the upper (carbonate) part of the Indian Springs Formation and the lower part of the Bird Spring Formation (spanning the mid-Carboniferous boundary). A total number of 68 samples were taken from virtually every distinct lithologic unit and thin sections or peels were made, after staining with Alizarin Red S and Potassium ferricyanide (as described by Adams *et al.*, (1984)).

Standard microfacies as described by Wilson (1975), modified by Flügel (1982) and Stevens and Armin (1983) were employed. Ten microfacies are recognised across the mid-Carboniferous at Arrow Canyon.

Description of microfacies

Siltstone microfacies microfacies (ss)

No fossils are present in this facies. It comprises siltstone or fine grained sandstone, with quartz grains ranging from 0.1 mm-1 mm in size (Plate 8.4). The grains are commonly subrounded to subangular. Lithoclasts from a metamorphic source, and pyroxene grains are present. Quartz overgrowths are present. Bimodality is seen in one sample with a matrix of fine grained anhedral quartz grains (0.1mm) with rare 1 mm rounded to subrounded quartz grains. A small amount of micrite is present in the matrix of some samples.

Occurrence: (Sample numbers) AC101, AC103, XAC1

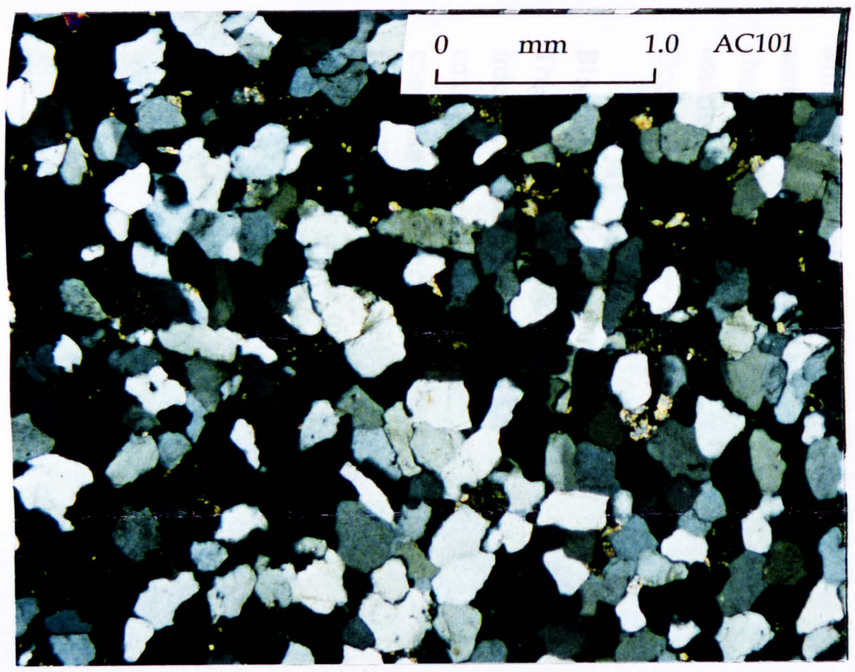

Plate 8.4 Photomicrograph showing siltstone microfacies (ss).

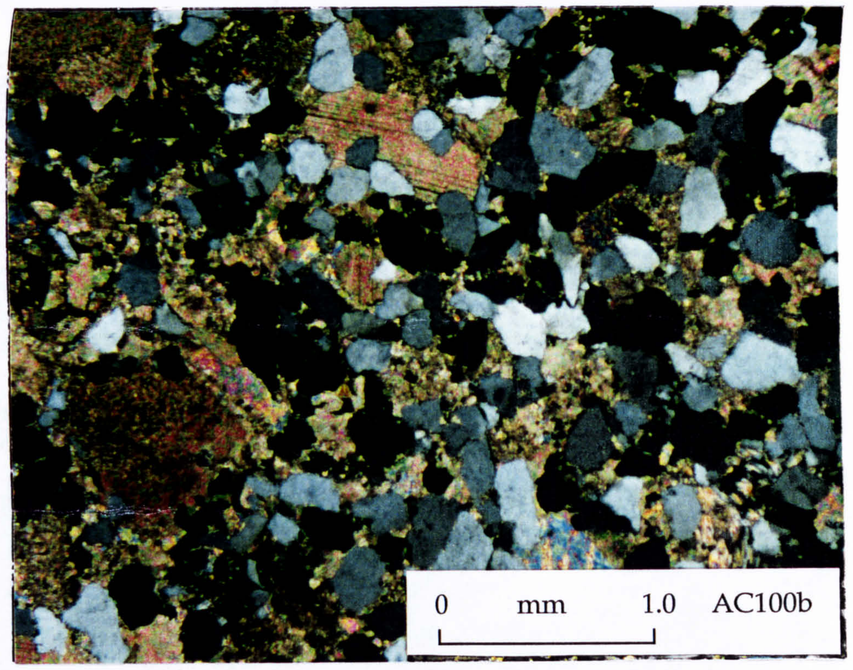

Plate 8.5 Photomicrograph showing fossiliferous siltstone microfacies (ssf).

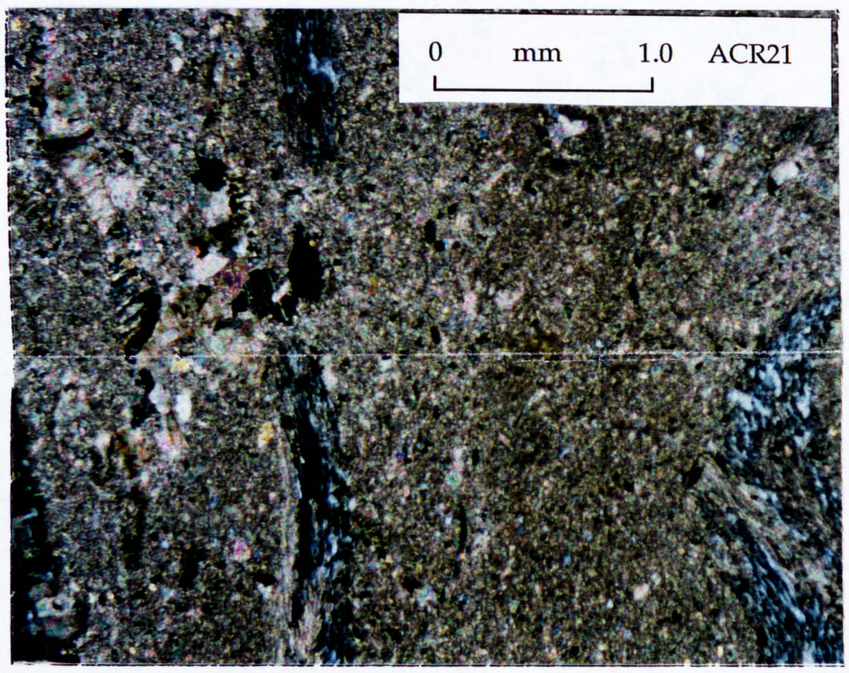

Plate 8.6 Photomicrograph showing whole fossil wackestone (smf-8).

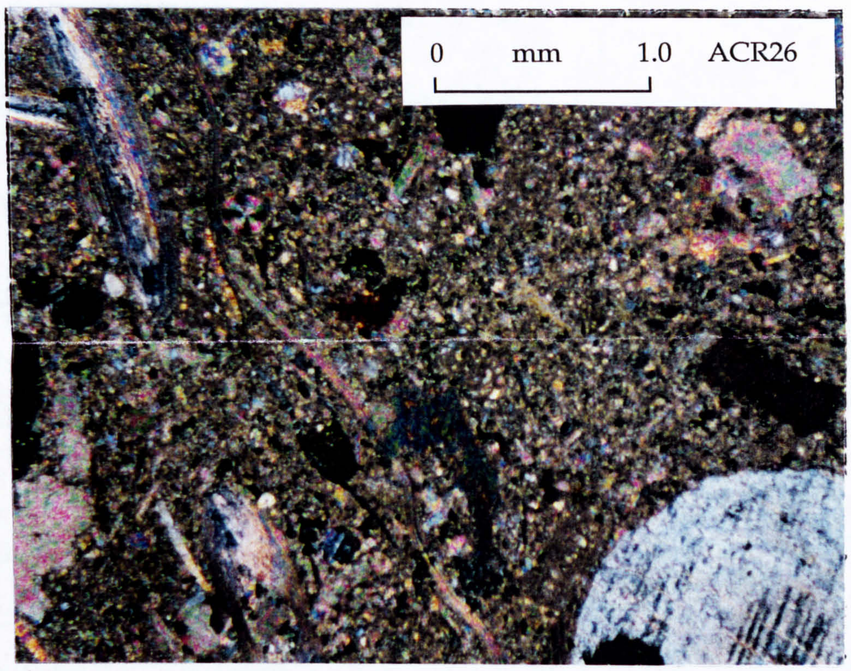

Plate 8.7 Photomicrograph showing bioclastic wackestone microfacies (smf-9).

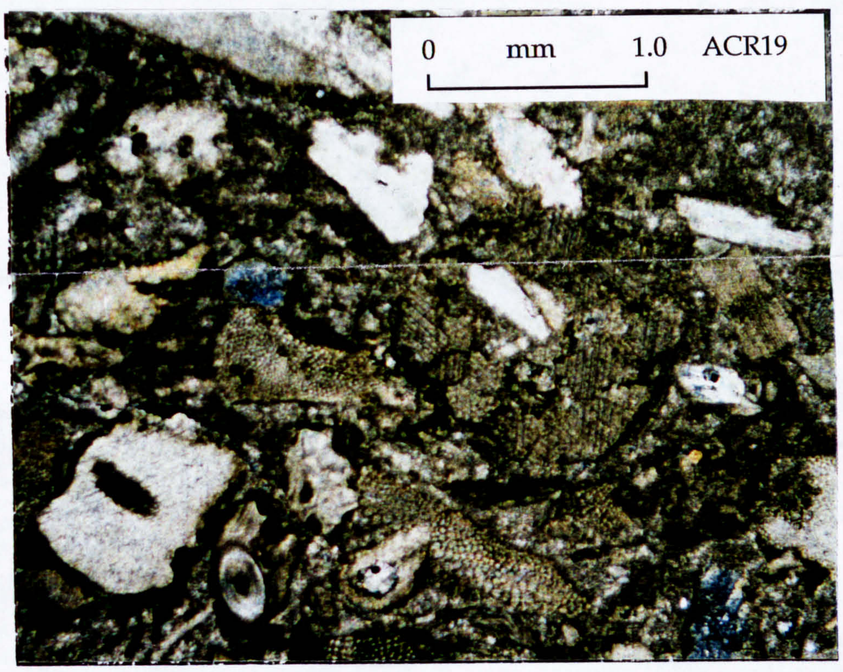

Plate 8.8 Photomicrograph showing packstone-wackestone with coated and worn bioclasts microfacies (smf-10).

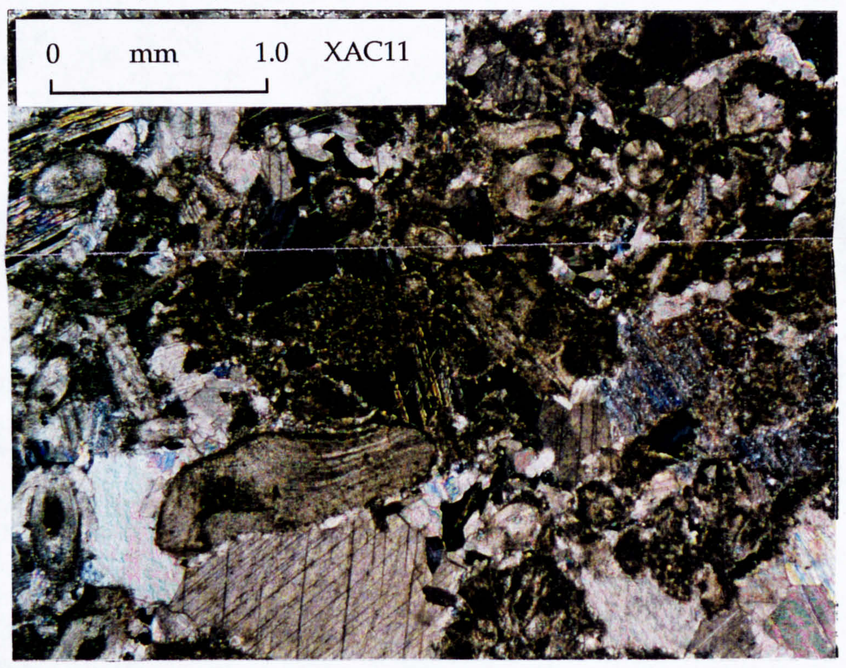

Plate 8.9 Photomicrograph showing coated bioclasts in sparite, grainstone microfacies (smf-11).

N.B. All photomicrographs are taken under crossed nicols

Peloidal siltstone microfacies (ssp)

Microfacies ssp is a siltstone containing peloids or highly micritized grains. The quartz grains are up to 0.25 mm in size and are angular-subrounded. The micrite clasts occur as small ovoid and circular clasts and also as stringers up to 1 cm long. Micrite is present in the matrix of the rock, together with a small amount of drusy calcite.

Occurrence: AC102, AC104, AC105, AC106.

Fossiliferous siltstone microfacies (ssf)

This microfacies consists of siltstone or fine-grained sandstone containing bioclasts (Plate 8.5). Quartz grains range from 0.25 - 0.5 mm in size and are subangular to rounded. Some irregular boundaries to the grains are visible and may indicate aggressive carbonate precipitation. Quartz overgrowths are present. Fossils are generally worn, rounded and often micritized, they comprise bryozoa fragments, crinoid ossicles, brachiopod and bivalve fragments. Syntaxial cements are commonly present on the crinoid ossicles. The matrix is predominantly micritic although some marine (acicular) and burial (drusy and poikilotopic) cements are also present.

Occurrence: AC100b, ACR 1, ACR1b.

Whole fossil wackestone microfacies (smf-8)

Microfacies smf-8 shows a carbonate mudstone containing only a few scattered very large fragments of brachiopod and recrystallized bivalve shells. Also present are rare bryozoan and algal fragments and crinoid ossicles (Plate 8.6).

Occurrence: ACR7, ACR21, ACR27, ACR45

Bioclastic wackestone microfacies (smf-9)

This microfacies shows relatively high amounts of bioclasts present in a micrite or micrite and psuedospar matrix (Plate 8.7). A small amount of coarser calcite cement may be present in intraparticle pores. Bioclasts comprise brachiopod and bryozoan debris, recrystallized bivalve shells and foraminifera. Frequently the shell debris is highly fragmented. A small amount of silt grade quartz is present in a few samples.

Occurrence: AC111b, AC111, AC117, AC119a, ACR5, ACR15, ACR16, ACR18, ACR18b, ACR24, ACR26, ACR32b, ACR34, ACR42, ACR43, ACR51, ACR54, ACR59, XAC3, XAC9.

Packstone-wackestone with coated and worn bioclasts microfacies (smf-10)
Microfacies smf-10 shows rounded and micritized bioclasts in a micrite or mixed micrite/sparite matrix (Plate 8.8). Bioclasts comprise heavily micritized, commonly rounded, foraminifera, crinoid ossicles and bryozoan, brachiopod and bivalve fragments. Superficial ooids (showing random oriented micrite), and Intraclasts are also present. Up to 10% silt sized quartz grains are present in one sample. The matrix is dominantly micrite although syntaxial cements and a minor amount of drusy cement are visible.
Occurrence: ACR8, ACR8a, ACR19, ACR30, ACR38, ACR50.

Coated bioclasts in sparite, grainstone microfacies (smf-11)
This microfacies comprises highly-abraded, micritized bioclasts (bryozoan fragments, crinoid ossicles, brachiopod debris and bivalve fragments), in a coarse sparite matrix (Plate 8.9). The sparite matrix comprises marine (prismatic) and burial cements (poikilotopic and drusy). Syntaxial overgrowths are omnipresent.
Occurrence: AC109, AC113, XAC11, XAC12.

Coquina, bioclastic grainstone or rudstone, shell hash microfacies (smf-12)
This microfacies is dominated by bioclastic debris consisting of either a mixed assemblage of bioclasts, or an assemblage dominated by one type of organism in a pseudospar or micrite matrix. The former assemblage includes brachiopod, bryozoa and recrystallized bivalve fragments together with occurrences of foraminifera, crinoid ossicles and intraclasts (Plate 8.10). Fragmentation may be high and clasts are commonly rounded to subrounded; micritization is low. Syntaxial, prismatic and drusy cements are common, and silt may make up 5% of the matrix.

The assemblage dominated by one group often has a finer grained matrix (Plate 8.11). Brachiopod fragments are the most common single element represented, although crinoids may also dominate. Bioclast may show some micritization.
Occurrence: AC108, AC110a, AC110b, AC111, AC112, AC112b, AC116, AC119, AC121, AC122, AC123, ACR4, ACR10, ACR17, ACR25, ACR29, XAC2, XAC4, XAC5, XAC7, XAC8.

Oolite microfacies (smf-15)
The oolite microfacies shows random micritic ooids together with superficial ooids (Plate 8.12). The nuclei comprise brachiopod and

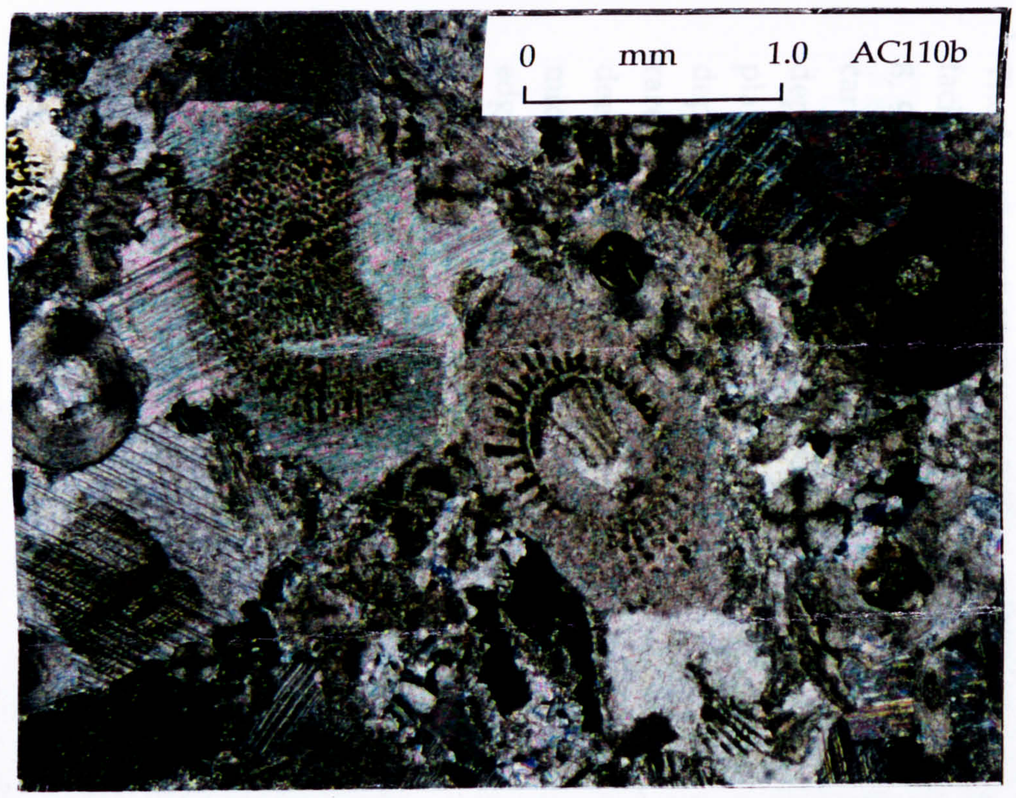

Plate 8.10 Photomicrograph showing coquina, bioclastic grainstone, shell hash microfacies (smf-12).

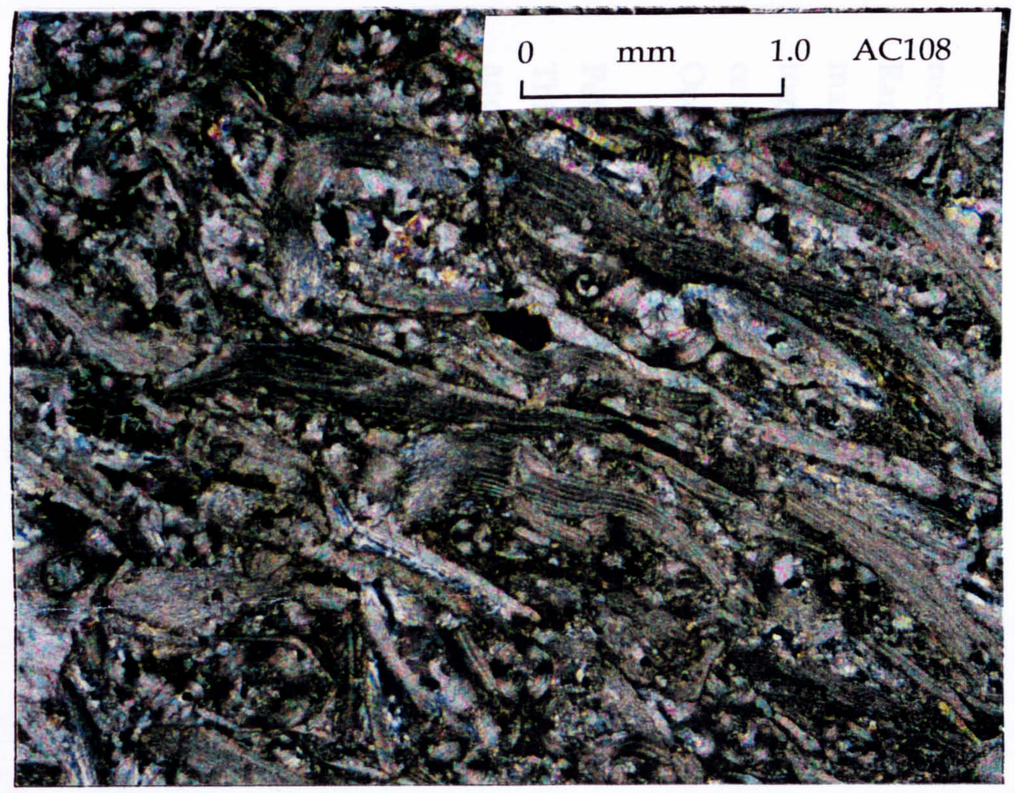

Plate 8.11 Photomicrograph showing coquina, bioclastic grainstone, shell hash microfacies (smf-12).

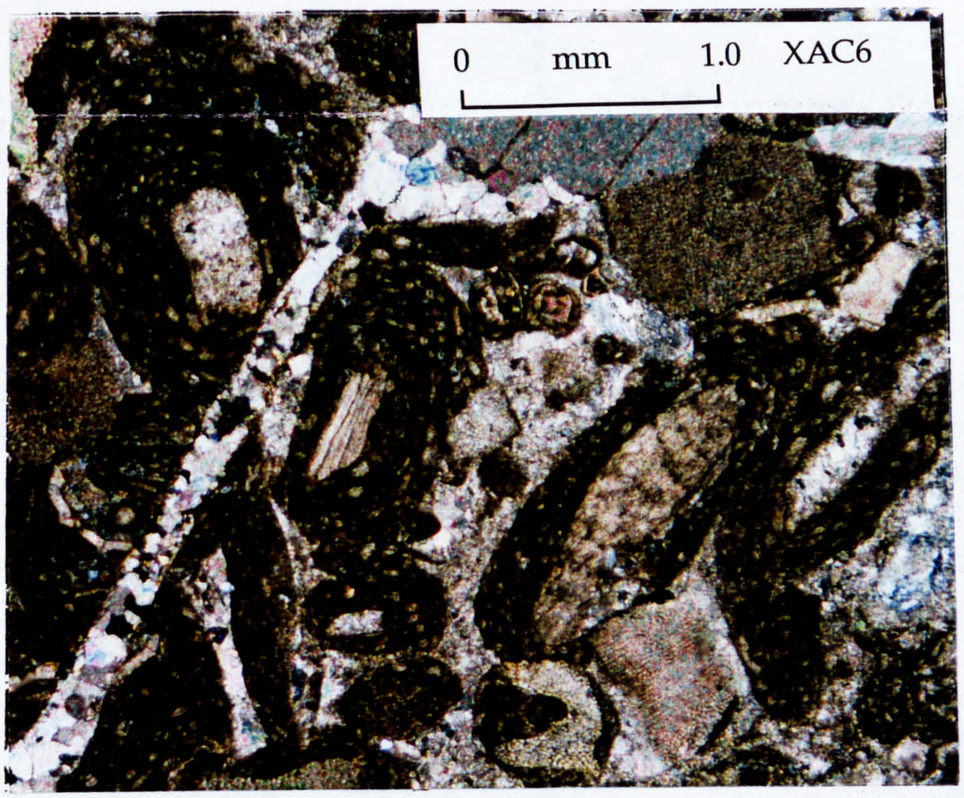

Plate 8.12 Photomicrograph showing oolite microfacies (smf-15).

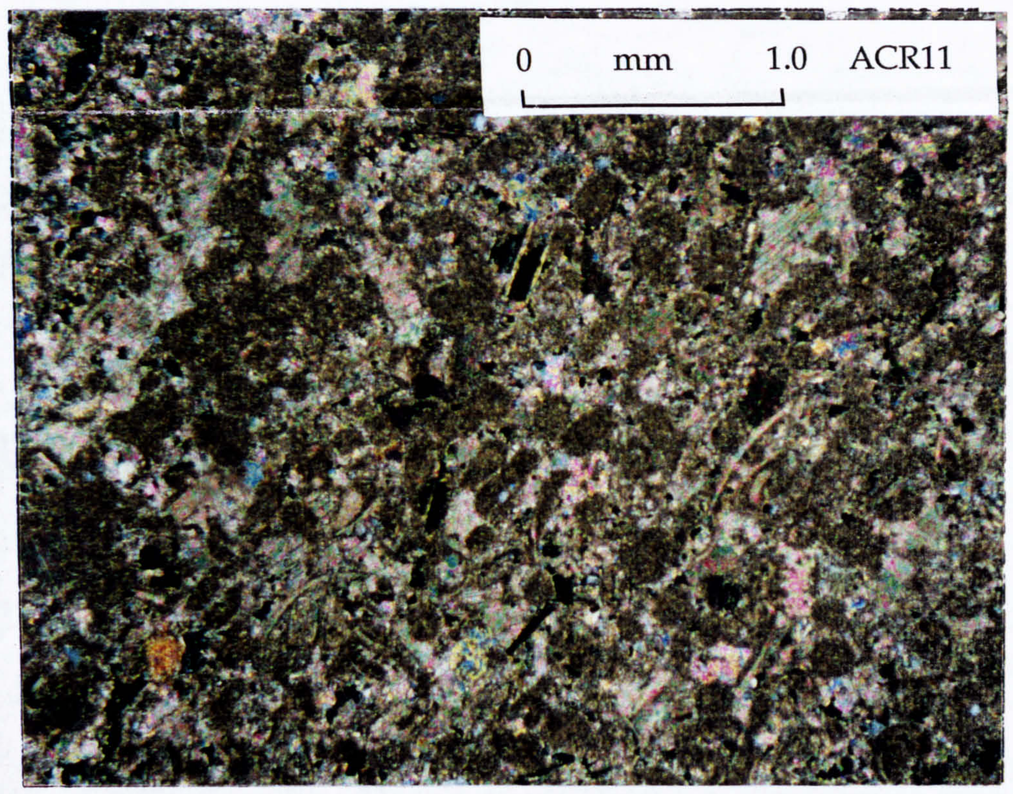

Plate 8.13 Photomicrograph showing pelgrainstone microfacies (smf-16).

N.B. All photomicrographs are taken under crossed nicols

recrystallized bivalve fragments, crinoid ossicles, and bryozoa fragments. Rare tiny quartz grains are also present within the ooids and also within the matrix of the rock. The matrix comprises minor amounts of micrite together with minor marine (prismatic) and burial (drusy and poikilotopic) cement. The nuclei of the ooids are well rounded.
Occurrence: ACR48b, XAC6.

Pelgrainstone microfacies (smf-16)

This microfacies is characterised by high amounts of small (0.2 mm) peloids and highly micritized coated grains with a burial cement matrix (equant, poikilotopic and drusy) (Plate 8.13). Highly fragmented bioclastic debris also appears together with foraminifera and crinoid ossicles.
Occurrence: ACR11, ACR35, ACR36, ACR49, ACR57.

Paleoenvironmental interpretation

Standard facies zones as described by Wilson (1975), Flügel (1982) and Stevens and Armin (1983) were applied to the microfacies (Table 8.1, Figure 8.4).

The lower part of the studied section is dominated by winnowed platform facies zone 6 with smf types 11 and 12 with a minor occurrences of smf types 8, 9, and 15 (Enclosures 2 and 3). These highly bioclastic, coarse-grained, carbonates and the minor oolitic occurrences are likely to have been deposited in a high energy environment at the edge of the carbonate platform possibly on carbonate bars or shoals with reworking of bioclasts deposited in deeper water. Minor deepening events are represented by the rare occurrences of smf 8 and 9 indicating deposition within the slightly deeper waters of facies zone 7 (open platform). Deposition of these microfacies was probably in open lagoons and bays behind the platform edge.

The mid-Carboniferous boundary is located within deposits pertaining to smf-12 (winnowed platform). The succeeding conglomerate horizon and mixed carbonate clastic interval is assigned to facies zone 8 (restricted platform) and represents the most proximal deposits encountered. Deposition of these sediments would have been in a marginal marine environment, possibly a beach or shallow lagoon with reworking of bioclasts at the shoreline.

Standard	Microfacies	Facies Zone	Interpretation of microfacies
ss	Siltstone	8- Restricted platform	Nearshore sublittoral sandsheets, beaches, and subaerial or submarine deltaic deposits
ssp	Peloidal siltstone	8- Restricted platform	Low energy beach to slightly subtidal environment.
ssf	Fossiliferous siltstone	8- Restricted platform	Moderately high energy nearshore bar or beach environment.
smf-8	Whole fossil wackestone	7- Open platform	Quiet water below normal wave-base
smf-9	Biowackestone	7- Open platform	Shallow neritic water at or below normal wave-base
smf-10	Coated/worn biopackestone/biowackestone	7- Open platform	High energy particles moved out of thier environmnet of formation, into water at or below normal wave-base.
smf-11	Coated/worn biograinstone	6- Winnowed platform	Shallow water high energy environment with particles formed in ares of constant wave action, at or above normal wave-base
smf-12	Biograinstone/coquina	6- Winnowed platform	Shallow water high energy environment with deposits formed in areas of constant wave action, at or above normal wave-base
smf-15	Oolite	6- Winnowed platform	Shallow water high energy environment with grains formed in ares of constant wave action, at or above normal wave-base
smsf-16	Pelgrainstone	7- Openplatform	Shallow water at or below normal wave-base.

Table 8.1 Standard microfacies zones. (After Wilson, 1975, Flügel, 1982 and Stevens and Armin, 1983).

Facies Zone		
6- Winnowed platform	7- Open platform	8- Restricted platfrom

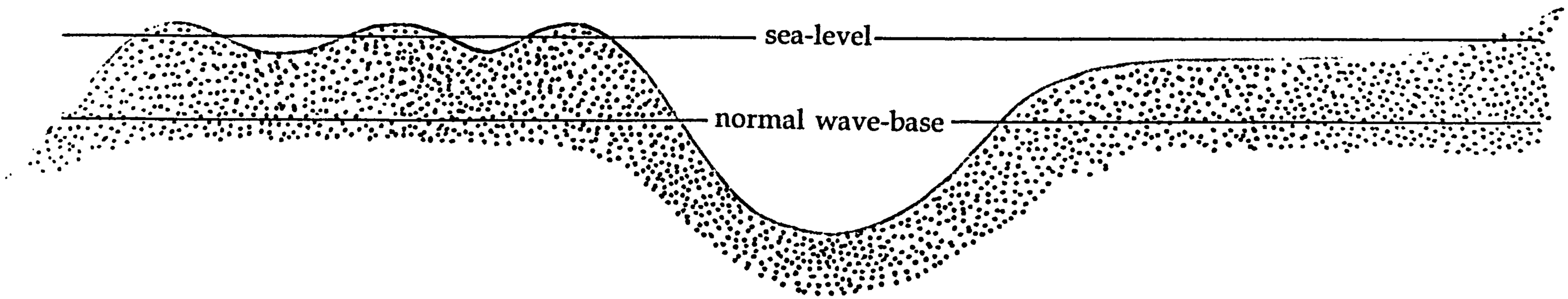

SMF types		
11, 12, 15	8, 9, 10, 16	ss, ssp, ssf
Facies belts		
Winnowed carbonate sands on shoals, bars or coastal areas. Shallow water, high energy within wave-base.	Bays and open lagoons behind the outer platform edge. Deposition at or below wave-base.	Beach or nearshore bar at proximal edge of platform. Subaerial and submarine deposits.

Figure 8.4 Standard microfacies types and their interpreted depositional environment. (After Wilson, 1975, Flügel, 1982 and Stevens and Armin, 1983).

The strata immediately succeeding the clastic interval show a return to winnowed platform deposits with increasing intercalations of the deeper water deposits of the open platform deposited at and below fair-weather wave-base. Shallow water deposits of smf-12 and smf-16 types become intercalated towards the top of this interval which shows fluctuations from the high energy platform margin sediments (smf-12) and the slightly lower energy lagoonal pelleted facies (smf-16). A return to the open platform deposits follows, although there is still evidence for periodic increases in the environmental energy with oolitic and pelleted deposits.

In summary, the upper part of the Indian Springs Formation and the lower part of the Bird Spring Formation (beneath the conglomerate) are mostly shallow, high energy facies from the winnowed edge of a carbonate platform with reworking of bioclasts deposited within more open regions of the platform and on the slope. Following the deposition of clastics in a paralic setting a return to the winnowed platform deposits is followed by a sequence of deep water, open platform deposits which shallow up to more winnowed deposits once again. A further deepening is seen at the top of the section. The mid-Carboniferous boundary therefore falls towards the top of a regressive interval at 85.6m above the base of the logged section.

Unlike the work of Stevens and Armin (1983) no distinct repetitions of smf-types are recognised. However, a similar relationship with the upper Mississippian strata representing shallow winnowed platform deposits followed by a transgression during the lowermost Pennsylvanian (producing open platform deposits) has also been recognised from microfacies studies at other locations in southern Nevada by Wilson (1985) .

8.4.4 Faunal Diversity across the mid-Carboniferous Boundary at Arrow Canyon

To investigate faunal diversity across the mid-Carboniferous boundary the entire amount of bioclastic components in a 20 x 10 mm area have been counted from sixty thin sections spanning the lower part of the Bird Spring Formation. Various statistical functions have then been applied to the data.

To calculate the faunal diversity there has to be some amount of community reconstruction, but as noted by Lasker (1976), there will always be a bias in the palaeocommunity reconstruction due to selective fossilisation, taphonomy and also time-averaging of faunas. These include:-

1) Selective preservation

Staff and Powell (1988) observed from modern sediments that between 20 and 40% of benthic species are preservable.

2) Biostratinomic processes

Biostratinomic processes are those occurring between the death of the organism and its subsequent burial. These processes are predominantly reorientation and transport, disarticulation, fragmentation and corrasion.

3) Early diagenetic processes

Early diagenetic processes include dissolution, compaction and mineralization (see Brett and Baird, (1986) and Parsons and Brett (1991) for a full review of the various aspects of taphonomy).

4) Time averaging

Time averaged populations contain the remains of organisms which may have lived under different ecological conditions. Time averaging therefore can alter the species composition, the relative abundance and diversity of the community by telescoping relic hardparts from different time planes (Fürsich and Aberhan, 1990). Fürsich and Aberhan (1990) expect that true community 'relics' are common in shallow water where net sedimentation rates are high with only short-term time-averaging being expected on shelf areas.

8.4.4.1 Data analysis

When considering the obtained data, it has proven impossible to correct for biostratinomic processes. Although it may be possible to provide a correction to calculate the number of individuals represented by crinoid ossicles (Meyer and Meyer, 1986), there is no way of estimating the number of individual brachiopods represented by the variety of shell fragments, as it is impossible to gauge how many fragments a brachiopod shell will fragment into and out of those how many are likely to contribute to the rock record! Obviously no correction can made for selective preservation in the results calculated from Arrow Canyon.

The statistics (described below) applied in this study use numbers of individuals. Unfortunately it is impossible to determine individual species (except for foraminifera) in thin section. Therefore all individual parts of organism have been treated as a whole, i.e. as representing all the brachiopods in the community, therefore all foram data is treated as a group rather than individual species. The statistics will therefore include the diversity of the total brachiopod community within the total fauna.

As individuals cannot be computed each occurrence of an organism at a horizon is assigned into one of four quartile classes:-absent, rare, common and abundant (Table 8.2). Quartiles were defined statistically to obtain a quarter of the data generated (omitting 'absences'). The lower quartile is restricted so that 1/4 of the data is lower than the 'cut-off' value for the 'rare' category. The medial quartile ('common') represents the following 50% of data points, and the upper quartile ('abundant' represent the top 25% of the data points (Medenhall, 1979, p42.).

Table 8.2 Numbers of fragments defining classes per faunal element (calculated statistically using quartiles)

Faunal element	Rare	Common	Abundant
Crinoids	0-8	9-51	>51
Brachiopods	0-20	21-87	>87
Bivalves	0-1	2-4	>4
Bryozoa	0-2	3-16	>16
Algae	0-1	1-7	>7
Foraminifera	0-1	2-13	>13

Coral fragments, calcispheres and worm tubes all have very low occurrences of fragments and thus are treated as 'rare'

Thus, in all computations 'abundant' is assigned a value of 3, 'common' 2 and rare a value of 1 (Table 8.3). Although defining the classes by quartiles may skew the results in that the 'common' class contains the greatest number of representatives, it was found that when the classes were defined subjectively they were found to coincide with the statistically-defined boundaries in the majority of cases. Thus there appears to be no gradation in between faunal element values and specific classes can be defined. By using the quartile method for all fauna then any bias will be applied to all the data.

Additionally, an advantage of the semi-quantitative method is that inflation of sample numbers due to differential disintegration is minimalized, as each group is treated separately. Additionally there will be no distortion due to counting both associated and non-associated elements as all elements are counted as belonging to a group of individuals rather than separate individuals.

Slide	Crinoids	Brach debris	Bivalve	Coral	Bryozoa	Algae	Foram total	Calcisphere	Worm tubes?	N	S	H	Hmax	E	E%
ACR59	2	1	0	0	2	0	2	0	0	7	4	1.352	1.386	0 975	97 511
ACR54	2	1	2	0	2	0	0	0	0	7	4	1.352	1.386	0 975	97.511
ACR51	2	2	0	0	1	0	0	0	0	5	3	1.055	1.099	0 960	96.023
ACR50	2	1	0	0	0	0	2	0	0	5	3	1.055	1.099	0 960	96.023
ACR49	1	2	1	0	0	0	1	1	0	6	5	1.561	1.609	0 970	96.972
ACR48b	1	2	3	0	0	0	1	0	0	7	4	1.277	1.386	0 921	92.119
ACR45	1	2	1	0	0	0	0	0	0	4	3	1.040	1.099	0 946	94.639
ACR43	2	2	0	0	1	0	3	0	0	8	4	1.321	1.386	0 953	95 282
ACR42	3	1	0	0	1	0	3	0	0	8	4	1.255	1.386	0.906	90.5o4
ACR38	2	3	1	0	2	0	2	0	0	10	5	1.557	1.609	0 9o7	96.749
ACR34	3	2	0	0	2	0	0	0	0	7	3	1.079	1.099	0 982	98 214
ACR32b	2	2	1	0	1	0	1	0	0	7	5	1.550	1.609	0 963	9o.296
ACR30	2	1	0	0	2	0	2	0	0	7	4	1.352	1.386	0.975	97.511
ACR29	2	2	0	0	0	2	3	1	0	10	5	1.557	1.609	0.967	96.749
ACR27	2	1	1	0	0	0	0	0	0	4	3	1.040	1.099	0.946	94.639
ACR26	3	2	2	0	0	0	3	1	0	11	5	1.547	1 609	0 961	96 096
ACR25	3	2	0	0	2	0	2	0	0	9	4	1.369	1.386	0 987	98.747
ACR24	3	2	0	0	1	0	0	0	0	6	3	1 011	1.099	0.921	92.0o2
ACR21	1	1	0	0	1	2	0	0	0	5	4	1.332	1.386	0 961	96 096
ACR19	3	2	2	0	2	3	1	0	0	13	6	1.738	1.792	0 970	96 999
ACR18b	1	1	0	0	0	2	0	0	0	4	3	1.040	1.099	0.946	94.639
ACR18	1	1	0	0	1	1	0	0	0	4	4	1.386	1.386	1.000	100 000
ACR17	3	3	0	0	2	0	2	0	0	10	4	1.366	1.386	0.985	98.548
ACR15	1	1	0	0	0	0	2	0	0	4	3	1.040	1.099	0 946	94 639
ACR11	1	1	0	0	1	0	0	0	0	3	3	1.099	1.099	1.000	100 000
ACR10	2	3	3	0	2	0	2	0	0	12	5	1.589	1.609	0.987	98.732
ACR8a	2	2	2	0	2	0	3	0	0	11	5	1.594	1.609	0 991	99 051
ACR8	2	1	2	0	2	0	3	1	0	11	6	1.720	1.792	0.960	96.006
ACR7	1	1	0	0	0	0	0	0	0	2	2	0.693	0 693	1.000	100.000
ACR5	2	2	1	0	1	0	0	0	0	6	4	1.330	1.386	0.959	95 915
ACR4	2	2	0	0	0	0	0	0	0	4	2	0.693	0.693	1.000	100.000
ACR1	2	2	3	0	3	0	0	0	0	10	4	1.366	1.386	0 985	98.548
AC100b	2	2	2	0	2	0	0	0	0	8	4	1.386	1.386	1.000	100.000
AC108	1	3	0	0	1	0	0	0	0	5	3	0 950	1.099	0 8o5	8o.497
AC109	2	2	2	0	3	0	2	0	0	11	5	1.594	1.609	0.991	99.051
AC110a	3	3	1	0	3	2	0	0	0	12	5	1.545	1.609	0.960	9o 023
AC110b	3	3	2	0	3	0	0	0	0	11	4	1.373	1.386	0 990	99.041
AC111	2	2	2	0	2	0	0	0	0	8	4	1.386	1.386	1.000	100.000
AC111b	0	1	1	0	2	0	0	0	0	4	3	1.040	1.099	0 946	94.639
AC111c	2	2	2	1	3	0	0	0	0	10	5	1.557	1.609	0.967	96.749
AC112b	1	2	0	0	2	3	1	0	0	9	5	1.523	1.609	0 946	94.627
AC113a	1	1	0	0	2	1	1	0	0	6	5	1.561	1.609	0 970	96.972
AC116	1	3	0	0	1	0	0	0	0	5	3	0.950	1.099	0.8o5	86.497
AC117	1	3	1	0	2	0	0	0	0	7	4	1.277	1.386	0.921	92.119
AC119	2	2	0	0	3	0	0	0	0	7	3	1.079	1.099	0.982	98.214
AC119a	2	2	1	0	3	1	0	0	0	9	5	1.523	1.609	0 946	94.627
AC121	2	2	0	0	2	0	0	0	0	6	3	1.099	1.099	1.000	100.000
AC122	3	3	0	0	3	0	1	0	0	10	4	1.314	1.386	0 948	94.773
AC123	2	2	0	0	2	0	0	0	0	6	3	1.099	1.099	1.000	100.000
AC126	2	3	0	0	2	0	0	0	0	7	3	1.079	1.099	0.982	98.214
XAC12	3	3	2	0	3	0	0	0	0	11	4	1.373	1.386	0.990	99.041
XAC11	2	2	0	0	2	1	2	1	0	10	6	1.748	1.792	0.976	97.561
XAC9	2	3	0	0	2	0	0	0	0	7	3	1.079	1 099	0.982	98.214
XAC8	1	3	0	0	0	0	0	0	0	4	2	0.562	0.693	0.811	81.128
XAC7	3	3	2	0	3	2	1	1	1	16	8	1.981	2.079	0.953	95.282
XAC6	2	1	0	0	1	0	0	0	0	4	3	1.040	1.099	0.946	94.639
XAC5	2	2	0	0	2	3	2	0	0	11	5	1.594	1.609	0.991	99 051
XAC4	3	2	0	0	2	0	0	0	0	7	3	1.079	1.099	0 982	98.214
XAC3	3	2	1	0	2	0	0	1	0	9	5	1.523	1.609	0.946	94.627
XAC2	2	2	0	0	1	1	0	0	0	6	4	1.330	1.386	0 959	95 915

Table 8.3 Table showing total fauna and calculated diversity and eveness values for each sample taken over the mid-Carboniferous boundary interval at Arrow Canyon.

The values given to each occurrence of a particular faunal element will also then reflect the taphonomic pathway the organism follows to fossilisation as well as community diversity. This pathway is controlled by factors in the palaeoenvironment: the environmental energy, sedimentation rate and bottom water/sediment chemistry. Therefore any calculated diversity results will also be a reflection of the palaeoenvironmental factors influencing the organisms, both during life and en route to fossilisation.

8.4.4.2 Methods of quantification

Shannon-Wiener function

$$H = -\sum_{n=1}^{n=S} (p_i)(\log_2 p_i)$$

where:

H = index of species diversity

S = number of species

pi = proportion of sample belonging to i^{th} species

The base of logarithm chosen is immaterial as this only affects the unit of diversity (Reyment, 1991). The terminology is:

Nats for logarithms to the base e

Bits for logarithms to the base 2

Decits for logarithms to the base 10.

A higher value of H indicates greater diversity as the function measures the amount of uncertainty in predicting the next sample to be drawn from a population.

e.g. a population contains two species, one with 99 individuals and the other with one individual

thus $H = -(p1(\log_2 p1) + (p2)(\log_2 p2)$

$= 0.99(\log_2 0.99) + (0.01(\log_2 0.01)$

$= 0.081$

if a population consists of two species with 50 individuals each, then

$H = -(0.5(\log_2 0.5) + (0.5(\log_2 0.5)$

$= 1$

The higher value shown by the second example shows that the population is more diverse and that the uncertainty is greater.

Thus, two components of diversity are combined in the Shannon-Wiener function, the number of species and the eveness of allotment of individuals among the species. A greater number of species increases species diversity, and a more even distribution among species will also increase species diversity.

The maximum value possible in the community if all species were equal in abundance is H_{max}, this occurs when $p_i = 1/S$, i.e. when all species are present in the equal proportions.

$$H_{max} = -S\,(1/S\,(\log_2 1/S))$$

$$H_{max} = \log_2 S$$

Equitability (ie. the eveness of the population) is defined as E (Lloyd and Ghelardi, 1964).

$$E = \frac{H}{H_{max}}$$

E will range from 0-1, and will have the maximum value when all individuals are evenly allotted throughout the population (ie. no one species is dominant).

In calculations it was found that natural logs were easier to compute and thus all results are in nats.

8.4.4.3 Results

Table 8.3 shows the results per sample, with Enclosure 2 showing the computed values of H and E (as a percentage) plotted against the sedimentary log and microfacies of the upper part of the Indian Springs Formation and the lower part of the Bird Spring Formation.

Diversity H

There do not appear to be any distinct trends in the diversity coefficient, and neither is there any definite relationship to the microfacies or Facies zones. However three distinct minima (samples ACR7, ACR4 and XAC8) and one distinct maximum value are observed (Enclosures 2 and 3).

The minimum XAC8 shows extremely high occurrences of brachiopod debris and a sole occurrence of a crinoid ossicle. ACR 4 shows a similar assemblage, although distribution is more even between the fauna. ACR7 shows an impoverished fauna of crinoids and brachiopods.

The maximum XAC7 contains a diverse and abundant fauna of brachiopod debris, crinoid debris, bivalve shells, bryozoa fragments, calcispheres, and foraminifera.

Eveness (E)

Again, no general trend is identified, although three distinct minima are observed (XAC8, AC116, AC108). Both AC108 and AC116 show assemblages dominated by brachiopod debris together with bryozoan fragments and crinoid ossicles.

8.4.4.4 Discussion

As previously discussed the calculated values for diversity will reflect not only the biological diversity of the environment, but also the physical regime to which the dead organism is subjected. The physical regime of the palaeoenvironment is reflected in the nature of the limestone deposits, and their microfacies identified in thin section.

Samples ACR4 and XAC8 showing low diversity values reflect essentially monospecific assemblages; both samples are assigned to smf-12 (biograinstone/shell hash/coquinas). These values may reflect low community diversity, however it is possible that the preserved assemblages are highly altered from the actual living community and reflect the physical regime that the organisms were subjected to, ie. selective winnowing and removal of fines. An 'artificial' value of diversity is then calculated due to over-representation of individuals and/or groups.

The third minimum value ACR7 occurs in a lime mudstone; this produces a low value of H due to the low number of both individuals and species. The low energy environment in which the lime mudstone was deposited is more likely to produce a 'true' diversity value due to the lack of winnowing and therefore fossil accumulation. However, the low diversity value of this assemblage is likely to be a function of the limited fauna living within this

facies zone (Wilson, 1975) rather than a faunal turnover induced minimal value.

The high diversity XAC7 is again a biograinstone and the high value obtained may be due to a high community diversity, but is likely to reflect reworking and winnowing of the sediment with the amalgamation of debris from a mixture of communities.

The three assemblages showing low eveness values are all dominated by one group. This group may be dominant due to the palaeocommunity having an extremely limited or specialised fauna or due to selective reworking. Again all three samples belong to smf-12 (biograinstones/shell hash/coquinas) and it is probable that there is some alteration between the actual living assemblage and the observed fossil assemblage.

8.4.4.5 Diversity and eveness across the mid-Carboniferous boundary

The mid-Carboniferous boundary as defined by Lane, Baesemann, *et al.*, (1985) lies between samples AC108 and AC109. As demonstrated above there is a distinct low E value directly after the Mississippian-Pennsylvanian boundary possibly reflecting a specialised and/or limited fauna. However, although it is tempting to assign the low value to the supposed extinction at the mid-Carboniferous (Saunders and Ramsbottom, 1986) it is more likely that this may reflect the physical regime with accumulation and selective winnowing of biodebris. However, it is not known whether the actual increased environmental energy associated with the physical regime is associated with the eustatic fall at the mid-Carboniferous boundary. If this is an event truly linked to the eustatic fall or extinction, it is a very short-lived event, with no gradual decline or recovery from the event.

It does not appear possible to use the Shannon-Wiener function in this instance to measure diversity across the mid-Carboniferous boundary as there are too many additional factors to take into account (e.g., palaeoenvironment and environmental energy). To obtain a realistic measure of diversity across the mid-Carboniferous boundary, the palaeoenvironment needs to be constant. It is also probable the better results will be obtained from identification of separate taxa rather than groups.

8.5 COMPARATIVE SECTIONS ACROSS THE MID-CARBONIFEROUS BOUNDARY IN THE SOUTHERN ANTLER BASIN

Stevens *et al.*, (1991) have defined three facies belts developed in the Antler Basin during the late Mississippian: inner limestone, outer limestone and quartzose siltstone facies belts. The inner limestone facies belt represents a carbonate platform consisting of predominantly shallow water limestones, with the outer belt exhibiting deeper water limestones and calciturbidites. The quartzose siltstone facies belt reflect a change from shallow water deposits of the early Mississippian to deep water siliclastics in the later part.

Arrow Canyon lies within the outer limestone facies belt during the upper Mississippian. Three other sections have been visited in the southern part of the Antler Basin for comparison with the section at Arrow Canyon (Figure 8.1). A section at Frenchman Mountain represents marginal marine deposits of the inner limestone facies belt during the upper Mississippian. A section at Indian Springs is similar to the section at Arrow Canyon in that it reflects deposition in the outer limestone facies belt. The Kane Springs Wash locale is the most basinal section encountered during this study and deposition during the upper Mississippian was within the quartzose siltstone facies belt.

8.5.1 Frenchman Mountain

The section at Frenchman Mountain lies on the outskirts to the north-east of Las Vegas (c.f Webster *et al*, 1985). Frenchman Mountain is a fault block of eastward dipping Palaeozoic to Cenozoic sedimentary rocks lying on a Precambrian crystalline basement (Rowland, 1987). The boundary between the Mississippian and Pennsylvanian is exposed in a gully at the top of the mountain. A section approximately 32 m in thickness has been logged across the mid-Carboniferous Boundary (Plate 8.14, Enclosure 1, Figure 8.1).

The lowest 2.67 m of the section expose a coarse, creamy-buff dolomite, pertaining to the Yellowpine Limestone of the Monte Cristo Group. An unconformity separates the Yellowpine Limestone and the succeeding 22.79 m thick Indian Springs Formation. At Frenchman Mountain the Indian Springs comprises an interbedded sequence of limestone, conglomerate, siltstone, and sandstone. No fauna was observed in the lower part of the Indian Springs whilst rare shell, bryozoan and crinoid debris is present

Plate 8.14 View south-east of the section exposed at Frenchman Mountain.

towards the top of the unit. The basal 6m of the overlying Callville Limestone comprises biowackestones passing up into biograinstones.

The Frenchman Mountain section is probably displaced 30-40 km west from its Carboniferous palaeogeographic position (Longwell, 1960) and thus represents a marginal marine environment developed at the edge of the Antler Basin during the mid-Carboniferous. Numerous unconformities are present through the section, with a major unconformity separating the Indian Springs and Yellowpine Limestone, removing the Battleship Wash Formation (Poole and Sandberg, 1991) together with further unconformities within the Indian Springs Formation.

The Mississippian-Pennsylvanian boundary has been placed within an interbedded sequence of limestone conglomerate and limestone by Webster *et al.*, (1985) and appears to be equivalent to the logged interval between 14.4 m and 17.5 m above the top of the Yellowpine Limestone. Webster *et al.*, (1985) noted the lower of the two conglomerate horizons yielded *Rhachistognathus muricatus* zone conodonts together with reworked Late Chesterian conodonts. The limestone between the conglomerates yields *R. primus* and *D. noduliferus*, as well as reworked Chesterian conodonts. Webster *et al.*, (1985) have suggested that the upper part of the *muricatus* zone, and the basal part of the *primus-noduliferus* zones are missing at the unconformity at the top of the lower conglomerate. Further reworked faunas were noted to occur up to base of the *Idiognathoides sinuatus* zone (Webster *et al.*, 1985, p 67), which appears to correspond to the base of the conglomerate at 20.36 m above the base of the Indian Springs Formation. This zone continues into the Callville Limestone Formation.

8.5.2 Indian Springs

The section at Indian Springs lies in low hills south-west of Indian Springs, in north-west Clark County approximately 65 km north-west of Las Vegas. The section lies 2.5 km from a jeep track that leads from the Indian Springs U.S. Air Force Base on Highway 95, and is described by Gordon (1969). A 91 m thick section in south-easterly dipping strata has been logged across the mid-Carboniferous boundary (Plate 8.15, Enclosure 1, Figure 8.1).

The lowest part of the section shows wackestones belonging to the Yellowpine Limestone. These are overlain unconformably by a 3.06 m thick fining-up, fine-grained sandstone at the base of the Indian Springs

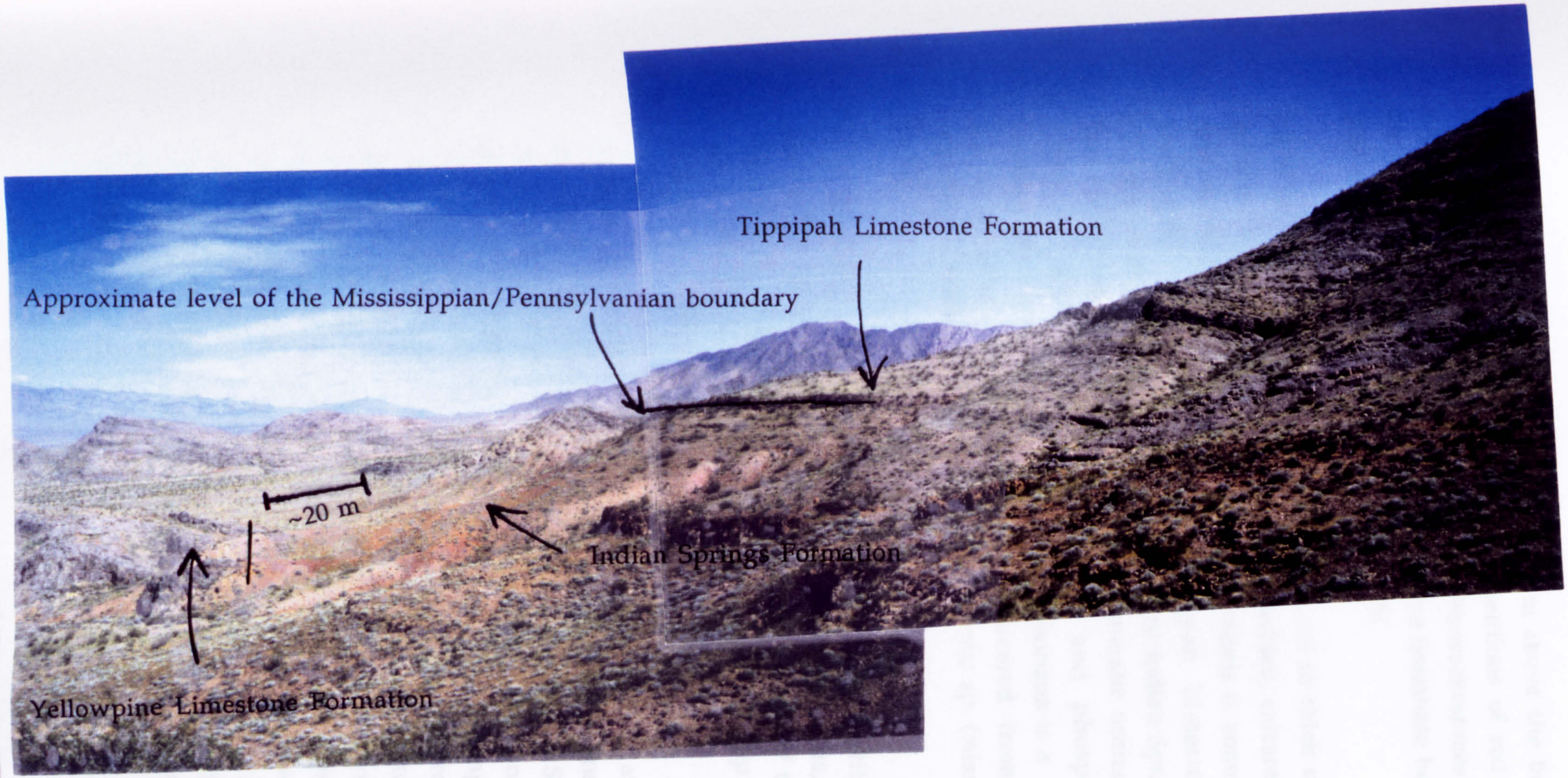

Plate 8.15 View south-west of the section at Indian Springs.

Formation. From this horizon until 57 m above the base of the logged section, there occurs relatively cyclic repetitions of red shales and marls capped by 1-3 m thick orange weathering biowackestones to packstones, the top surfaces showing phosphatic clasts. One limestone horizon in the lower part of the section appears to be stromatolitic.

At 57 m above the base of the section a 3.9 m thick clastic bed forms a prominent ridge. This bed shows cross-bedded, calcareous, coarsening-up fine-coarse grained sandstone. Bioclastic debris is common and comprises shell and crinoid hash. The Tippipah Limestone is developed unconformably on this top sandstone of the Indian Springs Formation and the contact shows an 11 cm thick conglomeratic horizon with well sorted clasts of chert, limestone, sandstone and phosphate. Developed conformably on top of this conglomeratic horizon is a 43 cm thick, fining-up grainstone. Ammonoids were recovered from this horizon and comprise *Glaphyrites* sp., and *Paraphaneroceras* sp. (Alan Titus, pers comm., 1992).

The following 24.8 m of section shows marl-micrite alternations. The limestone in the cycles are very poorly fossiliferous, although rare shell hash and crinoid debris is visible towards the top of the unit. *Teichichnus* sp. biorturbation is visible at one horizon. The top 4.8 m of the section comprises cherty micrite.

Gordon and Poole (1968) investigated the section at Indian Springs and recognised that the Mississippian-Pennsylvanian boundary is represented by a disconformity at the contact between the Indian Springs formation and overlying Tippipah Limestone Formation. The contact between the two formations occurs at the base of the conglomeratic horizon. *Rhachistognathodus muricatus* has been recovered from beneath the clastic interval whilst the ammonoid-containing limestone has yielded *Declinognathodus* and *Idiognathoides* sp conodonts (Alan Titus, pers comm., 1992). Further ammonoids noted as occurring at this level include *Glaphyrites lanei, Bisatoceras nevadense, Paraphaneroceras peroccidens* and *Stenopronorites sp.* (Gordon, 1969). Thus a late Chesterian (late Arnsbergian) age is assigned to the upper Indian Springs, with an upper Morrowan (lower Westphalian age) being shown by the Tippipah Limestone.

8.5.3 Kane Springs Wash

The Kane Springs Wash section lies approximately 160 km north of Las Vegas, 2 km from a dirt track (following the wash), which leads from the US Highway 93 (cf. Webster, 1969).

The boundary between the Mississippian and Pennsylvanian is exposed in easterly dipping strata on the east side of the wash. A section approximately 119 m in thickness has been logged across the mid-Carboniferous boundary (Figure 8.1, Enclosure 1). Many of the shaly units of the Chainman and Indian Springs Formations are very poorly exposed and therefore pits were dug.

The lowest 15.59 m of logged section are assigned to the Chainman Shale (Webster, 1969). However, the top of the Chainman Formation is drawn at the top of the highest sandstone bed below the 'marker conglomerate', and a higher sandstone bed is recognised in this study at 27.4 m above the base of the logged section. The upper part of the Chainman Formation comprises grey-green shales, with interbedded thin bioclastic limestones and orange weathering sandstones. The sandstones show a variety of sedimentary structures including hummocky cross stratification. Trace fossils are also common at one horizon comprising *Skolithos sp.*, *Diplocraterion sp.*, *Asterosoma sp.*, *Lockeia sp.* and *Rhizocorallium sp.* indicative of a shallow marine ichnofacies.

The succeeding Indian Springs Formation is 53.9 m thick and comprises grey shales, mudstones and interbedded thin bioclastic limestones in the lower half of the Formation. The 'marker conglomerate' occurs 18.1 m above the base of the Indian Springs Formation.

The upper half shows interbedded khaki-coloured siltstones, grey shales and biograinstones. A 9.8m thick laterally impersistant sandstone body occurs 34.6 m above the base of the Indian Springs Formation and comprises a conglomeratic base passing up into medium to coarse grained, tabular and trough cross bedded horizons passing up into fine to coarse grained, symmetrically rippled sandstone.

The base of the Bird Spring is drawn at the first occurrence of cherty limestones, at 82.2 m above the base of the logged section. The lower part of the Bird Spring Formation consists of biowackestones to grainstones with

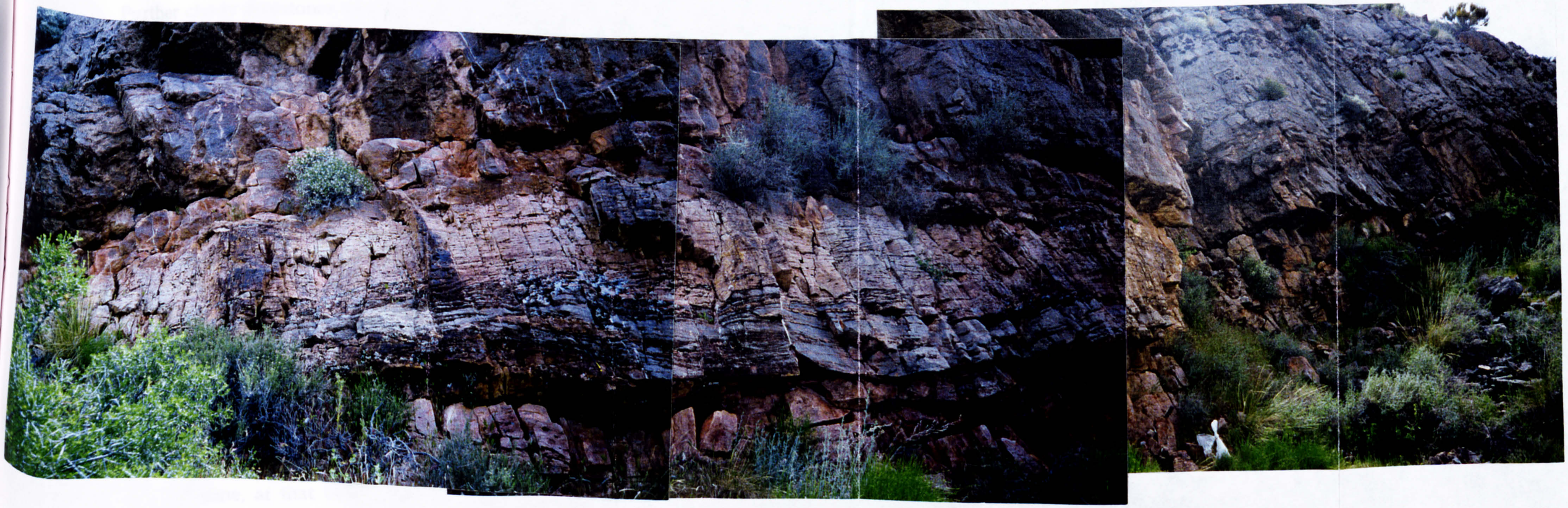

Plate 8.16 View east of the sand development at the Mississippian/Pennsylvanian boundary at Kane Springs Wash. (Large plastic food bag for scale in the bottom right of the Plate).

chert present as nodules and as horizons. However, at 8.45 m above the base of the Bird Spring, there a orange-grey weathering clastic interval (Plate 8.16). The base of the clastics shows a poorly exposed 1.5 m thick grey-green shale. This is followed by a 3 m thick interval of calcareous fine to medium grained sandstone. Indistinct tabular cross bedding is evident. The central part of this unit shows a channelized sandy limestone, containing large amounts of bioclastic hash at the base. This is overlain by cross-bedded sandstone, which shows symmetrical rippling towards the top of the bed. Further cherty limestones follow to the top of the logged section.

From work by Webster (1969, p15) at a nearby locality (Kane Springs Wash West), it is shown that the base of the Bird Spring Formation at Kane Springs coincides with the top of the *unicornis* conodont zone. The lower part of the *muricatus* zone appears to be absent, with *Adetognathodus lautus* and *Rhachistognathodus muricatus* occurring at the same level. There was no note of any disconformable contact between the Indian Springs and Bird Springs Formation and thus it may be that facies control of *Rhachistognathus* is a major factor (cf. Titus, 1992).

The Mississippian-Pennsylvanian boundary as delineated by the first occurrence of *Declinognathodus noduliferus* is placed at approximately 70 m above the base of the Bird Spring Formation (Webster, 1969, p15) However, the boundary was placed at the base of the clastic interval by Webster (1969), as it was thought that the top of the *Rhipodomella nevadensis* brachiopod zone correlated to the top of the *Gnathodus girtyi simplex* zone, at that time. This conodont zone is now defunct and has been replaced by the *muricatus* zone, the top of which shows the last occurrence of *Adetognathus unicornis;* this occurs directly below the clastic interval at Kane Springs Wash West (Webster, 1969, p15). Thus, the lower part of the *primus-noduliferus* zone appears to be unrecorded in the 54.5 m thick clastic and overlying limestone interval at Kane Springs Wash West. Unfavourable facies may explain the absence of *D. noduliferus* above the clastic interval. It is therefore probable that a similar relationship exists at the section logged in this study (equivalent to Kane Springs Wash East of Webster, (1969)), with the Mississippian-Pennsylvanian boundary being represented by an unconformity at the base of the clastic interval.

Although the section at Kane Springs Wash was deposited towards the centre of the Antler Basin, the Mississippian-Pennsylvanian boundary is represented by an unconformity.

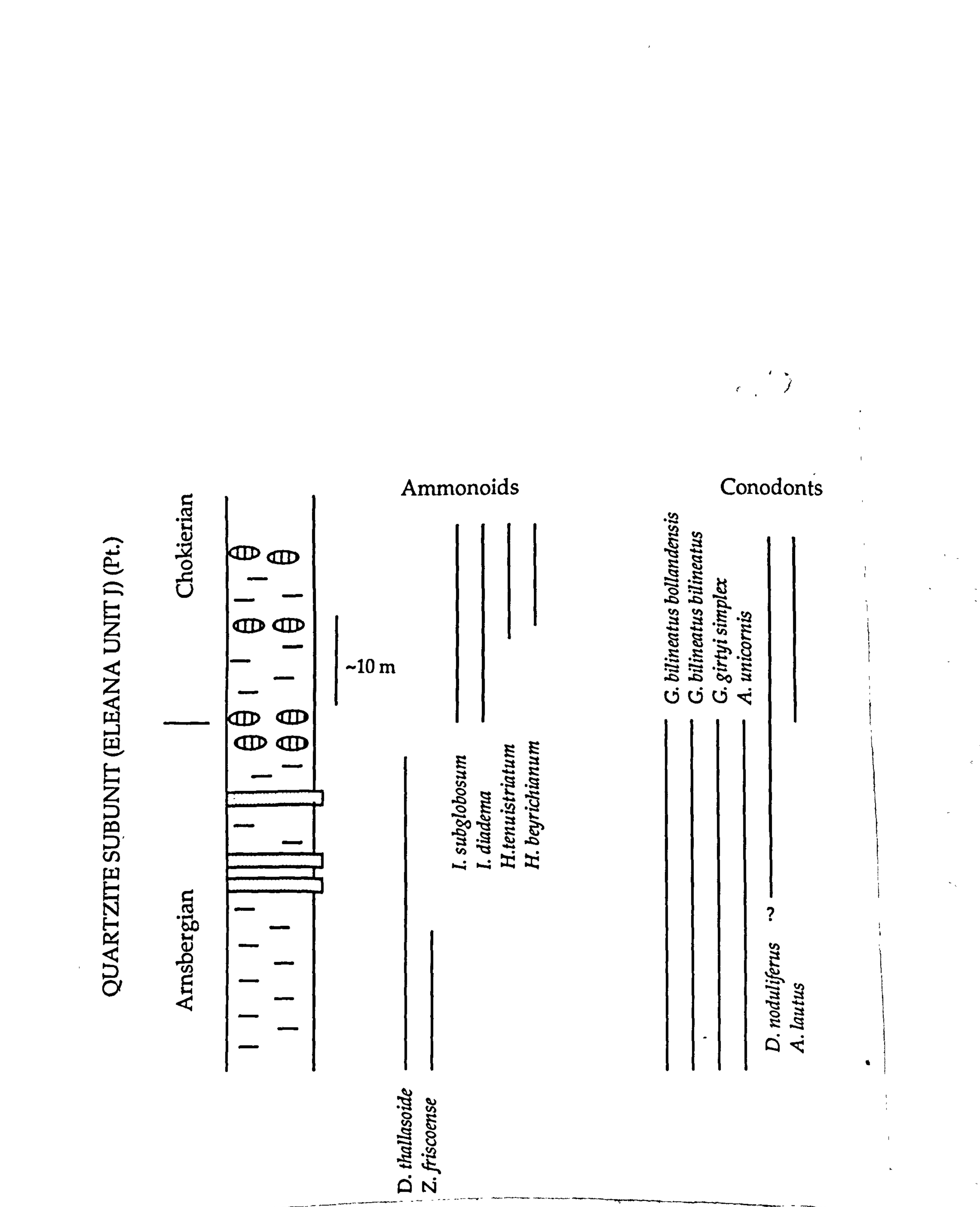

Stratigraphic log of the section through the mid-Carboniferous at South Syncline Ridge, Nevada Test Site (modified from Titus, 1992).

8.5.4 Nevada Test Site

The Nevada Test Site section has not been visited (due to restricted access to foreign nationals). However, it has been documented by Titus (1992) and Titus and Manger (1992). The section lies at South Syncline Ridge in the northern part of the Test Site in Nye County, Nevada. This locality has yielded the only *Isohomoceras* and *Homoceras* faunas ever found in the U.S.A. and therefore is of utmost importance to facilitate correlation with European sections. The fossils were recovered from the deep basinal deposits of the upper Quartzite Subunit of unit J of the Eleana Formation (equivalent to the Chainman Shale and Indian Springs Formations) and comprise in addition to ammonoids, crinoid debris, articulate and inarticulate brachiopods, bryozoans, bivalves, gastropods, conularids, corals, trilobites and nautiloids (Titus, 1992).

The lower part of the section provide ammonoids of the *Eumorphoceras bisulcatum-Euroceras* assemblage. This probably represents an E_2b fauna (Titus, 1992). The *Delepinoceras thalassoide-Zephyroceras friscoense* assemblage follows and is comparable to the late Arnsbergian (E_2c) of Britain, (Riley, 1987). Conodonts occurring with these ammonoid fauna include *G. bilineatus bilineatus, G. bilineatus bollandensis, G. girtyi simplex, G. girtyi sp.*, and *A. unicornis*. Titus (1992) suggested that facies control of *Rhachistognathus muricatus* precluded its occurrence at Syncline Ridge where *Gnathodus bilineatus* persisted in these basinal facies up to the Arnsbergian-Chokierian boundary (as in European basinal sections).

The *Isohomoceras subglobosum-Isohomoceras diadema* assemblage occurs 2 m above the previous assemblage and contains the first reported occurrence of *Isohomoceras subglobosum* in the western hemisphere. This assemblage is H_1a (early Chokierian in age). 15 m above the base of this assemblage ammonoids indicative of a late Chokierian age appear and they are assigned to the *Homoceras beyrichianum-Homoceras coronatum* zone. A hiatus is present at the top of the section spanning the Alportian (H_2), to lower Westphalian.

Recent work by Titus (pers. comm., 1995) has led to the discovery of the mid-Carboniferous boundary defining conodont (*Declinognathodus noduliferus*) **beneath** the Arnsbergian-Chokierian boundary (exact level undisclosed). The Arnsbergian-Chokierian boundary now appears to coincide with the lower-upper *muricatus* boundary (as defined by

Baesemann and Lane, 1985). Obviously, this section shows the most complete section across the Mississippian-Pennsylvanian boundary in the United States and this new data will now necessitate a complete revision of the American conodont biostratigraphy. The implications of this remarkable find to the choice of the mid-Carboniferous boundary stratotype are discussed in chapter 9.

8.6 DISCUSSION

It is shown that only the section at Arrow Canyon out of those visited is complete at the level of the mid-Carboniferous boundary (Enclosure 1). The basin margin section at Frenchman Mountain shows a marginal marine environment, whilst the Indian Springs and Kane Springs Wash sections display an unconformity at the boundary with sand or conglomerate development. The Kane Springs section is thought to be a more basinal section than Arrow Canyon, yet still shows an unconformity at the boundary.

The only section which shows the ammonoid-defined Arnsbergian-Chokierian boundary is that at Syncline Ridge in the Test Site. Here however, this horizon coincides with the upper *muricatus* boundary, with *Declinognathodus* appearing **below** this boundary.

As discussed in chapter 2, conodonts are facies controlled, with *Declinognathodus* typically being a deep water faunal element and *Adetognathus* representing a shallow water fauna. Therefore, it is not surprising that *Declinognathodus* appears to be present earlier than *Adetognathus* in the basinal section at the Test Site. As the two conodonts are facies controlled it is very hard to draw actual timelines between the sections at Arrow Canyon and the Nevada Test Site. However, there are two ways of interpreting the data (Figure 8.5):

Scenario 1. If it is assumed that the appearance of *Adetognathus* occurs at the same level at both localities then the Arnsbergian-Chokierian boundary at Arrow Canyon occurs at the first occurrence of *Adetognathus lautus* (*Adetognathus lautus* defines the upper *muricatus* boundary). The appearance of *Declinognathodus* at Arrow Canyon will then be much higher than the Arnsbergian-Chokierian boundary as shown by ammonoids, and thus the mid-Carboniferous boundary at Arrow Canyon is currently placed too high.

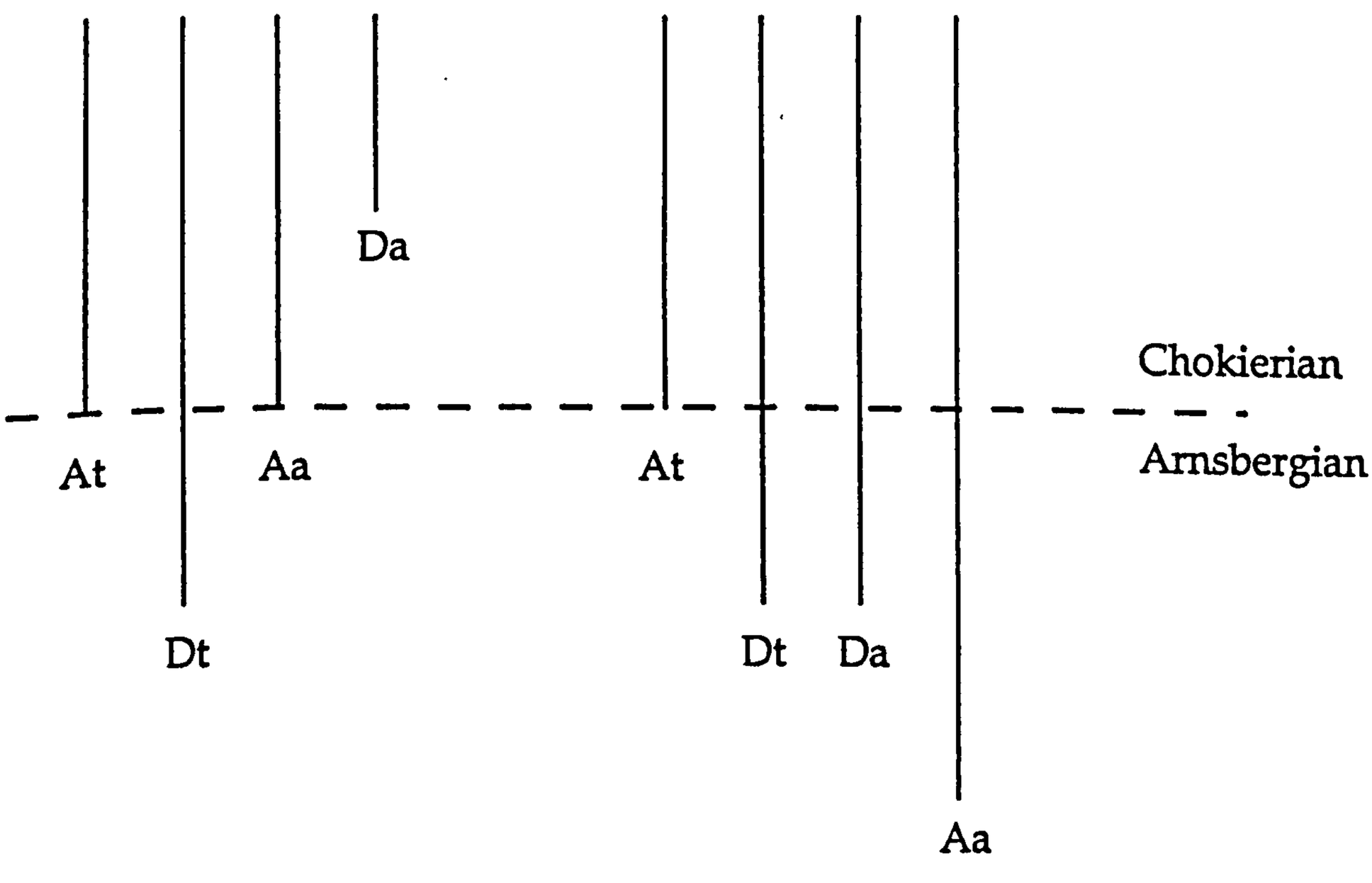

Where A and D are *Adetognathus* and *Declinognathodus* respectively

and t and a represent Test Site and Arrow Canyon occurrences respectively

Figure 8.5 Hypothetical relationships between Arrow Canyon and the Nevada Test Site for the conodonts *Adetognathus* and *Declinognathodus*.

Scenario 2. If it is assumed that the appearance of *Declinognathodus noduliferus* is synchronous between exposures, then the appearance of *Declinognathodus noduliferus* is also pre-Chokierian at Arrow Canyon, as well as at the Test Site.

It would appear that the upper *muricatus* boundary at Arrow Canyon lies 10.27m below the mid-Carboniferous boundary (Lane, Baesemann *et al.*, 1985 p 433). Startlingly this occurs (when plotted against the sedimentary log measured in this study) at XAC8, the sample showing both lowest diversity and evenness. The question must be asked could this be the true Arnsbergian-Chokierian boundary in the Arrow Canyon section? At the Test Site *Declinognathodus* appears below the Arnsbergian-Chokierian boundary, with such facies-control of the conodont assemblage in the carbonate platform deposits of Arrow Canyon, it may be impossible to predict the true first evolutionary occurrence of the conodont, thus can the first occurrence at Arrow Canyon possibly represent fauna from winnowed and reworked deeper water sediments?

The choice of such a facies-controlled organism as the defining fauna for the mid-Carboniferous boundary is questioned in chapter 9.

8.7 CONCLUSIONS

1) The mid-Carboniferous boundary interval at Arrow Canyon lies on a carbonate platform. The late Mississippian deposits were formed in shallow high energy water at the winnowed edge of the carbonate platform and show reworking of bioclasts deposited within more open regions of the platform and on the slope. Immediately following the mid-Carboniferous boundary itself (as defined by Lane, Baesemann *et al.*, 1985), a marginal marine clastic interval was deposited and followed by a return to the winnowed platform deposits. The lower part of the Pennsylvanian shows a sequence of deep water open platform deposits which shallow up to more winnowed deposits once again. A further deepening is seen at the top of the section.

2) No drop in faunal diversity is seen at the mid-Carboniferous boundary, although a reduction in the equitability of the sample immediately following the level of the boundary is shown, whether this relates to selective winnowing of bioclasts or the presence of a limited specialised fauna is unknown.

3) The mid-Carboniferous boundary at three other visited sites in the southern Antler Basin all show unconformities at the boundary interval including the section (Kane Springs Wash) which is presumed to be more basinal than Arrow Canyon.

4) Re-evaluation of the section at Arrow Canyon in the light of recent work by Alan Titus on the Nevada Test Site section, may show that the chosen stratotype section is incomplete. It is possible that the Arnsbergian-Chokierian boundary at Arrow Canyon actually occurs at the lower-upper *muricatus* boundary or that the occurrence of *Declinognathodus noduliferus* is pre-Chokierian. Facies control appears to be a dominant influence on *Declinognathodus,* and thus the first occurrence of that genus at Arrow Canyon may not be its true first evolutionary occurrence, and it may be much higher than that seen in both the Nevada Test Site and Europe. With the occurrence of the conodont in such high energy deposited limestone it may be that the conodont is reworked into this environment.

Chapter 9

DISCUSSION ON THE MID-CARBONIFEROUS BOUNDARY

9.1 INTRODUCTION

The selection of the mid-Carboniferous boundary stratotype section should reconcile problems between the different mid-Carboniferous biostratigraphies developed throughout the world. The ultimate aim in determining a stratotype section is that it represents a unique instant in time and a standard against which other sequences can be correlated. Thus, with the decision on the choice of mid-Carboniferous boundary stratotype at Arrow Canyon, Nevada, ideally the problems of correlating the different biostratigraphic schemes that exist between America and western Europe should be solved. Following recent developments in mid-Carboniferous stratigraphy a cross-correlation between American and western European zonations is presented.

However, since the inception of a search for a global stratotype in 1983 there has been much progress in mid-Carboniferous stratigraphy. This chapter examines whether the original choice of defining fauna (and choice of boundary) is still a valid choice after these developments.

9.2 CROSS-CORRELATION BETWEEN THE EUROPEAN AND AMERICAN BIOSTRATIGRAPHIES

9.2.1 Correlation between ammonoid zonations

Cross-correlation between Britain and the U.S.A. is hampered by problems of provinciality and palaeogeography, particularly during the eustatic sea-level low of the mid-Carboniferous when marine connections were limited. Additionally, in Britain ammonoid occurrences are associated predominantly with shaly 'marine band' deposits produced at maximum flooding. Thus facies control is exerted on the ammonoids, and the

ammonoid record is effectively punctuated by decreases in salinity during the upper regressive part of each cyclothem (Ramsbottom *et al*, 1962; Ramsbottom, 1977, 1979, 1980). American sections have continuous occurrences whilst western European sections show more sporadic occurrences (Ramsbottom, 1980).

The composite American succession (as shown in section 2.2.2.1) is used against which the western European succession is correlated (Table 9.1). As the correlations with the American biostratigraphical zones are primarily based on major associations of faunal elements, it is probable that the full sequence of ammonoid zones (as shown in western Europe) may not be present within the correlative zone of the U.S.A. Therefore only major discrepancies in the ammonoid stratigraphy are mentioned in the following text. Saunders *et al.*, (1979) have suggested that the Arkansas occurrences (on which the Pennsylvanian ammonoid stratigraphy is based) in fact are separated by numerous hiatuses, and that the ammonoid occurrences represent the later parts of each of Ramsbottoms' mesothems.

***Goniatites multiratus* zone**

The Goniatites multiratus zone contains *Girtyoceras meslerianum* in the United States. Both this species and the zonal name bearer are found in the *Goniatites crenistria* (P1a) of Britain.

***Lusitanoceras granosus* zone**

Both *Lusitanoceras granosus* and *Neoglyphioceras subcirculare,* present within the American zone occur within the lower part of the P_2 zone of Britain.

***Syngastrioceras barnettense* zone**

The *Syngastrioceras barnettense* zone in Nevada contains species assigned to the genera *Eumorphoceras, Tumulites, Pronorites* and *Cravenoceras*. A similar faunal association occurs within the Pendleian (E1) of Great Britain.

***Cravenoceras hesperium* zone**

The *Cravenoceras hesperium* zone contains *Eumorphoceras cf. grassingtonense, Fayettevillea* sp. and *Glaphyrites nevadensis.*

AMERICAN AMMONOID ZONATION		WESTERN EUROPEAN AMMONOID ZONATION		
PENNSYLVANIAN (pt.)	*Verneulites pygmaeus*	G_1b^1	*Cancelloceras cumbriense*	YDN
		G_1a^1	*Cancelloceras cancellatum*	
		R_2c^2	*Verneulites sigma*	MRDN
	Arkanites relictus	R_2c^1	*Bilinguites superbilinguis*	
	Quinnites henbesti	R_2b^5	*Bilinguites metabilinguis*	
		R_2b^4	*Bilinguites eometabilinguis*	
		R_2b^3	*Bilinguites bilinguis*	
		R_2b^2	*Bilinguites bilinguis*	
		R_2b^1	*Bilinguites bilinguis*	
	Retites semiretia	R_2a^1	*Bilinguites gracilis*	
		R_1c^4	*Reticuloceras coreticulatum*	KINDERSCTN
		R_1c^3	*Reticuloceras reticulatum*	
		R_1c^2	*Reticuloceras reticulatum*	
		R_1c^1	*Reticuloceras reticulatum*	
		R_1b^3	*Reticuloceras stubblefieldi*	
		R_1b^2	*Reticuloceras nodosum*	
		R_1b^1	*Reticuloceras eoreticulatum*	
		R_1a^5	*Reticuloceras dubium*	
		R_1a^4	*Reticuloceras todmordenense*	
		R_1a^3	*Reticuloceras subreticulatum*	
		R_1a^2	*Reticuloceras circumplicatile*	
		R_1a^1	*Hodsonites magistrorum*	
		H_2c^2	*Homoceratoides prereticulatus*	AP
		H_2c^1	*Vallites eostriolatus*	
		H_2b^1	*Homoceras undulatum*	
		H_2a^1	*Hudsonoceras proteum*	
	Homoceras beyrichianum - Homoceras coronatum	H_1b^2	*Isohomoceras sp. nov.*	CHKRN
		H_1b^1	*Homoceras beyrichianum*	
	Isohomoceras suglobosum - Isohomoceras diadema	H_1a^3	*Isohomoceras subglobosum*	
		H_1a^2	*Isohomoceras subglobosum*	
		H_1a^1	*Isohomoceras subglobosum*	
MISSISSIPPIAN (pt.)	*Delepinoceras thalassoide - Zephyroceras friscoense*	E_2c^4	*Nuculoceras nuculum*	ARNBGN
		E_2c^3	*Nuculoceras nuculum*	
		E_2c^2	*Nuculoceras nuculum*	
		E_2c^1	*Nuculoceras stellarum*	
		E_2b^3	*Cravenoceratoides nititoides*	
		E_2b^2	*Cravenoceratoides nitidus*	
	Stenoglaphyrites involutum	E_2b^1	*Cravenoceratoides edalensis*	
	Eumorphoceras bisulcatum - Cravenoceras richardsonianum	E_2a^3	*Eumorphoceras yatesae*	
		E_2a^{2a}	*Cravenoceras gressinghamense*	
	Richardsonites merriami	E_2a^2	*Eumorphoceras ferrimontanum*	
	Cravenoceras hesperium	E_2a^1	*Cravenoceras cowlingense*	
	Syngastrioceras barnettense	E_1c^1	*Cravenoceras malhamense*	PN
		E_1b^2	*Tumulites pseudobilinguis*	
		E_1b^1	*Cravenoceras brandoni*	
		E_1a^1	*Cravenoceras leion*	
	Lusitanoceras granosus	P_2c	*Lyrogoniatites georgiensis*	BGTN
		P_2b	*Neoglyphioceras subcirculare*	
		P_2a	*Lusitanoceras granosus*	
	Goniatites multiratus	P_1d	*Paraglyphioceras koboldi*	
		P_1c	*Paraglyphioceras elegans*	
		P_1b	*Arnsbergites falcatus*	
		P_1a	*Goniatites crenistria*	

Table 9.1 Cross-correlation on ammonoid zonations for America and western Europe.

Eumorphoceras grassingtonense is an early E_2 species in Britain (occurring with *Cravenoceras* sp. in the E_2a^1 marine band) and following Gordon, (1964, 1970) and Titus, (1993), this zone is assigned to early E_2.

***Richardsonites merriami* and *Eumorphoceras bisulcatum-Cravenoceras richardsonianum* zones**

The lower of these two zones in America contains occurrences of *Eumorphoceras* cf. *girtyi, E.* aff. *bisulcatum, Pronorites* sp., and *Syngastrioceras walkeri.* *Eumorphoceras bisulcatum* occurs in the E_2a^2 marine band

The upper zone (*Eumorphoceras bisulcatum-Cravenoceras richardsonianum* zone) also contains *Eumorphoceras* sp. which are very similar to the *E. bisulcatum ferrimontanum* and *E. bisulcatum erinense* which occur at the base of the E_2 (E_2a^2) (Saunders, 1973).

Due to the occurrence of *E. bisulcatum* in both these zones, they correlate to E_2a^2 and E_2a^3 zones of Britain. However, as it appears that the upper (as well as the lower) American zone contains ammonoids also indicative of the E_2a^2 horizon, in this work therefore these two zones are not assigned to the two particular horizons (cf. Titus, 1992) but the range E_2a^2 to E_2a^3.

***Stenoglaphyrites involutum* zone**

The association of *Eumorphoceras* cf. *bisulcatum,* and *Glaphyrites sp.,* seen the American zone occurs in Britain at the base of the E_2b^1, and thus the base of this zone is correlated with that horizon.

***Delepinoceras thalassoide-Zephyroceras friscoense* zone**

This zone contains *Eumorphoceras richardsoni, Eumorphoceras imoense,* and *Fayettevillea* sp. The association of *Eumorphoceras* and *Fayettevillea* sp. is seen in Britain in the E_2b^2 marine band and the base of the American assemblage is assigned to this level. Forms described as *Eumorphoceras beta* and *Eumorphoceras sp.* from the E_2c^3 in Britain by Riley (1987), have been likened by that author to *Eumorphoceras imoense* and *Eumorphoceras richardsoni,* respectively. However, this work follows Titus (1992) who correlated the upper limit of the zone horizon as latest Arnsbergian in age

(E_2c^4) in age due to the fact that this assemblage occurs without a break below the *Isohomoceras* faunas at the Test Site.

***Isohomoceras suglobosum-Isohomoceras diadema* zone**

The *Isohomoceras suglobosum-Isohomoceras diadema* zone correlates with the appearance of *Isohomoceras subglobosum* in the earliest Chokierian faunas of Britain and are H_1a in age.

***Homoceras beyrichianum-Homoceras coronatum* zone**

The H_1b equivalent strata in Nevada contain *Homoceras tenuistriatum, Isohomoceras subglobosum, Isohomoceras diadema, Euroceras leedomi* and *Proshumardites colei.* The first appearance of *Homoceras beyrichianum* in western Europe occurs in the H_1b^1 marine band, and thus the base of this American zone is correlated with that horizon. The top of this zone is removed by erosion, however the co-occurrence of *Isohomoceras subglobosum* with *Homoceras beyrichianum* is similar to that found in the H_1b^2 marine band in Ireland and thus the top of the zone is correlated with the H_1b^2 horizon.

***Retites semiretia* zone**

The zone contains *Swintoceras tiro* and *Swintoceras wainwrighti* in the U.S.A. Work by Saunders and Ramsbottom (1993) have found these forms closely allied to *Swintoceras spiraloides* (found in the R_1b^2 marine band). The genus *Hudsonoceras* is also represented at both horizons (by *H. ornatum* in the U.K. and *H. moorei* in America). Thus the base of the zone corresponds to R_1b^2. Manger and Saunders (1980) in comparing ornamentation between the reticuloceratids infer that there is a probable gap in the American ammonoid succession following this zone.

***Quinnites henbesti* zone**

There are no comparative fauna known in Britain similar to those found in this zone. Manger and Saunders (1980) have assigned a R_2b age to this zone (due to the gastrioceratid-like suture of the zonal name-bearer).

Arkanites relictus **zone**

Arkanites relictus (which is very similar to *Bilinguites superbilingue*) co-occurs in the upper part of its range with *Cancelloceras huntsvillense* in the U.S.A. (Manger and Saunders, 1980). This association is seen in the R_2c^1 (*Bilinguites superbilingue*) in Britain (Paul Wignall, pers comm., 1995).

Verneulites pygmaeus **zone**

Verneulites sigma appears in Britain in the R_2c^2 marine band along with *Cancelloceras* sp.. A similar relationship is seen in the United States in the *Verneulites pygmaeus* zone. However, in Britain *Bilinguites superbilingue* also occurs within the zone, unlike the U.S.A.

9.2.2 Cross-correlation between the European and American conodont stratigraphies

There are many problems when trying to correlate the western European conodont zonation with the many proposed schemes of the U.S.A. In attempting to correlate the European with North American conodont stratigraphies in particular, Grayson (1990) notes a few drawbacks to the current schemes.

1) Zones have been erected on the ranges of only one or two taxa without a phylogenetic base. Lineage's must be known since if the taxa defining a zone are different from those above or below it, there is no way of knowing whether the events represented by zonal boundaries reflect environmental or evolutionary signals.
2) The existing zonations reflect differences in paleoenvironments and therefore facies control.
3) There are differences in conodont taxonomy.
4) Various species constituting the multielement organism should be known.

Additionally there are the same problems with provinciality and paleogeography as there are for ammonoids. However, unfortunately, facies control of conodonts both in the Mississippian and Pennsylvanian is evident from many studies, both in western Europe and America, and particularly affects the conodonts that are common within mid-Carboniferous strata.

Within the British biostratigraphical record facies restriction has been noted by various workers, although no biofacies scheme has been forthcoming. It has been noted (Austin, 1974, 1976; Higgins and Varker, 1982; Austin and Davies, 1984) that shelf faunas are typically characterized by *Cavusgnathus*, and the basin exhibiting a dominant fauna of *Gnathodus* conodonts (Metcalfe, 1981). Higgins (1975) also noted that *Apatognathodus* and *Rhachistognathus* may represent shallower water faunas of the Namurian.

Various works have focused on the development of conodont biofacies schemes in the U.S.A. (e.g., Merrill, 1973; Merrill and von Bitter, 1976, 1984; Driese *et al.*, 1984), with the biofacies thought to relate to either depth stratification (Druce, 1973), or to distance away from a palaeoshoreline/water depth (Barnes and Fåhraeus (1975)). It is more likely that the conodonts are more susceptible to other physical environmental parameters (e.g., salinity and hydraulic energy). Particularly important may be hydraulic energy in selective winnowing of the conodont apparatus, thus the observed biofacies may not be a true representation of the conodont community. The most recent biofacies scheme, applicable to both the upper Mississippian and lower Pennsylvanian is that described from the mid-Carboniferous of Montana by Davies and Webster (1985). They defined four biofacies (shown in Table 9.2.)

Table 9.2 Mid-Carboniferous biofacies scheme of Davies and Webster (1985).

Biofacies	Dominant fauna	Palaeoenvironment
Adetognathus	*e.g. Adetognathus gigantus, A. lautus, A. spathus*	Lagoonal, tidal flat and barrier bar. Highly variable salinities
Declinognathodus - *Idiognathoides*	*e.g. Declinognathodus noduliferus, D. inequalis, Idiognathoides sinuatus, I. sulcatus*	Open, offshore, shallow marine. Normal salinity
Rhachistognathus	e.g. *Rhachistognathus primus*	Shallow, high energy. Possibly fluctuating salinities
Neognathodus	e.g. *Neognathodus symmetricus*	Shallow water bay lagoon. Unknown salinity level.

Thus a very shallow water or low salinity section (e.g. in the *Adetognathus* biofacies) spanning the mid-Carboniferous boundary may not in fact show the boundary-defining *Declinognathodus noduliferus* and the biostratigraphic age of the section will be mis-interpreted.

Using the known published ranges of conodonts, range charts have been constructed for selected conodonts in both the western European and American successions (outlined in sections 2.2.1.2 and 2.2.2.2 respectively) (Figures 9.1 and 9.2, Enclosure 4). These charts help compare the conodont successions of America and western Europe (Table 9.3). It is assumed in this correlations that the biozonations are complete for each region (cf. Manger and Sutherland, 1992).

Major changes in faunal content are shown to occur in the British succession at the end of the *Gnathodus girtyi collinsoni* and *Gnathodus bilineatus bollandensis* zones and the beginning of the *Declinognathodus noduliferus* and *Idiognathoides corrugatus-Idiognathoides sulcatus* zones. In the American succession major changes occur at the end of the upper *muricatus* and the beginning of the upper *noduliferus-primus* zones.

The *bilineatus*-Upper *Cavusgnathus* zone shows the appearance of *Lochreia commutata* and *Cavusgnathus charactus* in the United States, however, this association occurs in the Arundian in Europe (Riley, 1993). By definition the *bilineatus*-Upper *Cavusgnathus* zone is defined at the base by the appearance of *Gnathodus bilineatus* (C. Sandberg, pers comm., 1994). Thus the base of the this American zone is correlated with the *Gnathodus bilineatus* zone of Europe.

Some resemblance is seen between the assemblage comprising *Gnathodus bilineatus, Lochreia commutata, Cavusgnathus naviculus, Gnathodus girtyi simplex* and *Adetognathus unicornis* of the *naviculus, unicornis and muricatus* zones of the United States and that seen in the *Gnathodus bilineatus bollandensis* zone of Britain. Thus the base of the *naviculus* zone is correlated with the base of the *Gnathodus bilineatus bollandensis* zone.

It is likely that due to the shared presence of *Adetognathus lautus* (a paired element with *Adetognathus gigantus*) that the upper part of the *muricatus* zone correlates with the *minutus* zone of western Europe.

Figure 9.1 Range chart for selected conodonts in the western European succession.

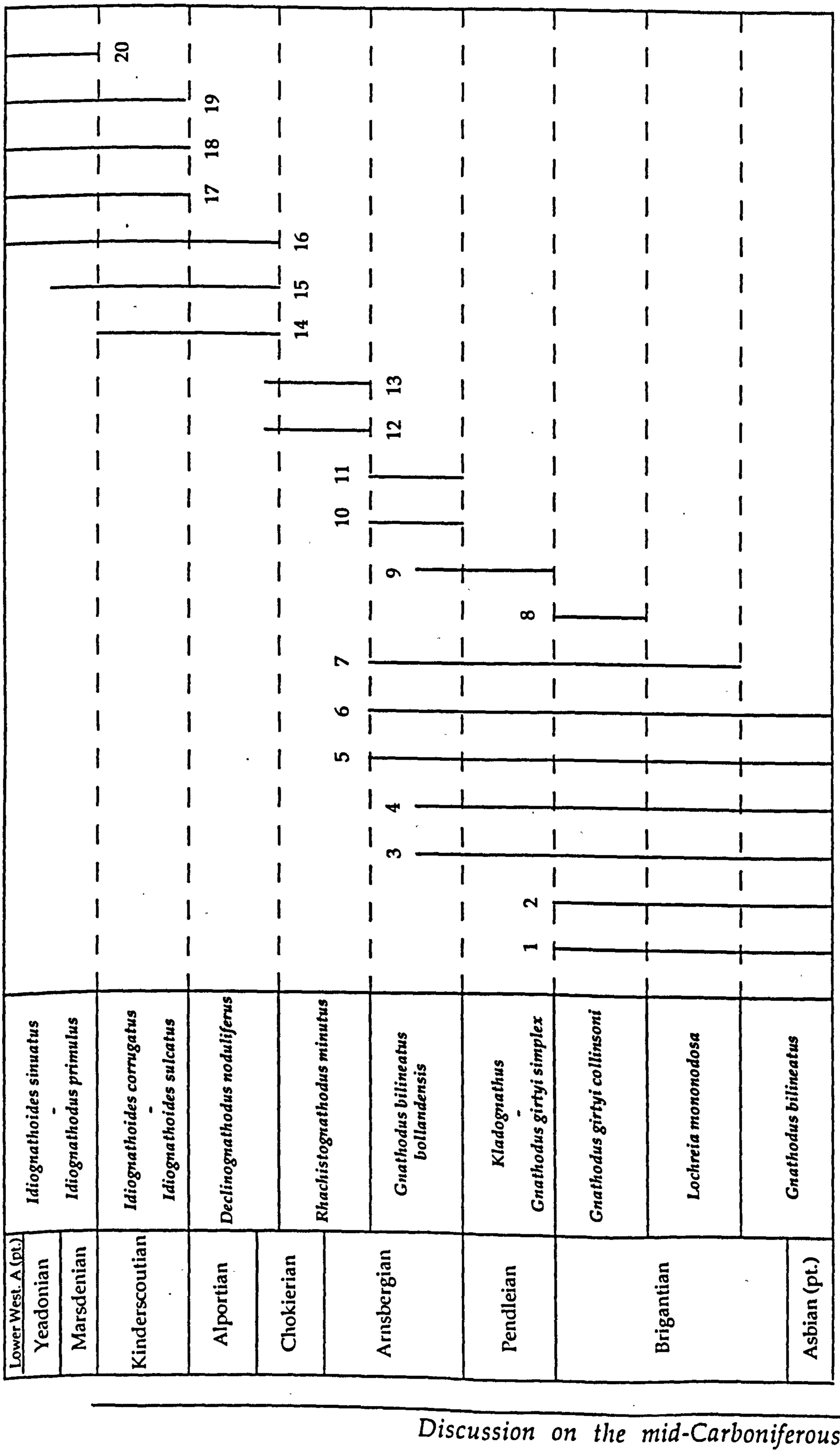

Figure 9.2 Range chart for selected conodonts in American succession.

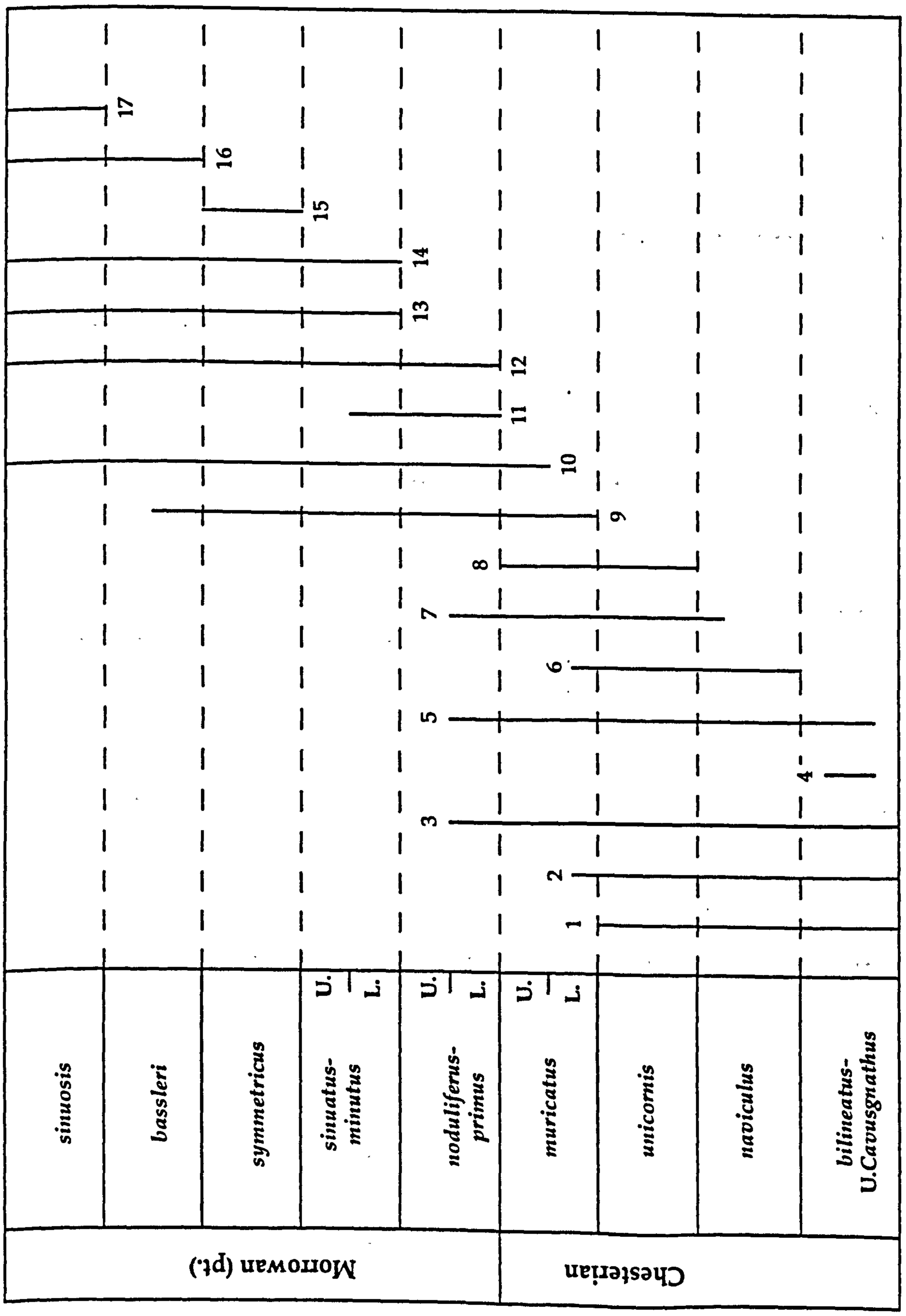

1 Cavusgnathus regularis; 2 Cavusgnathus unicornis; 3 Gnathodus bilineatus; 4 Cavusgnathus charactus; 5 Lochreia commutata; 6 Cavusgnathus naviculus; 7 Gnathodus girtyi simplex; 8 Adetognathus unicornis; 9 Rhachistognathus muricatus; 10 Adetognathus lautus; 11 Rhachistognathus primus; 12 Declinognathodus noduliferus; 13 Rhachistognathus minutus; 14 Idiognathoides sinuatus; 15 Neognathodus symmetricus; 16 Neognathodus bassleri; 17 Idiognathodus sinuosis.

U.S. CONODONT ZONE	WESTERN EUROPEAN CONODONT ZONE
symmetricus	*Idiognathoides sinuatus* - *Idiognathodus primulus*
sinuatus - *minutus*	*Idiognathoides corrugatus* - *Idiognathoides sulcatus*
noduliferus - *primus*	*Declinognathodus noduliferus*
muricatus	*Rhachistognathus minutus*
unicornis	*Gnathodus bilineatus bollandensis*
naviculus	
bilineatus - *Upper Cavusgnathus*	*Kladognathus-Gnathodus girtyi simplex*
	Gnathodus girtyi collinsoni
	Lochriea mononodosa
	Gnathodus bilineatus

Table 9.3 Cross-correlation on conodont zonations for America and western Europe.

The Pennsylvanian zones show much less coincidence of species between the two areas. However, by definition of the mid-Carboniferous boundary, the appearance of *Declinognathodus noduliferus* is isochronous (Cowie, 1990). Therefore the base of the *noduliferus-primus* and *noduliferus* zones of the U.S.A. and Europe are coincident.

Correlation between the Morrowan conodont scheme and that of the Namurian of Britain is very sketchy, due to the lack of similarities in the range of certain conodont elements:-

1) Overlap of lower Carboniferous faunas (e.g., *Gnathodus bilineatus, Lochreia commutata, Gnathodus girtyi simplex*) is seen with later Carboniferous forms such as *Rhachistognathus muricatus, Declinognathodus noduliferus* and *Rhachistognathodus primus* in America.
2) *Rhachistognathodus minutus* occurs prior to the appearance of *Declinognathodus noduliferus* in western Europe.
3) *Neognathodus bassleri* occurs much earlier in western Europe than in America, co-occurring with *Declinognathodus* near the base of the Chokierian.
4) The range of *Declinognathodus noduliferus* in Europe is much shorter than that of the species in U.S.A.

Using the definition for the base of the *sinuatus-minutus* zone i.e., that it corresponds to the first appearance of the *Idiognathoides sinuatus* then the *sinuatus-minutus* zone of the U.S.A. is correlated with the base of the base of the *Idiognathoides corrugatus-Idiognathoides sulcatus* zones of Europe, and probably ranges into the *Idiognathoides sinuatus-Idiognathodus primulus* zone of Europe.

9.2.3 Cross-correlation using both conodont and ammonoid stratigraphies

Riley (1993) stated the influence of facies effects in correlation is reduced by comparing different zonation schemes. Therefore a cross-correlation is attempted utilising both schemes. To the author's knowledge cross correlation using both ammonoid and conodont zonations has not been attempted before.

As ammonoids show an identical succession of genera in both areas it is implied that their occurrence in the stratigraphic record is heavily influenced by rapid worldwide flooding events (see section 9.1.2.2). It is

therefore more likely that the ammonoids represent time-planes in the succession. As proven in section 9.2.2 it is extremely difficult to correlate the American and European successions based on conodont data alone, especially for post-boundary strata. Thus, ammonoid successions are correlated and the conodont zones related to the ammonoid succession for each region (Table 9.4). Although the correlation is primarily based on ammonoids the correlation is effectively forced due to the assumption that *noduliferus* is isochronous at its first appearance (which defines the mid-Carboniferous boundary), yet it does not affect the ammonoid data, thus two separate zonations are effectively compared for the two regions.

Table 9.4 shows how, as surmised in section 9.2.2, that the upper *naviculus*, *unicornis* and *muricatus* zones of the U.S.A. compare to the *Gnathodus bilineatus bollandensis* zones of Europe. Additionally the *bilineatus*-Upper *Cavusgnathus* zone of the U.S.A. compares with the *Gnathodus bilineatus* to lower *Kladognathus-Gnathodus girtyi simplex* zones of Britain.

It is implied by the cross-correlation that the upper *muricatus* zone is probably coincident with the *Rhachistognathus minutus* zone of Europe (the conodont record shows this with the occurrence of *Adetognathus lautus* (=*A. gigantus*) at the same level in both regions.

By definition the appearance of *Declinognathodus noduliferus* is isochronous. This provides a correlation with the goniatite record in the U.S.A. (which was not available prior to the recent findings of Alan Titus, (discussed later)).

However, a major difference in correlation (to that suggested in the correlation based primarily on conodonts in section 9.2.2) is seen in the Pennsylvanian zones where the *noduliferus-primus* zone is coincident with the *Idiognathoides corrugatus-Idiognathoides sulcatus* and *Declinognathodus noduliferus* zones of Europe. The correlation of the separate zonations for ammonoids and conodonts also provides a much better correlation for the later Morrowan conodont zones (where it is extremely difficult to correlate the conodont data).

Additionally this Table (when overlain with conodont ranges) and Figures 9.1 and 9.2 show how disparate the ranges of certain conodont taxa are between regions. Some of the major anomalies are listed below:-

---

Discussion on the mid-Carboniferous boundary

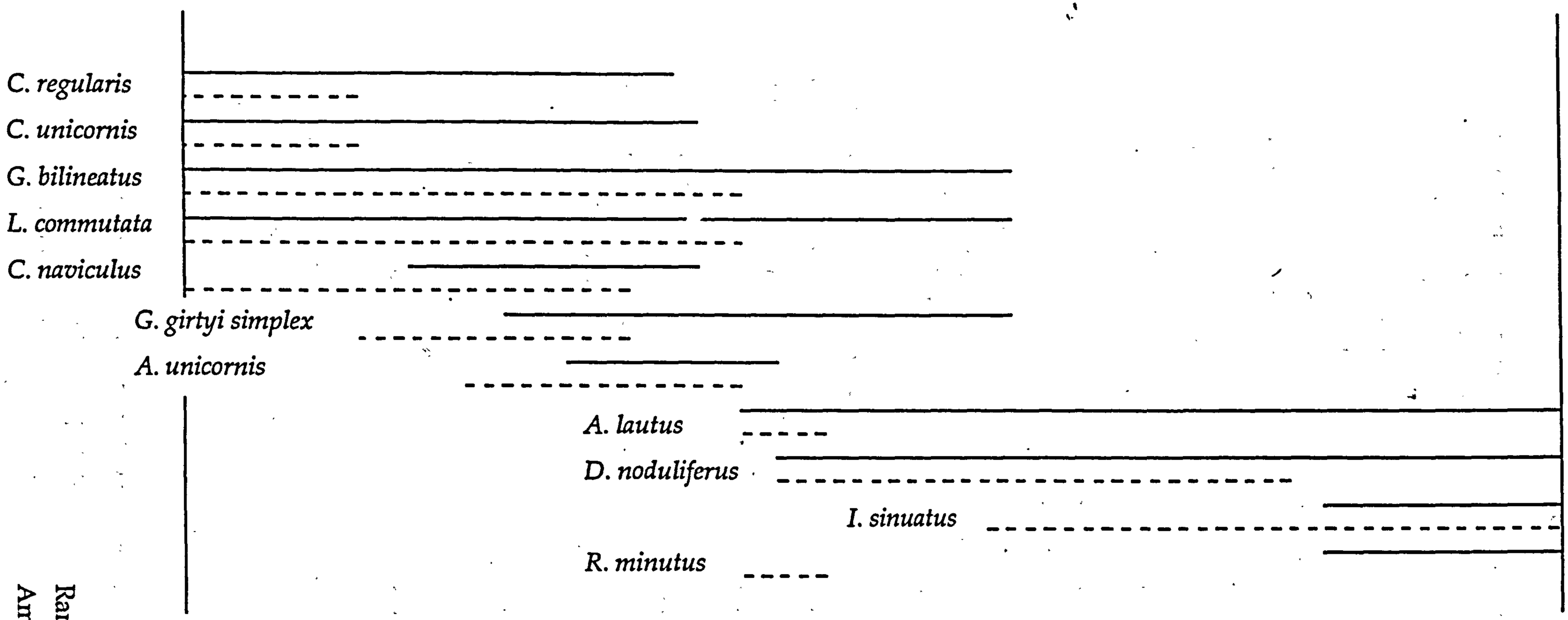

Ranges for conodont species in America shown in solid line, and in western Europe as dashed line).

U.S. CONODONT ZONE	U.S. AMMONOID ZONE	EUR.AMM. INDEX	EUR CONODONT ZONE
symmetricus (pt.)	*Verneulites pygmaeus*	G_1b^1	*Idiognathoides sinuatus* - *Idiognathodus primulus* (pt.)
		G_1a^1	
		R_2c^2	
	Arkanites relictus	R_2c^1	
sinuatus - *minutus*	*Quinnites henbesti*	R_2b^5	
		R_2b^4	
		R_2b^3	
		R_2b^2	
		R_2b^1	
noduliferus - *primus*	*Retites semiretia*	R_2a^1	
		R_1c^4	*Idiognathoides corrugatus* - *Idiognathoides sulcatus*
		R_1c^3	
		R_1c^2	
		R_1c^1	
		R_1b^3	
		R_1b^2	
	[redacted]	R_1b^1	
		R_1a^5	
		R_1a^4	
		R_1a^3	
		R_1a^2	
		R_1a^1	
		H_2c^2	*Declinognathodus noduliferus*
		H_2c^1	
		H_2b^1	
		H_2a^1	
	Homoceras beyrichianum - *Homoceras coronatum*	H_1b^2	
		H_1b^1	
	Isohomoceras suglobosum - *Isohomoceras diadema*	H_1a^3	
		H_1a^2	
muricatus		H_1a^1	*Rhachistognathus minutus*
unicornis	*Delepinoceras thalassoide* - *Zephyroceras friscoense*	E_2c^4	*Gnathodus bilineatus bollandensis*
		E_2c^3	
		E_2c^2	
		E_2c^1	
		E_2b^3	
		E_2b^2	
	Stenoglaphyrites involutum	E_2b^1	
naviculus	*Eumorphoceras bisulcatum* - *Cravenoceras richardsonianum*	E_2a^3	
		E_2a^{2a}	
	Richardsonites merriami	E_2a^2	
	Cravenoceras hesperium	E_2a^1	
bilineatus - Upper *Cavusgnathus*	*Syngastrioceras barnettense*	E_1c^1	*Kladognathus* - *Gnathodus girtyi simplex*
		E_1b^2	
		E_1b^1	
		E_1a^1	
	Lusitanoceras granosus	P_2c	*Gnathodus girtyi collinsoni*
		P_2b	*Lochreia mononodosa*
		P_2a	*Gnathodus bilineatus*
	Goniatites multiratus	P_1d	
		P_1c	
		P_1b	
		P_1a	

Table 9.4 Cross-correlation on conodont and ammonoid zonations for America and western Europe.

U.S. CONODONT ZONE	U.S. AMMONOID ZONE	EUR. AMM. INDEX	EUR. CONODONT ZONE
symmetricus (pt.)	*Verneculites pygmaeus*	C1b C1a R2c^2	*Idiognathoides sinuatus* - *Idiognathodus primulus* (pt.)
	Arkanites relictus	R2c	
sinuatus - minutus	*Quinnites henbesti*	R2b^5 R2b^4 R2b^3 R2b^2 R2b^1	
noduliferus - primus	*Retites semiretia*	R2a^1 R1c^4 R1c^3 R1c^2 R1c^1 R1b^3 R1b^2	*Idiognathoides corrugatus* - *Idiognathoides sulcatus*
		R1b^1 R1a^5 R1a^4 R1a^3 R1a^2 R1a^1	
		H2a^2 H2c^1 H2b^1 H2a^1	*Declinognathodus noduliferus*
	Homoceras beyrichianum - Homoceras coronatum	H1b^2 H1b^1	
	Isohomoceras suglobosum - Isohomoceras diadema	H1a^3 H1a^2 H1a^1	*Rhachistognathus minutus*
muricatus	*Delepinoceras thalassoides*	E2c^4 E2c^3	*Gnathodus bilineatus bollandensis*
unicornis	*Zephyroceras friscoense*	E2c^2 E2c^1 E2b^3	
	Stenoglaphyrites involutum	E2b^2 E2b^1	
napiculus	*Eumorphoceras bisulcatum - Cravenoceras richardsonianum*	E2a^3 E2a^{2a}	
	Richardsonites merriami	E2a^2	
	Cravenoceras hesperium	E2a^1	
bilineatus	*Syngastrioceras barnettense*	E1c^1 E1b^2 E1b^1 E1a^1	*Kladognathus* - *Gnathodus girtyi simplex*
Upper *Cavusgnathus*	*Lusitanoceras granosus*	P2c	*Gnathodus girtyi collinsoni*
		P2b	*Lochreia mononodosa*
		P2a	*Gnathodus bilineatus*
	Goniatites multiratus	P1d P1c P1b P1a	

C. regularis — *C. unicornis* — *G. bilineatus* — *Li. ornatus* — *C. navicullus* — *G. girtyi simplex* — *A. unicornis* — *D. noduliferus* — *R. minutus*

Table 14 Cross correlation on conodont and ammonoid zonations for America and western Europe. Ranges for conodont species in America shown in solid line, and in western Europe as dashed line).

1) Comparing the ranges of *Cavusgnathus unicornis* and *C. regularis,* these faunas are confined to the Dinantian in Britain but range up to near the top of the Arnsbergian in the States.
2) *Rhachistognathus minutus* appears briefly in the European succession over the Arnsbergian-Chokierian boundary. In the United States this conodont element does not appear until the Marsdenian.
3) *Neognathodus bassleri* first occurs in the Westphalian in U.S.A. whilst it makes its first appearance very near to the base of the Chokierian in Europe.
4) *Declinognathodus noduliferus,* by definition occurs at the same level in the two areas, however, it ranges until the Westphalian in the United States, but does not survive past the top of the Kinderscoutian in western Europe.
5) *Idiognathoides sinuatus* appears in the Kinderscoutian in Europe, and not until one stage higher in the States.

9.2.3.1. Previous correlations

It has been thought by many workers that there is possibly a gap in the conodont succession of the United States (commonly believed to be at the lower/upper *muricatus* boundary or at the base or within the *noduliferus-primus zone*), however, even if gaps are inferred, the sequence of conodont faunal appearances is unchanged.

Some of the various cross correlations with conodonts and ammonoids are shown in Table 9.5. Most commonly either favour the presence of an unconformity within the American sequence or facies control of the faunas as explaining the differences in the zonations. Lane, Baesemann and Groves, (1985) however, unusually invoked an unconformity within the British succession within the middle part of the Namurian to explain the differences in stratigraphy (Figure 9.3). This appears to be quite absurd as there is no evidence of an unconformity at the most complete British section (Stonehead Beck) where a complete sequence of ammonoid horizons is known.

The attempted correlation in this study, shown in Table 9.4, therefore indicates that there are still problems trying to correlate between regions, even with the decision on the choice of stratotype and the level of the mid-Carboniferous boundary. The Mississippian does show some similarities between the United States and western European zonations, however, it appears that provincialism and facies control of conodont faunas is much

	Western Europe	Higgins (1981)	Grayson *et al.*, (1985)	Manger and Sutherland (1992)
West. A (pt.)	*Idiognathoides sinuatus* - *Idiognathodus primulus* (pt.)			*bassleri*
Yeadonian				*symmetricus*
Marsdenian				*sinuatus* - *minutus*
Kinderscoutian	*Idiognathoides corrugatus* - *Idiognathoides sulcatus*	*primus* - *noduliferus*	*primus* - *noduliferus*	
Alportian	*Declinognathodus noduliferus*		*muricatus*	*noduliferus* - *primus*
Chokierian	*Rhachistognathus minutus*	*muricatus*		
Arnsbergain	*Gnathodus bilineatus bollandensis*	*unicornis*	*muricatus*	*muricatus*
		naviculus	*unicornis*	*unicornis*
				naviculus
Pendleian	*Kladognathus* - *Gnathodus girtyi simplex*			

Table 9.5 Three of the previously suggestion correlations between conodont zonations for America and western Europe.

<table>
<tr><th>AMERICA</th><th>WESTERN EUROPE</th></tr>
<tr><td>klapperi</td><td>Idiognathoides sinuatus
-
Idiognathodus primulus (pt.)</td></tr>
<tr><td>sinuosis</td><td rowspan="2">Idiognathoides corrugatus
-
Idiognathoides sulcatus</td></tr>
<tr><td>bassleri</td></tr>
<tr><td>symmetricus</td><td>Declinognathodus noduliferus</td></tr>
<tr><td>sinuatus
-
minuatus</td><td>Rhachistognathus minutus</td></tr>
<tr><td>noduliferus
-
primus</td><td rowspan="3"></td></tr>
<tr><td>muricatus</td></tr>
<tr><td>unicornis</td><td rowspan="2">Gnathodus bilineatus
bollandensis</td></tr>
<tr><td>naviculus</td></tr>
</table>

Figure 9.3 Suggested correlation between conodont zonations of America and western Europe by Lane, Baesemann and Groves (1985).

more rife after the mid-Carboniferous boundary. Discrepancies between the conodont record from America and Europe are likely to be due to facies control, both within and between the regions. If, as shown in Table 9.4 that there are discrepancies in the ranges of virtually every conodont species between the U.S.A. and Europe, is it tangible to force a correlation by assuming *Declinognathodus noduliferus* is isochronous in its first appearance?

9.2.3.2. New data from the Nevada Test Site

Very recent work by Alan Titus (pers. comm., 1995) has led to the discovery of the mid-Carboniferous boundary defining conodont (*Declinognathodus noduliferus*) ***beneath*** the Arnsbergian-Chokierian boundary (see also section 8.6). The Arnsbergian-Chokierian boundary now appears to coincide with the lower-upper *muricatus* boundary (as defined by the appearance of *Adetognathus lautus*). At Arrow Canyon, on the other hand, *Adetognathus lautus* occurs earlier than *Declinognathodus noduliferus*.

The Nevada Test Site section shows the most complete succession across the Mississippian-Pennsylvanian boundary in the United States and this new data will now necessitate a complete revision of the American conodont biostratigraphy (beyond the scope of this work).

At first sight the Nevada Test Site data appear to correlate well with the data from western Europe. It is this author's opinion that it is probable that the *Adetognathus/Rhachistognathus* fauna developed across the Arnsbergian/Chokierian boundary in western Europe represents a shallow water conodont facies equivalent to that of *Declinognathodus noduliferus*. In this case it is the shallow water conodont record that is showing the change at the mid-Carboniferous boundary. This may be not totally unexpected if, as has been suggested in this work (section 7.4.4) and by other authors (Saunders and Ramsbottom, 1986) the mid-Carboniferous 'faunal event' is marking a substantial sea-level fall, then in fact it will be the shallow water faunas that will show the most immediate drastic change, with possibly deeper water faunas becoming affected only towards the later parts of the eustatic fall. However, obviously the only stratigraphic sections to survive the regression would represent deep water deposition.

The new data of Alan Titus's also invokes questions on the time-relationship between this section and that at Arrow Canyon. *Adetognathus*

is a shallow water fauna and thus is likely to be a lateral equivalent to a deeper water *Declinognathodus* fauna, but by definition of the mid-Carboniferous boundary the appearance of *Declinognathodus noduliferus* must be synchronous worldwide. This therefore implies that the mid-Carboniferous at Arrow Canyon is also pre-Chokierian in age, yet here *Adetognathodus lautus* occurs before the first occurrence of *Declinognathodus noduliferus*...**but** the lower-upper *muricatus* boundary (and thus the Arnsbergian/Chokierian boundary) occurs at the first appearance of *Adetognathus lautus*. It must be implied that facies control of the faunas is taking place between the basinal section at the Nevada Test Site and the shallow water carbonate shelf at Arrow Canyon. Whether the Arnsbergian/Chokierian boundary occurs at the same level (with the appearance of *Adetognathus lautus*) is unknown due to the lack of ammonoid control at Arrow Canyon. It is this authors opinion that at least part of the upper *muricatus Adetognathus* biofacies at Arrow Canyon is likely to be a lateral equivalent to the *Declinognathus* biofacies in the basin centre, and thus the boundary at Arrow Canyon may be later Chokierian in age.

Further work will clarify the situation between the carbonate shelf and the basin centre in the Antler Basin and also the relationship between the Nevadan *Isohomoceras* faunas and the corresponding level within the H_1 of Europe. However, it appears that:-

1) If *Declinognathodus noduliferus* occurs in pre-Chokierian strata then its first evolutionary occurrence is not related to the 'faunal event' at the base of the Chokierian.

2) The first occurrence of *Declinognathodus noduliferus* at Arrow Canyon may not be its true first occurrence in the stratigraphic record.

3) *Declinognathodus noduliferus* is not isochronous in its first appearance.

It could be argued that these points detailed above involve the use of calibration against a ammonoid datum (in which ammonoid occurrences are assumed to be synchronous and worldwide) and the assumption that the *Isohomoceras subglobosum* faunas at the Test Site are earliest Chokierian in age. Removing the ammonoid stratigraphy and assuming that the appearance of *Declinognathodus noduliferus* is isochronous throughout the world invokes a facies-controlled shallow water fauna after the mid-Carboniferous boundary at the Nevada Test Site (and before the boundary at Arrow Canyon) and assumes that *Declinognathus* nevertheless is not facies controlled. This does not seem a viable option.

9.3 DISCUSSION ON THE MID-CARBONIFEROUS BOUNDARY AND THE CHOICE OF STRATOTYPE.

Cowie (1990) following the work of the International Committee on Stratigraphy listed the following criteria as being important in selecting a stratotype for a particular boundary:-

1) Correlation on a global scale. A marker horizon has to be globally significant and be proved to be isochronous within the limits of precision attainable by stratigraphic methods.

2) Completeness of exposure. The section should not display an isolated position (of the boundary) but a succession that can be easily followed.

3) Adequate thickness of sediments.

4) Abundance and diversity of well-preserved fossils. Appearances and disappearances of single fossil species may be diachronous and therefore a bad guide to the location of the boundary. Taxa which are palaeoecologically tied to facies should be excluded from consideration. Ideally selection of a point within an evolutionary lineage is desirable.

5) Favourable facies for widespread and reliable correlation. i.e., the boundary stratotype should not be in or close to conglomerates, breccias, turbidites etc. Thus, the variation of chronostratigraphic age within the stratotype section is eliminated.

6) Freedom from structural complication and metamorphism.

7) Amenability to magnostratigraphy and geochronometry

8) Accessibility and conservation. The site should be protected to deter over-excessive collecting. There must be no physical or political obstacles to the stratotype site.

9) Continuity of sedimentation. A monotonous succession will reduce errors resulting form stratigraphic gaps. Additionally occurrences are likely to relate to biological rather than environmental factors.

10) Freedom from unconformities. The change may imply a timebreak. No disconformities, unconformities, cryptic paraconformities or time breaks in sedimentation any longer than a brief diastem can be tolerated close to the boundary.

Point 1 is discussed in section 9.3.1 below and the other points are applied to the three sections selected as potential stratotype sections in 1993 (Aksu-1, Stonehead Beck and the eventual chosen stratotype at Arrow Canyon) in section 9.3.2.

9.3.1 Choice of biostratigraphic marker fauna

The decision to recognise the actual mid-Carboniferous boundary on conodonts marks a departure for the first time, to the principle established at the first Carboniferous Congress in 1927, that divisions at least of the lower part of the Carboniferous should be based on goniatites (Ramsbottom, 1991). This decision was based on the fact that one of the ammonoid genera (*Homoceras*) that is present in mid-Carboniferous strata was thought to have had limited distribution (Lane, Baesemann, *et al.*, 1985). However, it is now known that both groups have worldwide distribution, and are present in a wide variety of facies and show changes at the Mississippian-Pennsylvanian boundary. This section examines the advantages and disadvantages of each group.

9.3.1.1 Conodonts

The major advantage of using conodonts to define the mid-Carboniferous boundary is that they were extremely widespread during the middle Carboniferous. However, the inherent problem with using conodonts as the defining fauna for the mid-Carboniferous boundary is their extreme facies variability which hampers cross-correlation (see section 9.2.2 above). Appearances of certain conodonts (e.g. *Neognathodus* sp., *Rhachistognathus* sp.) also occur much earlier in different regions and this is probably related to facies control.

Another problem is that the platform element *Declinognathodus noduliferus* represents only one part of a multielement species, at the time of proposing the conodont as the faunal marker the entire multielement species was not known and now there are doubts on phylogeny of the species. It was thought that *Gnathodus girtyi simplex* was the ancestor of *Declinognathodus noduliferus.* But at present there are two interpretations for the origin of *Declinognathodus:-*

1) Dunn (1970), Lane and Baesemann (1982), Lane, Baesemann, *et al* (1985) and Lane and Manger (1985b) suggest that *Declinognathodus* evolved from *Gnathodus girtyi.*

2) Grayson *et al* (1987) suggested that *Declinognathodus* evolved from *Gnathodus bilineatus.* More recently workers have started to recognise this transition in European and Russian successions. Nigmadganov and

Nemirovskaya (1992) have recognised transitional forms (*Gnathodus postbilineatus* and *Declinognathodus praenoduliferus*) between *Gnathodus bilineatus* and *Declinognathodus noduliferus* from the Aksu-1 section. Work by Varker (1994) has now also recognised this transition in northern England strata. Additional support for the hypothesis that *Gnathodus bilineatus* is the ancestor for *Declinognathodus* comes from the reconstruction of the multielement species for *Gnathodus bilineatus*. (Norby, 1976) . The multielement species contains the elements *Ozarkodina deliculata, Synprioniodina microdentata, Hibbardella acuta, Hindeodella simplex; H. ibergensis,* and *H. uncata. Gnathodus bilineatus* is not known from strata younger than Arnsbergian in age, yet Austin (1972), Higgins (1975) and this study (section 4.4.2) have recognised the above association of non-platform elements from strata that are dated as Chokierian and Alportian in age. Thus, with only modification of the platform elements it is easy to envisage the transition from *Gnathodus bilineatus* to *Declinognathodus noduliferus* such that the multielement *Declinognathodus noduliferus* species would essentially comprise of modified platforms together with other elements inherited from its *bilineatus* ancestor.

A third problem is the long time-range for each conodont zone and thus the possibility of intra-zone unconformities that are not marked by the conodont record.

9.3.1.2 Ammonoids

Carboniferous ammonoids, although showing an elemental of provinciality show wide geographic spread, developed at times of glacio-eustacially-driven maximum flooding. It is envisaged that ammonoid occurrences effectively represent isochronous time-planes within a succession (Ramsbottom, 1980; Maynard and Leeder, 1992; Riley *et al.*, 1994).

Therefore the ammonoid record provides a high resolution stratigraphic timescale. There are 46 marine bands known from the Namurian succession which is estimated to last 5.5 Ma (Riley *et al.*, 1994) which gives a duration of 120 000 years per marine band (interestingly, close to the eccentricity value for Milankovitch cyclicity). Obviously the ammonoid biostratigraphy provides much higher resolution than the conodont zonation, in which single zones may last up to 1 Ma and show diachronicity.

When the selection criteria for the choice of mid-Carboniferous stratotype were drawn up it was thought that the homoceratid genera were limited in distribution. Known occurrences at that time were from northern Europe, the C.I.S. and Algeria. It is now known that the range is much greater and also encompasses western U.S.A.

However, one problem with the use of ammonoids in definition of the mid-Carboniferous boundary is that the Namurian ammonoids seemed to prefer more basinal successions rather than shallow water carbonates.

9.3.1.3 Discussion

It would seem that with hindsight, the choice of an ammonoid species (presumably *Isohomoceras subglobosum*) rather than the use of conodonts as the defining fauna for the mid-Carboniferous boundary would have provided much greater resolution to the chronostratigraphic mid-Carboniferous boundary. The use of the conodont *Declinognathodus noduliferus* and the related conodont zonation schemes in correlation, is fraught with difficulties due to facies control and the long time range of zones. One of the early papers relating to the choice of conodont by Lane himself (Lane and Baesemann, 1982) indicated that there were four important considerations to be taken into account:-

1) Are ancestor-descendant relationships clearly understood?
2) Can the same evolutionary sequence be shown to appear widely?
3) Does the defining taxa occur abundantly?
4) Does the defining horizon approximate the boundary utilised at the appearance of *Rhachistognathus primus*?

Obviously points 1 and 2 are now not applicable. The recent discovery that required repositioning of the horizon at the stratotype at Arrow Canyon (see section 2.3.4) now also casts doubts on the answers to points 3 and 4.

The entire purpose of the mid-Carboniferous boundary is to aid correlation between areas and set a standard against which other sections can be compared. The boundary is based on numerous significant changes within the fossil record and records the biostratigraphic expression of a major worldwide floral and faunal event (Lane and Manger, 1985a). The choice of an appropriate boundary level (and therefore defining fauna) is only

possible where a marker horizon has been proved to be isochronous within the limits of precision attainable by stratigraphic methods (Hedberg, 1976; Cowie 1990).

It is shown that the major change in fauna occurs at the Arnsbergian/Chokierian boundary (itself defined by ammonoids) (Ramsbottom, *et al.*, 1982), however, the conodont defined mid-Carboniferous boundary does not occur until one marine (ammonoid) bands above this level (in western Europe). Following Wagner and Winkler Prins (1993), who stressed that evolutionary changes apparent in the geological record are related to an external event it is assumed that the mid-Carboniferous faunal change was related to same evolutionary catalyst for all groups (e.g., eustatic sea-level minima) then it would be expected that changes are synchronous. However, the absence of *Declinognathodus* in western Europe is probably related to facies control during the sea-level low at the beginning of the Chokierian. Thus, although it is the base of the Chokierian that shows a major faunal change it is not marked by *Declinognathodus*. The section at Arrow Canyon lacks ammonoids and thus the appearance of *Declinognathodus* cannot be calibrated against the ammonoid record, however surely the presence of this deep-water conodont in a predominantly extremely shallow water section must be anomalous? The recent discovery of *Declinognathodus noduliferus* below the Arnsbergian/Chokierian boundary (Titus, pers. comm., 1995) implies that the appearance of this conodont is not synchronous worldwide, neither is it related to the mid-Carboniferous 'faunal event'.

Thus, it has to be questioned whether the appearance of *Declinognathodus* really does mark the mid-Carboniferous faunal event, surely the only species that represents the level at which the faunal turnover occurred, and also shows worldwide synchronous appearance is that of the ammonoid *Isohomoceras subglobosum*? At present the appearance of *Isohomoceras* only roughly marks the boundary, it being defined precisely by *Declinognathodus*. It is the author's opinion that the boundary would be better defined if the roles of the two species were reversed.

9.3.2 Choice of stratotype.

For various reasons (e.g., imprecise boundary location, political instability etc.) many of the sections were discounted leaving three main candidates from which the eventual stratotype was chosen:-

1) Aksu-1, Gissar Range, South Tien Shan, Uzbekistan.
2) Stonehead Beck, Cowling, North Yorkshire, U.K.
3) Arrow Canyon, Nevada, U.S.A.

9.3.2.1 Aksu-1

The 20 m thick section at Aksu-1 has been only recently proposed (Nigmadganov and Nemirovskaya, 1993) as a potential stratotype and as a consequence relatively little work has been published on the site. The conodont faunas have been described, and there is only a little work on the poorly preserved ammonoids. No sedimentological or geochemical has been undertaken.

As in the British sections ammonoids are restricted to certain horizons. The section at Aksu-1 does not contain any representatives of the terminal Arnsbergian ammonoid genus *Nuculoceras*. The overlap of *Eumorphoceras* and *Isohomoceras* faunas at Aksu-1 may represent a condensed/reworked horizon. However, this section does show the transition from *Gnathodus bilineatus to Declinognathodus noduliferus* faunas, and thus, no gap is shown in the conodont record.

The situation of the section in a country liable to political unrest also has to be considered as undesirable

9.3.2.2 Stonehead Beck

The section at Stonehead Beck has been well documented and extensively studied, with geochemistry and the sedimentology being described as well as the biostratigraphy. It is the only section containing palynological evidence of the boundary. Most importantly the section is accurately constrained geochronometrically (314 Ma) and displays high resolution ammonoid biostratigraphy.

The section at Stonehead Beck is already the boundary stratotype for the Arnsbergian/Chokierian boundary (Ramsbottom *et al.*, 1981) and the type locality for *Isohomoceras subglobosum* (Bisat, 1924; Riley, 1987) and is protected having being designated a Site of Special Scientific Interest.

Some American workers (e.g. Lane and Baesemann, 1982; Baesemann and Lane, 1985) conclude that there must be a hiatus developed at the level

* Approximately at the level of sample 60 on Figure 2.2.

between the *Gnathodus bilineatus bollandensis* and *Rhachistognathus minutus* zones in the British Isles (see section 9.2.3.1 above). Yet there is no lithological evidence for an unconformity at the proposed section at Stonehead Beck, also there are no sections elsewhere that show a more complete ammonoid zonation record. Thus, the presumed hiatus is probably the result of environmental faunal control and provincialism.

However, the conodont defined boundary at this section unfortunately does not coincide with the Arnsbergian /Chokierian boundary. This is probably due to a shallow water conodont fauna spanning the Arnsbergian-Chokierian boundary and representing the lowstand of sea-level at this point. As detailed in section 9.1.2.3 it should be expected that *Declinognathodus* should occur at the base of the Chokierian, thus it is likely that the occurrence of *Declinognathodus* s.l. at H_1a^2 is not its earliest global occurrence. Additionally although the fauna at Stonehead Beck is quite diverse for a dysoxic basin setting, it is confined to 'marine bands' (except conodonts) and thus faunal changes outside these time planes are unclear.

9.3.2.3 Arrow Canyon

The section at Arrow Canyon is extensively exposed and contains abundant and varied fauna and has been extensively studied. After being recognised as one of the most depositionally complete exposures of Late Mississippian-Early Pennsylvanian strata in the U.S.A., much biostratigraphic work has resulted in the section becoming the basis for conodont zonation in the U.S.A. (e.g., Lane and Baesemann, 1982). However, recent work has shown that the original level as indicated in the proposal for Arrow Canyon as a stratotype is too high and in fact *Declinognathodus noduliferus* occurs at the base of the bed rather than within the top.* Surely if work at this late-stage still leads to new discoveries of the level of the first appearance of *D. noduliferus,* more work needs to be undertaken to establish the true first occurrence of *Declinognathodus*?

Another drawback to the section is that the actual boundary shown by the presence of *Declinognathodus noduliferus* occurs " less than 1m below a conglomeratic horizon" (Lane, Baesemann, *et al,*. 1985). The temporal extent of this unconformity is at present unclear, although as presented in chapter 8, the conglomerate very probably is represented by a 4.5 m thick sandstone body in more distal regions. Additionally the boundary is

situated in shallow water high energy carbonate deposits that were formed at the winnowed edge of a carbonate platform (see section 8.4.2). These show reworking of bioclasts deposited within more open regions of the platform and on the slope.

Foraminiferal and brachiopod zonation schemes have been erected for the Arrow Canyon section, however they do not coincide with each other nor with the conodont zonation. Examination of the biostratigraphic log in Baesemann and Lane (1985) (Figure 9.4) also reveals that there is a complication in later Morrowan conodont zone succession at this locality, with the occurrence of *Idiognathoides sinuatus* (ie., the base of the *sinuatus-minutus* zone) in sample 89, followed by the first occurrence of *Idiognathoides convexus*, less than one metre higher in a sample 90. *Idiognathoides convexus* usually occurs in the American succession two zones higher than the youngest zone described in this study (*sinuosus*) this implies that there may be a considerable gap in the sequence at Arrow Canyon.

This work (section 8.6) also casts doubt on the age of the first appearance of *Declinognathodus noduliferus* at Arrow Canyon, due to the discovery of this species in association with Arnsbergian ammonoids at the Nevada Test Site by Alan Titus (pers. comm., 1995). It is possible that the first appearance of *Declinognathodus noduliferus* at Arrow Canyon may then be later Chokierian in age.

9.3.2.4 Discussion

Table 9.6 shows the various criteria for consideration in a choice of stratotype against the three stratotype candidates.

It is shown that the section at Aksu-1 is primarily unsatisfactory due to a possible unconformity (represented in the ammonoid record) and possible doubts over the accessibility and preservation of the site. Additionally the site lacks the extensive documentation of the other candidates.

The Stonehead Beck section appears to fulfil all the criteria for selection as a stratotype. Although, as the boundary is conodont defined, it is this author's opinion that the section does not display the true first occurrence of *Declinognathodus* s.l. due to the persistence of a shallow water conodont fauna during the lower Chokierian.

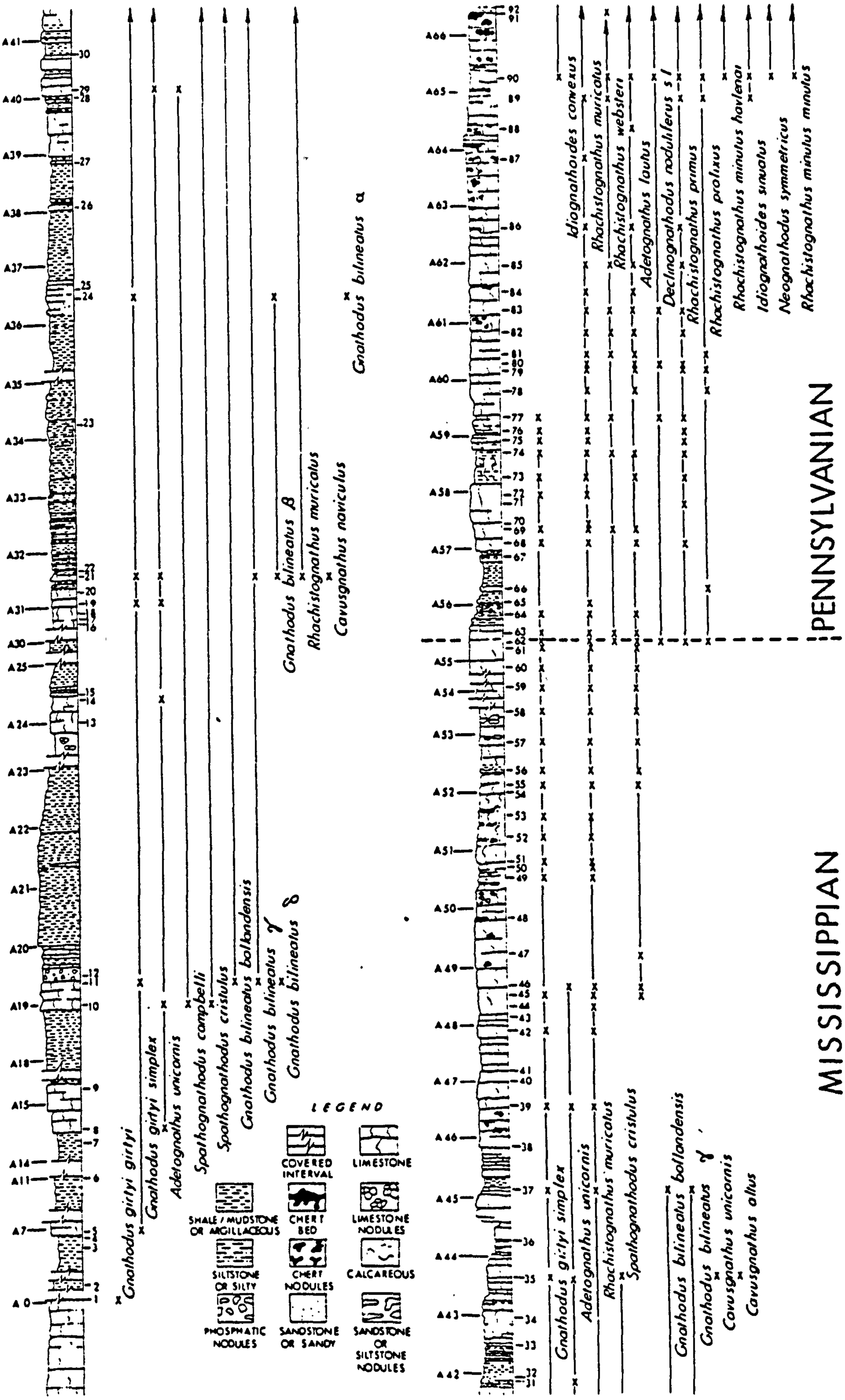

Figure 9.4 Biostratigraphic log for the lower Pennsylvanian of Arrow Canyon. (From Baesemann and Lane, 1985).

CRITERIA	AKSU-1	STONEHEAD BECK	ARROW CANYON
Completeness of exposure.	✓	✓	✓
Adequate thickness of sediments.	✓	✓	✓
Abundance and diversity of well-preserved fossils.	✓	✓	✓
Favourable facies for widespread and reliable correlation.	✓	✓	✗
Freedom from structural complication and metamorphism.	✓	✓	✓
Amenability to magnostratigraphy and geochronometry.	?	✓	✓
Accessibility and conservation.	✗	✓	✓
Continuity of sedimentation.	✓	✓	✗
Freedom from unconformities.	✗	✓	✗

Table 9.6 Criteria considered important in the choice of stratotype.

Although the Arrow Canyon section has been chosen as the stratotype section, Table 9.6 shows there are many problems with the section. The section shows a prominent unconformity in very close proximity to the boundary and an absence of the lower Morrowan conodont zones is also noted. The shallow water facies exposed across the boundary interval is liable to facies control of faunas and also to winnowing and reworking of faunas. Although the section has been extensively studied the late-stage modification of the level of the boundary must still indicate that further work should be conducted on the site.

The opinion given in this work is that the section at Arrow Canyon is an extremely unwise choice for a boundary stratotype (as additionally are the other two candidate sections). The search for a stratotype section spanning the mid-Carboniferous should continue if conodonts are to be kept as the defining fauna.

9.4 CONCLUSIONS

Cowie (1990) stated that "the correctly selected Global Boundary Section and Point, gives an actual point in the rock which defines an instant in time. The main criterion is that is that any horizon and point selected must be capable of being correlated over wide areas by any or all available methods. The choice of an appropriate boundary level for the point is only possible where a marker horizon has been proved to be isochronous within the limits of precision attainable by stratigraphic methods".

It is this authors opinion that the chronostratigraphic mid-Carboniferous boundary has been incorrectly selected:-

a) The purpose of the mid-Carboniferous boundary is to solve the problems of cross-correlation between regions and set a standard against which correlation can be made. An attempt has been made to produce at correlation chart for America and western Europe. It is extremely difficult to produce a correlation scheme on conodont data alone (due to the disparate ranges of species) therefore to reduce any facies effects the conodont schemes were also correlated against the ammonoid record for the two regions. Ranges for certain conodonts have been superimposed on this chart and shows facies control and provincialism of these organisms was prevalent during the mid-Carboniferous. Therefore it does not seem tenable that for only one conodont species (that marking the mid-

Carboniferous boundary - *Declinognathodus noduliferus*) it is thought that facies control did not apply and that its appearance was isochronous worldwide. Recent work in the Nevada Test Site by Alan Titus suggests that it is not.

b) The conodont *Declinognathodus noduliferus* was chosen to define the mid-Carboniferous boundary due to its widespread and known common evolutionary lineage. There are now doubts over the lineage of this species and also its abundance at the stratotype section at Arrow Canyon.

c) It is the author's opinion that the ammonoid record would provide much greater resolution to the chronostratigraphic mid-Carboniferous boundary. It is commonly thought that the ammonoid record represents the development of a widespread faunal phase at maximum transgression. It has been shown that sea-level fluctuations during mid-Carboniferous times were glacio-eustatically controlled, and thus the ammonoid succession effectively represents timeplanes. It is now shown that the mid-Carboniferous goniatite *Isohomoceras subglobosum* has much wider spread than previously thought. The mid-Carboniferous boundary is based on numerous significant changes within the fossil record and records the biostratigraphic expression of a major worldwide floral and faunal event, however it appears that it is the ammonoid record (and in particular the appearance of *Isohomoceras subglobosum*) that marks this change, not the heavily facies-controlled conodont record.

d) The mid-Carboniferous boundary stratotype has been chosen at Arrow Canyon in Nevada. There are many problems with this section, not least that there is a conglomerate within 1 m of the boundary level. Additionally this study has shown by facies analysis that the section lay on a winnowed carbonate platform in Carboniferous times. These show reworking of bioclasts deposited within more open regions of the platform and on the slope.

Recent work at the section has redefined the level of the mid-Carboniferous boundary, this indicates that more work may be needed to unequivocally define the first true occurrence of *Declinognathodus noduliferus* at Arrow Canyon. Although it may be implied that the conodont record is complete at the boundary there is a considerable gap higher in the sequence which omits five of the standard conodont zones of America.

Chapter 10

CONCLUSION

10.1 INTRODUCTION

This chapter presents a summary of the findings of this work, it also addresses the relevance of the work to other studies and provides suggestions for further investigations.

10.2 SUMMARY OF THE MAIN FINDINGS OF THIS THESIS.

As chapters 7 and 9 effectively act as conclusion chapters for the investigation of mid-Carboniferous deposition in County Clare and the choice of mid-Carboniferous stratotype respectively, the main findings of this work are listed in summary form.

- The stratigraphy of the Clare Basin has been investigated with a view to examining the expression of the mid-Carboniferous boundary in this basin. The main controls on mid-Carboniferous deposition were basin configuration, the extent of sea-level changes and sediment supply. A model of deposition through the mid-Carboniferous has been formulated. It is shown that during the earliest Namurian a widespread transgression flooded the shelves of the basin and created an environment favourable to phosphate authigenesis. Repeated regressions during the Pendleian and lower/middle Arnsbergian led to reworking of the phosphate into lags. The base of the Chokierian is marked by a sea-level low with phosphate lag formation on the shelves. Later Chokierian deposition is during a relative highstand of sea-level, with the *Homoceras beyrichianum* marine band marking a particularly highstand of sea-level.

- The section exposed at Inishcorker shows the most biostratigraphically complete section through the mid-Carboniferous

in Ireland. The high erosion rates at this locality make it a perfect candidate for intensive geochemical investigation. By comparison of various geochemical techniques a chart has been constructed to infer the relationship between the various geochemical parameters and relative sea-level. The section at Inishcorker although showing continuous deposition through the mid-Carboniferous boundary displays the geochemical expression of the relative sea-level lowstand at the beginning of the Chokierian. Additionally geochemical analysis has shown that the presumption that deposition outside 'marine' bands is in fresh- or low salinity waters is incorrect in this instance. It is likely that marine band formation may also partly be related to oxygen levels within the water column.

- The mid-Carboniferous boundary stratotype has been chosen within a section at Arrow Canyon. This succession has been investigated and it is shown that deposition during the mid-Carboniferous was on a winnowed carbonate platform. The diversity and eveness of the fauna through the mid-Carboniferous has also been studied and a drop in eveness is seen at the conodont defined boundary. However, this is a sudden drop and may reflect the increased environmental energy at this level (and thus winnowing of bioclasts) rather than the presence of a specialised fauna.

- Cross-correlation between the conodont biostratigraphies of western Europe and America has been attempted but is seriously hampered by the strong facies variability of the organism. This facies control of the conodont faunas is amplified when comparing both the ammonoid and conodont schemes for the two regions, and thus shows the true influence of facies control on the conodont faunas.

- It does not seem plausible to infer that the appearance of *Declinognathodus noduliferus* (the conodont defining the mid-Carboniferous boundary) is isochronous when virtually all other mid-Carboniferous conodont species show disparate ranges between the two regions. Additionally there are doubts over the phylogeny of the species and thus it is thought that the choice of this conodont fauna is an unwise choice for delimiting the mid-Carboniferous boundary. The actual faunal change at the mid-Carboniferous boundary is calibrated to the ammonoid record and it is this fauna (in particular *Isohomoceras subglobosum*) that defines the mid-

Carboniferous boundary, with the lowstand at the beginning of the Chokierian being reflected in the conodont record by a shallow water facies. The ammonoid record effectively represents timeplanes within a succession and thus provides much better calibration to the chronostratigraphic mid-Carboniferous boundary.

- The section at Arrow Canyon is an unwise choice for the mid-Carboniferous boundary stratotype. Not only does this section display carbonate sediments liable to exhibit reworking of bioclasts, there is also a conglomerate horizon within 1 m of the boundary level. Recent work at a more basinal locality within the same basin also questions the true first occurrence of *Declinognathodus noduliferus*.

10.3 RELEVANCE TO OTHER WORK

Holdsworth and Collinson (1988) and Martinsen (1990, 1993) have recognized the succession in the Craven Basin as showing a condensed sequence from E_2c^2 to H_1b^1. They correlated this to a highstand of sea-level. This is almost certainly true for late Arnsbergian and middle and late Chokierian times, but not for the lowest Chokierian in the Clare Basin. It is likely that the sea-level at the base of the Chokierian showed such a rapid fall that it was not matched by a sudden influx of sediment into the basin (possibly due to channel avulsion). However, although the lowest Chokierian deposits are condensed it is shown geochemically that this is related to an absence of sediment supply during a low- rather than highstand of sea-level. Thus, this work supports the inference of a lowstand at the base of the Chokierian by Ramsbottom (1977), Saunders and Ramsbottom (1986) and Riley *et al.*, (1987).

Martinsen (1990, 1993) also suggests a major lowstand at the end of the Chokierian (shown by an influx of clastics). However, Clare Basin deposits infer a highstand throughout the interval. Additionally late Chokierian marine bands show significantly high global geographic spread. It may well be that the eustatic signal is masked in the Craven Basin by high sediment influx or is due to a differing subsidence history to that of the Clare Basin.

It has previously been thought by many workers, (e.g. Ramsbottom, *et al.*, 1962) that barren strata outside marine band development represents

deposition in low salinitites. Geochemical investigation in the Clare Basin suggests that rather than the entrance of freshwater instaneously flushing the basin of marine waters, in fact it is possible that the presence of freshwater induces stronger stratification in the water column. Therefore, marine waters may be present in the water column outside marine band formation; only towards the ends of cyclothems do freshwaters become fully mixed into the water column. It is likely therefore that other environmental factors (e.g. oxygen levels) play a major role in influencing marine band formation. This work supports the work of Riley *et al.*, (1987) and Varker (1994) in their finding of conodonts outside marine bands, and thus the suggestion that marine waters are evident in the basin at times outside marine band formation.

10.4 SUGGESTIONS FOR FUTURE WORK

Sulphur isotope work on samples taken from Inishcorker would add to the model of deposition throughout the mid-Carboniferous interval. The work should clarify the source of the sulphate involved in pyrite formation, and thus show the extent of water exchange with the open sea (Sælen *et al.*, 1993). Additionally the work would provide an estimation as to the level of pyrite formation within the water column.

Greater integrated geochemical investigation should verify how chemofacies can be used in the rock record. The use of the relative sea-level versus geochemical parameter chart formulated in this study should be tested in other basins of both the same and differing ages as the Clare Basin. The determination of chemofacies in the rock record will lead to improved correlation between stratigraphic sections when biostratigraphic control is not available (i.e. by the use of unweathered rock cuttings in the oil industry.)

Although a biostratigraphic correlation chart between western Europe and America has been constructed, further work on the ammonoid and conodont succession will refine the correlation. In particular work should be focussed on the level of the base of the *Isohomoceras subglobosum-Isohomoceras diadema* and base of the *Verneulites pygmaeus* ammonoid zones and within the upper *muricatus* condont zone.

Further work can be attempted to examine the possiblity of a temporal lag between extreme eustatic minima and the entrance of clastics into a

depositional basin. However, this model can only be tested where a high resolution biostratigraphic framework is in place.

Obviously, as this work has shown there needs to be further search for a complete section spanning the mid-Carboniferous boundary if conodonts are kept as the defining fauna, so that the level of the boundary truely marks the faunal turnover on which it is based.

Do I belong to some ancient race?
I like to walk in ancient places,
These are things that I can't understand.
But I don't believe in your modern ways,
Don't care about the things you say,
Your policies have failed the test of time,
'Cos you sold them down the river.

The Levellers, 'Sell out.'

REFERENCES

ABED, A.M. and AL-AGHA, M.R. 1989. Petrography, geochemistry and origin of the NW Jordan phosphorites. *Journ. Geol. Soc. London, 146: 499-506.*

ADAMS, A.E., MacKENZIE, W.S. and GUILFORD, C. 1984. *Atlas of sedimentary rocks under the microscope. Longman Scientific Press. 104 pp.*

ADAMS, J.A.S. and WEAVER, C.E. 1958. Thorium to Uranium ratios as indicators of sedimentary processes; example of the concept of geochemical facies. *Bull. Am. Ass. Petrol. Geol., 42: 387-430.*

ADAMS, J.A.S., OSMOND, J.K. and ROGERS, J.J.W. 1959. The geochemistry of uranium and thorium. *Physical Chemistry of the Earth 3: 299-328.*

AL-BIATTY, H.J. 1990. *Aspects of carbon-sulphur-iron geochemistry and diagenesis. Ph.D. Thesis. (Unpubl)., Univ. Leeds: 428 pp.*

AMES, L.L. 1959. The genesis of carbonate apatites. *Economic Geology, 54: 829-841.*

ANDERSON, R.F., FLEISCHER, M.Q., and LEHURRAY, A.P. 1989a. Concentration, oxidation state, and particulate flux of uranium in the Black Sea. *Geochim. Cosmochim. Acta, 53: 2215-2224.*

ANDERSON, R.F., LEHURRAY, A.P., FLEISCHER, M.Q., and MURRAY, J.W. 1989b. Uranium deposition in Saanich Inlet sediments, Vancouver Island. *Geochim. Cosmochim. Acta, 53: 2201-2213.*

ANTIA. D.D.J. and WOOD, B.A. 1977. Some aspects of the palaeoecology of the E1b Zone of the Edale Shales (Namurian) in the Edale Valley, Derbyshire. *Mercian Geol., 6, (3): 179-196.*

ARTHUR, M.A. and JENKYNS, H.C. 1981. Phosphorites and paleoceanography. *Proceedings 26th International Geological Congress, Geology of Oceans symposium, Paris, July 7-17, 1980, Oceanologica Acta 1981: 83-96.*

ARTHUR, M.A. and SAGEMANN, B.B. 1994. Marine black shales: Depositional Mechanisms amd Environments of Ancient deposits. *Ann. Rev. Earth Planet. Sci., 22: 499-551.*

AUSTIN, R.L., 1972. Problems of conodont taxonomy with special reference to Upper Carboniferous forms. *Geologica et Palaeontologica, SB1: 115-126.*

AUSTIN, R.L. 1973. Modification of the British Avonian Conodont zonation and a re-appraisal of European Dinantian conodont zonation and correlation. *Ann. Soc. Géol. Belge, 96: 523-532.*

AUSTIN, R.L. 1974. The biostratigraphic distribution of conodonts in Great Britain and the Republic of Ireland. In: Bouckaert, J. and Streel, M. (Eds.). *Int. Symp. on Belgian Micropalaeontological Limits from Emsian to Viséan, Namur, 3, Geological Survey of Belgium: 1-17.*

AUSTIN, R.L. 1976. Evidence from Great Britain and Ireland concerning West European Dinantian conodont palaeoecology. In: Barnes, C.R. (Ed.). *Conodont Palaeoecology, Spec. Paper Geol. Assoc. Can., 15: 201-204.*

AUSTIN, R.L. 1987. *Condonts: investigative techniques and applications. British Micropalaeontological Society/Ellis Horwood Ltd.: 210 pp.*

AUSTIN, R.L. and DAVIES, R.B. 1984. Problems of conodont recognition and implications of Dinantian conodont biofacies in the British Isles. In: Clark, D.L. (Ed.). *Conodont biofacies and Provincialism. Geol. Soc. Am Spec. Paper 196: 195-229.*

BADGLEY, C. 1986. Counting individuals in Mammalian Fossil Assemblages from Fluvial Environments. *Palaios, 1: 328-338.*

BAESEMANN, J.F. and LANE, H.R. 1985. Taxonomy and evolution of the genus *Rhachistognathus* Dunn (Conodonta; Late Mississippian to early Middle Pennsylvanian). In: Lane. H.R. and Ziegler, W. (Eds.). *Toward a*

Boundary in the Middle of the Carboniferous: Stratigraphy and Palaeontology. Cour. Forsch. -Inst. Senckenberg, 74: 93-136.

BAIRD, G.C. and BRETT, C.E. 1986. Erosion on an aerobic seafloor: Significance of reworked pyrite deposits from the Devonian of New York State. *Palaeogeog., Palaeoclimat., Palaeoecol., 57: 157-193.*

BAIRD, G.C. and BRETT, C.E., 1991. Submarine erosion on the anoxic sea floor: stratinomic, palaeoenvironmental and temporal significance of reworked pyrite bone deposits. In: Tyson, R.V. and Pearson, T.H. (Eds.). *Modern and ancient continental shelf anoxia. Geol. Soc. Spec. Publ., 58: 233-259.*

BAIRD, G.C., BRETT, G.C. and KIRCHGASSER, W.T., 1988. Genesis of black shale-roofed discontinuities in the Genesee Formation, western New York State. In: McMillan, N.J., Embry, A.F. and Glass, D.J. (Eds.). *Devonian of the World, Can. Soc. Petrol. Geol. Mem., 14, 2: 357-375.*

BARNES, C.R. and FÅHRAEUS, L.E. 1975. Provinces, communities, and the proposed nektobenthic habit of Ordovician conodontophorids. *Lethaia 8: 133-149.*

BASSETT, M.G. 1990. International Commission on Stratigraphy. In: Briggs, D.E.G. and Crowther, P.R. (Eds.) *Palaeobiology, a synthesis. Blackwell Scientific: 468-469.*

BASSLER, R.S. 1925. Classification and stratigraphic use of the conodonts. *Geol. Soc. Am. Bull., 36: 218-220.*

BATURIN, G. N. 1970. Recent authigenic phosphorite formation on the South-West African Shelf. In: *The Geology of the East Atlantic Continental Margin, ICSU/SCOR Working Party 31 Symposium, Cambridge, Inst. Geol. Sci. Rep., 70/13: 88-97.*

BATURIN, G. N. 1971. Formation of phosphate sediments and water dynamics. *Oceanology, 11, (3): 372-376.*

BATURIN, G. N. 1974. New data on the Upper Quaternary phosphorite concretions on the continental shelf of South-West Africa. *Oceanology, 14 (6): 1040-1044.*

BATURIN, G. N. 1988. Disseminated Phosphorus in Oceanic sediments. *Marine Geology, 84; 95-104.*

BERNER, R.A. 1970. Sedimentary pyrite formation. *Am. Journ. Sci., 268: 1-23.*

BERNER, R.A. 1982. Burial of orgnic carbon and pyrite sulphur in modern oceans: Its geochemical and environmental significance. *Am. Journ. Sci., 282: 451-473.*

BERNER, R.A. 1984. Sedimentary pyrite formation: An update. *Geochim, Cosmochim., Acta, 48: 605-615.*

BERNER, R.A. and RAISWELL, R. 1983. Burial of organic carbon and pyrite sulphur in sediments over Phanerozoic time: a new theory. *Geochim., Cosmochim., Acta, 47: 855-862.*

BERNER, R.A. and RAISWELL, R. 1984. C/S method for distinguishing freshwater from marine sedimentary rocks. *Geology, 12: 365-368.*

BERNER, R.A. and WESTRICH, J.T., 1985. Bioturbation and the early diagensis of carbon and sulphur. *Am. Journ. Sci., 285: 193-206.*

BESLEY, B.M. 1988. Late Carboniferous sedimentation in north-west Europe: an introduction. In: Besley, B.M. and Kelling, G. (Eds.). *Sedimentation in a synorogenic basin complex: The Upper Carboniferous of north-west Europe. Blackie, Glasgow and London: 1-8.*

BISAT, W.S., 1924. The Carboniferous goniatites of the north of England and their zones. *Proc. Yorks. Geol. Soc., 20: 40-124.*

BISAT, W.S., 1928. The Carboniferous Goniatites of England and their Continental Equivalents. *Cong. de Strat. Carb., Heerlen: 117-133.*

BISAT, W.S., 1940. An early *Gastrioceras* (*G. branneroides* sp. nov.) from North Wales. *Trans. Leeds. Geol. Ass. 330.*

BISAT, W.S. and HUDSON, R.G.S., 1943. The Lower Reticuloceras (R_1) Goniatite Succession in the Namurian of the North of England. *Proc. Yorks. Geol. Soc., 24: 383-446.*

BOARDMANN, D.R. II and HECKEL, P.H. 1989. Glacio-eustatic sea level curve for early Late Pennsylvanian sequence in north-central Texas and biostratigraphic correlation curve for Midcontinent North America. *Geology, 17: 802-805.*

BOROVEC, Z., KRIBEK, B., and TOLAR, V. 1979. Sorption of uranyl by humic acids. *Chemical Geology, 27: 324-338.*

BOTT, M.P.H. and JOHNSON, G.A.L. 1967. The controlling mechanism of Carboniferous cyclic sedimentation. *Quart. Journ. Geol. Soc. Lond., 122: 421-441.*

BOUROZ, A., EINOR, O.L., GORDON, M., MEYEN, S.V. and WAGNER, R.H. 1978a. Proposals for an international Chronostratigraphic Classification of the Carboniferous. *Industrie Minerale, 60, (10): 469-483.*

BOUROZ, A., EINOR, O.L., GORDON, M., MEYEN, S.V. and WAGNER, R.H. 1978b. Proposals for an International Chronostratigraphic Classification of the Carboniferous. *Compte Rendu, 8th International Congress on Carboniferous Stratigraphy and Geology, Moscow 1975, vol. 1:36-69.*

BOUROZ, A., WAGNER, R.H., EINOR, O.L., GORDON, M. and MEYEN, S.V. 1977. Proposals for an International Chronostratigraphic Classification of the Carboniferous. *Izvestiya Akademiya nauk SSSR, Seriya geologicheskaya, Moscow, 2: 5-24.*

BOUROZ, A. WINKLER PRINS, C.F. and SAUNDERS, W.B. 1980. The I.U.G.S. Subcommission on Carboniferous Stratigraphy: its past, present and future. In: Winkler Prins, C.F. (Ed.), 1980. *Newsletter on Carboniferous Stratigraphy, 1: 1-7.*

BOYCE, A.J., ANDERTON, R. and RUSSEL, M.J., 1983. Rapid subsidence and early base-metal mineralization in Ireland. *Trans. Inst. Mineralogy and Metallurgy (Sect. B: Applied Earth Sci.), 92: 55-66.*

BRAITHWAITE, K. 1993. The stratigraphy of a section spanning the mid-Carboniferous at Inishcorker, County Clare, Ireland. *Ann. Soc. geol. Belg., T116: 209-221.*

BRENCKLE, P.L. 1973. Smaller Mississippian and Lower Pennsylvanian calcareous foraminifera from Nevada. *Cushman Found. Foram. Res. Spec. Pub., 11: 82 pp.*

BRENCKLE, P.L., GROVES, J.R., and SKIPP, B. 1982. A Mississippian-Pennsylvanian (mid-Carboniferous) boundary in North America based on calcareous Foraminifera. In: Ramsbottom, W.H.C., Saunders, W.B. and Owens, B. (Eds.). *Biostratigraphic data for a mid-Carboniferous boundary. I.U.G.S. Subcommission on Carboniferous Strat., Leeds., 1981: 42-51.*

BRENCKLE, P., LANE, H.R., MANGER, W.L. and SAUNDERS, W.B. 1977. The Mississippian-Pennsylvanian boundary as an intercontinental biostratigraphic datum. *Newsl. Strat., 6 (2): 106-116.*

BRENNAND, T.P., 1965. The Upper Carboniferous (Namurian) stratigraphy north-east of Castleisland, County Kerry, Ireland. *Proc. Roy. Irish Acad., 64B: 41-63.*

BRETT, C.E. and BAIRD, G.C. 1986. Comparative Taphonomy: A Key to Palaeoenvironmental Interpretation Based on Fossil Preservation. *Palaios, 1: 207-227.*

BRILL, K.G. JR. 1963. Permo-Pennsylvanian stratigraphy of western Colorado Plateau and eastern Great Basin regions. *Bull Geol. Soc. Am., 74: 307-330.*

BRINDLEY, J.C. and GILL, W.D., 1958. Summer Field Meeting in Southern Ireland, 1957. *Proc. Geol. Ass., 69: 244-261.*

BROWN,J., COLLING, A., PARK, D., PHILLIPS, J., ROTHERY, D. AND WRIGHT. J. 1993. *Ocean Circulation. Pergamon Press: 238 pp.*

BROWN, T. 1841. Description of some new species of fossil shells, found chiefly in the Vale of Todmorden, Yorkshire. *Trans. Man. Geol. Soc., 1: 212.*

BURCHFIELD, B.C. and ROYDEN, L.H., 1991. Antler orogeny: a Mediterranean-type orogeny. *Geology, 19: 66-69.*

BURNETT, W.C. 1977. Geochemistry and origin of phosphorite deposits off Peru and Chile. *Geol. Soc. Am. Bull., 88: 813-823.*

BUSCH, R.M. and ROLLINS, H.B. 1984. Correlation of Carboniferous strata using a hierarchy of transgressive-regressive units. *Geology, 12: 471-474.*

CALVER, M.A. 1969. Westphalian of Britain. *Compte Rendu 6me Cong. Int. Strat. Geol. Carb. (Sheffield, 1967), vol. 1: 233-254.*

CALVERT, S.E. 1987. Oceanographic control on the accumulation of organic matter in marine sediments. In: Brooks, J. and Fleet, A.J. (Eds.) *Marine petroleum source rocks. Geol Soc. Lond. Spec. Pub., 26: 47-67.*

CANFIELD, D.E., 1989. Reactive iron in marine sediments. *Geochim., Cosmochim., Acta, 53: 619-632.*

CANFIELD, D.E. and RAISWELL, R. 1991. Pyrite formation and fossil preservtion. In: Allison, P.A. and Briggs, D.E.G. (Eds.) *Taphonomy: Releasing the data locked in the Fossil Record. Plenum, New York: 337-387.*

CANFIELD, D.E., RAISWELL, R., and BOTTRELL, S. 1992. The reactivity of sedimentary iron minerals toward sulphide. *Am. Journ. Sci., 292: 659-683.*

CANFIELD, D.E., RAISWELL, R., WESTRICH, J.T., REAVES, C.M. and BERNER, R.A. 1986. The use of chromium reduction in the analysis of reduced inorganic sulphur in sediments and shales. *Chemical Geology, 54: 149-155.*

CAPUTO, M.V. and CROWELL, J.C. 1985. Migration of glacial centres across Gondwana during the Palaeozoic era. *Geol. Soc. Am. Bull., 96: 1020-1036.*

CASSITY, P.E. and LANGENHEIM, R.L. JR. 1966. Pennsylvanian and Permian fusulinids of the Bird Spring Group from Arrow Canyon, Clark County, Nevada. *Journ. Pal., 40: 931-968.*

CLARKE, M.J., 1966. *Orionastrea* in Ireland. *Irish Nat. Journ., 15: 177-178.*

CLAOUÉ-LONG, J.C., ROBERTS, J. and JONES, P.J. 1993. Carboniferous time. *Early Carboniferous stratigraphy, Liege, 1993. Abstr. with program.*

COCHRAN, J.K., CAREY, A.E., SHOLKOVITZ, E.R., and SURPRENANT, L.D. 1986. The geochemistry of uranium and thorium in coastal marine sediments and sediment porewaters. *Geochim., Cosmochim., Acta., 50: 663-680.*

COLLER, D.W., 1984. Variscan structures in Upper Palaeozoic rocks of west central Ireland. In: Hutton, D.H.W. and Sanderson, D.J. (Eds.). Variscan Tectonics of the North Atlantic Region. *Geol. Soc. London Spec. Publ., 14: 185-194.*

COLLIER, R.E.Ll., LEEDER, M.R. and MAYNARD, J.R. 1990. Transgressions and regressions: a model for the influence of tectonic subsidence, deposition and eustasy, with application to Quaternary and Carboniferous examples. *Geol. Mag., 127, (2): 117-128.*

COLLINSON, C. 1963. Collection and preparation of conodonts through mass production techniques. *Ill. State Geol. Surv. Circ., 343: 1-16.*

COLLINSON, C. REXROAD, C.B. and THOMPSON, T.L. 1971. Conodont zonation of the North American Mississippian. In: Sweet, W.C. and Bergstrom, S.M. (Eds.). Symposium on Conodont Biostratigraphy. *Geol. Soc. Am. Mem., 127: 353-394.*

COLLINSON, C., SCOTT, A.J. and REXROAD, C.B. 1962. Six charts showing biostratigraphic zones and correlation's based on conodonts from the Devonian and Mississippian rocks of the upper Mississippi Valley. *Ill. State Geol. Surv. Circ., 328: 32pp.*

COLLINSON, J.D. 1988. Controls on Namurian sedimentation in the Central Province Basins of northern England. In: Besley, B.M. and Kelling, G. (Eds.). *Sedimentation in a synorogenic basin complex: The Upper Carboniferous of north-west Europe. Blackie, Glasgow and London: 85-102.*

COLLINSON, J.D., MARTINSEN, O., BAKKEN, B. and KLOSTER, A., 1991. Early fill of the western Irish Namurian Basin: a complex relationship between turbidites and deltas. *Basin Research, 3: 223-242.*

CONYBEARE, W.D. and PHILLIPS, W. 1822. *Outlines of the Geology of England.*

COOGAN, A.H. Early Pennsylvanian history of the Ely Basin, Nevada. *Bull. Am. Assoc. Petrol. Geol., 48: 487-495.*

COOK, P.J. and SHERGOLD, J.H., 1986. Proterozoic and Cambrian phosphorites: nature and origin. In: Cook, P.J. and Shergold, J.H. (Eds.). *Phosphate deposits of the World. Proterozoic and Cambrian Phosphorites: 369-386.*

COWIE, J.W. 1990. Global Boundary Stratotypes. Overview. In: Briggs, D.E.G. and Crowther, P.R. (Eds.) *Palaeobiology, a synthesis. Blackwell Scientific: 471-475.*

CROKER, P.F. 1994. The Clare Basin - a geological and geophysical outline. The Petroleum Geology of Ireland's Offshore Basins, Dublin, April 1994. *Technical Programme and Abstracts of Papers: 42-43.*

CROWELL, J.C. 1978. Gondwanan glaciation, cyclothems, continental positioning and climate change. *Am. Journ. Sci., 278: 1345-1372.*

CROWELL, J.C. 1982. Continental glaciation through geologic time. In: Berger, W.H. and Crowell, J.C. (Eds.) *Climate in Earth History. Studies in Geophysics. Nat. Research Council. Nat. Academic Press: 77-82*

CURTIS, C.D., 1980. Diagenetic alteration in black shales. *Journ. Geol. Soc. London, 137: 189-194.*

DAVIES , S. and ELLIOT, T, 1994a. The gamma-ray response of high resolution key surfaces and system tracts; examples form the Upper Carboniferous Clare basin, western Ireland. *Abs. High Resolution sequence stratigraphy: innovations and applications, Univ. Liverpool.*

DAVIES , S. and ELLIOT, T, 1994b. *High resolution sequence stratigraphy of an Upper Carboniferous Basin-fill succession, County Clare, western Ireland Fieldguide to trip B2, High Resolution sequence stratigraphy: innovations and applications, Univ. Liverpool. 67pp.*

DAVIES, L.E. and WEBSTER, G.D. 1985. Late Mississippian to Early Pennsylvanian conodont biofacies in central Montana. *Lethaia 18: 67-72.*

DEAN, S.P. 1994.. *A study of the organic and inorganic geochemistry of sulphur in shales. Ph.D. Thesis. (Unpubl)., Univ. Leeds: 292 pp.*

DEENY, D.E., 1982. Further evidence for Devono-Carboniferous rifting in Central Ireland. *Geologie en Mijnbouw, 61: 243-252.*

DONALDSON, D. and SIMPSON, S. 1962. *Chromatichnus*, a new ichnogenus, and other trace-fossils of the Wegber Quarry. *L.pool Manchr. Geol. Journ., 3, (1): 73-81.*

DOUGLAS, J.A. 1909. The Carboniferous Limestone of County Clare. *Quart. Journ. Geol. Soc. London, 65: 538-586.*

DOW, V.E. 1960. Magnetic separation of conodonts. *Journ. Pal., 34 (4): 738-743.*

DRIESE, S.G., CARR, T.R. and CLARK, D.L. 1984. Quantitative analysis of Pennsylvanian shallow-water conodont biofacies, Utah and Colorado. In: Clark, D.L.(Ed.) Conodont biofacies and Provincialism. *Geol. Soc. Am Spec. Paper, 196: 233-250*

DRUCE, E.C. 1973. Upper Palaeozoic and Triassic conodont distribution and the recognition of biofacies. In: Rhodes, F.H.T. (Ed.) *Conodont Palaeozoology. Geol. Soc. Am. Spec. Paper, 141: 191-238.*

DUNN, D.L. 1970. Conodont zonation near the Mississippian-Pennsylvanian Boundary in Western United States. *Geol. Soc. Am. Bull., 81: 2959-2974.*

EAGER, R.M.C. 1956. The non-marine lamellibranch fauna of the Lower Coal Measures of the Leinster Coalfield-Appendix in Nevill (1956). *Proc. Roy. Ir. Acad., 58B: 11-15.*

ELLIOT, T. and PULHAM, A.J. 1990. Incised valley fills, and the sequence stratigraphy of Upper Carboniferous deltaic cyclothems. *Bull. Am. Ass. Petrol. Geol., 75: 874-889.*

ENGEL, B.A. 1989. S.C.C.S. ballot results. In: Engel, B.A. (Ed.) *Newsletter on Carboniferous stratigraphy, 7: 6-7.*

ENGEL, B.A. 1990 Mid-Carboniferous boundary group meeting, September 30, 1989. In: Engel, B.A. (Ed.) *Newsletter on Carboniferous Stratigraphy, 8: 12*

ENGEL, B.A. 1995. Subcommision vote on the mid-Carboniferous boundary. In: Engel, B.A. (Ed.) *Newsletter on Carboniferous Stratigraphy, 13: 3.*

FLÜGEL, E. 1982. *Microfacies analysis of limestones. Springer Verlag: 633 pp.*

FÖLLMI, K.B., 1990. Condensation and phosphogenesis: example of the Helvetic mid-Cretaceous (northern Tethyan margin). In: Notholt, A.J.G. and Jarvis, I. *Phosphorite Research and Development. Geol. Soc. London Spec. Publ., 52: 237-252.*

FOORD, A.H., 1897-1903. Monograph on the Carboniferous Cephalopoda of Ireland. *Palaeont. Soc. London.*

FOOT, F.J. 1859. Explanations to accompany sheets 150 and 151. *Mem. Geol. Surv. Ireland. 16pp.*

FOOT, F.J. 1860a. Explanations to accompany sheets 131 and 132. *Mem. Geol. Surv. Ireland. 21pp.*

FOOT, F.J. 1860b. Explanations to accompany sheets 140 and 141. *Mem. Geol. Surv. Ireland. 16pp.*

FOOT, F.J. 1863. Explanations to accompany sheets 114, 122 and 123. *Mem. Geol. Surv. Ireland. 32 pp.*

FOSSING, H., GALLARDO, V.A., JORGENSEN, B.B., PUTALL, N., NIELSON, L.P., SCHULTZ, H., CANFIELD, D.E., FORSTER, S., GLUD, R.N., GUNDERSTEN, J.K., KUVER, J., RAMSING, N.B., TESKE, A., THAMDRUCK, B., and ALLOA, O. 1995. Concentration and transport of nitrate by the mat forming sulphur bacteria *Thioploca. Nature, 374: 713-715.*

FRAKES, L.A., FRANCIS, J.E. and SYKTUS, J.I. 1992. *Climate Modes of the Phanerozoic. The history of the Earth's climate over the past 600 million years. Cambridge University Press: 274 pp.*

FRASER, A.J. and GAWTHORPE, R.L. 1990. Tectono-stratigraphic development and hydrocarbon habitat of the Carboniferous in Northern England. In: Hardman, R.F.P. and Brooks, J. (Eds.) *Tectonic events responsible for Britains oil and gas reserves. Geol. Soc. London Spec. Pub. 55: 49-86.*

FÜRSICH, F.T. and ABERHAN, M. Significance of time-averaging for palaeocommunity analysis. *Lethaia, 23: 143-152.*

GADE, H.G. and EDWARDS, A. 1980. Deep water renewal in fjords. In: Freeland, H.J., Farmer, D.M. and Levings, C.D. (Eds.). *Fjord oceanography. Nato Conference on fjord Oceanography, Victoria, B.C., Part IV Marine Sciences, Vol. 4: 453-491.*

GAWTHORPE, R.L., GUTTERIDGE, P. and LEEDER, M.R., 1989. Devonian and Dinantian basin evolution in northern England and north Wales. In: Arthurton, R.S. and Nolan, S.C. (Eds.) *The role of Tectonics in Devonian and Carboniferous sedimentation in the British Isles. Occ. Publ. Yorks. Geol. Soc., 6: 1-23.*

GEORGE, T.N., JOHNSON, G.A.L., MITCHELL, M., PRENTICE, J.E., RAMSBOTTTOM, W.H.C., SEVASTOPULO, G.D. and WILSON, R.B. 1976. A correlation of Dinantian rocks in the British Isles. *Geol. Soc. London Spec. Rep., 7: 1-87.*

GILL, W.D. and KEUNEN, P.H., 1958. Sand volcanoes on slumps in the Carboniferous of County Clare, Ireland. *Quart. Journ. Geol. Soc. London, 113: 441-460.*

GILL, W.D., 1979. Syndepositional sliding and slumping in the west Clare Namurian Basin, Ireland. *Geol. Survey Ireland Spec. Paper, 4: 31pp.*

GIRTY, G.H. 1909. The fauna of the Caney Shale of Oklahoma. *U.S.G.S. Bull., 37: 106 pp.*

GIRTY, G.H. 1910. New genera and species of fossils from the Fayetteville shale of Arkansas. *New York Acad. Sci. Annals, 20: 189-238.*

GLENN, C.R. and ARTHUR, M.A. 1990. Anatomy and origin of a Cretaceous phosphorite-greensand giant, Egypt. *Sedimentology, 37: 123-154.*

GOEBEL, K.A. 1991. Paleogeographic Setting of the Late Devonian to Early Mississippian Antler Foreland, Eastern Nevada and Western Utah. S.E.P.M., S.E.G, S.P.W.L.A., Pacific Section Meeting, Association Round Table 1991. *Bull. Am. Assoc. Petrol. Geol., 75 (2): 365.*

GOLDHABER, M.B. and KAPLAN, I.R. 1974. Controls and consequences of sulphate reduction in Recent sediments. *Soil Sci., 119: 42-55.*

GORDON, M. JR. 1964. Carboniferous cephalopods of Arkansas. *U.S.G.S. Prof. Pap., 460: 322 pp.*

GORDON, M. JR. 1968. An early Reticuloceras fauna from the Hale Formation in north-western Arkansas. *U.S.G.S. Prof. Pap., 6132: A1-A21.*

GORDON, M. JR. 1969. Early Pennsylvanian Ammonoids from Southern Nevada. *U.S.G.S. Prof. Pap., 613-C: 1-13.*

GORDON, M. JR. 1970. Carboniferous ammonoid zones of the south-central and western United States. Xième Congrès International de Stratigraphie et Géologie du Carbonifère, Sheffield. *Compte Rendu, 2: 817-826.*

GORDON, M. JR. and MAMET, B.L. 1978. The Mississippian-Pennsylvanian boundary. In: Cohee, G.V. (Ed.) Contributions to the geologic time scale. *A.A.P.G. Studies in Geology, 6: 327-335.*

GORDON, M. JR., and POOLE, F.G. 1968. Mississippian-Pennsylvanian Boundary in south-western Nevada and south-eastern California. In: Eckel, E.B. (Ed). Nevada Test Site. *Geol. Soc. Am. Mem., 110: 157-168.*

GRAHAM, J., SEVASTOPULO, G.D., MacDERMOT, C. and BOLDY, S. 1986. *Carboniferous Geology of west County Clare. A field guide prepared for Amerada Hess Ltd: 44 pp.*

GRAYSON, D.K. 1978. Reconstructing mammalian communities: a discussion of Shotwell's method of palaeoecological analysis. *Palaeobiology, 4: 77-81.*

GRAYSON, R.C., JR 1990. Canyon creek: A significant exposure of a predominantly mudrock succession recording essentially continuous deposition from the Late Devonian through Middle Pennsylvanian. In Ritter, S.M. (Ed.). *Early to Middle Palaeozoic Conodont Biostratigraphy of the Arbuckle Mountains Southern Oklahoma. Oklahoma Geol. Surv. Guidebook, 27: 85-106.*

GRAYSON, R.C., JR. MERRILL, G.K. and MILLER, J.F. 1987. Early and Late Palaeozoic conodont faunas of the Llano uplift region, central Texas - Biostratigraphy, systematic boundary relationships and stratigraphic importance. *Geol. Soc. Am. Guidebook, South Central Section, Fieldtrip 1: 151pp.*

GRIFFITH, R. 1814. *Geological and Mining Report on the Leinster Coalfield. Dublin. 135 pp.*

GRIFFITH, R. 1838. Geological structure of Ireland. In: Larcom, T.A. *A general map of Ireland to accompany the report of the Railway Commissioners, showing the Principle Physical Features and Geological Structure of the Country.*

GULBRANDSEN, R.A. 1969. Physical and chemical factors in the formation of marine apatite. *Econ. Geol., 64 (4): 365-382.*

GULBRANDSEN, R.A., ROBERSON, C.E. and NEIL, S.T. 1984. Time and the crystallisation of apatite in seawater. *Geochim., Cosmochim., Acta, 48: 213-218.*

HARBAUGH, D.W. and DICKINSON, W.R. 1981. Depositional facies of Mississippian clastics, Antler foreland basin, central Diamond Range, Nevada. *Journ. Sed. Pet., 51: 1223-1234.*

HARDMAN, E.T. 1881. Explanatory memoir on the Geology of the Leinster Coalfield. *Mem. Geol. Surv. Ireland: 96 pp.*

HARLAND, W.B., ARMSTRONG, R.L., COX, A.V., CRAIG, L.E., SMITH, A.G. and SMITH, D.G. 1990. *A Geologic Time Scale. Cambridge Univ Press: 263 pp.*

HASS, W.H. 1947. Conodont zones in the Upper Devonian and Lower Mississippian Formations of Ohio. *Journ. Pal., 21: 131-141.*

HASZELDINE, R.S., 1984. Carboniferous North Atlantic palaeogeography: stratigraphic evidence for rifting, not megashear or subduction. *Geol. Mag., 121: 443-463.*

HASZELDINE, R.S., 1988. Crustal lineaments in the British Isles: their relationship to Carboniferous Basins. In: Besley, B.M. and Kelling, G. (Eds.) *Sedimentation in a synorogenic basin complex: The Upper Carboniferous of north-west Europe. Blackie, Glasgow and London: 53-68.*

HATCHER, .R.D. JR. 1988. Basement-cover relationships in the Appalachian-Caledonian-Variscan orogen: mid Devonian (end of Acadian orogeny) to end of the Permian. In: Harris, A.L. and Fettes, D.J. (Eds.). *The Caledonian-Appalachian Orogen. Geol. Soc. London Spec. Pub. 38: 507-514.*

HAUG, E. 1898. Études sur les Goniatites. *Mem. Geol. Soc. Fr. Paléont., 18: 112 pp.*

HAYS, J.D., IMBRIE, J. and SHACKLETON, N.J. 1976. Variations in the Earth's orbit: pacemaker of the Ice Ages. *Science, 194: 1121-1132.*

HECKEL, P.H. 1977. Origin of phosphatic black shale facies in Pennsylvanian cyclothems of Mid-Continent North America. *Bull. Am. Ass. Petrol. Geol., 61: 1045-1068.*

HECKEL, P.H. 1986. Sea-level curve for Pennsylvanian eustatic marine transgressive depositional cycles along the midcontinent outcrop belt, North America. *Geology, 14: 330-334.*

HECKEL, P.H. 1990. Evidence for global (glacial-eustatic) control over Upper Carboniferous (Pennsylvanian) cyclothems in the mid-Continent of North America. In: Hardman, R.F.P. and Brooks, J.(Eds.). *Tectonic events Responsible for Britain's Oil and Gas Reserve. Geol. Soc. London Spec. Publ., 55: 35-47.*

HECKEL, P.H. 1991. Thin widespread Pennsylvanian black shales of Midcontinent North America: a record of a cyclic succession of widespread pycnoclines in a fluctuating epeiric sea. In: Tyson, R.V. and Pearson, T.H. (Eds.) *Modern and ancient continental shelf anoxia. Geol. Soc. London Spec. Publ., 58: 259-273.*

HEIER, K.S and BILLINGS, G.K. 1972. Potassium. In: Wedepohl, A. (Ed.) *Handbook of Geochemistry. Berlin. Springer-Verlag., Vol 11-2, pt 19-b-n.*

HESS, J.C. AND LIPPOLT, H.J. 1986. $^{40}Ar/^{39}Ar$ ages of tonstein and tuff sanidines: new calibration points for the improvement of the Upper Carboniferous timescale. *Chem. Geol., 59: 143-154.*

HIGGINS, A.C. 1975. Conodont zonation of the late Viséan - early Westphalian strata of the South and Central Pennines of Northern England. *Bull. Geol. Surv. Gt. Brit., 53: 1-90.*

HIGGINS, A.C. 1985. The Carboniferous System: Part 2 - Conodonts of the Silesian Subsystem of Great Britain and Ireland. In: Higgins, A.C. and Austin, R.L. (Eds.). *A Stratigraphical Index of Conodonts. British Micropalaeontological Society Series. Ellis Horwood Ltd, Sussex: 210-236.*

HIGGINS, A.C. and VARKER, W.J. 1982. Lower Carboniferous conodont faunas from Ravenstonedale, Cumbria. *Palaeontology, 25: 145-166*

HIGGS, K, 1986. The stratigraphy of the Namurian rocks of the Leinster Coalfield. *Geol. Survey Ireland Bull., 3: 257-277.*

HIND, W., 1905. Notes on the homotaxial equivalent of the beds which immediately succeed the Carboniferous Limestone in the West of Ireland. *Proc. Roy. Irish Acad., 25B: 93-116.*

HINDE, G.J. 1900. Notes and descriptions of new species of Scotch Carboniferous conodonts. *Trans. Nat. Hist. Soc. Glasgow, 5: 338--346.*

HODSON, F, 1954a. The beds above the Carboniferous limestone in north-west County Clare, Eire. *Quart. Journ. Geol. Soc. London, 109: 259-283.*

HODSON, F, 1954b. The Carboniferous rocks of Foynes Island, County Limerick. *Geol. Mag., 91: 153-160.*

HODSON, F. 1957. Marker horizons in the Namurian of Britain, Ireland, Belgium and Western Germany. *Pub. Assoc. Étud. Paléont. Strat. Houill., 24: 1-26.*

HODSON, F and LEWARNE G.C., 1961. A mid-Carboniferous (Namurian) basin in parts of the counties of Limerick and Clare, Ireland. *Quart. Journ. Geol. Soc. London, 117: 307-333.*

HOLDSWORTH, B.K. 1966a. A preliminary study of the palaeontology and palaeoenvironment of some Namurian limestone 'bullions'. *Mercian Geology, 1: 315-337.*

HOLDSWORTH, B.K. 1966b. Radiolaria from the Namurian of Derbyshire. *Palaeontology, 9: 319-329.*

HOLDSWORTH, B.K. 1965. The Namurian goniatite *Nuculoceras stellarum* (BISAT). *Palaeontology, 8 (2): 226-230.*

HOLDSWORTH, B.K. and COLLINSON, J.D., 1988. Millstone Grit cyclicity revisited. In: Besley, B.M. and Kelling, G. (Eds.) *Sedimentation in a synorogenic basin complex: The Upper Carboniferous of north-west Europe. Blackie, Glasgow and London: 132-151*

HUDSON, R.G.S. 1945. The goniatite zones of the Namurian. *Geol Mag., 82: 1-9.*

IMBRIE, J., HAYS, J.D., MARTINSON, D.G., McINTYRE, A., MIX, A.C. MORLEY, J.J., PISISA, N.G., PRELL, W.L., and SCHAKLETON, N.J. 1984. The orbital theory of Pleistocene climate: support from a revised chronology of the marine $\partial^{18}O$ record. In: Berger, A.L., Imbrie, J., Hays, J., Kukla, G. and Saltzman, B. (Eds.) *Milankovitch and Climate, Part 1. Dordrecht Reidel: 269-305.*

JACKSON, J.S. 1965. The Upper Carboniferous (Namurian and Westphalian) of Kingscourt, Ireland. *Sci. Proc. Roy. Dublin Soc. Ser., A2: 131-152.*

JARVIS, I. 1980. The initiation of phosphatic chalk sedimentation-The Senonian (Cretaceous) of the Anglo-Paris Basin. In: Bentor, Y.K., (Ed.) *Marine Phosphorites-Geochemistry, Occurrence, Genesis. Soc. Econ. Pal. Min. Spec. Publ., 29: 167-192.*

JARVIS, I. 1992. Sedimentology, geochemistry and origin of phosphatic chalks: the Upper Cretaceous deposits of NW Europe. *Sedimentology, 39: 55-97*

JEWELL, P.W. 1993. Water column stability, residence times and anoxia in the Cretaceous North American Seaway. *Geology, 21: 579-582.*

JOHNSTON, I.S. and HIGGINS, A.C. 1981. Conodont faunas from the Lower Carboniferous rocks at Hook Head, County Wexford. *Journ. Earth. Sci. Roy. Dublin Soc., 4: 83-96.*

JUKES, J.B., KINAHAN, G.H and O'KELLY, J. 1859. Explanations to accompany sheet 128. *Mem. Geol. Surv. Ireland: 32pp.*

KAZAKOV, A.V. 1939. The phosphate facies: origin of the phosphorites and the geologic factors of formation of the deposits. *Proc. Sci. Inst. Fert. Insectofung., 145: 1-106.*

KINAHAN, G.H. and FOOT, F.J. 1860. Explanations to accompany sheet 142. *Mem. Geol. Surv. Ireland: 41pp.*

KLEIN, G. deVries 1990. Pennsylvanian time scales and cycle periods. *Geology, 18: 455-457.*

KLEIN, G. deVries and WILLARD, D.A. 1989. Origin of the Pennsylvanian coal-bearing cyclothems of North America. *Geology, 17: 152-155.*

KOSS, J.E., ETHERIDGE, F.G. and SCHUMM, S.A. 1994. An experimental study of the effects of base-level change on fluvial, coastal plain and shelf systems. *Journ. Sed. Research, B64 (2): 90-98.*

KROM, M.D. and BERNER, R.A. 1980. Adsorption of phosphate in anoxic marine sediments. *Limnol. Oceanog., 25(5): 797-806.*

KROM, M.D. and BERNER, R.A. 1981. The diagenesis of phosphorus in nearshore marine sediment. *Geochim., Cosmochim., Acta, 45: 207-216.*

KROM, M.D. and BERNER, R.A. 1983. A rapid method for the determination of organic and carbonate carbon in geological samples. *Journ. Sed. Pet., 53: 660-663.*

LAMBOY, M. 1990. Microbial mediation in phosphatogenesis: new data from the Cretaceous phosphatic chalks of northern France. In: Notholt, A.J.G. and Jarvis, I. (Eds.). Phosphorite Research and Development. *Geol. Soc. Spec. Publ., 52: 157-167.*

LANE, H.R. 1967. Uppermost Mississippian and Lower Pennsylvanian conodonts from the type Morrowan region: Arkansas. *Journ. Pal., 41: 920-942.*

LANE, H.R. 1977. Morrowan (Early Pennsylvanian) conodonts of north-western Arkansas and north-eastern Oklahoma. In: Sutherland, P.K. and Manger, W.L. (Eds.) *Upper Chesterian-Morrowan Stratigraphy and the Mississippian-Pennsylvanian boundary in north-eastern Oklahoma and north-western Arkansas. Oklahoma Geological Survey Guidebook, 18: 177-181.*

LANE, H.R. 1988. Working group on the mid-Carboniferous boundary. In: Engel, B.A. (Ed.) *Newsletter on Carboniferous Stratigraphy, 6: 18-19*

LANE, H.R. 1995. Mid- Carboniferous boundary Working Group. In: Engel, B.A. *Newsletter on Carboniferous Stratigraphy, 13: 3.*

LANE, H.R. and BAESEMANN, J.F. 1982 A mid-Carboniferous Boundary based on conodonts and revised intercontinental correlation's. In: Ramsbottom, W.H.C, Saunders, W.B. and Owens, B., (Eds.). *Biostratigraphic data for a mid-Carboniferous boundary. Subcommission on Carboniferous Stratigraphy, Leeds, 1982: 6-13.*

LANE, H.R. and MANGER, W.L. 1985a. The basis for a mid-Carboniferous boundary. *Episodes, 8: 112-115.*

LANE, H.R. and MANGER, W.L. 1985b. Toward a boundary in the middle of the Carboniferous (1975-1985): ten years of progress. In: Lane. H.R. and

Ziegler, W. (Eds.) *Toward a Boundary in the Middle of the Carboniferous: Stratigraphy and Palaeontology. Cour. Forsch. -Inst. Senckenberg, 74: 15-34.*

LANE, H.R. AND STRAKA II, J.J. 1974. Late Mississippian and Early Pennsylvanian conodonts, Arkansas and Oklahoma. *Geol. Soc. Am. Spec. Paper, 152: 144 pp.*

LANE, H.R., BAESEMANN, J.F. and GROVES, J.R. 1985. Is the base of the *Reticuloceras* Zone a reliably recognisable biostratigraphic level? In: Lane. H.R. and Ziegler, W. (Eds.) *Toward a Boundary in the Middle of the Carboniferous: Stratigraphy and Palaeontology. Cour. Forsch. -Inst. Senckenberg, 74: 137-148.*

LANE, H.R., BAESEMANN, J.F., BRENCKLE, P.L. and WEST, R.R. 1985. Arrow Canyon, Nevada - A potential mid-Carboniferous boundary stratotype. *Compte Rendu, 10th Int. Cong. Carb Strat. and Geol., Madrid, 1983, Vol 4: 429-439.*

LANE, H.R., BOUCKAERT, J., BRENCKLE, P., EINOR, O.L., HAVLENA, V., HIGGINS, A.C., JING-ZHI, Y., MANGER, W.L., NASSICHUK, W., NEMIROWSKAYA, T., OWENS, B., RAMSBOTTOM, W.H.C., REITLINGER, E.A., and WEYANT, M. 1985. Proposal for an international mid-Carboniferous boundary. *Compte Rendu, 10th Int. Cong. Carb Strat. and Geol., Madrid, 1983, Vol 4: 323-339.*

LANE, H.R., BRENCKLE, P. and HIGGINS, A.C. 1994. Mid-Carboniferous Boundary Working Group Decision. In: Engel, B.A. (Ed.) *Newsletter on Carboniferous Stratigraphy, 12: 3.*

LANE, H.R., MERRILL, G.K., STRAKA II, J.J. and WEBSTER, G.D. 1971. North American Pennsylvanian Conodont Biostratigraphy. In: Sweet, W.C. and Bergstrom, S.M. (Eds.) *Symposium on Conodont Biostratigraphy. Geol. Soc. Am. Mem., 127: 395-414.*

LANGENHEIM, R.L. JR., CARSS, B.W., KENNERLEY, J.B., McCUTCHEON, V.A. and WAINES, R.H. 1962. Palaeozoic section in Arrow Canyon Range, Clark County, Nevada. *Bull. Am. Assoc. Petrol. Geol., 46 (5): 592-609.*

LANGENHEIM, V.A.M. and LANGENHEIM, R.L. JR. 1965. The Bird Spring Group, Chesterian through Wolfcampian at Arrow Canyon, Arrow

Canyon Range, Clark County, Nevada. *Trans. Ill. State Acad. Sci., 58: 225-240.*

LARKIN, J., AHARON., P. and HENK, M.C. 1994. *Beggiatoa* in microbial mats at hydrocarbon vents in the Gulf of Mexico and warm mineral springs, Florida. *Geomarine Letters, 14: 97-103.*

LARSON, E.R. and LANGENHEIM, R.L., JR. 1979. The Mississippian and Pennsylvanian (Carboniferous) systems in the United States - Nevada. *U.S.G.S. Prof. Paper, 1110 - M- BB: 1-19.*

LASKER, H. 1976. Effects of differential preservation on the measurement of taxonomic diversity. *Palaeobiology, 2: 84-93.*

LEEDER, M.R., 1982. Upper Palaeozoic basins of the British Isles-Caledonian inheritance versus Hercynian plate margin processes. *Journ. Geol. Soc. London, 139: 479-491.*

LEEDER, M.R., 1988a. Recent developments in Carboniferous geology: a critical review with implications for the British Isles and north-west Europe. *Proc. Geol. Ass., 99: 73-100.*

LEEDER, M.R., 1988b. Devono-Carboniferous river systems and sediment dispersal from the orogenic belts and cratons of north-west Europe. In: Harris, A.L. and Fettes, D.J. (Eds.). *The Caledonian -Appalachian Orogen. Geol. Soc. Spec. Publ., 38: 549-558.*

LEEDER, M.R. and McMAHON, A.H., 1988. Upper Carboniferous (Silesian) basin subsidence in northern Britain. In: Besley, B.M. and Kelling, G.(Eds.). *Sedimentation in a synorogenic basin complex: The Upper Carboniferous of north-west Europe. Blackie, Glasgow and London: 43-52.*

LEMOSQUET, Y., LYS, M., and PAREYN, C. 1983. La transgression du Carbonifére moyen et ses rapports avec la paléokarst Serpukhovian dans la Bassin de Bechar (Algérie). *Int. Cong. Carb. Strat. and Geol. 10th, Madrid. Abst: 184.*

LEMOSQUET, Y., LYS, M., PAREYN, C. and WEYANT, M. 1983. The Mid-Carboniferous Boundary in Bechar Basin (Algeria). In: Saunders, W.B. 1983. *Newsletter on Carboniferous Stratigraphy, 4: 13.*

LEWARNE, G.C. 1959. *The junction of the Upper and Lower Carboniferous of County Clare and County Limerick, Eire. Ph.D. Thesis. (Unpubl.) Univ. Reading: 158 pp.*

LEWY, Z. 1990. Pebbly phosphate and granular phosphorite (Late Cretaceous, southern Israel) and their bearing on phosphatization processes. In: Notholt, A.J.G. and Jarvis, I. (Eds.) *Phosphorite Research and Development. Geol. Soc. London Spec. Publ., 52: 167-178.*

LIPPOLT, H.J, HESS, J.C. and BURGER, K. 1984. Isotopische alter Pyroklastischen Sanidinen aus Kaolin-Kohlentonsteinen ab Korrelationsmarken für das Mitteleleuropäische Oberkarbon. *Fortscr. Geol. Rheinld. Westf., 32: 119-150.*

LLOYD, G.E. 1987. Atomic number and crystallographic contrast images with the S.E.M.: a review of backscattered electron techniques. *Min. Mag., 51: 3-19.*

LLOYD , M. and GHELARDI, R.J. 1964. A table for calculating the 'equitability' component of species diversity. *Journ. Anim. Ecol., 33: 217-225.*

LONGWELL, C.R. 1960. Possible explanantions of diverse structural patterns in southern Nevada. *Am. Journ. Sci., 258A: 192-203.*

LOUGHMAN, D.L. 1984. Phosphate authigenesis in the Aramachay Formation (Lower Jurassic) of Peru. *Journ. Sed. Pet., 54 (4): 1147-1156.*

MANGER, W.L. and SAUNDERS, W.B. 1980. Lower Pennsylvanian (Morrowan) ammonoids from the North American Midcontinent. *Pal. Soc. Mem., 10: 1-56.*

MANGER, W.L. and SAUNDERS, W.B. 1982. An ammonoid based Middle Carboniferous boundary. In: Ramsbottom, W.H.C., Saunders, W.B. and Owens, B. (Eds.) *Biostratigraphic data for a mid-Carboniferous boundary. Subcommission on Carboniferous stratigraphy, Leeds, 1982: 95-101.*

MANGER, W.L. and SUTHERLAND, P.K. 1992. Analysis of Sections presumed to be complete across the Mississippian-Pennsylvanian boundary,

Southern Midcontinent. In: Sutherland, P.K. and Manger, W.L. (Eds.) Recent Advances in Middle Carboniferous Biostratigraphy - A Symposium. *Oklahoma Geological Survey, 944: 69-79.*

MANGER, W.L. WEYANT, M. and PAREYN, C. 1985 Mid-Carboniferous ammonoid Biostratigraphy, Bechar Basin, Algeria. *Cour. Forsch. -Inst. Senckenberg, 74: 181-196.*

MARTENS, C.S, and HARRISS, R. 1970. Inhibition of apatite precipitation in the marine environment by magnesium ions. *Geochim., Cosmochim., Acta, 34: 621-625.*

MARTINSEN, O.J., 1989. Styles of soft-sediment deformation on a Namurian (Carboniferous) delta-slope, Western Irish Namurian Basin, Ireland. In: Whateley, M.K.G. and Pickering K.T. (Eds.) *Deltas: Sites and Traps for Fossil Fuels. Geol. Soc. London Spec. Publ., 41: 167-177.*

MARTINSEN, O.J., 1990. Interplay between eustatsy, tectonics and sedimentation with particular reference to the Namurian E_{1c} to H_{2c} of the Craven-Askrigg area, northern England. *Dr. Scient. thesis, Univ. Bergen, 490 pp.*

MARTINSEN, O.J., 1993. Namurian (Late Carboniferous) depositional systems of the Craven-Askrigg area, northern England: implications for sequence stratigraphic models. *Spec. Publ. Int. Ass. Sed., 18: 247-281.*

MARTINSEN, O.J. and BAKKEN, B. 1990. Extensional and compressional zones in slumps and slides in the Namurian of County Clare, Ireland. *Journ. Geol. Soc., 147: 153-164.*

MAYNARD, J.R. 1991. Upper Carboniferous marine transgressions and their deposits. *Ph.D. Thesis. (Unpubl.) Univ. Leeds: 273 pp.*

MAYNARD, J.R. and LEEDER, M.R. 1992. On the periodicity and magnitude of Late Carboniferous glacio-eustatic sea-level changes. *Journ. Geol. Soc. London, 149: 303-311.*

MEDENHALL, W. 1979. *Introduction to probability and statistics. Duxbury Press: 594.pp*

MEERE, P.L., 1988. *The Geology of the Slieve Elva, Knochaunus Mountain area, north-west County Clare. B.Sc. (Hons) thesis (Unpubl.), NUI, University College, Galway.*

MERRILL, G.K. 1973. Pennsylvanian conodont palaeoecology. In: Rhodes, F.H.T. (Ed.) *Conodont Palaeozoology. Geol. Soc. Am. Spec Paper, 141: 239-274.*

MERRILL, G.K. and VON BITTER, P.H. 1976. Revision of conodont biofacies nomenclature and interpretations of environmental controls in Pennsylvanian rocks of eastern and central north America. *Royal Ontario Museum, Life Sciences Contribution, 108: 46 pp.*

MERRILL, G.K. and VON BITTER, P.H. 1984 Facies and frequencies among Pennsylvanian conodonts: apparatuses and abundances. In: Clark, D.L. (Ed.) Conodont biofacies and Provincialism. *Geol. Soc. Am Spec. Paper, 196: 251-262.*

METCALFE, I. 1981. Conodont zonation and correlation of the Dinantian and early Namurian strata of the Craven lowlands of Northern England. *Inst. Geol. Sci. Rep., 80/10: 1-70.*

MEYER, D.L. and MEYER, K.B. 1986. Biostratinomy of Recent Crinoids (Echinodermata) at Lizard Island, Great Barrier Reef, Australia. *Palaios, 1: 294-302.*

MILLER, K.B. 1991. High resolution correlation within a storm dominated muddy eperic sea: taphofacies of the Middle Devonian Wanakah Member, western New York. In: Landing, E. and Brett, C.E. (Eds.) *Dynamic stratigraphy and depositional environments of the Hamilton Group (Middle Devonian) in New York State, part II. Bull. New York State Museum, 469: 129-152.*

MILLER, K.B., BRETT, C.E. and PARSONS, K.M. 1988. The palaeoecological significance of storm generated disturbance within a Middle Devonian muddy epeiric sea. *Palaios, 3: 35-52.*

MIDDLEBURG, J.J. 1991. Organic carbon, sulphur and iron in recent semi-euxinic sediments of Kau Bay, Indonesia. *Geochim., Cosmochim., Acta, 55: 815-828.*

MISI, A. and KYLE, J.R. 1994. Upper Proterozoic Carbonate Stratigraphy, Diagenesis, and stromatolitic Phosphorite Formation, Irecê Basin, Bahia, Brazil. *Journ. Sed. Pet., A64 (2): 299-310.*

MOORE, C. 1863. On the palaeontology of mineral veins and on the secondary age of some of the mineral veins in the Carboniferous limestone. *Rep. Brit. Assoc. Adv. Sci: 82-83.*

MOORE, E.W.J. 1945. The Carboniferous goniatite genera *Girtyoceras* and *Eumorphoceras. Proc. York. Geol. Soc., 25: 387-442.*

MOORES, E. 1970. Ultramafics and orogeny, with models of the U.S. cordillera and the Tethys: *Nature, 228: 837-842.*

MORTON, W.H. 1965. The Carboniferous stratigraphy of the area north-west of Newmarket, Co. Cork. *Sci. Proc. Roy. Dublin Soc. Ser A2: 47-65.*

MULLINS, H.T. and RASCH, R.F. 1985. Sea-Floor Phosphorites along the Central California Continental Margin. *Economic Geology, 80: 696-715.*

MYERS, K.J. and WIGNALL, P.B. 1987. Understanding Jurassic Organic-rich Mudrocks-New Concepts using Gamma-ray Spectrometry and Palaeoecology: Examples from the Kimmeridge Clay of Dorset and the Jet Rock of Yorkshire. In: Leggett, J.K. and Zuffa, G.G. (Eds.) *Marine Clastic Sedimentology: 172-189.*

NATHAN, Y. 1990. Humic substances in phosphorites: occurrence, characterisation and significance. In: Notholt, A.J.G. and Jarvis, I. *Phosphorite Research and Development. Geol. Soc. London Spec. Publ., 52 :49-58.*

NEMIROVSKAYA, T.I. and NIGMADGANOV, I. 1992. Stratotype candidate, Gissar Ridge, Aksu River, South Tian Shan, Central Asia. In: Engel, B.A. (Ed.) *Newsletter on Carboniferous stratigraphy, 10: 11.*

NEMIROVSKAYA, T.I., POLETAEV, V.I.. and VDOVENKO, M.V. 1990. The Kal'mius Section, Donbass, Ukraine, U.S.S.R.: A Soviet Proposal For The Mid-Carboniferous Boundary Stratotype. In Brenckle, P.L. and Manger,

W.L. (Eds.) Intercontinental Correlation and Division of the Carboniferous System. *Cour. Forsch. -Inst. Senckenberg, 130: 247-273.*

NEVILL, W.E. 1956. The Millstone Grit and Lower Coal Measures of the Leinster Coalfield. *Proc. Roy. Ir. Acad., 58B: 1-16.*

NEVILL, W.E. 1957. The geology of the Summerhill Basin, Co. Meath. *Proc. Roy. Ir. Acad., 58B: 293-303.*

NIGMADGANOV, I., AND NEMIROVSKAYA, T.I. 1992. Mid-Carboniferous Boundary Conodonts from the Gissar Ridge, South Tienshan, Middle Asia. *Cour. Forsch. -Inst. Senckenberg, 154: 253-275.*

NISSENBAUM, A. 1979. Phosphorus in marine and non-marine humic substances. *Geochim., Cosmochim., Acta, 43: 1973-1978.*

NORBY, R.D. 1976. *Conodont apparatuses from chesterian (Mississippian) strata of Montana and Illinois. Ph.D. thesis (Unpub.) Univ. Illinois at Urbana-Champaign: 295 pp.*

NORRIS, R.D. 1986. Taphonomic gradients in shelf fossil assemblages: Pliocene Purisma Formation, California. *Palaios 1: 256-270.*

NUDDS, J. and PALMER, D. 1990. Societies, Organizations, Journals and Collections. In: Briggs, D.E.G. and Crowther, P.R. (Eds.) *Palaeobiology, a synthesis. Blackwell Scientific: 522-537.*

O'BRIEN, M.V. 1953. Phosphatic horizons in the Upper Carboniferous of Ireland. *Compte Rendu XIX Int. Geol. Congr. Algiers, 1952, sect 11: 135-143.*

O'CONNOR, P.J. and PYNE, J.F., 1986. Radioelement and R.E.E. content of Namurian phosphorites, County Clare, Ireland. *Trans. Inst. Mineralogy and Metallurgy (Sect. B: Applied Earth Sci.) 95: 211-213.*

OAKLEY, K.P. 1942. Occurrences of Phosphate in Pre-Cretaceous Rocks. British Phosphates, Part IV. *Wartime Pamphlet, 8. Geol. Surv. Great Britain: 9-10*

OWENS, B. 1982. Palynological zonation of mid-Namurian strata in northern England. In: Ramsbottom, W.H.C., Saunders, W.B. and Owens, B.

(Eds.) *Biostratigraphic data for a mid-Carboniferous boundary. Subcommission on Carboniferous stratigraphy, Leeds, 1982: 22-27.*

OWENS, B. , VARKER, W.J. and HUGHES, R.A. 1990. Lateral biostratigraphical consistency across the mid-Carboniferous boundary in northern England. In: Brenckle, P.L. and Manger, W.L. (Eds.) *Intercontinental Correlation and Division of the Carboniferous System. Cour. Forsch. -Inst. Senckenberg, 130: 237-247.*

OZRETICH, R.J. 1975. Mechanisms for deep water renewal in Lake Nitinat, a permantly anoxic fjord. *Estuarine Coastal Marine Sci., 3: 189-200.*

PARSONS, K.M. AND BRETT, C.E. 1991. Taphonomic processes and biases in modern marine environments: an actualistic perspective on fossil assemblage preservation. In Donovan, S.K. (Ed.) *The Processes of Fossilisation. Belhaven Press: 22-66.*

PEDERSON, T.F. and CALVERT, S.E. 1990. Anoxia vs. productivity: What controls the formation of organic carbon-rich sediments and sedimentary rocks? *Bull. Am. Ass. Pet. Geol., 74: 454-466.*

PERRET, M-F. 1992. Field notes on the High Pyrénées Field Excursion. In: Engel, B.A. (Ed.) *Newsletter on Carboniferous Stratigraphy, 10: 8-9.*

PFEFFERKORN, H.W. 1972. Distribution of *Stigmaria wedingtonensis* (Lycopsida) in the Chesterian (Upper Mississippian) of North America. *American Midland Naturalist , 88: 225-231.*

PHILCOX, M.E., 1961. Namurian shales near Buttevant, north County Cork. *Sci. Proc. Roy. Dublin Soc. Series A, 1: 205-209.*

PHILLIPS, J. 1832 *Illustrations of the Geology of Yorkshire: 192 pp.*

PHILLIPS, J. 1836. *Illustrations of the Geology of Yorkshire, Part II, the Mountain Limestone District.*

PHILLIPS, J. 1841. Palaeozoic fossils of Cornwall, Devon, and West Somerset. *Mem. Geol. Surv. London.*

POCOCK, Y.P. 1968. Carboniferous schizophoriid brachiopods from western Europe. *Palaeontology, 11: 64-93.*

POLETAEV, V.I., MAKAROV, I.A. NEMIROVSKAYA, T.I. and MASLO, A.I. 1988. (Compilers). The guidebook to excursion to the Lower/Middle Carboniferous boundary deposits of Donbass. *Inst. Geol. Sci., Ukrainian Acad. Sci. Kiev: 92 pp.*

POOLE, F.G. 1974. Flysch deposits of the Antler foreland basin, western United States. In: Dickinson, W.R. (Ed.) *Tectonics and sedimentation: Soc. Econ. Pal. Min. Spec. Pub., 22: 58-82.*

POOLE, F.G. and SANDBERG, C.A. 1977. Mississippian paleogeography and tectonics of the western United States. In: Stewart, J.H., Stevens, C.H., and Fritsche, A.E. (Eds.) *Paleozoic paleogeography of the western United States: Soc. Econ. Pal. Min., Pacific Section, Pacific Coast Paleogeography Symposium 1: 181-215.*

POOLE, F.G. and SANDBERG, C.A. 1991. Mississippian Paleogeography and Conodont Biostratigraphy of the Western United States. In: Cooper, J.D. and Stevens, C.H. (Eds.) *Palaeozoic Paleogeography of the Western United States-II, Vol. 1. Soc. Econ. Pal. Min., Pacific section: 107-136.*

PULHAM, A.J., 1989. Controls on internal structure and architecture of sandstone bodies within Upper Carboniferous fluvial-dominated deltas, County Clare, western Ireland. In: Whateley, M.K.G. and Pickering K.T. (Eds.,). *Deltas: Sites and Traps for Fossil Fuels. Geol. Soc. London Spec. Publ., 41: 179-203.*

RAISWELL, R. and BERNER, R.A. 1985. Pyrite formation in euxinic and semi-euxinic sediments. *Am. Journ. Sci, 285: 710-724.*

RAISWELL, R. and BERNER, R.A. 1987. Organic carbon losses during burial and thermal maturation of normal shales. *Geology, 15: 853-856.*

RAISWELL, R., BUCKLEY, F., BERNER, R.A. and ANDERSON, T.F. 1988. Degree of Pyritization of Iron as a Palaeoenvironmental Indicator of Bottom-Water Oxygenation. *Journ. Sed. Pet. 58 (5): 812-819.*

RAISWELL, R., CANFIELD, D.E., and BERNER, R.A. 1994. A comparison of iron extraction methods for the determination of degree of pyritization and the recognition of iron-limited pyrite formation. *Chemical Geology, 111: 101-110.*

RAMSBOTTOM, W.H.C., 1969. The Namurian of Britain. *Compte Rendu 6me Cong. int. Carb. Strat. Géol. Carb. (Sheffield 1967), 1: 71-77.*

RAMSBOTTOM, W.H.C., 1977. Major cycles of transgression and regression (mesothems) in the Namurian. *Proc. Yorks. Geol. Soc., 41: 261-291.*

RAMSBOTTOM, W.H.C., 1979. Rates of transgression and regression in the Carboniferous of North West Europe. *Quart. Journ. Geol. Soc. London, 136: 147-154.*

RAMSBOTTOM, W.H.C. 1980. Eustatic control in Carboniferous Ammonoid Biostratigraphy. In: House , M.R. and Senior, J.R. (Eds.) *The Ammonoidea. Systematics Association Special Volume, 18. Academic Press, London and New York: 369-388.*

RAMSBOTTOM, W.H.C. 1981. (Ed.) *Field guide to the Boundary Stratotypes of the Carboniferous stages in Britain. Subcommission on Carboniferous stratigraphy.*

RAMSBOTTOM, W.H.C. 1991. A History of the Carboniferous Congress. *Onzième Congrès International de Stratigraphie et de Géologie du Carbonifère, Beijing 1987, Compte Rendu 1 (1991): 20-27.*

RAMSBOTTOM, W.H.C., CALVER, M.A., EAGER, R.M.C., HODSON, F., HOLLIDAY, D.W., STUBBLEFIELD, C., and WILSON, R.B., 1978. A correlation of Silesian rocks in the British Isles. *Spec. Rep. Geol. Soc. London, 10: 81 pp.*

RAMSBOTTOM, W.H.C., HIGGINS, A.C. and OWENS, B. 1983. Recognition of a mid-Carboniferous boundary in the Pennine Province, England. In: Saunders, W.B. (Ed.) *Newsletter on Carboniferous Stratigraphy, 4:12.*

RAMSBOTTOM , W.H.C., RHYS, G.H. and SMITH, E.G., 1962. Boreholes in the Carboniferous rocks of the Ashover district, Derbyshire. *Bull. Geol. Surv. G.B., 19,: 75-168.*

RAMSBOTTOM, W.H.C., SAUNDERS, W.B. and OWENS, B. 1982. *Biostratigraphic data for a mid-Carboniferous Boundary. Subcommission on Carboniferous Stratigraphy Publication 8, Leeds, U.K., 156 pp.*

RAYMOND, A., KELLEY, P.H. and BLANTON-LUTKEN, C. 1989. Polar glaciers and life at the equator: The history of Dinantian and Namurian (Carboniferous) climate. *Geology, 17: 408-411.*

READ, W.A. 1991. The Millstone Grit (Namurian) of the southern Pennines viewed in the light of eustatically controlled sequence stratigraphy. *Geol. Journ., 26: 157-165.*

REXROAD, C.B. and MERRILL, G.K. 1985. Conodont Biostratigraphy and palaeoecology of Middle Carboniferous Rocks in Southern Illinois. In: Lane. H.R. and Ziegler, W. (Eds.) *Toward a Boundary in the Middle of the Carboniferous: Stratigraphy and Palaeontology. Cour. Forsch. -Inst. Senckenberg, 74: 35-65.*

REXROAD, C.B. AND THOMPSON, T.L. 1979. A spathognathodont lineage of Mississippian conodonts. *Lethaia, 12: 235-243.*

REYMENT, R.A. 1991. *Multidimensional palaeobiology, Pergamon Press: 377 pp.*

RHODES, F.H.T., AUSTIN, R.L. and DRUCE, E.C. 1969. British Avonian conodont faunas and their value in local and intercontinental correlation. *Bull. Br. Mus. Nat. History, Geol. Supp., 5: 1-313.*

RIDER, M.H., 1974. The Namurian of west County Clare. *Proc. Roy. Irish Acad., 74B: 125-142.*

RIGGS, S.R. 1979. Phosphorite sedimentation in Florida-A model Phosphogenic System. *Journ. Geol. Soc. London, 137: 285-314.*

RILEY, N.J. 1990. Revision of the Beyrichoceras Ammonoid Biozone (Dinantian) of NW Europe. *Newsletter on Strat., 21(3): 149-156*

RILEY, N.J. 1993. Dinantian (Lower Carboniferous) biostratigraphy and chronostratigraphy in the British Isles. *Journ. Geol. Soc., London, 150: 427-446.*

RILEY, N.J., CLAOUE-LONG, J, HIGGINS, A.C., OWENS, B., SPEARS, A., TAYLOR, l., and VARKER, W.J., 1994. Geochronometry and geochemistry of the European mid-Carboniferous global stratotype proposal, Stonehead Beck, North Yorkshire, U.K.*Ann. Soc. geol. Belg., T116: 275-291.*

RILEY, N.J., VARKER, W.J., OWENS, B., HIGGINS, A.C., and RAMSBOTTOM, W.H.C. 1987. Stonehead Beck, Cowling, North Yorkshire, England: A British proposal for the Mid-Carboniferous boundary Stratotype. *Cour. Forsch. -Inst. Senckenberg, 98: 159-178.*

ROBESON, D., BURNETT, R.D. and CLAYTON, G. 1988. The Upper Palaeozoic geology of the Porcupine, Erris and Donegal Basins, offshore Ireland. *Ir. Journ. Earth Sci, 9: 153-175*

ROSS, C.A. and ROSS, J.R.P. 1985a. Carboniferous and Early Permian biogeography. *Geology, 13: 27-30.*

ROSS, C.A. and ROSS, J.R.P. 1985b. Late Palaeozoic depositional sequences are synchronous and worldwide. *Geology, 13: 194-197.*

ROSS, C.A. and ROSS, J.R.P. 1988. Late Palaeozoic transgressive-regressive deposition. In: Wilgus, C.K. et al., (Eds.) *Sea-level changes: An integrated Approach., Soc. Econ. Pal Min. Spec. Pub., 42: 227-247.*

ROSSENBERG, R.. and DIAZ, R.J. 1993. Sulphur bacteria (*Beggiatoa* spp.) mats indicate hypoxic conditions in the inner Stockholm archipelago. *Ambio, 22: 32-36*

ROUNDY, P.V. 1926. Part 2. The microfauna. In: Roundy, P.V., Girty, G.H. and Goldman, M.I. (Eds.) *Mississippian Formations of San Saba County, Texas. U.S.G.S. Prof. Pap., 146: 5-23.*

ROWLAND, S.M. 1987. Palaeozoic stratigraphy of Frenchman Mountain, Clark County, Nevada. *Geol. Soc. Am. Centennial Field Guide-Cordilleran Section, Field trip 12: 53-56.*

SÆLEN, G., RAISWELL, R., TALBOT, M.R., SKEI, J.M. and BOTRELL, S.H. 1993. Heavy sedimentary sulfur isotopes as indicators of super-anoxic bottom-water conditions. *Geology, 21: 1091-1094.*

SANDBERG, C.A. 1979. Devonian and Lower Mississippian Conodont Zonation of the Great Basin and Rocky Mountains. In: Sandberg, C.A. and Clark, D.L. (Eds.) *Conodont Biostratigraphy of the Great Basin and Rocky Mountains. Brigham Young University Geology Studies, 26, (3): 87-107.*

SANDBERG, C.A. and GUTSCHICK, R.C. 1980. Sedimentation and biostratigraphy of Osagean and Meramecian starved basin and foreslope, western United States. In Fouch, T.D. and Magathan, E.R. (Eds.) *Paleozoic paleogeography of the west-Central United States. Soc. Econ. Pal. Min. Rocky Mountain Section, Rocky Mountains Paleogeography Symposium, 1: 129-147.*

SANDBERG, C.A., POOLE, F.G. and GUTSCHICK, R.C. 1980. Devonian and Mississippian Stratigraphy and Conodont zonation of Pilot and Chainman Shales, Confusion Range, Utah. In Fouch, T.D. and Magathan, E.R. (Eds.) *Paleozoic paleogeography of the west-Central United States. Soc. Econ. Pal. Min. Rocky Mountain Section, Rocky Mountains Paleogeography Symposium, 1: 71-82.*

SANDERSON, D.J., 1984. Structural variation across the northern margin of the Variscides in north-west Europe. In: Hutton, D.H.W. and Sanderson, D.J. (Eds.) *Variscan Tectonics of the North Atlantic Region. Spec Publ. Geol. Soc. London, 14: 149-166.*

SAUNDERS, W.B. 1973. Upper Mississippian ammonoids from Arkansas and Oklahoma. *Spec. Pap. Geol. Soc. Am., 145: 1-110.*

SAUNDERS, W.B. 1975. The Upper Mississippian Eumorphoceras richardsoni-Cravenoceras friscoense ammonoid assemblage, North American Midcontinent. *Compte Rendu, 7eme Cong. int. Strat. Geol. Carb., Krefeld. 1971, 1: 201-207.*

SAUNDERS, W.B. 1984. Report of the IUGS Subcommission on Carboniferous Stratigraphy. In: Saunders, W.B. (Ed.) *Newsletter on Carboniferous Stratigraphy, 5: 1-8.*

SAUNDERS, W.B. and RAMSBOTTOM, W.H.C. 1986. The mid-Carboniferous eustatic event. *Geology, 14: 208-212.*

SAUNDERS, W.B. and RAMSBOTTOM, W.H.C. 1993. Re-evaluation of two early Pennsylvanian (middle Namurian) ammonoids and their bearing on mid-Carboniferous correlations. *Journ. Pal., 67 (6): 993-999.*

SAUNDERS, W.B., MANGER, W.L. and GORDON, M. Jr. 1977. Upper Mississippian and lower and Upper Pennsylvanian ammonoid biostratigraphy of northern Arkansas. In: Sutherland, P.K. and Manger, W.L. (Eds.) *Upper Chesterian-Morrowan stratigraphy and the Mississippian-Pennsylvanian boundary in northeastern Oklahoma and northwestern Arkansas. Oklahoma Geol. Survey Guidebook, 18: 117-137.*

SAUNDERS, W.B., RAMSBOTTOM, W.H.C., and MANGER, W.L. 1979. Mesothemic cyclicity in the mid-Carboniferous of the Ozark shelf region? *Geology, 7: 293-396.*

SCHAFFER, G. 1986. Phosphate pumps and shuttles in the Black Sea. *Nature, 321: 515-517.*

SEVASTOPULO, G.D., 1981. Upper Carboniferous. In: Holland, C.H. (Ed.) *A Geology of Ireland. Scottish Academic Press, Edinburgh: 173-187.*

SHAW, T.J., SHOLKOVITZ, E.R., KLINKHAMMER, G. 1994. Redox dynamics in the Chesapeake bay: The effect on sediment/water uranium exchange. *Geochim., Cosmochim., Acta, 58: 2985-2995.*

SHELFORD, P.H., 1963. The structure and relationship of the Namurian outcrop between Duntryleague, County Limerick and Dromlin, Co. Tipperary. *Proc. Roy. Ir. Acad., 62B: 255-266.*

SHELFORD, P.H., 1967. The Namurian and Upper Viséan of the Limerick Volcanic Basin, Eire. *Proc. Geol. Ass., 78: 121-136.*

SKIPP, B. BAESEMANN, J.F., and BRENCKLE, P.L. 1983. Possible Mid-Carboniferous Boundary Stratotype in South Central Idaho. In: Saunders, W.B. (Ed.) *Newsletter on Carboniferous Stratigraphy, 4: 15-16.*

SKIPP, B. BAESEMANN, J.F., and BRENCKLE, P.L. 1985. A reference area for the Mississippian-Pennsylvanian (mid-Carboniferous) boundary in East-Central Idaho, USA. *Compte Rendu Xeme Int. Cong. Carb., Madrid (1983), 4: 403-428.*

SKIPP, B.A., BRENCKLE, P.L., POLETAEV, V.I., NEMIROVSKAYA, T.I., LANE, H.R. and MANGER, W.L. 1989. The continuing international search for a Mid-Carboniferous boundary Stratotype - Donets Basin, USSR, 1988. *Episodes, 12 (3): 179-183*

SLANSKY, M. 1986. *Geology of Sedimentary Phosphates. Elsevier Science Publishing Co.: 210 pp.*

SMITH, J. 1900. Conodonts from the Carboniferous Limestone strata of the West of Scotland. *Trans. Nat. Hist. Soc. Glasgow. 5: 336-338*

SMITH, J.T. 1896. Marine fossils from the Coal Measures of Arkansas. *Am Philos. Soc. Proc. 35, (152): 214-285.*

SMITH, J.T. 1903. The Carboniferous ammonoids of America. *U.S.G.S. Mon., 42: 211 pp.*

SMITH, M.T., DICKINSON, W.R. and GEHRELS, G.E. 1993. Contractional nature of Devonian-Mississippian Antler tectonism along the North American continental margin. *Geology, 21: 21-24.*

SOPER, N.J., WEBB, B.C. and WOODCOCK, N.H., 1987. Late Caledonian (Acadian) transpression in north-west England: timing, geometry and geotectonic significance. *Proc. Yorks. Geol. Soc., 46: 175-192.*

SOUDRY, D. 1979. Intervention de schizophytes dans la phospimicritisation des débris osseux. *Compte Rendu Acad. Sci. Ser. D, 288: 669-671.*

SOUDRY, D. AND CHAMPETIER, Y. 1983. Microbial processes in the Negev phosphorites, Southern Israel. *Sedimentology, 30: 411-423.*

SOUDRY, D. and LEWY, Z. 1988. Microbially influenced formation of phosphate nodules and megafossil moulds (Negev, Israel). *Palaeogeogr. Palaeoclimat. Palaeoecol., 64: 15-34.*

SOUDRY, D. and LEWY, Z. 1990. Ommission-surface incipient phosphate crusts on early diagenetic calcareous concretions and their possible origin, Upper Campanian, southern Israel. *Sedimentary Geology, 66: 151-163.*

SOUTHGATE, P.N. 1986. Cambrian phoscrete profiles, coated grains, and microbial processes in phosphogenesis: Georgina Basin, Australia. *Journ Sed. Pet., 56: 429-441.*

SPEED, R.C. and SLEEP, N.H. 1982. Antler orogeny and foreland basin: A model. *Bull. Geol. Soc. Am., 93: 815-828.*

SPEYER, S.E. and BRETT, C.E. 1988. Taphofacies models for epeiric sea environments: middle Palaeozoic examples. *Palaeogeog., Palaeoclimat., Palaeoec., 63: 225-262.*

STAFF, G.M. and POWELL, E.N. 1988. The palaeoecological significance of diversity: the effect of time-averaging and differential preservation of macroinvertebrate species richness in death assemblages. *Palaeogeog., Palaeoclimat., Palaeoec., 63: 73-89.*

STEVENS, C.H. and ARMIN, R.A. 1983. Microfacies of the middle part of the Oquirrh Group, central Utah. *Geol. Soc. Am., Mem., 157: 83-100.*

STEVENS, C.H., STONE, P. and BELASKY, P. 1991. Paleogeographic and structural significance of an Upper Mississippian facies boundary in southern Nevada and east-central California. *Bull. Geol. Soc. Am., 103: 876-885.*

STROGEN, P., 1988. The Carboniferous lithostratigraphy of south-east County Limerick, Ireland, and the origin of the Shannon Trough. *Geol. Journ., 23: 121-137.*

STROGEN, P., 1994. *Field seminar on Sedimentation in the Namurian Clare Basin, Ireland. Geology Department, University College Dublin. 27pp.*

TANABE, K., SHIGETA, Y. and MAPES, R.H. 1995. Early life history of Carboniferous ammonoids inferred from analysis of shell hydrostatics and fossil assemblages. *Palaios, 10: 80-86.*

TATE, M.P., 1993. Structural framework and tectono-stratigraphic evolution of the Porcupine Seabight Basin, offshore western Ireland. *Marine and Petroleum geology, 10: 95-123.*

THORN, E.R.S. 1958. *The Carboniferous Limestone succession in north-west Co. Limerick, Eire. Ph.D. thesis (Unpubl.). Univ. Reading: 215 pp.*

TIEH, T.T., LEDGER, E.B. and ROWE, M.W. 1980. Release of uranium from granitic rocks during in-situ weathering and initial erosion (Central Texas), *Chemical Geology, 29: 227-248*

TITUS, A. L. 1992. *Mid-Carboniferous biostratigraphy and ammonoid paleontology of the Upper Eleana Formation (Unit J-Upper Quartzite Subunit), Syncline Ridge, Central Nevada Test Site, Nye County, Nevada. M.S. Thesis (Unpub.), Univ. Arkansas: 134 pp.*

TITUS, A.L. 1993. Biostratigraphic implications of the first north American occurrence of the Upper Mississippian ammonoid *Platygoniatites. Journ. Pa., 67 (2): 310-313.*

TITUS, A.L. and MANGER, W.L. 1992. Mid-Carboniferous (E_2c-H_1b) Ammonoid Biostratigraphy, Nevada Test Site, Nye County, Nevada. *Abstracts with Programs, Rocky Mountain Section Annual Meeting Geol. Soc. Am., 24 (6): 66.*

TREXLER, J.H. and NITCHMAN, S.P. 1990. Sequence stratigraphy and evolution of the Antler foreland basin, east-central Nevada. *Geology, 18; 422-425.*

TYSON, R.V. 1987. The genesis and palynofacies characteristics of marine petroleum source rocks. In: Brooks, J. and Fleet, A.J. (Eds.) *Marine Petroleum Source Rocks. Geol. Soc. London Spec. Pub., 26: 47-68.*

TYSON, R.V. and PEARSON, T.H. 1991. Modern and ancient continental shelf anoxia: A review. In: Tyson, R.V. and Pearson, T.H. (Eds). *Modern and ancient Continental Shelf anoxia. Geol. Soc. London Spec. Pub., 58: 1-24.*

VAIL, P.R. 1987. Seismic stratigraphic interpretation using sequence stratigraphy. Part 1. Seismic stratigraphic procedure. In: Bally, A.W. (Ed.) *Atlas of seismic stratigraphy, vol. 1. A.A.P.G. Studies in Geology, 27: 1-10.*

VARKER, W.J. 1964. *The conodont faunas and stratigraphy of the Yoredale Series in the Askrigg and Alston regions. Ph.D. thesis (Unpub.) Univ. Sheffield.*

VARKER, W.J. 1987. A method of extracting conodonts from non-calcareous shale samples using parafin (kerosene). In: Austin, R.L. (Ed.) *Conodonts Investigative Techniques and Applications. British Micropalaeontological Society/Ellis Horwood Ltd.: 43-44.*

VARKER, W.J. 1994. Multielement conodnt faunas from the proposed mid-Carboniferous boundary stratotype locality at Stonehead Beck, Cowling, North Yorkshire, England. *Ann. Soc. geol. Belg., T116: 301-321.*

VARKER, W.J. and AUSTIN, R.L. 1974. The significance of *Adetognathodus unicornis* (Rexroad and Burton) in the Mirk Fell Beds (E2a) of the North of England. *Trans. Leeds. Geol. Assoc., 8: 399-408*

VARKER, W.J., OWENS, B. AND RILEY, N.J. 1990. Integrated biostratigraphy for the proposed mid-Carboniferous boundary stratotype, Stonehead Beck, Cowling, North Yorkshire. *Cour. Forsch. -Inst. Senckenberg, 130: 221-235.*

VARKER, W.J. and SEVASTOPULO, G.D. 1985. The Carboniferous System: Part 1 - Conodonts of the Dinantian Subsystem from Great Britain and Ireland. In: Higgins, A.C. and Austin, R.L. (Eds.). *A Stratigraphical Index of Conodonts. British Micropalaeontological Society Series. Ellis Horwood Ltd, Sussex: 167-209.*

VAUGHAN, A. 1905. The palaeontological sequence in the Carboniferous Limestone of the Bristol area. *Quart. Journ. Geol. Soc. London, 61: 181-307.*

VEEVERS J.J. and POWELL, C. McA. 1987. Late Palaeozoic glacial episodes in Gondwanaland reflected in transgressive-regressive depositional sequences in Euramerica. *Geol. Soc. Am. Bull., 98: 475-489.*

WAGNER, R.H. and WINKLER PRINS, C.F. 1991. Major subdivisions of the Carboniferous system. *Compte Rendu XIeme Cong. Int. Strat. Géol. Carb., Beijing, 1987, 1 (1991): 213-245.*

WAGNER, R.H. and WINKLER PRINS, C.F. 1993. General overview of Carboniferous Stratigraphy. *Ann. Soc. geol. Belg., T. 116 - 1993 (fascicule 1): 163-174.*

WANLESS, H.R. AND SHEPARD, F.P. 1936. Sea level climatic changes related to late Palaeozoic cycles. *Bull. Geol. Soc. Am., 47: 1177-1206.*

WEAVER, T. 1940. On the geological relations of the south of Ireland. *Trans. Geol. Soc. London, 2 (5): 1-68.*

WEBSTER, G. 1969. Chester through Derry conodonts and stratigraphy of northern Clark and southern Lincoln Counties, Nevada. *Univ. of California Pub. in Geol. Sci., 79: 121 pp.*

WEBSTER, G.D. and LANE, N.G. 1967. Mississippian-Pennsylvanian Boundary in Southern Nevada. In Teichert, C. Yochelsen, E.L. (Eds.) *Essays in Paleontology and Stratigraphy, R.C. Moore Commerative Volume, Dept. Geology, Univ. of Kansas, Spec. Publ., 2: 503-522.*

WEBSTER, G.D., BRENCKLE, P., GORDON, M., Jr., LANE, H.R., LANGENHEIM, R.L. Jr., SANDERSON, G.A. and TIDWELL, W.D. 1984. The Mississippian-Pennsylvanian boundary in the eastern Great Basin: *Compte Rendu, 9eme Cong. Int. Strat. Geol. du Carb., Washington, D.C. and Champaign-Urbana, 1979., 2: 406-418.*

WEBSTER, G.D., GORDON, M. JR., LANGENHEIM, R.L., JR. and HENRY, T.W. 1985. *Road Logs for the Mississippian-Pennsylvanian Boundary in the Eastern Great Basin: Salt Lake City, Utah, to Las Vegas, Nevada (Field Trip 1). 1-73.*

WEIBEL, C.P. and NORBY, R.D. 1992. Paleopedology and Conodont Biostratigraphy of the Mississippian-Pennsylvanian Boundary Interval, Type Grove Church Shale Area, Southern Illinois. In: Sutherland, P.K. and Manger, W.L. (Eds.) *Recent Advances in Middle Carboniferous Biostratigraphy-A symposium Oklahoma Geological Circular 94: 39-54.*

WESTRICH, J.T., 1983. *The consequences and controls of bacterial sulphate reduction in marine sediments. Ph.D. Thesis (Unpub.) Yale Univ: 289 pp.*

WIGNALL, P.B. 1991. A model for transgressive black shales? *Geology, 19: 167-170.*

WIGNALL, P.B. 1994. *Black shales. Oxford Monographs on Geology and Geophysics, 30: 127pp.*

WIGNALL, P.B. and HALLAM, A. 1991. Biofacies, stratigraphic distribution and depositional models of British onshore Jurassic black shales. In: Tyson, R.V. and Pearson, T.H. (Eds.) *Modern and ancient continental shelf anoxia. Geol. Soc. London Spec. Pub., 58: 291-309.*

WIGNALL, P.B. and MAYNARD, J.R. 1993. The sequence stratigraphy of transgressive black shales. In: Katz, B.J. and Pratt, L.M. (Eds.) *Source rocks in a Sequence Stratigraphic Framework. A.A.P.G. Studies in Geology 37.*

WIGNALL, P.B. and MYERS, K.J. 1988. Interpreting benthic oxygen levels in mudrocks - a new approach. *Geology, 16: 452-455.*

WILLIAMS, L.A. and REIMERS, C. 1983. Role of bacterial mats in oxygen deficient marine basins and coastal upwelling regimes: preliminary report. *Geology, 11: 267-276.*

WILSON, J.L., 1975. *Carbonate facies in geologic history. Springer Verlag: 458 pp.*

WILSON, M.A. 1985. Conodont biostratigraphy and paleoenvironments at the Mississippian-Pennsylvanian boundary (Carboniferous: Namurian) in the Spring Mountains of southern Nevada. *Newsletter in Strat., 14 (2): 69 -80*

WOOD, L.J., ETHRIDGE, F.G. and SCHUMM, S.A. 1993. The effects of base-level fluctuation on coastal plain, shelf and slope depositional systems: an experimental approach. *Spec. Publ. Int. Assoc. Sediment., 18: 43-52.*

YATES, P.J. 1962. The palaeontology of the Namurian rocks of Slieve Anierin, County Leitrim, Eire. *Palaeontology, 5: 355-443.*

YOUNG, J. 1880a. Notes on Scottish Carbonifeorus microzoa and the methods by which they can be collected and mounted. *Trans. Edin. Geol. Soc., 3: 300-302.*

YOUNG, J. 1880b. On a group of fossil organisms termed conodonts. *Proc. Trans. Nat. Hist. Soc. Glasgow, 4: 5-7.*

ZIEGLER, P.A. 1982. *Geological Atlas of Western and Central Europe. Shell Int. Elsevier: 130 pp.*

APPENDIX A

LOCATION OF GEOCHEMISTRY SAMPLES/GAMMA-RAY READING

The following stratigraphic logs show the positions of where cores were taken and/or the position of gamma-ray readings.

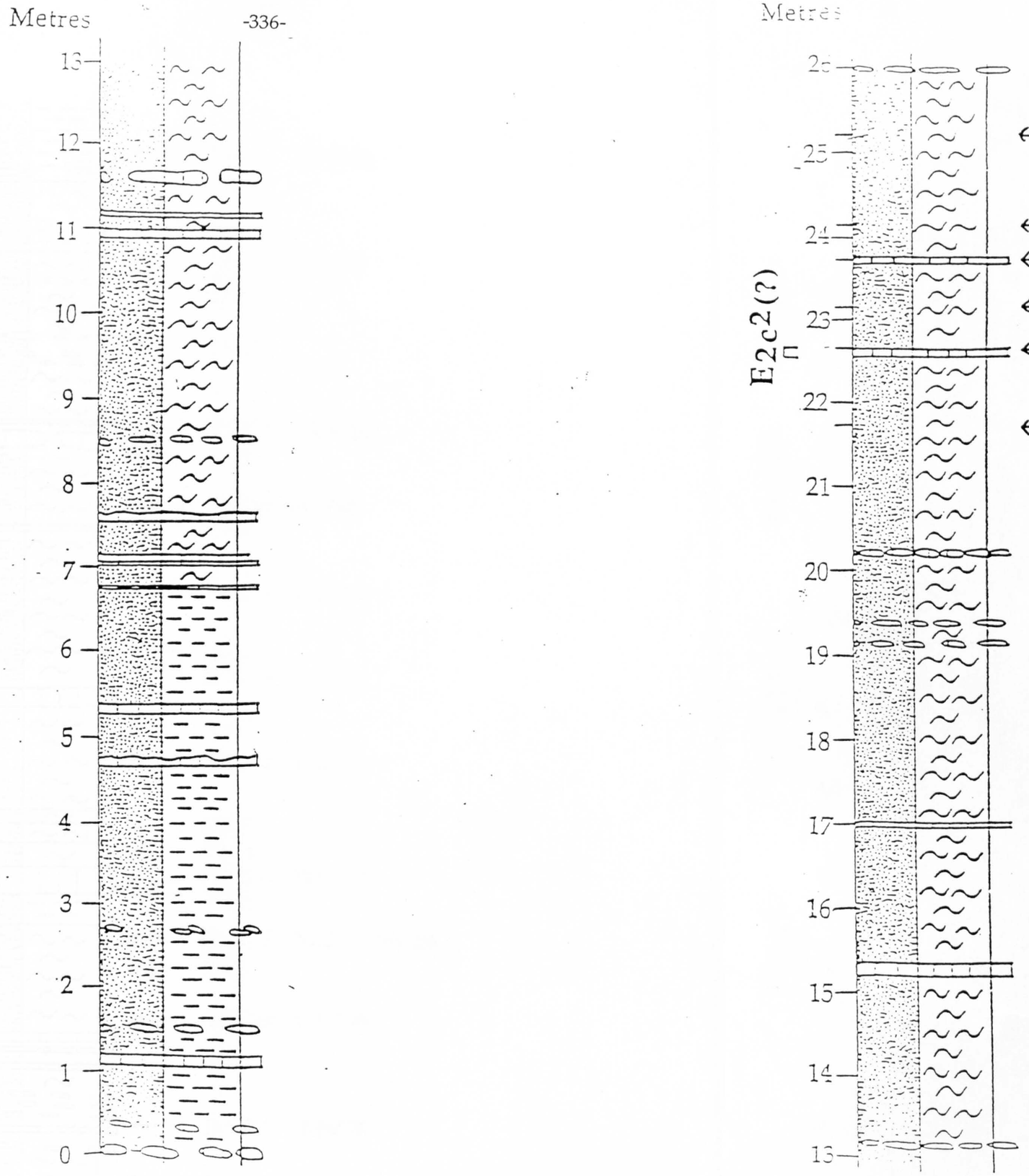

INISHCORKER

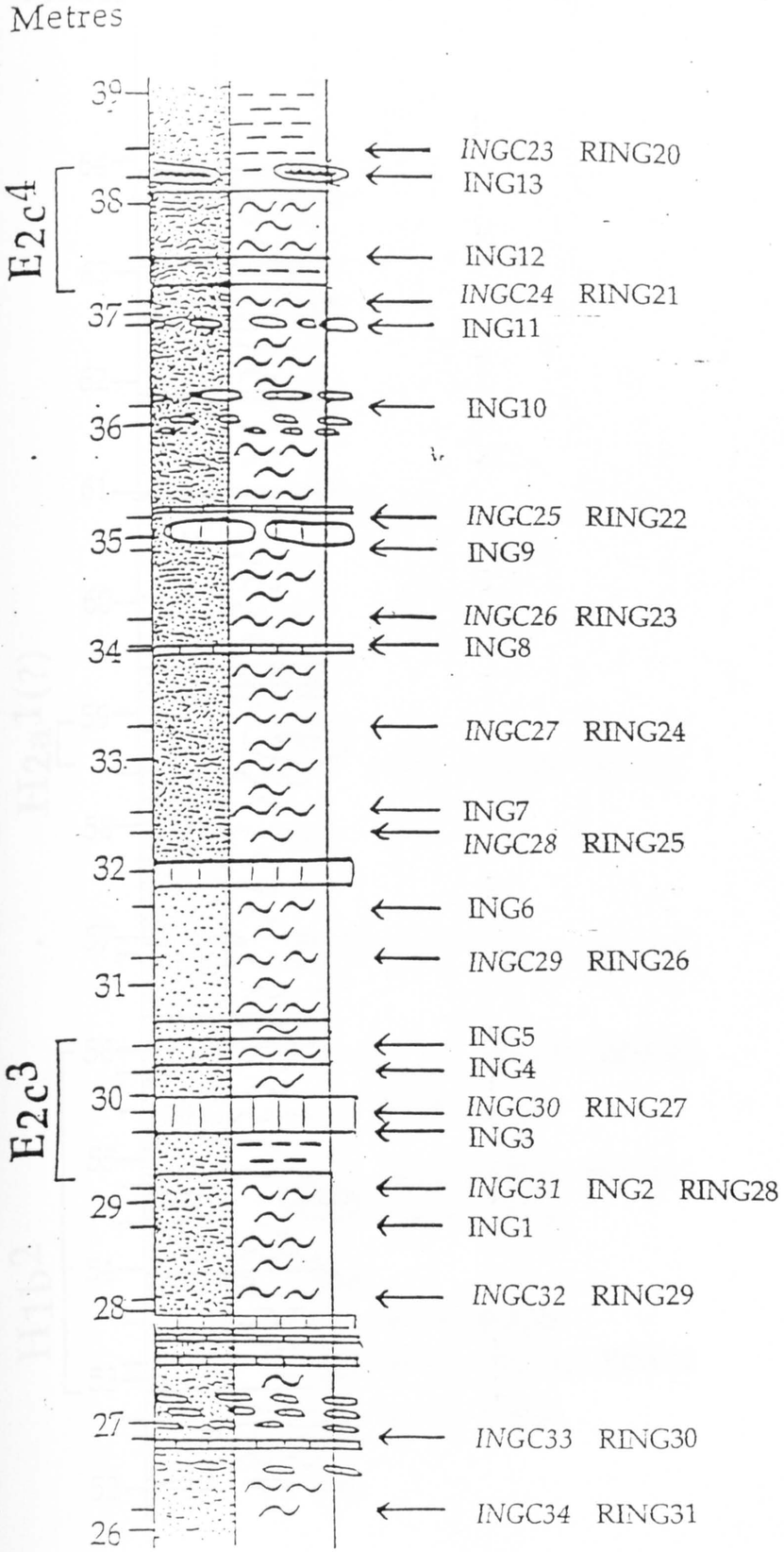
Metres
E2c4
E2c3
39
38
37
36
35
34
33
32
31
30
29
28
27
26
INGC23 RING20
ING13
ING12
INGC24 RING21
ING11
ING10
INGC25 RING22
ING9
INGC26 RING23
ING8
INGC27 RING24
ING7
INGC28 RING25
ING6
INGC29 RING26
ING5
ING4
INGC30 RING27
ING3
INGC31 ING2 RING28
ING1
INGC32 RING29
INGC33 RING30
INGC34 RING31

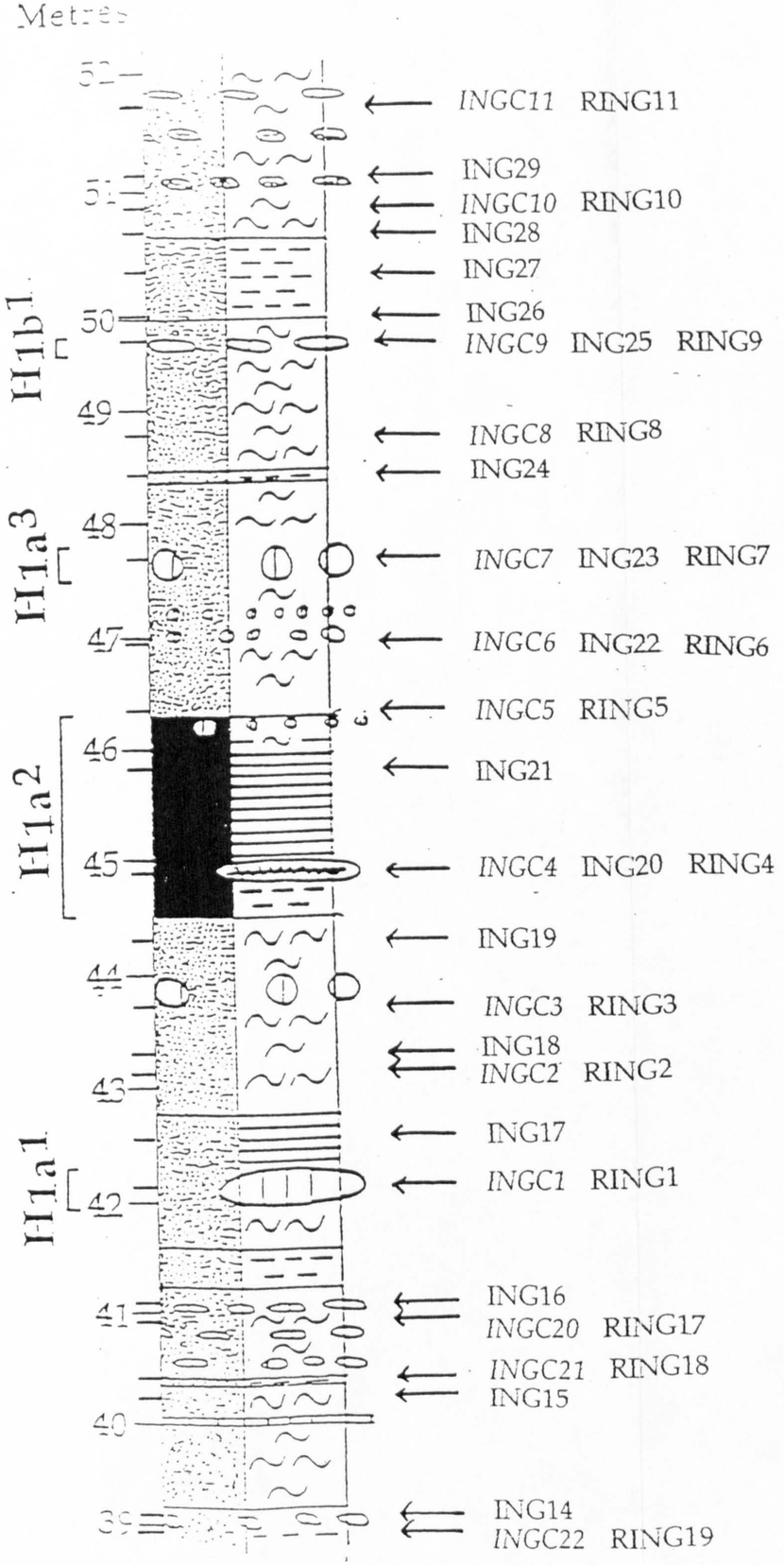
Metres
H1b1
H1a3
H1a2
H1a1
52
51
50
49
48
47
46
45
44
43
42
41
40
39
INGC11 RING11
ING29
INGC10 RING10
ING28
ING27
ING26
INGC9 ING25 RING9
INGC8 RING8
ING24
INGC7 ING23 RING7
INGC6 ING22 RING6
INGC5 RING5
ING21
INGC4 ING20 RING4
ING19
INGC3 RING3
ING18
INGC2 RING2
ING17
INGC1 RING1
ING16
INGC20 RING17
INGC21 RING18
ING15
ING14
INGC22 RING19

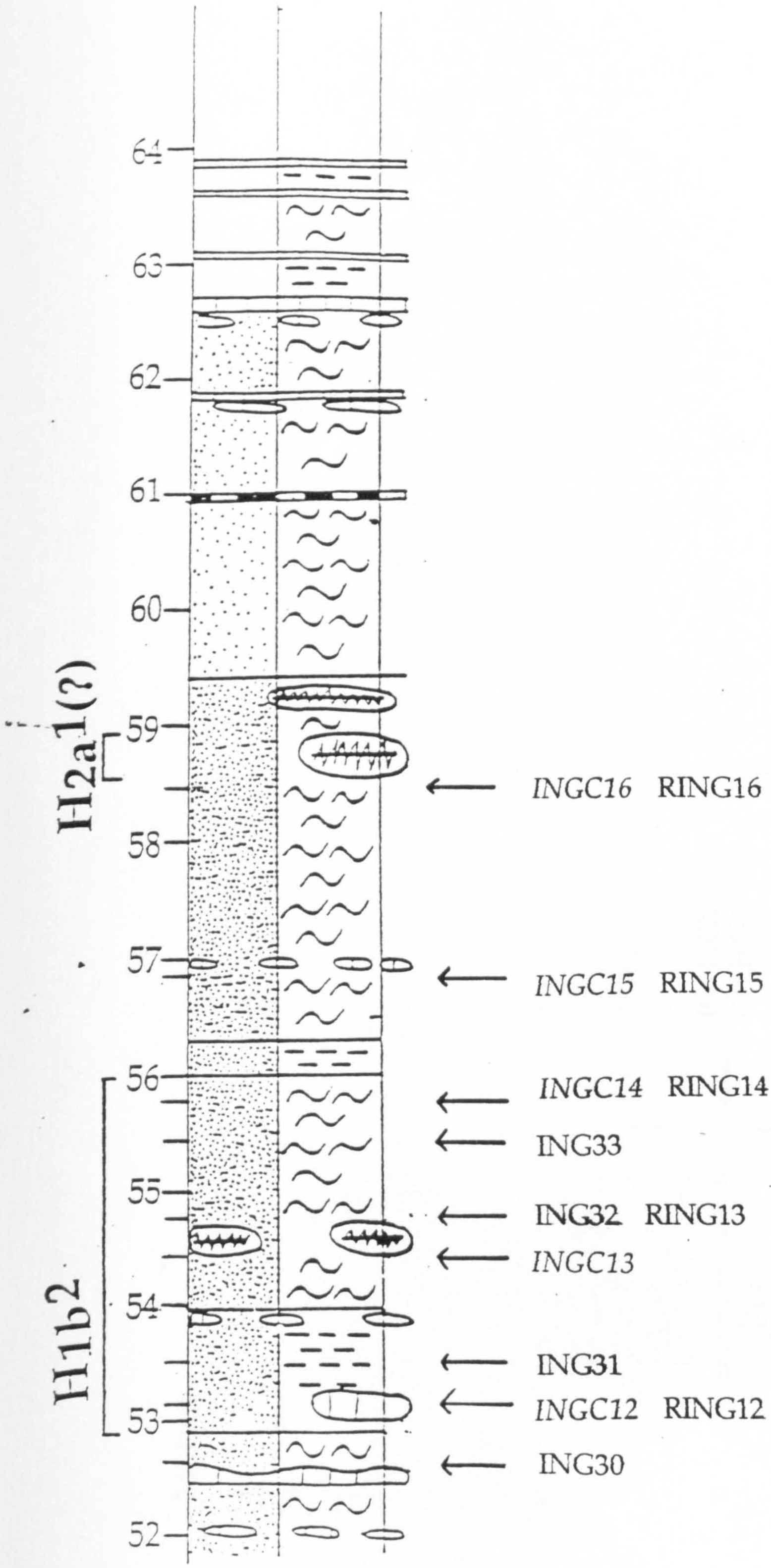
Metres
64
63
62
61
60
59
58
57
56
55
54
53
52
H2a1(?)
H1b2
INGC16 RING16
INGC15 RING15
INGC14 RING14
ING33
ING32 RING13
INGC13
ING31
INGC12 RING12
ING30

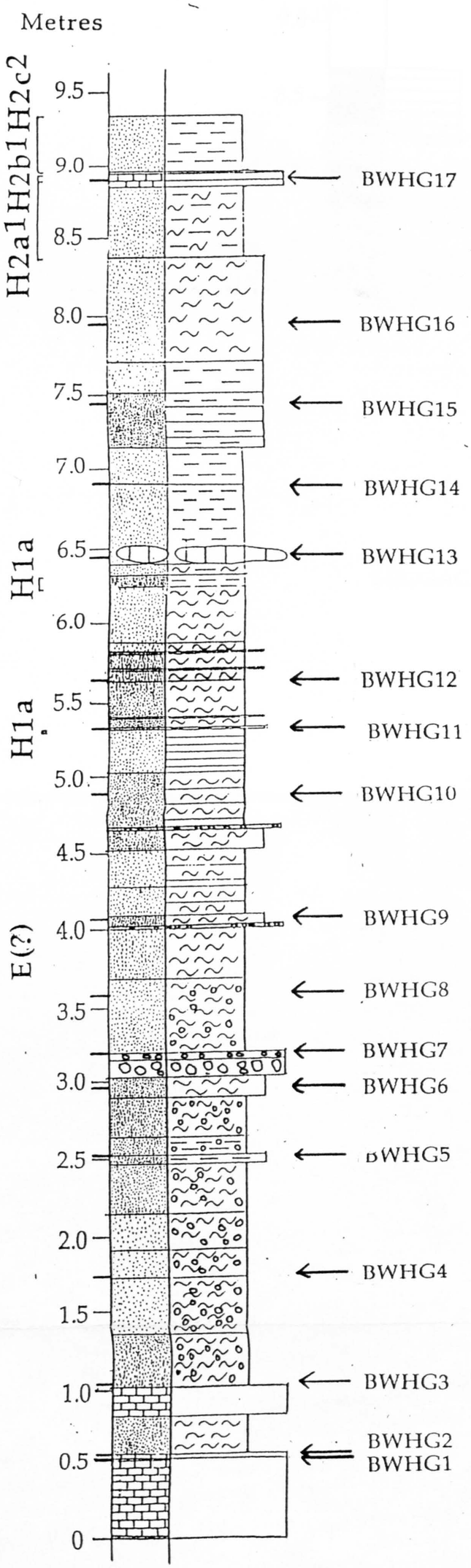

BALLYSHANNY HOUSE

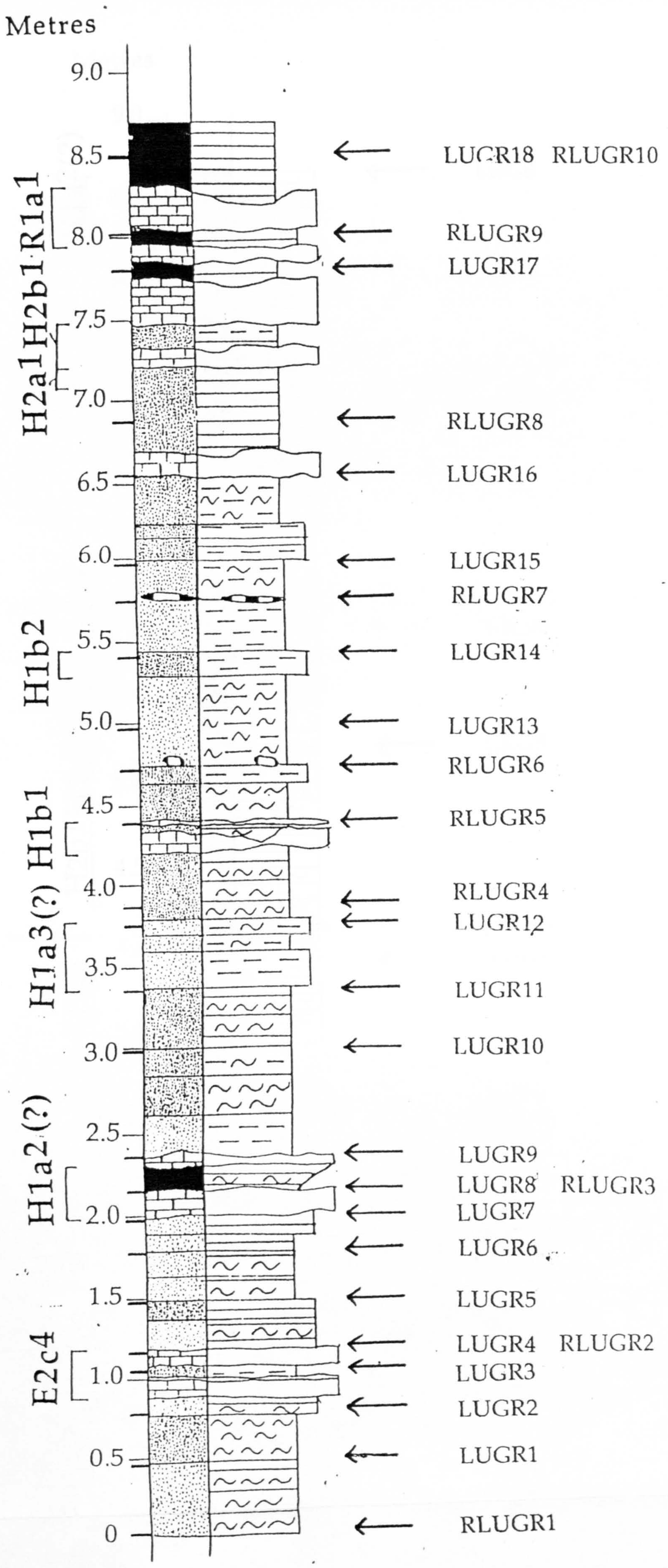

LUGGACURREN

LOUGH RAHA

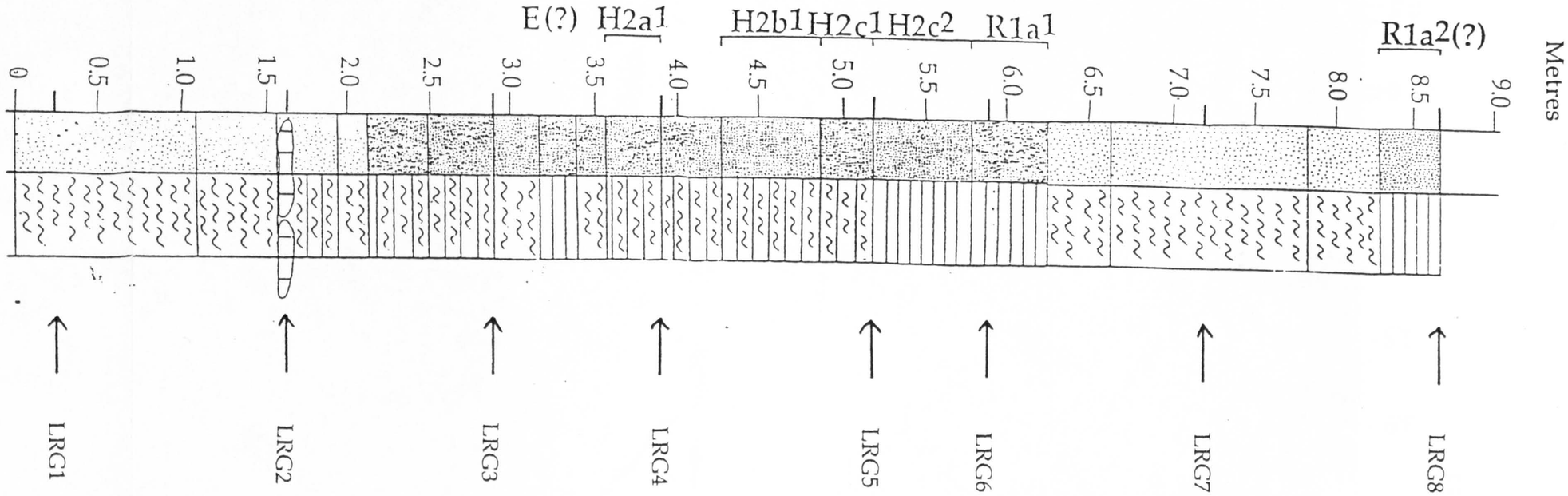

LRG1 LRG2 LRG3 LRG4 LRG5 LRG6 LRG7 LRG8

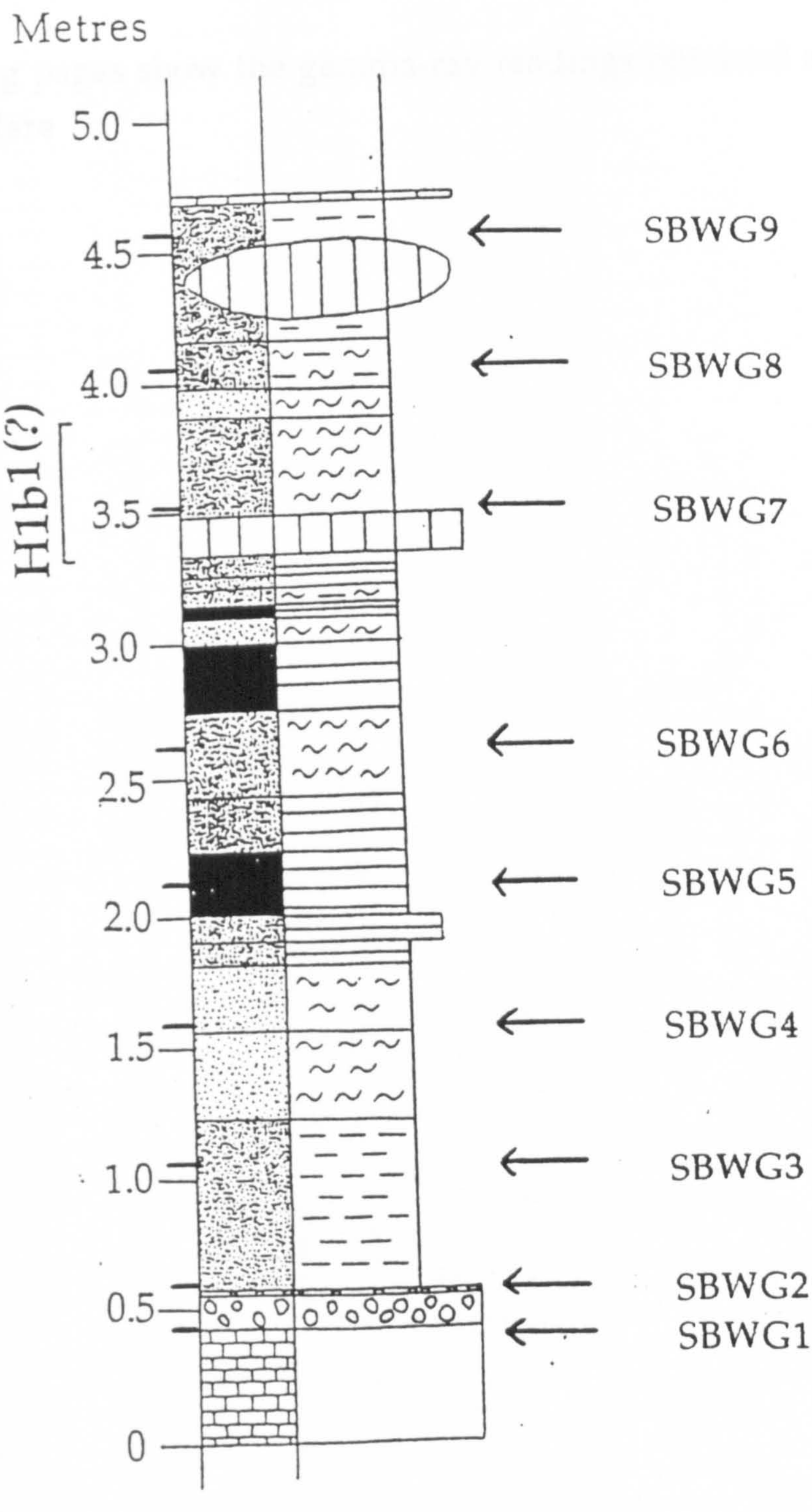

ST BRENDANS WELL

APPENDIX B

GAMMA-RAY VALUES

The following pages show the gamma-ray readings obtained at the localities in County Clare

Locality	Reading no.	Total	K	Utot	Th	Uaut	Udet
Ballyshanny House	BWHG1	5.10	0.40	3.60	1.00	3.27	0.33
	BWHG2	12.10	0.40	9.20	2.30	8.43	0.77
	BWHG3	21.80	0.80	16.70	3.60	15.50	1.20
	BWHG4	31.60	1.80	23.10	6.80	20.83	2.27
	BWHG5	39.80	1.60	30.80	7.90	28.17	2.63
	BWHG6	62.60	2.00	51.40	8.20	48.67	2.73
	BWHG7	103.30	2.00	89.60	11.20	85.87	3.73
	BWHG8	41.10	3.50	23.00	12.20	18.93	4.07
	BWHG9	40.90	3.10	24.60	12.20	20.53	4.07
	BWHG10	37.00	3.50	13.40	12.50	9.23	4.17
	BWHG11	32.50	3.20	15.80	12.30	11.70	4.10
	BWHG12	27.90	3.40	14.20	10.70	10.63	3.57
	BWHG13	25.20	2.80	10.90	11.30	7.13	3.77
	BWHG14	33.80	3.20	16.90	13.60	12.37	4.53
	BWHG15	33.60	3.10	16.80	15.20	11.73	5.07
	BWHG16	29.60	2.30	16.20	13.40	11.73	4.47
	BWHG17	26.30	3.30	13.30	10.80	9.70	3.60
Lough Raha	LRG1	26.60	3.60	18.40	14.40	13.60	4.80
	LRG2	33.00	3.70	13.80	16.70	8.23	5.57
	LRG3	40.00	4.10	19.50	16.20	14.10	5.40
	LRG4	32.10	3.00	17.40	11.10	13.70	3.70
	LRG5	24.10	2.60	11.00	10.80	7.40	3.60
	LRG6	25.10	3.00	11.90	10.50	8.40	3.50
	LRG7	21.40	2.70	8.50	9.20	5.43	3.07
	LRG8	25.30	3.40	11.50	9.70	8.27	3.23
Inishcorker	ING1	21.40	1.60	7.40	14.90	2.43	4.97
	ING2	21.20	1.10	11.00	7.40	8.53	2.47
	ING3	20.80	1.30	8.90	10.50	5.40	3.50
	ING4	22.60	1.00	11.50	7.70	8.93	2.57
	ING5	25.30	1.90	9.30	14.40	4.50	4.80
	ING6	29.30	1.80	12.10	13.90	7.47	4.63
	ING7	27.90	1.90	9.80	15.70	4.57	5.23
	ING8	28.40	2.00	9.80	16.00	4.47	5.33
	ING9	21.00	1.50	7.80	9.80	4.53	3.27
	ING10	22.50	1.50	8.70	11.40	4.90	3.80
	ING11	22.60	1.70	7.90	12.80	3.63	4.27
	ING12	23.10	1.30	11.80	17.70	5.90	5.90
	ING13	23.10	1.20	11.00	9.30	7.90	3.10
	ING14	23.60	1.30	11.20	9.60	8.00	3.20
	ING15	25.40	1.60	9.60	13.30	5.17	4.43
	ING16	27.10	1.90	9.60	15.80	4.33	5.27
	ING17	32.40	1.60	15.60	15.00	10.60	5.00
	ING18	28.30	1.80	12.60	13.20	8.20	4.40
	ING19	32.90	1.90	13.30	15.60	8.10	5.20
	ING20	14.20	0.60	7.40	6.00	5.40	2.00
	ING21	19.70	1.00	9.50	8.10	6.80	2.70
	ING22	22.20	1.40	9.60	7.80	7.00	2.60
	ING23	24.10	1.30	11.10	12.50	6.93	4.17
	ING24	31.40	1.70	13.30	16.00	7.97	5.33
	ING25	26.30	1.70	9.00	14.20	4.27	4.73
	ING26	26.80	1.70	10.80	13.00	6.47	4.33
	ING27	23.70	1.20	11.40	9.60	8.20	3.20
	ING28	32.50	2.00	11.80	17.40	6.00	5.80
	ING29	27.80	2.00	9.50	16.10	4.13	5.37
	ING30	29.80	2.10	11.40	14.30	6.63	4.77
	ING31	23.50	1.60	10.70	10.50	7.20	3.50
	ING32	21.10	1.30	9.30	9.90	6.00	3.30
	ING33	23.30	1.70	9.10	11.00	5.43	3.67
Inishcorker	RING1	29.80	3.50	11.10	15.20	6.03	5.07
	RING2	31.00	3.70	12.90	15.30	7.80	5.10
	RING3	29.00	3.20	13.30	11.40	9.50	3.80
	RING4	28.70	2.50	14.80	10.80	11.20	3.60
	RING5	14.20	1.10	3.40	5.20	1.67	1.73
	RING6	23.10	2.80	10.10	9.70	6.87	3.23
	RING7	23.60	2.40	11.40	10.50	7.90	3.50
	RING8	30.60	3.60	11.50	16.00	6.17	5.33
	RING9	24.70	3.00	9.70	13.60	5.17	4.53

	RING10	26.00	3.30	9.30	14.70	4.40	4.90
	RING11	27.00	3.40	13.50	10.60	9.97	3.53
	RING12	24.40	2.30	12.40	10.70	8.83	3.57
	RING13	23.50	2.50	10.90	10.50	7.40	3.50
	RING14	24.70	3.00	10.30	11.40	6.50	3.80
	RING15	25.30	2.90	10.20	13.80	5.60	4.60
	RING16	21.80	2.60	8.10	10.90	4.47	3.63
	RING17	26.50	3.10	9.10	15.20	4.03	5.07
	RING18	25.80	3.40	9.10	13.10	4.73	4.37
	RING19	28.10	3.10	11.90	13.60	7.37	4.53
	RING20	21.00	1.50	13.10	4.60	11.57	1.53
	RING21	23.10	3.10	7.80	14.40	3.00	4.80
	RING22	22.80	2.80	8.60	11.70	4.70	3.90
	RING23	27.00	3.60	8.50	16.70	2.93	5.57
	RING24	29.70	3.90	9.50	18.50	3.33	6.17
	RING25	29.30	3.60	10.20	14.90	5.23	4.97
	RING26	25.50	3.70	7.90	13.90	3.27	4.63
	RING27	27.30	1.30	22.20	4.20	20.80	1.40
	RING28	23.70	3.10	7.90	13.50	3.40	4.50
	RING29	22.20	2.70	7.50	15.40	2.37	5.13
	RING30	22.00	2.70	7.20	14.70	2.30	4.90
	RING31	25.20	3.60	5.60	15.00	0.60	5.00
	RING32	30.30	3.80	10.90	16.40	5.43	5.47
	RING33	28.60	3.30	11.10	15.00	6.10	5.00
	RING34	23.40	3.50	10.80	10.50	7.30	3.50
	RING35	24.50	3.40	7.60	15.40	2.47	5.13
Luggacurren	LUG1	28.50	1.60	11.80	13.40	7.33	4.47
	LUG2	29.50	1.40	13.10	13.80	8.50	4.60
	LUG3	30.50	1.40	15.50	11.30	11.73	3.77
	LUG4	34.90	1.50	18.80	13.20	14.40	4.40
	LUG5	35.80	2.00	15.20	16.00	9.87	5.33
	LUG6	26.50	1.80	10.60	12.80	6.33	4.27
	LUG7	28.60	1.20	15.10	11.20	11.37	3.73
	LUG8	30.00	1.30	14.90	12.90	10.60	4.30
	LUG9	26.20	1.40	13.50	11.20	9.77	3.73
	LUG10	32.30	2.00	14.10	16.00	8.77	5.33
	LUG11	26.20	1.20	12.40	12.10	8.37	4.03
	LUG12	31.50	1.40	17.00	11.70	13.10	3.90
	LUG13	26.30	1.20	12.80	13.20	8.40	4.40
	LUG14	30.60	1.60	14.10	13.00	9.77	4.33
	LUG15	30.10	2.00	13.30	13.60	8.77	4.53
	LUG16	28.40	1.30	14.10	14.10	9.40	4.70
	LUG17	28.40	1.20	13.70	14.60	8.83	4.87
	LUG18	29.10	1.60	14.30	14.10	9.60	4.70
	RLUG1	38.80	2.40	27.00	10.40	23.53	3.47
	RLUG2	25.00	3.10	7.60	13.30	3.17	4.43
	RLUG3	35.80	2.10	23.80	11.00	20.13	3.67
	RLUG4	31.90	2.40	18.50	11.10	14.80	3.70
	RLUG5	25.00	2.70	9.50	14.00	4.83	4.67
	RLUG6	25.90	3.10	15.30	9.20	12.23	3.07
	RLUG7	29.90	2.10	18.30	9.40	15.17	3.13
	RLUG8	28.60	2.50	15.20	11.20	11.47	3.73
	RLUG9	30.70	2.70	15.90	13.80	11.30	4.60
	RLUG10	27.90	2.60	12.80	11.30	9.03	3.77
St. Brendans Well	SBWG1	15.60	0.70	7.50	5.20	5.77	1.73
	SBWG2	150.00	5.20	79.40	47.30	63.63	15.77
	SBWG3	49.90	2.30	23.50	17.50	17.67	5.83
	SBWG4	48.10	2.40	24.10	14.90	19.13	4.97
	SBWG5	39.60	1.80	19.90	14.90	14.93	4.97
	SBWG6	32.30	1.70	14.60	13.20	10.20	4.40
	SBWG7	26.70	1.50	12.10	11.10	8.40	3.70
	SBWG8	32.50	1.90	13.80	16.50	8.30	5.50
	SBWG9	30.00	1.90	11.80	15.10	6.77	5.03

APPENDIX C

CORE DATA

The following page shows the amount of details of the coring carried out at Inishcorker.

Sample number(conodont/core)	Bedding (strike/dip °)	Attitude of core (°)	Depth cleaned off (cm)	Depth drilled (cm)
CORE1I	042/21N	26	6	11
CORE2I	039/21N	54	5	12
CORE3I	041/24N	62	7	12
CORE4I	041/22N	10	3	10
CORE5I	039/22N	73	12	9
CORE6I	044/22N	34	10	10
CORE7I	045/23N	47	10	12
CORE8I	049/25N	36	12	14
CORE9I	047/24N	38	10	12
CORE10I	042/24N	20	15	11
CORE11I	039/22N	22	18	10
CORE12I	039/26N	39	15	8
CORE13I	041/20N	52	14	9
CORE14I	045/22N	41	12	10
CORE15I	051/27N	8	17	8
CORE16I	041/39N	6	16	10
CORE20I	049/24N	49	7	10
CORE21I	040/22N	9	16	8
CORE22I	038/20N	38	12	5
CORE23I	042/22N	74	8	4
CORE24I	040/22N	33	15	8
CORE25I	037/19N	23	9	10
CORE26I	045/16N	9	6	12
CORE27I	039/22N	7	8	11
CORE28I	037/18N	8	12	10
CORE29I	033/18N	5	8	13
CORE30I	039/22N	85	10	9
CORE31I	035/18N	41	10	12
CORE32I	037/20N	12	12	8
CORE33I	036/19N	58	8	7
CORE34I	033/23N	16	15	8
CORE35I	032/23N	0	10	12
CORE36I	041/23N	18	12	12
CORE37I	038/16N	23	13	11

APPENDIX D

DESCRIPTIONS OF PHOSPHORITE THIN SECTIONS

To save space, descriptions of thin sections of the phosphorite samples obtained from County Clare are to be found on a disk enclosed within the back cover. MicrosoftWord version 5 (Macintosh) is needed to read them.

APPENDIX E

DESCRIPTIONS OF ARROW CANYON LIMESTONE THIN SECTIONS

To save space, descriptions of thin sections of the limestone samples obtained from Arrow Canyon are to be found on a disk enclosed within the back cover. MicrosoftWord version 5 (Macintosh) is needed to read them.

APPENDIX F

FAUNAL COUNTS PER LIMESTONE THIN SECTIONS

To save space, a spreadsheet showing occurrences of different faunal elements per sample of the limestone obtained from Arrow Canyon is to be found on a disk enclosed within the back cover. MicrosoftExcel version 3 (Macintosh) is needed to read it.

APPENDIX G

AMMONOID OCCURRENCES PER MARINE BAND

A spreadsheet has been established showing occurrences of ammonoids per marine band. The stratigraphy of Riley *et al.*, (1994) has been used. Ammonoid occurrences have been taken from a variety of literature including B.G.S. memoirs, theses and other works. To save space this spreadsheet is contained on a disk enclosed within the back cover. MicrosoftExcel version 3 (Macintosh) is needed to read it.